

Investigating the role of tumour-derived Interleukin-35 in the regulation of M2 macrophage polarisation in Head and Neck Squamous Cell Carcinomas

A thesis submitted to Cardiff University in partial fulfilment
of the requirements for the degree of
Doctor of Philosophy



September 2022



**CANCER
RESEARCH
WALES**

Richard Ali
School of Dentistry
Cardiff University
United Kingdom

DECLARATION

This work has not been submitted in substance for any other degree or award at this or any other university or place of learning, nor is being submitted concurrently in candidature for any degree or other award.

Signed: *Richard Ali*

Date: 21/09/2022

STATEMENT 1

This thesis is being submitted in partial fulfillment of the requirements for the degree of PhD (*Philosophiae Doctor*; Doctor of Philosophy).

Signed: *Richard Ali*

Date: 21/09/2022

STATEMENT 2

This thesis is the result of my own independent work/investigation, except where otherwise stated, and the thesis has not been edited by a third party beyond what is permitted by Cardiff University's Policy on the Use of Third Party Editors by Research Degree Students. Other sources are acknowledged by explicit references. The views expressed are my own.

Signed: *Richard Ali*

Date: 21/09/2022

STATEMENT 3

I hereby give consent for my thesis, if accepted, to be available online in the University's Open Access repository and for inter-library loan, and for the title and summary to be made available to outside organisations.

Signed: *Richard Ali*

Date: 21/09/2022

STATEMENT 4: PREVIOUSLY APPROVED BAR ON ACCESS

I hereby give consent for my thesis, if accepted, to be available online in the University's Open Access repository and for inter-library loans **after expiry of a bar on access previously approved by the Academic Standards & Quality Committee.**

Signed: *Richard Ali*

Date: 21/09/2022

Acknowledgements

I would like to express my gratitude to my supervisors Dr Xiaoqing Wei and Dr Adam Jones for your guidance, expertise, unwavering patience and understanding. I also extend my gratitude to Dr Elaine Ferguson for providing your time and guidance. I would also like to acknowledge Cancer Research Wales for funding my PhD studentship.

I wish to thank all members of staff who taught and guided me both professionally and personally, especially during particularly difficult personal moments. I fully appreciate the experiences I have shared with friends and colleagues I have met throughout this project, from whom I have learned a lot.

As a sufferer of chronic illness, I am particularly grateful for the support I have received from Cardiff University and staff at the School of Dentistry. I will never forget how understanding and gracious you have been in providing the time and resources for me to complete my PhD whilst managing my symptoms.

Finally, I would like to thank my close friends and family for their support throughout my PhD.

Abstract

HNSCC is the 6th most common cancer worldwide. Despite advances in treatment, responses to immunotherapies and overall survival remain unsatisfactory. Immunity in the tumour microenvironment of inflamed HNSCC is often dysfunctional. Studies have shown that macrophages therein exist preferentially in the M2 activation state, which potently suppresses anti-tumour immunity and promotes tumour aggressiveness. To improve anti-tumour immunity, it is important to identify novel regulators of M2 macrophage polarisation, which could potentially be targeted for immunotherapy.

Interleukin-35 (IL-35) is an immunosuppressive cytokine overexpressed in cancers that has been shown to reprogram immune cells to immunosuppressive phenotypes. Limited information is present on expression of IL-35 in HNSCC and its role in M2 macrophage polarisation. Preliminary studies indicated that gene expression of IL-35 subunits (EBI3 and p35) is low in HNSCC cell lines but becomes upregulated in response to stimulation with pro-inflammatory cytokines, suggesting a potential feedback response to anti-tumour immunity. This study aimed to further evaluate the upregulation of IL-35 expression in HNSCC cells in response to inflammatory stimuli, and investigate the potential role of HNSCC-derived IL-35 in the repolarisation of M1 macrophages to the prevalent M2 phenotype.

Stimulation of the hypopharyngeal carcinoma (FaDu) and oral carcinoma (H357) cell lines, with IFN γ and TNF α , elevated gene expression of IL-35. These cytokines concurrently upregulated expression of IL-35 receptors in FaDu cells. IL-10 nor IL-35 stimulation affected IL-35 endogenous gene expression. Using conditioned medium (CM) from transfected FaDu cells that overexpress IL-35 (FaDu-IL-35), and mixed culture with M1 macrophages, HNSCC-derived IL-35 was found to suppress TNF α secretion. CM from EBI3-overexpressing FaDu cells showed similar effects. IL-35 overexpression did not downregulate expression of the M1 markers HLA-DR (antigen presentation) CD80 or CD86 (T cell activation), nor did it upregulate M2 cytokines (IL-10, VEGF-A), surface markers (CD206, CD163) or candidate M2-TAM markers (PD-L1, CD204, B7-H4). Notably, FaDu-IL-35 CM downregulated PD-L1 expression in M1 macrophages, which may have implications in responses to immunotherapy. CM from p35-overexpressing FaDu cells upregulated IL-10 secretion.

These studies suggest that inflammation may induce IL-35 expression in hypopharyngeal carcinoma cells, and may also prime them to respond to exogenous IL-35 to further increase expression. IL-35 produced may not repolarise M1 macrophages to M2, but may suppress inflammation and affect responses to anti-PD-1/PD-L1 therapy. Further studies are required to confirm these findings, and to evaluate potential roles of individual IL-35 subunits in immunoregulation.

Table of Contents

Chapter 1 General Introduction	1
1.1 Head and neck squamous cell carcinomas (HNSCC)	2
1.1.1 Anatomy.....	2
1.1.2 Epidemiology and aetiology	3
1.1.3 Conventional treatment.....	4
1.1.4 Immunotherapy	5
1.2 Cancer and the Immune System	11
1.2.1 History	11
1.2.2 Cancer Immunoediting	13
1.3 Immunoediting and escape in HNSCC	13
1.3.1 Immune escape via defective antigen presentation.....	14
1.3.2 Immune escape via overexpression of immune checkpoint proteins	15
1.3.3 Immune escape through development of an immunosuppressive TME..	15
1.4 The HNSCC tumour microenvironment (TME)	15
1.4.1 Innate immune cells	16
1.4.2 Adaptive immune cells	17
1.4.3 Myeloid cells.....	18
1.5 Macrophages	19
1.5.1 History	19
1.5.2 Ontogeny.....	19
1.5.3 Macrophage activation.....	20
1.5.4 Macrophage functions.....	21
1.6 Tumour Associated Macrophages (TAMs).....	23
1.7 Roles of M2-TAMs in tumour progression	25
1.7.1 Angiogenesis.....	25
1.7.2 Invasion and metastasis	25
1.7.3 Resistance to chemotherapy and radiotherapy.....	26
1.7.4 Suppression of anti-tumour immunity	27
1.8 TAMs in HNSCC	28
1.8.1 Targeting via inhibition of TAM recruitment.....	29
1.8.2 Targeting via induction of TAM cell death	30
1.8.3 Targeting via repolarisation of TAMs from M2 to M1	31

1.9	Interleukin-35	35
1.10	Interleukin-35 in cancer.....	36
1.10.1	Role of IL-35 in tumourigenesis.....	37
1.10.2	Role of IL-35 in tumour cell growth and resistance to apoptosis.....	37
1.10.3	Role of IL-35 in angiogenesis.....	38
1.10.4	Role of IL-35 in metastasis.....	38
1.10.5	Anti-tumour roles of IL-35	38
1.10.6	Role of IL-35 in the suppression of anti-tumour immunity.....	40
1.11	Interleukin-35 in HNSCC.....	44
1.12	Project hypothesis.....	45
1.13	Project aims	45
Chapter 2 Materials and Methods		47
2.1	Cell Culture Materials	48
2.1.1	Established cell lines.....	48
2.1.2	Developed cell lines.....	48
2.1.3	Routine tissue culture materials.....	48
2.1.4	Recombinant cytokines.....	49
2.1.5	Materials for stable transfection	49
2.1.6	Equipment for general tissue culture	53
2.2	Assay Materials	53
2.2.1	Reverse Transcription quantitative PCR (RT-qPCR) materials	53
2.2.2	SDS-PAGE/Western Blot materials	54
2.2.3	Immunoprecipitation/co-immunoprecipitation materials	55
2.2.4	ELISA kits and materials.....	55
2.2.5	Flow Cytometry materials	55
2.2.6	Miscellaneous	55
2.3	General Methods	56
2.3.1	Cell Culture.....	56
2.3.2	Reverse Transcription – Quantitative Polymerase Chain Reaction (RT-qPCR)	58
2.3.3	Protein detection via Western Blotting.....	64
2.3.4	Immunoprecipitation/Co-immunoprecipitation.....	66
2.3.5	Enzyme-Linked Immunosorbent Assay (ELISA).....	68
2.3.6	Transfection	69
2.3.7	Macrophage differentiation models.....	70
2.3.8	3D tumour spheroids.....	72

2.3.9	Flow Cytometry	73
Chapter 3 Regulation of IL-35 expression in HNSCC cells by inflammatory cytokines in the tumour microenvironment80		
3.1	Introduction	81
3.1.1	Immunoediting	81
3.1.2	Interleukin 35 (IL-35)	83
3.1.3	IL-35 in HNSCC	84
3.1.4	Aims and Objectives	85
3.2	Chapter Methods	86
3.2.1	Evaluation of the effects of proinflammatory cytokines on IL-35 expression in stimulated HNSCC cell lines	86
3.2.2	Assessment of IL-35 gene upregulation in response to anti-inflammatory cytokine stimulation	92
3.2.3	RT-qPCR optimisation - Selecting a stable reference gene, calculation of primer qPCR efficiencies and RNA integrity	93
3.3	Results	94
3.3.1	Evaluation of IL-35 upregulation in response to stimulation with pro-inflammatory cytokines	94
3.3.2	Evaluation of IL-35 upregulation in response to anti-inflammatory cytokine stimulation	109
3.3.3	Assessment of changes in IL-35 receptor chain expression in response to pro-inflammatory cytokine stimulation	111
3.4	Discussion	117
3.4.1	IL-35 gene upregulation in HNSCC cell lines in response to stimulation with pro-inflammatory cytokines	117
3.4.2	Effects of anti-inflammatory cytokines on IL-35 gene expression in stimulated HNSCC cell lines	125
3.5	Conclusions	128
Chapter 4 Establishment of a HNSCC cell line that overexpresses and secretes human Interleukin 35 (IL-35)130		
4.1	Introduction	131
4.2	Aims and objectives	134
4.3	Chapter Methods	135
4.3.1	Expression plasmids	135
4.3.2	Development of a CHO cell line that overexpresses and secretes human IL-35	135
4.3.3	Development of a FaDu cell line that overexpresses and secretes human IL-35	138

4.4	Results	141
4.4.1	Development of a CHO cell line that overexpresses and secretes human IL-35	141
4.4.2	Development of a FaDu cell line that overexpresses and secretes human IL-35	150
4.5	Discussion	161
4.5.1	Chapter Methodology	161
4.5.2	Development of a CHO cell line that overexpressed human IL-35.....	164
4.5.3	Generation of FaDu cell line that overexpress IL-35	167
4.5.4	Conclusions.....	170
Chapter 5 Investigating the role of HNSCC-derived IL-35 in M1 to M2 macrophage repolarisation via suppression of the M1 macrophage phenotype.....		172
5.1	Introduction	173
5.1.1	Tumour associated macrophages (TAMs).....	173
5.1.2	M1-TAMs	173
5.1.3	M2-TAMs	175
5.1.4	Rationale of the study	176
5.1.5	Aims and objectives.....	177
5.2	Methods	177
5.2.1	Macrophage differentiation and polarisation protocols	177
5.2.2	Validation of macrophage differentiation.....	178
5.2.3	Validation of M1 and M2 macrophage models	178
5.2.4	Assessment of the role of HNSCC-derived IL-35 in the suppression of TNF α secretion by M1 macrophages	179
5.2.5	Assessment of the role of HNSCC-derived IL-35 in the downregulation of HLA-DR, CD80 and CD86 in M1 macrophages	181
5.2.6	Assessment of the role of HNSCC-derived IL-35 in suppression of M1-mediated tumour cell death	182
5.3	Results	184
5.3.1	Macrophage models	184
5.3.2	Assessment of the role of HNSCC-derived IL-35 in suppression of the M1 phenotype.....	194
5.4	Discussion	209
5.4.1	Macrophage models	210
5.4.2	Assessment of the role of HNSCC-derived IL-35 in suppression of the M1 phenotype.....	214
5.5	Conclusions	219

Chapter 6 Investigating the role of HNSCC-derived IL-35 in M1 to M2 macrophage repolarisation via promotion of the M2-TAM phenotype .221

6.1	Introduction	222
6.1.1	M2-TAMs	222
6.1.2	M2 surface markers	223
6.1.3	M2 cytokines.....	223
6.1.4	M2-TAM markers.....	224
6.2	Aims and objectives	225
6.3	Methods	226
6.3.1	Upregulation of M2 cytokine production	226
6.3.2	Upregulation of M2 surface marker expression	227
6.3.3	Upregulation of M2-TAM biomarker expression.....	228
6.4	Results	230
6.4.1	Upregulation of M2 cytokine production	230
6.4.2	Upregulation of M2 surface marker expression	234
6.4.3	Upregulation of M2-TAM biomarker expression.....	238
6.5	Discussion	242
6.5.1	Upregulation of M2 cytokine production	242
6.5.2	Upregulation of M2 surface marker expression	246
6.5.3	Upregulation of M2-TAM biomarker expression.....	248
6.5.4	Limitations	250
6.6	Conclusions	251
Chapter 7 General Discussion		253
7.1	Overview	254
7.2	Evaluation of the thesis studies	255
7.2.1	Regulation of IL-35 expression in HNSCC cells by inflammatory cytokines.....	255
7.2.2	Establishment of a HNSCC cell line that overexpresses and secretes human Interleukin 35 (IL-35).....	260
7.2.3	Investigation of the role of HNSCC-derived IL-35 in M1 to M2 macrophage repolarisation via suppression of the M1 phenotype	261
7.2.4	Investigation of the role of HNSCC-derived IL-35 in M1 to M2 macrophage repolarisation via promotion of the M2-TAM phenotype	263
7.3	Conclusion.....	266
7.4	Future studies	267
7.5	Contribution of the thesis study.....	269

References.....	80
Supplementary Data.....	301
9.1 Supplementary data 1 - RNA Integrity Scores (Chapter 3).....	301
9.2 Supplementary data 2 - Selection of a stable reference gene for qPCR normalisation (Chapter 3).....	302
9.3 Supplementary data 3 - Primer Efficiencies for gene targets in Chapter 3	303
9.4 Supplementary data 4 - Estimations of basal gene expression by RT-qPCR (Chapter 3).....	304
9.5 Supplementary data 5 – RT-qPCR Dissociation (Melt) Curves.....	305
9.6 Supplementary data 6 - Immunoprecipitation/Western blot detection of p35 in FaDu cells stimulated with IFN γ	311
9.7 Supplementary data 7 – Co-immunoprecipitation/Western blot to detect EBI3 and p35 using the Veriblot antibody	311
9.8 Supplementary Data 8 – Gating strategy to identify single, live THP1 or M1/M2 macrophages in monoculture when validating M1 or M2 polarisation ..	312
9.9 Supplementary Data 9 – Gating strategy to identify single, live CD326- macrophages when co-cultured with FaDu or FaDu-IL-35 cells	312
9.10 Supplementary Data 10 – Gating strategy to identify single, CD326+ CD14- FaDu cells when co-cultured with M1 or M2 macrophages	313
9.11 Supplementary Data 11 – 3D tumour spheroids.....	313
9.12 Supplementary data 12 - Morphology and scatter data for M1 and M2 macrophages	316
9.13 Supplementary data 13 – TNF α secretion in the M1-like cell model	317
9.14 Supplementary data 14 – Preliminary IL-10 ELISA data	318

Abbreviations

AF	Amplification Factor
ANG2	Angiopoietin 2
APCs	Antigen Presenting Cells
APM	Antigen Presentation Machinery
BCA	Bicinchoninic Acid Assay
BFA	Brefeldin A
Bregs	Regulatory B cells
BSA	Bovine Serum Albumin
CAR	Chimeric Antigen Receptors
CAR-M	Chimeric Antigen Receptor-Macrophage
CCL2	C-C motif ligand 2
CD	Cluster of differentiation
CD326	EpCAM
cGAMP	Cyclic guanosine adenosine monophosphate
CHO	Chinese Hamster Ovary
CM	Conditioned Medium
CRISPR	Clustered Regularly Interspaced Short Palindromic Repeats
CSF1	Colony-Stimulating Factor 1
CTLA-4	Cytotoxic T-Lymphocyte Associated Protein 4
CXCL	C-X-C motif chemokine ligands
DC	Dendritic Cell
DCT	Delta CT
DDCT	Delta Delta CT
dH2O	Distilled Water
DMSO	Dimethyl Sulfoxide
DTT	Dithiothreitol
EBI3	Epstein-Barr virus-induced gene 3
ECACC	European Collection of Authenticated Cell Cultures
ECL	Enhanced Chemiluminescence
EGFR	Epidermal Growth Factor Receptor
EMT	Epithelial-to-Mesenchymal Transition
EpCAM	Epithelial cell adhesion molecule
ER	Endoplasmic Reticulum
FACS	Fluorescence-activated Cell Sorting
FBS	Fetal Bovine Serum
Fc	Fragment Crystallisable
FDA	Food and Drug Administration
FMO	Fluorescence Minus One
FoxP3	Forkhead box P3
GAPDH	Glyceraldehyde 3-Phosphate Dehydrogenase
GM-CSF	Granulocyte-Macrophage Colony-Stimulating Factor
HCC	Hepatocellular Carcinoma
HIV	Human Immunodeficiency Virus
HLA	Human Leukocyte Antigen
HNSCC	Head and Neck Squamous Cell Carcinoma

HPV	Human Papillomavirus
HRP	Horseradish Peroxidase
HRPT1	Hypoxanthine Phosphoribosyltransferase 1
IDO1	Indoleamine 2,3-Dioxygenase 1
IFN γ	Interferon- γ
IgG	Immunoglobulin G
IL	Interleukin
IL-35	Interleukin-35
IRF3	Interferon Regulatory Factor 3
iTr35	Induced Regulatory T cell (via IL-35)
iTregs	Induced Regulatory T cell
JAK	Janus kinase
LAG-3	Lymphocyte Activating 3
LDH	Lactate Dehydrogenase
LDS	Lithium Dodecyl Sulfate
LILRB1	Leukocyte Immunoglobulin-Like Receptor subfamily B member 1
LMP	Low-Molecular-Weight Protein
LPS	Lipopolysaccharide
M-CSF	Macrophage Colony-Stimulating Factor
MDMs	Monocyte-Derived Macrophages
MDSC	Myeloid Derived Suppressor Cells
MET	Mesenchymal-Epithelial Transition
MHC	Major Histocompatibility Complex
MMP	Matrix Metalloproteinase
MPS	Mononuclear Phagocyte System
MSR	Macrophage Scavenger Receptor
MTT	3-(4,5-dimethylthiazol-2-yl)-2,5-diphenyl-2H-tetrazolium bromide
NC	Nitrocellulose
NCBI	National Center for Biotechnology Information
NK	Natural Killer
NTC	Negative Transfection Control
OPSCC	Oropharyngeal Squamous Cell Carcinoma
OS	Overall Survival
PAH	Polycyclic Aromatic Hydrocarbons
PBS	Phosphate Buffered Saline
PD-1	Programmed Cell Death Protein-1
PD-L1	Programmed Death-Ligand 1
PI	Propidium Iodide
PKC	Protein Kinase C
PMA	Phorbol 12-myristate 13-acetate
Poly I:C	Polyinosinic:polycytidylic acid
qPCR	Quantitative Polymerase Chain Reaction
R/M	Recurrent/Metastatic
RAG-1/RAG-2	Recombination-Activating Genes

RIN	RNA Integrity Number
RIPA	Radioimmunoprecipitation assay
RPMI	Roswell Park Memorial Institute
SD	Standard Deviation
SDS-PAGE	Sodium Dodecyl Sulfate - Polyacrylamide Gel Electrophoresis
SEM	Standard Error of the Mean
SIRP α	Signal Regulatory Protein- α
SRA	Scavenger Receptor A
STAT	Signal Transducer and Activator of Transcription
STING	Stimulator of Interferon Genes
TAM	Tumour Associated Macrophage
TAP1	Transporter Associated with Antigen Processing Gene 1
TBST	Tris-buffered saline with Tween 20 detergent
TCR	T Cell Receptor
TGF- β	Transforming Growth Factor β
Th	T helper
TIM-3	T cell immunoglobulin domain and mucin domain 3
TLR	Toll-Like Receptor
TME	Tumour Microenvironment
TMEM	Tumour Microenvironment for Metastasis
TNF α	Tumour necrosis factor-alpha
TRAIL	TNF-Related Apoptosis-Inducing Ligand
Tregs	Regulatory T cells
VEGF	Vascular Endothelial Growth Factor
WNT7B	Wingless/Integrated 7B
β 2M	Beta-2-Microglobulin

Chapter 1
General Introduction

This thesis focused on the potential role of Interleukin-35 in the suppression of anti-tumour immunity in HNSCC by repolarising M1 macrophages, which are pro-inflammatory and function to support tumour cell elimination, to an M2-like phenotype, that suppresses anti-tumour immunity and promotes tumour progression. This introduction provides a review of HNSCC, how HNSCCs evade host immunity, tumour associated macrophage (TAM) biology and therapeutic targeting, and the current understanding of IL-35 and its role in cancer. By evidencing that IL-35 can suppress anti-tumour immunity via macrophage repolarisation, the thesis research could implicate IL-35 as a novel target for immunotherapy, potentially improving poor treatment responses and survival rates.

1.1 Head and neck squamous cell carcinomas (HNSCC)

Mucosal head and neck cancers, 90% of which are head and neck squamous cell carcinomas (HNSCC), represent the sixth most common cancer worldwide, with approximately 600,000 new cases per year (Bray et al. 2018). The term HNSCC describes a variety of cancers that originate from the transformation of cells that line the surfaces (squamous epithelium) of anatomical sites within the head and neck region. These include the oral and nasal cavities, the larynx and pharynx. Collectively, HNSCC has had a devastating impact on world health, accounting for 380,000 reported deaths per year (Bray et al. 2018; Sung et al. 2021; Sun et al. 2022). While treatment options have improved over the last twenty years, patient survival rates remain poor (Siegel et al. 2017; Siegel et al. 2020; Sung et al. 2021). To improve this, novel therapies are needed.

1.1.1 Anatomy

Head and neck cancers can be subcategorised by site of origin (**Figure 1.1**). These include (1) nasal cavity and paranasal sinus cancers – that originate from the hollow spaces found inside the nose, and the air-filled spaces that surround the cavity, respectively. (2) Oral cancers – originating from the lips, gingivae, retromolar (mandible rear), anterior tongue, buccal mucosa, floor of the mouth and hard palate (which incorporates the palatal part of the maxilla). (3) Pharyngeal cancers – which initiate from three potential subsites – the nasopharynx, found superiorly, which joins

the oropharynx, and ends inferiorly at the hypopharynx. (4) Laryngeal cancers - which represent the most inferior extent of HNSCCs.

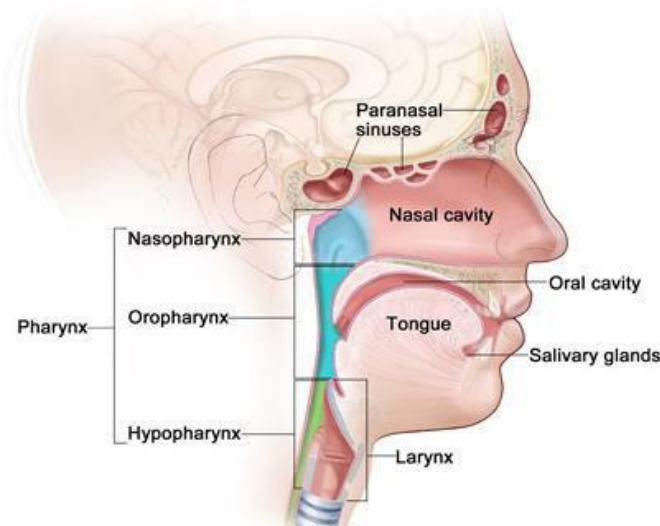


Figure 1.1 - Anatomy of the head and neck

(Image adapted from (Cancer.gov, 2017))

1.1.2 Epidemiology and aetiology

Geographically, HNSCC incidence is high in areas including India, Bangladesh and Australia (particularly oral cancer), France, Southern Africa and Central and Eastern Europe. Regarding gender, incidence is higher in men (2:1) when compared to women (1:4). Incidence is rising internationally, with nearly all countries demonstrating increased human papillomavirus (HPV) associated oropharyngeal cancer incidence, partly due to its increased recognition, as cancers of unknown origin are frequently identified in the oropharynx (Ferlay et al. 2019; Johnson et al. 2020; Sun et al. 2022).

Aetiologically, over the last 30 years, HPV infection has become regarded as a major risk factor for HNSCC (Snijders et al. 1992; Haraf et al. 1996; Vokes et al. 2015). Of all the HNSCC subtypes, HPV infection is most commonly associated with oropharyngeal squamous cell carcinoma (OPSCC) (Chaturvedi et al. 2011). Patients with HPV-associated HNSCC are often younger, non-smokers, male and Caucasian.

Prognostically, patients with HPV-associated HNSCC tend to exhibit more favourable survival rates when compared to non-HPV HNSCC (D'Souza et al. 2007; Ang et al. 2010; Benson et al. 2014).

Where HNSCC is not associated with HPV infection, tobacco and alcohol use are the two main risk factors (Sankaranarayanan et al. 1998; Pezzuto et al. 2015). Smoking tobacco (cigarettes, cigars or pipes) is associated with a 5-25% increase in risk of HNSCC diagnosis, where risk increases with the amount consumed. This may in part be due to the DNA-damaging effects of polycyclic aromatic hydrocarbons (PAH) that are present within these products (Gelboin 1980; Blot et al. 1988; Lewin et al. 1998; Wyss et al. 2013). Alcohol consumption doubles the risk of HNSCC independently of tobacco use, but also has multiplicative effects when combined with tobacco consumption (Hashibe et al. 2009; Dal Maso et al. 2016). Other aetiological factors have also been reported. Chewing of betel nut is a rising epidemic in Asia and carries a 2-15 fold increase in risk of oral HNSCC (Guha et al. 2014; Wang et al. 2018b). Poor diet choices and oral health have also been attributed to an increased risk of HNSCC (Goldenberg et al. 2004; Farquhar et al. 2017; Mazul et al. 2017).

1.1.3 Conventional treatment

For local primary tumours, treatment usually consists of surgical resection or radiation, alone or in combination with chemotherapy as a radiosensitiser (Karabajakian et al. 2017). The general aim is to remove as much of the tumour as possible whilst preserving physiological function and quality of life (Yao et al. 2007; Rivera 2015). Where patients present with small primary tumours without lymph node involvement, cure rates using these modalities are above 80% (Lee et al. 2018b).

Most patients however, present with advanced recurrent/metastatic (R/M) HNSCC (Foster et al. 2018). For R/M disease, cases where the tumour has spread outside the confines of the lymph node (extranodal), or where there is involvement of the surgical margin, systemic platinum-based chemotherapy is employed in combination with the anti-EGFR (epidermal growth factor receptor) antibody cetuximab. Though, due to resistance, response rates remain dismal, with a median overall survival (OS) of 10.1 months and a high relapse rate (Jayaram et al. 2016). Until 2016, this was the standard

course of treatment. It was at this time where the application of immunotherapies changed the landscape of HNSCC treatment.

1.1.4 Immunotherapy

HNSCC is among the most inflamed cancers, with tumours often containing a high number of immune cells (Mandal et al. 2016). The immunogenicity of tumour cells can arise from neoantigen formation. Neoantigens can originate from mutated proteins, overexpressed native proteins, or the elevated presence of HPV-derived viral antigens (E6 and E7) (Lawrence et al. 2013; Parfenov et al. 2014; Chabanon et al. 2016; Zolkind et al. 2018). These neoantigens are recognised by the immune system, resulting in the recruitment of immune cells and an anti-tumour response. However, a hallmark characteristic of malignant tumours, is that they contain tumour cells which can escape detection and/or elimination from the immune system (immunotolerance), which promotes accelerated cancer progression. Immunotherapies are designed to break this immunotolerance, reversing the underlying mechanisms in order to strengthen the host anti-tumour immune response. Advances in such therapies have revolutionised the treatment of R/M HNSCC.

1.1.4.1 Immune checkpoint inhibitors

The immunotherapy revolution began with the identification and targeting of immune checkpoint proteins. Immune checkpoints are “brake” mechanisms that normally protect the host from chronic inflammation or autoimmunity. For effector T cells to become fully activated, they first use the T cell receptor (TCR) to recognise their cognate antigen, which is bound in a complex with Major Histocompatibility Complex (MHC) molecules (Human Leukocyte Antigen (HLA) in humans) on the surface of an antigen presenting cell. A second activation signal is then required. This can be derived from expression of co-stimulatory molecules such as the B7 genes CD80 (B7-1) or CD86 (B7-2), which interact with CD28 molecules on the engaged T cell to send activation signals that lead to effector T cell functionality and tumour cell elimination. Immune checkpoints carry out the reverse function of these co-activator molecules. Instead of activating T cell responses, they instead inhibit them. Immune checkpoint proteins interact with molecules on T cells. This sends inhibitory signals that are transduced by the T cell to attenuate or prevent their activity. Thus, in cancers

including HNSCC, overexpression of these proteins describes a mechanism by which tumour cells can negate anti-tumour immunity (Mei et al. 2020).

The most studied immune checkpoint in HNSCC involves the Programmed cell death protein-1/programmed death-ligand 1 (PD-1/PD-L1) axis. PD-1 is a transmembrane protein belonging to the CD28 family of receptors. It is expressed on the surface of cytotoxic CD8⁺ T cells (Ferris 2015; Green et al. 2020). Overexpression of its cognate ligands, PD-L1 and PD-L2, has frequently been observed in HNSCC, with PD-L1 overexpressed in 60-70% of HNSCCs, most commonly when there is HPV involvement (Lyford-Pike et al. 2013; Zandberg and Strome 2014). Tumour cells can overexpress PD-L1 as an adaptive response to inflammation (particularly in response to interferon γ (IFN γ) stimulation) or via intrinsic oncogene activity (Ritprajak and Azuma 2015; Concha-Benavente et al. 2016).

Overexpression of PD-L1 enables CD8⁺ T cells that engage with tumour cells via antigen recognition, to facilitate PD-1/PD-L1 interactions. These send inhibitory signals that prevent T cells from killing the tumour cell (Sunshine and Taube 2015). Thus, by targeting this axis therapeutically, cytotoxic T cell function may be restored. Development of monoclonal antibodies that block the PD-1/PD-L1 axis was a major breakthrough in immunotherapy, and later led to two drugs being approved by the FDA (Food and Drug Administration) for the treatment of HNSCC – nivolumab and pembrolizumab.

Nivolumab was the first anti-PD-1 agent to improve overall survival in recurrent/metastatic (R/M) HNSCC. This was based on findings from the Checkmate 141 clinical trial, where patients with platinum-refractory HNSCC were shown to have reduced risk of death and improved overall survival when nivolumab treatment was used versus standard chemotherapy (7.7 months and 5.1 months, respectively) (Ferris et al. 2016; Ferris et al. 2018).

Pembrolizumab is the other major anti-PD1 drug approved for HNSCC treatment. Initially, findings of the Keynote 0-40 trial demonstrated that, in patients with R/M HNSCC whose disease recurred or progressed after previous standard treatment, median overall survival was improved to 8.4 months when patients were treated with pembrolizumab versus 6.9 months with standard chemotherapy (Cohen et al. 2019). Later, data from the Keynote-048 trial led to the approval of pembrolizumab as a first-

line monotherapy for R/M HNSCC that overexpress PD-L1. This trial showed that, in HNSCC patients with a high percentage of PD-L1 expressing cells (in both tumour and immune cells), pembrolizumab monotherapy, or when applied in combination with platinum-based chemotherapy, significantly increased median overall survival with less toxicity when compared to standard treatment (Burtneess et al. 2019).

While improvements in survival were achieved, a drawback to these drugs is that most patients do not respond, or acquire resistance which prevents the durability of responses. To improve this, many other approaches have been explored. Other immunotherapeutic modalities are detailed in the following sections. As it pertains to PD-1/PD-L1, using the aforementioned drugs in combination with alternative drugs is a commonly employed method. Pembrolizumab was found to be more effective when used in combination with other therapies (Burtneess et al. 2019). As such, additional trials are being performed which involve the use of pembrolizumab in combination with radiotherapy and chemotherapy (NCT02641093), colony-stimulating factor receptor kinase inhibitors (NCT02452424) and histone deacetylase inhibitors (NCT02538510). Nivolumab is also being assessed in combination with other treatments such as HPV vaccines (Massarelli et al. 2019) and radiotherapy (McBride et al. 2021). Aside from nivolumab and pembrolizumab, alternative antibodies, including durvalumab (anti-PD-1) and avelumab (anti-PD-L1), are also being evaluated in clinical trials for HNSCC (Wang et al. 2021).

CTLA-4 (Cytotoxic T-Lymphocyte Associated Protein 4) is another immune checkpoint protein implicated in HNSCC. It is expressed on the surface of regulatory T cells (Tregs) and activated CD4+ and CD8+ T cells. When CD4+ T cells bind to antigen presenting cells (APCs) via antigen MHC/TCR interactions, T cells can transduce activation signals from CD28, or inhibitory signals from CTLA-4. Which of these signals predominate depends on interactions with their shared binding partners - the B7 molecules CD80 and CD86. How this is regulated is not fully understood, but CTLA-4 can bind to B7 molecules with higher affinity than CD28. Inhibition of T cell activity that results from CTLA-4/B7 interactions can be beneficial when preventing autoimmunity. In cancers such as HNSCC however, CTLA-4 is often overexpressed, leading to an accumulation of exhausted T cells that cannot eliminate tumour cells. To favour inhibitory CTLA-4 activity over CD28 interactions, tumour

cells or resident regulatory T cells secrete TGF- β (Transforming growth factor β), which promotes CTLA-4 overexpression in stimulated T cells (Sullivan et al. 2001; Wing et al. 2014; Rowshanravan et al. 2018). Tremelimumab and ipilimumab are antibodies developed against CTLA-4 that are currently in clinical trials for the treatment of HNSCC (Siu et al. 2019; Ferris et al. 2020; Wang et al. 2021).

1.1.4.2 Adoptive T cell Transfer

Adoptive T cell transfer is an alternative immunotherapeutic method that aims to increase the number of activated T cells that can attack tumour cells in the patient. T cells are first isolated from surgically removed tumour tissue or peripheral blood. Ex-vivo, extracted T cells are then activated and expanded. These T cells are finally reinfused back into the patient, where they assist in tumour cell elimination. Oftentimes, the activity of adoptive T cells can be negated by tumour microenvironments that are immunosuppressive. To combat this, isolated T cells can be genetically engineered. Genetic material is added to promote expression of T cell receptor chains that have a greater affinity to tumour-associated antigens, or express chimeric antigen receptors (CAR).

Cells that express CAR receptors are termed CAR-T cells. The CAR receptor is a synthetic peptide that contains three modules - an extracellular antibody domain with a high specificity and affinity to a particular tumour antigen, a transmembrane domain, and an intracellular T-cell signalling domain, that transmits strong activation signals. These domains enable reinfused T cells to target specific tumour cells, engage with high affinity, and become strongly activated. T cell activity then functions to support tumour cell elimination. This approach is particularly useful in tumours that have developed mechanisms to restrict antigen presentation, as CAR receptors are able to bind intact surface antigens and become activated without the need for co-stimulatory signals. A drawback however, is that this restricts CAR-T cells to target tumour cells that express intact surface antigens (Kalos and June 2013; Fesnak et al. 2016). While CAR-T cells have been shown to be effective in treating haematological malignancies, they have yet to show such promise in solid cancers including HNSCC (Canning et al. 2019; Feins et al. 2019; Chen et al. 2021).

1.1.4.3 Targeting immunomodulators

Other target molecules that regulate the immune system have been targeted for HNSCC immunotherapy. Drugs developed include the IDO1 (Indoleamine 2,3-Dioxygenase 1) inhibitors navoximod and epacadostat. IDO1 and IDO2 are immunosuppressive enzymes that are overexpressed in some HNSCCs. They help catabolise tryptophan into immunosuppressive catabolites such as kynurenine (Lin et al. 2021). IDO overexpression is associated with T cell inhibition and poor patient prognoses (Godin-Ethier et al. 2011; Liu et al. 2018a; Prendergast et al. 2018). Inhibitors developed against IDO enzymes have shown promise in HNSCC treatment (Mitchell et al. 2018; Nayak-Kapoor et al. 2018; Prendergast et al. 2018). Alternatively, TLR8 (Toll-Like Receptor 8) agonists, which function to potently stimulate the anti-tumour activity of immune cells, have also shown promise (Wang et al. 2021).

1.1.4.4 Cancer Vaccines

Cancer vaccines serve to immunise patients with tumour antigens to increase the number of functional CD4⁺ and CD8⁺ T cells that specifically target and eliminate tumour cells. Prophylactic vaccines are used for disease prevention, working by inducing humoral (antibody-mediated) responses that protect the host from tumour occurrence. Therapeutic cancer vaccines treat existing tumours by stimulating cell-mediated (adaptive) immune responses against tumour cells (Wierzbicka et al. 2014). Therapeutic vaccines generally contain peptide epitopes belonging to specific tumour antigens known to be expressed in tumour cells detected in the patient. These vaccines are infused into the patient, where they are detected and captured by specialised antigen presenting cells. Dendritic cells (DC) are crucial APCs for presenting tumour antigens to cytotoxic T cells. DCs process captured tumour antigens into short peptide epitopes. They carry these antigens to lymphoid organs, where they present antigenic epitopes on their surfaces in association with MHC molecules. Exogenous antigens are normally presented by APCs bound to MHC Class II molecules, which allows engagement with specific TCRs and subsequent priming of naïve CD4⁺ T cells. IFN γ and IL-12 produced by the DCs polarise the naïve CD4⁺ T cell to the Th1 lineage (Type 1 T helper cells). Now active, these cells produce cytokines to help activate

CD8⁺ T cells, and travel to the tumour, where they enhance immune responses by producing pro-inflammatory cytokines. DCs can also present exogenous tumour antigens to naïve CD8⁺ T cells via cross-presentation. CD8⁺ TCR engagement with MHC I/antigen complexes results in cell activation and differentiation into cytotoxic CD8⁺ T cells. These cells use MHC I/antigen recognition to specifically target tumour cells. They then eliminate them via cytokine secretion, perforin or granzyme release. Alternatively, vaccines may promote T cell differentiation into memory T cells, which provide protection from tumour recurrence (**Figure 1.2**) (Shibata et al. 2021; Sun et al. 2022).

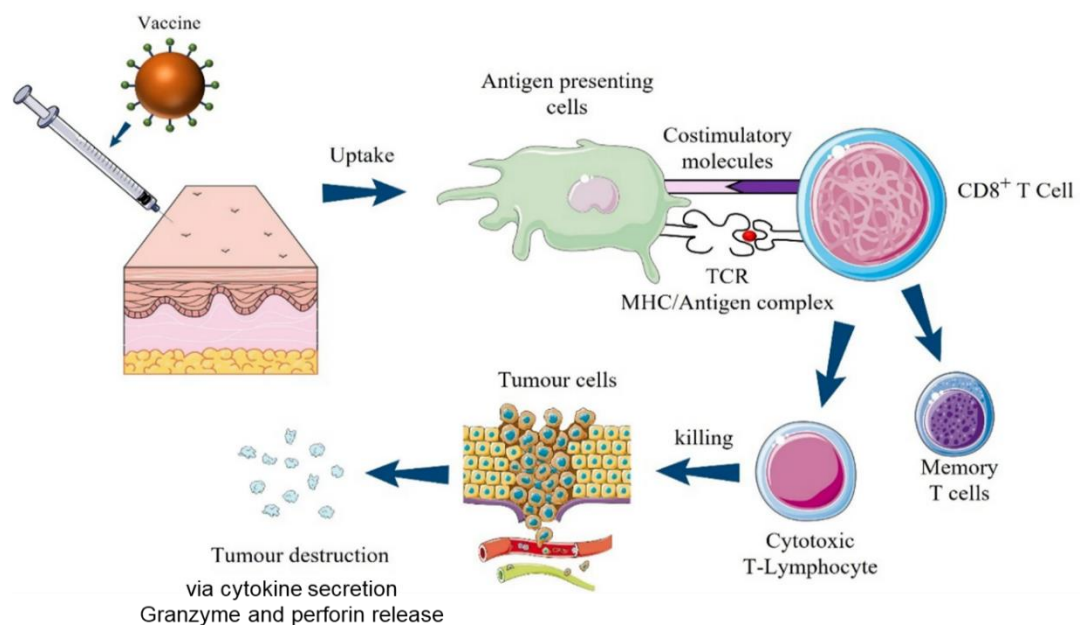


Figure 1.2 Tumour killing by cancer vaccines.

Vaccines containing tumour associated antigens are infused into patients. These are captured by dendritic cells, which cross-present tumour antigens to naïve CD8⁺ T cells. Upon engagement, they are activated and differentiate into cytotoxic T cells that kill tumour cells, or memory T cells, which protect the host from future tumour formation. Adapted from (Sun et al. 2022).

Cancer vaccines can be developed using several platforms including cell-based, gene-based or protein/peptide-based vaccines. Cell-based vaccines use tumour cells from the patient, or tumour cell lines or lysates. These contain tumour antigens that are not overexpressed in normal cells. They are exposed to autologous dendritic cells ex-vivo, which when re-infused into patients, present tumour antigens to naïve T cells. Autologous DC vaccines can be derived as such, or by loading them directly with specific tumour antigens prior to re-infusion. The advantage of this is that they

immediately present tumour antigens in the host without the need for antigen capture and processing (De Gruijl et al. 2008; Tagliamonte et al. 2014).

Gene-based vaccines include DNA and RNA vaccines. These involve the delivery of plasmids containing genes that encode specific tumour antigens. When infused into the patient, they are captured by DCs. DCs then overexpress the tumour antigen, process it into epitopes and present them to naïve T cells (Shibata et al. 2021).

Peptide vaccines generally involve the infusion of synthetic long peptides that come from specific tumour antigens. These are captured, processed and presented by DCs. Peptide vaccines are the most commonly used cancer vaccine modality as they are deemed safe and easy to store long-term (Rosalia et al. 2013; Li et al. 2017; Bezu et al. 2018; Shibata et al. 2021; Sun et al. 2022).

For HNSCC, prophylactic vaccines have been FDA-approved. Gardasil and Gardasil 9 are prophylactic vaccines derived from HPV particles which are used in the prevention of oropharyngeal and other HPV-associated HNSCCs. These vaccines enable the generation of neutralising antibodies that target and prevent infection from HPV 6/11/16/18 – Gardasil, or HPV 6, 11, 16, 18, 31, 33, 45, 52, and 58 - Gardasil 9. While preventative, the antibodies these vaccines produce cannot access intracellular HPV antigens in patients already diagnosed with HPV+ HNSCC, and so efforts have been made to develop therapeutic vaccines (von Witzleben et al. 2020).

Many therapeutic vaccines have been or are being investigated in clinical trials (Sun et al. 2022). Though, despite the potential of these novel approaches, no therapeutic peptide vaccines have been approved for clinical use in HNSCC treatment. Therefore, there is a requirement for novel immunotherapies that may improve overall survival in HNSCC patients. To develop such therapies, there needs to be a greater understanding of how tumour cells dysregulate immune cells in the HNSCC TME.

1.2 Cancer and the Immune System

1.2.1 History

The relationship between tumour cells and the immune system is complex. Today, it is understood that the host immune system can act as a double-edged sword, able to detect and eliminate tumour cells, but also protect them and promote cancer

development. The investigations leading to this consensus are long and somewhat controversial, and so only the major findings will be reviewed here.

Early studies by Paul Ehrlich suggested that the growth of carcinomas could be inhibited by the host immune system (Ehrlich 1909). Though, due to a lack of relevant biological models at the time, experiments to evidence this could not be performed. Over the course of the following century, this would be resolved as inbred mouse strains became available. Syngeneic transplantation studies using these mice indicated that tumour cells can express antigens which are able to trigger immune responses (Old and Boyse 1964). This led Burnet and Thomas to propose the concept of “cancer immunosurveillance” – the idea that “thymus-dependent” cells (now known as T cells) can act as sentinels, patrolling tissues of the body to seek and destroy newly transformed cells that express these antigens (Burnet 1964; Burnet 1970). However, the validity of this concept came under challenge, as later experiments using athymic mice, thought immunologically deficient, produced results that suggested the immune system had no role in the regulation of cancer (Stutman 1974; Stutman 1979). As a consequence, the theory of immunosurveillance was abandoned. It was not until later, following improvements in mice genetics, when it became understood that athymic mice still possessed natural killer (NK) cells and a small number of functional T cells. Therefore, anti-tumour responses were still possible, and this cast doubt over the conclusions drawn from these experiments (Ikehara et al. 1984; Maleckar and Sherman 1987).

In the 1990’s, the availability of immunologically deficient mice led to a resurgence in the investigation of cancer immunosurveillance. Key experiments used mouse strains lacking expression of recombination-activating genes (RAG-1/RAG-2), required for the generation of mature B, T and natural killer T cells (Shinkai et al. 1992). Following chemical induction of tumour formation, RAG-2-deficient mice displayed an earlier occurrence and increased frequency of spontaneous tumours when compared to wildtype, age-matched mice (Shankaran et al. 2001). Thus, these results confirmed that the immune system can contribute to the elimination of tumour cells. It was these findings that led to the theory of cancer immunoediting (Dunn et al. 2002; Dunn et al. 2004).

1.2.2 Cancer Immunoediting

Cancer immunoediting describes three phases (Elimination, Equilibrium and Escape), whereby nascent tumours that are initially targeted by the immune system, develop mechanisms that enable them to escape immunosurveillance, and manipulate immune cells to promote immune suppression and accelerate tumour development.

Elimination broadly describes the immunosurveillance paradigm, where newly transformed cells expressing high-affinity neoantigens are detected and destroyed by cells of the immune system (Dunn et al. 2004; Mittal et al. 2014). Less immunogenic tumour cells can survive Elimination and proceed to the Equilibrium phase. Here, tumours are held dormant as tumour cell outgrowth is modulated by the immune system. Constant exposure to immune cells and cytokines creates a selective pressure on tumour cells, causing some cells to adapt. These tumour cells “edit” themselves or immune cells around them, acquiring traits that inhibit immune cells from detecting or eliminating them. The balance between tumour cells that are successfully controlled by the immune system, and the development and outgrowth of immunotolerant subclones, describes Equilibrium. This state of tumour dormancy can last for several years (Koebel et al. 2007; Eyles et al. 2010; Teng et al. 2012; Wu et al. 2013).

Eventually, tumours can progress to Escape. Here, positive selection leads to the accelerated outgrowth of tumour subclones that possess mechanisms which allow them to escape immunosurveillance. Multiplication of these subclones within the presence of immune cells leads to the formation of clinically detectable tumour masses (Dunn et al. 2004).

1.3 Immunoediting and escape in HNSCC

Several studies have evidenced the existence of immunoediting in HNSCC. Reports have shown that, when compared to healthy individuals, there is an increased incidence of HNSCC in immunocompromised individuals, such as those infected with human immunodeficiency virus (HIV), or immunosuppressed recipients of transplantation (Bhatia et al. 2001; Haigentz 2005). This supports the anti-tumour role the immune system plays in preventing HNSCC formation. However, immunocompetent HNSCC patients commonly present with tumours that contain a high number of immune cells. Yet, these cells have a reduced capacity to eliminate

tumour cells (Mandal et al. 2016). Tumour cells facilitate this by employing Escape mechanisms. Several mechanisms have been described for HNSCC. These can broadly be categorised into three groups: (1) defects in antigen presentation, (2) overexpression of immune checkpoint proteins and (3) development of an immunosuppressive tumour microenvironment (TME).

1.3.1 Immune escape via defective antigen presentation

Effector CD8⁺ T cells target tumour cells via recognition of specific antigens that are expressed on their cell surface bound to HLA/MHC I molecules. Once engaged, the cytotoxic activity of the T cell eliminates the tumour cell. HNSCC cells can evade detection by downregulating expression of the tumour antigen, preventing presentation of the antigen via downregulation of HLA/MHC I expression, or by altering expression or the activity of the antigen presentation machinery (APM). This machinery contains proteins that process tumour antigens into short peptides, and that load these peptides onto HLA Class I molecules, which are then translocated to the cell surface for recognition by CD8⁺ T cells.

APM defects in HNSCC include the dysregulation of LMP2 and LMP7 (low-molecular-weight protein 2 and 7), which are members of the antigen-processing proteasome complex, tapasin and TAP1 (transporter associated with antigen processing gene 1) of the translocation machinery, and mutations in the β 2M (Beta-2-Microglobulin) subunit of the HLA/MHC I complex (Ferris et al. 2005; Ferris et al. 2006; López-Albaitero et al. 2006; Seliger et al. 2020). The consequence of these defects is the reduced expression of HLA/MHC I and bound antigens on the cell surface. Therefore, these tumour cells use these mechanisms to escape detection and elimination by CD8⁺ T cells.

It is important to note that complete loss of HLA/MHC I expression would normally provide a strong stimulus for the activation of NK cells, which in turn would eliminate the tumour cell (Ljunggren and Kärre 1990). HNSCC cells bypass this by promoting the downregulation, but not complete absence, of HLA/MHC I expression (Ferris 2015). These mechanisms therefore enable HNSCC cells to escape the cytotoxic activity of both CD8⁺ T cells and NK cells.

1.3.2 Immune escape via overexpression of immune checkpoint proteins

As previously described, T cells that engage with tumour cells via antigen presentation require co-stimulatory signals to promote their expansion and activity. Immune checkpoint proteins act as co-inhibitory signals, preventing or attenuating the activity of bound T cells. The most studied immune checkpoints that are overexpressed in HNSCC include PD-1, PD-L1, and CTLA-4 (reviewed above). Overexpression of checkpoint proteins by tumour cells or immune cells in the HNSCC TME thus suppresses the ability of the immune system to eliminate detected tumour cells, and can also result in an abundance of dysfunctional T cells.

1.3.3 Immune escape through development of an immunosuppressive TME

In an inflamed TME, tumour cells can alter the behaviour of cells around them to sculpt an immunosuppressive microenvironment. To facilitate this, tumour cells produce chemokines that recruit immunosuppressive cells, secrete cytokines that either negate the activity of anti-tumour immune cells, or reprogram them in such a manner that they instead function to suppress immunity (Whiteside 2002; Ferris et al. 2006; Zandberg and Strome 2014). By creating an TME with cells and mediators that negate anti-tumour immunity, tumours can evade immunosurveillance, but also become resistant to immunotherapies. Thus, to improve immunotherapies, it is important to better understand the immune components of the HNSCC TME and how they are regulated.

1.4 The HNSCC tumour microenvironment (TME)

Cancers are no longer viewed as a bulk of accumulated tumour cells, but rather a complex ecosystem containing tumour cells and a plethora of additional cell types and structures that together form a self-sufficient entity known as the tumour microenvironment. Cells found include non-immune types such as fibroblasts. Fibroblasts are important as they provide growth factors and promote metastasis via matrix remodelling. They also promote blood vessel formation, providing oxygen and nutrient supplies. However, immune cells in the TME are of high importance as it pertains to tumour development and immunotherapy (Peltanova et al. 2019; Baghban et al. 2020).

The HNSCC TME can be heterogenous, which may affect responses to therapy. Generally, TMEs have been classified into three groups based on their immunological profile. (i) “hot” or inflamed tumours. These are rich in pro-inflammatory cytokines and effector immune cells such as CD8+ T cells and natural killer cells. (ii) “Cold” or non-inflamed tumours. These contain a paucity of the aforementioned immune cells, but a high density of immunosuppressive cytokines and immune cells such as regulatory T cells and myeloid derived suppressor cells (MDSCs). (iii) Immune deserted tumours. These generally lack immune cells. HPV+ HNSCCs are often inflamed but contain an array of dysfunctional or immunosuppressive immune cells that do not eliminate tumour cells, and may contribute to immunotherapy resistance (Allen et al. 2015; Chen and Mellman 2017; Trujillo et al. 2018; Canning et al. 2019). By understanding the regulation of the immune cells in the HNSCC TME, new and effective immunotherapies can be developed. A summary of the immune cell constituents in the HNSCC TME, and their prognostic significance, is given below.

1.4.1 Innate immune cells

Neutrophils are recruited as early responders to nascent tumour cell formation. They use chemotactic signals to migrate from the bloodstream into the tumour. Here, depending on the nature of the cytokine milieu, neutrophils can exhibit polarised functional states broadly categorised as N1 or N2. N1 neutrophils antagonise tumour development, using mechanisms including tumour cell phagocytosis, production of anti-microbial products and enhancement of immune responses through secretion of pro-inflammatory cytokines. Conversely, N2 neutrophils support tumour development by promoting genetic instability, angiogenesis and immune suppression. High densities of neutrophils, regardless of polarisation state, have been associated with poor HNSCC prognoses. Though, to better understand the role of these neutrophils, studies may benefit from the identification of biomarkers that can be used to subclassify N1 and N2 neutrophils in-vivo (Dumitru et al. 2013; Zhang et al. 2016b; Masucci et al. 2019).

Natural killer cells are cytotoxic cells of the innate immune system that play an important role in tumour elimination. Within tumours, they detect and eliminate cells under stress that do not express HLA Class I molecules on their surface. Additionally, they enhance immune responses by producing pro-inflammatory cytokines. Clinically,

high densities are associated with better overall survival, which is in line with their inflammatory and cytotoxic functions. Nevertheless, in some cases they have been shown to exhibit altered functionality, whereby they can suppress immunity and promote tumour development. How the NK phenotype can be regulated in the HNSCC TME requires further investigation before their impact can be fully assessed (Mandal et al. 2016; Concha-Benavente et al. 2018; Wondergem et al. 2020).

1.4.2 Adaptive immune cells

Naïve CD8+ T cells are activated in lymph nodes following engagement with their cognate antigen and subsequent cytokine stimulation. Once activated, they differentiate into memory or cytotoxic T cells that circulate and enter the tumour tissue, seeking and destroying resident tumour cells (Zhang and Bevan 2011). Due to their cytotoxic nature, like NK cells, they are regarded key players in the anti-tumour response. Many reports have associated high CD8+ T cell infiltrates with improved survival in HNSCC (reviewed by (Wondergem et al. 2020)). However, density alone does not give a clear picture of their role, as their functionality can be inhibited by immunosuppressive cells and cytokines in immunoedited TMEs.

CD4+ T cells are a heterogeneous cell type. When activated, naïve CD4+ T cells differentiate into effector cells that are categorised into various subtypes. These include, Th1 (T helper type 1), Th2, Th9, Th17, Tregs and follicular T cells (Kim and Cantor 2014). This heterogeneity creates a degree of complexity when evaluating the prognostic effect of infiltrating T cells identified using CD4+ staining. This is evident, as studies have reported contrasting associations between CD4+ density and patient prognoses (Wondergem et al. 2020). As their functions vary, use of biomarkers to differentiate between subtypes may be beneficial. Regulatory T cells can be identified using CD4+ and FoxP3+ (Forkhead box P3) double staining (Kim and Cantor 2014). Within the TME they function as potent suppressors of anti-tumour immunity. Hence, meta-analyses have shown that in several cancers, high densities of FoxP3+ Tregs are associated with disease progression and poor survival. In HNSCC however, several reports have suggested that high CD4+ FoxP3+ Treg densities are associated with better overall survival. It is not yet understood why this occurs (Badoual et al. 2006; Liang et al. 2011; Shang et al. 2015; Seminerio et al. 2019).

B cells are a key part of the adaptive immune response against tumours. When mature, functional B cells that infiltrate into the tumour produce antibodies. These antibodies bind onto tumour cells and label them for elimination (Deola et al. 2008). Accordingly, B cells that facilitate this are regarded friendly, as they oppose tumour development. Nonetheless, B cell function can be edited within the TME. A cytokine milieu that is strongly immunosuppressive can reprogram B cells into regulatory B cells (Bregs). Bregs can perform immunosuppressive functions, including the secretion of anti-inflammatory cytokines, inhibition of Th1/Th17 differentiation, and the promotion of tumour-promoting Th2 and FoxP3+ Treg differentiation (Gavrielatou et al. 2021). As B cell phenotype can vary, the overall association between B cell density and HNSCC prognoses is not yet clear (Wondergem et al. 2020; Gavrielatou et al. 2021).

1.4.3 Myeloid cells

Myeloid cells that infiltrate the HNSCC TME include dendritic cells, MDSCs and macrophages. Myeloid dendritic cells circulate through the bloodstream and migrate into tumour tissue, where they can capture and internalise tumour-associated antigens. They transport these antigens from the tumour site to the draining lymph nodes. During transport, myeloid DCs undergo maturation, upregulating genes such as CD80, CD86 and MHC II, which enables them to present captured antigens to naïve T cells and subsequently activate them. These activated T cells then migrate to the tumour tissue, where they help to eliminate tumour cells. Studies in HNSCC have shown that high densities of myeloid DCs in the TME are associated with high lymphocyte infiltrates, lower rates of both metastases and tumour recurrence, and increased survival (Gallo et al. 1991; Goldman et al. 1998). More recent studies have also supported these findings (Karpathiou et al. 2017; Jardim et al. 2018).

However, in tumours with an abundance of immunosuppressive factors, DC function can be edited. These factors can prevent DC maturation and their ability to present antigens. This leads to the accumulation of immature DCs in tumours which, instead of repressing tumour development, assist in promoting it, through mechanisms including the secretion of additional immunosuppressive factors (Gabrilovich 2004). It is unsurprising therefore, that some reports associate high myeloid DC infiltrates with poor prognoses in HNSCC (Wondergem et al. 2020). These conflicting findings may be in part due to the opposing roles of mature and immature dendritic cells, but

could also be affected by patient heterogeneity and differences in the TME between HNSCC subsites.

Infiltrating MDSCs are potent suppressors of anti-tumour immunity. They inhibit both the innate and adaptive immune systems by secreting immunosuppressive cytokines (Almand et al. 2001; Ostrand-Rosenberg and Sinha 2009). High densities have been described in HNSCC when compared to normal mucosa (Bu et al. 2016; Ma et al. 2017), and their accumulation has been correlated with high clinical stage and pathological grade (Ma et al. 2017). Aside from the myeloid cells mentioned, macrophages and their role in HNSCC immunity represents a major part of this thesis. Therefore, a more extensive review of macrophages and their role in HNSCC is given below.

1.5 Macrophages

1.5.1 History

Macrophages are large phagocytes that are integral to the immune system. The term macrophage ($M\Phi$) was introduced following early experiments by Elie Metschnikoff. In these experiments, he demonstrated the ability of digestive cells to ingest foreign material (Metschnikoff 1878). He later described these cells as phagocytes (originating from the Greek words “phago” meaning devour, and “cytos” meaning cell) (Metschnikoff 1884). These phagocytes were subclassified as macrophages (big eater) and microphages (small eater) (now known as neutrophils). In his seminal work, he also showed that macrophages use phagocytosis to contribute to host immunity against pathogens, but also to perform scavenger functions – the devouring and removal of dying/dead cells (Metschnikoff 1887). The importance of these findings in the field of immunology were later recognised, as Metschnikoff was granted the Nobel Prize in 1908, and is considered the father of innate immunity (Gordon 2008; Kaufmann 2008).

1.5.2 Ontogeny

Over the last decade, the field of macrophage ontogeny has developed substantially. Macrophages, circulating monocytes, dendritic cells and bone marrow precursors make up the mononuclear phagocyte system (MPS) proposed by van Furth and

colleagues (van Furth et al. 1972; Taylor and Gordon 2003). The traditional view of the MPS suggested that bone marrow precursor cells give rise to monocytes, which migrate from peripheral blood into tissues. It is here they differentiate into tissue-resident macrophages. Thus, the prevailing dogma was that circulating monocytes act as reservoirs of cell precursors, readily replacing tissue macrophages that have died (van Furth and Cohn 1968).

In more recent times, accumulating evidence challenged this perception. Fate mapping studies elucidated that tissue-resident macrophages describe a distinct cellular entity present before birth, which originate in the yolk sac during early haematopoiesis. These cells also demonstrate the capacity for self-renewal, used to maintain their numbers in tissues of adults. This therefore negated the idea that tissue-resident macrophages require replenishment from circulating monocyte precursors (Schulz et al. 2012; Sieweke and Allen 2013). It is now understood that tissue-resident macrophages can be sourced from either, yolk sac progenitors, foetal liver monocytes or infiltrating bone marrow-derived monocytes (Schulz et al. 2012; Gomez Perdiguero et al. 2015).

1.5.3 Macrophage activation

As it pertains to monocyte-derived macrophages, monocytes are first recruited to sites of tissue damage or inflammation, such as tumours. Here, they differentiate into macrophages. The phenotype and function (known as the activation state) of these macrophages can differ depending on the nature of their environmental cues. Furthermore, macrophages display functional plasticity, that is, their activation state is not fixed and can change dynamically in response to alterations in the nature of the surrounding cytokine signals (Gordon 2003; Mosser 2003; Auffray et al. 2007; Benoit et al. 2008).

A large body of research has attempted to subclassify the activation states a macrophage can undertake. Two polarised activation states were first described - M1 and M2, also known as classically activated and alternatively activated macrophages, respectively. These terms were coined from early studies by Nathan and Gordon. They observed phenotypic differences in macrophages that were treated with interleukin-4 (IL-4), when compared to that following stimulation with IFN γ and

lipopolysaccharide (LPS) (Nathan et al. 1983; Stein et al. 1992; Martinez and Gordon 2014). IL-4-stimulated macrophages were described as ‘alternatively activated’, whereas those stimulated with IFN γ and LPS were termed ‘classically activated’. More recently, the term classically activated macrophages has been broadened to describe those stimulated by IFN γ and/or agents that trigger toll-like receptor activation.

M1/M2 nomenclature was later introduced by Mills. This was based on the Th1/Th2 helper T cell paradigm. Th1 cells produce pro-inflammatory cytokines such as IFN γ , whereas Th2 cells secrete anti-inflammatory cytokines including IL-4 and IL-13 (interleukin-13), each promoting M1 and M2 macrophage activation states, respectively (Mills et al. 2000). Beyond these classifications, a third set of nomenclature was devised by Mantovani. This disregarded the notion that macrophage activation states were binary and purported a spectrum of different activation states. Classically activated macrophages (via treatment with IFN γ and LPS or tumour necrosis factor alpha, TNF α) were termed M1. Alternatively activated macrophages induced by IL-4/IL-13 were termed M2a. Those activated by engagement of Fc (fragment crystallisable) receptors with immune complexes were named M2b. Finally, macrophages stimulated with IL-10, TGF β and glucocorticoids were described as M2c (Gordon 2003; Martinez et al. 2008). Other classifications were suggested after this, such as that made by Joshi, who defined M1 and M2 polarisation based the phenotype of cells that were stimulated by the growth factors granulocyte-macrophage colony-stimulating factor (GM-CSF) and macrophage colony-stimulating factor (M-CSF) respectively (Joshi et al. 2014).

Currently, it is generally believed that macrophage activation states represent a large spectrum of phenotypes in which M1 and M2 represent inflammatory and anti-inflammatory extremes, respectively. Phenotypes that exist between these extremes are thus described as M1-like, M2-like or an M1/M2 hybrid state.

1.5.4 Macrophage functions

M1-like macrophages are activated by Th1 cell-derived IFN γ , TNF α and agonism of toll-like receptors. The IFN γ signal is transduced by its receptor on the cell surface, resulting in the increased activity of the downstream transcription factors STAT1

(signal transducer and activation of transcription 1) and IRF3 (interferon regulatory factor 3) (Biswas and Mantovani 2010; Xue et al. 2014). These transcription factors increase the expression of genes that promote the pro-inflammatory phenotype of M1-like macrophages. The functions of M1-like macrophages include, the ability to uptake and eliminate foreign material by phagocytosis, and to present captured exogenous antigens via upregulation of MHC II expression. They promote T cell activation via expression of the co-stimulatory molecules CD80 and CD86. They also secrete pro-inflammatory cytokines such as TNF α , IL-6 (Interleukin 6) and IL-1 β (interleukin 1 β), which enhance immune responses, and reactive oxygen and nitrogen species, which eliminate pathogens and tumour cells (Zheng et al. 2017; Orecchioni et al. 2019; Jayasingam et al. 2020). Considering these roles, M1-like macrophages are regarded as having anti-tumour behaviour. Macrophage functions have been summarised in **Figure 1.3**.

M2-like macrophages are activated by Th2 cell-derived cytokines such as IL-4 or IL-13. These cytokines induce a different intracellular signalling cascade, generally resulting in activation of STAT6 and IRF4 (Biswas and Mantovani 2010). Functionally, M2 macrophages resolve inflammation via production of immune-suppressing mediators such as IL-10 and TGF β , and by scavenging residual inflammatory markers and dead cells. They also have roles in allergy and parasite clearance and promote wound healing via tissue remodelling and angiogenesis (**Figure 1.3**). As such, M2 macrophages can promote tumour development (Sica and Mantovani 2012). Markers of M2 macrophage polarisation include the scavenger receptor CD163, the mannose receptor (CD206), CD209 (DC-SIGN), IL-10, VEGF (vascular endothelial growth factor), TGF β and genes involved in arginine metabolism (Orecchioni et al. 2019).

The ability of macrophages to alter polarisation states in response to changing stimuli enables them to coordinate the course of an inflammatory response. This includes inducing pathogen killing and the engulfing and digestion of cellular debris, and later promoting wound healing and tissue regeneration post-inflammation (Stout et al. 2005; Biswas and Mantovani 2010; Orecchioni et al. 2019; Jayasingam et al. 2020).

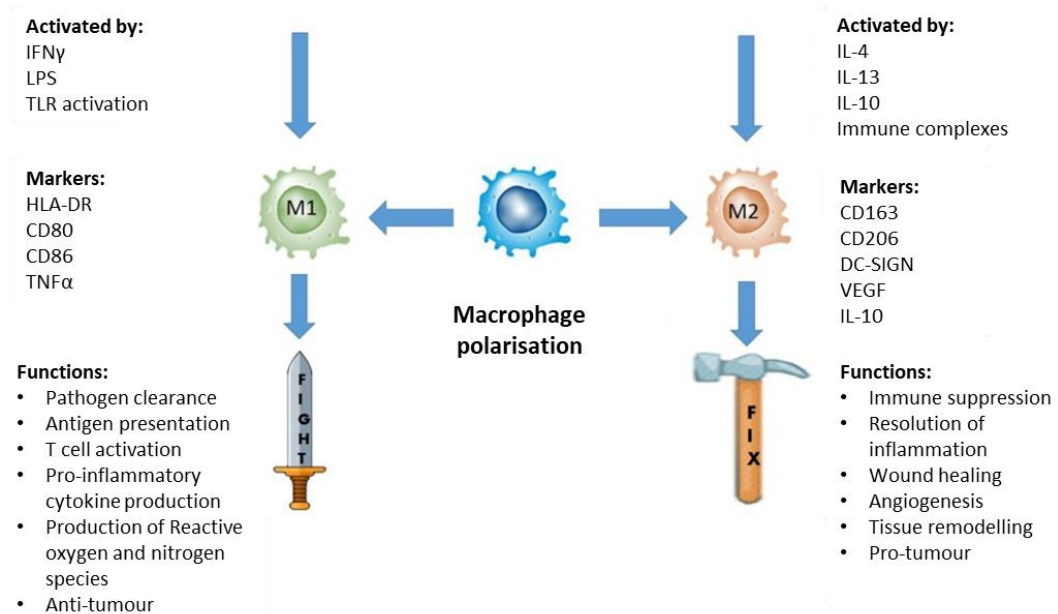


Figure 1.3 Macrophage polarisation.

Illustration of macrophage polarisation into either M1 or M2 activation states, their identification markers and biological functions. Adapted from (Jayasingam et al. 2020).

1.6 Tumour Associated Macrophages (TAMs)

Macrophages that populate solid tumours are termed tumour-associated macrophages (TAMs). TAMs are a vital component of the TME, comprising the most abundant population of tumour-infiltrating immune cells, and up to 50% of all cells (Morrison 2016; Azizi et al. 2018). As such, they play important roles in cancer progression and clinical outcome. Oftentimes, a higher density of TAMs is observed at more advanced stages of tumour progression. This has been shown in oesophageal cancer (Li et al. 2019a), ovarian cancer (Yuan et al. 2017), breast cancer (Qiu et al. 2018) and pancreatic cancer (Di Caro et al. 2015). In line with this, TAM densities are positively correlated with poor clinical outcomes. This has been reflected in oesophageal (Li et al. 2019a), pancreatic (Yu et al. 2019), breast (Zhao et al. 2017a), lung (Wu et al. 2016b), gastric (Wu et al. 2016b) and oral cancers (Hu et al. 2016). Therefore,

understanding the roles and regulation of TAMs is important if they are to be targeted for immunotherapy.

TAMs can originate from tissue resident macrophages that are already present prior to tumour formation, or from circulating monocytes that are recruited into the tumour. Circulating monocytes are recruited via environmental cues including local anoxia (absence of oxygen), inflammation, high levels of lactic acid and chemokine attraction. Chemotactic signals include the major macrophage recruitment molecule C-C motif ligand 2 (CCL2), colony-stimulating factor 1 (CSF1) also known as M-CSF, cytokines and complement components (Hao et al. 2020; Zhou et al. 2020). Once these monocytes infiltrate the TME, the milieu of environmental signals enable them to become differentiated into macrophages.

After differentiation, TAMs can display a wide spectrum of activation states. The state they exhibit is dependent on a number of factors, such as the overall nature of the environmental signals within the tumour, the tumour site and stage. Predominance of pro-inflammatory signals induces M1-like macrophage polarisation (Noy and Pollard 2014). M1-like TAMs are anti-tumour in function. They antagonise tumour development directly, by eliminating tumour cells through phagocytosis and release of reactive oxygen and nitrogen species, or via secretion of TNF α . Alternatively, macrophages can indirectly control tumour progression via the secretion of pro-inflammatory cytokines. These help recruit and activate cytotoxic immune cells that target and destroy tumour cells. The most commonly attributed role of M1-TAMs however, is their ability to capture and present tumour antigens to resident effector CD4⁺ T cells using MHC II, and to enhance the anti-tumour activity of bound T cells through engagement with the co-stimulatory molecules CD80 and CD86 (Zheng et al. 2017; Jayasingam et al. 2020; Muntjewerff et al. 2020).

While M1 polarisation is possible in tumours, TAMs are generally synonymous with an immunosuppressive M2-like activation state. This state is commonly detected in tumours, and can be derived from the exposure of macrophages to an abundance of immunosuppressive cells and cytokines that are present in immunoedited TMEs at advanced disease stages. When prevalent, M2-TAMs are potent promoters of tumour progression. Mechanisms they use to contribute to this are detailed below and summarised in **Figure 1.4**.

1.7 Roles of M2-TAMs in tumour progression

1.7.1 Angiogenesis

As development progresses, tumours reach a size where they can no longer grow. To continue, they require a vascular network, which provides oxygen and nutrition, and enables the removal of waste products. The formation of this vascular network describes the angiogenic switch. During angiogenesis, new blood vessels are created within the tumour. Dilation of these vessels is promoted to increase influx of nutrients. Perivascular cells are also recruited to regulate blood flow (Bergers and Benjamin 2003; Bruno et al. 2014). M2-TAMs partake in this process by secreting pro-angiogenic factors such as VEGF-A and the C-X-C motif chemokine ligands, CXCL8 and CXCL12 (Lin and Pollard 2007; Hughes et al. 2015). Recruitment of endothelial cells, fibroblasts and pericytes are promoted by additional M2-TAM derived factors such as WNT7B (wingless/integrated 7B), TGF- β , TNF and thymidine phosphorylase. Together, these cells and signals contribute to the generation of vascular networks within the TME (Hirano et al. 2001; Yeo et al. 2014).

The angiopoietin 1 receptor TIE2 (also known as TEK) is an important regulator of tumour angiogenesis. TIE2 is a receptor tyrosine kinase expressed on a subpopulation of TAMs that localise near blood vessels. The interaction of TIE2 with its ligand, angiopoietin 2 (ANG2), triggers the process of new vessel formation (neovascularisation) (Venneri et al. 2007; Mazziери et al. 2011). Under hypoxic conditions, such as within growing tumours, both these genes are overexpressed, and provide a cascade whereby new blood vessels replenish the supply of oxygen. In line with this, the subpopulation of TIE2 expressing TAMs comprise the majority of myeloid-derived angiogenic activity within the TME (De Palma et al. 2005; Mazziери et al. 2011).

1.7.2 Invasion and metastasis

Invasive tumour cells are defined by their ability to leave the primary tissue site and enter the bloodstream (intravasation), where they migrate to distant locations and establish secondary tumours (metastasis) (Kitamura et al. 2015). M2-TAMs can play a role in this process by producing enzymes such as serine proteases, MMP2 (matrix metalloproteinase-2) and MMP9 (matrix metalloproteinase-9), and cathepsins. These

enzymes disrupt cell-cell and cell-to-basement membrane interactions, enabling tumour cells to detach from the primary tissue site, degrade extracellular matrix and enter the bloodstream (Liguori et al. 2011; Cassetta and Pollard 2018; Chen et al. 2019).

M2-TAMs also promote invasion and metastasis via epithelial-to-mesenchymal transition (EMT). During EMT, tumour cells reduce their expression of epithelial markers such as E-cadherin, and upregulate mesenchymal genes that promote invasiveness and increased cell migration, including slug, snail, and fibronectin (Aras and Raza Zaidi 2017). This transition helps disseminated tumour cells migrate through the bloodstream and reach secondary tissue sites. Tumour cell migration can be assisted directly by M2-TAMs. A positive feedback loop occurs, where migration-promoting EGFs produced by macrophages are transduced by tumour cells, which in return secrete M-CSF, further activating these macrophages (Wyckoff et al. 2004; Goswami et al. 2005).

Circulating tumour cells also localise towards TIE2⁺ macrophages near blood vessels. These TAMs produce VEGF-A to increase vascular permeability, which provides greater capacity for tumour cell motility and nutrient uptake within the bloodstream. This network of vessels, TIE2⁺ TAMs and circulating tumour cells have been described as the tumour microenvironment for metastasis (TMEM) (Rohan et al. 2014; Harney et al. 2015).

1.7.3 Resistance to chemotherapy and radiotherapy

Tumour cells can acquire resistance to chemotherapy and radiotherapy (Meng et al. 2010; Leblond et al. 2017; Wang et al. 2018c). Growing evidence has implicated TAMs in this process. Paulus et al. showed that inhibition of macrophage recruitment and activation, via administration of an M-CSF neutralizing antibody, increased the chemosensitivity of human breast cancer cells in xenograft models (Paulus et al. 2006). Several reports also showed that secretion of IL-6 from TAMs confers anti-apoptotic effects on tumour cells, and can contribute to resistance to chemotherapeutic drugs (Kong et al. 2016; Xu et al. 2019).

1.7.4 Suppression of anti-tumour immunity

M2-TAMs can suppress anti-tumour immune responses. For example, they can activate inhibitory receptors on infiltrating immune cells. They express non-classical MHC class I molecules such as HLA-E and HLA-G. These HLA molecules present antigens and engage NK and T cells via association with CD94 and LILRB1 (leukocyte immunoglobulin-like receptor subfamily B member 1, also known as ILT2) receptors on their respective cell surfaces. Rather than activating them, engagement of these HLA molecules instead instigates inhibitory signalling, thus preventing the anti-tumour activity of these cells. HLA-G engagement has been reported to inhibit CD4+ T cell proliferation, promote induction of anergy, and differentiation into Tregs (Morandi and Pistoia 2014; Obrique et al. 2017).

M2-TAMs also express ligands for checkpoint receptors on T cells, including PD-L1 and PD-L2, that inhibit their activity within the TME. This is important in HNSCC, as overexpression of PD-L1 may inhibit the efficacy of anti-PD1 immunotherapies (Arlaukas et al. 2017). Despite being co-stimulatory molecules, CD80 and CD86 expression in TAMs can also trigger T cell inhibition upon favoured interactions with the checkpoint receptor CTLA-4 on engaged T cells (Santarpia and Karachaliou 2015; Buchbinder and Desai 2016). M2-TAMs also suppress immunity via secretion of cytokines, such as IL-10 and TGF β , which repress CD4+ and CD8+ T cell activity and promote induction of Treg differentiation. M2-TAMs further increase Treg density by secreting chemokines that promote their recruitment into the tumour (Noy and Pollard 2014).

M2-TAMs can directly inhibit cytotoxic CD8+ T cells by releasing the arginine-metabolising enzyme arginase I. Arginine is important for the re-expression of the T cell receptor following activation. Therefore, expression of arginase I by TAMs reduces repeated T cell responses within tumours. Furthermore, TAMs can induce expression of IDO enzymes in CD4+ T cells. IDO enzymes can metabolise tryptophan into products that drive differentiation of CD4+ T cells into potently immunosuppressive Tregs (Mellor et al. 2002; Mbongue et al. 2015).

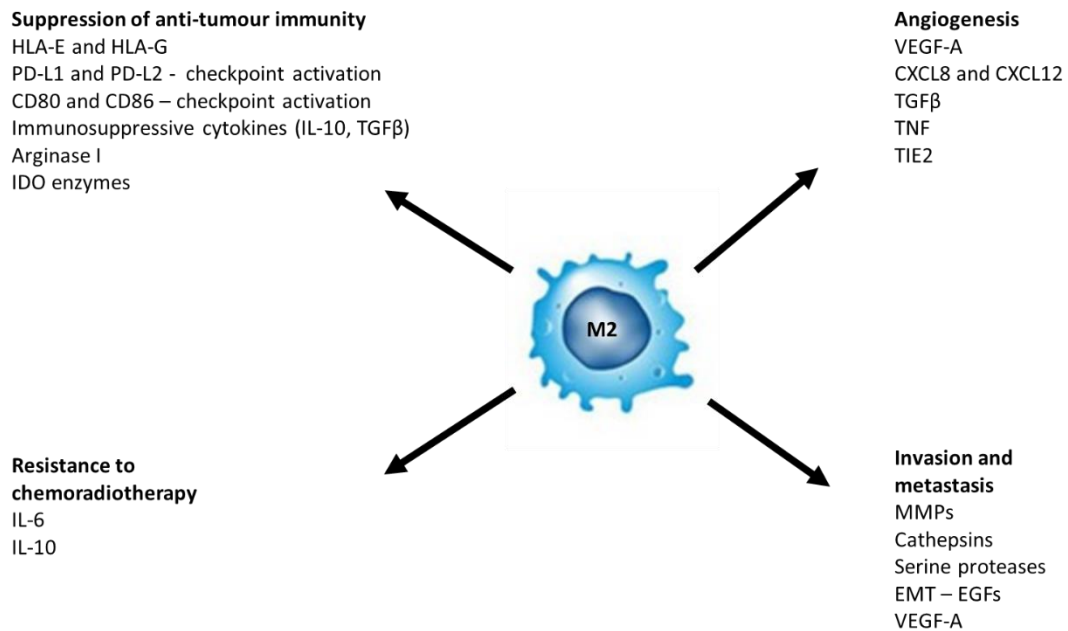


Figure 1.4 Roles of M2-TAMs in tumour progression.

M2-TAMs are involved in many hallmarks of tumour development. Factors produced by M2-TAMs that facilitate each of these are summarised here and explained in full in the text.

1.8 TAMs in HNSCC

TAMs are a crucial component of the HNSCC TME. Regardless of activation state, TAMs can be detected in-vivo by expression of the pan-macrophage marker CD68. CD68⁺ macrophage levels are elevated in HNSCC when compared to normal mucosa, suggesting that they commonly infiltrate tumour tissue and may have a role in tumour development (Ni et al. 2015; Seminerio et al. 2018; Wondergem et al. 2020). A pro-tumour role for these TAMs in HNSCC was indicated, as high CD68⁺ TAM concentrations were commonly correlated with lymph node metastases and poor survival (Hu et al. 2016; Seminerio et al. 2018). Other studies however, linked CD68⁺ infiltrates with better outcomes (Nguyen et al. 2016; Oguejiofor et al. 2017). Such discrepancies may have arisen because studies using CD68 as a sole macrophage marker did not account for differences in macrophage activation states. From a broad perspective, these CD68⁺ TAMs could exhibit anti-tumour M1-like or pro-tumour M2-like phenotypes in the TME (Qian and Pollard 2010). In HNSCC, TAMs most

commonly exhibit M2-like phenotypes. This somewhat explains why the majority of reports link high CD68+ infiltrates with poor outcomes (Weber et al. 2014).

M2-TAMs can be identified against other TAM subtypes via detection of CD68 along with expression of known M2 biomarkers. Many markers have been used for this purpose, though the co-expression of CD68 with the M2 marker CD163, has been shown to be prevalent in HNSCC TAMs and has prognostic significance (Marcus et al. 2004; Weber et al. 2014). These M2-TAMs are present in higher number than their CD68+ CD163- counterparts, and strongly influence tumour development. Reported functions include – promotion of tumour cell migration and invasion (Chang et al. 2011; Pirilä et al. 2015), angiogenesis, and resistance to therapy (Mori et al. 2011; Okubo et al. 2016; Alves et al. 2018). In line with these roles, a large body of reports have positively correlated the density of M2-TAMs in HNSCC with disease severity and poor survival (He et al. 2014; Petruzzi et al. 2017; She et al. 2018; Kumar et al. 2019; Troiano et al. 2019; Li et al. 2020; Wondergem et al. 2020).

How macrophages become polarised to the M2 phenotype is of importance in this thesis. By identifying novel regulators that promote M2 polarisation in HNSCC, novel therapies can be created that improve the effectiveness of existing immunotherapies. As a major component of the TME, a variety of anti-macrophage therapeutic approaches have been developed and are detailed below and summarised in **Table 1.1**. By eliminating or reprogramming TAMs, immunotolerance may be reversed, and tumour elimination by the host immune system enhanced.

1.8.1 Targeting via inhibition of TAM recruitment

Macrophages are recruited into tumours via chemotaxis. Tumour cells produce chemokines such as CCL2 and CSF1. These signals are sensed by, and promote the recruitment of, circulating monocytes into the tumour. Here, both CCL2 and CSF1 also promote M2 macrophage polarisation (Peña et al. 2015; Hao et al. 2020). Preclinical studies have shown that HNSCC cells produce CCL2, which indeed recruits and promotes the M2 polarisation of macrophages. As previously mentioned, these macrophages produce EGF, which increases the proliferative and migration capacity of tumour cells, but also their expression of CCL2, culminating in a positive feedback loop (Gao et al. 2016). Several attempts have been made to block monocyte

recruitment and M2 polarisation by inhibiting the interaction between CCL2 and its receptor CCR2. Approaches in HNSCC include the use of the anti-inflammatory compound curcumin (Gao et al. 2016), the CCL2 inhibitor bindarit, and neutralising antibodies (Gazzaniga et al. 2007; Loberg et al. 2007). While the effects of these treatments have been positive, it was found that when removed, rebound relapses often occur. Thus, to improve this approach, further research is required.

CSF1 and its receptor CSF1R, which also recruit monocytes and promote M2 TAM polarisation, have been targeted using inhibitors and neutralising antibodies. Positive results have been shown in cancer models, including reduction of macrophage recruitment and M2 polarisation, reduced tumour growth and increased CD8+ T cell influxes (Aharinejad et al. 2004; Paulus et al. 2006; Mitchem et al. 2013; Ries et al. 2014). Antibodies and small molecule inhibitors that target this axis are currently in clinical trials for HNSCC (NCT02526017).

1.8.2 Targeting via induction of TAM cell death

Another approach developed is intended to induce TAM apoptosis. By decreasing the overall number of TAMs, this approach, in principle, reduces the capacity of M2-TAMs to suppress anti-tumour immunity and promote tumour development. Trabectedin (ET-743) is a drug that is cytotoxic to macrophages. When administered, it binds to and activates the death receptors Fas and TRAIL (TNF-related apoptosis-inducing ligand), leading to cell death by apoptosis. Neutrophils and T cells within the TME are spared from trabectedin-mediated apoptosis via the expression of decoy death receptors. This approach therefore, is effective in specific targeting of TAMs (Germano et al. 2013). Thus far however, no reports have described its use in the treatment of HNSCC. Biphosphonates, especially those that have been encapsulated into liposomes, are compounds which are selectively taken up by macrophages through phagocytosis. Upon internalisation, these compounds induce cell apoptosis. Clodronate is an example of a liposomal biphosphonate, where its application has been shown to result in macrophage depletion and suppression of tumour progression (Zeisberger et al. 2006).

While induction of apoptosis can be effective, a drawback of the aforementioned agents is that they target all TAMs regardless of their polarisation state. This can

inadvertently result in depletion of anti-tumour M1-TAMs and tissue-resident macrophages. Therefore, anti-macrophage approaches that selectively target M2-TAMs are considered the gold standard. M2pep is a M2-targeting peptide construct. M2pep application in mice models as originally designed, or when edited to contain apoptosis-inducing peptides, has been shown to selectively target and eliminate M2 TAMs (Cieslewicz et al. 2013; Ngambenjawong et al. 2016; Kakoschky et al. 2018). Though, while promising, studies using M2pep are still in its infancy.

Alternative M2-selective approaches include the targeting of surface molecules that are preferentially expressed in M2 macrophages. An example of this is legumain, which is highly expressed on M2-TAMs in breast cancer. A DNA vaccine, that promotes immune responses against cells expressing legumain, has been demonstrated to reduce M2-TAM density, stimulate CD8⁺ T cell activity, reduce angiogenesis and metastases, and increase survival in mouse cancer models (Luo et al. 2006). CD204 (scavenger receptor A) is a scavenger receptor and a highly expressed biomarker of M2-TAMs. Treatment of mice ovarian cancer models with anti-CD204 immunotoxins caused elimination of M2-TAMs and suppressed tumour progression (Bak et al. 2007). CD163 is a classical M2 macrophage marker. As described earlier, its expression in TAMs has been associated with pro-tumour effects in HNSCC, amongst several other cancers (Shiraishi et al. 2018; Pinto et al. 2019). Use of anti-CD163 monoclonal antibodies, conjugated with doxorubicin-loaded lipid nanoparticles (which prevents DNA replication and causes cell death), has been shown to selectively deplete CD163⁺ macrophages in a mice melanoma model (Etzerodt et al. 2019). Inhibition of the CSF1-CSF1R axis has also been shown to affect M2-TAMS. Emactuzumab (RG7155) is an anti-CSF1R antibody which, when used in pre-clinical studies, decreased TAM density, whilst increasing CD8⁺ T cell numbers (Ries et al. 2014). Emactuzumab is currently in clinical trials for the treatment of advanced HNSCC (NCT01494688) (Gomez-Roca et al. 2019).

1.8.3 Targeting via repolarisation of TAMs from M2 to M1

TLRs are expressed by APCs including macrophages. Upon engagement with their ligands, macrophages become activated, displaying M1-like phenotypes and functions (Mantovani et al. 2017). As drivers of M1 polarisation, stimulation of TLRs is an attractive approach for the reprogramming of M2-TAMs. Generally, developed agents

have been designed to stimulate TLR3, TLR7, TLR8 and TLR9, which are intracellular. As of yet, only imiquimod, a TLR7 agonist and topical agent, has been FDA-approved for the treatment of squamous cell carcinomas (Hanna et al. 2016). It is currently in clinical trials for HNSCC (NCT04883645). Clinical trials have also been performed for other TLR agonists, of which polyinosinic:polycytidylic acid (poly I:C) is of particular note. When compared to imiquimod, poly I:C has been shown to display greater efficacy in the reprogramming of tumour-conditioned M2-TAMs towards an M1 phenotype (Maeda et al. 2019). Furthermore, to promote selective targeting of M2-TAMs, arginine-based poly (I:C)-loaded nanocomplexes were developed. Application of this agent induced greater T cell recruitment and tumour cell killing, presumably following successful M2-TAM depletion (Dacoba et al. 2020). An analogue of poly (I:C) is currently in clinical trials for the treatment of head and neck cancers (NCT03789097).

Stimulator of interferon genes (STING) is a protein involved in innate immunity that has become an attractive target in cancer therapy. It is a cytoplasmic DNA-sensor that becomes activated in response to detection of viral nucleotides. Upon activation, it triggers the activity of IRF3 and the subsequent production of pro-inflammatory cytokines. These cytokines enhance the immune response leading to elimination of the virus. Therefore, as a stimulator of immunity, STING presents an attractive target to promote M1-like macrophage behaviour (Ishikawa et al. 2009; Fuertes et al. 2011; Schiavoni et al. 2013; Li et al. 2019b; Miao et al. 2020). STING agonists, including the cyclic dinucleotide cGAMP (Cyclic guanosine adenosine monophosphate), have been evaluated in preclinical and clinical trials (Downey et al. 2014; Corrales et al. 2015). When encapsulated into liposomes, cGAMP administration was shown to successfully induce TAM reprogramming, increase CD8+ T cell density and reduce tumour growth in mouse breast cancer models (Cheng et al. 2018). STING agonists for treatment of solid tumours, including HNSCC, are currently in clinical trials (NCT03937141, NCT04220866) (Amouzegar et al. 2021).

Several monoclonal antibodies have also been investigated. Macrophages express the CD40 receptor on their surface. They can interact with its ligand, CD40L, expressed on CD4+ T cells. CD40 agonism has been shown to increase the M1 activity of macrophages, evidenced by upregulation of MHC II, CD86 and pro-inflammatory

cytokine secretion (Beatty et al. 2011; Zhang et al. 2018). Exploiting this axis with anti-CD40 agonists have resulted in successful reprogramming of TAMs towards anti-tumour activity (Beatty et al. 2011; Vonderheide 2020). Furthermore, treatment of TAMs using a combination of CD40 agonists with anti-CSF1R antibodies has been shown to synergistically reprogram TAMs towards a pro-inflammatory phenotype and inhibit macrophage infiltration. These reprogrammed TAMs were also able to stimulate T cell responses (Hoves et al. 2018; Perry et al. 2018). In HNSCC, expression of CD40 and CD40L have been negatively correlated with tumour stage (Sathawane et al. 2013). The anti-CD40 agonist Selicrelumab is currently in clinical trials for the treatment of solid tumours including HNSCC (NCT02665416).

CD47 is a ubiquitous surface protein expressed on “self-cells” that functions to protect them from macrophage-mediated phagocytosis. Self-cells use CD47 to engage with signal regulatory protein- α (SIRP α) molecules on macrophage surfaces. This interaction educates macrophages not to phagocytose these cells, thus preventing autoimmunity (Murata et al. 2014). Tumour cells in several cancers overexpress CD47 as a means of escaping phagocytosis (Jaiswal et al. 2009; Zhang et al. 2015a). In preclinical cancer models, pharmacological inhibition of CD47 restored the ability of macrophages to phagocytose and kill tumour cells (Gu et al. 2018; Schürch et al. 2019; Yang et al. 2019a). Sustained TAM reprogramming has also been achieved by combining anti-SIRP α with anti-CSF1R (Kulkarni et al. 2018; Ramesh et al. 2019). Several agents targeting this pathway are under clinical trials, either alone or in combination with other agents, for cancers including HNSCC (Li et al. 2020).

The PI3-kinase γ isoform is a signalling molecule that can act as a switch in macrophages, promoting immune suppression rather than inflammation. This is overactive in M2-TAMs, and its activity can be used as a prognostic indicator in cancer. Genetic and pharmacological targeting of PI3 γ in TAMs restores an immunostimulatory M1-like transcriptional profile, resulting in the expression of MHC II, IL-12 and decreased secretion of IL-10. In turn, reprogrammed TAMs were shown to promote the recruitment of anti-tumour immune cells and inhibit tumour growth in several cancers including HNSCC (Kaneda et al. 2016). The use of the PI3-kinase γ inhibitor IPI-549, combined with nivolumab, is currently in clinical trials for advanced solid tumours (NCT02637531) (Sullivan et al. 2018).

Novel genetic and epigenetic approaches have also been developed to reprogram M2-TAMs. These include nanoparticle-based delivery of M1 genes (including CD80, CD86, IL-12 and IFN γ) (Haabeth et al. 2019; Zhang et al. 2019), and CRISPR (clustered regularly interspaced short palindromic repeats) or siRNA-mediated knockout/knockdown of M2 gene expression (such as VEGF-A and CSF-1R) (Cieslewicz et al. 2013; Song et al. 2018). Alternatively, CAR-M (Chimeric Antigen Receptor-Macrophage) cells are being studied. CAR-M therapy involves the introduction of genetic material into M2-TAMs, that results in expression of chimeric receptors that both detect specific tumour antigens and potently trigger phagocytosis and antigen presentation. CAR expression in M2-TAMs thus provides them with anti-tumour roles and enhances T cell responses. While a promising approach, studies involving CAR-M for the treatment of solid tumours are still at an early stage (Klichinsky et al. 2020; Chen et al. 2021).

There are high densities of M2-TAMs in HNSCC, where they promote tumour aggressiveness and are associated with poor patient outcomes. While there are many anti-macrophage treatments under assessment, more research is required to identify novel mechanisms tumour cells use to promote M2-macrophage polarisation in HNSCC. Identification and blocking of such mechanisms, in combination with other immunotherapies, may promote M1-TAM polarisation and reverse immunotolerance. By improving host anti-tumour immune responses, patient survival rates may be improved. This project sought to help achieve this aim by investigating the role of the immunosuppressive cytokine Interleukin-35 (IL-35) in the repolarisation of M1-TAMs, which may be present in an inflamed HNSCC TME, towards an M2-like phenotype.

Table 1.1 Anti-TAM therapies

Anti-TAM approach	Agent
Inhibition of macrophage recruitment and M2 polarisation	CCL2/CCR2 inhibitors (curcumin, bindarit, antibodies) CSF1/CSF1R inhibitors
Induction of TAM apoptosis	Trabectedin Liposomal bisphosphonates (clodronate)
M2-TAM targeting	M2-pep Legumain targeting Anti-CD204 immunotoxins Anti-CD163 antibodies Emactuzumab
M2 to M1-TAM reprogramming	TLR agonists Iquimimod (TLR7) Poly I:C STING agonists (cGAMP) anti-CD47 (phagocytosis) Anti-SIRP α (phagocytosis) PI3K γ inhibitors (IPI-549) Nanocomplexes for M1 gene expression Gene Knockout/knockdown of M2 genes CAR-Macrophages

1.9 Interleukin-35

Interleukin-35 is a heterodimeric cytokine belonging to the IL-12 family. Structurally, it is composed of an EBI3 (Epstein-Barr virus-induced gene 3) chain joined non-covalently to a p35 chain. It was discovered during an investigation to identify potential binding partners for the EBI3 chain, that when bound, could be secreted as a heterodimer. Using co-immunoprecipitation, Devergne and others found that when both EBI3 and p35 were overexpressed in the same cell (by means of transfection), they were able to interact and become secreted as a heterodimer (Devergne et al. 1997).

At this time, the function of this heterodimer was unknown, but there were early indications that it had immunomodulatory roles. The EBI3 chain had been reported to be highly expressed in the spleen and placental trophoblasts, and is located in the genome near the Tyk2 gene (a regulator of IL-6, IL-10 and IL-12 signalling) (Devergne et al. 1996; Devergne et al. 2001). However, it was not until seminal work by Collison in 2007, where the principal function of the EBI3/p35 heterodimer was uncovered, and it was given the name Interleukin-35 (Collison et al. 2007). This study demonstrated that EBI3 and p35 were constitutively expressed and secreted by Tregs.

Tregs are potent immunosuppressive cells. Though, when both the EBI3 and p35 genes were removed by knockout, the ability of Tregs to suppress immunity was significantly impaired. This suggested that the EBI3/p35 heterodimer may function as a critical immunosuppressive cytokine. As it shared structural chains from the IL-12 family, but was functionally distinct from previously discovered members, the EBI3/p35 heterodimer was given the name Interleukin-35 (Collison et al. 2007).

After a decade of further research, IL-35 is understood today to function as a potent suppressor of immunity. It is expressed mainly by Tregs, but also regulatory B cells (Bregs) and less so by endothelial cells, smooth muscle cells, macrophages, monocytes, tolerogenic dendritic cells and cancer cells (Banchereau et al. 2012; Long et al. 2013; Shen et al. 2014; Tedder and Leonard 2014; Dixon et al. 2015; Hao et al. 2018; Lee et al. 2018a; Zhu et al. 2020). As an immunosuppressive cytokine, its expression has been implicated in many immunological diseases. Of these diseases, a large body of research has investigated the roles of IL-35 in cancer.

1.10 Interleukin-35 in cancer

IL-35 overexpression has been detected in tumour tissue and patient serum from several cancers. As a suppressor of immunity, its somewhat unsurprising that its concentration is commonly positively correlated with disease severity and poor patient survival. This has been reported in a plethora of cancers including - prostate cancer (Chatrabnous et al. 2019; Zhu et al. 2019; Zhu et al. 2020), gastric cancer (Gu et al. 2021), pancreatic ductal adenocarcinoma (Jin et al. 2014; Nicholl et al. 2014), colorectal cancer (Zeng et al. 2013; Ma et al. 2016), acute myeloid leukaemia (Tao et al. 2015; Ahmed et al. 2019), non-small-cell lung cancer (Gu et al. 2015; Zhang et al. 2021), renal cell carcinoma (Jin et al. 2015), breast cancer (Chen et al. 2016; Zhao et al. 2017b) and B cell lymphoma (Larousserie et al. 2019). These findings indicate that IL-35 may have important roles in cancer, and its expression may also serve as an effective prognostic biomarker.

The origin of IL-35 production in cancer may be important to consider. In patient studies, IL-35 is detected both in the tumour tissue and serum. Though, some reports have shown that both IL-35 and Treg counts are depleted following tumour resection, which suggests that IL-35 production is largely of tumour origin, and that resident

Tregs may be the principal producers within the TME (Zeng et al. 2013; Wu et al. 2017). Aside from Treg production, studies have also shown that tumour cells themselves can produce IL-35 (Long et al. 2013; Zeng et al. 2013; Hao et al. 2018; Zhu et al. 2020). This may be significant, as it suggests that tumour cells could use IL-35 secretion as an immune escape mechanism via suppression of anti-tumour immune cells. The role of IL-35 in cancer is not restricted to the regulation of immunity. The variety of roles attributed to IL-35, that rather controversially either favour or antagonise tumour development, are explored below (summarised in **Table 1.2**).

1.10.1 Role of IL-35 in tumourigenesis

A study by Wang and others showed that IL-35 can directly promote tumourigenesis. Melanoma and plasmacytoma cell lines were transfected, resulting in IL-35 overexpression. These cell lines were then injected into immunocompetent or immunocompromised mice. Compared to untransfected controls, IL-35 overexpression accelerated tumourigenesis in both types of mice. Furthermore, these effects were abrogated when mice were simultaneously injected with IL-35 and a blocking antibody (Wang et al. 2013).

1.10.2 Role of IL-35 in tumour cell growth and resistance to apoptosis

Nicholl and others showed that stimulation of pancreatic carcinoma cell lines with recombinant IL-35-Fc resulted in increased cell proliferation and survival in a dose-dependent manner. Addition of an anti-IL-35 antibody prior to stimulation blocked these effects, indicating that IL-35 can directly promote proliferation in these cancer cell lines (Nicholl et al. 2014). A study by Wang and others also showed, through co-culture of activated cytotoxic T lymphocytes with IL-35-overexpressing mouse plasmacytoma cell lines, that IL-35 conferred resistance to T-cell mediated cytotoxicity (Wang et al. 2013). Zhu demonstrated that in prostate cancer, IL-35 overexpression in tumour tissue was associated with increased tumour cell proliferation, as shown via elevation of Ki67 expression (Zhu et al. 2020). Fan also showed this to occur in gastric tumour tissue (Fan et al. 2015). Thus, these studies demonstrate that IL-35 may not only regulate surrounding immune cells, but also promote tumour development by increasing the proliferation and survival of tumour cells.

1.10.3 Role of IL-35 in angiogenesis

Using immunocompromised mice injected with plasmacytoma or melanoma cells that overexpress IL-35, Wang and others showed IL-35 contributed to an increase in expression of VEGF and CD31, markers of angiogenesis. Analysis of tissue sections also detailed an increase in the infiltration of MDSCs (CD11b⁺Gr1⁺) in IL-35+ tumours. Injection of an anti-Gr1 antibody depleted MDSC count, and coincided with reduced tumour growth to a level matching that of controls, indicating that IL-35 production promotes the infiltration of MDSCs into the TME, and that these MDSCs are largely responsible for the observed increase in tumour growth and angiogenesis (Wang et al. 2013). A study in prostate cancer also demonstrated that IL-35 overexpression correlated with increased CD31 expression and microvessel density, further evidencing its role in promoting angiogenesis (Zhu et al. 2020).

1.10.4 Role of IL-35 in metastasis

In mice breast cancer models, TAMs present within metastases show an M2-like activation state. In contrast, TAMs within primary tumour tissue were skewed towards an M1 phenotype. M2 macrophages present at metastatic sites produced IL-35 at much higher levels than peripheral macrophages, and this was confirmed in-vitro. In addition, this study showed that tumour cells may upregulate IL-35 receptor chains in response to inflammation-induced epithelial-to-mesenchymal transition, which may prepare these cells to respond to IL-35 during metastasis. TAM-secreted IL-35 may promote metastatic colonisation of these tumour cells via mesenchymal-to-epithelial transition. Knockout of EBI3, injection of an IL-35 antibody or an anti-CSF1R antibody (to block macrophage differentiation), confirmed these findings as metastatic colonisation was reduced (Lee et al. 2018a).

1.10.5 Anti-tumour roles of IL-35

IL-35 is commonly described as a pro-tumour cytokine, especially considering the large body of evidence associating its expression with poor prognoses. However, some reports have contradicted this idea. Research in hepatocellular carcinomas (HCC) and colon cancers have suggested that IL-35 expression may antagonise tumour development. In an study by Long and others, it was shown that IL-35 overexpression in HCC cell lines arrested them in the G1 phase of the cell cycle, and increased their

sensitivity to apoptosis (Long et al. 2013). In a later study, Long also demonstrated that reduced levels of IL-35 were correlated with disease progression in HCC. Following use of transfection, IL-35 overexpression in HCC cell lines resulted in reduced invasiveness and capacity for cell migration. Furthermore, in direct contrast to its role as an immunosuppressive cytokine, IL-35 overexpression was also associated with the increased expression of HLA-ABC (MHC-I) on the cell surface, which sensitises these tumour cells to destruction by cytotoxic T cells (Long et al. 2016).

IL-35 may also antagonise colon cancer progression. Zhang and others showed that when compared to healthy controls, tissue sections from colon cancer patients contained a significant reduction in IL-35 expression. Low IL-35 was also strongly associated with metastases and poor clinical outcome. This was supported by in-vitro studies, whose results conveyed that treatment of colon cancer cell lines with recombinant IL-35 reduces cell proliferation and migration. These cells also displayed an increased sensitivity to chemotherapeutic agents. These effects may have been mediated by a reduction in the expression of β -catenin, known to promote the development of colon cancer (Zhang et al. 2017; Jiang et al. 2018). Thus, it seems that despite reports linking IL-35 to pro-tumour roles, it also possesses anti-tumour functions, and this functional heterogeneity may depend in part on tissue site.

Table 1.2 Pro-tumour and anti-tumour roles attributed to IL-35

Pro-tumour roles of IL-35	Anti-tumour roles of IL-35
Tumourigenesis	Tumour cell G1 cycle arrest
Growth and resistance to apoptosis	Increased tumour cell sensitivity to apoptosis
Resistance to chemotherapy	Downregulation of β -Catenin in tumour cells
Angiogenesis	Reduced invasiveness and migration of tumour cells
Suppression of anti-tumour immunity	Reduced cell proliferation

1.10.6 Role of IL-35 in the suppression of anti-tumour immunity

IL-35 is a potent immunosuppressive cytokine (Collison et al. 2007). Within the cancer setting, this implicates it as a promoter of immune escape and tumour progression. In the TME, IL-35 can accumulate due to the variety of cells therein that produce it. These include tumour cells (Long et al. 2013; Hao et al. 2018; Zhu et al. 2020), regulatory T cells (Collison et al. 2007), induced Tregs (Collison et al. 2010), regulatory B cells (Shen et al. 2014; Tedder and Leonard 2014; Wang et al. 2014), immature dendritic cells (Dixon et al. 2015) and macrophages (Terayama et al. 2014; Lee et al. 2018a). When secreted from these cells, IL-35 can stimulate and modulate the behaviour of surrounding immune cells in the TME. This can result in suppression of anti-tumour immunity. The immune cells that receive this signal, and how they are regulated by IL-35, are described below and summarised in **Table 1.3**.

CD4+ T cells – IL-35 in the TME can inhibit the anti-tumour activity of resident CD4+ T cells. Several studies have shown that CD4+ T cells stimulated with IL-35 derived from tumour cells, Tregs, or in recombinant form, can inhibit cell proliferation and suppress Th1 cytokine production (Collison et al. 2007; Turnis et al. 2016; Hao et al. 2018; Liu et al. 2021b; Mirlekar and Pylayeva-Gupta 2021). A number of reports have also revealed that IL-35 can induce CD4+ T cell exhaustion (progressive loss of differentiation capacity, function and vitality). Turnis and others generated mice cancer models via injection with melanoma or colon cancer cells. When comparing wildtype and EB13-knockout mice, it was observed that IL-35 contributed to CD4+ T cell exhaustion within tumours, as depicted by the increased expression of the immune-inhibitory receptors PD1, TIM-3 (T cell immunoglobulin domain and mucin domain 3) and LAG-3 (Lymphocyte Activating 3) (Turnis et al. 2016). Hao also found that CD4+ T cells treated with conditioned medium from breast cancer cell lines that

expressed IL-35, or recombinant IL-35, induced upregulation of the exhaustion marker CD73 (Hao et al. 2018). Liu and others recently revealed that mouse CD4⁺ T cells respond to IL-35 treatment by increasing their expression of PD1 and LAG-3 (Liu et al. 2021b).

Another major function of IL-35 is to convert conventional CD4⁺ T cells into FOXP3⁺ Tregs. These are termed induced Tregs or iTregs (iTr35 when induced by IL-35). Functionally, they do not secrete IL-10 or TGF β , instead primarily exerting immune suppression via secretion of IL-35, resulting in a positive feedback loop (Collison et al. 2010; Sullivan et al. 2020). This is important as it enables the propagation of the suppressive IL-35 signal from the secreting cell, to the receiving CD4⁺ T cells and beyond. This is known as infectious tolerance (explained in detail below). Studies have mostly shown iTr35 conversion to occur in naïve CD4⁺ T cells that would not commonly be present within tumour tissue (Collison et al. 2010). However, other reports have evidenced that mature effector CD4⁺ T cells, present within the TME, can also be converted to iTr35 cells (Ma et al. 2016; Hao et al. 2018). This phenotypic switch acts as a potent immunosuppressive signal, both by inhibiting the anti-tumour activity of CD4⁺ T cells within the tumour, and by enabling the production of additional IL-35 to propagate immunosuppression.

Th17 cells - IL-35 has been shown to inhibit the differentiation of naïve T cells into Th17 cells, instead promoting iTreg differentiation (Collison et al. 2007; Niedbala et al. 2007; Collison et al. 2010). In non-small cell lung cancers, IL-35 can suppress anti-tumour immunity by inhibiting Th17 responses (Wang et al. 2018a). **Thymus-derived Tregs** – These Tregs differ from iTregs in that they express the FOXP3 transcription factor. They are recruited into the TME, where they are key suppressors of anti-tumour immunity. IL-35 overexpression in tumours has been associated with the increased presence of these FOXP3⁺ Tregs (Collison et al. 2010; Heim et al. 2019; Liu et al. 2021b).

CD8⁺ T cells - CD8⁺ T cells eliminate tumour cells. IL-35 within tumours can block their activity in several ways. IL-35 assists in the recruitment of IL-35-producing Tregs and MDSCs. These cells produce signals that inhibit the recruitment of CD8⁺ T cells (Wang et al. 2013; Zhu et al. 2020). Using HNSCC mice models, Jiang recently showed that IL-35 can repress the activation of CD8⁺ T cells within the TME by

reducing the expression of the co-activator molecule CD28 (Jiang et al. 2019). Functionally, CD8⁺ T cells are cytotoxic to tumour cells and can produce pro-inflammatory cytokines to enhance anti-tumour immune responses. When CD8⁺ T cells extracted from tumours were treated with IL-35, expression of cytolytic genes were reduced. LDH (lactate dehydrogenase) co-culture assays also showed that these cells were less capable of inducing tumour cell death (Wang et al. 2018a; Liu et al. 2019a; Yang et al. 2019b). Several studies have also demonstrated that IL-35 can promote CD8⁺ T cell exhaustion (Turnis et al. 2016; Sawant et al. 2019; Liu et al. 2021b). Regarding cytokine production, Liu showed that CD8⁺ T cells isolated from osteosarcoma patients, that were then treated with IL-35, showed reduced expression of Th1 cytokines (Liu et al. 2019a). This was also shown to occur in HCC and HNSCC (Jiang et al. 2019; Yang et al. 2019b). Thus, IL-35 is a potent suppressor of CD8⁺ T cell activity in cancer.

B cells - Similar to CD4⁺ T cells, IL-35 can convert infiltrating B cells, that are anti-tumour in nature, to regulatory B cells, which produce IL-35 and propagate immune suppression. IL-35 also promotes the proliferation of these cells (Shen et al. 2014; Wang et al. 2014; Sullivan et al. 2020). **Dendritic cells** - IL-35 can prevent the maturation of dendritic cells by reducing expression of MHC II and co-stimulatory molecules. This represses their ability to present tumour antigens to naïve T cells within lymph nodes, and therefore reduces the number of activated anti-tumour T cells that are produced. Furthermore, these immature dendritic cells secrete immunosuppressive cytokines including IL-35, further promoting immunotolerance (Dixon et al. 2015; Haller et al. 2017; Liu et al. 2018b). **Neutrophils** - Neutrophils in the TME can exist in polarised phenotypes broadly described as N2 (immunosuppressive and pro-tumour) and N1 (pro-inflammatory and anti-tumour). Zou and others showed that IL-35 can facilitate N1 to N2 reprogramming, which, as a result of immune suppression, lead to increases in tumour growth (Zou et al. 2017). **Macrophages:-** Previous reports have described that, as with T cells, B cells, dendritic cells and neutrophils, IL-35 may reprogram M1 macrophages to an immunosuppressive M2 phenotype (Peng et al. 2019; Jiang et al. 2020; He et al. 2021). Together, these findings underline the potent immunosuppressive effects of IL-35 within the TME and implicate it as a major contributor to immune escape.

Table 1.3 Immune suppressing effects of IL-35 on immune cells within the TME

Target immune cells in the TME	Immune-regulatory effects of IL-35
CD4+ T cells	Inhibition of cell proliferation. Inhibition of Th1 cytokine production. Promotion of exhaustion. Conversion to suppressive induced Tregs (iT _h 35)
Th17 cells	Inhibition of Th17 differentiation and activity
Regulatory T cells	Increased density in tumours
CD8+ T cells	Reduced recruitment into tumours. Reduced capacity for activation via downregulation of CD28. Reduced cytotoxicity. Promotion of exhaustion. Reduced Th1 cytokine production.
B cells	Conversion to IL-35-producing regulatory B cells
Dendritic cells	Inhibition of maturation. Supports production of IL-35 from immature dendritic cells.
Neutrophils	Conversion to immunosuppressive N2 subtype
Macrophages	Conversion to immunosuppressive M2

The molecular mechanism underlying the secretion of immunosuppressive cytokines (such as IL-35) from one cell type, and the functional inhibition and further secretion of these cytokines from transducing cells, is not yet fully understood. This phenomenon describes infectious tolerance (Gershon and Kondo 1971; Qin et al. 1993). As described above, IL-35 can achieve this in the TME through induction of IL-35-expressing T cells, B cells, dendritic cells and macrophages. Recent research has uncovered a potential mechanism by which the IL-35 signal is propagated. Sullivan and others showed that IL-35 subunits can be loaded onto and secreted via extracellular vesicles from Tregs, the main producers of IL-35. Here, it accumulates and is transferred to a larger number of surrounding immune cells such as T and B cells that transduce this signal. T cells that become inhibited by this signal, appear to recycle IL-35 to the cell surface. Here, it repeatedly engages with its receptor, resulting in T cell exhaustion. In addition, free surface bound IL-35 may stimulate and inhibit other immune cells that come into close proximity. Therefore, the IL-35 signal can be

passed between cell populations in the TME, from a small number of Tregs, which produce many IL-35-coated extracellular vesicles, to a larger number of surrounding immune cells, which themselves recycle and use IL-35 to stimulate additional cells. This may therefore explain how, despite low stability, IL-35 is able to propagate its signal in cancer (Sullivan et al. 2020).

1.11 Interleukin-35 in HNSCC

IL-35 has been linked to several cancers, where it suppresses anti-tumour immunity using the mechanisms described above. Investigation into the expression and role of IL-35 in HNSCC however, is currently lacking. Wang has shown, using immunohistochemical techniques, that IL-35 expression is detected in tumour tissue taken from nasopharyngeal carcinoma patients. This expression appeared to be sourced mainly from stromal cells rather than from tumour cells (Wang et al. 2013). Zhang and others also found that IL-35 was overexpressed in nasopharyngeal tumours. In contrast to Wang's study, IL-35 was found to be overexpressed within the tumour cells. In addition, IL-35 expression was positively correlated with disease progression and poor survival (Zhang et al. 2015b). Wu and others examined IL-35 expression in laryngeal carcinomas. In preoperative patients, IL-35 overexpression was detected both from cells within the tumour tissue and in peripheral blood. Following surgical resection, expression was reduced significantly, suggesting that IL-35 mostly originated from within the tumour tissue (Wu et al. 2017). The findings from these studies indicate that IL-35 may play an important role in HNSCC development.

As described earlier, tumour cells can respond to immunosurveillance by producing signals that alter the phenotype of immune cells, such that function to suppress immunity in the TME. Numerous reports have shown that cancer cell lines express IL-35 (Long et al. 2013; Zhang et al. 2015b; Hao et al. 2018; Zhu et al. 2020). However, there was a gap in the literature pertaining to the expression of IL-35 by HNSCC cells, and how this is regulated by inflammation in the TME. This is important as, if IL-35 is upregulated in response to inflammation, this would reveal a novel mechanism by which HNSCC cells could escape anti-tumour immunity.

To begin to fill this gap, preliminary studies were performed in our laboratory group. HNSCC cell lines were analysed by RT-qPCR to detect IL-35 gene expression. The

data showed that the IL-35 subunits, EBI3 and p35, were expressed in all tested cell lines in varying amounts. Notably, within the hypopharyngeal cell line, FaDu, baseline mRNA levels of EBI3 and p35 were low. However, when placed under pro-inflammatory conditions akin to an anti-tumour immune response, these cells adapted by elevating IL-35 expression. IFN γ stimulation induced upregulation of p35, whereas TNF α induced EBI3 upregulation. Combined stimulation with both IFN γ and TNF α , commonly present in an inflamed TME, resulted in overexpression of both IL-35 subunits.

The results from the preliminary studies suggested that HNSCC cells may produce IL-35 as an adaptive response to inflammation in the TME. It is possible therefore, that in an inflamed TME rich in immune cells, tumour cells produce IL-35, which may suppress anti-tumour immunity from surrounding cells. As macrophages are often polarised to M2 in HNSCC, it is conceivable that HNSCC-derived IL-35 may promote immune escape by repolarising M1 macrophages, which may initially be polarised by pro-inflammatory cytokines in the inflamed TME, to the prevalent M2 phenotype. It was both the preliminary data, and these inferences, that formed the rationale of this study and led to the following hypothesis.

1.12 Project hypothesis

HNSCC cells within an inflamed microenvironment are under stimulation by inflammatory cytokines. Tumour cells respond by upregulating expression of EBI3 and p35, culminating in IL-35 production. As an immunosuppressive cytokine, IL-35 protects tumour cells from anti-tumour immunity by repolarising M1 macrophages, which are pro-inflammatory, to the immunosuppressive M2 phenotype, which are prevalent in HNSCC.

1.13 Project aims

To test this hypothesis, the following project aims were devised.

- By using pro-inflammatory and anti-inflammatory cytokine stimulation, investigate the effects of inflammation in the TME on IL-35 expression in HNSCC cell lines (Chapter 3).

- To investigate the immunosuppressive roles of HNSCC-derived IL-35, establish an HNSCC cell line that stably overexpresses IL-35 in its native form (Chapter 4).
- Investigate the role of HNSCC-derived IL-35 in the repolarisation of M1 macrophages to an M2 phenotype via suppression of the M1 phenotype (Chapter 5).
- Investigate the role of HNSCC-derived IL-35 in the repolarisation of M1 macrophages to an M2 phenotype via upregulation of classical M2 and candidate M2-TAM markers (Chapter 6).

Should the hypothesis be proven, this would reveal a potential mechanism used by HNSCC cells to escape anti-tumour immunity. This could implicate IL-35 as a potential target for immunotherapy. When targeted in combination with existing immunotherapies, this may improve patient responses and overall survival.

Chapter 2
Materials and Methods

2.1 Cell Culture Materials

2.1.1 Established cell lines

The FaDu cell line was derived from a hypopharyngeal squamous cell carcinoma taken from a 56 year old Caucasian male. The H357 cell line was derived from a human oral squamous cell carcinoma taken from the tongue of a 74 year old male. Both cell lines were gifted from Dr Simon Whawell (The University of Plymouth). CHO (Chinese Hamster Ovary) cells were purchased from the European Collection of Authenticated Cell Cultures (ECACC) (Wiltshire, United Kingdom). The acute monocytic leukaemia cell line (THP1) was purchased from Thermo Fisher Scientific (Loughborough, United Kingdom). Cryovials containing each cell line were stored in liquid nitrogen until use.

2.1.2 Developed cell lines

CHO-EBI3 and FaDu-EBI3 cell lines, which overexpress human EBI3, were established following stable transfection of CHO and FaDu cells with a plasmid containing the human EBI3 gene. The FaDu-p35 cell line, that overexpresses human p35, was developed via stable transfection of FaDu cells with a plasmid containing the human p35 gene. CHO-IL-35 and FaDu-IL-35 cell lines, which overexpress both human EBI3 and p35 and secrete IL-35, were established following stable transfection of CHO-EBI3 and FaDu-EBI3 cell lines with an expression plasmid containing the human p35 gene. FaDu-NTC and CHO-NTC cell lines were developed following stable transfection with a negative transfection control (NTC) plasmid, which contains a stuffer sequence in the open reading frame. Full transfection methods are detailed in **Section 2.3.6**.

2.1.3 Routine tissue culture materials

RPMI-1640 (Roswell Park Memorial Institute) culture medium and Penicillin/Streptomycin (P/S) were obtained from Thermo Fisher Scientific. Fetal Bovine Serum (FBS) was also purchased from Thermo Fisher Scientific, and heat inactivated by incubating in a water bath at 56 °C for 30 min prior to storage. Phosphate Buffered Saline (PBS) was obtained from Thermo Fisher Scientific and reconstituted in distilled water to make a 1X working solution. Trypsin-EDTA

(0.25%), TrypLE Express and Brefeldin A were also purchased from Thermo Fisher Scientific. Trypan Blue was acquired from Sigma-Aldrich (Poole, United Kingdom). Dimethyl Sulfoxide (DMSO) was purchased from Fisher Scientific (Leicestershire, United Kingdom).

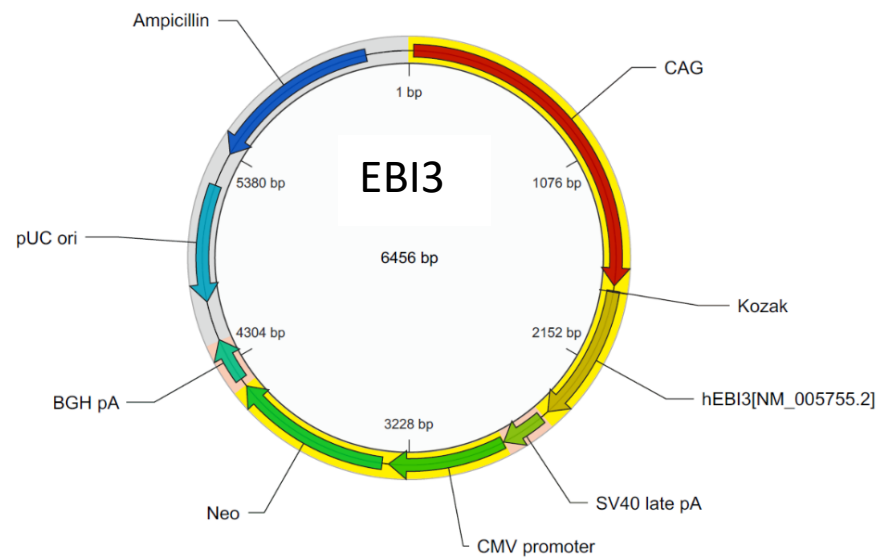
2.1.4 Recombinant cytokines

Recombinant human interferon- γ (IFN γ), Tumour Necrosis Factor alpha (TNF α), human Interleukin-10 (IL-10), human Interleukin-4 (IL-4) and human Interleukin-35 (IL-35) were obtained from Peprotech (London, United Kingdom). Human IL-35-Fc was purchased by R&D Systems (Minneapolis, United States). Human granulocyte-macrophage colony-stimulating factor (GM-CSF) and macrophage colony-stimulating factor (M-CSF) were both purchased from ImmunoTools (Friesoythe, Germany). Phorbol 12-myristate 13-acetate (PMA, code 1585) was purchased from Sigma-Aldrich. All cytokines were diluted as instructed by the manufacturer and stored at -20 °C or -80 °C until required.

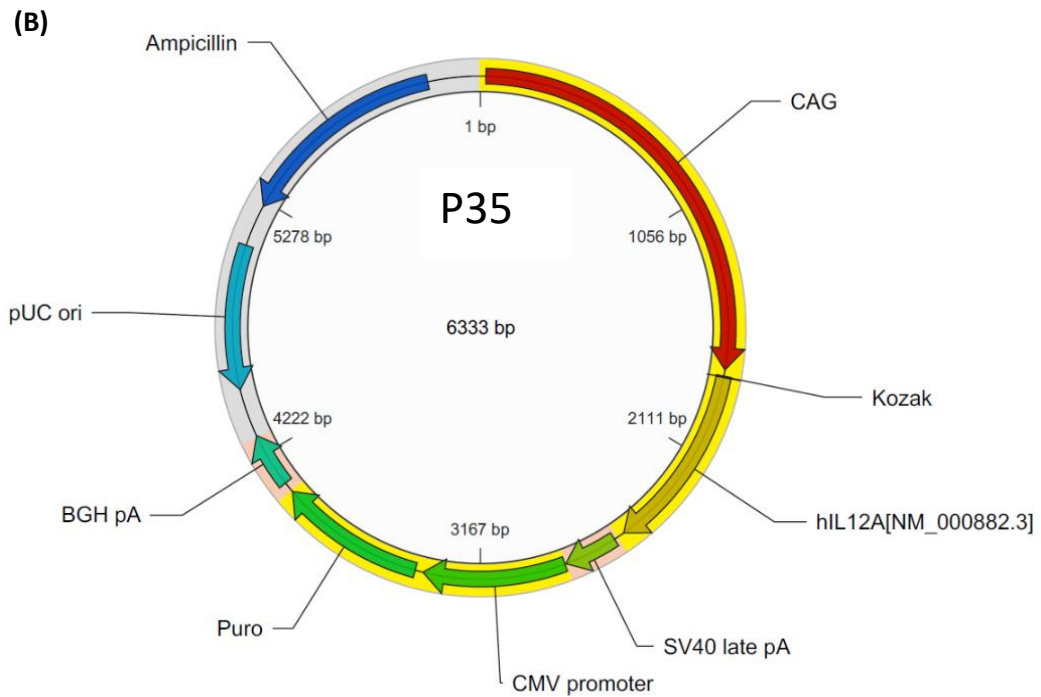
2.1.5 Materials for stable transfection

Expression plasmids encoding the human EBI3 (EBI3 expression plasmid) (**Figure 2.1A**) or human p35 (p35 expression plasmid) (**Figure 2.1B**) genes were designed by Dr Xiaoqing Wei. The negative transfection control plasmid (NTC) (**Figure 2.1C**) was designed by me. It was identical to the EBI3 expression plasmid but contained a non-coding stuffer sequence in place of the EBI3 coding region. All plasmids were manufactured by and purchased from Vector Builder Inc (Chicago, United States). cDNA for the human EBI3 and p35 expression plasmids were purified by the manufacturer. cDNA for the NTC plasmid was prepared by Maxi-prep purification of Ecoli stock, as instructed by the manufacturer (Qiagen, Hilden, Germany). Plasmid maps are shown below in **Figure 2.1**. The Lipofectamine 2000 transfection reagent, and the antibiotics used for selection - G418 and Puromycin, were purchased from Thermo Fisher Scientific.

(A)

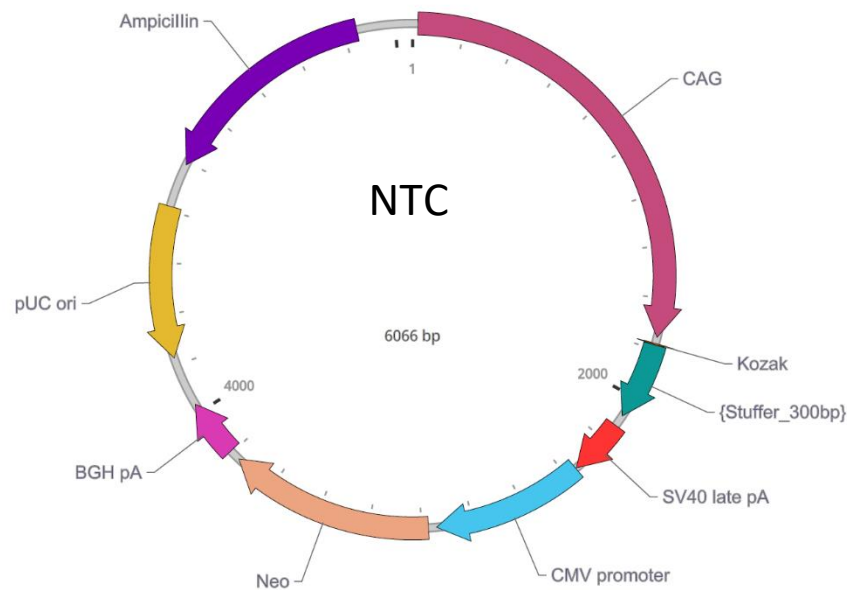


Component Name	Nucleotide Position	Full Name	Description
CAG	22-1754	CAG	Strong promoter
Kozak	1779-1784	Kozak	Facilitates translation initiation
hEBI3[NM_005755.2]	1785-2474	hEBI3[NM_005755.2]	EBI3 gene
SV40 late pA	2519-2740	SV40 polyadenylation signal	Allows transcription termination and polyadenylation of mRNA.
CMV promoter	2744-3331	Human cytomegalovirus immediate early promoter	Allows high-level expression of marker in mammalian cell lines.
Neo	3363-4157	Neomycin resistance gene	Allows to select stable expression clones using G418.
BGH pA	4201-4425	Bovine growth hormone polyadenylation	Allows transcription termination and polyadenylation of mRNA.
pUC ori (c)	5209-4621	pUC origin of replication	Permits high-copy replication and maintenance in E. coli.
Ampicillin (c)	6240-5380	Ampicillin resistance gene	Allows selection of the plasmid in E. coli.



Component Name	Nucleotide Position	Full Name	Description
CAG	22-1754	CAG	Strong promoter
Kozak	1779-1784	Kozak	Facilitates translation initiation
hIL12A[NM_000882.3]	1785-2546	hIL12A[NM_000882.3]	P35 gene
SV40 late pA	2591-2812	SV40 polyadenation signal	Allows transcription termination and polyadenylation of mRNA.
CMV promoter	2816-3403	Human cytomegalovirus immediate early promoter	Allows high-level expression of marker in mammalian cell lines.
Puro	3435-4034	Puromycin resistance gene	Allows to select stable expression clones using puromycin.
BGH pA	4078-4302	Bovine growth hormone polyadenylation	Allows transcription termination and polyadenylation of mRNA.
pUC ori	5086-4498	pUC origin of replication	Permits high-copy replication and maintenance in E. coli.
Ampicillin	6117-5257	Ampicillin resistance gene	Allows selection of the plasmid in E. coli.

(c)



Component Name	Nucleotide Position	Full Name	Description
CAG	22-1754	CAG	Strong promoter
Kozak	1779-1784	Kozak	Facilitates translation initiation
Stuffer_300bp	1785-2084	None	None
SV40 late pA	2129-2350	SV40 polyadenylation signal	Allows transcription termination and polyadenylation of mRNA.
CMV promoter	2354-2941	Human cytomegalovirus immediate early promoter	Allows high-level expression of marker in mammalian cell lines.
Neo	2973-3767	Neomycin resistance gene	Allows to select stable expression clones using G418.
BGH pA	3811-4035	Bovine growth hormone polyadenylation	Allows transcription termination and polyadenylation of mRNA.
pUC ori	4231-4819	pUC origin of replication	Permits high-copy replication and maintenance in E. coli.
Ampicillin	4990-5850	Ampicillin resistance gene	Allows selection of the plasmid in E. coli.

Figure 2.1 Expression plasmids used for stable transfection. Plasmid maps and component descriptions corresponding to (A) the EB13 expression plasmid (B) p35 expression plasmid (C) Negative Transfection Control (NTC) plasmid are shown.

2.1.6 Equipment for general tissue culture

General plastics including universal containers (30 mL), 0.22 µM sterile filters, serological pipettes, cryovials, culture plates and flasks were purchased from Sarstedt Ltd (Leicester, United Kingdom) unless otherwise stated. Microcentrifuge tubes (1.5 mL) were obtained from StarLab (Milton Keynes, United Kingdom). 100 mm/ 20 mm Cellstar petri dishes were purchased from Greiner Bio-One (Stonehouse, United Kingdom). 10 mL syringes were purchased from Fisher Scientific. For microscopy, an Eclipse TS100 microscope (Nikon, Tokyo, Japan) coupled to a Moticam BTW8 (Motic, Barcelona, Spain) camera system was used. Centrifugation steps were performed using a Precision Duraforce 200 (Cambridge Scientific, Massachusetts, USA). With the exception of centrifugation steps, all cell culture procedures were performed in Astec Microflow Class II laminar flow cabinets (Bioquell, Andover, UK). Cells were cultivated in incubators (BINDER GmbH, Tuttlingen, Germany) containing humidified air maintained at 37 °C, 5 % CO₂. Neubauer haemocytometer counting chambers were obtained from Marienfeld Superior (Lauda-Königshofen, Germany). Freezing containers were obtained from Nalgene (New York, USA) and filled with isopropanol (Sigma-Aldrich) prior to use.

2.2 Assay Materials

2.2.1 Reverse Transcription quantitative PCR (RT-qPCR) materials

RNAse Zap was purchased from Thermo Fisher Scientific. The RNAeasy mini kit used for RNA extraction was obtained from Qiagen. 2-mercaptoethanol and primers were purchased from Sigma-Aldrich. RNA concentrations were quantified using a NanoVue Plus spectrophotometer obtained from GE Healthcare (Chicago, United States). RNA quality was assessed using a Bioanalyser manufactured by Agilent Technologies (California, United States). For reverse transcription, Random primer, Moloney-Murine Leukaemia Virus (M-MLV) reverse transcriptase, dNTPs (deoxyribonucleotide triphosphate) and RNAsin were all purchased from Promega (Hampshire, United Kingdom). 0.1 mL PCR tubes were obtained from StarLab. cDNA synthesis was performed in a G-storm GS1 thermocycler manufactured by Gene Technologies Ltd (Essex, United Kingdom). For qPCR reactions, PowerUp SYBR Green mastermix was purchased from Thermo Fisher Scientific. 384-well plates were

loaded with samples using an automated EpMotion liquid handler, both purchased from Eppendorf (Stevenage, United Kingdom). qPCR reactions were performed using a QuantStudio 12K Flex thermocycler, acquired from Applied Biosystems (Massachusetts, United States).

2.2.2 SDS-PAGE/Western Blot materials

Radioimmunoprecipitation (RIPA) lysis buffer was purchased from Thermo Fisher Scientific and supplemented with Protease Inhibitor Cocktail (cOmplete™, Protease Inhibitor Cocktail) (Sigma-Aldrich). The following materials were purchased from Thermo Fisher Scientific. Protein concentrations within cell lysates were measured using a Pierce™ BCA (Bicinchoninic acid Assay) kit. For SDS-PAGE (Sodium dodecyl sulfate polyacrylamide gel electrophoresis), the NuPage™ bis-tris mini gel system was used, consisting of LDS (Lithium dodecyl sulfate), Reducing Agent and MES Running Buffer, precast 4-12% bis-tris polyacrylamide gels (1.0 mm thickness) and XCell SureLock mini gel tanks. The Novex Sharp PreStained Protein Standard was used as a molecular weight marker. For Western blotting, nitrocellulose mini stacks and the iBlot 2 dry blotting system were used. Tween-20 was purchased for use in washing buffers. SuperSignal™ West Atto Ultimate Sensitivity Substrate was acquired for signal detection of low abundance proteins. X ray films, the iBright imager and its corresponding software were also acquired from Thermo Fisher Scientific. Square petri dishes used for washing and staining steps were purchased from Sarstedt. Ponceau S sodium salt was obtained from Cell Signalling Technology (London, UK). To read plates during BCA assays, a FLUOstar Omega plate reader was used (BMG Labtech, Aylesbury, UK) and used in conjunction with the Omega and MARS data analysis software packages. Amersham Enhanced Chemiluminescence (ECL) reagent and hyperfilm cassettes were purchased from GE Healthcare. An autoradiographer used to detect protein bands was obtained from AGFA Healthcare (Mortsel, Belgium). The Veriblot detection reagent was purchased from Abcam (Bristol, United Kingdom). Antibodies and their sources are listed in **Table 2.6**.

2.2.3 Immunoprecipitation/co-immunoprecipitation materials

A microcentrifuge tube rotator mixer was purchased from StarLab. Sheep anti-mouse IgG dynabeads (clone M-280) were bought from Thermo Fisher Scientific. The Magnetic Particle Concentrator was acquired from Thermo Fisher Scientific. Reagent Diluent Concentration 2, used to prepare Bovine Serum Albumin (BSA) solutions, was purchased from R&D Systems.

2.2.4 ELISA kits and materials

Nunc Maxisorp 96-well microtitre plates, Tween-20 and Sulphuric acid were purchased from Thermo Fisher Scientific. Human IL-35 ELISA kits were obtained from Cusabio (Texas, USA), or Bio-Ocean (Minnesota, United States). Human TNF α and IL-10 ELISA kits were purchased from Thermo Fisher Scientific. Human EBI3 ELISA kits were obtained from R&D Systems. Where wash buffers were not provided, a wash buffer containing 0.05 % PBS/Tween-20 was made. Where Stop solution was not provided, it was prepared using dilution of sulphuric acid to 2N.

2.2.5 Flow Cytometry materials

The LSRFortessa cytometer, and the compensation beads kit - Anti-Mouse Ig, κ /Negative Control (BSA) Compensation Plus (7.5 μ m) Particles Set, were both from BD Biosciences (New Jersey, United States). Staurosporine was purchased from Sigma Aldrich. Round bottom polystyrene Fluorescence-activated Cell Sorting (FACS) tubes were obtained from Corning (New York, United States). Round bottomed 96-well plates were from Sarstedt. Flow Cytometry Staining Buffer and the LIVE/DEAD™ Fixable Green Dead Cell Stain Kit, were both acquired from Thermo Fisher Scientific. Antibodies, TruStain FcX, FluoroFix Buffer and the APC Annexin V Apoptosis Detection Kit with P/I, were all purchased from BioLegend (California, United States).

2.2.6 Miscellaneous

A Hanna HI2210 pH meter was acquired from Hanna Instruments (Leighton Buzzard, UK). A Scanvac freeze-dryer used during concentration of solutions was from Thistle Scientific (Uddingston, UK).

2.3 General Methods

This section provides a detailed description of the methods used throughout the project. Specific experimental details used in results chapters are described therein, along with a short summary of the methods performed.

2.3.1 Cell Culture

2.3.1.1 Cell culture media

Established cell lines were cultured in RPMI-1640 culture medium supplemented with 10 % FBS and 1 % P/S. Cell lines developed using stable transfection were maintained in the same medium but were also supplemented with antibiotics required to maintain selection pressure (**Table 2.1**).

Table 2.1 Transfected cell lines and antibiotics added to RPMI 1640

Developed Cell Line	Antibiotic Supplementation
CHO-EBI3	G418 (500 µg/mL)
CHO-NTC	G418 (500 µg/mL)
CHO-IL-35	G418 (500 µg/mL) + Puromycin (5 µg/mL)
FaDu-EBI3	G418 (500 µg/mL)
FaDu-NTC	G418 (500 µg/mL)
FaDu-p35	Puromycin (1 µg/mL)
FaDu-IL-35	G418 (500 µg/mL) + Puromycin (1 µg/mL)

2.3.1.2 General cell culture conditions

Actively used cell lines were maintained in a humidified incubator at 5 % carbon dioxide (CO₂) and 37 °C. Prior to use, all surfaces and equipment were cleaned with a 70 % v/v ethanol solution. Items that were not supplied pre-sterilised, such as PBS, distilled water (dH₂O) and Eppendorf tubes, were sterilised by autoclaving (120 °C, 15 lb/m², 15 min). Cell culture reagents were warmed to 37 °C before use. Culture experiments were performed in Class II laminar flow cabinets with aseptic technique.

2.3.1.3 Freezing and storage

FaDu, CHO, transfected cell lines, and H357 cells were resuspended in 90% RPMI-1640 (with FBS and P/S) diluted with 10% DMSO. THP1 cells were resuspended in 90% FBS and 10% DMSO. After resuspension, cells were evenly distributed into cryovials. Cryovials were slow-cooled overnight at -80 °C in freezing containers, before transfer to liquid nitrogen dewars for long-term storage.

2.3.1.4 Thawing

Frozen cells were rapidly thawed in a 37 °C water bath and transferred into a universal container containing 9 mL of RPMI medium before centrifugation at 350 xg (adherent cell lines) or 150 xg (suspension cell lines) for 5 min. Supernatants were discarded and the cell pellet resuspended in culture medium. Cell lines were then grown in tissue culture flasks. Cells that died during thawing were removed by replacement of culture medium the following day.

2.3.1.5 Subculture

Cells were routinely passaged upon reaching 80% confluency (adherent cell lines) or every 2-3 days (suspension cell lines). Adherent cells were washed with PBS and incubated with 1 mL/25 cm² flask or 2 mL/75 cm² trypsin -EDTA (0.25%) until cells had detached from the flask surface. Trypsinisation was stopped by addition of 5 mL/25 cm² or 10 mL/75 cm² culture medium, followed by centrifugation for 5 min at 350 xg. Cells were resuspended in fresh culture medium and counted using a Neubauer counting chamber. Cells were then resuspended into specific seeding densities for experimentation, or split 1:3-1:6 and subcultured in new flasks.

Suspension cell lines were passaged first by centrifugation (150 xg, 5 min) and resuspension of cells in fresh medium. Cells were then counted and reseeded in densities required for experimentation, or split 1:3-1:6 and subcultured.

All cell lines were routinely tested and determined to be free of mycoplasma contamination. This was performed by Dr Maria Stack (School of Dentistry, Cardiff University) via PCR analysis of supernatant samples taken from confluent flasks.

2.3.2 Reverse Transcription – Quantitative Polymerase Chain Reaction (RT-qPCR)

2.3.2.1 Cell lysis

To lyse adherent cells, monolayers were washed with PBS before adding 350 µL of RLT buffer (RNeasy Mini Kit) containing 2-mercaptoethanol. After a 5 min incubation, cells were scraped and resulting lysates collected into microcentrifuge tubes. Suspension cells were lysed by centrifugation (150 xg, 5 min) and resuspension in 350 µL RLT. Lysates were stored at -80 °C until required.

2.3.2.2 RNA extraction

Working surfaces and equipment were cleaned using RNase Zap. RNA extraction was then performed using the RNeasy mini kit as instructed by the manufacturer. No modifications or additional reagents were added. DNase I treatment was omitted. Concentrations of purified RNA were quantified using a NanoVue Plus spectrophotometer. 2 µL per sample was added, and absorbance was measured at 260 and 280 nm. Concentrations in ng/µL were calculated using the Lambert-Beer law. All samples used displayed A260/A280 ratios equal to or close to 2.0. RNA integrity numbers (RIN) of selected samples were obtained using a Bioanalyser instrument. 4 µL per RNA sample was provided to the Central Biotechnology Services at Cardiff University, where analyses were performed.

2.3.2.3 cDNA synthesis via reverse transcription

In 0.1 mL PCR tubes, the following was prepared. Volumes containing 1 µg, 500 ng or 250 ng of purified RNA were diluted with 50 ng of random primer and autoclaved Milli-Q water to make a total of 15 µL per sample. To melt secondary RNA structures and enable binding of random primer, sample tubes were heated at 70 °C for 5 min and cooled to 4 °C. Reverse transcription was then performed using the Moloney Murine Leukemia Virus (M-MLV) reverse transcriptase, as instructed by the manufacturer. Briefly, a reverse transcriptase mastermix was prepared in a sterile microcentrifuge tube. This contained a volume of 10 µL per sample comprised of - M-MLV buffer (1X), 200 units of M-MLV enzyme, 10 mM dNTPs, 25 units of RNAsin, and brought to total volume with autoclaved Milli-Q water. To make a mastermix,

these volumes were multiplied by the total number of samples, including supplementary amounts for pipetting variation. 10 μL of mastermix was then added to each RNA sample tube, producing a total reaction volume of 25 μL . For cDNA formation to occur, sample tubes were placed into a thermocycler and incubated at 37 $^{\circ}\text{C}$ for 1 h before cooling to 4 $^{\circ}\text{C}$. Produced cDNA samples were then stored at -20 $^{\circ}\text{C}$ until use. For each experiment, no-template-control samples were prepared, which included all reaction components used for reverse transcription except template RNA.

2.3.2.4 Primer Design

Primers were designed using the Primer BLAST tool from the National Center for Biotechnology Information (NCBI) database. Reference sequences were acquired by searching for target gene mRNA. If several isoforms were present, the longest isoform was selected. Where possible, the following parameters for primer design were applied:- Product size must be between 70 and 200 bp. Melting temperature must be a minimum of 59 $^{\circ}\text{C}$, optimum 62 $^{\circ}\text{C}$, and maximum of 65 $^{\circ}\text{C}$ with a maximum difference of 3 $^{\circ}\text{C}$ between primers. Primers must span exon-exon junctions. Primers must be between 18-25 base pairs. GC content must be between 50 and 60%. Primers must contain at least 1 GC clamp. Primers must contain a maximum of 4 oligonucleotide repeats. Primers sequences generated using these parameters were then assessed using the OligoEvaluatorTM software tool (Sigma-Aldrich, <http://www.oligoevaluator.com>). Primers were only selected for manufacture if they exhibited the following:- no modifications, a secondary structure of “Weak”, “Very Weak” or “None”, and no primer dimers. Primers were then purchased and manufactured from Sigma-Aldrich. Upon retrieval, they were reconstituted to 100 μM in autoclaved Milli-Q water as instructed, aliquoted and stored at -20 $^{\circ}\text{C}$ until use. All primer sequences used in this thesis are listed below (**Table 2.2**).

Table 2.2 qPCR Primers

<u>Gene</u>	<u>Primer (5' to 3')</u>	<u>Sequence</u>	<u>T_m (°C)</u>
B-Actin	Forward	AAGGATTCCTATGTGGGCGACG	69.9
	Reverse	GGCGTACAGGGATAGCACAG	64.5
GAPDH	Forward	CGACAGTCAGCCGCATCTTC	68.4
	Reverse	ACCAAATCCGTTGACTCCGAC	67.2
HPRT1	Forward	CCTGGCGTCGTGATTAGTGA	66.2
	Reverse	CGAGCAAGACGTTCAAGTCCT	64.6
EBI3	Forward	GAGCACATCATCAAGCCCGAC	69.2
	Reverse	AAGGACGTGGCTTCAATGGG	68.3
P35	Forward	TCCTCCTTGTTGGCTACCCTG	66.4
	Reverse	AGAGTTTGTCTGGCCTTCTGG	64.6
P19	Forward	GGGGAGCAGAGCTGTAATGC	66.0
	Reverse	TTCTCTTAGATCCATGTGTCCAC	65.1
P28	Forward	GAGGGAGTTCACAGTCAGCC	63.9
	Reverse	AGGTGAGATTCCGCAAAGC	64.3
P40	Forward	TGCCCAGAGCAAGATGTGTC	66.0
	Reverse	AGTTCATATGGCCACGAG	66.0
GP130	Forward	GCCATAGTCGTGCTGTTTGC	68.8
	Reverse	AATTGTGCCTTGAGGAGTGTG	67.3
IL-12Rβ2	Forward	CAGGCGACACGTGGAAGAATAC	67.7
	Reverse	GCTTCACAGTCACATCGCCTC	67.3
CD14	Forward	CGGAAGACTTATCGACCATGGAGC	70.4
	Reverse	GGAGAAGTTGCAGACGCAGC	67.5
CD68	Forward	TGTCTACCTGAGCTACATGGCG	66.3
	Reverse	CGAGAATGTCCACTGTGCTGC	68.3
CD11B	Forward	CCATGGCTCTCAGAGTCCTTCT	65.9
	Reverse	CTCCAACCACCACCCTGGAT	68.4
HLA-DR	Forward	AGCCTCTTCTCAAGCACTGGG	67.0
	Reverse	CCATCACCTCCATGTGCCTTAC	67.5
CD80	Forward	CATTGTGATCCTGGCTCTGCG	70.2
	Reverse	AGGTGTAGGGAAGTCAGCTTIG	63.4
CD86	Forward	TTAGGTCACAGCAGAAGCAGCC	67.7
	Reverse	AGCAGCACCAGAGAGCAGGAAG	69.3
CD206	Forward	ACAAGAACTGGGGCCAAGC	67.4
	Reverse	CACAGCCACGTCCCTTCAAC	68.0
CD163	Forward	AACAGGTCGCTCATCCCGTC	68.7
	Reverse	CTCTTGAGGAAACTGCAAGCCG	69.1
IL-10	Forward	GCGCTGTCATCGATTTCTTCCC	70.8
	Reverse	AGTCGCCACCCTGATGTCTC	66.7
VEGF-A	Forward	GTGCCCGCTGCTGTCTAATG	68.0
	Reverse	CCTCGGCTTGTCACATCTGC	68.3
PD-L1	Forward	TGCAGGGCATTCCAGAAAAGATG	70.3
	Reverse	CGTGACAGTAAATGCGTTCAGC	66.6
B7-H4	Forward	CCTGGGGCAGATCCTCTTCTGGAGCATAA	68.9
	Reverse	CAGGATTCCATCCTCCCAATGTTCCCA	67.8

2.3.2.5 qPCR using Powerup SYBR Green

Quantitative Polymerase Chain Reaction (qPCR) was performed in line with the MIQE guidelines (Bustin et al. 2009). In a total volume of 10 μ L per reaction, 8-10 ng of cDNA was mixed with 1X PowerUp SYBR Green mastermix and 500 nM of forward and reverse primers, all diluted in autoclaved Milli-Q water. cDNA and mastermix solutions were loaded into 384-well microplates using an automated EpMotion liquid handler. For each plate, in addition to samples, water only (water used in place of cDNA) and no-template controls were also loaded. Plates were then analysed for mRNA expression using the QuantStudio 12K Flex thermal cycler. PCR cycle conditions are shown in the tables below.

Table 2.3 qPCR cycling conditions

Step	Temperature	Duration	Cycles
UDG activation*	50	2 minutes	Hold
DNA Polymerase activation	95	2 minutes	Hold
Denaturation	95	1 second	40
Annealing/Extension	60	30 seconds	

* Uracil-DNA glycosylase – prevents mutagenesis by initiating degradation of uracil from misprimed or non-specific products

Table 2.4 Melt (Dissociation) Curve conditions

Step	Ramp rate	Temperature	Time
1	1.6°C/second	95	15 seconds
2	1.6°C/second	60	1 minute
3	0.15°C/second	95	15 seconds

2.3.2.6 *Relative quantification*

Product specificity was determined via melt curve analysis. Samples containing multiple, non-specific products were omitted from analyses. Relative quantification, used to compare gene expression versus untreated controls, was calculated using the Livak comparative $2^{(-\Delta\Delta CT)}$ method. First, target gene expression was normalised against stable reference genes via calculation of delta CT (DCT). To do so, CT values of the designated reference gene were subtracted from that obtained for the target gene. Mean DCT values (also known as delta delta CT (DDCT)) were then calculated in the control group. Expression levels of the target gene in the treatment group, relative to that in the control group, was then determined using the following equation: **Fold Change = $2^{(-DCT (\text{Treatment Group}) - DCT (\text{Control Group}))}$** . Mean Fold Changes (+ standard error of the mean (SEM) or standard deviation (SD)) were represented on the y-axes of bar graphs charts.

2.3.2.7 *Statistical Analysis*

Statistical analyses were performed on untransformed DCT values using the GraphPad Prism software (Dotmatics, San Diego, United States). Where three independent experimental repeats were performed, One Way ANOVA, followed by Dunnett's post-hoc test, were used to compare means between treatment and control groups.

2.3.2.8 *Selection of a stable reference gene for normalisation*

In Chapter 3, to optimise the data obtained by qPCR, a stable housekeeping gene was selected to normalise data during relative quantification. Three housekeeping genes - Hypoxanthine Phosphoribosyltransferase 1 (HRPT1), Glyceraldehyde 3-phosphate dehydrogenase (GAPDH) and β -Actin, were chosen as candidate reference genes as they are commonly used in the literature. Primer pairs were designed and purchased for each target. To test which gene was the most applicable for the Chapter studies, RNA was extracted from FaDu and H357 cells that were left untreated, or stimulated with either IFN γ and TNF α , or IL-10 and IL-35 (n=2). 1 μ g of extracted RNA was used to generate cDNA. 8 ng of cDNA from each sample was mixed with 500 nM of each primer pair and examined by qPCR (ran in triplicate). To select the gene with the most stable Ct values across each test condition, both an algorithm derived from the

Thermo Fisher Connect portal, and the qBase+ analysis software tool (Biogazelle, Ghent, Belgium) were used. The Thermo Fisher analysis tool generated a stability score for each gene across all test conditions, of which the highest was selected. Screenshots of the results are shown in **Supplementary data 2**. qBase+ generated a graph (Genorm M), which was used to confirm the gene with the highest stability score. Genorm M charts are also shown in **Supplementary data 2**. The most stable gene was then used as a reference for normalisation in Chapter 3.

2.3.2.9 Calculation of Primer efficiencies

As primers in Chapter 3 were used extensively, qPCR efficiencies and amplification factors were calculated for primer pairs. Two samples of HNSCC cell lines that were treated with cytokines, and shown to express the gene of interest, were selected for efficiency tests. From stored RNA, 1 µg was converted into cDNA and kept undiluted, or a dilution series prepared by sequentially diluting 1 µg of RNA in milliQ water in a 1 in 10 ratio, up to six times. 2 µL of each prepared dilution was loaded onto qPCR plates in duplicate. qPCR reactions were prepared by mixing sample cDNA with 500 nM forward and reverse primer. Primers were then amplified by qPCR using the cycling conditions described previously (**Section 2.3.2.5**). Standard curves were generated from outputs by plotting CT values for each primer against log DNA concentrations. Linear regression was used to generate lines of best fit. To calculate Amplification Factors (AF) and qPCR efficiencies, the slopes of these lines were applied to the equations shown below. The mean from two samples was then calculated, which was used to report Amplification Factor and Efficiency values for each primer. These values are shown in **Supplementary Data 3**.

$$\text{Amplification Factor (AF)} = 10^{(-1/\text{slope})}$$

$$\text{Efficiency} = (\text{AF}-1) \times 100$$

2.3.3 Protein detection via Western Blotting

2.3.3.1 Cell Lysis

Cells in flasks were first harvested by trypsinisation and centrifugation. Cell pellets were resuspended in 200 μ L ice-cold Radio-Immunoprecipitation Assay (RIPA) lysis buffer (containing protease inhibitors) and incubated for 5 min at room temperature before storage at -20 C. Cells in multi-well plates were washed with PBS before 200 μ L ice-cold RIPA was added. After 5 mins, cells were scraped with sterile pipette tips and resulting lysates collected into microcentrifuge tubes. Lysates were stored at -20 C.

During experiments that examined cell lysates for detection of proteins that can be secreted, the secretion blocker Brefeldin A (BFA) was used. 3.0 μ g/mL of BFA was added to cell culture 4-6 h prior to lysis. BFA inhibits secretion by blocking transport of proteins from the Endoplasmic reticulum (ER) to the Golgi apparatus. Thus, it was used to increase intracellular concentration of detectable target protein within cell lysates.

2.3.3.2 Quantification of protein concentration– Bicinchoninic acid (BCA) Assay

The Pierce™ BCA protein assay kit was used to quantify total protein concentration in cell lysates. Lysates were thawed and cell debris removed by centrifugation (15 min, 10,000 xg, 4 °C) and extraction of pellets with sterile pipette tips. BCA assays were then performed in 96-well microtitre plates as instructed by the manufacturer. Standards were prepared by serial dilution of BSA in PBS. 10 μ L of sample or standard were loaded into plates, and 200 μ L of working reagent added to all wells. Following gentle agitation for 30 s, plates were incubated at 37 °C for 30 min. Absorbance was immediately measured at 570 nm using a plate reader. Absorbance within samples and standards were blank-corrected before unknown protein concentrations were calculated using the gradients of standard curves.

2.3.3.3 SDS-PAGE

To separate proteins by molecular weight, SDS-PAGE analyses were performed using the NuPage™ bis-tris mini gel system, as instructed by the manufacturer. Firstly, samples were diluted to working concentrations in sample loading solutions. Sample

loading solutions consisted of sample protein, Lithium dodecyl sulfate (LDS) - to denature, linearise and provide proteins with a uniform negative charge, Reducing Agent – containing 500 nM dithiothreitol (DTT) to reduce disulphide bonds, and RIPA buffer to bring to total volume. Loading solutions were prepared at a 20% volume surplus to account for pipetting variation. Following a 10 min incubation at 70 °C, samples were briefly centrifuged and resuspended before loading into gels. Pre-cast polyacrylamide gels (10 wells, 4-12% gradient) were assembled into tanks filled with MES running buffer. Samples and pre-stained molecular weight ladder were carefully loaded into wells, and gels were run for up to 35 min at 200 V.

2.3.3.4 Western Blotting

Proteins were transferred from gels to nitrocellulose (NC) membranes using the iBlot 2 dry blotting system. Gels were assembled into NC stacks, placed into the machine and proteins transferred from gel to membrane as instructed by the manufacturer. Transfers were performed using the 7 min programme consisting of 20 V for 1 min, 23 V for 4 min and 25 V for 2 min. Membranes were then placed into square petri dishes containing distilled water.

To confirm protein transfer, NC membranes were incubated for 5 min in Ponceau S whilst agitated on a see-saw rocker. Lane positions were marked with a pencil. All traces of Ponceau S were removed by repeated washing with TBST. Membranes were blocked in 5% non-fat dried milk diluted in TBST (Tris-buffered saline with Tween 20 detergent) for 2 h, or overnight at 4 °C. Unbound material was removed using several wash steps on a see-saw rocker. To wash thoroughly, membranes were washed twice with TBST, twice using a high-salt wash buffer, and once more in TBS to remove excess Tween-20. Each wash step lasted 5 min. All subsequent washes were performed using this sequence. Composition of all buffers are shown in the table below (**Table 2.5**).

For staining of protein targets, membranes were incubated overnight at 4 °C in primary antibody (pre-diluted in 5% milk/TBST). Membranes were washed and incubated with horseradish peroxidase (HRP)-conjugated secondary antibody for 1 h at RT (room temperature). Unbound material was removed by washing. Membranes were stained with ECL reagent for 3 min in darkness at RT to enable visualisation of HRP. Protein

bands were detected on membranes using an iBright imager or alternatively, assembled into hypercassettes, exposed to x-ray films and developed using autoradiography.

In experiments where equal protein concentrations between samples were examined, detection of β -Actin was used to evidence equal protein loading. After detection of target protein, membranes were washed, and an HRP-conjugated anti β -Actin antibody (pre-diluted in 5% TBST) added. Membranes were incubated for 30 min to stain. They were then washed, and ECL reagent applied before signal detection by radiography or use of iBright equipment. A list of all antibodies used for Western Blotting is given in **Table 2.6**. Concentrations used in each experiment are described within the relevant results chapters.

Table 2.5 Western Blot Buffers

Buffer	Composition
TBS	25 mM Tris, 0.15 M NaCl
TBST	25 mM Tris, 0.15 M NaCl, 0.1% Tween 20
High salt wash buffer	10 mM Tris, 500 mM NaCl, 0.1% Tween 20
Blocking Buffer	5 g powdered milk in 100 mL TBS-T

Table 2.6 - Western Blot Antibodies

Target	Clonality	Isotype	Manufacturer	Clone
Primary Antibodies				
Anti-human EBI3	Monoclonal	Mouse IgG2b, κ	Biologend	A15058A
Anti-human p35	Monoclonal	Rabbit IgG	Abcam	EPR5736
Anti-human p35	Monoclonal	Mouse IgG ₁	R&D Systems	27537
Anti-human β -Actin (HRP)	Monoclonal	Mouse IgG3	Abcam	mAbcam 8224
Secondary Antibodies				
Anti-Rabbit IgG (HRP)	Polyclonal	Goat IgG	Abcam	ab205718
Anti-Mouse IgG (HRP)	Polyclonal	Rabbit	Abcam	ab6728
Anti-mouse IgG2b heavy chain (HRP)	Polyclonal	Goat	Abcam	ab97250

2.3.4 Immunoprecipitation/Co-immunoprecipitation

Immunoprecipitation was used to pull down p35 from cell lysates and supernatants. Western Blotting was then performed on eluted precipitates to detect p35 or co-immunoprecipitated EBI3, which indicated presence of the IL-35 heterodimer (EBI3/p35). To precipitate p35 from solution, 500 μ L to 1 mL of cell lysate or culture

supernatant per sample was transferred into microcentrifuge tubes and treated with 1-4 μg of mouse monoclonal anti-p35 (Clone, 27537) antibody. Samples were incubated overnight at 4 °C on a tube rotator to enable antibody-antigen interactions.

Sheep anti-mouse IgG dynabeads were prepared as instructed by the manufacturer. Briefly, the stock tube was vortexed for 30 s to resuspend beads in solution. The required total volume for a given experiment was then aliquoted into a sterile microcentrifuge tube. Dynabeads are magnetic, which enabled the use of a magnetic particle concentrator to isolate beads against the sides of microcentrifuge tubes. By repeatedly removing solution and resuspending beads in 0.1% BSA (prepared from Reagent Diluent Concentration 2, dissolved in PBS), beads were washed three times. To capture and provide a solid support for mouse IgG on anti-p35 antibodies, 50 μL of anti-mouse IgG dynabeads were added to each sample containing anti-p35. Bead-antibody-p35 complexes were left to form by incubating samples overnight at 4 °C on a tube rotator.

To elute protein complexes bound to beads, beads within each sample were first washed five times in ice-cold PBS to remove unbound material. Beads were then resuspended in SDS-PAGE sample loading solution. For immunoprecipitation experiments, this consisted of: Dynabeads (50 μL), 50% LDS (25 μL) and 1X reducing agent (10 μL), topped up to a total volume of 100 μL with PBS. Samples were heated for 10 min at 70 °C. Beads were isolated using the particle concentrator, and supernatants containing bead-free eluates transferred into sterile microcentrifuge tubes. Finally, sample eluates were loaded onto SDS-PAGE gels and analysed for the presence of EBI3 and p35 by Western Blotting (**Section 2.3.3.4**). Primary and secondary antibodies used to detect these proteins are described within relevant results chapters. A full list of antibodies is shown in **Table 2.6**.

2.3.4.1 Immunoprecipitation controls

Several controls were used during immunoprecipitation/Western Blotting experiments. Positive control samples were used to confirm antibody specificity during the detection of EBI3 and p35 protein by Western Blot. For this purpose, recombinant human IL-35, which was first reduced, and lysates or supernatants taken from transfected cell lines which overexpress these subunits, were examined alongside

test samples. Untransfected CHO or FaDu cells, in which subunits could not be detected, were used as negative controls.

Immunoprecipitation controls included the confirmation of pulldown, IgG, input and flowthrough controls. To confirm successful immunoprecipitation, p35 was detected in eluates by Western Blotting. IgG controls (termed IgG control (beads only) in Chapter results) involved the addition of anti-mouse IgG dynabeads to solute samples and the omission of anti-p35 pulldown antibody. Western Blot analysis of this control was used to detect cross reactivity of human protein to anti-mouse IgG. To generate input controls, a fraction of the total sample volume was reduced and analysed without antibody or bead incubations. 2% of the total sample volume was used in the thesis experiments. Flowthrough controls were generated by collecting and analysing the unbound fraction of the sample, taken after immunoprecipitation with the pulldown antibody. Following incubation with anti-p35, beads were isolated by magnetic particle concentration and the liquid flowthrough collected rather than discarded. A volume equal to that used for the input control was then reduced and analysed by Western Blot. Input and flowthrough controls were derived from the same sample, which was known to express the target proteins. Input and flowthrough controls are used to assess pulldown efficiency. This was done by relative signal comparison between the input control (before immunoprecipitation) and the flowthrough (after immunoprecipitation). The degree of signal depletion thus provided an indication of pulldown efficiency (Gerace and Moazed 2014).

2.3.5 Enzyme-Linked Immunosorbent Assay (ELISA)

ELISA assays were used to detect target proteins in solution. Each kit was performed as instructed by the manufacturer. Where these materials were not provided in kits, the following were used. Assays were performed in Nunc Maxisorp 96-well microtitre plates. Reactions were stopped by addition of 2 N sulphuric acid. Absorbances were measured using a plate reader before blank-correction and calculation of target solute concentration using the gradient of standard curves.

2.3.6 Transfection

2.3.6.1 *Transfection using Lipofection*

1×10^5 cells were seeded into 24-well plates and incubated overnight to enable cells to reach 70-90% confluency. They were then transfected with plasmid DNA using the Lipofectamine 2000 reagent as instructed by the manufacturer. Briefly, Lipofectamine 2000 reagent, prepared at two concentrations to optimise transfection efficiency, was diluted in 25 μ L of serum free RPMI 1640 culture medium in two separate microcentrifuge tubes. 1 μ g of plasmid DNA was diluted into 50 μ L of serum free medium in another tube. The p2000 reagent was added to diluted DNA and mixed well. 25 μ L of DNA mastermix was then added to each of the two tubes containing Lipofectamine 2000 and mixed, such that 500 ng DNA was added to each tube in a 1:1 volume ratio. After a 10 min incubation, mixtures were added to cells in a dropwise manner. Cells were incubated for 48 h to enable transfection and cell recovery to occur.

2.3.6.2 *Stable transfection via antibiotic selection*

The EBI3 and NTC plasmids both contain the gene for resistance to neomycin (**Figure 2.1A and Figure 2.1C**). The p35 expression plasmid contains the gene for resistance to puromycin (**Figure 2.1B**). Stable transfectants were therefore positively selected by treating cells with antibiotics. Culture medium from transfected cells was replaced with that containing G418 (for neomycin resistance), puromycin, or both. Concentrations of each antibiotic used for transfected CHO and FaDu cell lines are shown in **Table 2.1**. Cells underwent selection for 10-14 days, replacing culture medium every 2/3 days. At this time, untransfected cells and transfectants that did not express the required antibiotic resistance markers had died. Surviving cells were then expanded and split into two populations. One was stored frozen in liquid nitrogen as polyclonal stocks. The other was maintained in culture. The cells within this transfected population were polyclonal - some expressed the gene of interest, and some did not. To generate monoclonal cell lines derived from cells that expressed the gene of interest, the cell population was first diluted into single cell cultures by limiting dilution. This step was omitted for the NTC transfectants, as due to the plasmid not

containing a gene of interest, this was not required. These were instead frozen until use in experiments as a control.

2.3.6.3 Limiting dilution to generate monoclonal cell lines

Cells were resuspended at 5 cells/mL in 10 mL of culture medium. 100 µL of cell suspension was dispensed into wells of a 96-well plate using a multichannel pipette. Cells were incubated until colonies had formed. Wells containing single colonies, indicative of monoclonal populations, were labelled with numbers and cultured further until 70-90% confluency was reached. Each clone was then harvested and transferred into 24-well plates to increase in number. Once 70-90% confluency was reached, clones which had survived expansion were each split into two populations. Clones cultured in the first population were each expanded progressively into larger plates/flasks until grown to 70-90% confluency in T75 flasks. Frozen stocks were then prepared and stored in cryovials at -80 °C. Those in the second population were screened to identify which clones successfully overexpressed EB13 and/or p35.

2.3.6.4 Generation of conditioned medium (CM)

To study the effects of secreted IL-35, or its subunits, on the behaviour of cultured macrophages, treatments with CM taken from generated cell lines were used. To create stocks of CM from each cell line, 5×10^5 cells were seeded into two T25 flasks in 5 mL of culture medium. After 24 h, dead cells were removed by washing with PBS. Cells were then cultured in fresh medium for a further 48 h. Generated conditioned medium was pooled together from both flasks and debris removed by passing it through a 0.22 µM sterile filter. The flowthrough was then aliquoted into microcentrifuge tubes, which were stored at -80 °C. To account for possible protein stability issues, each aliquot was thawed only once before use and discarded afterwards.

2.3.7 Macrophage differentiation models

As commonly reported in the literature, THP1 cells were used to generate macrophage polarisation models (Chanput et al. 2014; Baxter et al. 2020). Models derived using stimulation with the phorbol ester PMA are henceforth termed M0, M1 and M2. An alternative M1 model was developed in our laboratory that did not use PMA for differentiation. To prevent ambiguity, these cells are described as M1-like.

2.3.7.1 Generation of M0, M1 and M2 models

Optimal cell seeding numbers and volumes of culture medium were determined in previous experiments. For RT-qPCR and ELISA experiments, 4×10^5 THP1 cells were seeded into single wells of 24-well plates within 500 μ L of culture medium. For Flow Cytometry experiments where a larger number was required, 2×10^6 cells were seeded into two wells per sample within 2.5 mL of culture medium. Cells from two wells were then pooled together prior to analyses. These culture conditions were determined in preliminary experiments.

As commonly reported, PMA was used to differentiate THP1 monocytes into macrophages followed by IFN γ or IL-4 stimulation to drive polarisation to M1 or M2, respectively (Daigneault et al. 2010; Chanput et al. 2014; Shiratori et al. 2017; Tedesco et al. 2018). To differentiate THP1 monocytes into resting M0 macrophages, seeded THP1 cells were treated with 50 ng/mL PMA and incubated for 24 h. Cells were washed gently three times and rested by addition of fresh culture medium. After a further 48 h, macrophages were termed M0. To generate M1 macrophages, THP1 cells were treated with PMA (100 ng/mL) and incubated for 24 h. They were rested for 48 h before stimulation with IFN γ (20 ng/mL) for an additional 48 h. To generate M2 macrophages, THP1 cells were treated with PMA (50 ng/mL) and incubated for 24 h. They were rested for 48 h before stimulation with IL-4 (20 ng/mL) for a further 48 h. Reagent concentrations, stimulation and rest times were determined empirically in previous experiments.

2.3.7.2 Generation of M1-like cells

M1-like cells were used as an alternative model to support data obtained from PMA derived M1 macrophage models. To generate M1-like cells, 2×10^5 THP1 cells were seeded in 24-well plates within 1 mL of culture medium. For M1 polarisation, cells were stimulated with GM-CSF (20 ng/mL) for 72 h. IFN γ (20 ng/mL) was then added, and cells incubated for a further 24 h before experimentation. Culture conditions were determined in previous experiments.

2.3.8 3D tumour spheroids

2.3.8.1 *Generation of 3D spheroids via hanging drops*

Hanging drops were used to create 3D spheroid models. These were generated to study the effects of FaDu-derived IL-35 on macrophage polarisation. FaDu/FaDu-IL-35 cell spheroids were made in monoculture, or mixed 1:20 with M1 or M2 macrophages (based on previous experiments). FaDu/FaDu-IL-35 cells were harvested, and cell density readjusted to 4×10^5 cells/mL. M1 or M2 macrophages were also harvested, and density adjusted to 2×10^5 cells/mL. To generate FaDu/FaDu-IL-35 spheroids, 25 μ L drops of cell suspension was added onto the inverted lids of petri dishes using a multichannel pipette. To cultivate hanging drops from FaDu/M1 or FaDu/M2 mixed cultures, after adjustment to the cell densities described above, 1:20 ratios were achieved by diluting macrophages 1:10 in FaDu/FaDu-IL-35 cells (final cell counts: approximately 2×10^4 macrophages to 4×10^5 FaDu/Fadu-IL-35 cells). 25 μ L drops of these mixtures were subsequently applied to petri dish lids. Lids were then placed onto dishes filled with PBS to ensure that cells did not dry out during incubation. 3D spheroids were left to form by incubating petri dishes at 37 °C 5 % CO₂ for up to 72 h.

2.3.8.2 *Imaging and calculation of spheroid surface area*

To visualise and capture images of 3D spheroids, lids containing hanging drops were transferred onto fresh, empty petri dishes. These dishes were inverted and placed onto a microscope stage. Spheroids were visualised at 4X magnification and ten images per sample captured using a Motic digital camera. The surface area of spheroids were measured using the Image J software (National Institute of Health, Maryland, USA). Images were first calibrated to a known measurement before the manual drawing tool was utilised to calculate spheroid surface area.

FaDu cells, and those that were mixed 20:1 with M1 or M2 macrophages successfully formed spheroids, which were used to measure changes in spheroid area caused by macrophage co-culture (**Supplementary Data 11**). However, spheroid formation could not be achieved using FaDu-IL-35 cells, nor could spheroid formation be replicated using FaDu cells. Thus, use of this method was ultimately abandoned.

2.3.9 Flow Cytometry

Flow cytometry was used to detect expression of surface proteins in cultured macrophages, and to detect apoptotic or necrotic FaDu/FaDu-IL-35 cells following mixed culture with macrophages.

2.3.9.1 *Development of antibody panels*

Two antibody panels were designed: one to detect an array of macrophage polarisation markers (**Macrophage Polarisation Panel – Table 2.7**), and the other to detect apoptotic and/or necrotic FaDu cells (**Apoptosis/Necrosis Panel – Table 2.8**). To build these panels, the FluoroFinder 2.0 tool (Biolegend) was used. As several colours were to be analysed, each panel was designed for use on the LSR Fortessa as configured in the Henry Wellcome Building, Cardiff University. The FluoroFinder tool enabled specific fluorophores to be assigned to each target antigen whilst minimising spectral overlap. To decide the brightness of the conjugated fluorophore for each antigen, expression levels were first inferred from qPCR data. Brighter fluorophores were selected for lesser expressed genes, and dimmer fluorophores for those highly expressed. Once antibodies were selected for each panel, they were purchased from Biolegend and tested both, to ensure that the antibodies worked correctly, and to determine antibody volumes to be used in subsequent experiments.

2.3.9.2 *Compensation matrices*

After validating each antibody, compensation matrices were generated to ensure minimisation of spectral overlap. To generate positive and negative signals for each individual antibody, anti-mouse Ig_k compensation beads were used, as instructed by the manufacturer. Briefly, one drop of unlabelled beads and Ig_k beads were added to microcentrifuge tubes containing 100 µL Flow Cytometry Staining Buffer. Antibodies were added to individual tubes at volumes equal to that used in final experiments. After a 30 min incubation at room temperature in the dark, tubes were washed once by addition of Flow Cytometry Staining Buffer, and fixed by resuspension in 500 µL FluoroFix Buffer. Samples were fixed for 1 h at room temperature in the dark. After, beads were pelleted by centrifugation (200 xG, 10 min) and washed once, before resuspension in 200 µL Flow Cytometry Staining Buffer. Tubes were stored at 4 °C in the dark for up to 72 h prior to analysis using an LSR Fortessa. Single-colour analyses

were first used to optimise voltages for positive and negative signals. Autocompensation was then applied to minimise spectral overlap.

Compensation beads cannot be used for live/dead staining. Therefore, to apply compensation for the Apoptosis/Necrosis panel, cells used in the applicable experiments were treated with staurosporine (1 μ M, 24 h) to induce cell death, and either left unstained, or stained with the Apoptosis/Necrosis Panel. The positive Annexin and P/I signals provided from this were used to apply autocompensation.

Table 2.7 Macrophage Polarisation Panel

Antigen	Conjugated Fluorophore	Clone	Isotype	Isotype Clone	Volume used per sample (µL)
<u>Surface Staining Mastermix</u>					
CD14	APCFire750	M5E2	Mouse IgG2a, k	MOPC-173	5
CD326 (EpCAM)	BV421	9C4	Mouse IgG2a, k	MPC-11	5
HLA-DR	PE/Cy7	L243	Mouse IgG2a, k	MOPC-173	2.5
CD80	PE	2D10	Mouse IgG1, k	MOPC-21	5
CD86	BV510	IT2.2	Mouse IgG2b, k	MPC-11	5
CD206	BV711	15.2	Mouse IgG1, k	MOPC-21	5
CD163	BV785	GH1/61	Mouse IgG1, k	MOPC-21	5
CD204	APC	7C9C20	Mouse IgG2a, k	MOPC-173	5
Flow Cytometry Staining Buffer	/	/	/	/	*To total 100 µL per sample
<u>Live/Dead Staining</u>					
LIVE/DEAD Fixable Green	/	/	/	/	100

Table 2.8 Apoptosis/Necrosis Panel

Antigen	Conjugated Fluorophore	Clone	Isotype	Isotype Clone	Volume used per sample (µL)
<u>Surface Staining Mastermix</u>					
CD14	APCFire750	M5E2	Mouse IgG2a, k	MOPC-173	5
CD326	BV421	9C4	Mouse IgG2a, k	MPC-11	5
Staining Buffer	/	/	/	/	*To total 100 µL per sample
<u>Live/Dead Staining</u>					
Annexin V	APC	/	Mouse IgG2a, k	MOPC-173	5
Propidium Iodide (P/I)	/	/	/	/	10
Annexin Binding Buffer	/	/	/	/	400

2.3.9.3 Sample preparation - Cell Culture, harvesting and Fc blocking

For experiments validating expression of M1 and M2 markers in M1 and M2 macrophage models, THP1 cells were differentiated and polarised into M1 and M2 macrophages within two wells of a 6-well plate (**Section 2.3.7**) to ensure a large number of cells for experiments. Polarised macrophages were lifted from well surfaces by treatment with TrypLE Express for 10 min, followed by repeated trituration to

ensure maximal detachment. TrypLE Express was used as a less cytotoxic alternative to trypsin, and to preserve surface marker expression. The minimum duration of TrypLE treatment required for maximal cell recovery was determined in previous experiments. Harvested cells were resuspended at a density of 1×10^5 cells/mL.

For mixed culture experiments, FaDu or FaDu-IL-35 cells were first resuspended at 4×10^5 cells/mL. 1 mL of FaDu or FaDu-IL-35 cells were then seeded into wells of fresh 6-well plates. 1 mL of M1 or M2 macrophages were mixed with seeded FaDu or FaDu-IL-35 cells within wells, resulting in a 4:1 FaDu/FaDu-IL-35 to macrophage cell ratio. Cell mixtures were seeded in two wells each, yielding a total of 8×10^5 FaDu/FaDu-IL-35 cells and 2×10^5 M1/M2 macrophages per sample. This ratio was selected to optimise effects of mixed culture, minimise potential loss of FaDu cell-cell and cell-surface adhesion, and to ensure enough macrophages were present per sample for Flow Cytometry analysis within the seeded cell count. Wells were topped up to a total volume of 5 mL with culture medium and plates gently agitated to ensure sufficient mixing. Cells were incubated at 37 °C for 48 h to provide sufficient time for potential changes to occur. Monocultures of each cell type were also maintained for the same duration for use as controls. After, cells were harvested via 10 min treatment with TrypLE Express. Collected cells were washed twice using Flow Cytometry Staining buffer and centrifugation (350 xg, 5 min).

For experiments validating M1 or M2 polarisation, and those involving mixed culture, Fc receptors were blocked by a 10 min incubation with TruStain FcX at room temperature. Cells were resuspended in 600 μ L PBS and aliquoted evenly into three wells of round bottomed 96-well plates per sample. This ensured that between 5×10^5 and 1×10^6 cells were either unstained (Well 1), stained with the relevant antibody panel (Well 2), or their corresponding isotype controls (Well 3). Approximately 1×10^6 cells or less ensured maximal antibody binding (as recommended by the antibody manufacturer).

2.3.9.4 Surface staining for macrophage polarisation experiments

Cells in wells of round-bottomed 96-well plates were first stained with a LIVE/DEAD™ Fixable Green Dead Cell Stain Kit for 30 min at 4 °C. Cells were washed three times using centrifugation (700 xG, 5 min, 4 °C) and resuspension in

Flow Cytometry Staining Buffer. Mastermixes were prepared for both the Macrophage Polarisation Panel and their corresponding isotypes (**Table 2.7**). Isotype controls were used to assess the efficiency of Fc blocking. Cells were then stained with the antibody mixture, or their corresponding isotypes, for 30 min in darkness at 4 °C. Post-staining, cells were transferred to microcentrifuge tubes and fixed in 500 µL FluoroFix fixation buffer for 1 h at room temperature in the dark. Cells were washed once and resuspended in 400 µL Flow Cytometry Staining Buffer before transfer to FACS tubes. Samples were stored at 4 °C in the dark for up to 72 h, whereby protein detection was analysed using an LSRFortessa. Up to 10,000 events were captured using the flow cytometer.

2.3.9.5 Surface Staining for Apoptosis/Necrosis experiments

Cells in 96-well plates were pelleted, and relevant wells stained with the Apoptosis/Necrosis panel or their corresponding isotype controls (100 µL per sample) (**Table 2.8**). Isotype controls were used to assess the efficiency of Fc blocking. Plates were incubated at 4 °C in the dark for 30 min. After, cells were washed three times with Flow Cytometry Staining Buffer and apoptotic/necrotic cells stained with an Annexin V Apoptosis Detection Kit with P/I, as instructed by the manufacturer. Samples were subsequently transferred to FACS tubes and fluorescence analysed immediately on an LSRFortessa. Up to 10,000 events per sample were captured using the flow cytometer.

2.3.9.6 Analysis of Flow Cytometry data

Data obtained from the LSR Fortessa was uploaded onto the FlowJo analysis software (BD Biosciences). Cells were gated via exclusion of debris. Doublets were excluded to gate on single cells. In experiments where Live/Dead stain was used, Live cells were obtained by gating the negative population. Cells were then gated to identify those that were positive or negative for expression of target markers. Positive/negative discrimination for each experiment – how it was determined where the uniform gate separating positive and negative cells was set between all test samples, is explained in detail in the section below. The percentage of cells that were positive for expression of the target marker was then calculated in FlowJo. The mean percentage across experimental repeats was displayed in bar charts (+SEM) generated in GraphPad

Prism. Percentages were compared between test samples to ascertain whether changes in target protein expression were associated with differences in culture conditions (macrophage polarisation protocols or mixed culture of macrophages with FaDu cells). Statistical tests were performed in GraphPad Prism to determine if differences observed were statistically significant (detailed in relevant chapter methods).

2.3.9.7 Positive/Negative discrimination

To best discriminate the population of cells that were positive or negative for expression of a target protein, uniform gates were set between all test samples. Gates were set in a manner that minimised exclusion of positive cells across all samples. Positive/negative discrimination for each experiment are described henceforth.

Validation of M1 or M2 polarisation in developed macrophage models - THP1, M1 or M2 monocultures were analysed for expression of their corresponding polarisation markers (M1 - HLA-DR, CD80, CD86, M2 – CD206, CD163). After gating on single live cells, dotplots were created using the target protein fluorescence on the x-axis, and Live/Dead fluorescence on the y-axis. Dotplots were smoothed to help identify populations of high and low fluorescence density. A gate was then set to separate cells that were positive for expression of the target protein from those that were negative. Positive/negative discrimination in this experiment was achieved by comparing plots between all test samples, gating on the boundaries of common regions of high signal density and ensuring that less than 1% of cells were stained in the unstained population. The gate was then applied in the same position for all test samples.

Measuring changes in expression of M1 and M2 markers following mixed culture with FaDu or FaDu-IL-35 cells - M1 or M2 macrophages were mixed in a 1:4 ratio with FaDu or FaDu-IL-35 cells and analysed by Flow Cytometry to assess whether IL-35 overexpression inhibited the M1 phenotype (Chapter 5) and promoted the M2 phenotype (Chapter 6) via regulating expression of surface markers. After gating on single, live cells, macrophages were identified by gating on the CD326- population, which excluded FaDu cells (confirmed to express CD326 in preliminary studies). From the CD326- macrophage population, cells that expressed each marker was determined by gating on the positive population. Positive/negative discrimination was

achieved by comparing plots from all test samples, and placing uniform gates with the assistance of the following: positive controls, previously tested M1 and M2 control samples and unstained cells. Gates were adjusted to minimise exclusion of positive events across all test samples. A uniform gate was then applied to all groups.

Measuring changes in apoptotic and necrotic FaDu/FaDu-IL-35 cells following mixed culture with M1/M2 macrophages. - FaDu or FaDu-IL-35 cells were cultured alone or mixed in a 4:1 ratio with M1 or M2 macrophages. After staining, single cells were identified. FaDu/FaDu-IL-35 cells were then gated by inclusion of CD326+ CD14- cells only. Positive/negative discrimination for Annexin V and P/I staining was then achieved using the boundaries of the unstained populations, and regions of high density between all test samples. A uniform gate was then set for all test samples.

Chapter 3

**Regulation of IL-35 expression in HNSCC cells by inflammatory
cytokines in the tumour microenvironment**

3.1 Introduction

Head and neck squamous cell carcinomas (HNSCC) are the sixth most common cancer worldwide. While the advent and use of immune checkpoint inhibitors as treatment prolonged survival, only a fraction of patients respond, and due to resistance, overall survival rates remain unsatisfactory (Ferris et al. 2016; Larkins et al. 2017; Canning et al. 2019; Galvis et al. 2020). Therefore, there is a need for new approaches that improve responses to immunotherapies.

To improve immunotherapies, research must elucidate novel mechanisms leveraged by tumour cells to dysregulate immune cells in a manner that facilitates immune escape. Such mechanisms may reveal targets, that when modulated, could reverse immune suppression and improve responses when used in combination with other immunotherapies. Research in this Chapter seeks to fill this gap by implicating the production of the immunosuppressive cytokine Interleukin 35 (IL-35), as a novel mechanism used by HNSCC cells to adapt to inflammation. By producing IL-35, tumour cells may use this cytokine to suppress the anti-tumour activity of immune cells in the TME, thus representing a novel escape mechanism that could potentially be targeted in novel immunotherapies.

3.1.1 Immunoediting

Responses to immunotherapies can be regulated in part by the nature of the immune infiltrate in the TME. HNSCCs (particularly HPV+) commonly show inflamed or immunologically “hot” TMEs, that is, those that are populated by immune cells and pro-inflammatory cytokines. However, these environments become edited by tumour cells to enable them to escape detection and elimination. The mechanisms leveraged to escape immune surveillance are thought to be involved in resistance to immunotherapies (Allen et al. 2015; Chen and Mellman 2017; Trujillo et al. 2018). The concept describing how tumours are able to manipulate the tumour microenvironment (TME) to escape immunosurveillance is named immunoediting (Dunn et al. 2004).

Immunoediting, described briefly, begins with cell transformation. Transformed cells express tumour antigens which alert the immune system. Infiltrating immune cells destroy tumour cells and secrete pro-inflammatory cytokines such as IFN γ and TNF α

(Elimination). IFN γ amplifies anti-tumour immune responses by enhancing antigen presentation, recruitment of additional immune cells, and by promoting apoptosis in tumour cells (Platanias 2005; Sharma et al. 2017; Jorgovanovic et al. 2020). TNF α also assists in inflammatory responses by recruiting and activating immune cells, and in some instances can cause tumour cell death (Laha et al. 2021). It is thought that this inflammatory response acts as a selective pressure, eliminating highly immunogenic tumour cells, and selecting for the survival of less immunogenic tumour cells. Outgrowth of cells that survive this phase are held dormant by the presence of immune cells and cytokines (Equilibrium). However, this can lead to chronic inflammation. Inflammation can damage tissues, promoting DNA damage and genetic instability (Pua et al. 2020). This provides an environment for surviving tumour cells to adapt to inflammation by acquiring traits which help them avoid detection and destruction from immune cells. They manipulate immune cells to behave in a way that blocks anti-tumour immunity and promotes tumour aggressiveness. Immune escape describes tumours that use these mechanisms to exhibit immunotolerance (Dunn et al. 2004; Benci et al. 2016; Greten and Grivennikov 2019).

In HNSCC, mechanisms that facilitate immune escape mechanisms include: - inhibition of detection by immune cells, through decreased expression and mutations in tumour antigens, or defective MHC I or antigen presentation machinery. Tumour cells can also increase expression of checkpoint proteins in their own cells or surrounding immune cells, preventing immune cell activity upon engagement with tumour cells. Additionally, they can recruit and reprogram immune cells using chemokines and immunosuppressive cytokines (such as IL-10). These mechanisms inhibit the activity of anti-tumour immune cells and help sculpt an immunosuppressive TME (Elmusrati et al. 2021) (reviewed in Chapter 1).

Tumour cells in HNSCC may leverage escape mechanisms to accelerate disease progression and confer resistance to immunotherapies. To improve responses to immunotherapies, it would therefore be beneficial to identify novel escape mechanisms that can be targeted, potentially as an adjuvant with existing therapies, to overcome resistance and strengthen the anti-tumour immune response.

3.1.2 Interleukin 35 (IL-35)

Interleukin 35 is an immunosuppressive cytokine belonging to the IL-12 family (Mirlekar and Pylayeva-Gupta 2021). Each cytokine in this family are heterodimers, structurally composed of a helical α -subunit similar to IL-6, and a β -subunit related to the IL-6 receptor (IL-6R α). These chains can dimerise interchangeably, potentially resulting in the formation of several cytokines. Cytokines in this family include IL-12 (p35/p40) IL-23 (p19/p40), IL-27 (p28/EBI3), IL-35 (p35/EBI3) and IL-39 (p19/EBI3) (Kobayashi et al. 1989; Devergne et al. 1997; Oppmann et al. 2000; Pflanz et al. 2002; Wang et al. 2016). Sharing of these chains enables highly flexible responses to immunological stimuli. IL-12, IL-23 and IL-39 are pro-inflammatory, while IL-27 and IL-35 are considered immunosuppressive (Mirlekar and Pylayeva-Gupta 2021).

IL-35 is expressed mostly in Tregs, induced Tregs and Bregs, but can also be expressed in macrophages and cancer cells (Long et al. 2013; Wang et al. 2013; Pylayeva-Gupta et al. 2016; Hao et al. 2018; Lee et al. 2018). When secreted from these cells, IL-35 can be transduced in target cells via four receptor combinations: gp130/IL-12R β 2, gp130/gp130, IL-12R β 2/IL-12R β 2 - in T cells, and IL-27R α /IL-12R β 2 in B cells (**Figure 3.1**) (Collison et al. 2012; Choi and Egwuagu 2021). How IL-35 interacts with these receptors and mediates downstream signalling is not well understood. In T cells, IL-35 can signal through gp130 and IL-12R β 2 homodimers or gp130/IL-12R β 2 heterodimers. Though, signalling through gp130/IL-12R β 2 heterodimers is thought to be required for maximal immune suppression (Collison et al. 2012). Furthermore, in human lung cell cancer cell lines, IL-35 is thought to require IL-12R β 2 for signal transduction resulting in mesenchymal-epithelial transition (MET) (Lee et al. 2018).

Downstream of the receptor, IL-35 is transduced using the Janus kinase/signal transducer and activator of transcription (JAK-STAT) signalling pathway. STAT1/STAT4 dimers are used T cells, and STAT1/STAT3 in B cells, to promote transcription resulting in immune suppression (**Figure 3.1**) (Collison et al. 2012; Wang et al. 2014). Alternatively, lung cancer cell lines were shown to use the JAK2-STAT6-Gata3 axis to facilitate metastatic colonisation (Lee et al. 2018). Importantly, IL-35 signal transduction has been shown to induce endogenous IL-35 expression in

T cells and some cancer cell lines (Collison et al. 2012; Wetzel et al. 2021). Therefore, it is possible that IL-35 expression may be accumulated by positive feedback in the HNSCC TME.

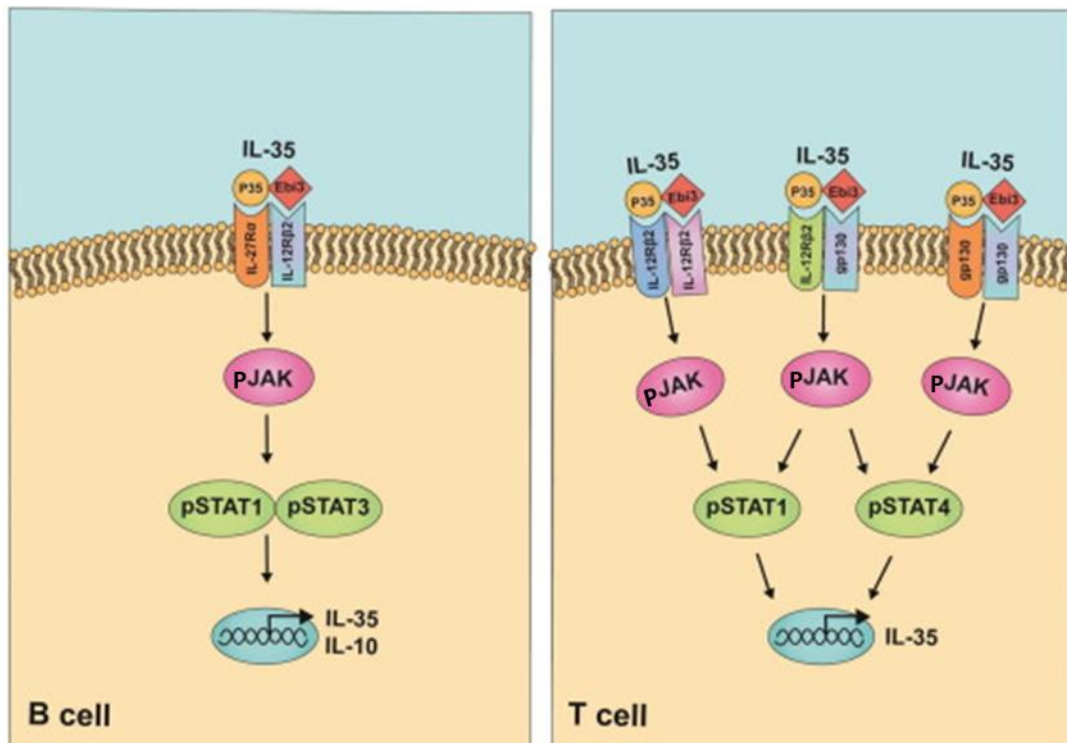


Figure 3.1 Interleukin 35 (IL-35) signalling in T and B cells.

Adapted from (Choi and Egwuagu 2021).

3.1.3 IL-35 in HNSCC

Research into the role of IL-35 in HNSCC is limited. In-vivo data has suggested that IL-35 is expressed in some HNSCCs (Wang et al. 2013; Zhang et al. 2015; Wu et al. 2017). However, there is a gap in the literature pertaining to its expression in tumour cells, and how this expression is regulated by inflammation in the TME. The purpose of this Chapter was to fill this gap by investigating whether inflammatory cytokines upregulate IL-35 expression in HNSCC cell lines.

Preliminary studies in Dr Xiaoqing Wei's laboratory group found that stimulation of HNSCC cells with IFN γ was able to cause an increase in gene expression of p35 expression. Furthermore, TNF α stimulation upregulated EBI3 expression. Addition of both IFN γ and TNF α culminated in overexpression of EBI3 and p35, indicating that IL-35 expression had been induced. As previous reports had shown that IL-35

concentrations increase with disease progression in several cancers (Nicholl et al. 2014; Larousserie et al. 2019; Gu et al. 2021; Zhang et al. 2021), and that IL-35 may be accumulated in producing cells by positive feedback (Collison et al. 2012; Wetzel et al. 2021), it is possible that in immunologically escaped tumours, tumour cell expression may also be regulated by immunosuppressive signals in the TME, including IL-35 itself.

Based on these findings, the following Chapter contributes to the research area by hypothesising the following: immune cells in the inflamed HNSCC TME produce pro-inflammatory cytokines including IFN γ and TNF α . These cytokines stimulate tumour cells, causing the upregulation of EB13 and p35 expression, and their association as the immunosuppressive IL-35 cytokine. Expression may also be increased by transduction of immunosuppressive signals including IL-35 produced in the TME. To obtain evidence supporting this hypothesis, the following aims and objectives were devised.

3.1.4 Aims and Objectives

- Evaluate whether stimulation with pro-inflammatory cytokines promotes the upregulation of IL-35 expression in HNSCC cell lines.
 - Using RT-qPCR, assess whether IFN γ and TNF α alone, or in combination, elevates EB13 and p35 gene expression in HNSCC cell lines using RT-qPCR.
 - Confirm EB13 and p35 upregulation is associated with IL-35 expression by assessing changes in gene expression of alternative IL-12 chains in response to pro-inflammatory cytokine stimulation.
 - Confirm EB13, p35 and IL-35 protein production in stimulated HNSCC cell lines.
- Evaluate IL-35 upregulation in response to anti-inflammatory cytokine stimulation.
 - Assess whether EB13 and p35 gene expression are elevated in response to stimulation with IL-10 and IL-35, alone or in combination.

This research has important implications as it may reveal a novel immunoediting mechanism used in HNSCC. If tumour cells respond to pro-inflammatory cytokines by increasing IL-35, which may also be elevated by exogenous IL-35 signal transduction, accumulated IL-35 in the TME could suppress anti-tumour immunity and may contribute to resistance to immunotherapies. This may implicate IL-35 as a biomarker of disease, and a potential target for use as an adjuvant to improve responses to immunotherapies.

3.2 Chapter Methods

In this Chapter, several general methods were used that are explained in detail in Chapter 2. Here, information relevant to chapter experiments are given. For detailed methods of the following assays, refer to the sections noted in parentheses. To detect changes in gene expression, RT-qPCR was used (**Section 2.3.2**). To detect protein expression, ELISAs (**Section 2.3.5**), SDS-PAGE/Western Blotting (**Section 2.3.3**), immunoprecipitation and co-immunoprecipitation (**Section 2.3.4**) techniques were performed.

3.2.1 Evaluation of the effects of proinflammatory cytokines on IL-35 expression in stimulated HNSCC cell lines

3.2.1.1 *Evaluation of IL-35 gene upregulation in response to stimulation with pro-inflammatory cytokines*

FaDu and H357 cell lines were used as HNSCC models. For 6 h stimulation studies with increasing doses of IFN γ and TNF α stimulation, FaDu cells were seeded at 2×10^5 cells/mL in 24-well plates. As they are larger, H357 cells were seeded at 0.5×10^5 cells/mL. For 48 h time-course studies, FaDu cells were seeded at 0.5×10^5 cells/mL in 12-well plates to prevent cells from reaching confluency. Seeded cell lines were then incubated overnight at 37 °C.

It was first assessed whether IFN γ , TNF α or both increased IL-35 (EBI3 and p35) gene expression in a dose-dependent manner. FaDu and H357 cells were treated for 6 h with 0 ng/mL (culture medium only), 1 ng/mL, 10 ng/mL, or 100 ng/mL of each cytokine alone or in combination. These conditions were selected as effects were seen using 100 ng/mL for 6 h in previous experiments in our laboratory. Next, to evaluate changes in gene expression over time, FaDu cells were treated with culture medium (mock-

treatment), or 100 ng/mL of each cytokine alone, or in combination (determined to induce changes in preliminary studies). Cells were incubated for 0 h, 6 h, 24 h or 48 h as previous studies showed variance in gene expression between these times (Maaser et al. 2004), and to assess early and late changes in gene expression. As FaDu cells were the main cell line used in this project, H357 cells were omitted from time-course analyses to limit costs.

Following stimulation, changes in gene expression of IL-35 (EBI3 and p35) were analysed by RT-qPCR. RNA was extracted from cultured cell lysates using spin columns. M-MLV reverse transcriptase was used to convert 1 µg of RNA per sample into cDNA. 8 ng of cDNA per sample was mixed with PowerUp SYBR green mastermix, along with primers for β-Actin (internal reference gene), EBI3, or p35 (forward and reverse primer sequences shown in **Table 2.2**). Primers were amplified on a QuantStudio 12K Flex thermocycler (conditions described in **Section 2.3.2.5**. All qPCR samples in this Chapter were loaded in triplicate. Sample number (n=3).

For data analysis – to obtain an estimation of basal gene expression for all genes studied in this Chapter, mean CT values obtained for the reference gene β-Actin in untreated cells, were divided by mean CT values for each target gene in untreated cells, and multiplied by 100. Basal gene expression in each cell line was then represented in bar charts as a percentage of β-Actin expression. To determine if cytokine treatments increased gene expression of target genes relative to untreated cells, output data was first normalised to the internal control reference gene. Increases in target gene expression were then represented in graphs as mean fold changes ($2^{(-\Delta\Delta CT)}$), relative to mRNA detected in untreated cells (0 ng/mL in dose-response studies, or untreated samples at each timepoint in time-course studies). One Way ANOVA and Dunnett's post hoc test were used to evaluate if differences in mean DCTs were statistically significant.

3.2.1.2 Evaluation of changes in gene expression of alternative IL-12 chains in response to pro-inflammatory cytokine stimulation

To provide evidence that stimulation of HNSCC cell lines with IFN γ , TNF α or both, upregulated gene expression of IL-35 and not that of alternative cytokines in the IL-12 family, induced changes in mRNA expression of p19, p28 and p40 subunit chains were investigated. 8 ng of stored cDNA from samples generated in **Section 3.2.1.1**,

were mixed with primer pairs for p19, p28 or p40 (**Table 2.2**). Changes in mRNA expression of each gene were analysed by qPCR as described above (n=3) (**Section 3.2.1.1**). In instances of significant gene downregulation, negative fold changes were calculated using the following equation: $-1/\text{Fold change}$ and represented in bar charts as values below zero. One Way ANOVA and Dunnett's post hoc test were used to evaluate if differences in mean DCTs were statistically significant.

3.2.1.3 Detection of EBI3 protein

To identify increased protein expression of EBI3 in stimulated FaDu cells, many methods were used. First, 5×10^6 cells were seeded into 6 well plates in 5 mL culture medium per well and incubated overnight. Dead cells were removed by replacing the culture medium. To create test samples, based on RT-qPCR data and to allow sufficient time for stable protein production, cells were treated with culture medium (untreated control), or culture medium containing IFN γ and TNF α (100 ng/mL), and incubated for 6 h, 24 h, 48 h or 72 h. 3.0 $\mu\text{g/mL}$ Brefeldin A was added 5 h before the end of each treatment to minimise protein secretion. After each timepoint had elapsed, cells were lysed using 200 μL of RIPA buffer. 20 μg of total protein per sample was loaded onto SDS-PAGE gels. 500 ng of total protein from transfected FaDu cells that overexpress IL-35 (FaDu-IL-35, generated in Chapter 4) was also loaded as a positive control. EBI3 protein was detected by Western Blotting using the following antibodies:- mouse monoclonal anti-EBI3 (Biolegend, 1 $\mu\text{g/mL}$) and rabbit polyclonal anti-mouse IgG (HRP) (Abcam, 0.2 $\mu\text{g/mL}$). Antibody concentrations were optimised prior to use. Next, to help identify EBI3, the experiment was repeated with the intent of increasing the amount of protein available for detection. Protein concentrations separated by SDS-PAGE were increased from 20 to 50 μg per sample. Blotted proteins were then probed for EBI3 expression using the antibody pair described.

As an alternative to Western Blotting, ELISA assays were also used to detect EBI3 secretion. FaDu cells were seeded and treated with IFN γ and TNF α as described above, with the exemption of Brefeldin A treatment. After each timepoint had elapsed, culture supernatant was collected and stored at -80°C . Upon completion of all treatments, frozen supernatants were thawed. Supernatants from transfected cell lines that overexpress IL-35 (Chapter 4) were also prepared as positive controls. To detect

expression and upregulation of secreted EB13 in supernatants, a commercial EB13 ELISA kit was used as instructed by the manufacturer (R&D Systems).

Next, as cytokine treatment may have been cytotoxic, to assist in protein detection by increasing cell viability and concentration of EB13 secreted into culture media, the following experiment was performed. 2×10^5 FaDu cells were seeded in 1 mL culture media within 24-well plates. Cells were stimulated with lower concentrations of IFN γ and TNF α (5, 10, 20, or 50 ng/mL) for 24 h, 48 h, or 72 h. Culture supernatants were collected and analysed by ELISA to detect secreted EB13.

After this, experimental parameters were changed to increase the concentration of EB13 produced from cells, and thus detectable by ELISA. 2×10^6 FaDu cells were seeded into T25 flasks and incubated until 90% confluency was reached. As IFN γ may be cytotoxic, it was omitted. As a potential inducer of EB13 in a time and concentration-dependent manner, higher concentrations and longer timepoints of TNF α stimulation were tested. After replacing medium, cells were treated with TNF α at 0 ng/mL, 100 ng/mL, 200 ng/mL or 500 ng/mL concentrations. Cells were incubated for 48 h, 72 h or 96 h. After, 5 mL of supernatant per sample was collected and frozen at -80 °C. Frozen supernatants were concentrated 10X by freeze-drying and reconstitution into 500 μ L of distilled water. Upon reconstitution, samples were immediately analysed for detection of EB13 by ELISA.

3.2.1.4 Detection of p35 protein

To detect upregulation of p35 protein in stimulated FaDu cells several approaches were used. First, as performed for EB13 detection, 5×10^5 FaDu cells were seeded into 6-well plates containing 5 mL culture medium per well and incubated overnight. FaDu cells were untreated, or stimulated with IFN γ and TNF α (100 ng/mL) for 6 h, 24 h, 48 h or 72 h. Lysates were collected in 200 μ L RIPA buffer per sample. 20 or 50 μ g of total protein per sample was loaded onto SDS-PAGE gels. 500 ng of lysate taken from FaDu-IL-35 cells (Chapter 4) was loaded as a positive control. P35 expression was analysed by Western Blotting using the following antibodies - Rabbit monoclonal anti-p35 (Abcam, 1:2000 dilution) and an HRP-conjugated goat anti-rabbit IgG secondary antibody (Abcam, 0.2 μ g/mL).

Next, experimental conditions were changed to increase p35 signal in sample lysates. 2×10^6 FaDu cells were seeded and grown in T25 flasks until 90% confluency was reached. As IFN γ may be cytotoxic at high concentrations, cells were untreated, or treated with 1 ng/mL or 10 ng/mL of IFN γ for 6 h, 12 h, 18 h, 24 h, 48 h or 72 h. Brefeldin A (3.0 μ g/mL) was added 5 h prior to cell lysis. Immunoprecipitation was used to enrich p35 before detection by Western Blotting. Lysates were collected into 500 μ L RIPA buffer as recommended by ThermoFisher Scientific. P35 was immunoprecipitated in samples via overnight incubation with 1 μ g of mouse monoclonal anti-p35 (R&D Systems) antibody, followed by overnight incubation with 50 μ L of sheep anti-mouse dynabeads. Lysate taken from FaDu-IL-35 (Chapter 4) cells were also treated as a positive control. Bound protein was eluted from beads, and the eluate analysed for precipitated p35 via Western Blotting. The following antibodies were applied:- rabbit monoclonal anti-p35 (Abcam, 1:500 dilution), HRP-conjugated goat anti-rabbit IgG secondary antibody (Abcam, 0.2 μ g/mL).

3.2.1.5 Detection of IL-35 protein

Several methods were used to detect IL-35 in stimulated FaDu cells. First, commercial human IL-35 ELISA kits were used. 1×10^6 FaDu cells were seeded into T25 flasks within 5 mL culture medium and incubated overnight. As performed for initial Western Blotting experiments to detect EBI3 and p35, cells were mock-treated by replacing medium, or stimulated with medium containing IFN γ and TNF α (100 ng/mL each) for 6 h, 24 h, 48 h or 72 h. Culture supernatant was collected and analysed for secretion of IL-35 using an ELISA kit purchased from Bio-Ocean. As the assay sensitivity had a minimum detection limit of 4 ng/mL, samples were also analysed using an alternative kit from Cusabio, which had a lower detection limit of 62.5 pg/mL. Both assays were performed as instructed by the manufacturer.

As an alternative to ELISA, co-immunoprecipitation/Western Blotting assays were also used to detect interacting EBI3 and p35 (IL-35) in concentrated lysates and supernatants. 5×10^6 FaDu cells were seeded into two T25 flasks per sample. Cells were cultured overnight and treated with 20, 50 or 100 ng/mL IFN γ and TNF α for 24 h or 48 h. A lower range of timepoints was used as proteins in each sample were concentrated, and due to limitations in available SDS-PAGE gel wells. Increasing cytokine concentrations were used to detect dose-dependent changes in protein

expression. Brefeldin A was added to the first set of T25 flasks to increase signal in lysates, and omitted from the remaining set to enable secretion into culture supernatant. To prepare lysate samples, cells were lysed in 1 mL RIPA and each sample divided into two 500 μ L aliquots (for separate detection of EBI3 and p35). To prepare supernatant samples, 5 mL was collected from cultured cells and frozen at -80°C , before concentrating 5X via freeze-drying and reconstitution in 1 mL ddH₂O. Each sample was divided into two 500 μ L aliquots for separate detection of EBI3 and p35. To perform co-immunoprecipitation, p35 was immunoprecipitated in all samples by adding 4 μ g of anti-p35 (R&D Systems) as described above. 500 μ L of lysate or supernatant taken from FaDu-IL-35 cells (Chapter 4) were used as positive controls. IgG controls, where a control sample was treated with anti-mouse dynabeads, but no antibody, were analysed as a negative control to assess antibody cross-reactivity (explained in detail in **Section 2.3.4.1**). To confirm p35 precipitation, Western Blotting was performed using an anti-p35 (Abcam, 1:2000) antibody paired with a goat anti-rabbit IgG secondary antibody (Abcam, 0.2 μ g). To detect co-immunoprecipitated EBI3, Western Blotting was performed using anti-EBI3 antibody (1 μ g/mL) and a goat anti-mouse IgG2b heavy chain (HRP) (1:5000) secondary antibody. The secondary antibody used was intended to prevent masking of EBI3 bands following detection of the IgG light chain from eluted anti-p35.

The experiment was next optimised to increase IL-35 gene expression and assay sensitivity. FaDu cells were seeded and grown to 90% confluence in pairs of T25 flasks as described above. Treatment parameters were adjusted to reduce cytotoxicity from IFN γ , and to maximise each cytokine's induction of EBI3 or p35 (based on RT-qPCR data). Cytokines were added at staggered timepoints. Cells were treated with TNF α (200 ng/mL or 500 ng/mL) for a total of 96 h to promote accumulation of EBI3. IFN γ (1 ng/mL or 10 ng/mL) was added in combination with, or 24 h, 48 h or 72 h after addition of TNF α , to induce p35 upregulation. Lysates and supernatants were collected as described above. Lysates and supernatants taken from CHO-IL-35 (Chapter 4) or FaDu-IL-35 cells (Chapter 4), were used as positive controls. Immunoprecipitation was performed using a lower amount of anti-p35 (1.5 μ g) to prevent saturation of dynabeads by unbound antibody. SDS-PAGE/Western Blotting was used to detect precipitated p35 within eluates. Initially, p35 was detected using a

mouse anti-p35 antibody (R&D Systems, 1 µg/mL) and the Veriblot secondary antibody (1:200 dilution). Blots were subsequently washed and probed with a higher concentration of the rabbit monoclonal anti-p35 (Abcam, 1:300) and the HRP-conjugated goat anti-rabbit IgG secondary antibody (Abcam, 0.4 µg/mL). Co-immunoprecipitated EB13 was detected using Western Blotting with a higher primary antibody concentration (anti-EB13, 1.7 µg/mL), combined with the Veriblot secondary antibody (Abcam, 1:200), used to prevent masking of EB13 bands by IgG light chains. After staining, to improve the sensitivity of signal detection, the SuperSignal™ West Atto Ultimate Sensitivity Substrate was used. This is designed to detect the capture of atto-gram concentrations of target protein. Bands generated were analysed to detect EB13 and p35 co-expression.

3.2.2 Assessment of IL-35 gene upregulation in response to anti-inflammatory cytokine stimulation

To investigate whether stimulation of HNSCC cell lines with anti-inflammatory cytokines affected IL-35 gene expression, FaDu cells were seeded at 2×10^5 cells/mL into 24-well plates. 0.5×10^5 cells/mL of H357 cells were seeded into 24-well plates. Seeded cell lines were incubated overnight. To match experimental conditions for pro-inflammatory cytokines, cells were treated with the recombinant anti-inflammatory cytokines IL-35, IL-10, alone or in combination (100 ng/mL, 6 h). RNA was extracted and converted to cDNA as previously described (**Section 2.3.2**). 8 ng of cDNA was added to β-Actin, EB13 or p35 primers. Primers were then amplified by qPCR in a thermocycler. Changes in expression of EB13 and p35 in stimulated cells were represented as fold changes relative to untreated cells (n=3). One Way ANOVA and Dunnett's post hoc test were used to evaluate if differences in mean DCTs were statistically significant.

3.2.2.1 Evaluation of IL-35 receptor expression in HNSCC cell lines

To evaluate whether the selected HNSCC cell lines were able to respond to IL-35, their expression of IL-35 receptor chains was investigated. 8 ng of cDNA from untreated cells was added to primers for β-Actin, gp130 and IL-12Rβ2, and amplified by qPCR (n=3). Basal gene expression was analysed as described above (**Section 3.2.1.1**), and expressed as a percentage of β-Actin-CT.

3.2.2.2 Assessment of changes in IL-35 receptor chain expression in response to pro-inflammatory cytokine stimulation

To investigate whether pro-inflammatory cytokines could increase expression of IL-35 receptor chains, cDNA generated from HNSCC cell lines treated with IFN γ , TNF α or both (**Section 3.2.1.1**), were mixed with gp130 and IL-12R β 2 primers. Primers were then amplified by qPCR. Changes in gene expression in a dose-dependent manner were shown as fold changes relative to untreated cells (0 ng/mL). Changes occurring at increasing timepoints were represented as fold changes relative to untreated cells at each timepoint. (n=3). One Way ANOVA and Dunnett's post hoc test were used to evaluate if differences in mean DCTs were statistically significant.

3.2.3 RT-qPCR optimisation - Selecting a stable reference gene, calculation of primer qPCR efficiencies and RNA integrity

To optimise the qPCR studies performed in this Chapter, the most stable reference gene under the conditions used, was selected for FaDu and H357 cells. To determine this, cDNA taken from FaDu and H357 cells treated with IFN γ and TNF α , or IL-35 and IL-10, were mixed with primers for three commonly used housekeeping genes. Primers were then amplified by qPCR. CT values were assessed using the ThermoFisher Connect portal and the qBase+ analysis software tool. The most stable housekeeping gene across the tested conditions was selected for FaDu and H357 studies. Data is shown in **Supplementary Data 2**. Detailed methods are given in Chapter 2 (**Section 2.3.2.8**).

Amplification factors and qPCR efficiencies were calculated for primers used in this chapter by serial dilution of selected RNA samples, followed by amplification of each primer (**Section 2.3.2.9**). Results were calculated from the slope of generated standard curves and are shown in **Supplementary Data 3**. To assess RNA integrity, RNA samples generated in this Chapter were selected to cover a range of test conditions. 4 μ L per sample was analysed using a Bioanalyser to verify maintenance of RNA integrity. All tested samples yielded a score of 9 or above (**Supplementary Data 1**).

3.3 Results

3.3.1 Evaluation of IL-35 upregulation in response to stimulation with pro-inflammatory cytokines

It was hypothesised that inflammation induces IL-35 expression in stimulated HNSCC cells. During an anti-tumour response, immune cells produce the pro-inflammatory cytokines IFN γ and TNF α . Preliminary data showed that IFN γ can induce p35 gene expression, and TNF α can induce EBI3 expression in stimulated FaDu cell lines. Stimulation with both cytokines increased gene expression of EBI3 and p35. To explore this further, the first Chapter aim was to evaluate the effects of the pro-inflammatory cytokines IFN γ and TNF α , alone or in combination, on expression of EBI3, p35 and IL-35 in multiple HNSCC cell lines.

3.3.1.1 Effects of IFN γ on EBI3 and p35 gene expression in HNSCC cell lines

The first objective was to investigate whether IFN γ stimulation can increase IL-35 gene expression by elevating that of both EBI3 and p35 in stimulated HNSCC cell lines. FaDu cells were shown to express EBI3 and p35 mRNA at low levels when unstimulated (**Supplementary data 4**). RT-qPCR data in **Figure 3.2A and B** shows that IFN γ stimulation significantly increased p35 gene expression. Stimulation for 6 h with 1 ng/mL IFN γ was sufficient to significantly increase p35 to levels 12-fold higher than in untreated cells ($p < 0.01$) (**Figure 3.2A**). Raising the applied dose did not correlate with further increases in expression, with similar levels detected across all tested concentrations (**Figure 3.2A**).

When assessing changes over time, data indicated that IFN γ stimulation induced p35 upregulation in FaDu cells as an early response. Relative to untreated cells, significant increases in p35 were highest after 6 h of treatment (13-fold, $p < 0.05$), reduced slightly after 24 h (9-fold, < 0.05) and had returned to baseline after 48 h (**Figure 3.2B**). IFN γ stimulation did not significantly increase gene expression of EBI3. Titrating the dose from 1 to 100 ng/mL (6 h treatment) did not correlate with elevations in EBI3 expression (**Figure 3.2A**). However, prolonged exposure to IFN γ did appear to increase EBI3 expression in a time-dependent manner, with the highest upregulation observed after 48 h (4-fold), though this was not statistically significant (**Figure 3.2B**).

Thus, the data suggested that IFN γ alone may not increase IL-35 gene expression in hypopharyngeal FaDu cells, as it increased p35 expression, but not that of EBI3.

When viewed under the microscope, reduced cell numbers and appearance of cell debris were present following stimulation of FaDu cells with IFN γ at increasing doses and times (**data not shown**). It is therefore possible that high concentrations and/or prolonged exposure to IFN γ was cytotoxic to hypopharyngeal carcinoma cells.

In unstimulated H357 cells, p35 is expressed at low levels. EBI3 is expressed also, but at higher levels than in FaDu cells (**Supplementary Data 4**). As shown in FaDu cells, IFN γ stimulation significantly upregulated p35 expression (**Figure 3.2C**). 1 ng/mL for 6 h was sufficient to induce a 4-fold increase ($p < 0.05$). Increases did not correlate with dosage applied, as similar magnitudes were observed at all tested concentrations. Similar to FaDu cells, IFN γ did not induce upregulation of EBI3 in H357 cells, regardless of increasing concentrations (**Figure 3.2C**). Therefore, data from both cell lines showed that stimulation with IFN γ may upregulate p35 in HNSCC cells, but may be insufficient to increase IL-35, as it did not significantly raise EBI3 expression.

3.3.1.2 Effects of TNF α on EBI3 and p35 gene expression in HNSCC cell lines

It was next investigated whether TNF α could stimulate upregulation of EBI3 and p35. RT-qPCR data acquired is shown in **Figure 3.3**. In FaDu cells, TNF α stimulation significantly increased EBI3 expression in positive correlation with time and dose applied. 1 ng/mL for 6 h was enough to cause a 10-fold increase ($p < 0.001$) (**Figure 3.3A**). Increasing the dose correlated with elevated expression, reaching levels 40-fold higher than untreated cells when 100 ng/mL was added ($p < 0.0001$). Increasing the duration of stimulation raised gene expression from 42-fold increases after 6 h ($p < 0.0001$), to 80-fold higher after 48 h ($p < 0.01$) (**Figure 3.3B**). TNF α did not increase p35 expression in FaDu cells regardless of increasing concentrations or time under stimulation (**Figure 3.3A, Figure 3.3B**). In H357 cells, TNF α stimulation did not affect gene expression of EBI3 or p35 (**Figure 3.3C**). The data therefore revealed that TNF α stimulation may induce gene upregulation of EBI3 in hypopharyngeal carcinoma cells, but not that of p35, and by extension, IL-35. Furthermore, TNF α stimulation may not affect EBI3 or p35 expression in oral carcinoma cells.

3.3.1.3 *Effects of IFN γ and TNF α on EBI3 and p35 gene expression in HNSCC cell lines*

As IFN γ upregulated p35, and TNF α EBI3, it was next evaluated whether combined stimulation with both cytokines could induce IL-35 upregulation in stimulated HNSCC cells. In treated FaDu cells, 1 ng/mL treatment for 6 h was sufficient to significantly increase expression of both EBI3 and p35. P35 upregulation was highest after a 6 h stimulation with 1 ng/mL of both cytokines (10-fold, $p < 0.001$), a magnitude which was maintained across all tested concentrations (**Figure 3.4A**). Similar to IFN γ alone, when testing changes over time, double stimulation induced significant increases in p35 after 6 h (11-fold, $p < 0.05$) which peaked after 24 h (14-fold, $p < 0.01$) and returned to baseline by 48 h. Similar to TNF α treatment, double stimulation significantly increased EBI3 in a dose-dependent manner, with the highest elevation observed after use of 100 ng/mL (34-fold, $p < 0.0001$) (**Figure 3.4A**). Increases also correlated with time under stimulation, ranging from 54-fold after 6 h ($p < 0.0001$) to 268-fold after 48 h ($p < 0.01$) (**Figure 3.4B**).

In H357 cells, double stimulation also increased p35 and EBI3 expression. P35 was significantly increased after stimulation with 1 ng/mL of both cytokines (4-fold, $p < 0.05$), a magnitude which was maintained with increasing doses of both cytokines (**Figure 3.4C**). Double stimulation caused a minor increase in EBI3 expression at 100 ng/mL which was statistically significant (1.9-fold, $p < 0.05$) (**Figure 3.4C**). Therefore, the data suggested that combined stimulation with IFN γ and TNF α in the TME may induce an adaptive response whereby IL-35 genes are significantly upregulated in stimulated hypopharyngeal and oral carcinoma cells.

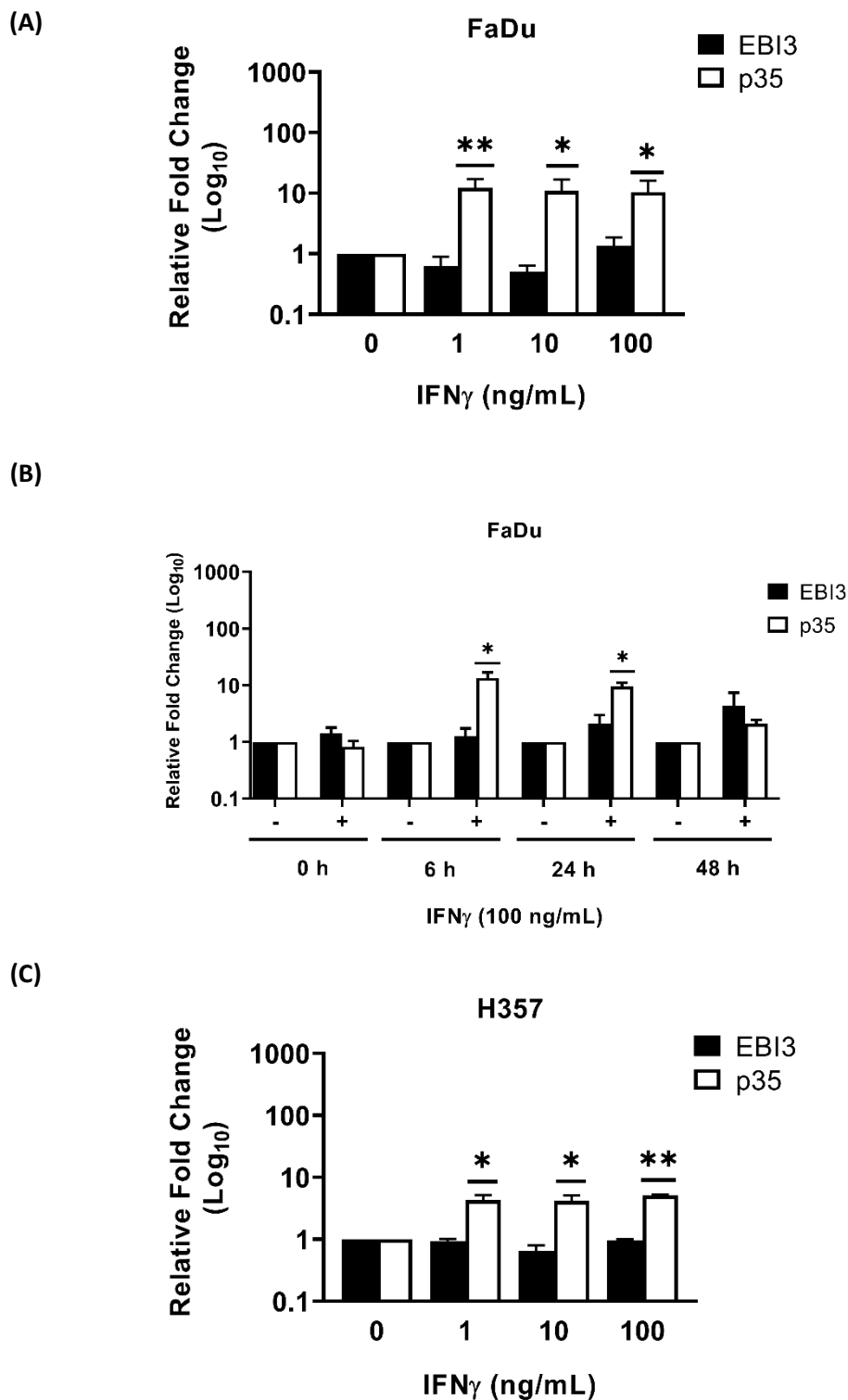
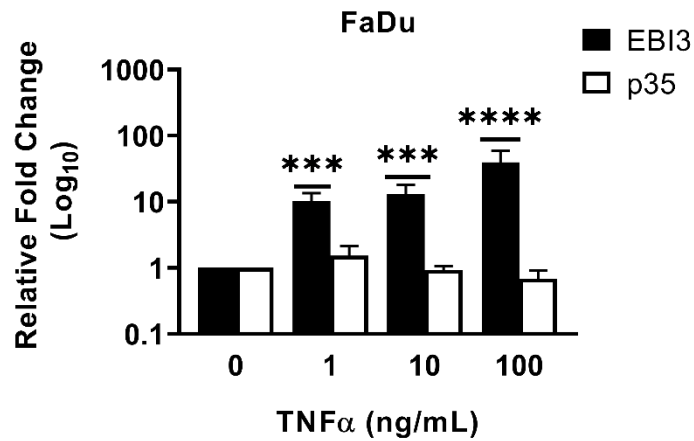
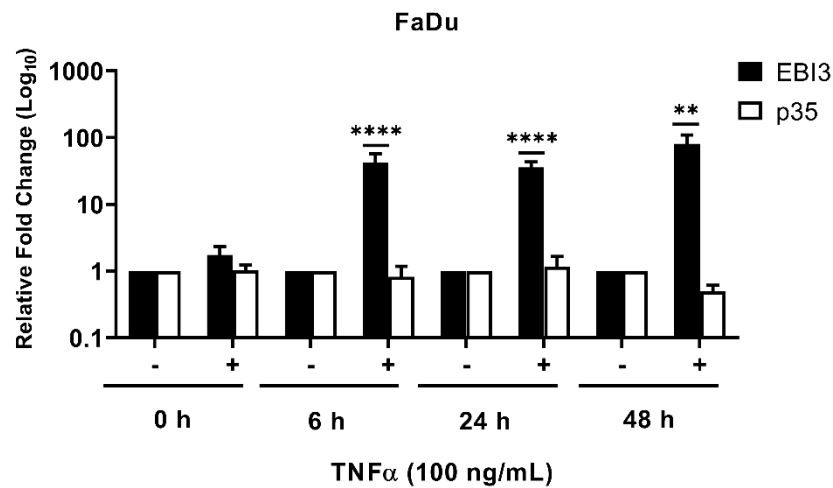


Figure 3.2 IFN_γ increases gene expression of p35 but not EBI3 in stimulated HNSCC cell lines. RT-qPCR data showing changes in gene expression of EBI3 and p35 in FaDu cells stimulated with IFN_γ (1, 10 or 100 ng/mL, 6h) (A), or 100 ng/mL for 6, 24 or 48 h (B). Data from H357 cells treated with IFN_γ (1, 10 or 100 ng/mL, 6 h) (C) are also shown. Fold changes shown are relative to untreated cells at each timepoint. Data represents mean + SEM. (n=3). Statistical analyses performed on DCT values using One Way ANOVA and Dunnett's test. Significance measured by comparing mean DCT from each treatment group to that in untreated cells. * = p < 0.05, ** = p < 0.01.

(A)



(B)



(C)

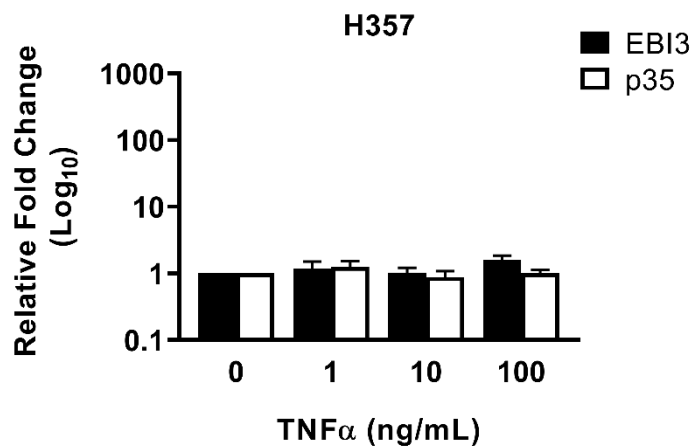


Figure 3.3 TNF α increases gene expression of EB13 in stimulated FaDu cells. RT-qPCR data showing changes in gene expression of EB13 and p35 in FaDu cells stimulated for 6 h with TNF α (1, 10 or 100 ng/mL) (A), or 100 ng/mL for 6, 24 or 48 h (B). Data from H357 cells treated for 6 h with TNF α (1, 10 or 100 ng/mL) (C) are also shown. Fold changes shown are relative to untreated cells at each timepoint. Data represents mean + SEM. (n=3). Statistical analyses performed on DCT values using One Way ANOVA and Dunnett's test. Significance measured by comparing mean DCT from each treatment group to that in untreated cells. ** = p < 0.01, *** = p < 0.001, **** = p < 0.0001.

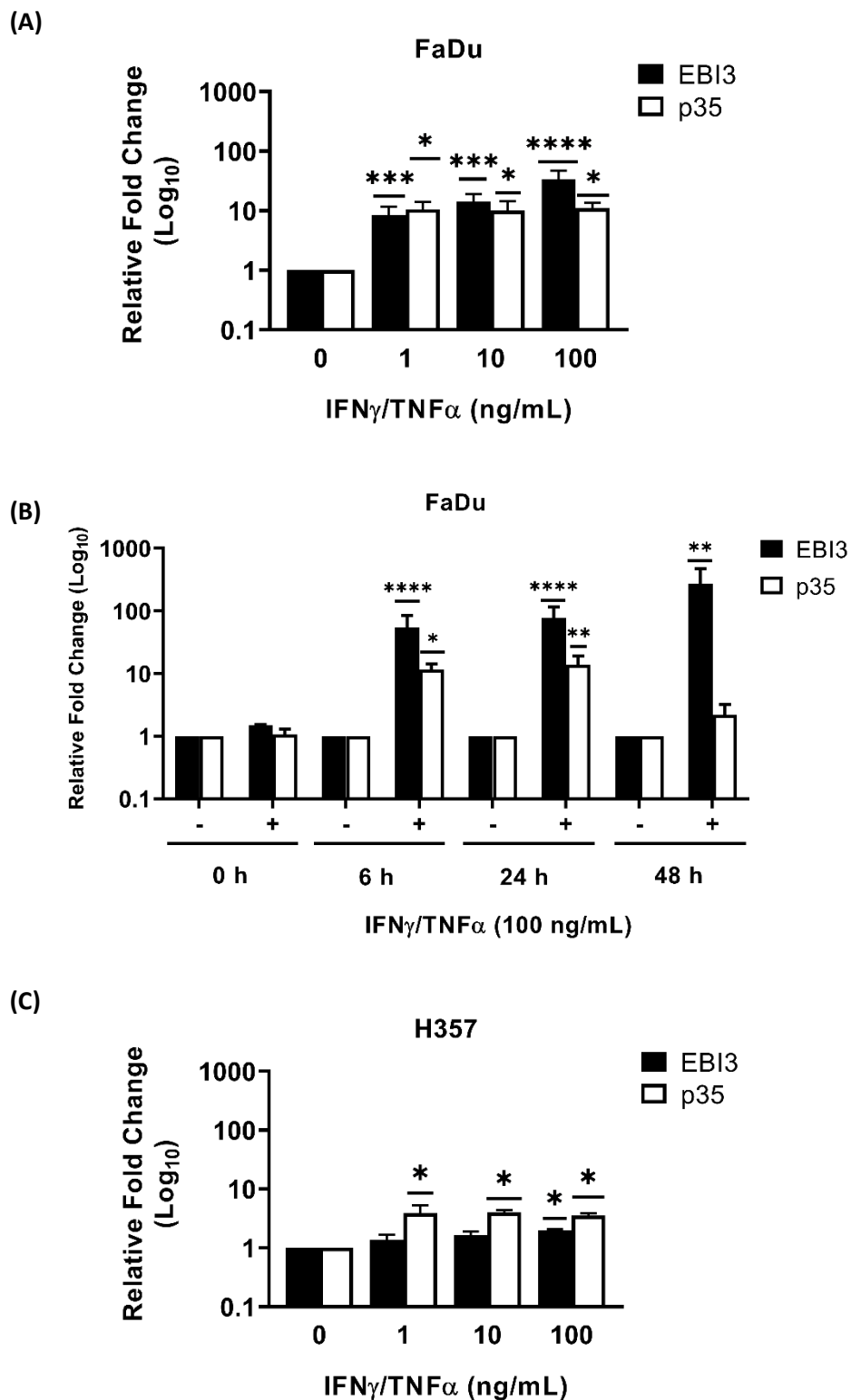


Figure 3.4 Stimulation with IFN γ and TNF α increases gene expression of EBI3 and p35 in FaDu cells. RT-qPCR data showing changes in gene expression of EBI3 and p35 in FaDu cells stimulated for 6 h with IFN γ +TNF α (1, 10 or 100 ng/mL) (A), or 100 ng/mL for 6, 24 or 48 h (B). Data from H357 cells treated for 6 h with IFN γ +TNF α (1, 10 or 100 ng/mL) (C) are also shown. Fold changes shown are relative to untreated cells at each timepoint. Data represents mean + SEM. (n=3). Statistical analyses performed on DCT values using One Way ANOVA and Dunnett's test. Significance measured by comparing mean DCT from each treatment group to that in untreated cells. * = p < 0.05, ** = p < 0.01, *** = p < 0.001, **** = p < 0.0001.

3.3.1.4 *Confirmation of IL-35 induction via assessment of inflammation-induced upregulation of alternative IL-12 family cytokines*

EBI3 and p35 chains associate with other subunits in the IL-12 family to form alternative cytokines. Following observations that p35 and EBI3 are upregulated by IFN γ and TNF α , it was important to assess whether these changes were associated with IL-35 upregulation, or potentially that of other cytokines. To determine this, it was investigated if stimulation of HNSCC cells with IFN γ and TNF α , alone or in combination, increased gene expression of the remaining IL-12 subunit chains (p19, p28 and p40).

The p19 chain can form the putative cytokine Interleukin 39 (IL-39) in association with EBI3 (Ecoeur et al. 2020). P19 is expressed at low mRNA levels in resting FaDu cells (**Supplementary data 4**). qPCR data depicting changes in p19 expression caused by pro-inflammatory cytokines is shown in **Figure 3.5A-C**. Treating FaDu cells with IFN γ (1 ng/mL) for 6 h did not increase p19 expression, instead causing a significant decrease (**Figure 3.5A**). Increasing the dose applied reduced the magnitude of p19 downregulation, with effects ranging from – 6-fold (1 ng/mL, $P < 0.01$) to - 3-fold (100 ng/mL IFN γ , $p < 0.01$) (**Figure 3.5A**). Prolonged exposure to IFN γ appeared to increase p19 expression, with a 3-fold increase in mRNA (relative to untreated cells) observed after 48 h of exposure, though this increase was not statistically significant (**Figure 3.5B**).

Similar to FaDu cells, p19 is expressed in resting H357 cells (**Supplementary Data 4**). IFN γ (1 ng/mL or 10 ng/mL) also significantly reduced expression after 6 h (**Figure 3.5C**). Thus, the results demonstrated that stimulation of HNSCC cell lines with IFN γ may not induce upregulation of p19, and therefore, IL-39.

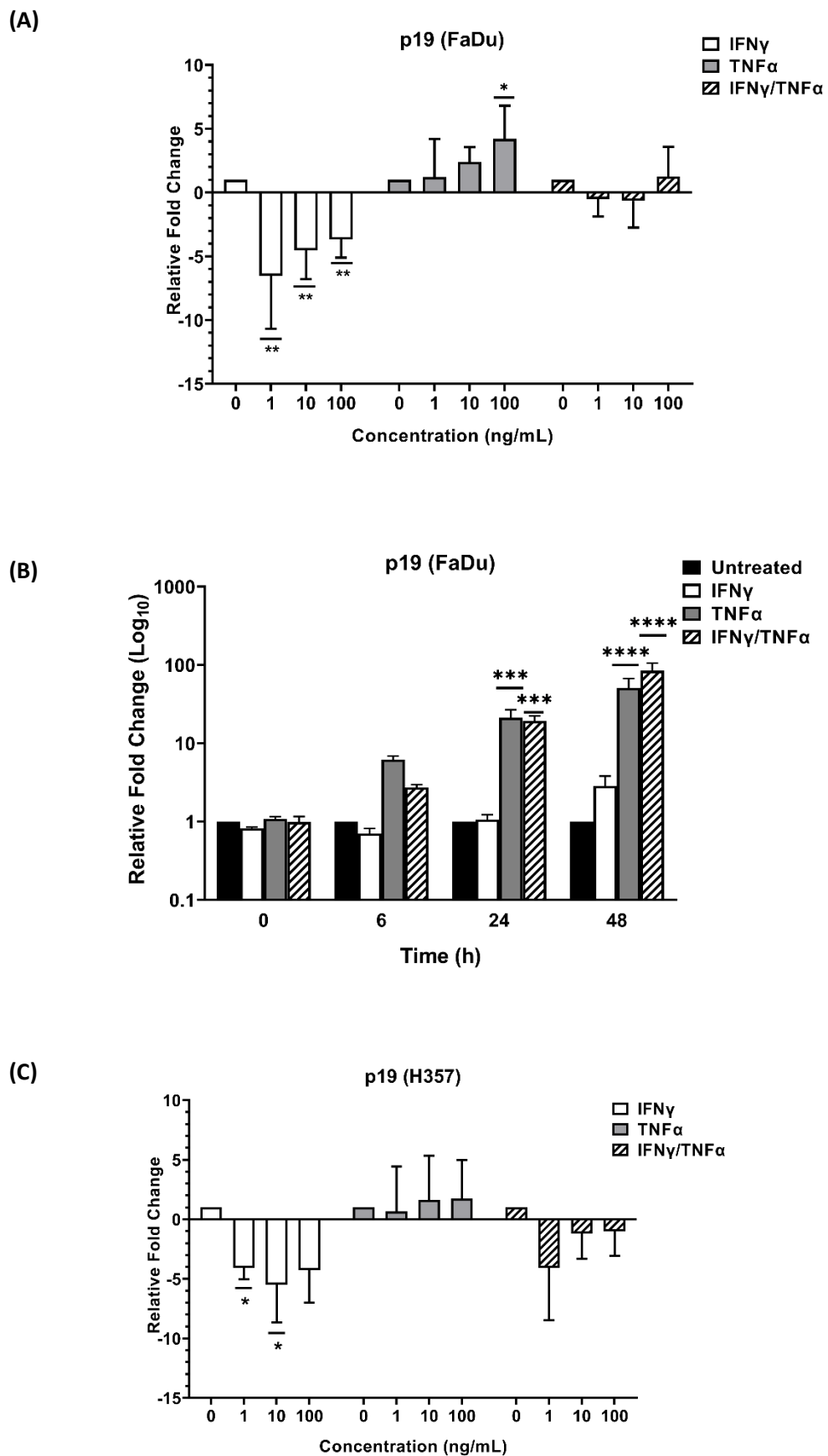
Treatment of FaDu cells with TNF α increased expression of p19 (relative to untreated cells) in a dose-dependent manner, with the highest increase (4-fold, $p < 0.05$) observed following exposure to 100 ng/mL TNF α (**Figure 3.5A**). This trend was similar to that observed with EBI3 expression (**Figure 3.2A**). Furthermore, like EBI3, p19 expression was also increased with time under stimulation, reaching a level 50-fold higher than unstimulated controls after 48 h ($p < 0.0001$) (**Figure 3.5B**, **Figure 3.2B**). As shown with EBI3, TNF α had no effect on p19 expression in H357 cells (**Figure 3.5C**, **Figure 3.2C**). The data therefore suggested that, in FaDu cells, but not H357

cells, as EBI3 and p19 expression are elevated, TNF α stimulation may induce IL-39 expression.

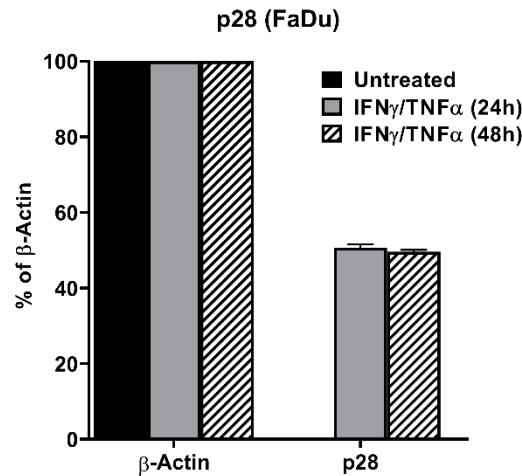
Stimulation of FaDu cells with both IFN γ and TNF α , caused a delayed but significant increase in p19 expression. After 6 h, double stimulation, at all tested concentrations, did not increase p19 expression beyond that in untreated cells FaDu cells (**Figure 3.5A, Figure 3.5B**). In a similar trend to TNF α treatment, p19 expression was significantly increased with prolonged exposure to both cytokines, reaching expression levels 84-fold higher than untreated cells after 48 h ($p < 0.0001$) (**Figure 3.5B**). In H357 cells, stimulation with both cytokines (6 h, 1-100 ng/mL ng/mL) did not increase p19 expression (**Figure 3.5C**). Thus, the data suggests that stimulation with IFN γ and TNF α together may result in increased p19 expression, potentially culminating in IL-39 (EBI3/p19) formation in FaDu (hypopharyngeal carcinoma) cells, but not H357 (oral carcinoma) cells, though time-course data may be required to confirm this.

P28 can associate with EBI3 to form the cytokine Interleukin-27 (IL-27) (Pflanz et al. 2002). Its gene expression could not be detected in untreated FaDu cells. IFN γ or TNF α alone had no effect on this. However, application of both cytokines enabled detection of very low levels of p28 expression after 24 h, which was maintained after 48 h (**Figure 3.5D**). In H357 cells, p28 is expressed at very low levels (**Supplementary Data 4**). IFN γ , TNF α , or stimulation with both cytokines (1-100 ng/mL), did not increase expression of p28 after 6 h (**Figure 3.5E**). The data therefore indicated that stimulation of HNSCC cells with pro-inflammatory cytokines may not significantly increase expression of p28, and thus may not induce IL-27 production.

P40 can associate with p35 to form IL-12 (Kobayashi et al. 1989). Its expression could not be detected in untreated nor treated FaDu or H357 cells (**data not shown**). Thus, the data suggested that IFN γ and/or TNF α may not induce IL-12 in these cell types.



(D)



(E)

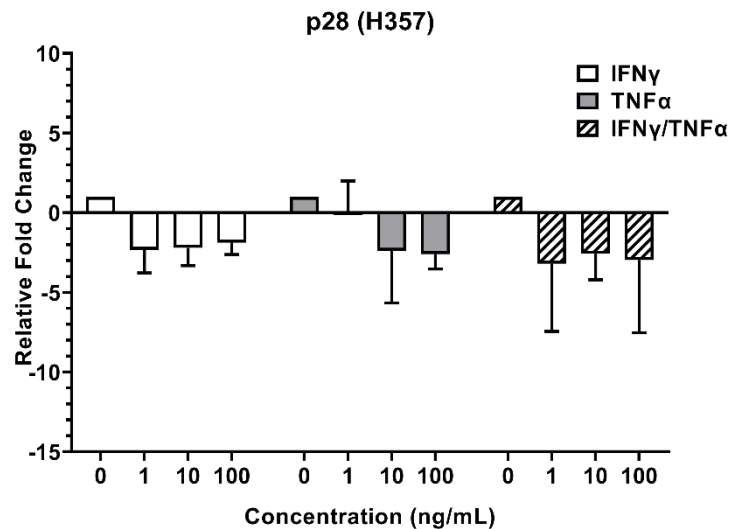


Figure 3.5 Changes in p19 and p28 expression in stimulated HNSCC cell lines. FaDu and H357 cells were treated with IFN γ and TNF α , alone or in combination (1, 10 or 100 ng/mL) for 6 h. FaDu cells were also treated with 100 ng/mL for 6, 24 or 48 h. Changes in gene expression of p19, p28 and p40 were examined by RT-qPCR. Fold changes in p19 expression in FaDu cells with increasing concentrations of cytokine are shown in (A), and time under stimulation in (B). Changes in p19 expression in H357 cells are shown in (C). Changes in expression of p28 in FaDu cells are shown in (D) as a percentage of mean CT (+SEM) relative to β -Actin (n=3). Changes in p28 expression in H357 cells are displayed in (E). Data showing Fold changes are relative to untreated cells. Data in those bar charts represent mean + SEM. n = 3. Statistical analyses were performed on DCT values using One Way ANOVA and Dunnett's test. Significance was measured by comparing mean DCT values from each treatment group to that in untreated cells. * = p < 0.05, ** = p < 0.01, *** = p < 0.001, **** = p < 0.0001.

3.3.1.5 *Confirmation of EBI3, p35 and IL-35 protein production in stimulated HNSCC cell lines*

As qPCR data showed that IFN γ and TNF α can upregulate p35 and EBI3 in stimulated FaDu cells, the next objective was to confirm protein production of each subunit, and formation of the (EBI3/p35) IL-35 cytokine. First, FaDu cells were examined for upregulation of EBI3 protein in response to pro-inflammatory cytokine stimulation. Following stimulation with IFN γ and TNF α (100 ng/mL, 6 to 72 h), EBI3 protein could not be detected using ELISA or Western Blotting, either in treated or untreated cells (**data not shown**). Despite repeating the experiment and lowering the concentration of each cytokine, which may have improved cell viability, EBI3 remained undetectable by ELISA (**data not shown**). To maximise EBI3 expression, FaDu cells were subjected to high concentrations of TNF α (100 ng/ml, 200 ng/mL or 500 ng/mL), and an increased duration of time under stimulation (48-96 h). Supernatants were also concentrated by a factor of 10. Under these conditions, EBI3 protein still could not be detected in any of the test samples by ELISA (**data not shown**). Therefore, assays performed in this study failed to detect upregulation of EBI3 in FaDu cells stimulated with TNF α , or a combination of IFN γ and TNF α .

Investigations were undertaken to detect upregulation of p35 protein in stimulated FaDu cells. Similar to EBI3, p35 protein could not be detected by Western Blotting in cells stimulated with both IFN γ and TNF α (100 ng/mL, 6-72 h). To reduce cytotoxicity, FaDu cells were next stimulated with lower concentrations of IFN γ (1 or 10 ng/mL). Regardless of using immunoprecipitation to enrich p35 from lysates, it could not be detected by Western Blotting (**Supplementary Data 6**). Thus, the assays performed could not detect upregulation of p35 protein expression in FaDu cells stimulated with pro-inflammatory cytokines.

It was also evaluated whether upregulation of the IL-35 heterodimer could be detected in stimulated FaDu cells. Commercial human IL-35 ELISA kits could not detect any IL-35 in supernatants taken from untreated FaDu cells, nor those stimulated with IFN γ and TNF α (100 ng/mL, 0-72 h) (**data not shown**). A kit purchased from Bio-Ocean did not detect any signal within samples. The kit from Cusabio was demonstrated non-specificity of antibodies as it detected signal in negative controls. Therefore, as an alternative approach, co-immunoprecipitation was attempted, with the intent of

detecting interacting EBI3 and p35. Lysates and supernatants from cells stimulated with increasing doses of IFN γ and TNF α were examined. Except for control samples, EBI3 and p35 could not be detected (**Figure 3.6**). EBI3 was detected in the IgG control sample within supernatants (**Figure 3.6D**), though this was likely due to spillover from a neighbouring lane, as it is absent in lysates and as antibody chains were also detected. To create conditions that may have maximised upregulation of both p35 and EBI3 based on qPCR data, FaDu cells were treated with lower concentrations of IFN γ and higher TNF α , added at staggered timepoints. Regardless of techniques used to increase sensitivity, including concentration of samples, and application of an ECL reagent that detects attogram protein concentrations, neither EBI3 nor p35 could be detected by co-immunoprecipitation/Western Blotting. Use of the Veriblot antibody failed to facilitate detection of EBI3 or p35 in control samples (**Supplementary data 7**). Re-staining of these samples with an alternative anti-p35 antibody enabled detection of p35, but only in control samples (**Figure 3.7A and B**). Faint bands detected at around 80 kDa in cell lysate samples were deemed non-specific, as they were artifacts of non-specific binding by the Veriblot antibody (**Figure 3.7A, Supplementary data 7**). In supernatant samples, bands around 62 kDa (labelled NS) and 50 kDa, corresponded to artifacts from non-specific binding of the Veriblot antibody to the IgG heavy chain and unintended targets (**Figure 3.7B, Supplementary data 7**). Similar non-specific bands were also observed in EBI3 blots (**Figure 3.7C and D**). In summation, increases in protein expression of EBI3, p35 or IL-35, could not be detected in FaDu cells stimulated with IFN γ and/or TNF α .

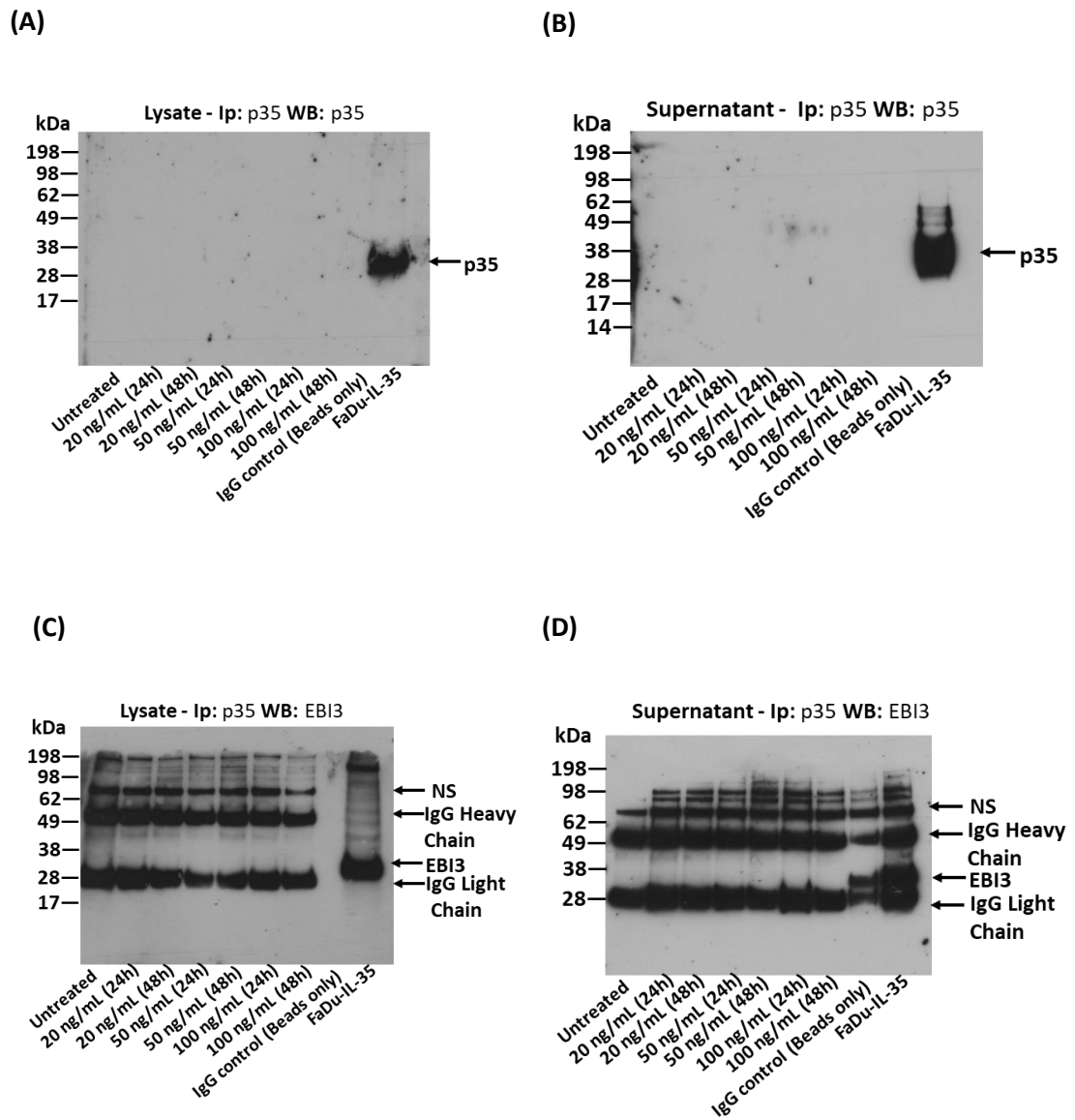
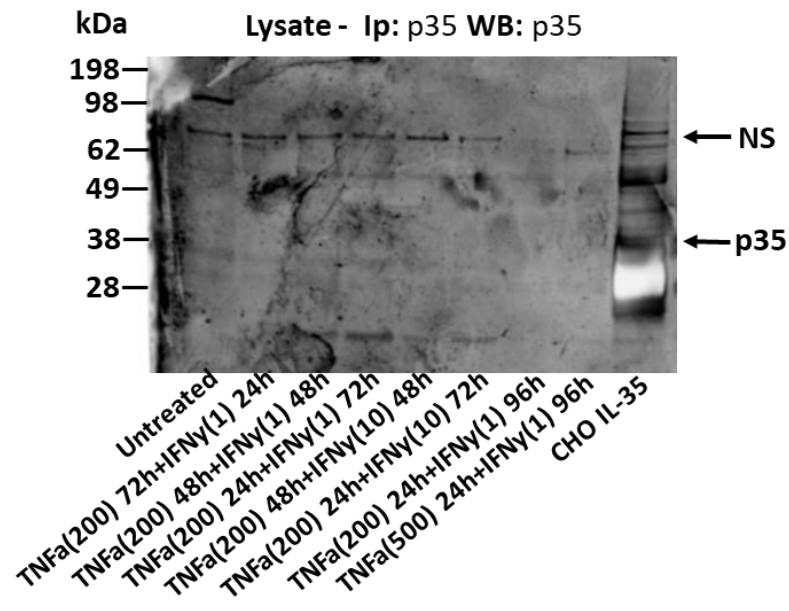
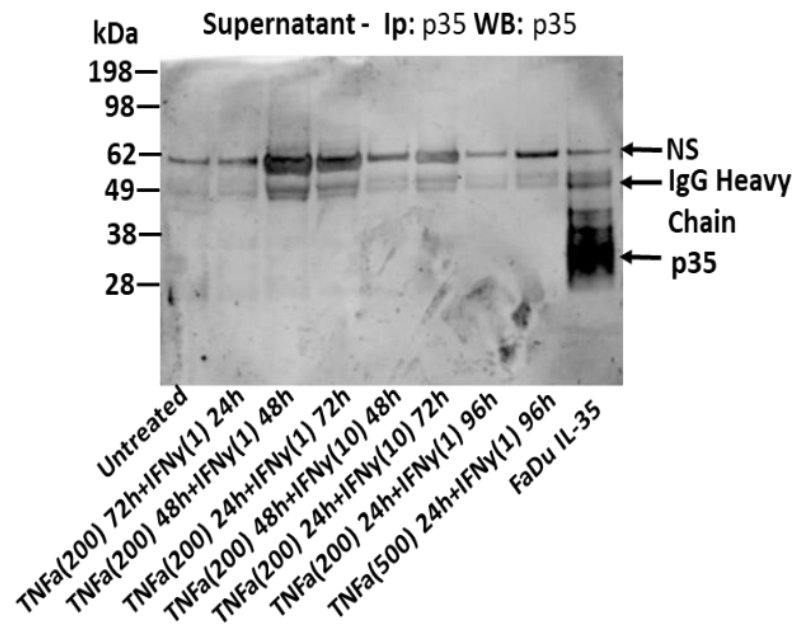


Figure 3.6 Detection of interacting EBI3 and p35 in FaDu cells stimulated with IFN γ and TNF α . FaDu cells were stimulated with IFN γ and TNF α for the concentrations and times shown. P35 was immunoprecipitated from lysates and supernatants. Western blotting was used to detect precipitated p35 (A and B) and co-immunoprecipitated EBI3 (C and D). NS; non-specific signal. Signals at approximately 28 and 50 kDa correspond to detection of the IgG light and heavy chains eluted from the anti-p35 antibody used for immunoprecipitation. (n=1).

(A)



(B)



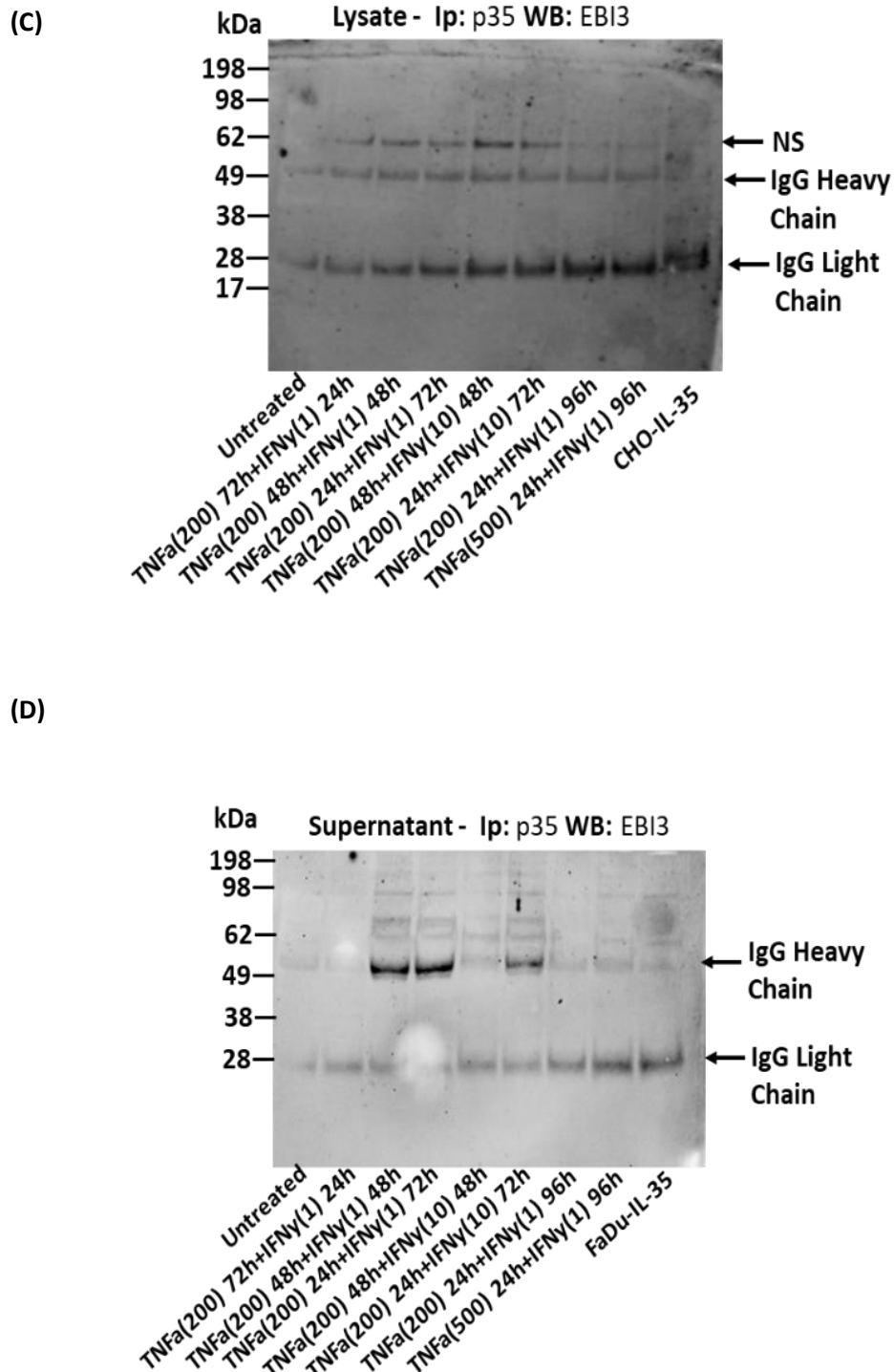


Figure 3.7 Detection of interacting EB13 and p35 in FaDu cells stimulated with IFN γ and TNF α . FaDu cells were stimulated with IFN γ and TNF α in a staggered manner using the concentrations (ng/mL) and times shown. Lysates and supernatants were concentrated. P35 was immunoprecipitated from lysates and supernatants. Western blotting was used to detect precipitated p35 (A and B) and co-immunoprecipitated EB13 (C and D) with the addition of Supersignal ECL. NS; non-specific signal. Signals at approximately 28 and 50 kDa correspond to detection of the IgG light and heavy chains eluted from the anti-p35 antibody used for immunoprecipitation. (n=1).

3.3.2 Evaluation of IL-35 upregulation in response to anti-inflammatory cytokine stimulation

The next aim was to investigate whether anti-inflammatory cytokines present in the tumour microenvironment could stimulate HNSCC cells causing upregulation of IL-35. IL-35 levels are high in immunosuppressive TMEs rich in anti-inflammatory cytokines. IL-35 has also been shown to stimulate its own gene expression in receiving cells (Collison et al. 2012; Wetzel et al. 2021). It is possible therefore, that anti-inflammatory cytokines may regulate IL-35 expression, and that exogenous IL-35 may elevate expression in tumour cells. To evaluate this, HNSCC cell lines were stimulated with IL-35 and IL-10, alone or in combination. RT-qPCR data shown in **Figure 3.8** demonstrated that neither cytokine was able to elevate gene expression of EB13 or p35 in FaDu (**Figure 3.8A**) or H357 cells (**Figure 3.8B**).

As stimulation with IL-35 had no effect on gene expression of EB13 or p35, it was investigated whether FaDu and H357 cells express the IL-35 receptor chains required to transduce the signal. RT-qPCR data shown in (**Figure 3.8C**) indicated that gp130 is expressed both in FaDu and H357 cell lines. IL-12R β 2 is expressed in FaDu cells but not in H357 cells. The data therefore suggested that when unstimulated, the tested HNSCC cell lines expressed at least one of the IL-35 receptor chains required to respond to IL-35. Stimulation with exogenous IL-35 did not result in elevation of endogenous gene expression. Furthermore, the anti-inflammatory cytokine IL-10 was unable to increase IL-35 expression in the tested HNSCC cells when added alone, or in combination with IL-35.

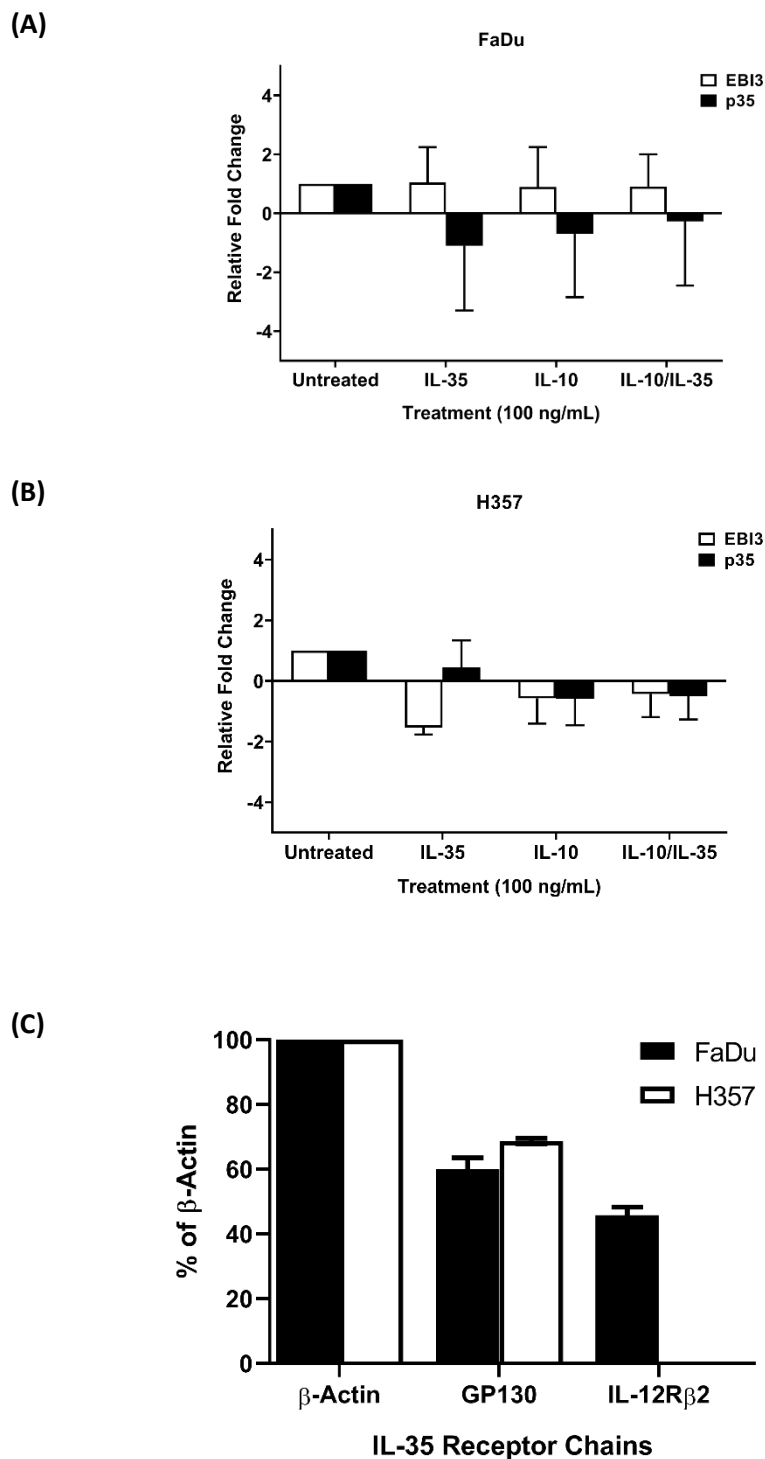


Figure 3.8 Effects of IL-10 and IL-35 stimulation on gene expression of EBI3 and p35. RT-qPCR data showing changes in EBI3 and p35 expression in FaDu (A) and H357 (B) cells treated with IL-10 and IL-35 (100 ng/mL, 6 h) alone or in combination. Fold changes shown are relative to untreated cells. Data represents mean + SEM. (n=3). Statistical analyses were performed on DCT values using One Way ANOVA and Dunnett's test. Significance was measured by comparing mean DCT from each treatment group to that in untreated cells. Untreated cells were examined for expression of the IL-35 receptor chains gp130 and IL-12R β 2 (C). Gene expression is represented as a mean percentage (+SEM) of β -Actin CT. (n=3).

3.3.3 Assessment of changes in IL-35 receptor chain expression in response to pro-inflammatory cytokine stimulation

Recombinant IL-35 had no effect on endogenous EB13 and p35 expression in resting HNSCC cell lines. These cells were also shown to express low or no IL-12R β 2 chain to help facilitate signalling. Previous studies have shown that, in several cancer cell lines, stimulation with TNF α upregulated expression of the IL-12R β 2 chain, which primed cells to respond to IL-35 signals (Lee et al. 2018). In addition, gp130/gp130 receptor signalling may only have biological roles in IL-6 signalling cascades (Adam et al. 2009; Suthaus et al. 2011). It was therefore hypothesised that, in addition to upregulating IL-35, pro-inflammatory cytokines may also induce increases in receptor chain expression. This may be necessary to facilitate transduction of autocrine and paracrine IL-35 signals. Signalling through IL-12R β 2 homodimers or gp130/IL-12R β 2 heterodimers may then result in further upregulation of endogenous IL-35 expression in HNSCC cell lines (Collison et al. 2012). To begin exploring this, the next objective was to investigate whether IFN γ , TNF α , or both, could increase expression of the IL-35 receptor chains gp130 and IL-12R β 2 in stimulated HNSCC cells.

3.3.3.1 *Effects of IFN γ on IL-12R β 2 and gp130 gene expression in HNSCC cell lines*

Relative to untreated cells, IFN γ was found to significantly increase gene expression of IL-12R β 2 and gp130 in FaDu cells. 1 ng/mL IFN γ was sufficient to increase IL-12R β 2 in FaDu cells after 6 h (12-fold, ns) (**Figure 3.9A and B**). Lower concentrations (1 and 10 ng/mL) caused maximal increases, with expression levels remaining at baseline when 100 ng/mL was applied (**Figure 3.9A**). However, when increasing the time cells were stimulated with 100 ng/mL, this positively correlated with elevations in IL-12R β 2 gene expression. Magnitudes of gene upregulation reached statistical significance after 24 h (19-fold, $p < 0.0001$) and increased further after 48 h (86-fold, $p < 0.0001$) (**Figure 3.9B**). IFN γ induced a delayed elevation in gp130 expression in FaDu cells. No increase was observed after 6 h, regardless of tested concentration (**Figure 3.9A**). When assessing effects over time, after 48 h, 100 ng/mL IFN γ caused a significantly increase in gene expression of gp130 in FaDu cells (2-fold, $p < 0.01$) (**Figure 3.9B**). Data from treated H357 cells also showed that IFN γ had no effect on

gp130 expression after 6 h (**Figure 3.9C**). It did not induce expression of IL-12R β 2, as expression remained undetectable (**data not shown**). Thus, the data demonstrated that in hypopharyngeal carcinoma cells, but not oral carcinoma cells, IFN γ may increase expression of both IL-35 chains, IL-12R β 2 and gp130.

3.3.3.2 *Effects of TNF α on IL-12R β 2 and gp130 gene expression in HNSCC cell lines*

In FaDu cells, TNF α stimulation did not increase IL-12R β 2 gene expression but did enhance that of gp130. None of the tested treatments significantly increased IL-12R β 2 expression (**Figure 3.10A and B**). Gp130 expression was not significantly increased after 6 h stimulations (1-100 ng/mL) (**Figure 3.10A**). Though, after 24 and 48 h, TNF α stimulation (100 ng/mL) increased gp130 to levels 2-fold higher than in untreated cells ($p < 0.05$) (**Figure 3.10B**). In H357 cells, TNF α stimulation did not affect gene expression of gp130 (**Figure 3.10C**), nor did it raise IL-12R β 2 expression to detectable levels (**data not shown**). The data therefore revealed that in FaDu cells, but not H357 cells, TNF α stimulation may increase gp130 gene expression, but not that of IL-12R β 2.

3.3.3.3 *Effects of IFN γ and TNF α on IL-12R β 2 and gp130 gene expression in HNSCC cell lines*

When added in combination, IFN γ and TNF α enhanced gene expression of both IL-12R β 2 and gp130 in stimulated FaDu cells. Non-significant increases were observed in IL-12R β 2 after 6 h of stimulation (**Figure 3.11A**). As with IFN γ treatment, maximal increases were observed at lower concentrations - 1 and 10 ng/mL (14-fold and 26-fold), and expression was maintained at baseline when 100 ng/mL was added (**Figure 3.11A, Figure 3.9A**). Increasing the time cells were stimulated with 100 ng/mL correlated with significant increases in IL-12R β 2 expression (**Figure 3.11B**). Previously, IFN γ was shown to cause increases ranging from 5-fold to 86-fold between 6 and 48 h of treatment (**Figure 3.9A**). Here, when both cytokines were added in combination, the effects of IFN γ may have been mitigated by TNF α , as upregulation ranged from 2-fold after 6 h, to 22-fold after 48 h ($p < 0.001$) (**Figure 3.11B**).

Combined IFN γ and TNF α stimulation may have synergistically increased gp130 expression in FaDu cells. Individually they had no significant effect after 6 h (**Figure**

3.9A, Figure 3.10A). Yet, double stimulation caused a significant 2-fold increase after 6 h ($p < 0.05$, **Figure 3.11A and B**). Extending the time cells were stimulated correlated with additional increases. $IFN\gamma$ previously caused a significant 2.5-fold increase after 48 h (**Figure 3.9B**). $TNF\alpha$ caused a significant 2-fold increase after 24 h, which was maintained after 48 h (**Figure 3.10B**). Here, double stimulation induced earlier significant increases which elevated further with time. This ranged from 2-fold after 6 h ($p < 0.05$), to 3.1-fold after 48 h ($p < 0.005$) (**Figure 3.11B**). The data therefore suggested that $IFN\gamma$ and $TNF\alpha$ may synergistically increase expression of the gp130 chain in stimulated FaDu cells.

In treated H357 cells, double stimulation for 6 h (1-100 ng/mL) had no effect on IL-12R β 2 expression as it remained undetectable (**data not shown**). It also had no effect on gp130 expression (**Figure 3.11C**). Therefore, the data supports that inflammation involving $IFN\gamma$ and $TNF\alpha$ may cause FaDu (hypopharyngeal carcinoma) cells, but not H357 (oral carcinoma) cells, to upregulate expression of the IL-35 receptor chains gp130 and IL-12R β 2. This may prime hypopharyngeal carcinoma cells to transduce IL-35 signals via IL-12R β 2 homodimers, or heterodimeric receptors, possibly resulting in endogenous IL-35 expression.

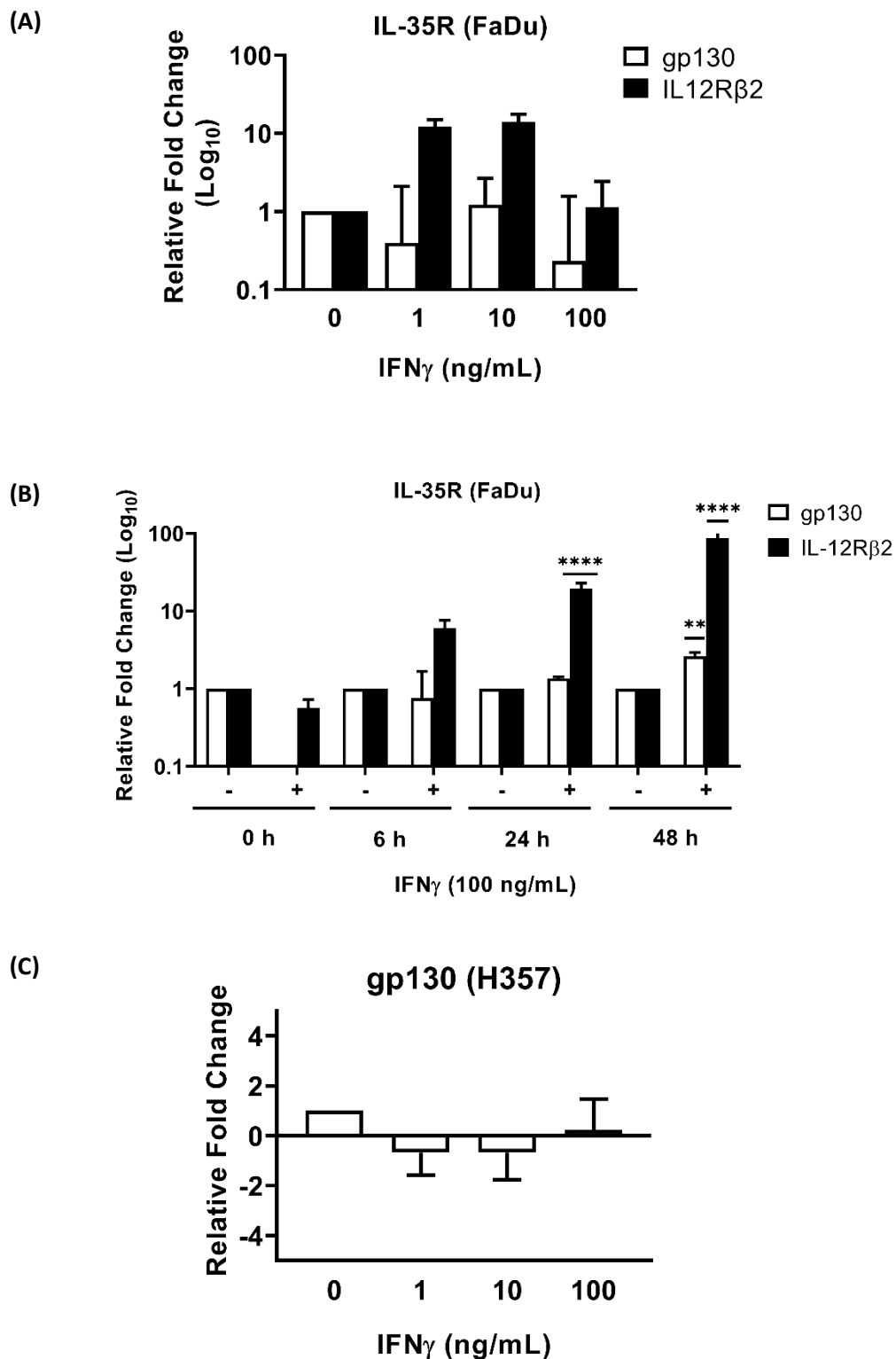


Figure 3.9 Effects of IFN γ stimulation on gp130 and IL-12R β 2 expression. RT-qPCR data showing changes in gene expression of gp130 and IL-12R β 2 in FaDu cells stimulated for 6 h with IFN γ (1, 10 or 100 ng/mL) (A), or 100 ng/mL for 6, 24 or 48 h (B). Data from H357 cells treated for 6 h with IFN γ (1, 10 or 100 ng/mL) are shown in (C). Fold changes shown are relative to untreated cells at each timepoint. Data represents mean + SEM. (n=3). Statistical analyses were performed on DCT values using One Way ANOVA and Dunnett's test. Significance was measured by comparing mean DCT from each treatment group to that in untreated cells. ** = $p < 0.01$, **** = $p < 0.0001$.

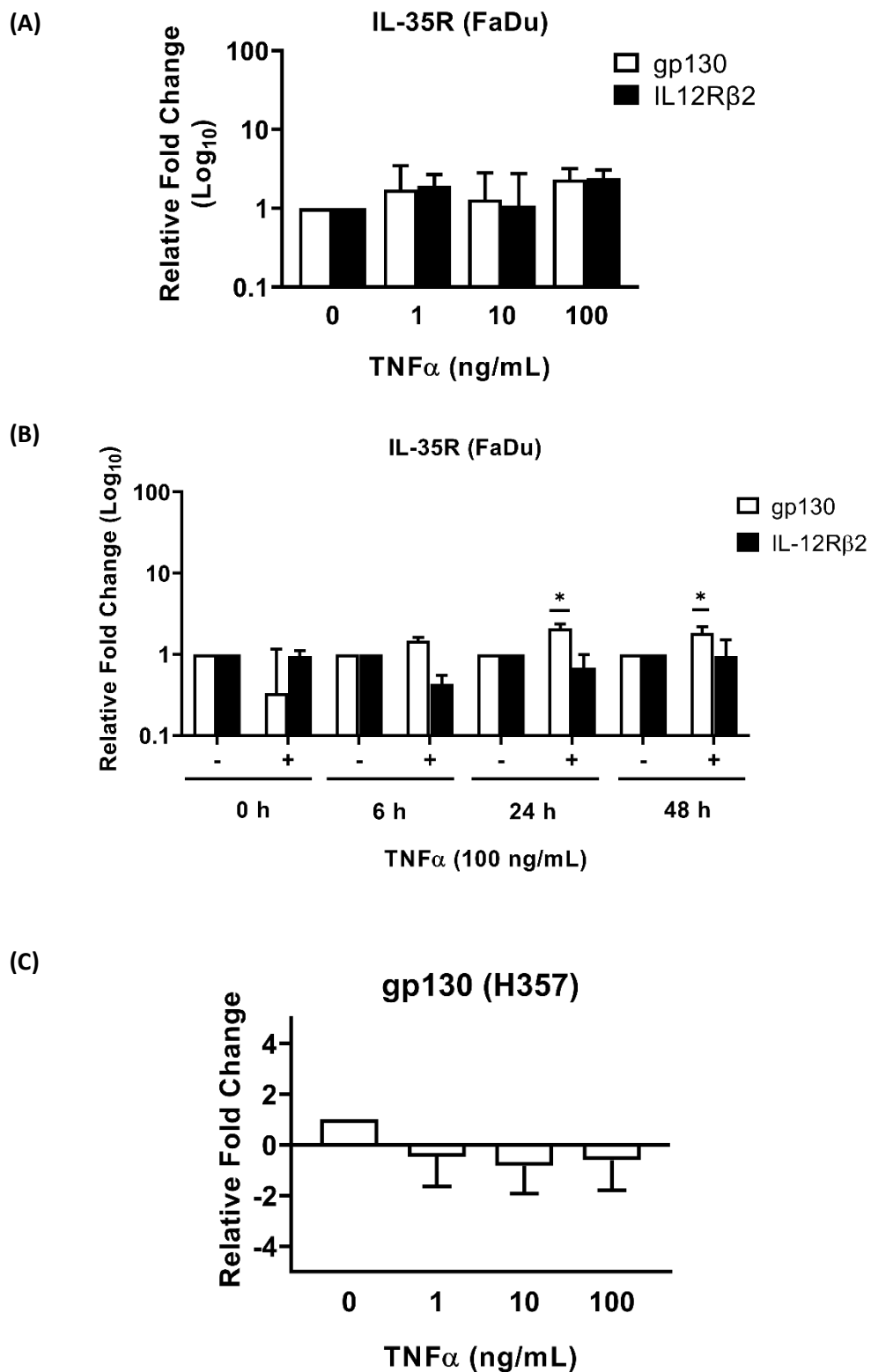


Figure 3.10 Effects of TNF α stimulation on gp130 and IL-12R β 2 expression. RT-qPCR data showing changes in gene expression of gp130 and IL-12R β 2 in FaDu cells stimulated for 6 h with TNF α (1, 10 or 100 ng/mL) (A), or 100 ng/mL for 6, 24 or 48 h (B). Data from H357 cells treated for 6 h with TNF α (1, 10 or 100 ng/mL) are shown in (C). Fold changes shown are relative to untreated cells at each timepoint. Data represents mean + SEM. (n=3). Statistical analyses were performed on DCT values using One Way ANOVA and Dunnett's test. Significance was measured by comparing mean DCT from each treatment group to that in untreated cells. * = p < 0.05.

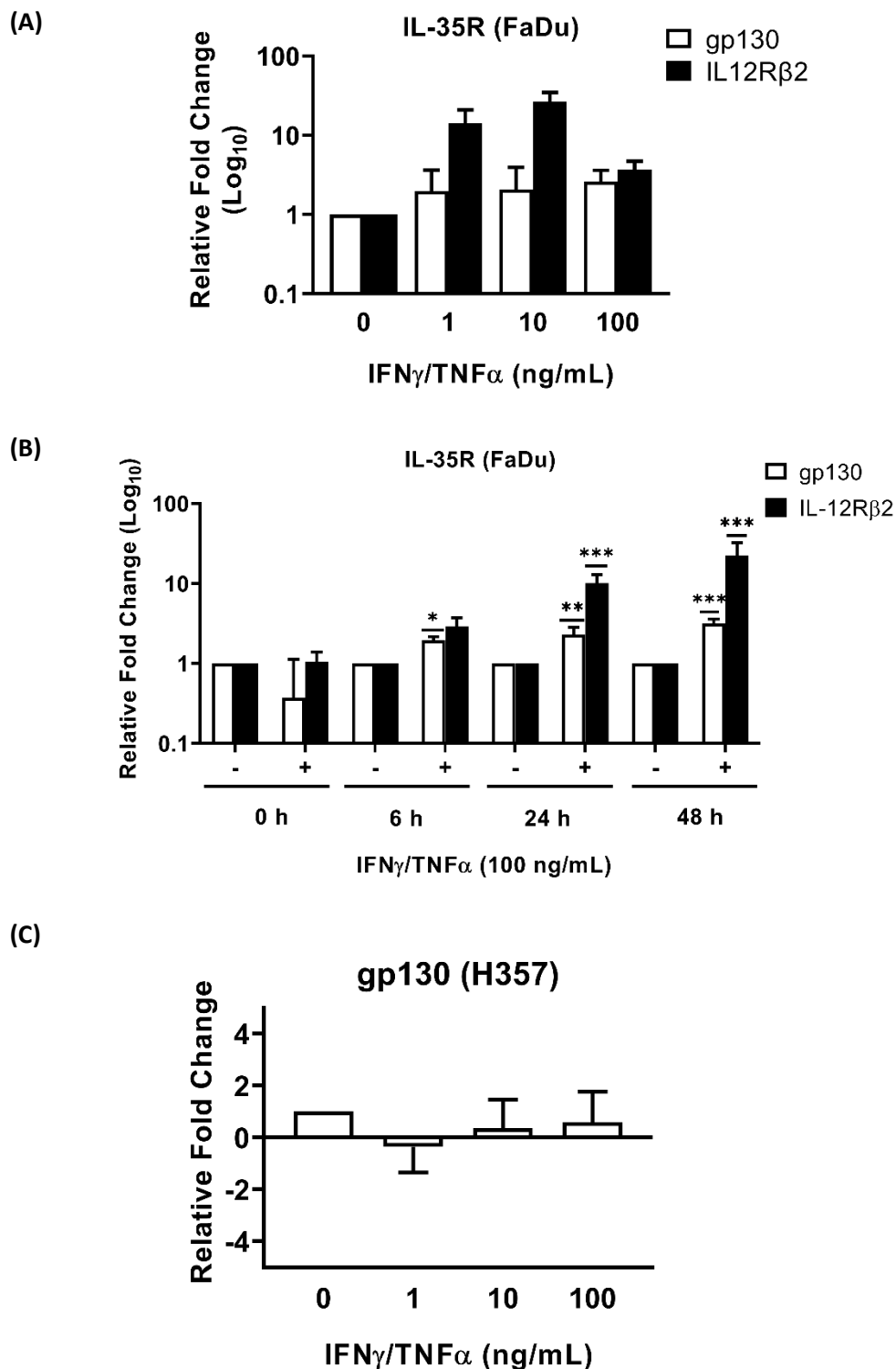


Figure 3.11 Effects of IFN γ and TNF α stimulation on gp130 and IL-12R β 2 expression. RT-qPCR data showing changes in gene expression of gp130 and IL-12R β 2 in FaDu cells stimulated for 6 h with IFN γ and TNF α (1, 10 or 100 ng/mL) (A), or 100 ng/mL for 6, 24 or 48 h (B). Data from H357 cells treated for 6 h with IFN γ and TNF α (1, 10 or 100 ng/mL) are shown in (C). Fold changes shown are relative to untreated cells at each timepoint. Data represents mean + SEM. (n=3). Statistical analyses performed on DCT values using One Way ANOVA and Dunnett's test. Significance was measured by comparing mean DCT from each treatment group to that in untreated cells. * = $p < 0.05$, ** = $p < 0.01$, **** = $p < 0.0001$.

3.4 Discussion

To improve responses to immunotherapy, there is a need to identify novel regulators of immune dysfunction in HNSCC. To date, the expression of the immunosuppressive cytokine IL-35 in tumour cells, and how this is regulated by the inflammatory nature of the TME, has not been well studied. In this chapter, it was hypothesised that HNSCC cells upregulate expression of IL-35 as a feedback response to stimulation with inflammatory cytokines present in an inflamed microenvironment. Preliminary results from Dr Xiaoqing Wei's laboratory group indicated that stimulation of HNSCC cell lines with IFN γ increases gene expression of p35, and that TNF α increases that of EBI3. When used in combination, elevated gene expression of both EBI3 and p35 was observed, indicating potential IL-35 production (Wei, unpublished).

Based on these results, the underlying hypothesis was that in an inflamed TME, pro-inflammatory cytokines, such as IFN γ and TNF α , stimulate tumour cells. This could result in an immunoediting event (Dunn et al. 2004). As an adaptive negative feedback response, tumour cells upregulate EBI3 and p35, which interact to form the immunosuppressive cytokine IL-35. Furthermore, IL-35 has been shown to stimulate its own gene expression in transducing cells (Collison et al. 2012; Wetzel et al. 2021). Therefore, it is possible that IL-35 expression in tumour cells could be increased by transduction of exogenous IL-35 produced from cells in the TME. This chapter sought to carry the preliminary research forward and test this hypothesis by further exploring the regulation of IL-35 gene expression in HNSCC cell lines in response to stimulation with pro- and anti-inflammatory cytokines found in an inflamed TME.

3.4.1 IL-35 gene upregulation in HNSCC cell lines in response to stimulation with pro-inflammatory cytokines

3.4.1.1 Induction of p35 and EBI3 gene expression by IFN γ and TNF α

The first aim was to evaluate and confirm IL-35 gene upregulation in response to stimulation with pro-inflammatory cytokines. The approach taken was to stimulate hypopharyngeal carcinoma cells (FaDu) and oral carcinoma cells (H357) with IFN γ and TNF α (used in preliminary studies) and use RT-qPCR to measure changes in gene expression of EBI3 and p35. FaDu cells were selected as they had been used in preliminary studies. H357 cells differ in that they have limited invasive capacity,

whereas FaDu cells are more invasive and aggressive. Using two cell lines enabled comparisons to be made and to prevent generalisations being taken from results in a single HNSCC cell line. In future, it may be prudent to evaluate additional HNSCC cell lines.

Previous data has shown constitutive gene expression of EBI3 and p35 across many cancer cell lines (Maaser et al. 2004; Long et al. 2013). The current study demonstrated that gene expression of EBI3 and p35 is low in unstimulated FaDu and H357 cells. Lack of signal in Western Blot and ELISA data suggested that gene expression was too low to result in detectable IL-35 protein when cells are unstimulated. This was in agreement with early studies suggesting that HNSCC cells require crosstalk with immune cells to induce expression of immunosuppressive cytokines (Pries et al. 2006). Regarding the effects of pro-inflammatory cytokines, it was first asked whether IFN γ could induce increases in IL-35 gene expression. Confirming preliminary findings, both cell lines showed that low concentrations of IFN γ caused early increases in p35 mRNA, but did not significantly increase EBI3 expression. Increases in p35 may have been in direct correlation to the dose applied and time under stimulation. Though, as maximal induction was observed at the lowest tested concentration (1 ng/mL) and time (6 h), this would need to be confirmed in future studies using lower doses and timepoints.

When analysing EBI3 expression, IFN γ had no major effect on expression in either cell line after 6 h. In FaDu cells, EBI3 expression appeared to increase with time under stimulation. Expression was increased 4-fold after 48 h, but when analysed statistically, expression was not deemed significantly different to untreated cells. However, as it pertains to IL-35, the time required for this increase (48 h) did not synchronise with early induction of p35 expression. Furthermore, by this time, p35 expression had returned to baseline. Therefore, the Chapter data suggested that stimulation of HNSCC cells with IFN γ in the TME may not be sufficient to induce IL-35 expression.

Compared to the available literature, no previous studies of this nature were performed on HNSCC cells. Though, similar results were observed in treated colorectal cancer cell lines (Maaser et al. 2004). Interestingly, IFN γ was sufficient to upregulate both p35 and EBI3 in the hepatocellular carcinoma cell line HepG2 (Long et al. 2013),

suggesting differential signalling between cell lines and/or tissue sites. Together, the data indicates that IFN γ in the HNSCC TME may stimulate tumour cells to increase p35 gene expression. This mechanism may also be common across several cancers. Though, as IFN γ does not significantly upregulate EBI3 at the same time as p35, it can be concluded that IFN γ may not cause upregulation of IL-35 in stimulated HNSCC cells as an adaptive response to inflammation.

In a notable observation, high concentrations and prolonged exposure to IFN γ appeared to be toxic to cultured FaDu cells when viewed under a microscope. This observation was in agreement with the idea that IFN γ at low concentrations favours tumour development, as shown with p35 data, but is cytotoxic at high concentrations (Jorgovanovic et al. 2020). However, it raises the possibility that cytotoxicity could have affected RNA quality, and thus the validity of the qPCR data. This can be disregarded, as when samples were analysed for RNA integrity, all scores were 9 or above, suggesting RNA was not degraded. It may be useful in future to assess the effects of IFN γ on HNSCC cell viability via MTT (3-(4,5-dimethylthiazol-2-yl)-2,5-diphenyl-2H-tetrazolium bromide) assay.

It was next investigated whether HNSCC cell lines upregulate IL-35 as an adaptive response to TNF α in the TME. Stimulation of FaDu cells with the lowest tested concentration (1 ng/mL) and stimulation time (6 h), significantly increased EBI3 expression. Expression increased further with higher doses and duration of stimulation. TNF α did not increase p35 expression and thus did not upregulate IL-35 in FaDu cells. In contrast, TNF α did not increase EBI3 or p35 expression in H357 cells. Differences observed may be due to heterogeneity in the genetic profile of each cell line, but may reflect differences in response based on site of tumour origin. It must be noted that, when H357 cells were stimulated with TNF α , expression levels of all genes tested in the chapter remained unchanged. It cannot be disregarded therefore, that H357 cells may not express the TNF α receptor chains required to transduce this signal. As there are currently no available literature investigating this, this could be confirmed in future qPCR studies. Additional HNSCC cell lines could also be assessed to evaluate possible causes for differences in responses to inflammatory stimuli.

TNF α -induced EBI3 upregulation may be common across several cancers, as similar results were observed in colorectal carcinoma cell lines (Maaser et al. 2004; Wetzel et

al. 2021). While this was apparent in a hepatocellular carcinoma cell line (Long et al. 2013), TNF α also upregulated p35 expression, suggesting potential differences in regulation of p35 between cancers. In conclusion, the current study indicated that HNSCC cells may not respond to TNF α in the TME by increasing IL-35 expression.

In-vivo, it is likely that both IFN γ and TNF α are present in an inflamed TME, rather than one in the absence of the other. Thus, it was investigated whether inflammation involving both IFN γ and TNF α induces an adaptive response in stimulated tumour cells, whereby IL-35 gene expression is increased. Stimulation of FaDu cells caused significant increases in gene expression of both EBI3 and p35. Stimulation for 6 h with 1 ng/mL of both cytokines was sufficient to significantly increase expression of both genes simultaneously. EBI3 expression increased further in correlation with dose and time. This trend was in concurrence with data from TNF α stimulation studies. P35 was also significantly increased early and was maintained after 24 h, after which expression returned to baseline by 48 h of stimulation (100 ng/mL). This trend matched data observed during IFN γ stimulation studies.

Double stimulation of H357 cells (100 ng/mL, 6 h) also resulted in increased p35 and EBI3 gene expression. This could indicate that H357 cells may respond to TNF α , perhaps when concurrently under IFN γ stimulation. Furthermore, it may suggest that these cytokines synergise to upregulate EBI3. However, it must be noted that while the increase in EBI3 was statistically significant, the magnitude of increase (1.9-fold), in addition to the low basal expression of EBI3, could indicate that this may have little or no biological significance. To confirm whether both EBI3 and p35 are upregulated in H357 cells, additional repeats, timecourse studies and protein detection assays, perhaps ELISA or co-immunoprecipitation, could be performed. Additionally, to test the hypothesis further, other pro-inflammatory cytokines could be used to assess upregulation of EBI3 and p35 in H357 cells.

Together, H357 and FaDu cell RT-qPCR data was in agreement with the chapter and thesis hypothesis and revealed that, in an inflamed HNSCC TME of hypopharyngeal and perhaps oral cell origin, IFN γ and TNF α may stimulate tumour cells and induce an adaptive response whereby IL-35 gene expression is elevated.

Regarding FaDu cells, it was interesting to ascertain whether IFN γ and TNF α signalled independently, increasing subunit expression individually, or synergistically, meaning

they together induced higher magnitudes of gene upregulation when compared to single cytokine stimulation. As it pertains to p35, all IFN γ stimulations yielded almost identical increases in gene expression when compared to double stimulation. This suggests that when both cytokines were applied, TNF α signalling may not have any effect on p35 transcription, and that induction of p35 may solely be a result of IFN γ stimulation. In contrast, EBI3 expression may have been impacted by convergence of IFN γ and TNF α signalling. IFN γ had no significant effect on EBI3 when added alone. However, when both cytokines were added together, EBI3 expression increased at higher magnitudes than when TNF α was added alone. This was also observed in double stimulated colorectal cancer cell lines (Maaser et al. 2004). Thus, the data suggests that when stimulated with IFN γ alone, signalling in hypopharyngeal carcinoma cells may not lead to significant changes in EBI3 expression, but when TNF α signalling is concurrently activated, these cascades possibly converge, multiplying the activation signals for EBI3 transcription, leading to increased expression.

In conclusion, RT-qPCR data in both FaDu and H357 cells agreed with the chapter and thesis hypotheses. The combination of IFN γ and TNF α in the TME may stimulate hypopharyngeal and oral carcinoma cells, invoking a potential negative feedback response via upregulation of IL-35 gene expression. In hypopharyngeal cells, IFN γ may induce an early increase in p35 expression which is depleted over time. Furthermore, IFN γ and TNF α may synchronise to induce early and sustained upregulation of EBI3. Together, both cell lines indicated that inflammation may induce EBI3 and p35 expression in HNSCC cells, which could result in production of the immunosuppressive cytokine IL-35. This response may be shared across HNSCC subtypes, though additional data using other cell lines is required to confirm this.

3.4.1.2 Inflammation-induced upregulation of other IL-12 family cytokines

EBI3 and p35 can dimerise with other chains to produce alternative cytokines within the IL-12 cytokine family: IL-12 (p35/p40), IL-23 (p19/40), IL-27 (p28/EBI3), IL-35 (p35/EBI3) and IL-39 (p19/EBI3). Switching of these subunit pairs enables highly flexible responses to various immunological stimuli. It was important therefore, to confirm that inflammation induced upregulation of EBI3 and p35 observed in HNSCC cells was likely causative of IL-35 production, and not that of other IL-12 cytokines.

The current study found that p19 gene expression was very low in resting FaDu and H357 cells. IFN γ stimulation reduced p19 expression in both cell lines. In FaDu cells, TNF α increased p19 in correlation with dose and time, similar to EBI3. This may be a response observed in several cancers, as other cancer cell lines also upregulated EBI3 and p19 in response to TNF α (Maaser et al. 2004; Wetzel et al. 2021). TNF α had no effect on p19 in H357 cells, further suggesting lack of TNF α receptor expression. In FaDu cells, stimulation with both cytokines had similar effects as TNF α stimulation, which suggests TNF α signalling potentially outcompeted negative signalling from IFN γ . Upregulation of p19 and EBI3 indicated that an inflamed TME in hypopharyngeal carcinomas may stimulate tumour cells to produce IL-39. This may be unlikely though, as the current literature has yet to confirm IL-39 formation in humans (Ecoeur et al. 2020).

P28 expression was only inducible in FaDu cells stimulated with IFN γ and TNF α after 24 and 48 h, though expression levels were likely too low to result in dimerisation with EBI3 to form significant levels of IL-27 cytokine. p28, while expressed at very low levels in resting H357 cells, was not upregulated by either cytokine alone, or in combination. Therefore, the data suggests that inflammatory cytokines in the HNSCC TME may not induce IL-27 in tumour cells as an adaptive response. P40 was not detectable at rest or following stimulation in either cell line, indicating that pro-inflammatory cytokines in the TME may not promote IL-12 expression in tumour cells.

Taken together, stimulation of tumour cells with IFN γ and TNF α in the hypopharyngeal carcinoma TME, but not that in oral carcinomas, may cause tumour cells to upregulate alternative IL-12 family chains. Though, of the chains upregulated, the IL-12 cytokines they could form include IL-35 or IL-39. As IL-39 has yet to be validated in humans, the data thus far supported the hypothesis by showing that pro-inflammatory cytokines in the TME causes HNSCC cells to upregulate gene expression EBI3 and p35, potentially resulting in IL-35 formation. Protein data is required to confirm this. In addition, other pro-inflammatory cytokines and HNSCC cell lines could be tested.

3.4.1.3 *EBI3, p35 and IL-35 protein detection*

Since IFN γ and TNF α significantly increased EBI3 and p35 gene expression in FaDu cells, it was important to validate that this resulted in protein formation, and heterodimerisation of these chains to form the IL-35 cytokine. In the current study, several assays were used to achieve this. Using inferences from qPCR experiments, FaDu cells were stimulated with IFN γ and TNF α at varying concentrations, and for a range of stimulation times. Despite varying experimental factors, and altering variables to increase assay sensitivity, including: - the increase of lysate or supernatant concentrations, antibody concentrations, and the use of highly sensitive detection reagents and kits, EBI3, p35 or IL-35 protein could not be detected. EBI3 could not be detected intracellularly by western blotting, or extracellularly by ELISA. p35 could not be detected regardless of stimulation conditions or the use of immunoprecipitation/western blotting assays to enhance signal detection.

Potential reasons why these proteins could not be detected are henceforth explored. EBI3 and p35 gene expression are low in unstimulated cells. Large fold increases in gene expression suggested that they could be expressed at the protein level, but despite concentrating samples, protein production may have remained too low to be detected within the sensitivity ranges of the assays used. In vivo, this may reflect that EBI3 and p35, in association as IL-35, may only be minimally produced by tumour cells, with the lion share of production deriving from Tregs, Bregs and M2 macrophages in the TME.

A limitation of this study is that the experiments performed analysed cultured tumour cells in isolation, stimulated with only two pro-inflammatory cytokines. This does not account for crosstalk with stromal cells, nor the effects of other pro-inflammatory cytokines that may be present in the TME in-vivo. These cytokines may increase IL-35 expression further. For example, IL-1 has previously been shown to synergise with IFN γ to induce upregulation of EBI3 and p35 in stimulated tumour cells (Maaser et al. 2004). Therefore, HNSCC-derived IL-35, induced by inflammation in the TME, may be at much higher concentrations in-vivo. This could be confirmed in future studies by analysing patient tissues using immunohistochemical techniques to detect expression of tumour cell-derived EBI3 and p35.

Previous reports have demonstrated protein detection of EB13 and p35 in cancer cell lines using western blotting (Zhu et al. 2020). A salient difference from this study to the current one however, is that protein concentrations separated by SDS-PAGE were much higher (30 mg) to that used in the current study (20 and 50 µg). While mg masses of protein may increase the amount of protein available to detect the targets, there is a risk of poor protein separation by SDS-PAGE and/or excessive background signal.

Another possibility for lack of detection is that proteins formed are in conformations with epitopes that are inaccessible to the antibodies used in this study. Other antibodies, such as polyclonal antibodies that target a range of epitopes, could be used to test this in future. The proteins formed may also be misfolded and/or degraded. Alternative methods rather than use of lysates or supernatant, including fixation and immunocytochemistry, or analysing live cells via flow cytometry, which were both successfully used by Long (Long et al. 2013), may enable protein detection in future. Finally, it cannot be disregarded that these genes are simply not translated due to mutations, and may therefore represent pseudogenes.

The IL-35 cytokine could not be detected using ELISA assays. Previous issues in IL-35 detection have been reported previously (Sakkas et al. 2018; Larousserie et al. 2019). Two kits were purchased but demonstrated either poor assay sensitivity (no signal), or lack of target specificity (signal in negative controls). As an alternative, co-immunoprecipitation/western blot assays were attempted. Neither immunoprecipitated p35, or interacting EB13, could be detected in concentrated lysates or supernatants. The assays did not fail as signal was detected in positive control samples taken from transfected cell lines that overexpress EB13 and p35. Of note, the final experiment attempted used a range of stimulation conditions to maximise gene expression. Lysates and supernatants were also concentrated. The Veriblot antibody, advertised to bind non-reduced antibody, was used to prevent capture of the antibody used for immunoprecipitation. The SuperSignal West Atto Ultimate Sensitivity Substrate was also used to increase signal by detecting proteins with atto-gram level sensitivity. Despite these optimisation strategies, immunoprecipitated p35 could not be detected. Notably, it was also undetected in control samples (**Supplementary data 7**). Washing the blot and reprobing with alternative antibody pairs enabled signal detection, albeit only in controls. Using

Veriblot, EBI3 could not be detected in control samples either, which suggested that this antibody failed to effectively capture primary antibodies. Ideally, in future, alternative antibody pairs would also be used to detect EBI3 under the same conditions tested. Though as p35 failed to be immunoprecipitated, it was unlikely that this would enable detection of co-immunoprecipitated EBI3.

Possible reasons why IL-35 could not be detected include those described for detection of individual subunits. Another potential possibility is that secreted IL-35 may have been recycled by its receptor and degraded. However, if it is an issue of assay sensitivity, IL-35 ELISA kits with a lower detection limit could be tried in future. In summary, qPCR data supported the chapter hypothesis that inflammation promotes IL-35 gene upregulation in HNSCC cells. However, a limitation of this study is that this could not be confirmed at the level of protein expression.

3.4.2 Effects of anti-inflammatory cytokines on IL-35 gene expression in stimulated HNSCC cell lines

3.4.2.1 IL-35 and IL-10 stimulation did not increase endogenous IL-35 gene expression in resting HNSCC cell lines

The effects of immunosuppressive cytokines on IL-35 expression in HNSCC tumour cells had not yet been investigated. IL-35 concentrations are high in immunosuppressive tumour microenvironments. In addition, exogenous IL-35 has been shown to stimulate endogenous gene expression in treated cells (Collison et al. 2012). Thus, it was hypothesised that immunosuppressive cytokines such as IL-35 and IL-10 in the HNSCC TME, could stimulate tumour cells to upregulate endogenous IL-35 as a means of enhancing immune suppression. To explore this, FaDu and H357 cells were treated with recombinant IL-10 and/or IL-35 (100 ng/mL each, 6 h). The data did not support the hypothesis, as neither cytokine increased IL-35 gene expression in either cell line.

It was considered whether the lack of changes in IL-35 expression was due to the cell's inability to respond to IL-35 signals. As such, expression of the IL-35 receptor chains (gp130 and IL-12R β 2) was examined. qPCR data showed that resting FaDu cells expressed gp130 and very low levels of IL-12R β 2. H357 cells expressed gp130 but did not express IL-12R β 2. Similarly, a study performed by Long and others showed

that IL-12R β 2 is either expressed at low levels or not at all in a range of cancer cell lines (Long et al. 2013). Gp130 is constitutively expressed in all human tissues. IL-35 can signal using gp130/gp130 homodimers, IL-12R β 2/ IL-12R β 2 homodimers, or gp130/IL-12R β 2 heterodimers. It was previously indicated that IL-35 signalling through homodimeric receptors may promote endogenous IL-35 expression. However, it must be considered that gp130 is ubiquitously expressed, and that previous studies have shown biological effects of gp130/gp130 homodimers in IL-6 signalling only (Adam et al. 2009; Suthaus et al. 2011). Furthermore, Lee and others showed that IL-35 signal transduction in tumour cells could be enhanced by increasing expression of IL-12R β 2 (Lee et al. 2018). It is therefore conceivable that recombinant IL-35 was unable to be transduced in a manner that promoted endogenous IL-35 expression, as the tested HNSCC cell lines did not express sufficient levels of IL-12R β 2.

3.4.2.2 Priming of HNSCC cells for IL-35 signal transduction via inflammation-induced receptor expression

While stimulation of resting HNSCC cell lines with exogenous IL-35 had no effect on endogenous gene expression, it was purported that inflammation in the HNSCC TME may not only upregulate IL-35 expression in tumour cells, but also its receptor chains. In doing so, upregulation of the minimally expressed IL-12R β 2 chain may prime these cells to respond to IL-35 signals using IL-12R β 2 homodimers, or gp130/IL-12R β 2 heterodimers. Signalling through these receptors could result in further upregulation of endogenous IL-35 expression. Experiments were hence performed to begin exploring this.

IFN γ was demonstrated to increase expression of both IL-12R β 2 and gp130 chains in stimulated FaDu cells. TNF α , similar to IFN γ , increased gp130 but did not increase IL-12R β 2 expression. When added in combination, IFN γ and TNF α elevated expression of both chains. Comparing data to that from single cytokine stimulation, these cytokines appeared to act in synergy, resulting in a higher magnitude of gp130 upregulation. Although, it appeared that TNF α signalling may have partially mitigated the effects of IFN γ -induced IL-12R β 2 upregulation.

Taking these results into consideration, the following could be inferred: - at rest, the IL-35 receptor, in the form of gp130 homodimers, may be expressed in FaDu cells. As IL-12R β 2 gene expression is low, it could be assumed that gp130/IL-12R β 2 and IL-

IL-12R β 2/IL-12R β 2 heterodimers are not expressed. Without IL-12R β 2, IL-35 signals may not be transduced in a manner that enables endogenous IL-35 expression. Conversely, in an inflamed TME, IFN γ stimulates tumour cells and causes increases in IL-12R β 2 expression, which could facilitate gp130/IL-12R β 2 heterodimer formation. When TNF α is also present in the TME, concurrent TNF α and IFN γ signalling may converge at the level of the gp130 transcription machinery, where they impart activation signals that increase gp130 transcription. In contrast, it is possible that TNF α and IFN γ may activate transcription factors that repress and activate transcription of IL-12R β 2, respectively. The effects of IFN γ may outcompete that of TNF α , culminating in increased gene expression of IL-12R β 2 in addition to gp130. In summation, data from FaDu cells provided evidence which suggested that inflammation may induce upregulation of IL-35 gene expression and its receptor chains in hypopharyngeal carcinoma cells.

A previous study by Lee and others also examined inflammation-induced IL-12R β 2 expression in tumour cells, and how it relates to IL-35 signalling (Lee et al. 2018). They cultured a variety of cancer cell lines, including human lung (A549), and three HNSCC cell lines (FaDu, SAS and OECM1), and stimulated them with TNF α (20 ng/mL, 24 h). Using RT-qPCR, immunohistochemistry, western blotting and flow cytometry, they examined the effects of TNF α on IL-12R β 2 expression. With regards to HNSCC, TNF α did not increase expression in treated FaDu cells, as observed in this study. In contrast, treated SAS, and particularly OECM1 cells, showed marked elevations in IL-12R β 2 expression. As H357 cells in the present study did not express IL-12R β 2, nor did gp130 or IL-12R β 2 expression alter in response to inflammation, it is possible that inflammatory signalling may differ between HNSCC cell lines and/or sites of tumour origin. A549 lung carcinoma cells were also shown to upregulate IL-12R β 2 in response to TNF α . Furthermore, induction of IL-12R β 2 expression primed A549 cells to transduce exogenous IL-35 signals. Therefore, while resting HNSCC cell lines did not respond to exogenous IL-35 by increasing endogenous expression, findings from Lee's study, together with data from the chapter results, suggests that inflammation in the TME may cause hypopharyngeal carcinoma cells to increase expression of IL-35 receptor chains. This may facilitate formation of IL-12R β 2

homodimeric and gp130/IL-12R β 2 heterodimeric receptors. Additional data such as protein expression studies are required to confirm this.

As the overall focus of the chapter was the regulation of IL-35 expression in inflamed tumour cells, the next logical question was whether increased receptor expression caused by inflammation enables hypopharyngeal carcinoma cells to transduce IL-35, resulting in enhanced IL-35 expression. Collison previously demonstrated the existence of such a positive feedback loop. Induced Tregs that produce IL-35 were shown to transduce IL-35, resulting in further endogenous expression (Collison et al. 2012). Wetzel's group recently showed that this could occur in tumour cells (Wetzel et al. 2021). They stimulated HCEC cells to induce IL-35 secretion, and used the conditioned medium produced to treat unstimulated cells. They observed significant increases in EBI3 and p35 expression, the latter of which was reversible by adding an anti-p35 antibody. While these findings suggest that this may be possible in inflamed hypopharyngeal carcinoma cells, this could be confirmed in future studies by adding recombinant IL-35 to IFN γ +TNF α -primed FaDu cells and examining whether gene expression of EBI3 and p35 are elevated. It would also have the added benefit of confirming whether inflammation-induced increases in EBI3 and p35 gene expression resulted in the formation of functional IL-35.

3.5 Conclusions

The current chapter hypothesised that pro-inflammatory cytokines in the HNSCC TME stimulate tumour cells, causing increased expression of the immunosuppressive cytokine IL-35. The data obtained partially supported this hypothesis, revealing the following:- IFN γ induced gene expression of p35 in both hypopharyngeal carcinoma cells (FaDu) and oral carcinoma cells (H357). TNF α induced EBI3 gene expression in FaDu but not H357 cells. Stimulation with both IFN γ and TNF α significantly increased gene expression of both EBI3 and p35 in FaDu and H357 cells. While these chains can associate with other IL-12 chains to produce alternative cytokines, of the remaining chains, inflammation was found to only significantly increase p19 expression in FaDu cells but not H357 cells. As IL-39 (EBI3/p19) has not been proven to exist in human studies, the data suggested that inflammation in the TME may promote upregulation of EBI3 and p35 to facilitate IL-35 production in both cell types.

A major limitation of this study however, was that EBI3, p35, nor the IL-35 cytokine, could not be detected at protein level in FaDu cells.

Exposure to immunosuppressive cytokines, including IL-10 and IL-35, did not cause increases in expression of IL-35 in resting FaDu or H357 cells. Regarding IL-35 receptors required to transduce IL-35, these cells were found to express very low (FaDu), or no (H357) IL-12R β 2 chain. However, when FaDu cells were exposed to IFN γ and TNF α , inflammation not only increased IL-35 expression, but also that of its receptor chains gp130 and IL-12R β 2. It is not yet known whether priming cells with such stimulation may enable them to transduce IL-35 in a manner that promotes endogenous expression. Future studies could explore additional pro-inflammatory cytokines. Furthermore, as findings varied between HNSCC cell lines, it may be important to evaluate the hypothesis further by testing additional cell lines sourced from different tissues sites and with different aetiological factors.

Nevertheless, taking these findings together, a potential mechanism may have been uncovered, at least in hypopharyngeal carcinomas. Inflammation in the TME may stimulate tumour cells to upregulate expression of both IL-35 and its receptor chains. IL-35 produced from tumour cells may be low in concentration, as it could not be detected in assays performed in this study. However, elevated receptor expression may prime tumour cells to receive IL-35 signals produced from its own cells (autocrine signalling) and that from highly producing Tregs, Bregs and M2 macrophages (paracrine signalling) in the TME. Transduction of IL-35 signals may then result in further increases in IL-35 expression.

The thesis aimed to investigate the potential roles of HNSCC-derived IL-35 in suppression of anti-tumour immunity via conversion of M1 macrophages to an M2 phenotype. To explore this robustly, the next chapter focused on the development of a hypopharyngeal FaDu cell line that overexpresses IL-35. This cell line could then be used in subsequent chapters to assess changes in macrophage polarisation.

Chapter 4

Establishment of a HNSCC cell line that overexpresses and secretes human Interleukin 35 (IL-35)

4.1 Introduction

Chapter 3 demonstrated that when stimulated with the pro-inflammatory cytokines IFN γ and TNF α , both the oral carcinoma cell line, H357, and to a greater extent, the hypopharyngeal carcinoma cell line FaDu, increase gene expression of the immunosuppressive cytokine Interleukin 35 (IL-35). This may depict an immunoediting mechanism used by tumour cells to suppress anti-tumour immunity and promote immune escape. To investigate the role of HNSCC-derived IL-35 in the regulation of anti-tumour immunity, a useful method is to establish a HNSCC cell model that constitutively overexpresses human IL-35. Previous overexpression models in the literature were limited, as IL-35 produced was not in its native form, and thus may not accurately mimic IL-35 in-vivo. The aim of this study was to develop a HNSCC cell line that overexpressed IL-35 in its native form. This model could then be used in mixed culture studies to elucidate whether HNSCC-derived IL-35 promotes M2 macrophage polarisation in the TME.

To develop a transfected cell line that overexpresses native human IL-35, its biological structure must be considered. IL-35 is a member of the IL-12 family of cytokines. These cytokines are derived from the heterodimerisation of α -helical chains and β -chains that are paired interchangeably, resulting in the formation of the following cytokines: - IL-12 (p35/p40), IL-23 (p19/p40), IL-27 (p28/EBI3), IL-35 (EBI3/p35) and IL-39 (p19/EBI3) (Kobayashi et al. 1989; Devergne et al. 1997; Oppmann et al. 2000; Pflanz et al. 2002; Wang et al. 2016b).

IL-35 is comprised of EBI3 (Epstein-Barr Virus Induced 3) and p35 subunits. Epstein-Barr virus-induced gene 3 (EBI3) is the β -subunit chain. It was discovered as a gene transcript in B cells infected with the Epstein-Barr virus (Devergne et al. 1996). The EBI3 gene is synthesised as a 229-amino acid precursor protein, which includes a 20-amino acid signal sequence required for protein secretion, and a 209-amino acid region (Devergne et al. 1997; Rousseau et al. 2010). This precursor protein is approximately 28 kDa in size before it is subjected to post-translational modifications, including N-linked glycosylation, that culminates in formation of the stable \approx 33 kDa EBI3 glycoprotein (Devergne et al. 1996; Devergne et al. 1997). EBI3 is structurally unique in the IL-12 family, as it does not contain an N-terminal IgG domain (Jones and Vignali 2011). In terms of trafficking and secretion, it is transiently held in the

endoplasmic reticulum (ER) in association with the molecular chaperone calnexin, before being readily secreted (Devergne et al. 1997; Pflanz et al. 2002; Jones et al. 2012).

P35 is the alpha chain of the IL-35 heterodimer. Regulation of p35 expression and trafficking of the produced protein are complex and not fully understood. Research has suggested the following: - EBI3 is readily secreted as its signal peptide is cleaved by signal peptidase to facilitate trafficking. In contrast, the signal peptide of p35 requires multiple cleavage events to facilitate trafficking and secretion. P35 is therefore not regarded a readily secreted protein. Initially, the p35 gene is transcribed. It can be transcribed from two distinct promoter regions resulting in the formation of precursor proteins approximately 27 or 30 kDa in size. In the ER, the precursor is glycosylated, increasing the molecular weight of each isoform to 32 or 35 kDa, respectively. These forms are only present transiently, as primary cleavage of the signal peptide occurs, yielding the dominant form of p35, which is ≈ 31 kDa regardless of isoform (Murphy et al. 2000). This form is held in the ER and has been described as unstable. Exactly how the following events are regulated is unknown, but to stabilise and enable secretion of p35, a sequence of events must occur. Co-expression of a binding partner is essential to increase the stability of p35 and enable translocation from the ER to the Golgi. Here, the signal p35 peptide is cleaved a second time. P35 is then subjected to additional glycosylation, creating a 36 kDa glycoprotein that is rapidly secreted (Murphy et al. 2000; Jalah et al. 2013).

Co-expression and interaction of p35 with a binding partner such as EBI3, is understood to stabilise and facilitate the secretion of heterodimeric IL-12 family cytokines including IL-35 (Devergne et al. 1997; Murphy et al. 2000; Jalah et al. 2013). Exactly how EBI3 stabilises p35 is unknown. It is possible that p35 is held in the ER by a chaperone protein, which when bound, signals for the degradation of p35, hence its low stability. Based on IL-12 studies, high expression of EBI3 may enable the retention of a sufficient amount of intracellular protein during its trafficking to the cell surface (Jalah et al. 2013). Binding of this intracellular EBI3 to p35, the unknown chaperone protein, or a combination of both, may liberate p35 from ER retention and labelling for degradation. With increased stability, p35 can translocate to the Golgi, where it is modified and later secreted in association with EBI3 as the IL-35 cytokine.

While this is plausible, more research is required to fully elucidate the formation and trafficking of the IL-35 heterodimer.

The interactions between EBI3 and other IL-12 chains are complex. Subunit chains that dimerise to form IL-12 (p35/p40) and IL-23 (p19/p40) interact covalently using disulphide bond linkages. EBI3 however, lacks the cysteine residues required to facilitate this. The EBI3-containing cytokines IL-27 and IL-35 are therefore not derived from disulphide-linked subunits (Jones and Vignali 2011). Exactly how EBI3 interacts with p28 (IL-27) and p35 (IL-35) is currently unknown, but these associations are thought to be non-covalent. As a weaker form of interaction, these cytokines are deemed relatively unstable (Devergne et al. 1997; Jones and Vignali 2011; Aparicio-Siegmund et al. 2014). This raised the question of how IL-35 signalling is maintained in-vivo. While this is not known, recent research has suggested that IL-35 may propagate its signal by transferring the ability to produce IL-35 between cells via extracellular vesicle transfer (infectious tolerance, reviewed in Chapter 1).

Poor stability of the IL-35 heterodimer has rendered it difficult to replicate in study models. To elucidate the biological roles of IL-35, research groups have often used transfection to induce IL-35 overexpression in model cell lines. Notably, vectors used encode EBI3 linked to p35 using a linker peptide. Linker peptides ensure EBI3 and p35 are held together by stable covalent interactions. These models have helped broadened knowledge of IL-35 and its functions (Niedbala et al. 2007; Nakano et al. 2015; Wang et al. 2016a; Haller et al. 2017). However, this approach has potential drawbacks. IL-35 formed using these vectors do not accurately represent the natural formation and structure of IL-35 in-vivo. By synthetically linking EBI3 and p35, certain aspects of their biology, such as their interactions with receptors and extracellular vesicles, may be affected. Furthermore, the linker peptides used may have unintended effects that could alter the functionality of IL-35, or the behaviour of cells that express or transduce its signal.

The rationale behind this study was the elucidation that stimulation with IFN γ and TNF α induces significant IL-35 gene upregulation in the hypopharyngeal carcinoma cell line FaDu (Chapter 3). To study whether HNSCC-derived IL-35 suppresses anti-tumour immunity via M2 macrophage polarisation, it was deemed beneficial to develop a HNSCC cell model that constitutively overexpresses and secretes IL-35 in

its native form. The objective of this Chapter therefore, was to utilise a novel methodology that could enable the development of a FaDu cell line that overexpresses IL-35 in its native form.

The Chapter hypothesis was as follows: - Stable transfection of FaDu cells with a plasmid encoding human EBI3 can be used to generate a monoclonal cell line that overexpresses EBI3. Subsequent stable transfection of this cell line with a plasmid encoding human p35, can be used to develop a cell line that co-expresses EBI3 and p35. These chains naturally interact, together becoming secreted as the IL-35 heterodimer in its native form. As such, a HNSCC cell line that overexpresses and secretes IL-35 will be developed as a study model.

4.2 Aims and objectives

- Validate the proposed methodology by developing a CHO cell line that overexpresses and secretes human IL-35.
 - Develop a CHO cell line that overexpresses human EBI3
 - Develop a CHO cell line that overexpresses both human EBI3 and p35
 - Detect secretion of the IL-35 heterodimer and establish a CHO-IL-35 cell line
 - Confirm EBI3, p35 and IL-35 overexpression in the established CHO-IL-35 cell line
- Develop a FaDu cell line that overexpresses and secretes human IL-35
 - Develop a FaDu cell line that overexpresses human EBI3
 - Develop a FaDu cell line that overexpresses human p35
 - Develop a FaDu cell line that overexpresses both human EBI3 and p35
 - Detect secretion of the IL-35 heterodimer and establish the FaDu-IL-35 cell line
 - Confirm EBI3, p35 and IL-35 overexpression in the established FaDu-IL-35 cell line

Should the FaDu-IL-35 model be created, it can be used to study the role of HNSCC-derived IL-35 in the regulation of macrophage polarisation in the HNSCC TME.

4.3 Chapter Methods

General methods used in this Chapter are described in full in the following sections of Chapter 2. Transfection (**Section 2.3.6**), generation of conditioned medium (**Section 2.3.6.4**). SDS-PAGE/Western Blotting (**Section 2.3.3**), co-immunoprecipitation (**Section 2.3.4**) and ELISA (**Section 2.3.5**). The following methods described are pertinent to investigations performed in the current Chapter.

4.3.1 Expression plasmids

Full plasmid maps are shown in Chapter 2 (**Section 2.1.5**). The EBI3 expression plasmid contains an open reading frame for the full length human EBI3 transcript, controlled by the CAG promoter. It also contains a neomycin resistance marker, controlled by the CMV promoter, to facilitate stable transfection using the G418 antibiotic. The negative control (NTC) plasmid contains the same elements, but with a stuffer sequence in place of the EBI3 open reading frame. The p35 expression plasmid contains the open reading frame for the full length human p35 transcript, controlled by the CAG promoter. It also has a puromycin resistance marker under the regulation of the CMV promoter.

4.3.2 Development of a CHO cell line that overexpresses and secretes human IL-35

4.3.2.1 Development of a CHO cell line that overexpresses human EBI3

To overexpress human EBI3, CHO cells were stably transfected with the EBI3 expression plasmid. As a negative control, they were also stably transfected with the NTC plasmid. To perform, 1×10^5 cells were seeded into 24-well plates and cultured overnight. The EBI3 expression plasmid, or the NTC plasmid, was then transfected into CHO cells using Lipofectamine 2000 as described in Chapter 2 (**Section 2.3.6**). Stable transfectants of both plasmids were selected by culturing cells in RPMI-1640 supplemented with G418 (500 $\mu\text{g}/\text{mL}$). After selection, CHO cells transfected with the NTC plasmid (now named CHO-NTC cells) were frozen until use. From the polyclonal pool of stable transfectants using the EBI3 expression plasmid, single

clones were isolated, numbered, and grown by limiting dilution. Clones that survived expansion were split into two populations. One population of clones were frozen. The other was examined for expression of human EBI3. To detect EBI3 expression, lysates were collected from cultured cells using RIPA buffer. 35 μ L of protein per sample was separated by SDS-PAGE. Recombinant human IL-35-Fc was used as a positive control. Clones expressing EBI3 were detected by Western Blotting using the following antibodies - mouse monoclonal anti-EBI3 (Biolegend, 1 μ g/mL), and a rabbit polyclonal anti-mouse IgG (HRP) secondary antibody (Abcam, 0.2 μ g/mL). The highest expressing clone was then designated the CHO-EBI3 cell line.

Generating representative data. After all transfected CHO cell lines in the Chapter were established, lysates and supernatants from each cell line were analysed to generate data representing EBI3 overexpression in developed cell lines.

To detect EBI3 overexpression by Western Blot, each cell line was thawed and subcultured. 5×10^5 cells were seeded into 6-well plates and cultured until 90% confluency was reached. 4-6 h prior to cell lysis, 3.0 μ g/mL Brefeldin A was added to culture to block protein secretion. Cells were lysed in RIPA buffer. 10 μ g of total protein per sample was separated by SDS-PAGE. Lysates from untransfected CHO and CHO-NTC cells were analysed as negative controls. Due to the unstable nature of recombinant IL-35, lysate from a double-transfected CHO cell clone (Clone 7), which tested positive for EBI3 and p35 overexpression during initial clone screening, was thawed and re-used as a positive control (labelled CHO-IL-35-C7 to prevent ambiguity). EBI3 expression was detected by Western Blotting using the same antibodies and concentrations as described above. A mouse monoclonal anti- β -Actin (Abcam, 0.1 μ g/ml) antibody, conjugated to HRP, was used to confirm equal loading of samples.

To confirm EBI3 secretion, conditioned medium was collected from confluent cell lines cultured in T25 flasks and stored at -80 °C (**Section 2.3.6.4**). Single use aliquots were thawed and examined for the presence of secreted EBI3 using an ELISA kit as instructed by the manufacturer (R&D Systems) (n=3). Conditioned medium collected from CHO-NTC and untransfected CHO cells were used as negative controls. One Way ANOVA and Dunnett's test were used to determine whether differences in mean

EBI3 concentrations detected in supernatants from transfected cell lines, versus that in untransfected controls, were statistically significant.

4.3.2.2 Development of a CHO cell line that overexpresses both human EBI3 and p35

The CHO-EBI3 cell line was seeded into 24-well plates and transfected with the p35 expression plasmid using Lipofectamine 2000 (**Section 2.3.6**). Stable transfectants were selected by culturing cells in medium containing both G418 (500 µg/mL) - to maintain selection pressure for EBI3 expression, and puromycin (5 µg/mL) - to simultaneously select for stable transfectants of the p35 plasmid. Single clones were isolated, numbered and grown using limiting dilution. Clones that survived expansion were screened for expression of p35 by SDS-PAGE/Western Blotting. Cells were lysed in RIPA buffer, and 35 µL per clone separated by SDS-PAGE. IL-35-Fc was also loaded onto SDS-PAGE gels as a positive control. P35 expression was detected by Western Blotting using the following antibodies - rabbit monoclonal anti-p35 (Abcam, 1:2000 dilution) primary antibody and an HRP-conjugated goat anti-rabbit IgG secondary antibody (Abcam, 0.2 µg/mL).

Selected clones were next screened to identify which clone expressed the highest concentration of p35, but also maintained expression of EBI3. Per clone, 3×10^5 cells were seeded into 6 well plates and cultured until 90% confluent. Brefeldin A was added prior to lysis with RIPA buffer. To enable comparison in expression levels, 10 µg of protein per sample was analysed for the co-expression of EBI3 and p35 by SDS-PAGE/Western Blotting using the previously described antibodies. Detection of EBI3 and p35 were performed on separate blots to prevent signal overlap.

4.3.2.3 Detection of the secreted IL-35 heterodimer and establishment of the CHO-IL-35 cell line

Co-immunoprecipitation was used to detect the IL-35 heterodimer via the association of co-expressed EBI3 and p35 in selected clones (**Section 2.3.4**) Candidate clones were seeded into 6-well plates and cultured until 90% confluent. 1 mL of supernatant was collected per sample. For 2% input and flowthrough controls (**fully explained in Section 2.3.4.1**), used to assess pulldown efficiency, extra supernatant was collected from the clone previously shown to express the highest amount of EBI3 and p35. P35

was immunoprecipitated from supernatants by incubating samples overnight in the presence of an anti-p35 antibody (2 µg/mL, R&D Systems), followed by an additional overnight incubation with anti-mouse IgG dynabeads. The IgG control (**Section 2.3.4.1**), used to assess antibody cross-reactivity, was generated by incubating the highest expressing clone in anti-mouse IgG dynabeads but omitting the anti-p35 incubation step. For all samples, beads were then washed five times and eluted. Eluates were separated by SDS-PAGE and both immunoprecipitated p35, and co-immunoprecipitated EBI3, detected by Western Blot using the antibodies and concentrations described above. Recombinant human IL-35 (rhIL-35, 10 ng) was used as a positive control. The clone expressing the highest concentrations of associated EBI3 and p35 was selected as the CHO-IL-35 cell line.

4.3.2.4 Confirmation of EBI3, p35 and IL-35 overexpression in the established CHO-IL-35 cell line

EBI3 overexpression in the CHO-IL-35 cell line was confirmed alongside other established CHO cell lines by Western Blotting and ELISA. Lysates and supernatants were prepared and analysed as described in **Section 4.3.2.1 – generating representative data**. Lysates were also assessed by Western Blotting to confirm p35 overexpression using antibodies previously described. A human IL-35 ELISA kit (Cusabio) was used to confirm IL-35 secretion in conditioned medium samples.

4.3.3 Development of a FaDu cell line that overexpresses and secretes human IL-35

4.3.3.1 Development of a FaDu cell line that overexpresses human EBI3

FaDu cells were transfected with the EBI3 expression plasmid or the NTC plasmid as described for CHO cells. Stable transfectants of each plasmid were selected using G418 (500 µg/mL). Stable NTC transfectants were frozen until use (named FaDu-NTC). Single clones from FaDu cells transfected with the EBI3 expression plasmid were isolated, numbered and grown by limiting dilution. Brefeldin A was added to cultures before lysis of surviving clones in RIPA buffer. Lysates were examined for expression of EBI3 by SDS-PAGE/Western Blotting using the same antibodies and concentrations as described for CHO cells. Recombinant human IL-35 (10 ng) was used as a positive control.

To confirm overexpression and select the model FaDu-EBI3 cell line, positive clones were subcultured, treated with Brefeldin A, and 10 µg of collected lysate analysed by Western Blotting (n=2). The clone expressing the highest concentration of EBI3 was named FaDu-EBI3. After all FaDu cell lines were created, representative data confirming EBI3 overexpression in established cell lines was obtained. Cell lines were cultured, and lysates and supernatants analysed by Western Blotting and ELISA as described for CHO cells (**Section 4.3.2.1 – generating representative data**).

4.3.3.2 Development of a FaDu cell line that overexpresses human p35

In addition to FaDu-EBI3, a FaDu-p35 cell line was established to provide IL-35-negative controls and to enable investigation into the potential roles of individual IL-35 subunits in the regulation of macrophage polarisation (Chapter 5 and 6). FaDu cells were transfected with the p35 expression plasmid. Stable transfectants were selected using puromycin (1 µg/mL). Single clones were isolated and grown by limiting dilution. Those that survived expansion were screened for expression of p35 by Western Blotting. 10 µg of protein per clone was separated by SDS-PAGE and analysed by Western Blot using an anti-p35 antibody (as described for CHO cells).

Two of the highest expressing clones were cultured further, lysed, and p35 expression confirmed by additional Western Blotting with equal protein loading (n=2). Untransfected CHO and FaDu cells were used as negative controls. The clone expressing the strongest p35 signal was selected as the FaDu-p35 cell line. Representative Western Blot data confirming p35 overexpression in developed FaDu cell lines was prepared as described for CHO cells (**Section 4.3.2.4**).

4.3.3.3 Development of a FaDu cell line that overexpresses both human EBI3 and p35

FaDu-EBI3 cells were transfected with the p35 expression plasmid. Stable transfectants were selected using both G418 (500 µg/mL, for EBI3 expression) and puromycin (1 µg/mL, for p35 expression). 10 µg of cell lysate from single clones (treated with Brefeldin A) were analysed by SDS-PAGE/Western Blotting to detect clones that overexpressed p35 and maintained EBI3 overexpression.

4.3.3.4 Detection of the secreted IL-35 heterodimer and establishment of the FaDu-IL-35 cell line

Co-immunoprecipitation/Western Blotting was used to identify IL-35 in supernatants from candidate double-transfected FaDu cell clones that co-expressed EBI3 and p35. Methods performed were as described for CHO cells with an alteration made to the secondary antibody used during detection of EBI3. To minimise potential masking of EBI3 bands by eluted immunoprecipitation antibody, a goat anti-mouse IgG2b heavy chain (HRP) (Abcam, 1:5000) secondary antibody was used. CHO-IL-35 cell lysate was used as a positive control. The clone displaying the highest concentrations of p35 and associated EBI3 was selected as the FaDu-IL-35 cell line.

4.3.3.5 Confirmation of EBI3, p35 and IL-35 overexpression in the established FaDu-IL-35 cell line

To generate representative data confirming overexpression of EBI3, p35 and IL-35 in the FaDu-IL-35 cell line, lysates and conditioned medium from established FaDu cell lines were prepared as described (**Section 4.3.2 – generating representative data**). EBI3 overexpression was confirmed by Western Blotting and ELISA. P35 overexpression was confirmed by Western Blotting. IL-35 secretion was confirmed using an ELISA kit as instructed by the manufacturer (Bio-Ocean) (n=1).

4.4 Results

4.4.1 Development of a CHO cell line that overexpresses and secretes human IL-35

4.4.1.1 *Development of a CHO cell line that overexpresses human EBI3*

The first aim of this Chapter was to use CHO cells to validate that successive stable transfection procedures, which result in a cell line that co-expresses human EBI3 and p35, leads to intrinsic heterodimerisation and secretion of the IL-35 heterodimer in its native form. The initial objective was to establish a CHO cell line that overexpressed human EBI3 (CHO-EBI3). CHO cells were transfected with an EBI3 expression plasmid, and stable transfectants selected using G418 (500 µg/mL).

Single clones were screened for expression of EBI3 by Western Blotting. Blot data is shown in **Figure 4.1A**. Of the tested clones, EBI3 expression was detected in Clone “1” only (**Figure 4.1A, Lane “1”**), evidenced by presence of a band at \approx 33 kDa, which corresponded to the glycosylated form of EBI3 (Devergne et al. 1997). Thus, the data showed that stable transfection of CHO cells with the human EBI3 plasmid successfully resulted in a cell line that overexpressed EBI3. As the only clone in which EBI3 was detected, Clone 1 was designated the CHO-EBI3 cell line.

After establishment of all transfected CHO cell lines, representative data confirming overexpression of human EBI3 in developed cell lines was obtained. Lysates (treated with secretion blocker Brefeldin A), and supernatants (untreated), were examined for expression and secretion of EBI3, respectively. EBI3 overexpression in CHO-EBI3 cells was confirmed by Western Blotting (**Figure 4.1B, Lane CHO-EBI3**) and its secretion by ELISA (**Figure 4.1C**). The data further confirmed the establishment of a CHO cell line that overexpresses and secretes human EBI3 (CHO-EBI3).

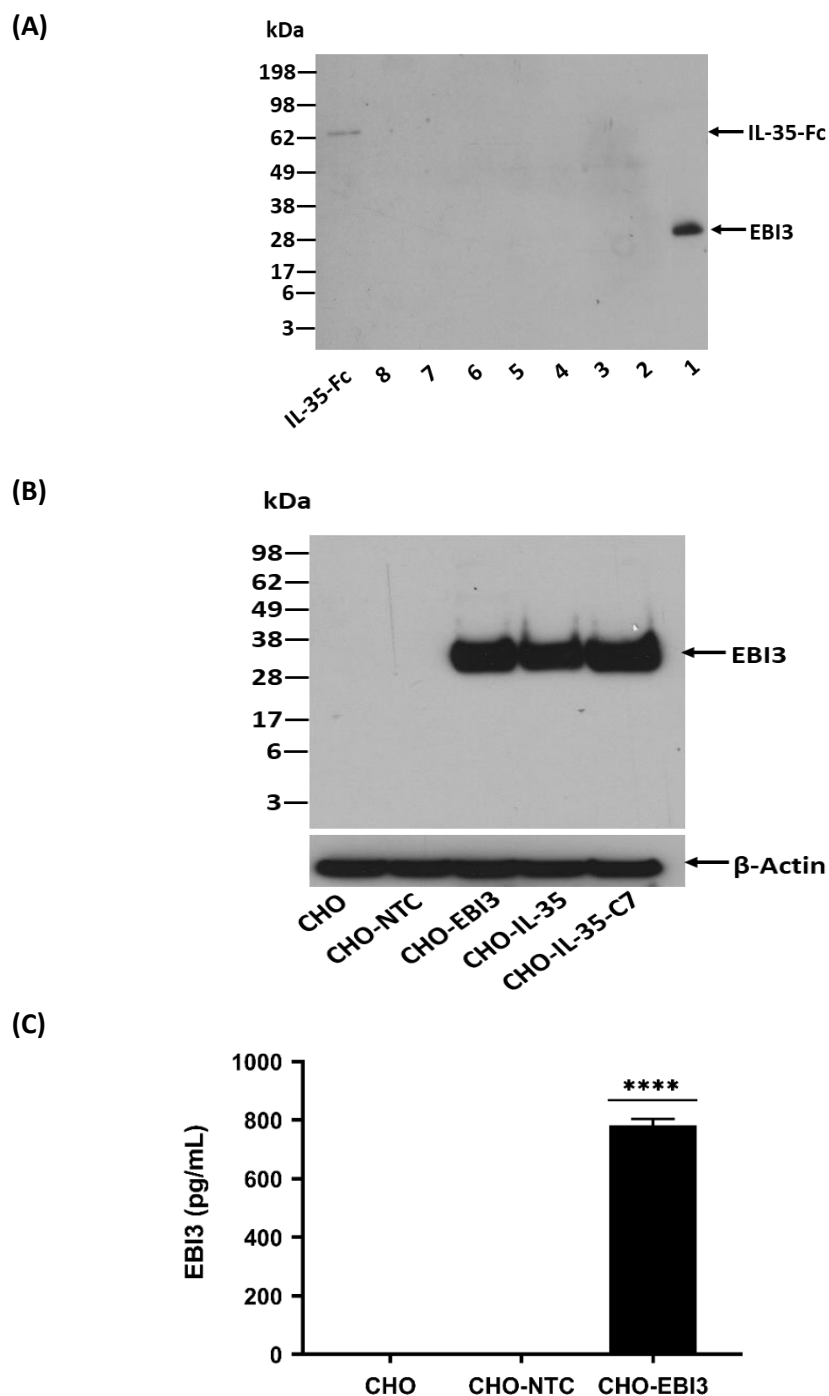


Figure 4.1 Detection of EB13 expression in CHO cells stably transfected with the human EB13 expression plasmid. CHO cells were stably transfected with EB13 expression plasmid. Single clones were screened for expression of EB13 by Western Blotting (recombinant IL-35-Fc (IL-35-Fc) was used as a control) (A). After development of CHO cell lines, lysates were analysed by Western Blotting to confirm EB13 overexpression (B). Supernatants from CHO-EB13 cells were analysed by ELISA to detect secreted EB13 (C). Untransfected CHO cells, or CHO cells transfected with an empty plasmid (CHO-NTC) were used as negative controls. Re-used lysate from a screened double-transfected CHO cell clone (CHO-IL-35-C7) was used as a positive control. β -Actin was used as a loading control. For the ELISA graph, bars represented mean+SEM. (N=3). Statistics were performed using One Way ANOVA and Dunnett's post-hoc test, to compare means against untransfected CHO cells. **** = $p < 0.0001$.

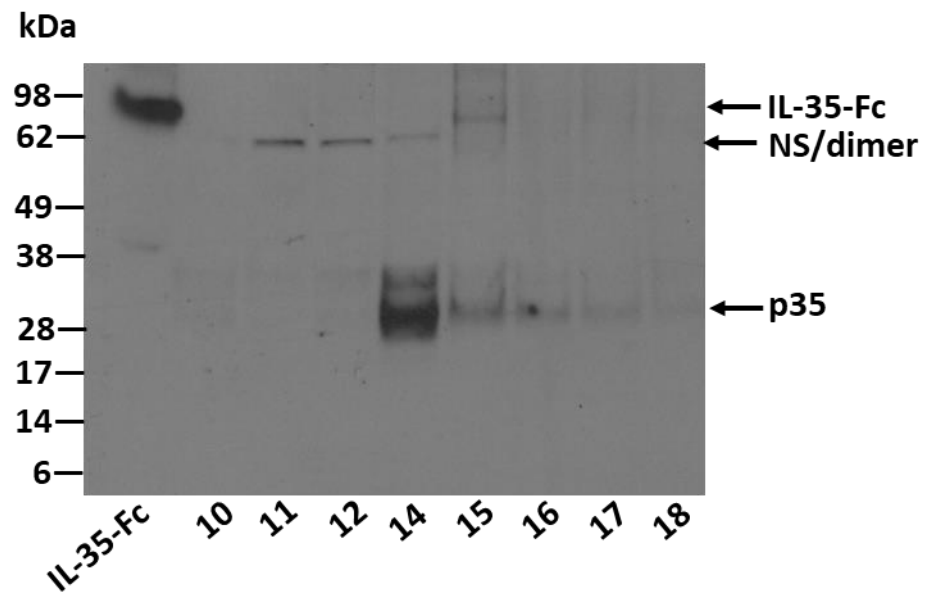
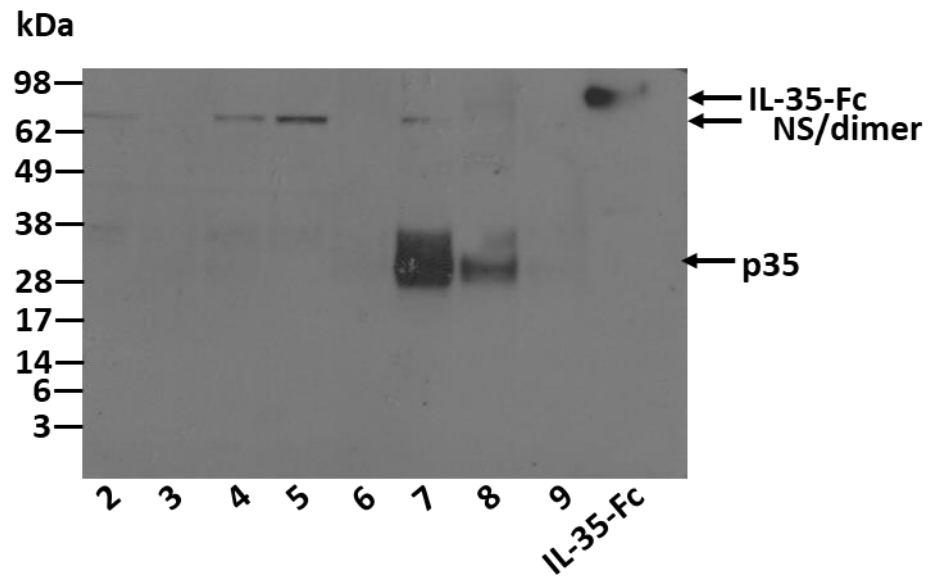
4.4.1.2 *Development of a CHO cell line that overexpresses both human EBI3 and p35*

The next objective was to develop a CHO cell line that overexpressed both EBI3 and p35, as co-expression may result in formation of the IL-35 heterodimer. CHO-EBI3 cells were transfected with the p35 expression plasmid. Stable transfectants were selected using both G418 (500 µg/mL – to maintain selection pressure for EBI3 expression) and puromycin (5 µg/mL, to select for cells stably transfected with the p35 plasmid).

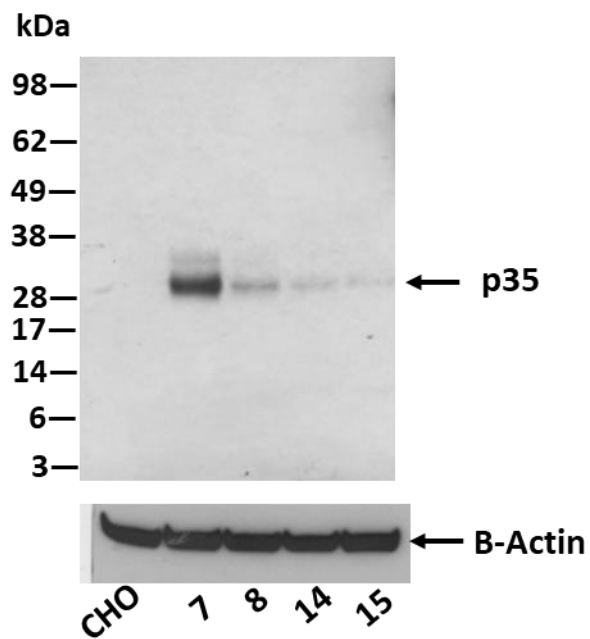
Lysates were taken from isolated clones and examined by Western Blot (**Figure 4.2A**). P35 expression was detected in Clones 7, 8, 14, 15, 16 and 17. This was evidenced by bands present at ≈ 31 kDa, corresponding to the dominant form of p35 (Murphy et al. 2000). Faint bands were also detected at ≈ 35 kDa in Clones 7, 8 and 14. These were indicative of the unstable p35 precursor protein, present prior to cleavage of the signal peptide (Murphy et al. 2000). Additional bands were also observed. Signals detected near the 62 kDa marker were deemed either artifacts of non-specific antibody binding, as they are also present in all negative CHO cell controls in a subsequent blot (**Figure 4.4B**), or p35 complexes (possible dimers) that failed to be reduced prior to SDS-PAGE (**Figure 4.2A**, “labelled NS/dimer”). Overall, the data suggested that p35 was successfully overexpressed in the following stably transfected CHO-EBI3 clones - 7, 8, 14, 15, 16 and 17.

It was prudent to both confirm p35 overexpression but also assess the maintenance of EBI3 expression in selected clones. As clones 7, 8, 14 and 15 displayed the highest signal intensity for p35 expression, they were subcultured further. Equal protein concentrations from collected lysates (10 µg) were examined by Western Blotting to confirm the co-expression of p35 (**Figure 4.2B**) and EBI3 (**Figure 4.2C**). Expression of p35 was confirmed in Clones 7, 8, 14 and 15, with bands present indicating expression of the dominant 31 kDa form of p35 (**Figure 4.2B**). EBI3 expression however, was only detectable in Clones 7, 8 and 14 (**Figure 4.2C**). Data therefore revealed that, in at least three clones, transfection of the p35 expression plasmid into CHO cells that overexpress EBI3 (CHO-EBI3), resulted in generation of single clones that co-expressed both proteins.

(A)



(B)



(C)

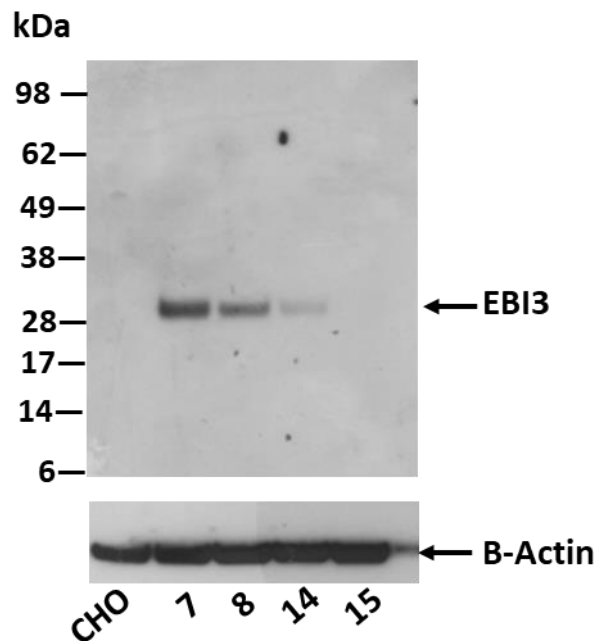


Figure 4.2 Western Blot detection of overexpressed p35 and EBI3 in clones from CHO-EBI3 cells stably transfected with p35 cDNA. CHO-EBI3 cells were transfected with the p35 expression plasmid. Stable transfectants were selected using both G418 (for EBI3 expression) and puromycin (for p35 expression). Single clones were screened for expression of p35 by Western Blot (A). Highest expressing clones were then analysed to confirm p35 expression (B) and maintenance of EBI3 expression (C). β -Actin was used as a loading control. NS, non-specific.

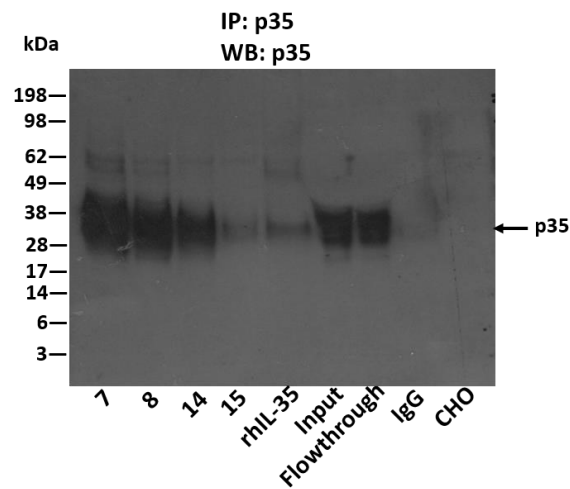
4.4.1.3 Detection of the secreted IL-35 heterodimer and establishment of the CHO-IL-35 cell line

The next objective was to detect the association and secretion of EBI3 and p35 as the IL-35 heterodimer, and to select a clone that will represent the CHO-IL-35 cell line. To detect EBI3/p35 in culture supernatants, clones from CHO-EBI3 cells transfected with the p35 expression plasmid (Clone 7, 8, 14, 15) were subcultured and supernatants collected. P35 was immunoprecipitated from solution and associated EBI3 detected by co-immunoprecipitation. Successful immunoprecipitation of p35 (**Figure 4.3A**) and capture of interacting EBI3 (**Figure 4.3B**) were detected by Western Blotting.

p35 was successfully immunoprecipitated in all tested clones (**Figure 4.3A**). Similar to intracellular Western Blot data, the highest signal of secreted p35 was detected in Clone 7, with the lowest in Clone 15. Western Blot data using the anti-EBI3 antibody confirmed successful co-immunoprecipitation of EBI3 in Clones 7, 8, 14 and less so in 15 (**Figure 4.3B**). EBI3 was also detected in the positive control lane (recombinant human IL-35), but at a slightly higher molecular weight, suggesting differential modifications in secreting cells. When assessing the efficiency of co-immunoprecipitation, band intensities observed were similar between 2% input and flowthrough controls, both for EBI3 and p35. This was likely indicative of very high concentrations of each protein in solution, rather than inefficiency of the assay to extract sufficient target protein. EBI3 was also detected in the IgG control. This was likely captured in residual sample supernatant that failed to be removed from beads or tubes during wash steps performed prior to elution.

Overall, the data confirmed the natural association between co-expressed human EBI3 and p35 in culture supernatants taken from double transfected CHO cells. This suggested that the devised methodology successfully culminated in establishment of CHO cell lines that overexpress human IL-35 in its native form. As Clone 7 had the highest signal strength detected for co-immunoprecipitated EBI3 and p35, it was selected as the CHO-IL-35 cell line.

(A)



(B)

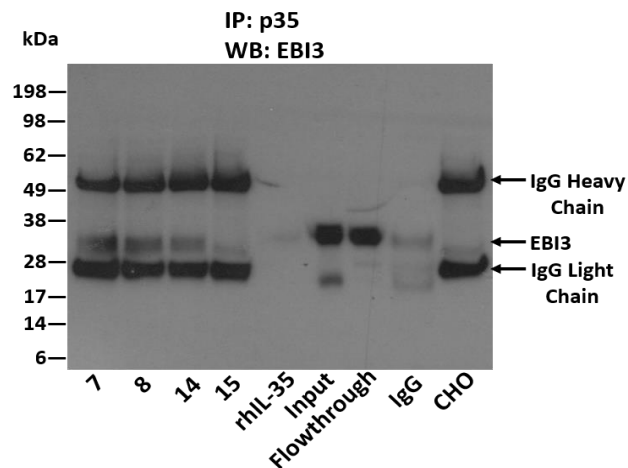


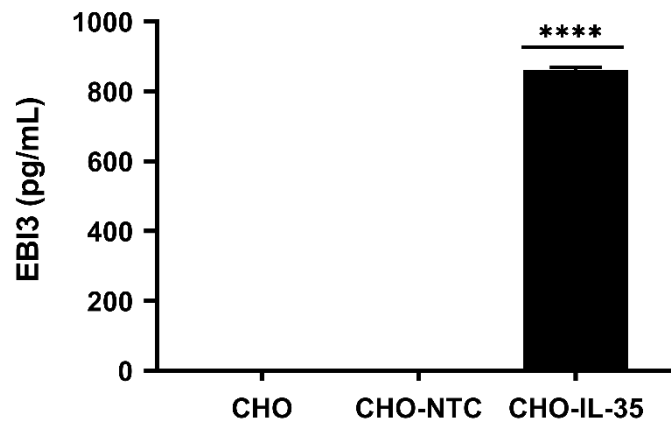
Figure 4.3 Detection of IL-35 in culture supernatants via interactions between co-expressed EB13 and p35. Supernatants were collected from clones of CHO-EB13 cells transfected with the p35 expression plasmid (Clone 7, 8, 14, 15). p35 was immunoprecipitated from solution using an anti-p35 antibody. Precipitated p35 (A) and co-immunoprecipitated EB13 (B) were detected by Western Blotting. IgG chains eluted from pulldown antibodies are shown at approximately 28 and 50 kDa. Input and flowthrough controls contain 2% volume of the Clone 7 sample taken before and after immunoprecipitation. IgG control contains Clone 7 supernatant treated with IgG dynabeads without the use of anti-p35 antibody.

4.4.1.4 Confirmation of EBI3, p35 and IL-35 overexpression in the established CHO-IL-35 cell line

Representative data confirming the overexpression of EBI3, p35 and IL-35 in the CHO-IL-35 cell line was next obtained. CHO-IL-35 cells were subcultured, and collected lysates (treated with brefeldin A) and supernatants (untreated) examined by Western Blot and ELISA, respectively. Western Blot data confirmed overexpression of EBI3 (**Figure 4.1B, Lane CHO-IL-35**). EBI3 ELISA data confirmed secretion of overexpressed EBI3 (**Figure 4.4A**). Co-expression of p35 was confirmed by Western Blotting (**Figure 4.4B**). Additional bands were also detected above 50 kDa in the CHO-IL-35 samples, which were likely capture of non-reduced p35 in protein complexes (**Figure 4.4B, labelled ***). Bands above 62 kDa (labelled NS/dimer), were presumed non-specific as they were detected in negative controls. Though, the non-specific target may also be cross-detected with dimers of 31 kDa p35 that failed to be reduced. Attempts to confirm IL-35 secretion using an ELISA kit failed, as due to lack of antibody specificity, the data was deemed unreliable (**data not shown**).

In summary, data thus far confirmed that stable transfection of CHO cells with the EBI3 expression plasmid, followed by that of the p35 expression plasmid, resulted in co-expression of both proteins. These proteins interacted naturally to form the IL-35 heterodimer. Thus, this methodology resulted in successful formation of a CHO cell line that overexpressed human IL-35 in its native form.

(A)



(B)

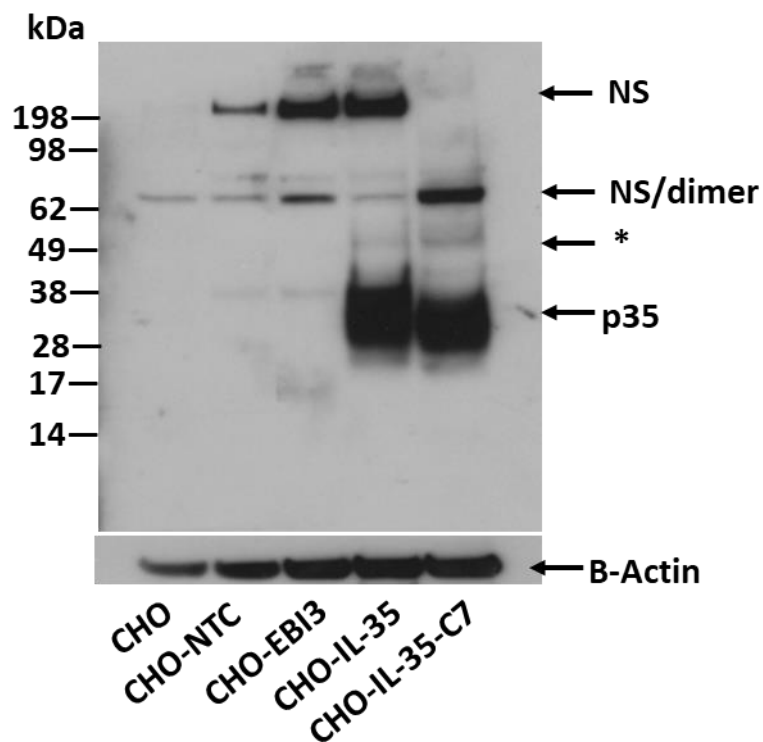


Figure 4.4 Confirmation of EB13 and p35 overexpression in the CHO-IL-35 cell line. Cell lysate and supernatant taken from developed cell lines were analysed to confirm overexpression of p35 by Western Blot and secretion of EB13 by ELISA. ELISA data is shown in (A). P35 overexpression was confirmed by blot data (B). Untransfected CHO cells, or those transfected with a control plasmid (CHO-NTC), were used as negative controls. A previously used cell lysate (CHO-IL-35-C7) was used as a positive control. β -Actin was used as a loading control. NS, non-specific. NTC, negative transfection control. * non-reduced p35 complexes. For the ELISA graph, bars represented mean+SEM. (N=3). Statistics were performed using One Way ANOVA and Dunnett's post-hoc test, to compare means against untransfected CHO cells. **** = $p < 0.0001$.

4.4.2 Development of a FaDu cell line that overexpresses and secretes human IL-35

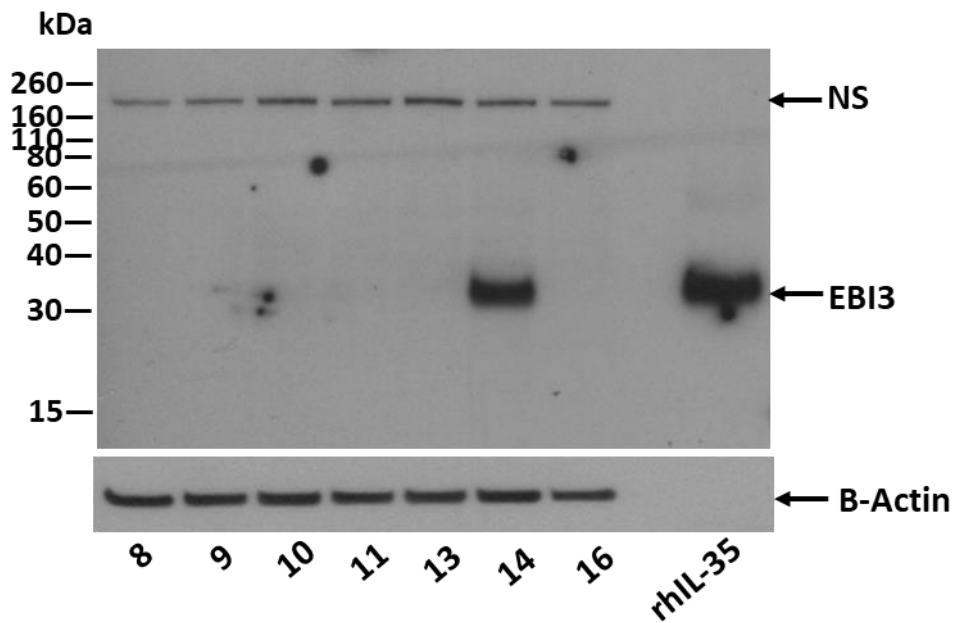
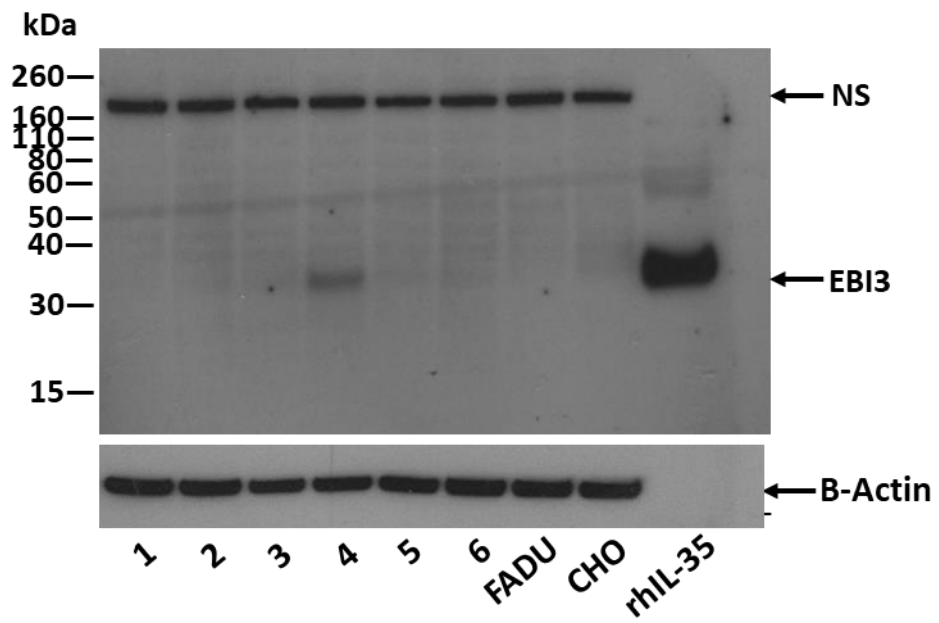
4.4.2.1 Development of a FaDu cell line that overexpresses human EBI3

The next Chapter aim was to use the same methodology to establish a FaDu cell line that overexpressed and secreted IL-35. To complete this, the first objective was to establish a FaDu cell line that overexpressed EBI3 (FaDu-EBI3). FaDu cells were transfected with the EBI3 expression plasmid and stable transfectants selected using G418 (500 µg/mL). Isolated single clones were then screened to detect those which overexpressed EBI3. Western Blot data confirmed EBI3 expression in Clones 4 and 14 (**Figure 4.5A**). Additional bands detected above the 160 kDa marker were assumed a result of non-specific binding of the anti-EBI3 antibody, as it was also present in the non-human CHO cell sample. Thus, stable transfection with the EBI3 expression plasmid resulted in two FaDu cell clones that successfully overexpressed EBI3.

To confirm overexpression of EBI3, and to select a clone that would represent the FaDu-EBI3 cell line, lysates were taken from Clones 4 and 14, and equal protein concentrations (10 µg) analysed by Western Blot (n=2). Data obtained confirmed that Clone 14 expressed high levels of EBI3, whereas EBI3 could no longer be detected in Clone 4 (**Figure 4.5B**). As Clone 14 was confirmed to overexpress EBI3, and at levels higher than in Clone 4, it was selected as the FaDu-EBI3 cell line.

After development of all transfected FaDu cell lines, representative data was generated to confirm EBI3 overexpression and secretion in relevant cell lines. Lysates and supernatants were collected and analysed. Western Blot data (**Figure 4.5C**) and ELISA data (**Figure 4.5D**) confirmed EBI3 overexpression and secretion in the FaDu-EBI3 cell line. The data therefore demonstrated that stable transfection of FaDu cells with the EBI3 expression plasmid successfully resulted in establishment of a FaDu cell line that overexpressed and secreted human EBI3 (FaDu-EBI3).

(A)



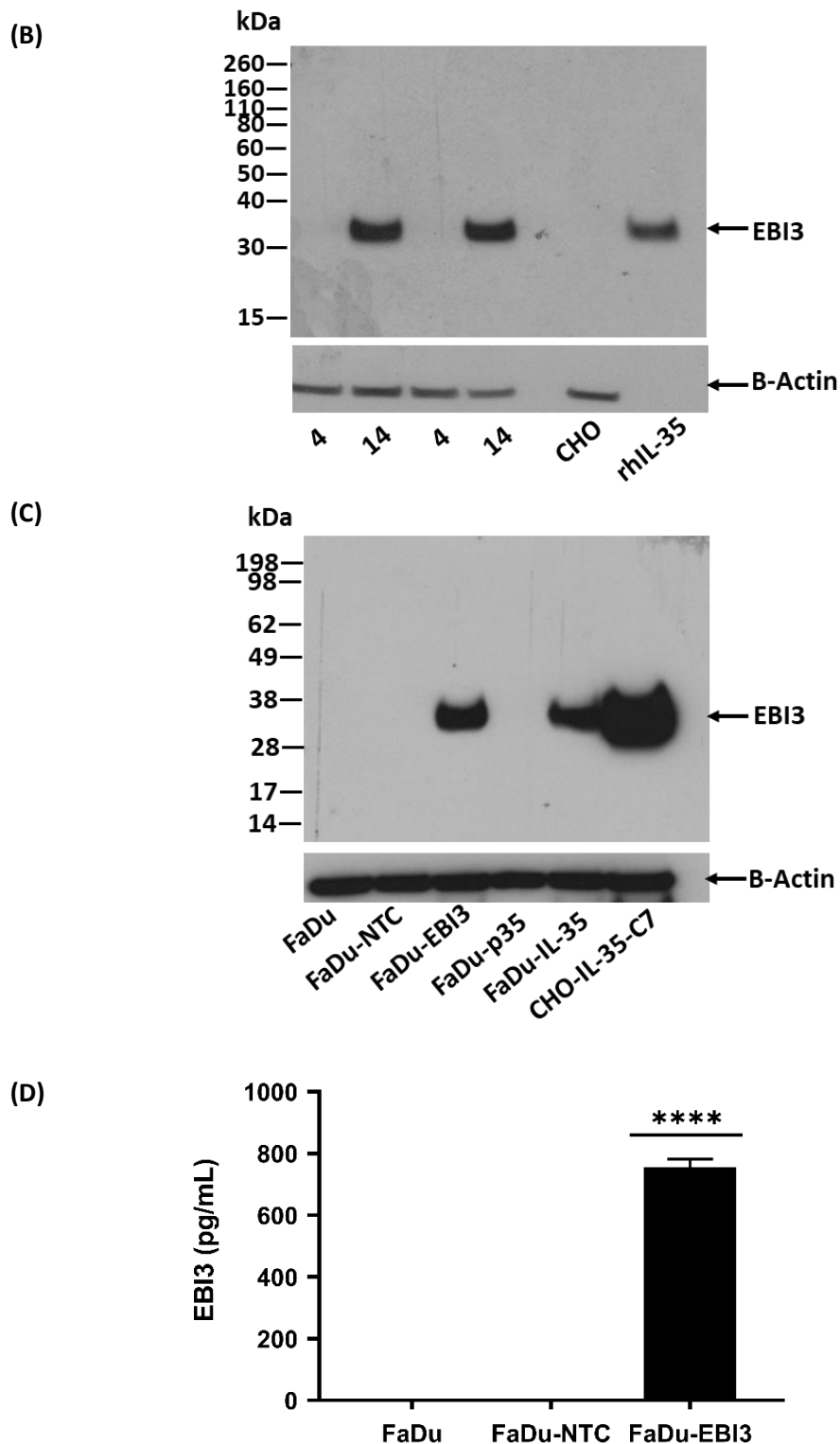


Figure 4.5 Detection of EBI3 overexpression in stably transfected FaDu cells. FaDu cells were stably transfected with the EBI3 expression plasmid. EBI3 expression was screened in single clones by Western Blot (A). Confirmation of expression was assessed in selected clones by Western Blot (n=2) (B). Overexpression and secretion of EBI3 in the FaDu-EBI3 cell line were confirmed by Western Blotting (C) and ELISA (D), respectively. NS, non-specific. For the ELISA graph, bars represented mean+SEM. (N=3). Statistics were performed using One Way ANOVA and Dunnett's post-hoc test, to compare means against untransfected FaDu cells. **** = $p < 0.0001$.

4.4.2.2 *Development of a FaDu cell line that overexpresses human p35*

To study the potential roles of individual IL-35 subunits in the regulation of anti-tumour immunity in HNSCC, and as a negative control of the IL-35 overexpression cell model, the next objective was to generate a FaDu cell line that overexpressed human p35. FaDu cells were transfected with the p35 expression plasmid and stable transfectants selected using puromycin treatment (1 µg/mL). To identify single clones that successfully overexpressed human p35, lysates were collected and analysed by Western Blot. Data showed that p35 was overexpressed in Clones 4, 5, 6, 7, 10 and 12 (**Figure 4.6A**). In each of these samples, both the ≈35 kDa transient precursor form, and the dominant 31 kDa forms of p35 were detected. Additional bands detected between 15 and 30 kDa markers (labelled with *) were presumed p35 degradation products. The data thus revealed the successful overexpression of p35 in several clones from stably transfected FaDu cells.

It was next assessed whether p35 overexpression could be confirmed, and which clone expressed the highest concentration of p35, that would subsequently represent the FaDu-p35 cell line. As Clone 7 and 12 displayed the highest p35 signal intensities in the previous experiment, they were subcultured and lysates from two separate cultures analysed for p35 expression by Western Blotting. p35 expression was confirmed in both clones (**Figure 4.6B**). Band intensity appeared to be highest in Clone 7. P35 detected was at a slightly lower molecular weight than in the recombinant IL-35 control, which may be due to additional glycosylation of the secreted form of p35 (Murphy et al. 2000). A band at a higher molecular weight was also detected in the control, and may represent a p35 dimer (**Figure 4.6B, Lane, rhIL-35**). Additional bands labelled NS (non-specific) were deemed so as they were detected in untransfected CHO cells which are not human. The results from these experiments conveyed that Clone 7 overexpressed the highest concentration of human p35 after stable transfection, and thus was designated the FaDu-p35 cell line.

Data representing p35 overexpression in the designated FaDu-p35 cell line was next acquired. The selected clone was subcultured, and lysate analysed by Western Blotting. The data confirmed overexpression of p35 in the FaDu-p35 cell line (**Figure 4.6C**). A faint band was detected, though this was likely a reflection of comparatively lower expression when compared to the FaDu-IL-35 and CHO-IL-35 lysate samples,

and possibly required a longer exposure time. Overall, the data suggested that stable transfection of FaDu cells with the p35 expression plasmid successfully resulted in overexpression of p35 and the establishment of a FaDu-p35 cell line.

4.4.2.3 Development of a FaDu cell line that overexpresses both human EBI3 and p35

As performed with CHO cells, FaDu-EBI3 cells were transfected with the p35 expression plasmid. Stable transfectants were selected in culture medium containing antibiotics for both EBI3 (G418, 500 µg/mL) and p35 (puromycin, 1 µg/mL) expression plasmids. To identify clones that overexpressed p35 and maintained expression of EBI3, lysates taken from isolated clones were analysed by Western Blotting. P35 expression was detected in Clones 9, 17 and 25 (**Figure 4.7A**). EBI3 expression was maintained in Clones 9, 17, 18 and 25, but was not detectable in Clones 1 and 13 (**Figure 4.7B**). Lack of EBI3 signal in the recombinant IL-35 sample was likely due to poor stability of the cytokine. The data therefore demonstrated that stable transfection of FaDu-EBI3 cells with the p35 expression plasmid successfully resulted in clones that co-expressed EBI3 and p35.

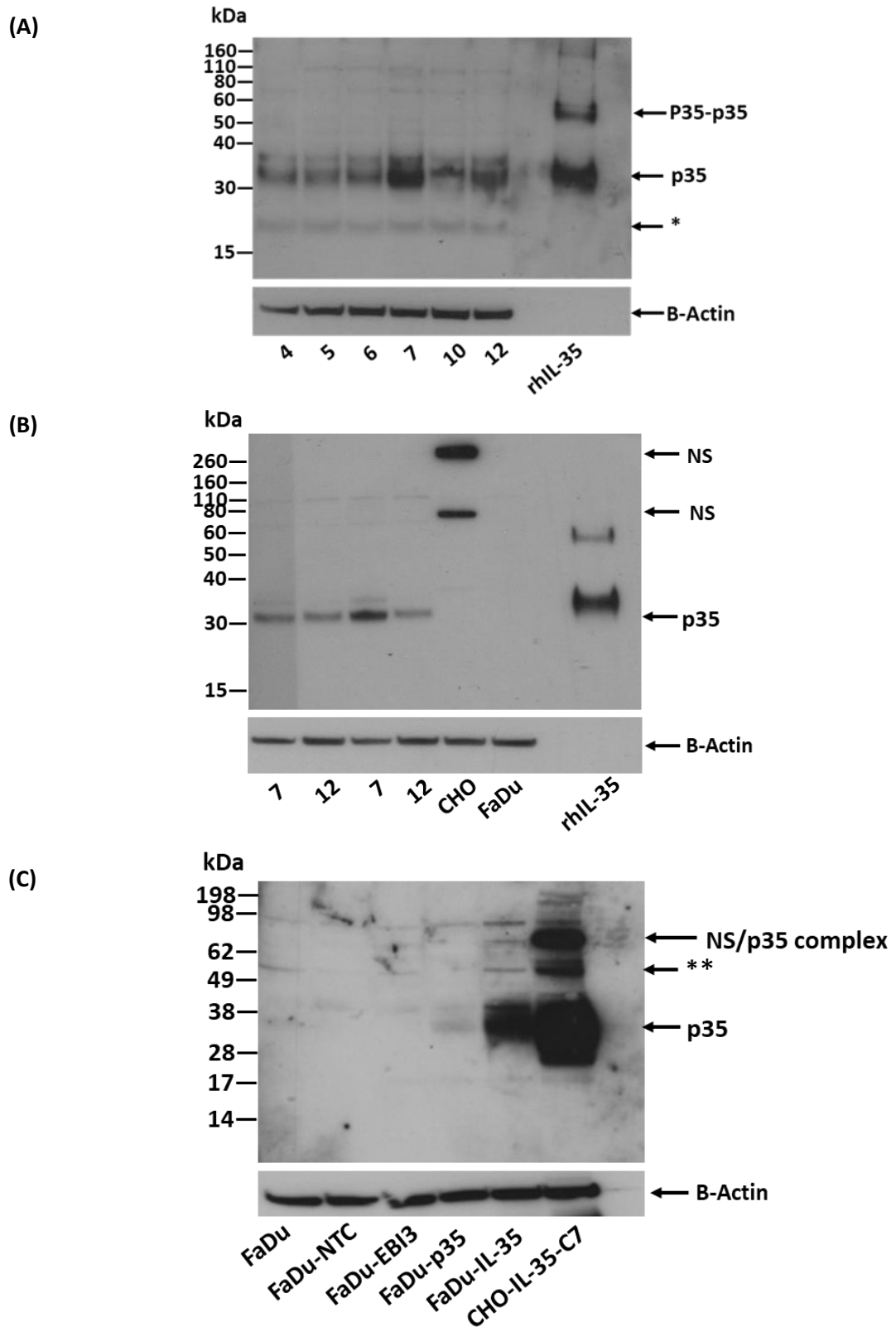


Figure 4.6 Detection of p35 overexpression in transfected FaDu cells. FaDu cells were transfected with the p35 expression plasmid and stable transfectants selected using puromycin. P35 expression was detected in single clones using Western Blotting (A). Expression was confirmed in selected clones by additional Western Blotting (n=2) (B). p35 expression was confirmed in the designated FaDu-p35 cell line by Western Blotting (C). * p35 degradation product. ** non-reduced p35/sample spillover

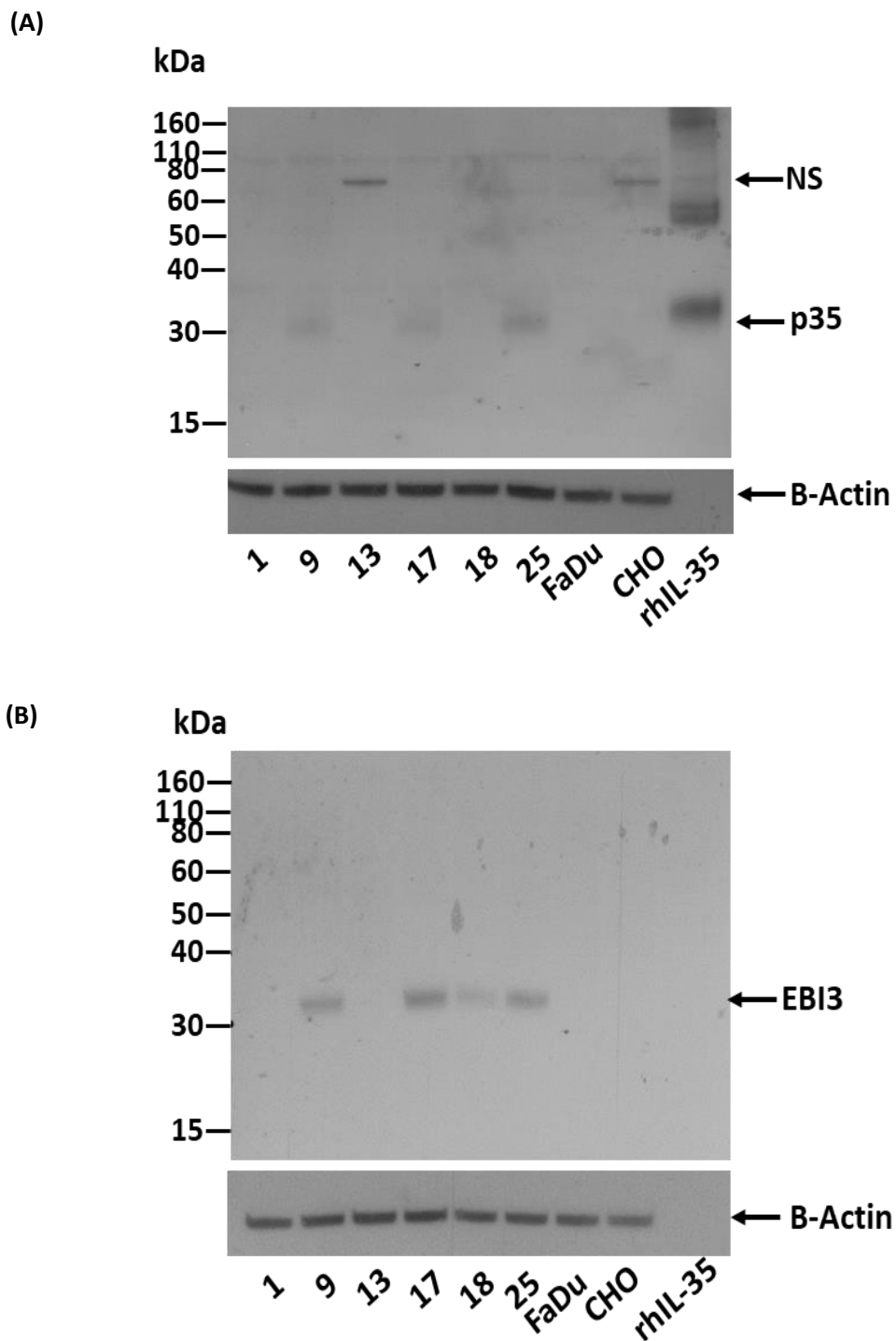


Figure 4.7 Detection of p35 and EB13 expression in FaDu-EBI3 cells transfected with p35. FaDu-EBI3 cells were transfected with the p35 expression plasmid. Single clones from stable transfectants were examined for expression of p35 (A) and EB13 (B) by Western Blot. β -Actin was used as a loading control.

4.4.2.4 *Detection of the secreted IL-35 heterodimer and establishment of the FaDu-IL-35 cell line*

Following detection of clones that co-expressed EBI3 and p35, the next objective was to identify in which of these clones EBI3 and p35 were secreted in association with each other as the IL-35 heterodimer, and to select the highest expressing clone as the model FaDu-IL-35 cell line. Clones 9, 17, 18 and 25, which co-expressed EBI3 and p35, were subcultured and their supernatants collected. p35 was immunoprecipitated from each sample using an anti-p35 antibody. To confirm immunoprecipitation of p35, and association of EBI3, anti-p35 and anti-EBI3 antibodies were used during Western Blotting, respectively.

Blot data using the anti-p35 antibody confirmed the successful immunoprecipitation of p35 from the supernatants of Clones 9, 17 and 25 (**Figure 4.8A**). Signal strength was high in Clones 9 and 25 but was much lower in Clone 17. Bands corresponding to p35 were higher in molecular weight when compared to that of the control (lysate from CHO-IL-35 cells), possibly reflecting additional glycosylation of the secreted form of p35 (Carra et al. 2000; Murphy et al. 2000). As with previous data, p35 could not be detected in Clone 18. Additional bands were detected in the control CHO-IL-35 lysate sample (**Figure 4.8A, Lane CHO-IL-35**). The signal proximal to the 75 kDa marker was observed previously and deemed either non-specific signal, or captured protein complexes containing non-reduced p35 (**Figure 4.7A, Figure 4.8A, Lane CHO-IL-35**). The band detected above 250 kDa may be a larger protein complex containing p35.

Co-immunoprecipitation of EBI3 was detected in Clones 9, 17, 18 and 25 (**Figure 4.8B**). As p35 was not detectable in Clone 18, EBI3 signal observed in this clone was likely either, co-immunoprecipitated EBI3 bound to p35, the latter of which was present but at concentrations too low to be detected, or free unbound EBI3 present in residual supernatant that had failed to be removed by wash steps before sample elution. The latter was also assumed of bands depicting the presence of EBI3 in the IgG control lane. Alternatively, this signal could have been produced via leakage of sample from the positive control during loading of SDS-PAGE gels. An additional band was also detected below the IgG light chain in Clones 9, 25 and the IgG control lane. These were likely transient signals of EBI3 that had been degraded through sample

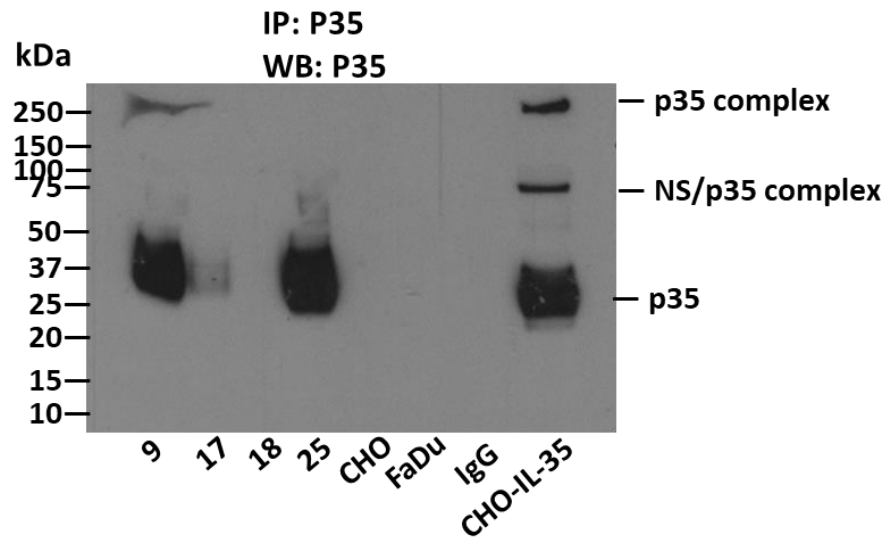
preparation, or via the possible activity of secreted proteases. Together, p35 and EBI3 data showed that Clone 25 expressed and secreted the highest concentration of associated EBI3 and p35 (IL-35). Clone 25 was therefore designated the FaDu-IL-35 cell line.

4.4.2.5 Confirmation of EBI3, p35 and IL-35 overexpression in the established FaDu-IL-35 cell line

The final objective of the chapter was to generate data that represented the overexpression of EBI3, p35 and IL-35 in the established FaDu-IL-35 cell line. After further subculture, lysates and supernatants were analysed by Western Blotting and ELISA. p35 expression in FaDu-IL-35 cells was confirmed by Western Blotting (**Figure 4.6C, Lane FaDu-IL-35**). Additional bands were also detected. In the FaDu-IL-35 and control CHO-IL-35-C7 samples, signal was detected at ≈ 50 kDa (marked **). This band had been detected previously in CHO-EBI3 cells transfected with the p35 plasmid (**Figure 4.4B**). As it had not been seen in previous FaDu cell blots detecting p35, it was possible that this band was derived from protein that had leaked from the CHO-IL-35-C7 lane into the FaDu-IL-35 lane during SDS-PAGE loading. Alternatively, as previously stated, it may depict a non-reduced p35 complex common to both cell lines. Another band was detected slightly under the 98 kDa marker in the FaDu-IL-35 sample. This was likely from background, non-specific staining that failed to be washed away, as this signal was faintly detectable in other lanes. A strong signal was also detected in the CHO-IL-35-C7 control lane above the 62 kDa marker (labelled “p35 complex”). This may depict dimerisation of the 35 kDa (glycosylated but not processed) or 36 kDa (ready to be secreted) forms of p35, or p35 in complex with EBI3, all of which may not have been completely reduced prior to SDS-PAGE.

EBI3 expression in the FaDu-IL-35 cell line was also confirmed by Western Blotting (**Figure 4.5C, Lane FaDu-IL-35**) and ELISA (**Figure 4.9A**). IL-35 formation and secretion was confirmed using a human IL-35 ELISA kit (**Figure 4.9B**). Therefore, the sum of data in this Chapter has validated the proposed methodology. It demonstrated that successive stable transfections of FaDu cells with the EBI3 expression plasmid, followed by that of the p35 expression plasmid, culminated in the development of a HNSCC cell line that overexpressed the IL-35 heterodimer in its native form.

(A)



(B)

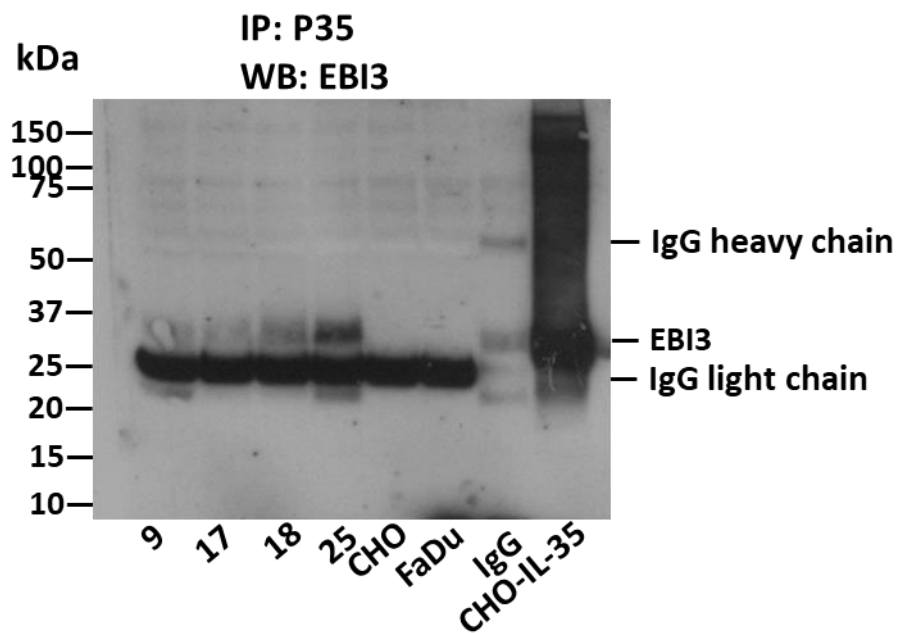
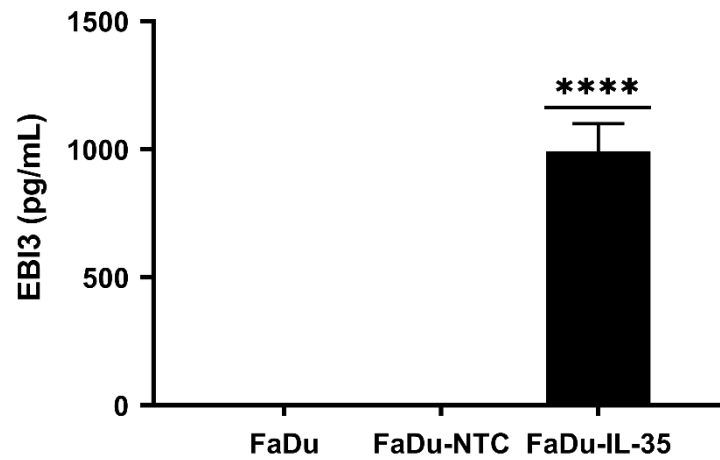


Figure 4.8 Detection of IL-35 secretion via association of EBI3 and p35 in FaDu cells that co-express EBI3 and p35. FaDu cell clones that co-expressed EBI3 and p35 were subcultured and supernatants collected. P35 was immunoprecipitated from solution using an anti-p35 antibody. Eluted protein was analysed for detection of precipitated p35 (A) and associated EBI3 (B) by Western Blotting.

(A)



(B)

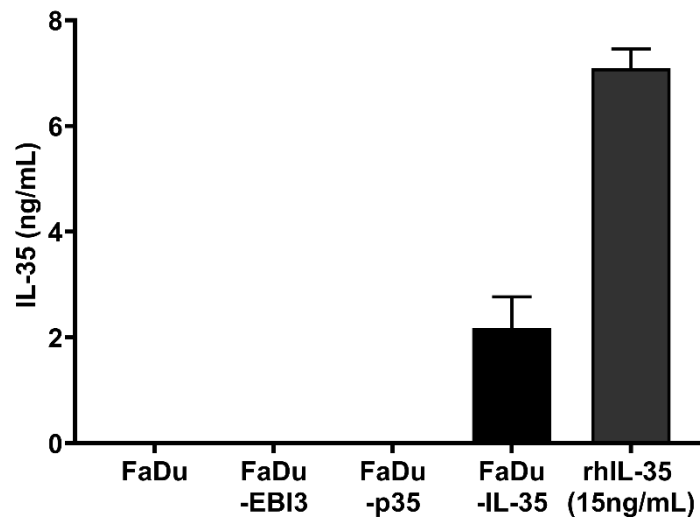


Figure 4.9 Confirmation of EB13 and IL-35 secretion in the FaDu-IL-35 cell line. The FaDu-IL-35 cell line was subcultured and lysates and supernatants collected. Lysates were examined by Western Blot to confirm overexpression of EB13 (shown in Figure 4.5C) and p35 (shown in Figure 4.6). Secretion of EB13 was confirmed by ELISA (A). Bars represented mean+SEM. N=3. Statistics were performed using One Way ANOVA and Dunnett's post-hoc test, to compare means against untransfected FaDu cells. **** = $p < 0.0001$. Secretion of IL-35 was confirmed by ELISA (B). N=1. Samples ran in duplicate. Data represents mean+SD.

4.5 Discussion

Interleukin 35 (IL-35) is an immunosuppressive cytokine that can inhibit anti-tumour immunity. Studies in Chapter 3 reported that the HNSCC cell lines FaDu and H357 significantly upregulate IL-35 gene expression in response to stimulation with IFN γ and TNF α . This may reveal a mechanism used by inflamed tumour cells to evade anti-tumour immunity. To study the potential role of HNSCC-derived IL-35 in the regulation of anti-tumour immunity, this Chapter sought to develop an IL-35 overexpression model using FaDu cells. Unlike those in previous reports, the model derived in this Chapter was intended to produce IL-35 in its native form. It was hypothesised that, by using stable transfection to develop a FaDu cell line that overexpressed EBI3, followed by stable transfection of these cells to establish a cell line which also overexpressed p35, co-expressed EBI3 and p35 would naturally associate within the cell. They would then become secreted together as the IL-35 heterodimer. Experiments performed verified that this methodology successfully created a FaDu cell line that overexpressed IL-35 (FaDu-IL-35).

4.5.1 Chapter Methodology

To develop the FaDu-IL-35 cell model, a detailed approach was used. Vector design was first considered. As FaDu cells may have been difficult to transfect, circular plasmids were used. DNA from circular plasmids are transfected at higher efficiencies than from linear plasmids. This is because, when entered into cells, linear plasmid DNA are vulnerable to destruction by cytoplasmic exonucleases (Von Groll et al. 2006; McLenachan et al. 2007).

Previous IL-35 cell models often use vectors encoding both EBI3 and p35 genes (Collison et al. 2007; Niedbala et al. 2007; Wang et al. 2016a). The current study employed two individual plasmids for the respective overexpression of EBI3 and p35. To promote high levels of transgene expression, and subsequent production of full-length, functional proteins, each plasmid incorporated open reading frames of either the EBI3 or p35 gene, both under the control of the strong CAG promoter. Each plasmid was also designed to contain genes that confer antibiotic resistance, necessary to generate stably transfected clones. Finally, to transfer plasmid DNA into target cells, the lipofection method, using the Lipofectamine 2000 reagent, was used as it yields

high transfection efficiencies whilst minimising detriment to cell health. Using these designs, it was expected that stable transfection would lead to the integration of plasmid DNA into the host cell genome. Here, transcription via the activity of the strong CAG promoter drives transgene overexpression, which is followed by production of full-length protein.

Following plasmid design, a novel approach was devised to develop cell lines that overexpressed IL-35 in its native form. IL-35 is a heterodimer of EBI3 and p35, which interact in a non-covalent manner. Previous reports have used a single transfection procedure, involving the transfer of a plasmid containing linker peptides that ensure covalent associations between EBI3 and p35 (Collison et al. 2007; Niedbala et al. 2007; Wang et al. 2016a). These interactions do not mimic the natural formation of the IL-35 heterodimer. To account for this in the current study, cells were transfected with two separate plasmids. Moreover, rather than transfecting both plasmids at the same time, it was proposed that a cell line that overexpressed EBI3 would be established first. These cells would then be stably transfected with the p35 plasmid, creating a cell line that co-expressed both subunits. Cells would then be assessed to determine the natural association of these subunits, and their secretion as the native IL-35 cytokine. CHO cells were used to validate the methodology prior to transfecting FaDu cells, as they are highly amenable to transfection and are considered a standard for recombinant protein production (Wurm 2004). Once validated, the same approach was applied to FaDu cells.

A gap between stable transfections with each plasmid was deemed important. This may have mitigated potential detrimental effects caused by adding both at the same time. Transfection of large amounts of exogenous DNA may have induced cell stress and affected cell viability. It may also have caused transgene silencing as a protective response. An advantage of the approach used, was that it enabled the development of FaDu cell lines that overexpressed EBI3 or p35, independently of one another. These could be used in future experiments to investigate the potential roles of each subunit in HNSCC, whilst also representing negative controls of IL-35 overexpression. Considering these points, the proposed approach was deemed suitable to achieve the Chapter aims.

There were limitations to the applied methodology. Transgene expression is predicated upon integration of plasmid DNA into the host cell genome. Integration occurs at random loci, which has several drawbacks. Circular plasmids require linearisation to generate loose DNA ends which are then integrated. Cleavage of the circular plasmid occurs at random sites (Finn et al. 1989; Wurm 2004). Should this happen at a locus which interrupts transgene coding regions or regulatory elements, correct protein production may not take place. A limitation therefore, is that approximately two months were required to isolate and expand single clones from polyclonal stable transfectants, and then screen which clones integrated the plasmid correctly resulting in protein overexpression.

There was also a risk that random integration of plasmid DNA occurred at loci which interrupted the coding region of important host genes. Mutations in these genes may cause unintended changes to cell health and/or behaviour. A common side effect of random integration is the occurrence of de novo transgene silencing. This may cause heterogeneous transgene expression in developed cell lines, which over time could lead to complete loss of expression (Wurm 2004). To circumvent these issues, alternative approaches could have been used. By acquiring the genomic sequence of the host cell line, site-specific integration technologies including Cre-lox (Bode et al. 2000; Hamaker and Lee 2018), Flp-FRT (Zhou et al. 2010; Turan et al. 2013) and zinc finger nucleases (Malphettes et al. 2010; Liu et al. 2017; Hamaker and Lee 2018), could have been adopted. Advantages of these include, improved integration efficiencies and high gene expression in several clones (Liu et al. 2017; Hamaker and Lee 2018). Loci-specific integration also minimises off-target effects caused by host gene mutations. These technologies are very lengthy and laborious though, and do not produce cell lines immune to genetic and epigenetic changes that could silence transgenes over time. Regardless of the limitations, the methodology applied in the Chapter successfully resulted in establishment of CHO and FaDu cell lines that overexpressed IL-35, and thus was fit for purpose.

4.5.2 Development of a CHO cell line that overexpressed human IL-35

4.5.2.1 *Development of a CHO cell line that overexpressed human EBI3 (CHO-EBI3)*

Stable transfection of CHO cells with the EBI3 expression plasmid resulted in generation of a monoclonal cell line that overexpressed human EBI3. After stable transfection, single clones were screened for EBI3 overexpression. This was only detected in a single clone. Lack of detection in other screened clones could indicate a limitation of low plasmid integration efficiency. This could be improved by using restriction enzymes to linearise plasmids, preferably at non-coding regions, prior to transfection. This would ensure that a higher number of clones which integrate plasmids overexpress EBI3. This approach would require optimisation of the transfection protocol to minimise cytoplasmic degradation of linear plasmid DNA.

It is also important to consider that EBI3 is readily secreted. During this particular experiment, secretion was not blocked using Brefeldin A. It is possible that EBI3 was overexpressed in other clones, but was mostly secreted, preventing detection of sufficient intracellular concentrations. Evidence supporting this came from subsequent analyses, where high EBI3 signals were detected in CHO-EBI3 lysates when secretion was blocked. Ideally, an ELISA would have been used further assess expression in other screened clones, but a kit was not available at the time of experimentation.

Nevertheless, data from the initial screen, and confirmation experiments which demonstrated intracellular overexpression and secretion of EBI3, provided evidence validating that stable transfection with the designed plasmid led to generation of a CHO cell line that overexpressed human EBI3 (CHO-EBI3).

4.5.2.2 *Development of a CHO cell line that co-expressed human EBI3 and p35.*

After stable transfection of CHO-EBI3 cells with the p35 expression plasmid, Western Blot data displayed p35 overexpression in several of the screened clones. Additional bands were also detected. A band was observed slightly above the 62 kDa marker (**Figure 4.2A**). This signal could have represented non-reduced dimers of the 31 kDa form of p35. Though, as this signal was also found in untransfected CHO cells in subsequent blots (**Figure 4.4B**), it could also be derived from the cross-reactivity of the anti-p35 antibody to a protein in CHO cells that shares a similar target epitope. A

band at a slightly higher molecular weight was also observed in lysate analysed from Clone 15 (**Figure 4.2A**). This could have been from non-reduced p35 dimers (secreted 36 kDa form) or non-reduced p35 bound to EBI3. The identity of these proteins could be confirmed by mass spectrometry. Alternatively, another antibody could have been tested to assess cross-reactivity. However, as these bands were not always present when detecting p35 in this Chapter, proteins that created this signal were possibly transient, products of incomplete sample reduction, non-specific, or very low in concentration. Despite detection of other signals, the data revealed that stable transfection of FaDu-EBI3 cells with the p35 expression plasmid successfully resulted in viable clones that overexpressed p35.

It was important to confirm that clones expressing p35 also maintained EBI3 expression. In a subsequent analysis, p35 overexpression was confirmed these clones, but not all of them maintained EBI3 expression. Expression was reduced in some clones (**Figure 4.2C, Clone 14**), and undetectable in others (**Figure 4.2C, Clone 15**). This raised the question of how EBI3 expression could have been reduced or lost in the stably transfected CHO-EBI3 cell line. Possible answers include –potential integration of p35 plasmid DNA into the genome at sites which interrupted EBI3 transcription, particularly if there was sequence similarity in design elements common to both plasmids. Also, loss of transgene expression within the clone could have been caused by epigenetic silencing, used to reduce cell stress from excess addition of exogenous DNA. Alternatively, the CHO-EBI3 cell line may not have been truly monoclonal, instead comprising a homogeneous population of cells that expressed EBI3, and some that either silenced, or integrated plasmid DNA in such a way that EBI3 was not transcribed. In turn, cells that lost transgene expression may have proliferated faster, eventually diluting out expressing cells.

To mitigate these possible limitations, plasmid design could have been altered to minimise sequence similarity. Alternatively, site directed integration technologies could have been utilised to avoid potential plasmid recombination. Silencing by methylation could have been minimised by switching promoters, perhaps instead using the EF-1 α promoter that has been reported to maintain stable transgene expression (Matzke et al. 2000; Wang et al. 2017). In the event that EBI3 was silenced

in some cells, limiting dilution could be repeated to re-establish monoclonal cell lines that overexpress EBI3.

Regardless of these limitations, the methods used generated more than one clone that co-expressed EBI3 and p35, and as such was successful in achieving the intended objective. Interestingly, when co-expressed, levels of EBI3 and p35 expression were in direct correlation (**Figure 4.2B, Figure 4.2C**). This could have been indicative of the role EBI3 plays in the stabilisation of p35 (Devergne et al. 1997).

4.5.2.3 Detection of IL-35 formation and establishment of a CHO cell line that overexpressed human IL-35

Similar to work by Devergne (Devergne et al. 1997), co-immunoprecipitation was used to identify the natural dimerisation of co-expressed EBI3 and p35 to form native IL-35. EBI3 is readily secreted with or without p35, whereas p35 is secreted in association with binding partners. To prevent saturation of Dynabeads with EBI3 that was not bound to p35, and to maximise detection of EBI3/p35 heterodimers, p35 was selected to be immunoprecipitated from sample supernatants before detection of associated EBI3. Co-immunoprecipitation data evidenced the success of the proposed methodology and validated the Chapter hypothesis. It revealed that when co-expressed, p35 was indeed secreted in association with EBI3 in all tested clones. This suggested that these subunits naturally interacted in cells, and that the IL-35 heterodimer secreted was in its native form.

Data was produced to represent overexpression of EBI3 and p35 in the designated CHO-IL-35 cell line. When detecting p35, signal was also detected slightly above the 49 kDa marker (**Figure 4.4B, marked ***). As this signal was only present in lysates from cells that overexpressed p35, it was likely derived from non-reduced p35 in complex with an unknown protein. As previously discussed, the signal detected above the 62 kDa marker may be non-specific, or from non-reduced p35 dimers, suggesting a possible need to alter sample reduction protocols. EBI3 overexpression and secretion were also confirmed in the CHO-IL-35 cell line. However, due to poor specificity, IL-35 secretion could not be confirmed using the ELISA kit purchased by Cusabio. Despite this, co-immunoprecipitation data, both from the current Chapter, and when used as a positive control in Chapter 3, sufficiently demonstrated enough evidence that EBI3/p35 dimers were formed in the culture supernatants of the established CHO-IL-

35 cell line. Overall, data from CHO cells supported the hypothesis and validated that the proposed methodology.

4.5.3 Generation of FaDu cell line that overexpress IL-35

4.5.3.1 Development of a FaDu cell line that overexpressed EBI3 (FaDu-EBI3)

Following validation of the methodology, the same approach was used in FaDu cells to develop a HNSCC cell line that overexpresses IL-35. A FaDu-EBI3 cell line was first established. After transfection, of the thirteen clones screened, EBI3 overexpression was only detected in two. The limitation of low transfection efficiency when using the EBI3 expression plasmid appeared to be common in both CHO and FaDu cells. As previously stated, this could be remedied by linearising the plasmid prior to transfection, using a different promoter, or by applying site-directed integration technologies.

From the two candidate clones, Clone 14 was confirmed to overexpress high levels of EBI3 and was thus designated the FaDu-EBI3 cell line. However, in the same experiment, Western Blot detection of EBI3 could not be replicated in Clone 4. EBI3 may have been expressed, just at a much lower level when compared to Clone 14, and thus required additional exposure of the blot to x-ray film to enable signal detection. Otherwise, EBI3 expression could have been reduced by epigenetic silencing, or diluting out of expressing cells by those which have lost or possibly never expressed the transgene.

The chosen FaDu-EBI3 cell line was confirmed to overexpress and secrete EBI3. Thus, regardless of poor integration efficiencies, the method was successful and supported the chapter hypothesis. In future, it may be prudent to freeze a large stock of low passage cells, and then assess the maintenance of EBI3 expression over several passages. This would provide evidence that overexpression is likely to be maintained during cell culture in upcoming experiments.

4.5.3.2 Development of a FaDu cell line that overexpressed p35 (FaDu-p35)

In addition to FaDu-EBI3, a FaDu cell line that overexpressed p35 (FaDu-p35) was also established. This was done to generate negative controls of IL-35 overexpression and to investigate roles of each subunit in HNSCC immunity. After stable transfection,

all tested clones overexpressed p35. This suggested a high plasmid integration efficiency. In addition to signal depicting p35 (31 or 35 kDa), Western Blot data also displayed bands in all clones at approximately 23 kDa (**Figure 4.6A, labelled ***). The identity of this signal is unknown. It was detected at too low a molecular weight to be the unglycosylated form of p35 (30 kDa) (Murphy et al. 2000). Considering this signal was not found when p35 expression was later confirmed (**Figure 4.6B**), and that p35 is unstable, this signal may correspond to processed p35 forms that are present transiently during degradation.

The highest expressing clone was designated the FaDu-p35 cell line. However, when p35 overexpression was tested alongside other developed cell lines, signal observed was low (**Figure 4.6C**). In this experiment, blots were exposed to x ray film for less than 15 seconds. This was done to prevent overexposure of signal detected in the CHO-IL-35 and FaDu-IL-35 samples. As equal protein was loaded between samples, low signal in the FaDu-p35 cell lysate was indicative of much lower expression levels when compared to CHO-IL-35 and FaDu-IL-35 cell lines. Nevertheless, positive data from three separate lysate samples provided sufficient evidence that stable transfection with the designed plasmid resulted in p35 overexpression in the FaDu-p35 cell line.

4.5.3.3 Development of a FaDu cell line that co-expressed EBI3 and p35

As with CHO cells, it was explored whether stable transfection of FaDu-EBI3 cells with the p35 plasmid results in co-expression of both proteins. After transfection, co-expression was detected in three of the tested clones, though signal strength was low. This was attributed to poor performance of the ECL substrate rather than lack of protein production, as when replaced, later blots showed stronger signal intensity. When analysing the data further, it was noted that p35 was detected in Clones 9, 17 and 25 (**Figure 4.7A**), while EBI3 protein was found in Clones 9, 17, 18 and 25, but lost in clones 1 and 13 (**Figure 4.7B**). EBI3 may not have been detected due to poor ECL performance. Other reasons include those given for CHO cells, consisting of reduction/loss of expression by recombination of the integrated EBI3 plasmid with p35 plasmid DNA, interruption of EBI3 expression by transfected p35 plasmid DNA, gene silencing, or polyclonality in the FaDu-EBI3 cell line. Despite loss of expression in some clones, the method successfully developed FaDu cell lines that co-expressed EBI3 and p35.

4.5.3.4 *Detection of IL-35 formation and establishment of a FaDu cell line that overexpressed IL-35*

As with CHO cells, it was investigated whether co-expressed EBI3 and p35 naturally associate in FaDu cells to generate the IL-35 cytokine in its native form. Three of four co-expressing clones were found to secrete p35 in association with EBI3. Immunoprecipitated p35 was detectable in Clones 9, 17 and 25, but was absent in Clone 18 (**Figure 4.8A**). EBI3 however, was detectable in supernatants from all four samples (**Figure 4.8B**). Detection of EBI3 in Clone 18, the sample in which immunoprecipitated p35 was not detected, was unexpected. It is possible that p35 was present, but at too low a concentration to be detected, and that EBI3 bound to p35 was at a concentration detectable by the applied anti-EBI3 antibody. Bead loss during wash steps, or poor elution of protein from beads in that sample, may also have contributed to reduction in detectable p35. Furthermore, EBI3 could have been detected in residual supernatant that may not have been removed from beads during wash steps.

When detecting co-immunoprecipitated EBI3, an additional band signal was identified in Clones 7 and 25 below the 25 kDa marker (**Figure 4.8B**). These were also detected in previous studies (Devergne et al. 1997) and were described therein as degradation products. As IL-35 is unstable, it is conceivable that the signal in this study was derived from the transient presence of degraded EBI3. EBI3 could have been degraded during sample preparation (freeze-thawing or sample heating prior to SDS-PAGE), or through the potential activity of secreted proteases. Should the latter have been the case, application of protease inhibitors to sample supernatants may have been beneficial.

As the clone displaying the highest co-expression of interacting p35 and EBI3, Clone 25 was selected as the FaDu-IL-35 cell line. Data was generated using lysates and supernatants from this cell line, which confirmed successful overexpression and secretion of EBI3, overexpression of p35, and secretion of IL-35 using a test ELISA kit purchased from Bio-Ocean. Moreover, lysates from this cell line were used in co-immunoprecipitation experiments in Chapter 3 (as a positive control). The Chapter thus confirmed that EBI3 and p35 naturally dimerise within FaDu cells prior to secretion as the IL-35 cytokine. Therefore, the Chapter studies successfully developed a HNSCC cell model that overexpressed IL-35 in its native form.

In future, it may be advantageous to ensure a large stock of frozen cell lines at a low passage number. Using them at a low passage numbers would reduce the likelihood of transgene silencing that may occur over time. It may also be prudent to assess whether transgene expression is lost over several passages. Should this occur, repetition of the limiting dilution procedure may be useful to re-establish monoclonal cell lines that overexpress the transgene. To investigate the role of IL-35 more robustly, generation of a knockout cell line would have been ideal. Studies using this cell line could have enabled comparisons to be made with untransfected and overexpression cell lines. While attempts were made to establish an EB13-knockout cell line using CRISPR-Cas9 technology, this could not be completed within the timeframe of the project.

4.5.4 Conclusions

The current Chapter aimed to generate a FaDu cell line that overexpressed IL-35 in its native form. This model cell line could then be used as a study tool to investigate the role of HNSCC-derived IL-35 in the regulation of anti-tumour immunity. It was hypothesised that, by using stable transfection techniques to develop a cell line that overexpressed EB13, and then transfecting these cells to generate a cell line that also overexpressed p35, their co-expression would result in natural association and secretion as the native IL-35 heterodimer. Data generated using CHO cells supported the hypothesis and validated the methodology. Stable transfection resulted in the establishment of CHO cell lines that overexpressed human EB13 (CHO-EB13) and co-expressed EB13 and p35 which were found to be secreted in association as the IL-35 heterodimer (CHO-IL-35). The method was then applied to FaDu cells, culminating in the establishment of FaDu cell lines that overexpressed EB13 (FaDu-EB13), p35 (FaDu-p35), and IL-35 in its natural form (FaDu-IL-35).

These cell lines are important regarding the study of IL-35 in cancer immunity. They can be used in co-culture with a variety of immune cells that are known to be present in the HNSCC TME. Should immunosuppressive effects be exerted by HNSCC-derived IL-35, these findings may implicate IL-35 not only as a disease biomarker, but as a potential therapeutic target which could improve patient responses to existing immunotherapies.

The following Chapters sought to use the developed cell lines to investigate the role of HNSCC-derived IL-35 in the repolarisation of anti-tumour M1 macrophages, to immunosuppressive M2 macrophages, which predominate in HNSCC.

Chapter 5

**Investigating the role of HNSCC-derived IL-35 in M1 to M2
macrophage repolarisation via suppression of the M1
macrophage phenotype**

5.1 Introduction

Poor survival in HNSCC is often attributed to dysfunctional immunity in the TME. Despite advances in immunotherapies, responses and overall survival remains unsatisfactory (Bray et al. 2018). To improve this, there is a need to identify novel mechanisms used by tumour cells to dysregulate immune cells in the TME. This may reveal new targets, which when modulated therapeutically, may improve anti-tumour immunity. Studies in Chapter 3 found that the hypopharyngeal cell line FaDu, and the oral carcinoma cell line H357, both upregulate gene expression of the immunosuppressive cytokine IL-35 when subjected to stimulation with IFN γ and TNF α . A FaDu cell line that overexpresses and secretes IL-35 was developed in Chapter 4. The current Chapter aimed to investigate the role of tumour-derived IL-35 in the negative regulation of anti-tumour immunity.

Macrophages are a major component of the TME. In HNSCCs they are often polarised to the immunosuppressive M2 phenotype, which suppresses anti-tumour immunity and promotes tumour progression (Wundergem et al. 2020). This and the following Chapters investigate whether tumour-derived IL-35 contributes to immune escape by repolarising pro-inflammatory M1 macrophages, which may be induced in inflamed HNSCC TMEs, to the prevalent M2 phenotype. Specifically, this Chapter focuses on the role of HNSCC-derived IL-35 in suppression of the M1 phenotype.

5.1.1 Tumour associated macrophages (TAMs)

In the TME, macrophages are known as tumour associated macrophages (TAMs) (Whiteside 2005; Saussez et al. 2010). TAMs transduce cytokine and chemokine signals in the TME to become activated. Broadly speaking, the activation state they exhibit can range between two polarised extremes - the pro-inflammatory M1 phenotype, and the anti-inflammatory M2 phenotype. However, macrophages exhibit functional plasticity. Changes in the signals they are exposed to can repolarise them to different activation states (Li et al. 2015; Yang and Zhang 2017).

5.1.2 M1-TAMs

TAMs exposed to pro-inflammatory cytokines such as IFN γ , produced by natural killer cells and Th1 (T helper type 1) cells are polarised to M1-like phenotypes.

Transduction of these signals increases expression of transcription factors such as STAT1 (signal transducer and activator of transcription 1) and IRF3 (interferon regulatory factor 3) (Biswas and Mantovani 2010; Xue et al. 2014). These promote gene expression of M1 genes, leading to M1 polarisation. M1 TAMs can be identified by expression of biomarkers including HLA-DR, CD80 and CD86, which have key roles in antigen presentation and T cell activation.

Functionally, M1-TAMs promote anti-tumour immunity. They produce pro-inflammatory cytokines including TNF α , IL-12 and IL-23, which promote the anti-tumour activity of CD4⁺ and CD8⁺ T cells, and natural killer cells (Anfray et al. 2020). They also capture and present tumour antigens to CD4⁺ T cells, and can directly eliminate tumour cells (Zheng et al. 2017; Aminin and Wang 2021).

Macrophages are professional antigen presenting cells (APC). They capture and internalise tumour antigens, process them into epitopes and present them on the cell surface in association with MHC Class II molecules. This enables recognition and engagement by CD4⁺ T cells (HLA, Human Leukocyte Antigens in humans) (Engelhard 1994; Wood 2011; Rock et al. 2016). To fully activate CD4⁺ T cells, three signals are required. CD4⁺ T cells use their unique TCRs to engage with antigenic peptides bound to MHC II on macrophage surfaces. CD3 chains on the CD4⁺ T cell then interact with MHC II. Both interactions are stabilised by the CD4 chain, which binds to non-polymorphic regions of MHC II molecules. The TCR-MHC synapse depicts the first signal. A secondary signal, provided by the ligation of co-stimulatory molecules (mainly CD80 and CD86) present on activated M1 TAMs, with CD28 on the surface of T cells, is required to trigger activation and expansion of bound T cells (Linsley et al. 1991; Sansom et al. 2003). Production and exposure to pro-inflammatory cytokines such as IL-2, IL-12, TNF α and IFN γ , promote further expansion and activation, and constitutes the third and final signal. Once fully active, CD4⁺ T cells function to enhance anti-tumour immunity (Guerriero 2019).

M1-TAMs can eliminate tumour cells. M1-TAMs can recognise tumour cells against normal cells. This can be accomplished via differences in cell membrane composition. Some tumour cells express tumour antigens, display elevated levels of membrane-bound phosphatidylserine, and alter the number and nature of carbohydrate chains present on their outer surface. These can act as recognition signals for macrophages,

allowing them to target tumour cells for elimination. While it is not fully understood how macrophages kill tumour cells, several mechanisms are believed to be utilised. Macrophages can produce factors to recruit and activate other immune cells which kill tumour cells. Secondly, they produce pro-inflammatory cytokines such as TNF α which, in some instances, can induce tumour cell death (Aminin and Wang 2021; Laha et al. 2021). Alternatively, they can phagocytose tumour cells that are either bound by antibodies (opsonisation) or are not. Once tumour cells are internalised, macrophages can kill them by producing nitrogen and oxygen species. These damage tumour cell DNA leading to apoptosis (Aminin and Wang 2021). These functions are important in supporting elimination of tumour cells by the immune system. As such, anti-TAM therapies have been developed to promote M1 macrophage polarisation in the TME (Chapter 1).

5.1.3 M2-TAMs

TAMs can be polarised to M2 via exposure to Th2 (T helper 2) cytokines, including IL-4, IL-13, IL-10 and TGF β (Mills et al. 2000; Gordon 2003; Martinez et al. 2008; Baxter et al. 2020). M2 macrophages can be identified via expression of biomarkers such as the mannose receptor CD206, the scavenger receptor CD163, and secretion of immunosuppressive cytokines including IL-10 and TGF β (Roszer 2015; Orecchioni et al. 2019).

Most TAMs detected in tumours exhibit M2-like functions. M2-TAMs suppress anti-tumour immunity and inflammation, and promote tissue remodelling and tumour angiogenesis. These functions are made possible by secretion of immunosuppressive cytokines including IL-10 and TGF β , and the pro-angiogenic factor VEGF-A (vascular endothelial growth factor A). Considering these roles, accumulation of M2-TAMs in tumours helps tumour cells escape immunosurveillance, and accelerates tumour progression (Hao et al. 2012; Sica and Mantovani 2012).

In-vivo, all macrophages are detected using the pan macrophage marker CD68. The density of M2 macrophages is assessed by detecting the co-expression of CD68 with other M2 markers. Immunostaining of CD68 with CD163 is commonly used to identify M2 macrophages in HNSCC (Minami et al. 2018; Kumar et al. 2019). A large body of evidence has suggested that CD68⁺ CD163⁺ TAMs are prevalent (Weber et

al. 2014), and often correlate with disease progression, de-differentiation, angiogenesis, relapse and decreased overall survival. Thus, high M2-TAM density is viewed as a biomarker of disease severity (Mori et al. 2011; Hu et al. 2016; Okubo et al. 2016; Alves et al. 2018; Kumar et al. 2019; Kalogirou et al. 2021).

It is important therefore, to identify novel factors produced by tumour cells in HNSCC which promote M2 TAM polarisation. These could be targeted in combination with existing immunotherapies to promote M1 polarisation and improve anti-tumour immunity. The current Chapter investigated the role of HNSCC-derived IL-35 in the promotion of M2 TAM polarisation.

5.1.4 Rationale of the study

Data from Chapter 3 demonstrated that FaDu cells upregulate IL-35 genes in response to IFN γ and TNF α stimulation. IL-35 is an immunosuppressive cytokine that has been shown to edit the behaviour of pro-inflammatory immune cells, altering their function so that they instead suppress immunity. Examples include the conversion of CD4 $^+$ T cells into regulatory T cells, B cells to immunosuppressive regulatory B cells, neutrophils from N1 to N2, and dendritic cells into tolerogenic dendritic cells (Liu et al. 2021).

What has not yet been studied, is the role of IL-35 in the regulation of macrophage polarisation in HNSCC, and whether it contributes to the greater ratio of M2:M1 macrophages reported in-vivo. The following Chapters attempt to fill this gap by investigating whether HNSCC-derived IL-35 can promote the repolarisation of M1 macrophages, which may be induced in an inflamed TME, to the prevalent M2-like phenotype.

The experimental approach used THP1 cells to generate macrophage models. Macrophage differentiation is often evidenced by increased cell size and granularity, and expression of both the bacteria-sensing co-receptor CD14, and the integrin CD11b. These macrophages are then polarised to M1 or M2 using different protocols (Genin et al. 2015; Baxter et al. 2020). Using conditioned medium and mixed culture of polarised macrophage models with a FaDu cell line that overexpresses IL-35 (FaDu-IL-35, Chapter 4), Chapter 5 investigated whether HNSCC-derived IL-35 suppresses the M1 phenotype of M1 macrophages. Chapter 6 follows this research by

assessing whether HNSCC-derived IL-35 promotes an M2-TAM phenotype in these M1 macrophages via upregulation of M2 markers.

Chapter 5 hypothesised that - HNSCC-derived IL-35 repolarises M1 macrophages to the M2 phenotype. This involves suppression of the M1 phenotype, which can be evidenced by inhibition of pro-inflammatory cytokine production, reduced expression of MHC II and the co-stimulatory molecules CD80 and CD86, and suppression of M1-mediated tumour cell death.

5.1.5 Aims and objectives

- Generate THP1-derived M1 and M2 macrophage models.
 - Differentiate THP1 cells into M0 macrophages.
 - Generate an M1 macrophage model.
 - Generate an M2 macrophage model.
- Assess the role of HNSCC-derived IL-35 in suppression of the M1 phenotype.
 - Assess suppression of pro-inflammatory cytokine secretion (TNF α).
 - Assess downregulation of HLA-DR, CD80 and CD86 expression.
 - Assess suppression of M1-mediated tumour cell death.

5.2 Methods

Several of the methods used in this Chapter are explained in detail in Chapter 2. The specific sections where these can be found are referenced using parentheses. Generation of macrophage models (**Section 2.3.7**). RT-qPCR and primer sequences (**Section 2.3.2**). Flow Cytometry and antibody panels (**Section 2.3.9**).

5.2.1 Macrophage differentiation and polarisation protocols

Detailed seeding and culture conditions used to generate macrophage models are described in Chapter 2 (**Section 2.3.7**). To differentiate THP1 cells into M0 macrophages, they were stimulated with PMA (50 ng/mL, 24 h) and rested for 48 h in fresh culture medium (Daigneault et al. 2010; Chanput et al. 2014; Shiratori et al. 2017; Tedesco et al. 2018). M1 macrophages were generated by treating THP1 cells with PMA (100 ng/mL, 24 h), followed by a 48 h rest. They were polarised to M1 via

IFN γ stimulation (20 ng/mL, 48 h) (Mantovani and Locati 2013; Genin et al. 2015; Smith et al. 2015; Baxter et al. 2020). Higher PMA concentrations were determined to improve M1 polarisation in preliminary studies. M2 macrophages were generated via stimulation of THP1 cells with PMA (50 ng/mL, 24 h) followed by a 48 h rest and subsequent treatment with IL-4 (20 ng/mL, 48 h) to induce M2 polarisation (Mantovani and Locati 2013; Genin et al. 2015; Smith et al. 2015; Baxter et al. 2020). During previous experiments prior to the project, an alternative M1-like model (termed M1-like cells) was developed without the use of PMA. To generate M1-like cells, THP1 cells were stimulated with GM-CSF (20 ng/mL) for 72 h, followed by application of IFN γ (20 ng/mL) and incubation for an additional 24 h. Culture conditions used (concentrations, rest times and timepoints) were determined in preliminary experiments.

5.2.2 Validation of macrophage differentiation

THP1 cells were differentiated to M0 macrophages as described above. To validate differentiation via detection of cell adhesion to the culture dish, cells were analysed under a light microscope. Light microscopy was also used to identify morphological changes (small round THP1 cells to large granular M0 macrophages). Increased cell size and granularity were identified by harvesting cultured cells and using Flow Cytometry to assess changes in forward and side scatter data.

To validate successful macrophage differentiation via changes in gene expression, 250 ng RNA was extracted from cultured THP1 or M0 macrophages and converted to cDNA. 8.5 ng of cDNA was analysed by RT-qPCR to identify increases in gene expression of the macrophage differentiation markers CD14, CD11b and CD68, relative to THP1 cells. Data was normalised to the reference gene β -Actin. N=1.

5.2.3 Validation of M1 and M2 macrophage models

M1 and M2 macrophages were generated as described and first validated using RT-qPCR. To validate M1 polarisation by RT-qPCR, THP1, M0 and M1 macrophages were cultured in 24-well plates (**Section 2.3.7**). 250 ng of RNA extracted from each model was converted to cDNA, 8.5 ng of which was analysed by qPCR to measure fold changes in gene expression of HLA-DR, CD80 and CD86, relative to THP1 cells. Data was normalised to the reference gene β -Actin. N=1. M2 polarisation was also

validated by RT-qPCR. Fold-changes in gene expression of CD206, CD163 and IL-10 were measured in RNA taken from cultured M0 or M2 macrophages, relative to THP1 cells (n=1).

Flow Cytometry was used to further validate M1 and M2 polarisation. THP1, M1 and M2 macrophages were generated in 6-well plates (**Section 2.3.7**). M0 macrophages were omitted due to limitations in antibody availability. Fc receptors were blocked using TruStain FcX. Cells were then stained using a LIVE/DEAD Fixable Green kit, followed by staining of M1 and M2 surface markers with the Macrophage Polarisation antibody panel (**Chapter 2 - Table 2.7**). Samples were fixed for up to 72 h in FluoroFix buffer, before up to 10,000 events per sample were captured in an LSRFortessa. Using FlowJo, single, live cells were first identified (representative gating strategy shown in **Supplementary Data 8**). Live cells in each test group were then gated to obtain those that expressed the M1 markers HLA-DR, CD80 or CD86, or the M2 markers CD206 or CD163. A detailed explanation of how populations were gated to discriminate cells positive for these markers against those that were negative, is given in Chapter 2 (**Section 2.3.9.7**). Successful M1 polarisation was determined by comparing the mean percentage of HLA-DR+, CD80+, or CD86+ cells between each test group (THP1 vs M1 vs M2). N=3. Successful M2 polarisation was determined by comparing the mean percentage of CD206+ or CD163+ cells between each test group (THP1 vs M1 vs M2). N=3. One Way ANOVA and Tukey's test was used to determine whether differences in means were statistically significant.

5.2.4 Assessment of the role of HNSCC-derived IL-35 in the suppression of TNF α secretion by M1 macrophages

To assess whether HNSCC-derived IL-35 could suppress the M1 phenotype via inhibition of TNF α secretion, cells were treated with CM from transfected cells and supernatants analysed using a human TNF α ELISA kit as instructed by the manufacturer. Two M1 models were used to provide evidence of trends observed, and for comparative purposes.

Before treatments, to confirm TNF α secretion in the M1-like model, M1-like cells were cultured. Supernatant was collected 24 h and 48 h after addition of IFN γ and analysed by ELISA. THP1 cells treated with IL-4 for 48 h were used as a negative control. Sterile-filtered CM used for treatments were prepared from transfected cell

lines in confluent T25 flasks (**Section 2.3.6.4**). CM from FaDu, FaDu-EBI3, FaDu-p35 and FaDu-IL-35 cells were analysed by ELISA to confirm absence of TNF α that may have affected results.

To test the suppressive effects of HNSCC-derived IL-35, M1-like cells were cultured and treated for 24 h or 48 h with fresh medium (mock treatment) or FaDu-IL-35 CM, at 10% of the culture volume (percentage selected to prevent serum starvation). Timepoints were selected based on previous laboratory experiments. As controls, M1-like cells were stimulated with FaDu CM, FaDu-p35 CM or FaDu-EBI3 CM (n=3 for all samples). Effects of each treatment were determined by comparing mean TNF α concentrations detected in treated cells to that of the mock treated control. One Way ANOVA with Dunnett's test was performed to validate whether differences observed at each timepoint were statistically significant.

Next, the M1 macrophages was analysed. Due to poor linearity of data points produced by standards, optical density readings were used for analyses rather than absolute concentrations. THP1 cells were differentiated and polarised to M1 macrophages within wells of 24-well culture plates. M1 macrophages were mock treated, or stimulated with 10% CM from FaDu-IL-35 cells, alone, or in combination with increasing concentrations of blocking antibody (monoclonal anti-EBI3 blocking antibody, 4 or 10 μ g, based on previous literature). As a control, M1 macrophages were stimulated with recombinant IL-35 (50 ng/mL). As negative controls, supernatants from cultured THP1 or M0 macrophages were analysed. For comparative purposes and as controls, M1 macrophages were also treated with FaDu CM, FaDu-EBI3 CM or CHO-EBI3 CM. 48 h after all treatments, supernatants were collected and assessed by ELISA to detect changes in TNF α secretion (n=1). 48 h was selected as significant effects were observed by this timepoint in previous experiments. Time course study was omitted due to limitations in assay availability.

To investigate the identity of secreted proteins that could interact with EBI3 and negatively regulate TNF α secretion, candidate EBI3 binding partners were identified using the proteomics database provided by the European Bioinformatics Institute (European Molecular Biology Laboratory, Heidelberg, Germany) (https://www.ebi.ac.uk/legacy-intact/interactors/id:Q14213*). The secretable proteins P19, p28 and p35 were selected for analysis as primers were readily available. It was

then evaluated whether these genes were upregulated when EBI3 was overexpressed in FaDu cells (FaDu-EBI3 cell line). FaDu, FaDu-EBI3, FaDu-p35 and FaDu-IL-35 cells were seeded and grown overnight in 24-well plates (n=3). 500 ng of extracted RNA was converted to cDNA. 8 ng was analysed by qPCR to assess fold changes in gene expression of p19, p28 or p35 in FaDu-EBI3, FaDu-p35 or FaDu-IL-35 cells, relative to untransfected FaDu cells. Negative fold changes were calculated using the following equation – negative fold change = (-1/Fold change). Differences observed were tested for statistical significance using One Way ANOVA with Dunnett's post hoc test.

5.2.5 Assessment of the role of HNSCC-derived IL-35 in the downregulation of HLA-DR, CD80 and CD86 in M1 macrophages

M1 macrophages were generated in 24-well plates (**Section 2.3.7**) and either mock treated with culture medium, stimulated with 10% FaDu-IL-35 CM, or double stimulated with 10% FaDu-IL-35 CM in combination with a blocking antibody at a mass determined experimentally to maximally block IL-35 (monoclonal anti-EBI3, 4 µg). Cells were incubated under these conditions for 48 h to match conditions used for flow cytometry. 250 ng of extracted RNA was converted to cDNA, 8 ng of which was analysed by qPCR to measure fold changes in gene expression of HLA-DR, CD80 and CD86, relative to mock treated M1 macrophages. Data was normalised to the reference gene β -Actin. (N=1). All samples were run in triplicate.

To validate RT-qPCR data and assess changes in protein expression, mixed culture experiments were prepared. This enabled cell crosstalk between macrophages and FaDu/FaDu-IL-35 cells that more closely resembles in-vivo cell interactions within a tumour. FaDu or FaDu-IL-35 cells were mixed 4:1 with M1 or M2 macrophages and incubated for 48 h as described in Chapter 2 (**Section 2.3.9.3**). M1 and M2 macrophages that were left untreated were used as controls. Thus, the samples generated were – M1, M1/FaDu, M1/FaDu-IL-35, or M2, M2/FaDu, M2/FaDu-IL-35. Fc receptors were blocked. Cells were stained with the Live/Dead stain kit and the Macrophage Polarisation antibody panel (**Chapter 2 - Table 2.7**). Samples were fixed for up to 72 h in FluoroFix buffer. 10,000 events per sample were captured in an LSRFortessa.

Using FlowJo, single, live cells were first identified. All macrophages were identified by gating on CD326⁻ cells, which excluded FaDu or FaDu-IL-35 cells shown to express CD326 in preliminary tests (representative gating strategy shown in **Supplementary Data 9**). In the CD326⁻ macrophage population, cells positive for HLA-DR, CD80 or CD86 were identified in each test sample by setting a uniform gate that discriminated positively stained cells from those that were negative (**Chapter 2 section 2.3.9.7**).

The effects of IL-35 overexpression were evaluated in M1 and M2 macrophages by comparing the mean percentages of CD326⁻ macrophages that were positive for each of these markers between the M1 test samples (M1 vs M1/FaDu vs M1/FaDu-IL-35) and M2 test samples (M2 vs M2/FaDu, M2/FaDu-IL-35). M1, (n=2). All other test samples, (n=3). One Way ANOVA and Tukey's test were used to evaluate whether differences observed between means were statistically significant.

5.2.6 Assessment of the role of HNSCC-derived IL-35 in suppression of M1-mediated tumour cell death

To evaluate whether M1 macrophages induced tumour cell death, and whether HNSCC-derived IL-35 could inhibit this, M1, and M2 macrophages (as controls), were generated in 6-well plates (**Section 2.3.7**) and harvested. They were then mixed in a 1:4 ratio with FaDu or FaDu-IL-35 cells and cultured for 48 h in fresh 6-well plates. FaDu and FaDu-IL-35 cells in monoculture were used as controls and for comparative purposes. This generated the following test groups – FaDu, FaDu/M1, FaDu/M2, FaDu-IL-35, FaDu-IL-35/M1, FaDu-IL-35/M2. (N=3). Fc receptors were blocked using TruStain FcX. Cells were stained with the Apoptosis/Necrosis panel or their corresponding isotype controls. 10,000 events were captured using an LSR Fortessa.

Using FlowJo, single cells were identified. FaDu or FaDu-IL-35 cells were isolated from the macrophage population by gating on CD326⁺ CD14⁻ cells (**Supplementary Data 10**). To identify apoptotic cells in the FaDu population, Annexin V⁺ PI⁻ cells were gated. To identify necrotic cells, Annexin V⁺ PI⁺ cells were gated. Positive/negative discrimination was determined as described in Chapter 2 (**Section 2.3.9.7**).

To determine whether M1 or M2 macrophages induced cell death in FaDu cells, differences in mean percentages of apoptotic and necrotic CD326+ CD14- cells were compared between the control group (FaDu) and the treatment groups FaDu/M1 or FaDu/M2. The same method was applied to determine whether M1 or M2 macrophages induced FaDu-IL-35 cell death. One Way ANOVA and Dunnett's post hoc test was used to determine if differences observed were statistically significant.

To determine whether overexpression of IL-35 affected sensitivity to apoptosis or necrosis in FaDu cells, mean apoptotic and necrotic CD326+ CD14- cells were compared between FaDu vs FaDu-IL-35 samples. A paired t-test was used to determine statistical significance.

5.3 Results

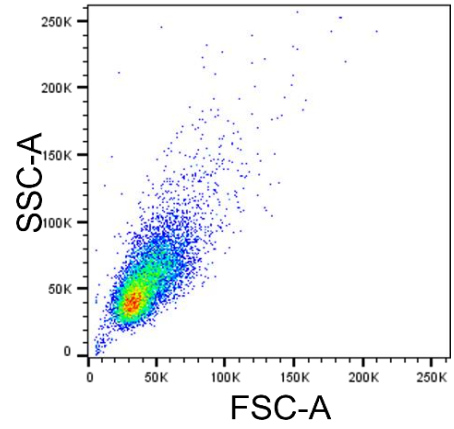
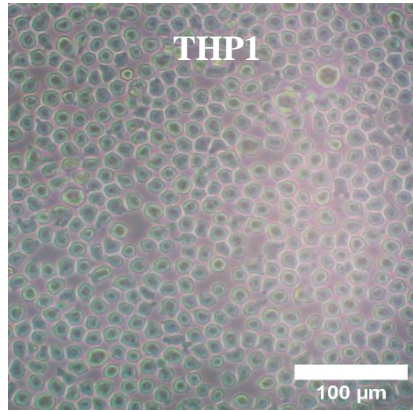
5.3.1 Macrophage models

5.3.1.1 Differentiation of THP1 cells into M0 macrophages

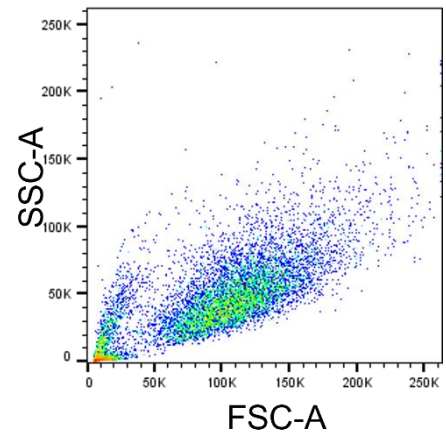
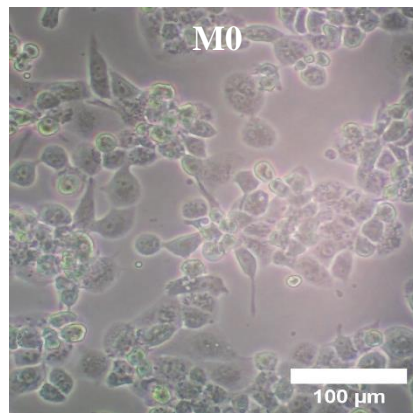
To generate M1 and M2 macrophage models, THP1 cells were first differentiated into macrophages. Macrophage differentiation is associated with hallmark changes including - cell adhesion to the culture plate, changes in morphology (spread morphology and increased granularity) and increased expression of macrophage biomarkers (Daigneault et al. 2010; Aldo et al. 2013; Baxter et al. 2020; He et al. 2021). THP1 cells were untreated or stimulated with PMA (50 ng/mL, 24 h) and rested for 48 h to generate M0 macrophages. Light microscopy analysis showed that, while THP1 cells remained in suspension, M0 macrophages became adherent after 24 h of PMA treatment, and maintained adhesion throughout the differentiation protocol (**data not shown**). Adhesion was also preserved following M1 and M2 macrophage polarisation (**data not shown**). Induction of cell adhesion therefore suggested that the selected protocol resulted in successful macrophage differentiation. Changes in cell morphology were analysed by light microscopy. Changes in cell size and granularity were examined by Flow Cytometry using forward and side scatter data. THP1 cells exhibited a small, rounded morphology, and presented low forward and side scatter data (**Figure 5.1A**). M0 macrophages were larger in size and displayed increased granularity (**Figure 5.1B**). Size and granularity increased further following M1 and M2 polarisation (**Supplementary data 12**). Thus, these data further support that macrophage differentiation was successful.

Differentiation of THP1 cells into macrophages is associated with increased expression of the toll-like receptor (TLR) CD14, the integrin molecule CD11b, and the intracellular glycoprotein CD68 (Aldo et al. 2013; Forrester et al. 2018; Starr et al. 2018). RT-qPCR data showed that, relative to THP1 cells, CD14 expression was 164-fold higher in the M0 macrophage model (**Figure 5.1C**). Gene expression of CD11b was elevated 6-fold (**Figure 5.1D**). Expression of CD68 was not increased (**Figure 5.1E**). Therefore, induction of cell adhesion, morphological changes, and elevation of macrophage marker gene expression (CD14 and CD11b), all suggested that differentiation of THP1 cells into macrophages was successful.

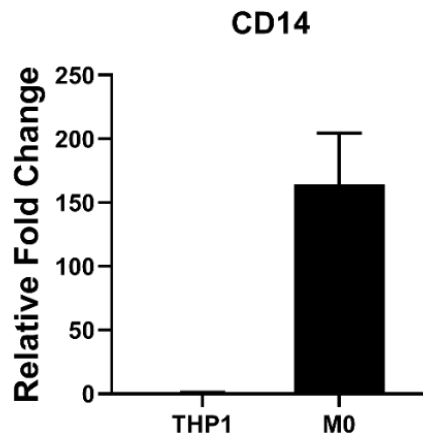
(A)



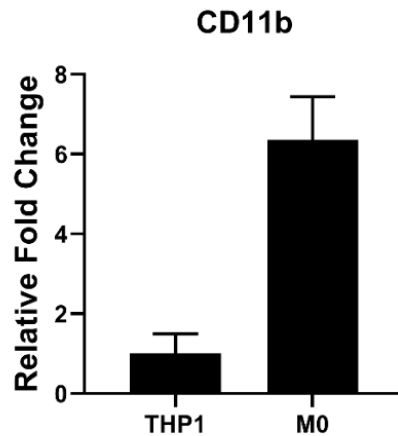
(B)



(C)



(D)



(E)

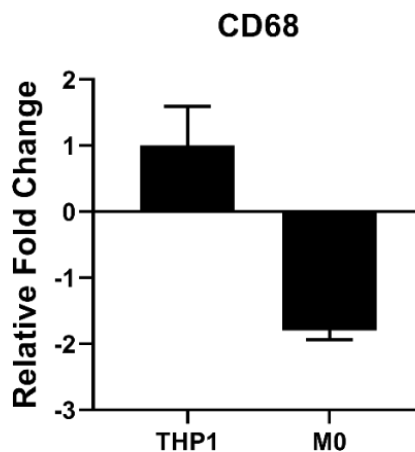


Figure 5.1 Validation of M0 macrophage differentiation in treated THP1 cells. THP1 cells were left untreated or stimulated with PMA (50 ng/mL, 24 h followed by 48 h rest) to induce M0 differentiation. Representative images are shown which depict changes in cell size and granularity from THP1 (A) to M0 (B) detected using a light microscope and forward and side scatter flow cytometric data. Microscopy images were acquired using a Nikon Eclipse TS100 inverted microscope coupled to a Moticon digital camera (Magnification x10). Forward scatter-area (FSC-A) x side scatter-area (SSC-A) plots were acquired by flow cytometry and analysed in FlowJo. RT-qPCR was also used to quantify fold changes in gene expression of the macrophage differentiation markers CD14 (C), CD11b (D) and CD68 (E) in M0 macrophages relative to THP1 cells. Data shown represents mean +SD. (n = 1).

5.3.1.2 M1 macrophage model

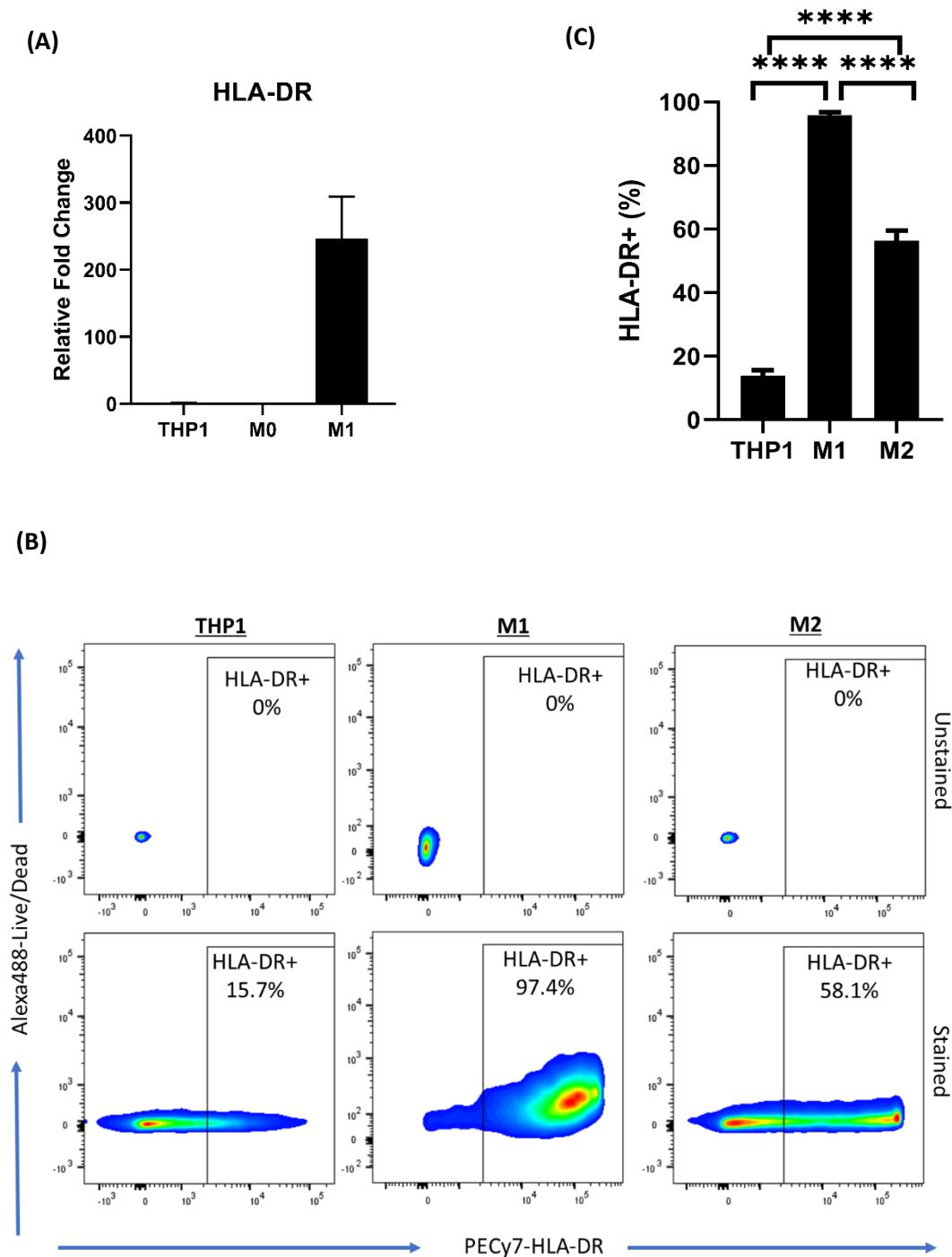
M1 macrophages were generated via PMA stimulation of THP1 cells followed by polarisation with IFN γ . To validate the M1 macrophage model, M1 macrophages were analysed alongside THP1 and M0 controls by RT-qPCR, or alongside THP1 and M2 macrophages by Flow Cytometry, to detect increases in expression of the M1 markers - HLA-DR, CD80 and CD86. M0 macrophages were omitted from Flow Cytometry analyses due to limitations in antibody availability.

RT-qPCR data showed that, relative to THP1 cells, M0 differentiation did not affect HLA-DR gene expression, whereas polarisation to M1 elevated gene expression (247-fold) (**Figure 5.2A**). HLA-DR upregulation in the M1 macrophage model was confirmed by Flow Cytometry (**Figure 5.2C**). From a minimum of 8500 events in the parent live cell population, the frequency of HLA-DR⁺ cells was significantly increased from 13% in THP1 cells, to 95% in the M1 macrophage population (n=3, p <0.0001). The HLA-DR⁺ population was also significantly higher in M1 macrophages than in control M2 macrophages (56%, p <0.0001). Thus, HLA-DR expression provided evidence of M1 polarisation in the developed model.

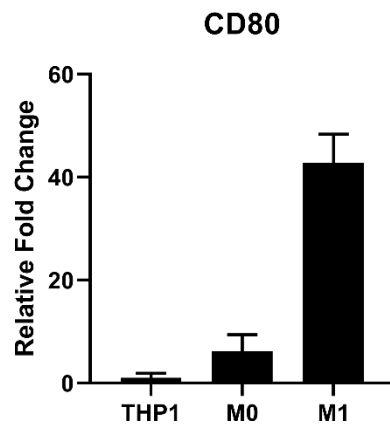
Relative to THP1 cells, M0 differentiation elevated gene expression of CD80 by a 6-fold magnitude M0 differentiation (**Figure 5.2D**). M1 polarisation induced a further increase, elevating expression 42-folds higher than in THP1 cells (**Figure 5.2D**). Flow cytometry data confirmed that M1 polarisation induced CD80 expression. The mean proportion of CD80⁺ cells was significantly higher in M1 macrophages (74%) when compared to THP1 cells (0.7%, p <0.0001), and M2 macrophages (36%, p <0.0001) (**Figure 5.2F**). Therefore, increased CD80 expression validated successful development of an M1 macrophage model.

M0 differentiation of THP1 cells increased CD86 gene expression (11-fold) (**Figure 5.2G**). M1 polarisation did not elevate gene expression further (5-fold higher than in THP1 cells). Flow cytometry data showed that the mean proportion of CD86⁺ cells was low in the M1 macrophage population (24%), though this was significantly higher than in THP1 cells (5%, p <0.05) (**Figure 5.2I**). The mean proportion of CD86⁺ cells was highest in M2 macrophages (32%) but this was not significantly different than in M1 (**Figure 5.2I**). While the polarisation protocol did not induce CD86 expression

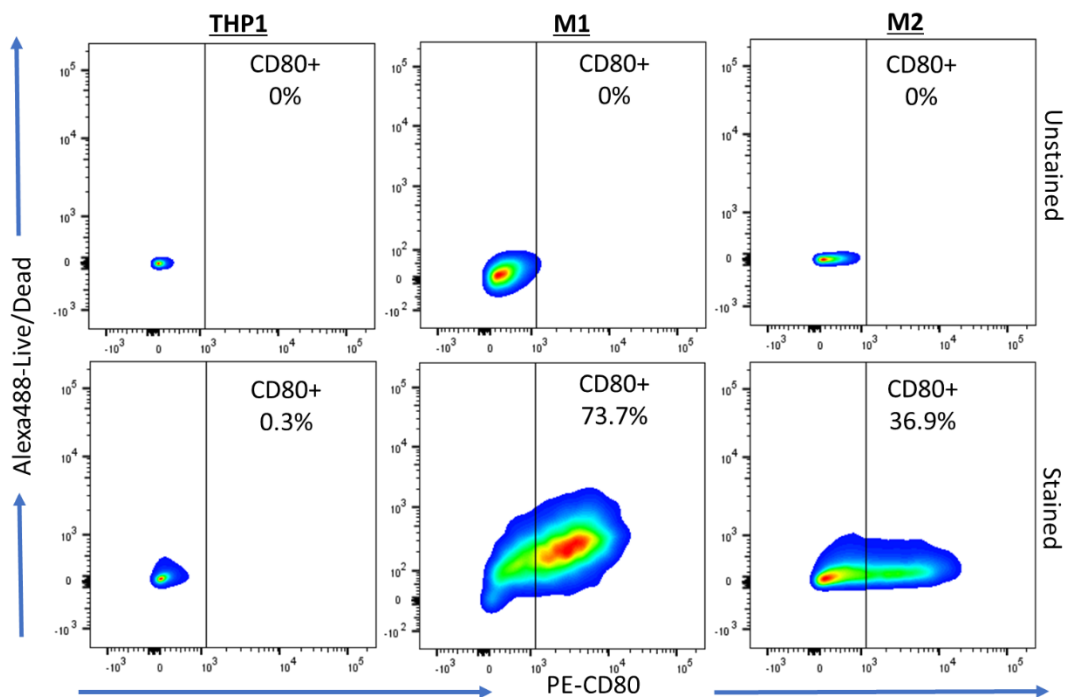
beyond M0 or M2 macrophage models, CD86 was still expressed in the M1 macrophage model.



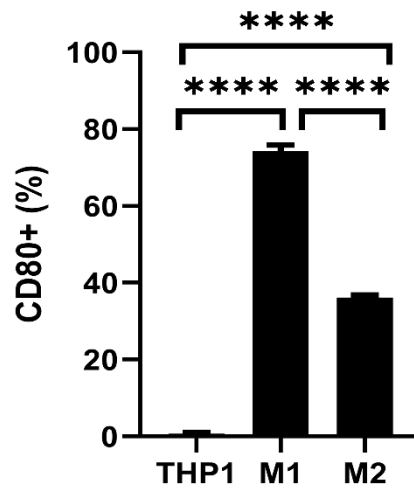
(D)



(E)



(F)



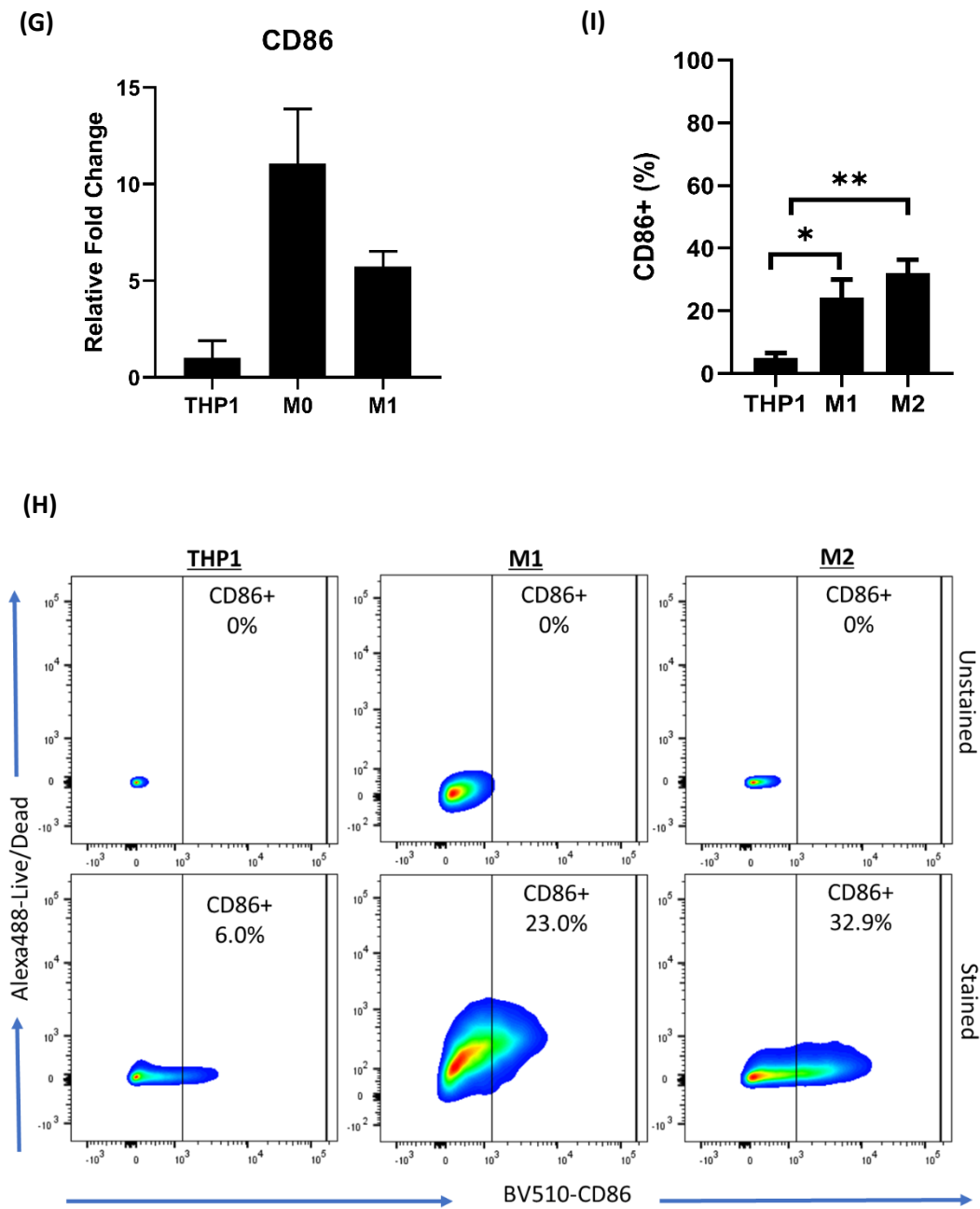


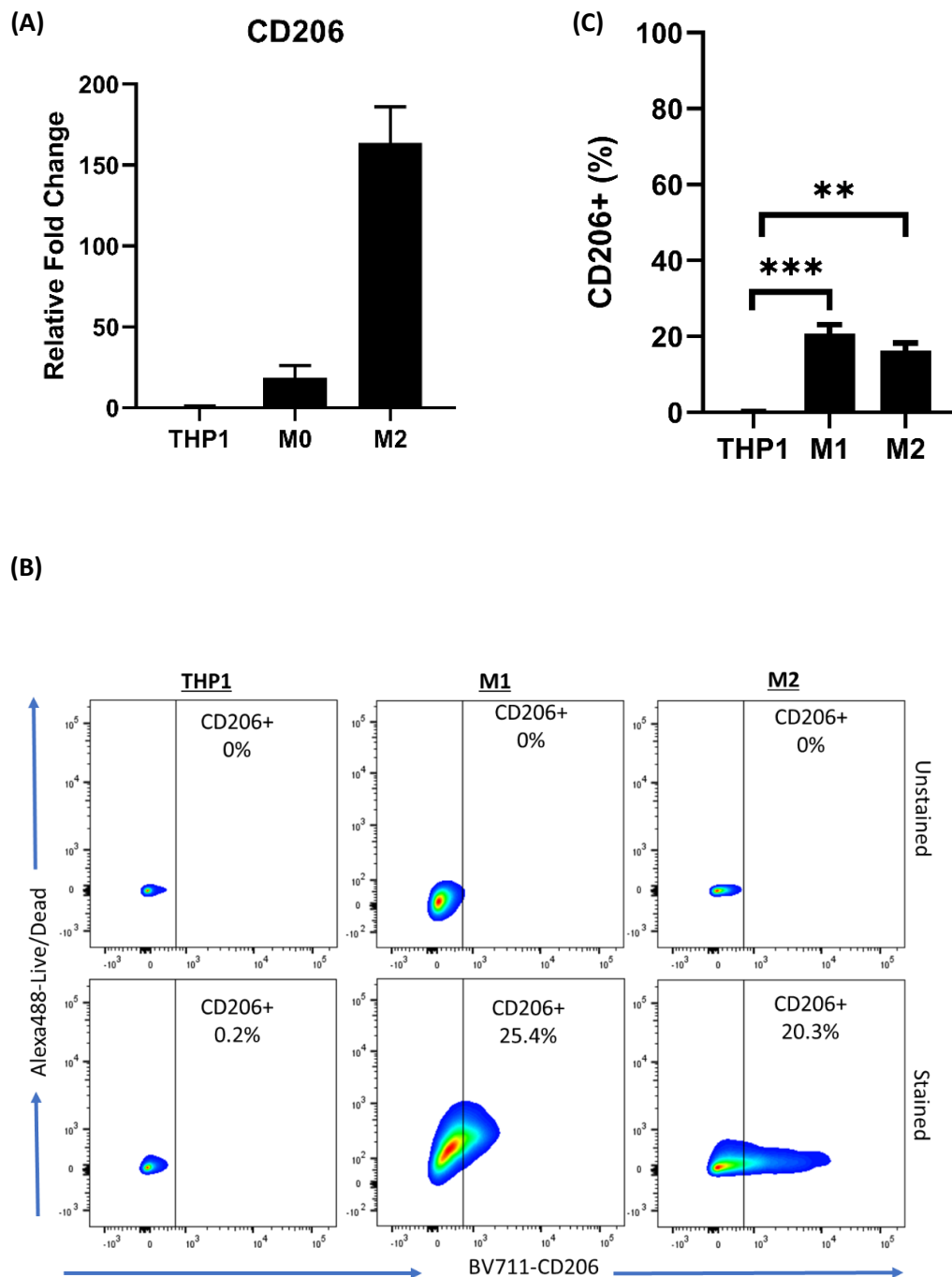
Figure 5.2 Validation of the M1 macrophage model. RNA taken from THP1, M0 or M1 macrophages were analysed by RT-qPCR to detect fold changes in gene expression of HLA-DR (A), CD80 (D) and CD86 (G), relative to THP1 cells. Data shown represents mean±SD. (n=1). THP1, M1 and M2 macrophages were cultured, stained with antibodies and analysed by Flow Cytometry. Representative dotplots are shown that depict the gating strategy used to discriminate positive and negative populations for expression of HLA-DR (B), CD80 (E) and CD86 (H). Mean percentages (+SEM) of HLA-DR+ (C), CD80+ (F) and CD86+ (I) from the parent population of live cells are shown in bar charts. (n=3). Statistics were analysed using One Way ANOVA with Tukey's post-hoc test to compare means between each group. * = $p < 0.05$, ** = $p < 0.01$, **** = $p < 0.0001$.

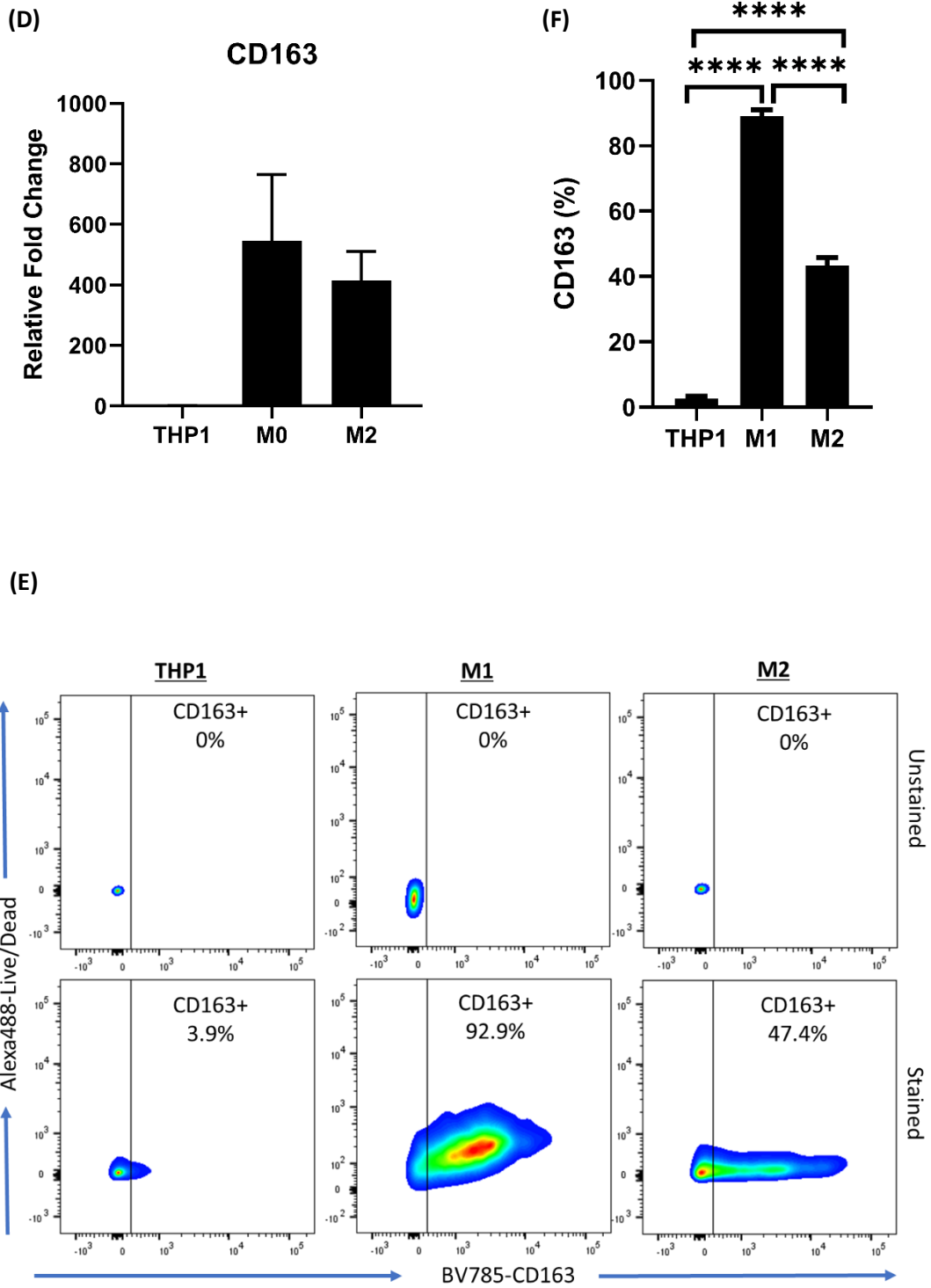
5.3.1.3 M2 macrophage model

M2 macrophages were generated by PMA stimulation of THP1 cells followed by polarisation with IL-4. RT-qPCR was first used to assess upregulation of the M2 markers CD206, CD163 and IL-10 (**Figure 5.3A**). Differentiation of THP1 cells induced CD206 gene expression (19-fold increase). M2 polarisation markedly increased CD206 expression to levels 168-fold higher than in THP1 cells. Flow cytometry was used to analyse protein expression of CD206 and CD163. The data showed that M2 polarisation did not significantly increase CD206 protein expression (**Figure 5.3C**). From a minimum of 8500 events, 0.1% of THP1 cells expressed CD206. While the mean proportion of CD206+ cells was higher in M2 macrophages (16%, $p < 0.01$), it was lower when compared to M1 macrophages (20%, ns). Thus, the M2 polarisation protocol markedly increased CD206 gene expression, but did not significantly increase protein expression beyond that observed in M1 macrophages. Nevertheless, while low, CD206 was expressed in the M2 macrophage model.

RT-qPCR data showed that differentiation with PMA potently increased CD163 expression in M0 macrophages relative to THP1 cells (546-fold) (**Figure 5.3D**). Polarisation to M2 did not elevate this further (414-fold higher than THP1). Flow cytometry data showed that protein expression followed a similar trend (**Figure 5.3F**). The mean proportion of CD163+ cells increased from 3% in THP1 cells, to 43% in M2 macrophages ($p < 0.0001$). However, the latter was significantly lower than in M1 macrophages (89%, $p < 0.0001$) (**Figure 5.3F**). Data therefore indicated that M2 polarisation with IL-4 did not upregulate CD163. Regardless, as an M2 marker, CD163 was still found to be moderately expressed in the M2 macrophage model.

Gene expression of IL-10 was not to be upregulated by M2 polarisation (**Figure 5.3G**). While PMA-induced M0 differentiation caused a 184-fold increase relative to THP1 cells, the magnitude of increase was much lower when compared to that following IL-4-stimulated M2 polarisation (91-fold). Thus, as with CD163, IL-4 did not appear to upregulate IL-10 gene expression. Nevertheless, the gene was highly expressed in the M2 model.





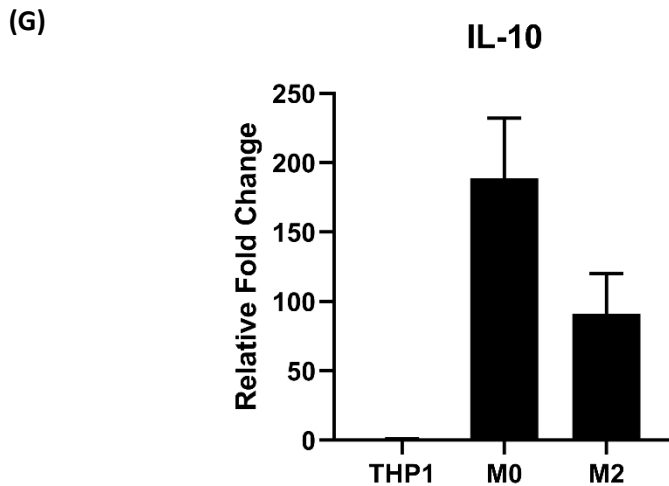


Figure 5.3 Validation of the M2 macrophage model. RNA taken from THP1, M0 or M2 macrophages were analysed by RT-qPCR to detect fold changes in gene expression of CD206 (A), CD163 (D) and IL-10 (G) relative to THP1 cells. Data shown represents mean+SD. (n=1). THP1, M1 and M2 macrophages were cultured, stained with antibodies and analysed by Flow Cytometry. Representative dotplots are shown that depict the gating strategy used to discriminate positive and negative populations for expression of CD206 (B) and CD163 (E). Bar charts are shown which display mean percentages (+SEM) of CD206+ (C), and CD163+ cells (F) within the live cell parent population (n=3). Statistics were analysed using One Way ANOVA with Tukey's post-hoc test to compare means between each group. ** = p <0.01, *** = p <0.001, **** = p <0.0001.

5.3.2 Assessment of the role of HNSCC-derived IL-35 in suppression of the M1 phenotype

5.3.2.1 Suppression of TNF α secretion

TNF α secretion is a function of M1 macrophages and promotes anti-tumour immunity. To assess whether HNSCC-derived IL-35 suppresses this function, M1 macrophages and M1-like cells were treated with 10% conditioned medium from FaDu-IL-35 or control cells and supernatants analysed for changes in TNF α secretion by ELISA. M1-like cells, developed by treating THP1 cells with GM-CSF and IFN γ , were confirmed to secrete TNF α 24 h and 48 h after application of IFN γ (**Supplementary data 13**). CM from transfected cell lines were confirmed not to contain any traces of TNF α , and thus did not affect the validity of data obtained from treatment studies (**data not shown**).

To test for suppression of TNF α in M1-like cells, cultured cells were treated with fresh culture medium (mock) or CM samples (10%) for 24 h or 48 h. Supernatants were collected and analysed by ELISA (**Figure 5.4A**). Relative to mock-treated cells,

FaDu-IL-35 CM significantly reduced the concentration of secreted TNF α , both after 24 h ($p < 0.01$) and more significantly so after 48 h ($p < 0.0001$). CM from FaDu and FaDu-p35 cells had no effect (**Figure 5.4A**). Intriguingly, FaDu-EBI3 CM also suppressed TNF α secretion in a similar manner to FaDu-IL-35 CM (**Figure 5.4A**). Thus, these data support the hypothesis that HNSCC-derived IL-35 may downregulate the M1 macrophage phenotype via suppression of TNF α secretion. It also indicates that the secretome of tumour cells that overexpress EBI3, but not p35, may induce the same effects.

To confirm these findings, the M1 macrophage model was also assessed. Cells were cultured and treated for 48 h with 10% CM. Changes in TNF α secretion were measured by ELISA (**Figure 5.4B**). Due to poor linearity of data points produced by standards, optical density readings were used for analyses rather than absolute concentrations.

The M1 macrophage model was shown to secrete TNF α (**Figure 5.4B**). FaDu CM increased TNF α secretion by approximately 3-fold (**Figure 5.4B**). This was in contrast to its lack of effect on the M1-like model (**Figure 5.4A**). In agreement with data from the M1-like model, 48 h treatment with FaDu-IL-35 CM was shown to suppress TNF α secretion (**Figure 5.4B**). Furthermore, blocking IL-35 by co-stimulation with an anti-EBI3 antibody prevented suppression, and yielded TNF α concentrations similar to that following FaDu CM treatment (**Figure 5.4B**). As comparable effects were observed regardless of increasing concentrations (4 or 10 μg), maximal blocking was likely achieved using 4 μg of antibody. As a control, M1 macrophages were stimulated with recombinant human IL-35 (50 ng/mL). This also suppressed TNF α secretion (**Figure 5.4B**). Thus, data generated from both M1 models suggested that HNSCC-derived IL-35 may suppress TNF α secretion from M1 macrophages.

It was previously shown that CM from FaDu-EBI3 cells suppressed TNF α secretion in M1-like cells (**Figure 5.4A**). Similarly, treatment of M1 macrophages with FaDu-EBI3 CM reduced TNF α production by approximately 50% (**Figure 5.4B**). It was considered whether these effects were due to the activity of secreted human EBI3 alone, or if FaDu cells also secreted an EBI3 binding partner, that when associated, enabled TNF α suppression. To investigate this, M1 macrophages were treated for 48 h with CM taken from a non-human cell line that overexpressed human EBI3, CHO-

EBI3 cells. The data showed that CHO-EBI3 CM did not suppress TNF α secretion from M1 macrophages (**Figure 5.4B**). Instead, it caused a 3.5-fold increase. This magnitude was similar to that observed following treatment with FaDu CM.

The data therefore suggested that the secretome of FaDu (and CHO-EBI3) cells may contain factors that stimulate M1 macrophages to increase production of TNF α . Overexpression and secretion of IL-35 from these tumour cells may suppress TNF α secretion. Moreover, secretion may not be negatively regulated by human EBI3 alone. But, when secreted with other factors derived from FaDu cells, overexpressed EBI3 may suppress TNF α production from M1 macrophages in a manner comparable to IL-35.

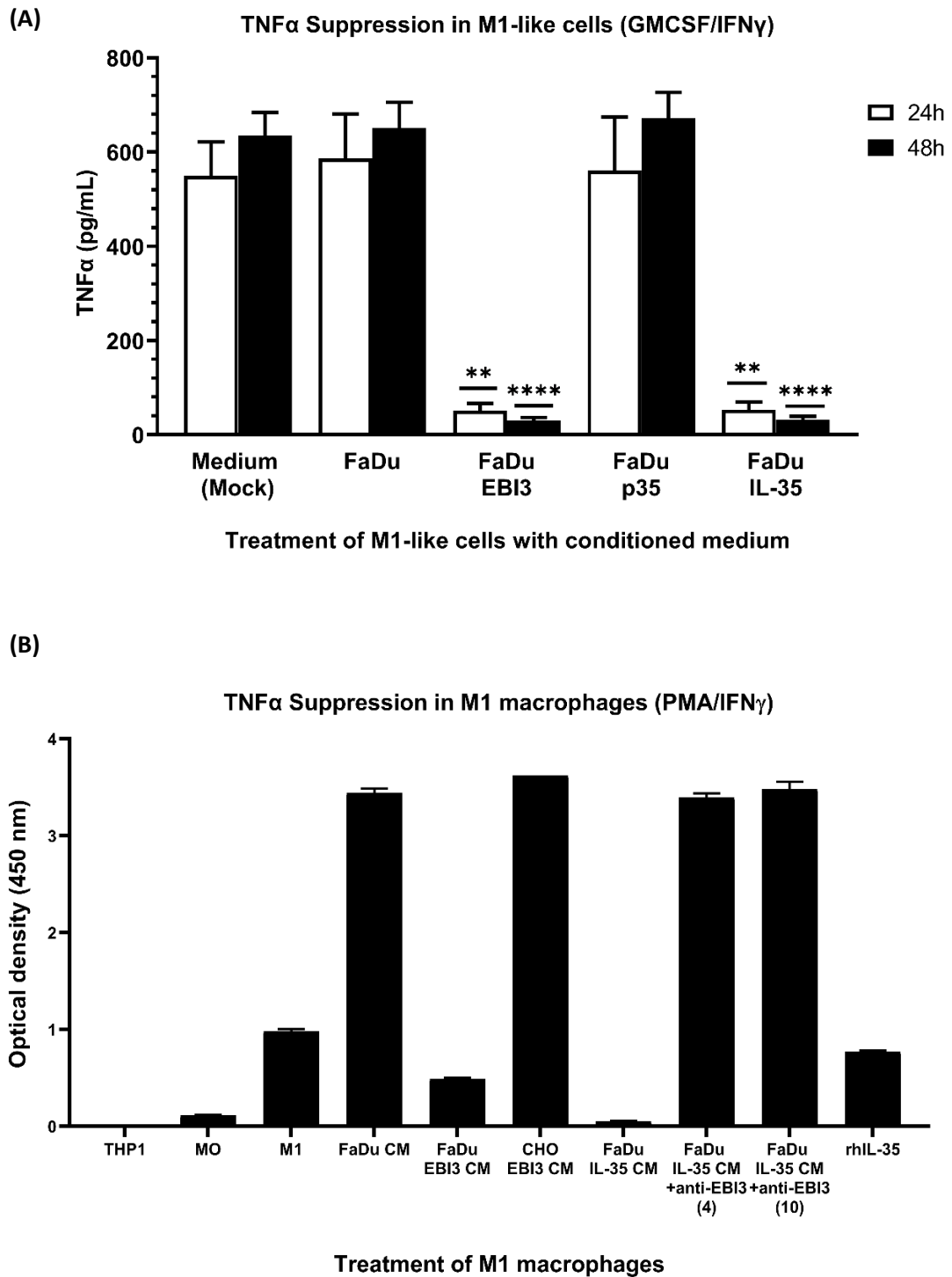


Figure 5.4 Suppression of TNF α secretion in M1 macrophages by HNSCC-derived IL-35. M1-like cells were stimulated for 24 h or 48 h with 10% conditioned medium taken from FaDu, FaDu-EBI3, FaDu-p35 or FaDu-IL-35 cells. Supernatant was collected and analysed by ELISA (A). Data shown represents mean TNF α concentration (pg/mL) + SEM. (N=3). Statistics were analysed using One Way ANOVA followed by Dunnett's post hoc test, with differences in means compared to that in the mock-treated control. ** = $p < 0.01$, **** = $p < 0.0001$. In addition, cultured M1 macrophages were treated with 10% FaDu, FaDu-EBI3, CHO-EBI3, FaDu-IL-35 CM, FaDu-IL-35 CM + anti-EBI3 (4 or 10 μ g), or recombinant human IL-35 (50 ng/mL). THP1 and M0 cells were cultured as controls. 48 h post-treatment, supernatants were collected and analysed by ELISA (B). Data shown represents mean optical density (OD) + standard deviation. (n=1).

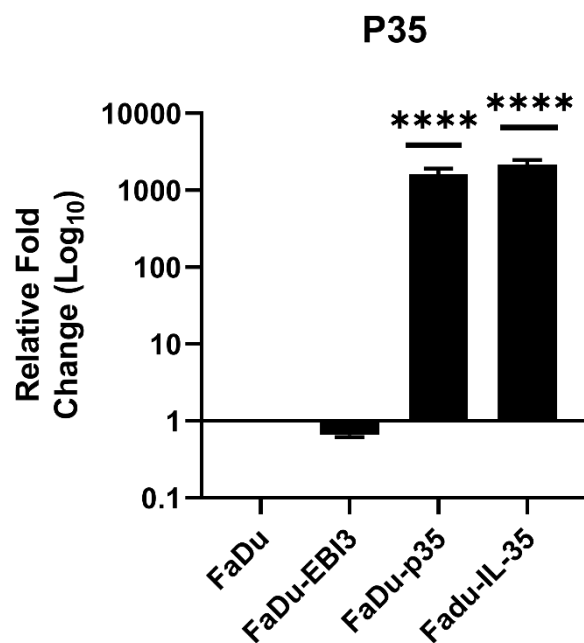
The identity of the secreted EBI3 binding partner was next investigated. EBI3 proteomics data identified the following candidate genes that may be secreted – HLA-G and the IL-12 family subunits p19, p35 and p28. As primers were available for p35, p19 and p28, RT-qPCR was used to assess whether these genes were upregulated in association with EBI3 in the FaDu-EBI3 cell line. Other transfected cell lines were analysed as controls.

p35 can dimerise with EBI3 to form the IL-35 cytokine. The p35 gene is expressed at low levels in untransfected FaDu cells (**Supplementary data 4**). Its expression was not elevated following overexpression of EBI3 in FaDu-EBI3 cells (**Figure 5.5A**). Hence, FaDu-EBI3 cells were unlikely to use IL-35 formation to suppress TNF α secretion in M1 macrophages.

P19 and EBI3 interact to form the IL-39 cytokine. P19 expression is very low in untransfected FaDu cells (**Supplementary data 4**). Data in **Figure 5.5B** revealed that overexpression of EBI3 in FaDu-EBI3 cells did not elevate expression of p19. It instead promoted a significant reduction (9-fold reduction, $p < 0.001$). This effect was also observed in FaDu-p35 and FaDu-IL-35 cell lines. Thus, FaDu-EBI3 cells may not suppress TNF α secretion via the activity of IL-39. EBI3 and p28 associate to form the IL-27 cytokine. However, RT-qPCR analysis could not detect gene expression of p28 in resting FaDu cells nor in any of the other transfected cell lines (**data not shown**). Therefore, EBI3 did not suppress TNF α secretion in M1 macrophages by interacting with p28.

Overall, the data suggested that FaDu-EBI3 cells possibly secrete an unknown protein that can interact with EBI3 to stimulate M1 macrophages, culminating in suppression of TNF α secretion. This binding partner is likely not an IL-12 family member. Therefore, its identity, and the mechanism of EBI3-mediated suppression, remain unknown.

(A)



(B)

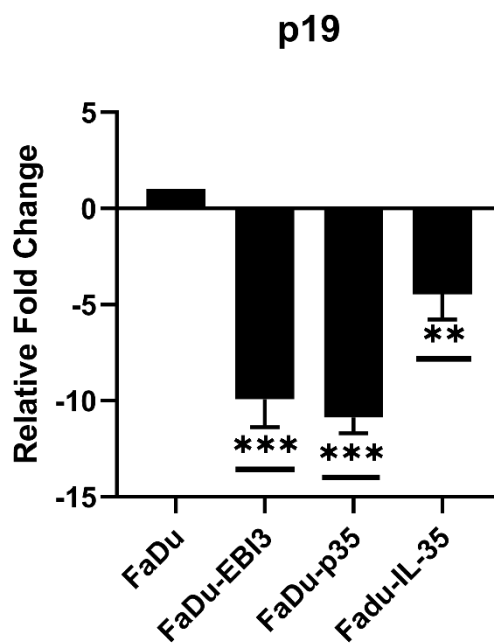


Figure 5.5 Identification of the secreted EBI3 binding partner in FaDu-EBI3 cells. P35 (A) and p19 (B) were examined for increases in gene expression in FaDu-EBI3 cells, relative to untransfected FaDu cells. FaDu-p35 and FaDu-IL-35 cells were also examined as controls. Data shown represents mean+SEM. N=3. Statistical analyses performed on DCT values using One Way ANOVA and Dunnett's post hoc test. ** = $p < 0.01$, *** = $p < 0.001$, **** = $p < 0.0001$.

5.3.2.2 Downregulation of HLA-DR, CD80 and CD86 in M1 macrophages

HLA-DR expression is used in M1-TAMs to present tumour antigens. CD80 and CD86 are co-stimulatory molecules used to activate T cells that engage with the macrophage via antigen presentation. To further assess the role of HNSCC-derived IL-35 in suppression of the M1 macrophage phenotype, cells were treated with FaDu-IL-35 CM, or mixed in culture with FaDu-IL-35 cells, and then evaluated for decreases in expression of these markers.

RT-qPCR data showed that treatment of M1 macrophages with FaDu-IL-35 CM (10%, 48 h) did not decrease HLA-DR gene expression (**Figure 5.6A**). Thus HNSCC-derived IL-35 may not reduce gene expression of HLA-DR in M1 macrophages. It was next investigated whether overexpression of IL-35 in HNSCC cells enabled the the downregulation of HLA-DR protein expression in M1 macrophages. M1 macrophages were cultured alone (M1), or mixed 1:4 with FaDu (M1/FaDu) or FaDu-IL-35 cells (M1/FaDu-IL-35). After 48 h, cells were stained and analysed using Flow Cytometry. All macrophages within each test group were gated using a CD326- gate (to exclude FaDu cells). In all M1 test groups (M1, M1/FaDu, M1/FaDu-IL-35), a minimum of 380 events were captured in the macrophage gate prior to analyses.

Population statistics shown in **Figure 5.6C** demonstrated that IL-35 overexpression had no significant effect on HLA-DR expression in co-cultured M1 macrophages. The mean percentage of CD326- HLA-DR+ macrophages in the M1/FaDu-IL-35 group (54%, n=3) was reduced when compared to both the M1/FaDu group (69%, n=3), and the M1 control group (65%, n=3). Though, One Way ANOVA analyses determined that none of these differences were statistically significant. Therefore, in agreement with findings using RT-qPCR, the data suggested that IL-35 overexpression in HNSCC cells may not enable the downregulation of HLA-DR expression in M1 macrophages.

HLA-DR downregulation was also assessed in M2 macrophages. M2 macrophages were cultured alone or mixed with FaDu or FaDu-IL-35 cells and analysed as described with M1 macrophages. Within the M2 test groups (M2, M2/FaDu, M2/FaDu-IL-35) a minimum of 500 events were captured in the CD326- macrophage gate. The resulting flow cytometry data conveyed that IL-35 overexpression in FaDu

cells did not correlate with reductions in HLA-DR expression (**Figure 5.6C**). Relative to M2 monoculture, M2/FaDu culture caused a slight increase in the mean frequency of CD326- HLA-DR+ macrophages (51% to 56%, n=3), though this difference was not statistically significant. Overexpression of IL-35 in the M2/FaDu-IL-35 group was not significantly different (61%, n=3) to any of the other test groups. Therefore, the data suggested that HNSCC-derived IL-35 had no effect on HLA-DR expression in M1 or M2 macrophages.

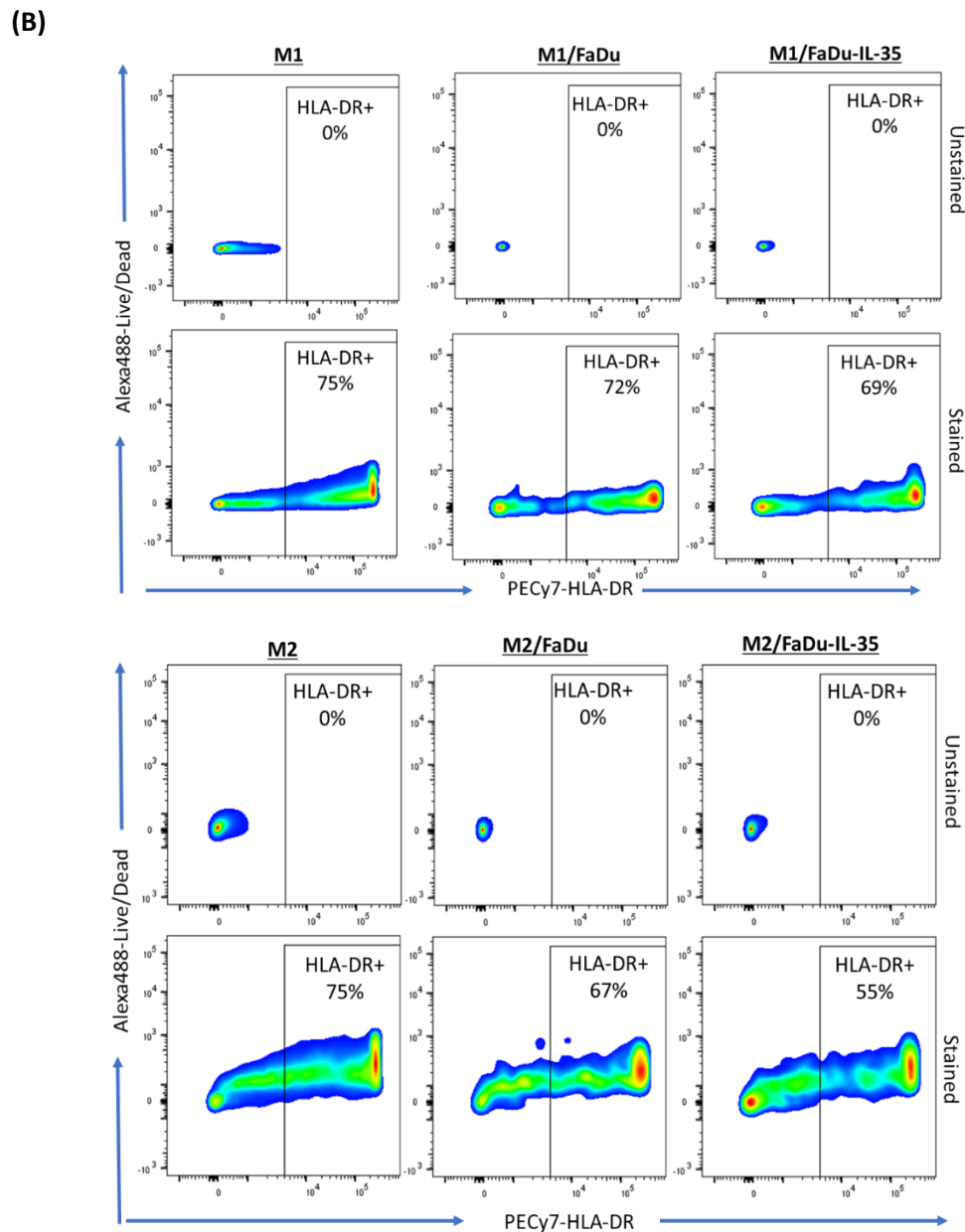
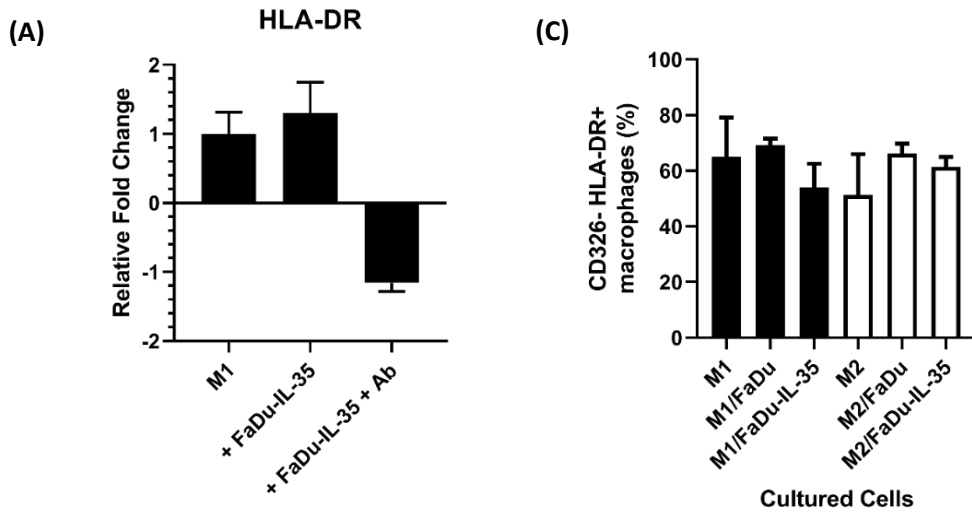


Figure 5.6 Effects of FaDu-derived IL-35 on HLA-DR expression in macrophages. M1 macrophages were stimulated for 48 h with 10% FaDu-IL-35 CM alone, or in combination with blocking antibody (anti-EBI3, 4 µg). RT-qPCR was used to measure changes in gene expression of HLA-DR, relative to that in untreated M1 macrophages (A). Data shown represents mean fold changes+SD. (N=1). The effects of HNSCC-derived IL-35 on HLA-DR protein expression was assessed in M1 and M2 macrophages. M1 or M2 macrophages were cultured alone, or mixed in a 1:4 ratio with FaDu or FaDu-IL-35 cells. Cells were stained with antibodies and analysed by Flow Cytometry. CD326- macrophages were identified and then gated to discriminate HLA-DR+ and HLA-DR- cells. A representative image of this discrimination in all test samples is shown (B). A bar chart is displayed which depicts mean percentages (+SEM) of CD326- HLA-DR+ macrophages within each test group (C). M1, (n=2). All other test samples (n=3). One Way ANOVA and Tukey's test was used to determine significance in differences observed between the following groups (M1 vs M1/FaDu vs M1/FaDu-IL-35) and (M2 vs M2/FaDu vs M2/FaDu-IL-35).

RT-qPCR data showed that treatment of M1 macrophages with FaDu-IL-35 CM alone, or in combination with a blocking antibody, had no effect on gene expression of CD80 (Figure 5.7A). Flow cytometry data revealed that IL-35 overexpression in FaDu cells had no significant effect on CD80 protein expression in co-cultured M1 macrophages (Figure 5.7C). The mean percentage of the CD326- CD80+ macrophage population in M1/FaDu-IL-35 culture (41%, n=3) was lower than in both FaDu/M1 culture (49%, n=3) and M1 monocultures (49%, n=2), though none of these differences were statistically significant. Thus, these findings, along with RT-qPCR data, suggested that HNSCC-derived IL-35 had no effect on CD80 expression in M1 macrophages.

Flow cytometry data demonstrated that IL-35 overexpression in FaDu cells had no effect on CD80 expression in M2 macrophages. When compared to M2 monoculture and M2/FaDu culture, co-culture with FaDu-IL-35 cells had no significant effect on the mean percentage of CD326- CD80+ macrophages (Figure 5.7C). This suggested that HNSCC-derived IL-35 did not negatively regulate CD80 expression in M1 or M2 macrophages.

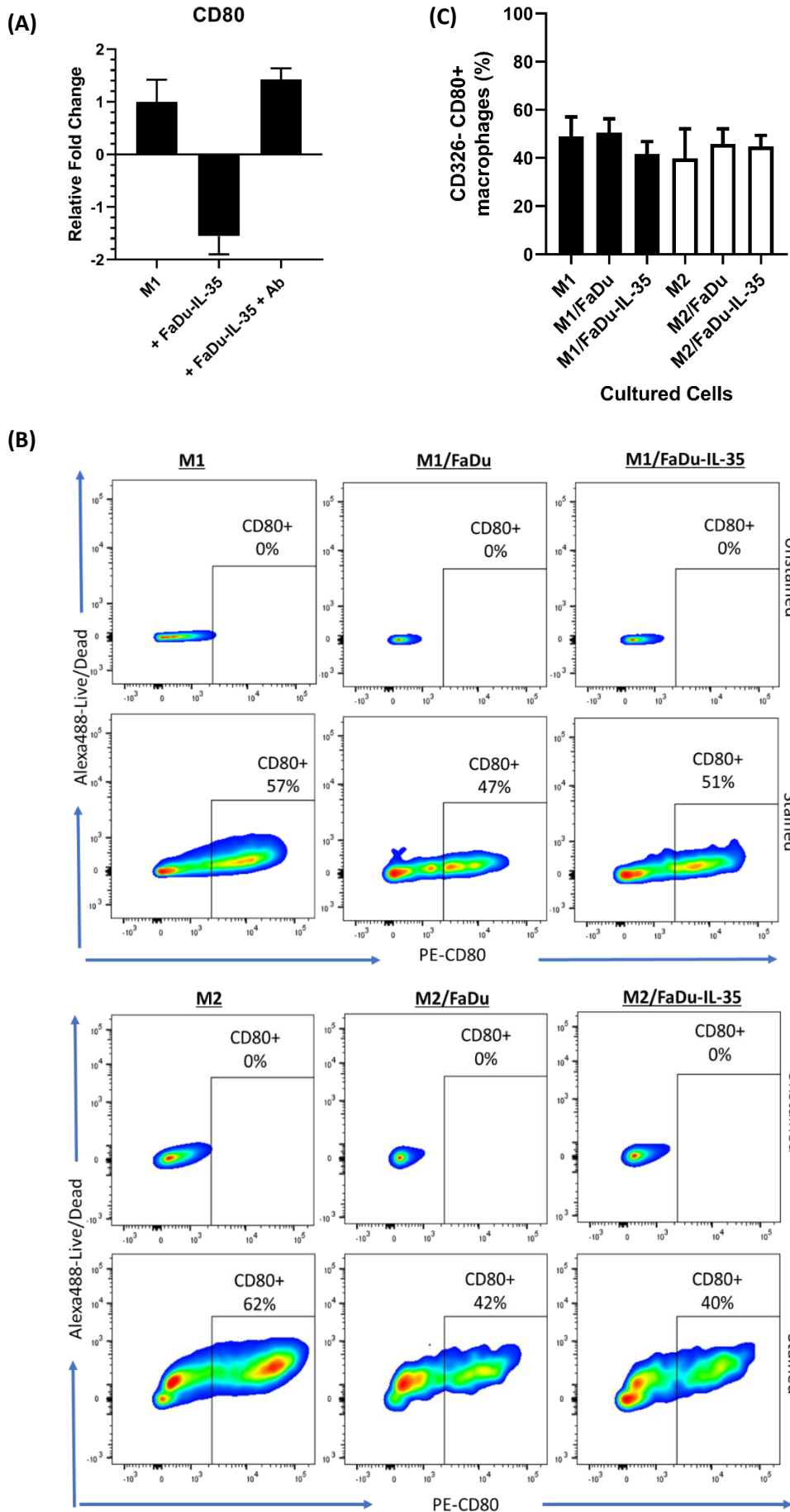


Figure 5.7 Effects of FaDu-derived IL-35 on CD80 expression in macrophages. M1 macrophages were stimulated for 48 h with 10% FaDu-IL-35 CM alone, or in combination with blocking antibody (anti-EBI3, 4 µg). RT-qPCR was used to measure changes in gene expression of CD80, relative to that in untreated M1 macrophages (A). Data shown represents mean + SD. (N=1). The effects of HNSCC-derived IL-35 on CD80 protein expression was assessed in M1 and M2 macrophages. M1 or M2 macrophages were cultured alone, or mixed in a 1:4 ratio with FaDu or FaDu-IL-35 cells. Cells were stained with antibodies and analysed by Flow Cytometry. CD326-macrophages were identified and then gated to discriminate CD80+ and CD80- cells. A representative image of this discrimination in all test samples is shown (B). A bar chart is displayed which depicts mean percentages (+SEM) of CD326- CD80+ macrophages within each test group (C). M1 (n=2). All other test samples (n=3). One Way ANOVA and Tukey's test was used to determine significance in differences observed between the following groups (M1 vs M1/FaDu vs M1/FaDu-IL-35) and (M2 vs M2/FaDu vs M2/FaDu-IL-35).

RT-qPCR data in **Figure 5.8A** demonstrated that treatment of M1 macrophages with FaDu-IL-35 CM did not reduce CD86 expression. Rather, gene expression was increased 2-fold when compared to untreated cells. Moreover, this increase was abolished when cells were co-stimulated with an anti-EBI3 blocking antibody. The data therefore suggested that HNSCC-derived IL-35 may elevate CD86 gene expression in M1 macrophages.

Flow cytometry data showed that co-culture of M1 macrophages with FaDu cells, nor those that overexpressed IL-35, had any significant effect on the percentage of M1 macrophages that expressed CD86 (**Figure 5.8C**). When compared to M2 macrophages in monoculture, FaDu cells caused a non-significant reduction in the mean percentage of macrophages that expressed CD86 (**Figure 5.8C**). IL-35 overexpression had no significant effect when compared to all M2 test groups (**Figure 5.8C**). Thus, HNSCC-derived IL-35 may increase gene expression of CD86 in M1 macrophages, but may not affect CD86 protein expression in either M1 or M2 macrophages.

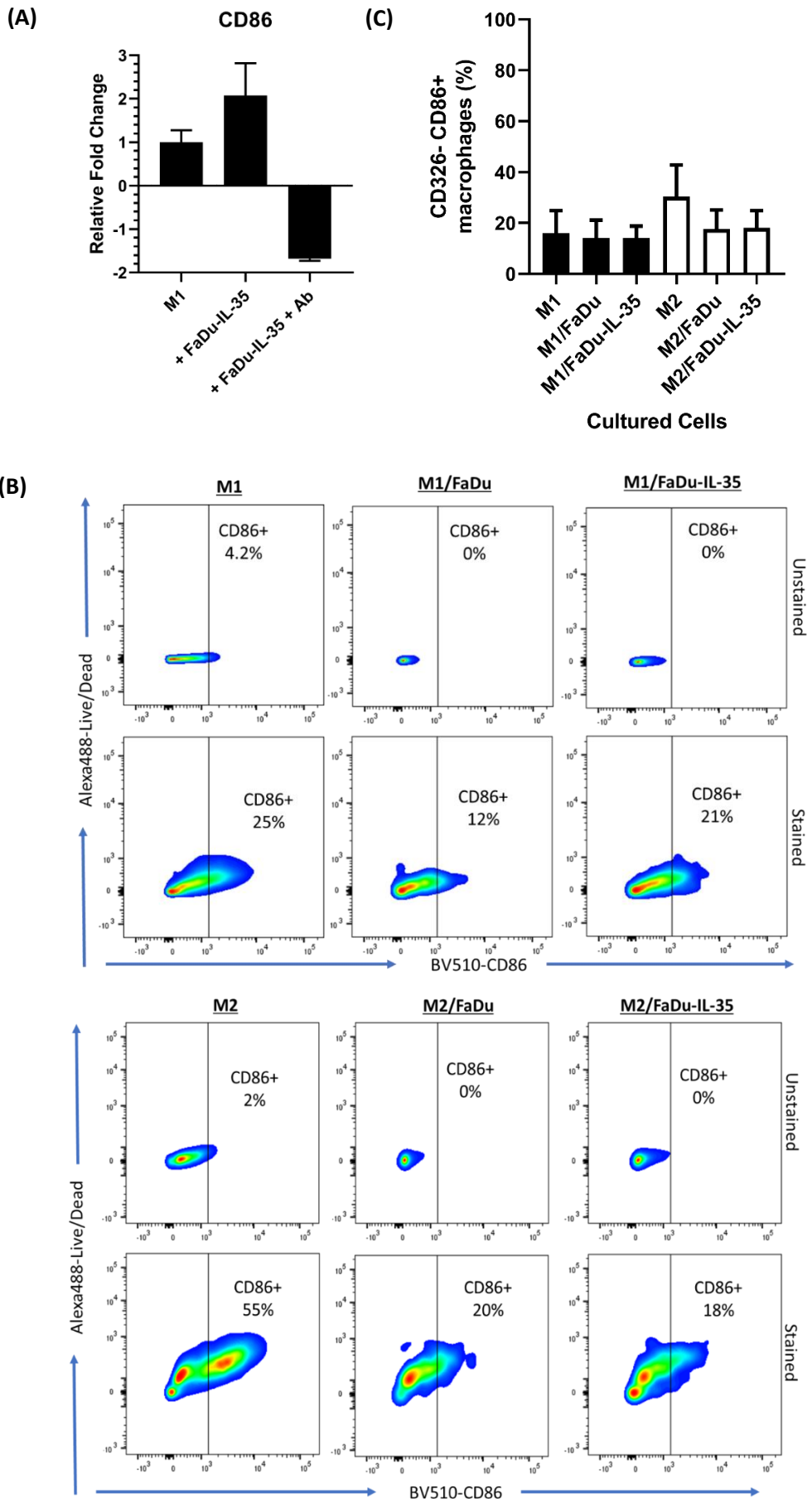


Figure 5.8 Effects of FaDu-derived IL-35 on CD86 expression in macrophages. M1 macrophages were stimulated for 48 h with 10% FaDu-IL-35 CM alone, or in combination with blocking antibody (anti-EBI3, 4 µg). RT-qPCR was used to measure changes in gene expression of CD86, relative to that in untreated M1 macrophages (A). Data shown represents mean fold changes + SD. (N=1). The effects of HNSCC-derived IL-35 on CD86 protein expression was assessed in M1 and M2 macrophages. M1 or M2 macrophages were cultured alone, or mixed in a 1:4 ratio with FaDu or FaDu-IL-35 cells. Cells were stained with antibodies and analysed by Flow Cytometry. CD326- macrophages were identified and then gated to discriminate CD86+ and CD86- cells. A representative image of this discrimination in all test samples is shown (B). A bar chart is displayed which depicts mean percentages (+SEM) of CD326- CD86+ macrophages within each test group (C). M1, (n=2). All other test samples (n=3). One Way ANOVA and Tukey's test was used to determine significance in differences observed between the following groups (M1 vs M1/FaDu vs M1/FaDu-IL-35) and (M2 vs M2/FaDu vs M2/FaDu-IL-35).

5.3.2.3 *Suppression of M1-mediated tumour cell death*

The next objective was to evaluate whether M1 macrophages could induce FaDu cell death, and whether FaDu-derived IL-35 could mitigate these effects. FaDu or FaDu-IL-35 cells were mixed 1:4 in culture with M1 or M2 macrophages. After 48 h, cells were harvested, stained and analysed by Flow Cytometry. FaDu cells were identified using a CD326+ CD14- gate (**Supplementary Data 10**). A minimum of 5000 events were captured within the CD326+ CD14- FaDu cell gate prior to analyses of apoptotic and necrotic populations. Apoptotic cells were identified by gating the Annexin V+ PI- population. Necrotic cells were found by gating the Annexin V+ PI+ population.

Population statistics showed that FaDu and FaDu-IL-35 cells in all samples were highly apoptotic (**Figure 5.9B**). A lower percentage of these cells in all samples were necrotic (**Figure 5.9C**). Neither M1 nor M2 macrophages elevated the percentage of apoptotic or necrotic FaDu cells (**Figure 5.9B and Figure 5.9C**). M1 nor M2 macrophages affected the percentage of apoptotic or necrotic FaDu-IL-35 cells (**Figure 5.9B and Figure 5.9C**). Therefore, the data suggested that the macrophage models used may not directly eliminate FaDu cells, and that IL-35 overexpression in FaDu cells did not affect susceptibility to macrophage-mediated cell death.

Interestingly, the percentage of apoptotic FaDu-IL-35 cells was higher than in FaDu cells. Conversely, the percentage of necrotic cells was reduced in FaDu-IL-35 cells (**Figure 5.9B and Figure 5.9C**). When assessed using a t-test though, neither of these differences were statistically significant. Overall, the data indicated that M1 nor M2 macrophages induce HNSCC cell death by apoptosis or necrosis. Moreover, IL-35 overexpression may not have any effect on the susceptibility of these tumour cells to macrophage-mediated apoptosis or necrosis.

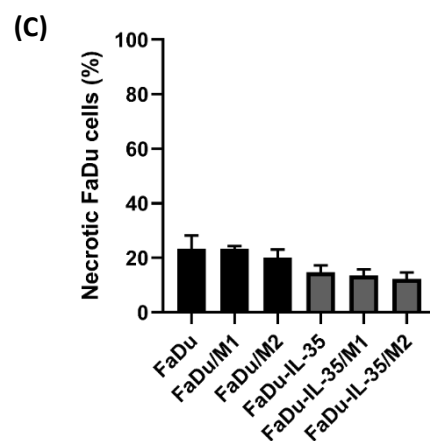
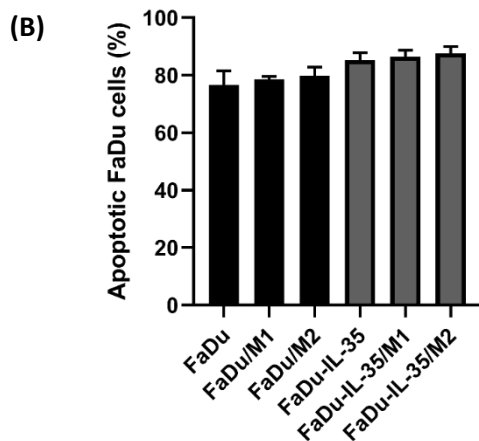
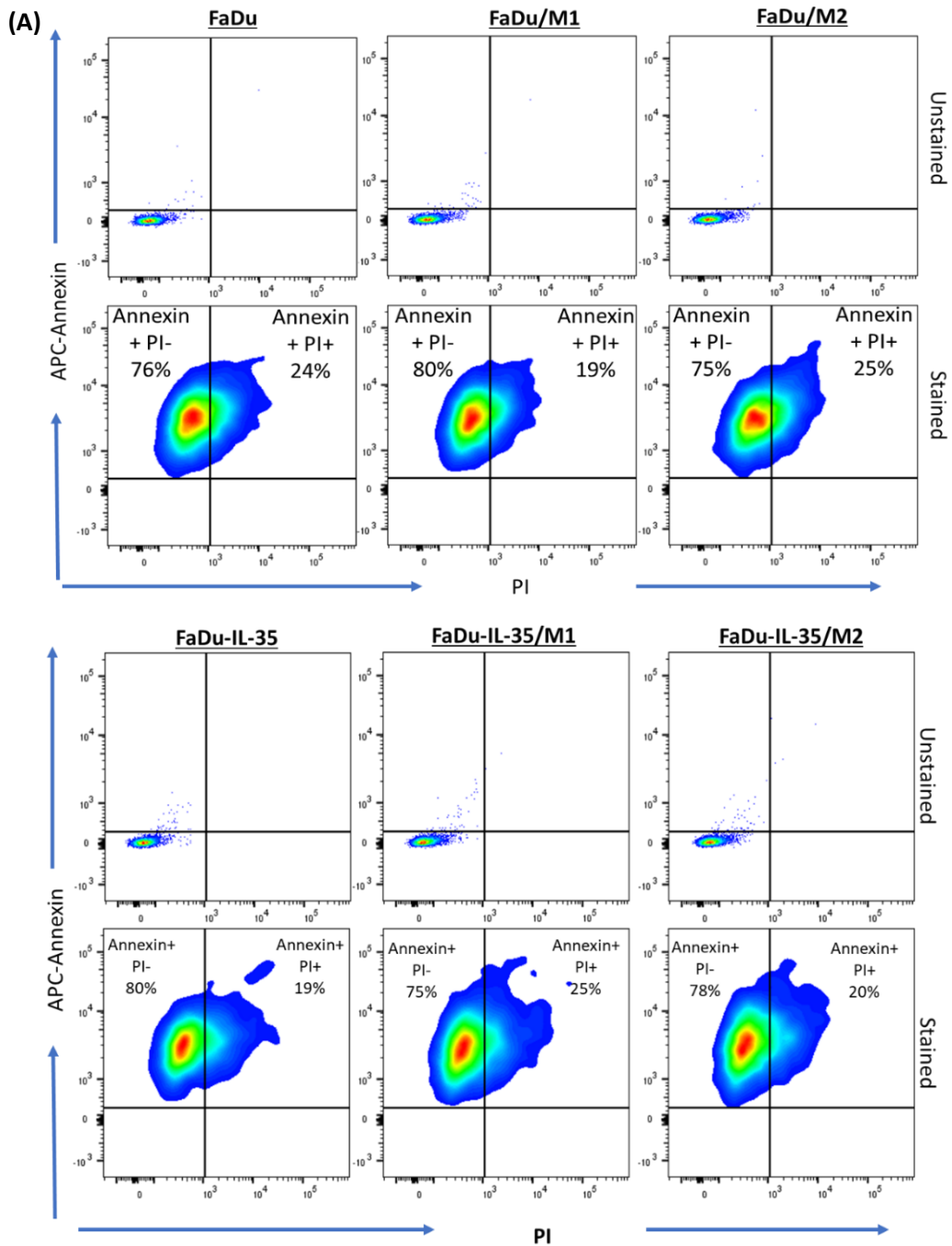


Figure 5.9 Assessment of M1-mediated FaDu cell death and regulation by FaDu-derived IL-35. FaDu or FaDu-IL-35 cells were cultured alone or mixed 4:1 with M1 or M2 macrophages. Cells were stained with antibodies and analysed by Flow Cytometry. FaDu/FaDu-IL-35 cells were identified by gating on the CD326+ CD14- population. These cells were then gated to identify apoptotic cells – Annexin V+ PI-, or necrotic cells – Annexin V+ PI+. A representative image of positive/negative discrimination is shown for each sample group (A). Bar charts are shown which display mean (+ SEM) percentages of apoptotic (B) and necrotic (C) cells. (n=3). One Way ANOVA was used to compare differences in means between the control group - FaDu vs FaDu/M1 and FaDu/M2, or the control group FaDu-IL-35 vs FaDu-IL-35/M1 and FaDu-IL-35/M2. A t-test was used to compare means between FaDu and FaDu-IL-35 sample groups.

5.4 Discussion

Anti-tumour immunity is often dysregulated in inflamed HNSCC. Suppression of immunity supports tumour progression and is associated with poor responses to treatment and overall survival. TAMs are regulators of immunity in the TME. Rather than the pro-inflammatory M1 phenotype, they are often polarised to the M2 phenotype in HNSCC, which promotes immunosuppression and tumour progression. Previous literature reports have described a role for IL-35 in the repolarisation of macrophages from M1 to M2 (Zhang et al. 2016; Peng et al. 2019; Jiang et al. 2020; He et al. 2021). However, there are currently no reports that investigate this role in the context of HNSCC. The thesis aimed to determine whether the immunosuppressive cytokine IL-35, which demonstrated increased gene expression in inflamed HNSCC cell lines (Chapter 3), promotes repolarisation of M1 macrophages, which may be polarised by pro-inflammatory cytokines in an inflamed TME, to the prevalent M2 phenotype. The current study began investigating this by determining whether HNSCC-derived IL-35 suppresses the M1 phenotype.

It was hypothesised that HNSCC-derived IL-35 suppresses the M1 phenotype via downregulation of pro-inflammatory cytokine secretion, HLA-DR, CD80 and CD86 expression – required to present antigens to, and activate T cells, and the ability of M1 macrophages to directly eliminate tumour cells. The Chapter studies revealed that HNSCC-derived IL-35 indeed suppressed the ability of M1 macrophages to secrete the pro-inflammatory cytokine TNF α . It however, did not significantly affect expression of HLA-DR, CD80 or CD86, nor did it significantly impact the susceptibility of tumour cells to macrophage-mediated cell death.

5.4.1 Macrophage models

5.4.1.1 *Macrophage differentiation in THP1 cells*

To test the thesis and Chapter hypotheses, physiologically relevant macrophage models were required. Previous studies have used primary monocyte-derived macrophages (MDMs) isolated from the blood of healthy volunteers, or the monocytic cell lines U937 and THP1 (Daigneault et al. 2010). It was initially intended for MDMs to be used in the current study. However, due to lockdown and social distancing rules put in place during the COVID-19 pandemic, it became difficult to obtain samples from volunteers. Therefore, THP1 cells, which are widely used and accepted as macrophage models, were used as an alternative (Chanput et al. 2014).

PMA was used to differentiate THP1 cells into macrophages. This method is used in most of the pertinent literature and has been reported to produce macrophage phenotypes that closest resemble human MDMs (Daigneault et al. 2010; Chanput et al. 2014; Shiratori et al. 2017; Tedesco et al. 2018). A limitation of this approach is that, dependent on the culture conditions used, such as the concentration of PMA (ranging from 1 to 400 ng/mL), duration of stimulation and rest times, the phenotype of the resulting macrophage model can vary significantly (Kohro et al. 2004; Park et al. 2007; Aldo et al. 2013; Tedesco et al. 2018). Therefore, preliminary experiments were performed to optimise a differentiation protocol that generated models relevant to the requirements of the project experiments. Differentiated cells were required to become adherent and remain so for the duration of culture times employed during Chapter experiments. They also needed to be easily harvested using a dissociation solution, without the need for harmful cell scraping. For these purposes, THP1 cells were differentiated to M0 macrophages using the following protocol – THP1 cells were stimulated with PMA (50 ng/mL, 24 h) followed by a 48 h rest to reduce off-target gene expression.

Data obtained in this Chapter verified macrophage differentiation using this protocol. The cells produced demonstrated hallmark features of macrophage differentiation including - cell adherence to the culture plate, changes in morphology (small and round monocytes to large and stellate macrophages) and increased cell size and granularity (Daigneault et al. 2010; Aldo et al. 2013; Baxter et al. 2020; He et al. 2021). Moreover, gene expression of the macrophage markers CD14 and CD11b were also

elevated, which was in agreement with previous studies (Aldo et al. 2013; Forrester et al. 2018; Starr et al. 2018; Jimenez-Duran et al. 2020). However, CD68 gene expression was not increased. This concurred with some previous studies (Pinto et al. 2021) while disagreeing with others (Genin et al. 2015), which reflects differences in models generated as a result of varied protocols. Nevertheless, data obtained provided sufficient evidence that a THP1-derived macrophage model had successfully been established.

5.4.1.2 M1 macrophage model

To test the hypothesis, M1 and control M2 macrophage models needed to be established. Previous studies commonly polarise M0 macrophages to M1 by treating cells with lipopolysaccharide (LPS) and/or IFN γ (Genin et al. 2015; Smith et al. 2015; Baxter et al. 2020). Preliminary studies showed that generation of M0 macrophages using higher concentrations of PMA was required to optimise M1 polarisation. Moreover, use of LPS was omitted, as both previous reports, and usage in the laboratory group, have shown it to negatively affect cell viability (Genin et al. 2015). Considering these points, M1 macrophages were generated by stimulating THP1 cells with PMA (100 ng/mL, 24 h) followed by a 48 h rest to induce M0 differentiation. M0 macrophages were then polarised to M1 by addition of IFN γ (20 ng/mL, 48 h). These concentrations and times were determined to be effective in preliminary studies. The generated M1 macrophage model was verified by detecting expression of M1 markers including HLA-DR, CD80 and CD86.

The Chapter studies revealed that IFN γ induced upregulation of HLA-DR gene and protein expression. M2 macrophages also expressed HLA-DR protein, but at a much lower level than in M1 macrophages. This suggested that, to a lesser extent, PMA and/or IL-4 may also have induced HLA-DR expression. CD80 expression was also upregulated following M1 polarisation. PMA may have increased expression initially, as both gene expression in M0, and protein expression in M2 macrophages, were found to be elevated. Nevertheless, IFN γ induced a further and more significant increase in HLA-DR expression in M1 macrophages. Raised expression of both HLA-DR and CD80 following M1 polarisation, was in line with previous reports using similar protocols (Genin et al. 2015; Shiratori et al. 2017). CD86 expression in contrast, was unaffected by IFN γ , which may suggest that IFN γ does not regulate CD86 gene

expression in PMA-differentiated macrophages. Concurrently, there are no literature reports that indicate the contrary.

Overall, increased HLA-DR and CD80 expression, and subsequent data demonstrating successful secretion of TNF α , all evidenced that the selected protocol resulted in a viable M1 macrophage model.

5.4.1.3 M2 macrophage model

IL-4 and/or IL-13 are commonly used to induce M2 polarisation in THP1-derived macrophage models (Genin et al. 2015; Smith et al. 2015; Baxter et al. 2020). In the current study, based on preliminary work, stimulation of THP1 cells with a lower concentration of PMA (50 ng/mL, 24 h followed by 48 h rest) and subsequent polarisation by addition of IL-4 (20 ng/mL, 48 h) was used. Previous studies have struggled to standardise a protocol for M2 polarisation (Baxter et al. 2020). Though, in agreement with the current protocol, Baxter recommended that PMA concentrations below 100 ng/mL were necessary for M2 polarisation using IL-4 or IL-13, as PMA can favour M1 polarisation (Baxter et al. 2020).

When validating M2 polarisation in the current study, it was expected that expression of the M2 markers CD163, CD206 and IL-10 would be elevated following treatment with IL-4. CD206 gene expression was markedly increased, which was in accordance with previous studies (Daigneault et al. 2010; Genin et al. 2015; Wheeler et al. 2018). However, this was not reflected in protein expression, levels of which were observed to be low, and similar to that in M1 macrophages. This may have been remedied by increasing the IL-4 concentration used, or by extending the duration of time cells were under stimulation.

CD163 expression was expressed in the M2 model. Its expression was strongly induced by the initial treatment of THP1 cells with PMA, but not at all by IL-4 stimulation used to polarise to M2. M0 macrophages demonstrated higher CD163 gene expression than M2 macrophages, which possibly reflected the dissipating effects of PMA treatment during the additional 48 h period cells were under IL-4 stimulation. This could be confirmed using time-course studies. Furthermore, protein expression was much higher in M1 macrophages than in M2, which may have been a consequence of higher concentrations of PMA used to generate M1 macrophages relative to M2.

Overall, it could be surmised that IL-4 did not affect CD163 expression in the developed model. This was in line with previous studies, which suggested that, for CD163 upregulation, THP1-derived macrophages needed to be stimulated with IL-10, or a combination of IL-4 and IL-13 (Baxter et al. 2020). Despite this possible limitation, as an M2 marker, its expression validated the M2 model.

As with CD163, IL-10 gene expression was expressed in the M2 model, but did not appear to be regulated by IL-4 stimulation. According to work by Genin and others, the current protocol may have required cells to be under IL-4 stimulation for a longer time, but may also require IL-13 co-stimulation (Genin et al. 2015). Despite the limitation of low expression observed for these M2 markers, it could still be assessed whether HNSCC-derived IL-35 affected this. As such, the M2 macrophage model was deemed fit for the purposes of the study.

A limitation of the study was that the same samples were not analysed using qPCR and Flow Cytometry experiments. Ideally, M0 macrophages would also have been analysed by Flow Cytometry. Though, due to antibody availability, the number of samples that could be analysed in the project was limited, and thus M0 macrophage controls were omitted.

A limitation of using THP1 cells is the plethora of differentiation and polarisation protocols reported and the varying phenotypes they produce. In future, it may be beneficial to develop standardised THP1-derived macrophage models, encompassing cell passage numbers, seeding densities, differentiation and polarisation conditions, that consistently induce expression of specific differentiation and polarisation markers. This would allow the researcher to select an established protocol for their particular research purposes. As a potent protein kinase C (PKC) activator, use of PMA can result in changes to gene expression of unintended targets. Therefore, in future studies, should PMA be used for differentiation, application of low concentrations, which may result in loss of adherence after short incubation times, followed by extended rest times, may be a preferable method, as this would minimise the influence of off-target genes in downstream studies. As an alternative, if other differentiation reagents, without the use of PMA, can induce similar morphological and gene expression profiles to that observed in MDMs, this would be beneficial in the development of standardised polarisation protocols.

5.4.2 Assessment of the role of HNSCC-derived IL-35 in suppression of the M1 phenotype

5.4.2.1 *Suppression of TNF α secretion by M1 macrophages*

After generation of M0, M1 and M2 macrophage models, the hypothesis that HNSCC-derived IL-35 suppresses the M1 phenotype was tested. M1 macrophages secrete pro-inflammatory cytokines such as TNF α , IL-12, IL-23, IL-1 β and IL-6 (Orecchioni et al. 2019). The Chapter studies found that, in two in-vitro M1 macrophage models, HNSCC-derived IL-35 directly suppressed TNF α secretion. Previous reports, albeit outside the context of HNSCC, also showed that IL-35 inhibits the M1 phenotype via suppression of TNF α and other pro-inflammatory cytokines. He showed that recombinant IL-35 reduced gene expression of TNF α in a similar PMA-differentiated THP1 model. Additionally, the alternative pro-inflammatory cytokines IL-6 and IL-1 β were also suppressed by IL-35 (He et al. 2021). Similar results were also observed in studies by Peng and Jiang (Peng et al. 2019; Jiang et al. 2020). Thus, the Chapter data adds to the body of literature, and suggests that HNSCC-derived IL-35 may suppress the M1-phenotype of TAMs via inhibition of TNF α secretion.

The current study could have been improved by repeating experiments performed using the M1 macrophage model. This would allow differences caused by treatments to be evaluated statistically. Though, as effects were observed using two different models, and confirmed statistically in the M1-like model, it can be considered that sufficient data was obtained. A limitation in this and other studies in the Chapter was the use of blocking antibody. As macrophages express Fc receptors, this may have affected results. Ideally isotype controls would have been used, or use of a control whereby CM samples are pre-treated with antibodies to remove EBI3 and p35.

In summary, in a novel finding, the study elucidated that HNSCC-derived IL-35 may suppress TNF α secretion in M1 macrophages, which could describe a mechanism used to downregulate the anti-tumour M1 phenotype in the TME. Future studies in this area could be focused on delineating how IL-35 signalling results in TNF α suppression. Also, it could be investigated whether HNSCC-derived IL-35 affects expression of other pro-inflammatory cytokines in M1 macrophages, such as IL-6 and IL-1.

The effects of the wildtype FaDu secretome on TNF α secretion was also investigated. It was found that, while CM from FaDu cells had no effect on treated M1-like cells, it elevated TNF α production in the M1 macrophage model. An explanation regarding this disparity is that, as different agents were used to induce differentiation, the resulting macrophage models exhibited different receptor and gene expression profiles. Otherwise, this finding could suggest that HNSCC cells which do not overexpress IL-35, may secrete soluble factors that stimulate immune responses from M1 macrophages. CHO-EBI3 CM had similar effects, which further suggests that treated M1 macrophages may have recognised and responded to foreign molecules in their secretomes.

A key novel observation in these studies, was that CM taken from FaDu cells that overexpressed EBI3, but not p35, was also able to suppress TNF α secretion in both M1 macrophages and M1-like cells. To test if these effects were attributed to secreted EBI3 alone, cells were treated with CM from non-human CHO cells that overexpressed human EBI3 after transfection. Such treatment did not suppress TNF α secretion. Ideally, additional repeats using CHO-EBI3 CM or recombinant EBI3 would have been performed in both M1 models, and trends validated statistically, to confirm this. Nevertheless, the data obtained suggested that EBI3 may require interactions with additional FaDu-produced factors to enable TNF α suppression.

When identifying potential EBI3-binding partners that facilitate this, candidate proteins were found using EBI3 proteomics data. When tested, it was found that gene expression of p19, p28 and p35 in FaDu-EBI3 cells were found to be too low to be attributed to this role. Regarding p35, it cannot be ruled out that EBI3 overexpression increased p35 protein stability, which could enable IL-35 production (Devergne et al. 1997). This would need to be confirmed in future using an ELISA, or co-immunoprecipitation.

Future studies could be performed to help identify proteins that associate with EBI3 in FaDu cells. From candidate genes found using the proteomics database, it was not analysed whether HLA-G is upregulated in FaDu-EBI3 cells. This could be determined by RT-qPCR. Interestingly, a new study has suggested that EBI3 could interact with p40 to form a novel cytokine that may negatively regulate TNF α expression (Lee et al. 2022). Thus, it may be prudent to assess co-expression of p40

in the FaDu-EBI3 cell line. Other candidates could be identified using techniques such as RNA sequencing or microarray, and comparing data from FaDu and FaDu-EBI3 cells, or using immunoprecipitation to pull down EBI3, followed by SDS-PAGE and mass spectrometry or Western Blotting to identify binding partners. It also cannot be disregarded that this phenomenon could be the result of unintended effects caused by random integration of EBI3 plasmid DNA into the genome during transfection. This could be validated by sequencing the FaDu-EBI3 genome and comparing it to FaDu cells.

Overall, what the novel data suggests, is that HNSCC cells may suppress the M1 TNF α secretion in M1 macrophages by not only secreting IL-35, but also EBI3 in association with another secreted protein.

5.4.2.2 Downregulation of HLA-DR, CD80 and CD86

HLA-DR, CD80 and CD86 are biomarkers of the M1 macrophage phenotype. HLA-DR is used to present tumour antigens to T cells. CD80 and CD86 are co-stimulatory molecules used to activate engaged T cells. It was evaluated whether HNSCC-derived IL-35 suppressed the M1 phenotype by downregulating expression of these markers. When searching the literature, no previous research had investigated this. In the current study, using both a contact independent approach (treatment with CM) to assess the direct effects of secreted IL-35, or a mixed culture approach which enabled cell crosstalk, the data obtained revealed that HNSCC-derived IL-35 had no significant effect on expression of HLA-DR, CD80 or CD86 in M1 macrophages. Co-culture with FaDu-IL-35 cells also had no significant effect on their expression in M2 macrophages.

As a control, macrophages were co-cultured with FaDu cells. FaDu cells did not affect expression of HLA-DR, CD80 or CD86 in M1 or M2 macrophages. This was in direct contrast to a study by Ishizu and others (Ishizu et al. 2021). It must be noted however, that this study used an MDM-derived M0 model treated with conditioned medium from FaDu cells. This promoted polarisation to a mixed M1/M2 phenotype, which displayed elevated levels of HLA-DR and CD86 but downregulation of CD80. Discrepancies in the results obtained when compared to the current study, could be due to differences in the macrophage model used, that the tested macrophages were

M0 and not M1 nor M2, or that the reported study did not incorporate cell-cell crosstalk which may have additional effects. In conclusion, the data from this Chapter suggested that HNSCC cells without influence of immune cells or cytokines, may not regulate HLA-DR, CD80 or CD86 expression in M1 or M2 macrophages.

FaDu-IL-35 CM did not affect gene expression of HLA-DR or CD80 in M1 macrophages, but did increase CD86 gene expression. Co-culture did not affect HLA-DR, CD80 or CD86 protein expression in M1 or M2 macrophages. Discrepancies in induction of CD86 gene expression but lack of protein upregulation could have occurred for several reasons. It is possible that changes in gene expression were not statistically significant (n=1). This would require additional repeats and statistical tests to confirm. Also, a longer culture time may have been required to see changes in protein expression on the cell surface. Time-course studies could be used to investigate this.

It must be noted that mean percentages of M1 and M2 macrophages that expressed these M1 markers was different when validating polarisation, compared to when assessed in co-culture studies. This may be due to the dissipating effects of cytokine stimulation used to polarise cells while they were left untreated for the 48 h mixed culture experiments. Time-course studies could be used to verify this in future. This may have been mitigated by increasing the doses of polarisation agents.

There were limitations in the Flow Cytometry experiments used in this study. To increase accuracy when gating on positive/negative populations, it would have been ideal to prepare fluorescence minus one (FMO) controls. However, due to the number of antibodies used in panels, the costs that would be required to do this rendered this approach unfeasible. Furthermore, it was difficult to assess whether trends observed were statistically significant. This was because, despite collecting 10,000 events in the cytometer, the number of live CD326⁻ macrophages identified in co-culture (1:4 with FaDu cells) ranged from 350 to 900 events. When gating positive populations for different markers within this range, the number of resulting events was very low, especially in lesser expressed markers. Therefore, in future, it may be beneficial to collect more than 10,000 events in the cytometer, which would in turn, increase the number of macrophages available for evaluation.

A CD326- gate was used to identify macrophages in mixed culture. CD326 (EpCAM) is a cell adhesion molecule that had been verified to be expressed in FaDu cells. However, it was possible that these macrophages may have reduced or eliminated CD326 expression as a means of increasing tumour cell invasiveness. While this may only be minimal, it may have affected results. In future it may be beneficial to use an additional macrophage marker to better gate on macrophages. CD14 was attempted in preliminary studies but was highly variable and could have been affected by IL-35 overexpression. An alternative marker such as the pan macrophage marker CD68 may be useful here, though a sufficient amount of time would be required to develop a new antibody panel and re-establish compensation matrices.

Overall, the results did not support the hypothesis, as it suggested that HNSCC-derived IL-35 may not suppress the M1 phenotype via downregulation of HLA-DR, CD80 or CD86. This means it may not inhibit antigen presentation or co-stimulation of T cells by M1 macrophages.

5.4.2.3 Regulation of M1-mediated tumour cell death

M1 macrophages can directly kill phagocytosed tumour cells via production of pro-inflammatory cytokines and reactive oxygen/nitrogen species (Chen et al. 2019; Pan et al. 2020). Research by Genin and others showed, using a THP1 model, that M1 macrophages can promote tumour cell death in-vitro (Genin et al. 2015). In the current study, it was purported that M1 macrophages induce HNSCC cell death, and overexpression of IL-35 may ameliorate this by repolarising M1 macrophages to M2. The results revealed that, unlike findings in Genin's group, neither M1 nor M2 macrophages promoted apoptosis or necrosis of FaDu or FaDu-IL-35 cells. It is possible that the M1 macrophage model could not recognise tumour cells in a manner that enabled phagocytosis. They may also not produce the oxygen or nitrogen species required to induce tumour cell death. A third possibility is that these M1 macrophages require tumour cells to be bound by antibodies to facilitate phagocytosis and tumour cell death. Alternatively, FaDu cells may possess intrinsic mechanisms that enable them to resist phagocytosis and macrophage-mediated cell death, possibly including expression of the don't-eat-me signal CD47 (Aminin and Wang 2021), which would need to be evaluated using RT-PCR or Flow Cytometry. What these results do

highlight however, is that TNF α produced by M1 macrophages does not induce FaDu cell apoptosis (Aminin and Wang 2021; Laha et al. 2021).

In an interesting observation, IL-35 overexpression increased the percentage of apoptotic FaDu cells. While the difference in apoptotic cells between FaDu and FaDu-IL-35 cell populations was not statistically significant when analysed using a t-test, this trend supported previous research which suggested that IL-35 overexpression increases the sensitivity of tumour cells to apoptosis (Long et al. 2013). It cannot be disregarded however, that this effect was a consequence of the stable transfection events used to overexpress EB13 and p35.

A limitation of this study was that there was a high percentage of both control and treated cells that were apoptotic. Cells may have become apoptotic during the several hours it took from harvesting cells to analysis by Flow Cytometry. Alternatively, a common feature of tumour cells is that they may naturally produce high amounts of phosphatidylserine, which is then bound by Annexin V (Aminin and Wang 2021). As such, the experiment may not have been fit for purpose. An alternative experiment to test the hypothesis could involve the use of transwell co-culture combined with an MTT assay (3-(4,5-dimethylthiazol-2-yl)-2,5-diphenyl-2H-tetrazolium bromide). While this experiment was attempted in preliminary studies, it could not be optimised in the time available.

Ultimately, the data produced in the performed experiment did not agree with the hypothesis. It suggested that macrophages may not directly induce HNSCC cell death, and that IL-35 overexpression in HNSCC cells has no effect on this. To continue the Chapter studies in the future, the effects of HNSCC-derived IL-35 on suppression of the M1 phenotype in MDM models could be analysed, as they more closely resemble in-vivo macrophages. It would also be ideal to examine whether IL-35 expression is negatively correlated with expression of M1 markers in TAMs in-vivo, and whether this changes with disease severity. Furthermore, how the IL-35 signal is transduced to suppress TNF α signalling may be explored.

5.5 Conclusions

The current Chapter hypothesised that HNSCC-derived IL-35 suppresses the M1 macrophage phenotype in the TME. The sum of the Chapter data did not agree with

this hypothesis. M0, M1 and M2 macrophage models were developed from THP1 cells. HNSCC-derived IL-35 suppressed the ability of M1 macrophage models to secrete the pro-inflammatory cytokine TNF α . This may be important, as lack of inflammation, which may be promoted by IL-35, is associated with poor outcomes in cancer. While this supported the hypothesis, HNSCC-derived IL-35 was found to have no significant effect on HLA-DR, CD80 or CD86 expression in M1 macrophages. Furthermore, the data suggested that M1 macrophages may not induce FaDu cell death, and as such, it was not determined whether IL-35 could mitigate this.

Thus, the Chapter data suggested that HNSCC-derived IL-35 may suppress pro-inflammatory cytokine production, but may not affect the ability of M1 macrophages to present tumour antigens to T cells, or to activate bound T cells via expression of the co-stimulatory molecules CD80 and CD86. While novel, studies in-vivo are required to elucidate these findings further, and to evaluate the prognostic significance of HNSCC-derived IL-35.

Regarding the thesis hypothesis, the current Chapter began investigating the role of HNSCC-derived IL-35 in repolarisation of M1 macrophages to M2 by analysing suppression of the M1 phenotype. To continue this research, the following Chapter evaluated whether HNSCC-derived IL-35 promotes M1 to M2 polarisation via upregulation of M2 markers.

Chapter 6

**Investigating the role of HNSCC-derived IL-35 in M1 to M2
macrophage repolarisation via promotion of the M2-TAM
phenotype**

6.1 Introduction

In HNSCC, TAMs are often polarised to the M2 activation state, which suppresses immunity and promotes tumour progression (Hao et al. 2012; Sica and Mantovani 2012; Kumar et al. 2019; Peltanova et al. 2019; Wondergem et al. 2020). As such, high densities of M2-TAMs are often associated with disease progression, angiogenesis, tissue remodelling and decreased overall survival (Mori et al. 2011; Weber et al. 2014; Hu et al. 2016; Okubo et al. 2016; Alves et al. 2018; Kumar et al. 2019; Kalogirou et al. 2021). To tackle this therapeutically, it is important to identify novel mechanisms employed by HNSCC tumour cells to promote M2-TAM polarisation.

A role for tumour-derived IL-35 on M2 macrophage polarisation in HNSCC has not yet been studied. Data from Chapter 3 elucidated that IL-35 expression may be upregulated in hypopharyngeal carcinoma cells (FaDu) in response to stimulation with IFN γ and TNF α . It was hypothesised that IL-35 produced from these cells may contribute to the prevalence of M2 TAMs in inflamed HNSCC by repolarising M1 macrophages to an M2-like phenotype. Using a developed FaDu cell line that overexpresses and secretes IL-35, data from Chapter 5 demonstrated that HNSCC-derived IL-35 may suppress the M1 phenotype by blocking their ability to secrete TNF α . The current Chapter aimed to continue testing the thesis hypothesis by investigating whether HNSCC-derived IL-35 promotes M1 to M2 repolarisation by upregulating expression of M2 markers. The potential impact of this research is that it may validate IL-35 as a biomarker of immune dysfunction and disease severity in HNSCC. Furthermore, it may implicate IL-35 as a prospective target to improve host immunity when used in combination with current immunotherapies.

6.1.1 M2-TAMs

TAMs are polarised to an M2 activation state via exposure to Th2 (T helper 2) cytokines (such as IL-4, IL-13, IL-10 and TGF β). M2 macrophages can be identified in-vitro via expression of classical M2 biomarkers. These include surface markers such as CD206, CD163 and secretion of immunosuppressive cytokines including IL-10. In-vivo, they can be identified via co-expression of the pan macrophage marker CD68, and the M2 surface marker CD163 (Kumar et al. 2019; Peltanova et al. 2019).

However, in cancers, several M2-TAM subtypes have been described which express different biomarkers (termed M2-TAM markers henceforth) that can be attributed to their roles (Lin et al. 2019). These consist of CD204, PD-L1 and B7-H4 (explained below), which are involved in immunity, and TAM receptor tyrosine kinases (TYRO3-AXL-MERTK) which are proto-oncogenes that may have roles in disease progression and therapeutic resistance in HNSCC (Verma et al. 2011; Brand et al. 2015; von Mässenhausen et al. 2016; von Mässenhausen et al. 2017; Ruicci et al. 2020). Thus, identifying expression of such TAM markers may provide insights into the roles of M2-TAMs in HNSCC. Within the current Chapter, M1 macrophage models exposed to HNSCC-derived IL-35 were evaluated for increased expression of classical M2 surface markers, M2 cytokines, and candidate M2-TAM markers.

6.1.2 M2 surface markers

There are several proteins expressed on the surface of M2 macrophages that are used for their identification. Of these proteins, CD163 and CD206 are commonly used to identify M2 macrophages in in-vitro studies. CD163 is a scavenger receptor (binds and removes inflammatory ligands from the bloodstream) that is upregulated by macrophages during the resolution of inflammation (Schaer et al. 2006). In HNSCC, CD163 is used to identify M2-TAMs in-vivo, though its role therein is not well understood (Kumar et al. 2019; Suárez-Sánchez et al. 2020; Wondergem et al. 2020). CD206, also known as the mannose receptor, is a carbohydrate-binding protein (C-type lectin). When expressed in M2 macrophages, it assists in resolution of inflammation by removing excess pro-inflammatory markers (Gazi and Martinez-Pomares 2009). It may also regulate immunity by inhibiting CD8+ T cell function (Schuette et al. 2016). However, its role in HNSCC is not well researched.

6.1.3 M2 cytokines

Interleukin-10 (IL-10) is a potent immunosuppressive cytokine. Secreted by M2-TAMs, it inhibits antigen presentation, pro-inflammatory cytokine production and T cell activity. Hence, its overexpression in cancers can contribute to immune escape (Mosser and Zhang 2008; Smith et al. 2018). IL-10 is expressed by M2-TAMs in HNSCC, and predominance of these expressing M2-TAMs is correlated with poor prognoses (Costa et al. 2013).

Vascular Endothelial Growth Factor A (VEGF-A) is also produced by M2-TAMs. It is a key mediator of tissue remodelling and angiogenesis in cancer, acting on endothelial cells to promote generation of new blood vessels. These vessels carry nutrients and oxygen which are integral for exponential tumour growth (Carmeliet 2005). TAMs in oral cancers have been shown to overexpress VEGF. Moreover, high densities of these TAMs in HNSCC have been correlated with disease progression and poor survival (Sun et al. 2018).

6.1.4 M2-TAM markers

CD204, also known as scavenger receptor A (SRA) or macrophage scavenger receptor (MSR), is highly expressed on M2-TAM surfaces. CD204 overexpression is often associated with tumour progression and poor prognoses in several cancers (Ohtaki et al. 2010; Kurahara et al. 2011; Shigeoka et al. 2013; Ichimura et al. 2014; Miyasato et al. 2017). In HNSCC, its co-expression with CD163 in TAMs is associated with PD-L1 and IL-10, suggesting a role of CD163+ CD204+ TAMs in T cell inhibition and immune suppression (Kubota et al. 2017).

M2-TAMs can suppress T cell activation via expression of immune checkpoint ligands. M1-TAMs promote anti-tumour immunity by capturing tumour antigens, processing them into small peptides, and presenting them on their surfaces in association with MHC II molecules. This facilitates the recruitment and engagement of CD4+ T cells. To help activate these cells, M1 macrophages express co-stimulatory molecules (such as CD80 and CD86). In contrast, to attenuate or suppress the activity of bound T cells, M2 macrophages express immune checkpoint proteins. These send inhibitory signals to engaged T cells, which, under normal conditions, prevents auto-immunity and chronic inflammation (Fife and Bluestone 2008). Overexpression of these proteins by tumour or immune cells within cancers can contribute to immunotolerance. In the current Chapter, it is explored whether HNSCC-derived IL-35 can promote M1 to M2 repolarisation via upregulation of the checkpoint proteins PD-L1 and B7-H4.

PD-1 is a well-studied co-inhibitory receptor expressed on activated T cells. Its ligand PD-L1 is commonly overexpressed in inflamed HNSCC, and can be induced in tumour cells stimulated with IFN γ (Tsushima et al. 2006; Ritprajak and Azuma 2015;

Qiao et al. 2020). PD-L1 has been shown to be overexpressed in M2-TAMs within oral cancers, where it was associated with elevated T cell apoptosis (Jiang et al. 2017). Mechanistically, PD-L1 on macrophage or tumour cell surfaces engages PD-1 on activated T cells. This sends inhibitory signals to the bound T cell, resulting in T cell exhaustion and apoptosis (Qiao et al. 2020). Thus, PD-L1 is a potent suppressor of T cell activity and anti-tumour immunity. HNSCC cells have been reported to induce PD-L1 expression in co-cultured TAMs via a mechanism dependent on IL-10 (Jiang et al. 2017). What was not known, and is explored in the Chapter research, is whether HNSCC-derived IL-35 can upregulate PD-L1 expression in M1 macrophages as a method of M2 repolarisation and suppression of anti-tumour immunity.

B7-H4 is another immune checkpoint protein. It is commonly overexpressed in tumour cells and TAMs (Choi et al. 2003), where it binds to and negatively regulates activated T cells in the TME (DeNardo and Ruffell 2019; Wang and Wang 2020). In oral cancers, B7-H4 has been shown to be highly expressed, where its prevalence is correlated with disease progression and poor survival. Its expression was also associated with that of CD11b and PD-L1, indicating this was of TAM origin (Wu et al. 2016a). By exploring the potential upregulation of these TAM markers in M1 macrophages under stimulation with HNSCC-derived IL-35, the Chapter research may provide insights into the immunoregulatory roles of IL-35-induced macrophages in HNSCC.

The purpose of the current Chapter was to expand on research in Chapter 5, by investigating whether HNSCC-derived IL-35 promoted the repolarisation of M1 macrophages to an M2-TAM phenotype via upregulation of M2 markers. The Chapter hypothesised that HNSCC-derived IL-35 promotes the repolarisation of M1 macrophages to an M2-TAM phenotype by upregulating M2 cytokine secretion, M2 surface marker expression and that of candidate immunosuppressive M2-TAM markers.

6.2 Aims and objectives

- Assess the role of HNSCC-derived IL-35 in promoting M1 to M2 repolarisation via upregulation of M2 cytokine production (IL-10 and VEGF-A).

- Assess the role of HNSCC-derived IL-35 in promoting M1 to M2 repolarisation via upregulation of M2 surface marker expression (CD206 and CD163).
- Assess the role of HNSCC-derived IL-35 in M1 to M2 repolarisation via upregulation of candidate M2-TAM marker expression (PD-L1, B7-H4 and CD204).

6.3 Methods

Several of the methods used in this Chapter are explained in detail in Chapter 2. The specific sections where these can be found are referenced using parentheses. Generation of sterile-filtered conditioned medium from transfected FaDu and CHO cell lines (**Section 2.3.6.4**). Generation of macrophage models (**Section 2.3.7**). RT-qPCR and primer sequences (**Section 2.3.2**). Flow Cytometry and antibody panels (**Section 2.3.9**).

6.3.1 Upregulation of M2 cytokine production

To investigate whether HNSCC-derived IL-35 affected IL-10 gene expression in M1 macrophages, RT-qPCR was used. Similar to experiments in Chapter 5, M1 macrophages were generated in 24-well plates (**Section 2.3.7**) and either mock treated with culture medium, stimulated with 10% FaDu-IL-35 CM, or double stimulated with 10% FaDu-IL-35 CM in combination with a blocking antibody (monoclonal anti-EBI3, 4 µg). Cells were incubated under these conditions for 48 h. 250 ng of extracted RNA was converted to cDNA, 8 ng of which was analysed by qPCR to measure fold changes in gene expression of IL-10, relative to mock treated M1 macrophages. Data was normalised to the reference gene β -Actin. (N=1). All samples were run in triplicate.

To investigate changes in IL-10 secretion, ELISA experiments were performed. As a preliminary test, M0, M1 and M2 macrophages were seeded into 24-well plates (**Section 2.3.7**). THP1 cells were also cultured as a control. Cells were mock treated with fresh culture medium, or FaDu-IL-35 CM at 10%, 20% or 50% of the culture volume. Alternatively, cells were treated with 20% CM from FaDu-EBI3 or FaDu-p35 CM as controls. Other concentrations were omitted due to limitations in

availability of wells in ELISA plates. 48 h post-treatment, all supernatants were collected and analysed to detect secreted IL-10 using an ELISA kit as instructed by the manufacturer (ThermoFisher Scientific). (N=1). Each sample was run in triplicate. For validation experiments performed three times with statistical analyses, M0, M1 and M2 macrophages were seeded and treated with 10% CM from FaDu-IL-35, FaDu, FaDu-EBI3, CHO-EBI3 and FaDu-p35 cells. 10% of the culture volume was selected to minimise the effects of serum starvation. THP1 cells were analysed as negative controls. 48 h post-treatment, supernatants were collected and analysed for IL-10 secretion by ELISA. (N=3). All samples were run in triplicate. For all IL-10 data, concentrations (pg/mL) were displayed in bar charts. Where large differences in concentrations were observed between samples, and concentrations were below the minimum detection limit of the assay (2 pg/mL), y-axes were split to show high and low IL-10 concentration data. Differences in mean IL-10 concentrations between the control groups (M0, M1 or M2) versus treatment groups, were analysed statistically using One Way ANOVA with Dunnett's post hoc test.

To provide an estimate of gene expression levels of VEGF-A in M1 macrophages, THP1 cells, M1 and M2 macrophages were cultured in 24-well plates (**Section 2.3.7**). 250 ng RNA was extracted and converted to cDNA. 8 ng cDNA was analysed by qPCR to measure fold changes in gene expression relative to untreated THP1 cells. Data was normalised to the reference gene β -Actin. (N=1). Samples were run in triplicate.

To investigate whether HNSCC-derived IL-35 can upregulate VEGF-A expression, M1 macrophages were treated with fresh culture medium (mock treatment) or 10% FaDu-IL-35 CM alone, or in combination with a blocking antibody (monoclonal anti-EBI3, 4 μ g). After 48 h of incubation, 8 ng cDNA was analysed by qPCR to measure fold changes in VEGF-A expression relative to mock treated M1 macrophages. (N=1). Samples were run in triplicate.

6.3.2 Upregulation of M2 surface marker expression

To investigate changes in gene expression, RT-qPCR was used with conditions similar to Chapter 5. M1 macrophages were generated in 24-well plates (**Section 2.3.7**) and treated with fresh culture medium (mock treatment), conditioned medium from FaDu-

IL-35 cells (FaDu-IL-35 CM) at 10% of the culture volume, or FaDu-IL-35 CM in combination with a blocking antibody (monoclonal anti-EBI3, 4 µg). After 48 h, 8 ng cDNA was analysed by RT-qPCR to detect changes in gene expression of CD206 and CD163 relative to mock-treated M1 macrophages. (N=1). Samples run in triplicate.

To evaluate the effects of HNSCC-derived IL-35 on protein expression of CD206 and CD163 in co-cultured macrophages, M1 or M2 macrophages were mixed 1:4 with FaDu or FaDu-IL-35 cells and incubated for 48 h (detailed methods in **Section 2.3.9.3**). M1 and M2 macrophages left untreated in monoculture were used as controls. Cells were harvested and Fc receptors blocked by addition of TruStain FcX. Cells were stained with a Live/Dead stain kit and the Macrophage Polarisation antibody panel (**Chapter 2 - Table 2.7**). Samples were fixed for up to 72 h in FluoroFix buffer. 10,000 events per sample were captured in an LSRFortessa. Using FlowJo, single, live cells were identified. Within this population, macrophages were captured by gating on CD326- cells (representative image of gating shown in **Supplementary Data 9**). Within the CD326- macrophage population, cells were gated to separate those positive and negative for CD206 or CD163 expression (detailed methods in **Section 2.3.9.7**). For each marker, a uniform gate was set for all sample groups. Where necessary, dotplot axes were adjusted to ensure all events were displayed. In all M1 test groups (M1, M1/FaDu, M1/FaDu-IL-35), a minimum of 380 events were captured in the CD326- macrophage gate prior to analyses. Within the M2 test groups (M2, M2/FaDu, M2/FaDu-IL-35) a minimum of 500 events were captured in this gate.

The effects of IL-35 overexpression in FaDu cells on the expression of these markers was evaluated by comparing the mean percentages of CD326- macrophages that were positive for CD206 or CD163 between the M1 test samples (M1 vs M1/FaDu vs M1/FaDu-IL-35) and M2 test samples (M2 vs M2/FaDu vs M2/FaDu-IL-35). M1 (n=2). All other test samples (n=3). One Way ANOVA and Tukey's test were used to evaluate whether differences in means were statistically significant.

6.3.3 Upregulation of M2-TAM biomarker expression

To provide an estimate of gene expression levels of the M2-TAM biomarkers PD-L1 and B7-H4 in M1 macrophages, THP1 cells, M0, M1 and M2 macrophages were cultured in 24-well plates (**Section 2.3.7**). 8 ng cDNA was analysed by qPCR to

measure fold changes in gene expression relative to untreated THP1 cells. Data was normalised to the reference gene β -Actin. (N=1). Samples were run in triplicate.

To investigate the effects of HNSCC-derived IL-35 on gene expression of the M2-TAM markers PD-L1 and B7-H4, M1 macrophages were generated in 24-well plates (**Section 2.3.7**) and treated with fresh culture medium (mock treatment) or 10% FaDu-IL-35 CM alone, or in combination with a blocking antibody (monoclonal anti-EBI3, 4 μ g). After 48 h, changes in PD-L1 and B7-H4 gene expression were analysed by RT-qPCR as described above. (N=1). Samples were run in triplicate.

To evaluate whether HNSCC-derived IL-35 could increase expression of the M2-TAM marker CD204 in macrophages, M1 or M2 macrophages were mixed 1:4 in culture with FaDu or FaDu-IL-35 cells, stained with fluorescent antibodies and analysed for differences in CD204 expression by Flow Cytometry as described for M2 surface markers. M1 (n=2). All other samples (n=3).

6.4 Results

6.4.1 Upregulation of M2 cytokine production

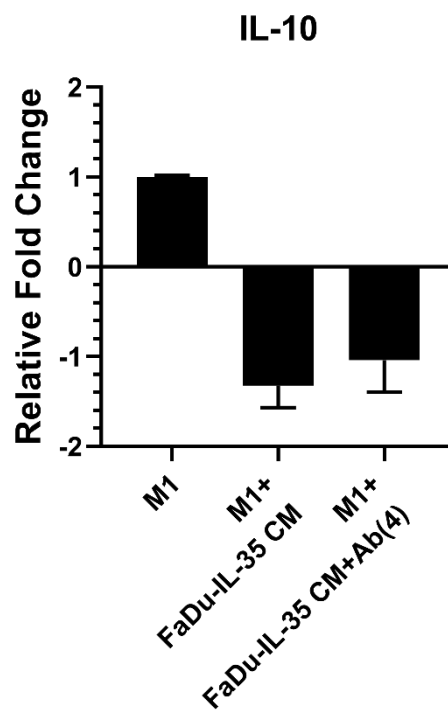
It was evaluated whether HNSCC-derived IL-35 increased IL-10 gene expression in M1 macrophages. RT-qPCR data showed that treatment of M1 macrophages with FaDu-IL-35 CM (10%) had no effect of IL-10 gene expression (**Figure 6.1A**).

As a preliminary test, M1, as well as M0 and M2 macrophages, were stimulated for 48 h with increasing concentrations of FaDu-IL-35 CM (10%, 20% or 50% of the culture volume). Supernatants were analysed by ELISA. Data obtained showed that M1 macrophages secreted very low levels of IL-10 which was reduced by FaDu-IL-35 CM. FaDu-IL-35 CM did not affect IL-10 levels secreted from M0 or M2 macrophages (**Supplementary data 14**).

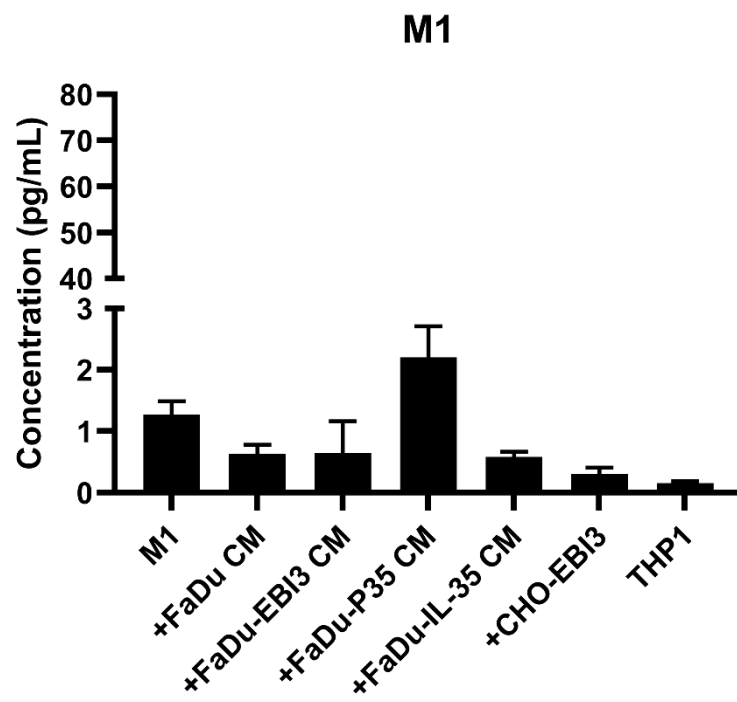
To validate these findings, experiments were performed using three independent repeats and statistical analyses. M1, M0 or M2 macrophages were treated for 48 h with 10% CM from transfected cell lines. Supernatants were analysed by ELISA. M1 macrophages secreted low levels of IL-10 (**Figure 6.1B**). Treatment with FaDu-IL-35 CM caused a non-significant decrease (**Figure 6.1B**). FaDu-p35 CM induced an increase in IL-10, but this was not statistically significant (**Figure 6.1B**). Similar to FaDu-IL-35 CM, FaDu CM, FaDu-EBI3 CM and CHO-EBI3 CM all induced non-significant reductions in IL-10 secretion (**Figure 6.1B**). The data therefore suggested that HNSCC-derived IL-35 may have no significant effect on gene expression or secretion of IL-10 in M1 macrophages.

M0 macrophages secreted trace levels of IL-10 (**Figure 6.1C**). Treatment with FaDu-IL-35 CM had no effect (**Figure 6.1C**). However, while FaDu-p35 CM caused non-significant increases in M1 macrophages, it was found to markedly increase IL-10 secretion in M0 macrophages ($p < 0.0001$) (**Figure 6.1C, supplementary data 14**). Stimulation with FaDu, FaDu-EBI3, or CHO-EBI3 CM had no effect (**Figure 6.1C**). Thus, the data showed that HNSCC-derived IL-35 may not upregulate IL-10 in M0 macrophages. The secretome from tumour cells that overexpress p35 however, may potentially induce IL-10 secretion in M0 macrophages.

(A)



(B)



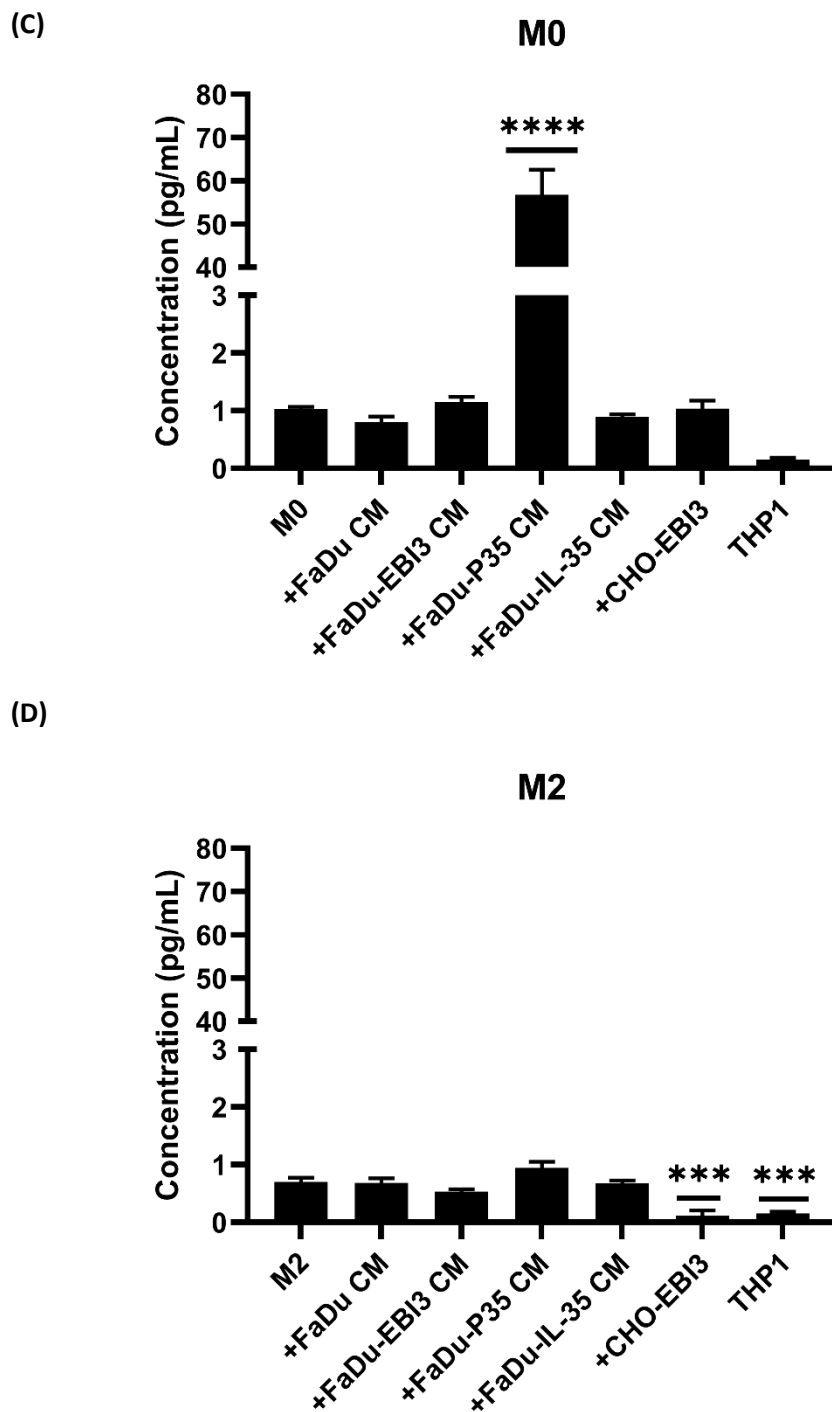


Figure 6.1 Effects of HNSCC-derived IL-35 on expression and secretion of IL-10 in cultured macrophage models. (A) M1 macrophages were treated for 48 h with 10% CM from FaDu-IL-35 cells alone or in combination with an anti-EBI3 monoclonal antibody (4 μ g). RT-qPCR was used to assess fold changes in IL-10 gene expression relative to untreated M1 macrophages. Data represents mean+SD. N=1. Alternatively, M1 (B), M0 (C) or M2 (D) macrophages were treated with 10% CM (from cells shown in Figure) for 48 h. Cultured THP1 cells were analysed as negative controls. Supernatants were collected and analysed by ELISA to assess changes in IL-10 secretion. Data represents mean concentration (pg/mL) + SEM. (N=3). Statistics were analysed using One Way ANOVA with Dunnett's post-hoc test to compare means of each treatment group to the control M1, M0 or M2 groups. *** = $p < 0.001$, **** = $p < 0.0001$.

M2 macrophages secreted very low levels of IL-10 (**Figure 6.1D**). Treatment with FaDu-IL-35 CM, nor that from FaDu, FaDu-EBI3 or FaDu-p35 cells, had any significant effect (**Figure 6.1D**). CHO-EBI3 CM induced a significant reduction in IL-10 secretion from M2 macrophages ($p < 0.001$) (**Figure 6.1D**). In summary, the data suggested that HNSCC-derived IL-35 may not promote M2 polarisation via upregulation of IL-10 expression. In contrast, the secretome of HNSCC cells that overexpress p35, but not EBI3, may elevate IL-10 secretion in M0 or M1 macrophages.

The effects of HNSCC-derived IL-35 on VEGF-A expression in M1 macrophages was investigated. RT-qPCR data from preliminary tests demonstrated that differentiation and polarisation to M1 macrophages increased VEGF-A expression 4-fold relative to untreated THP1 cells (**Figure 6.2A**). VEGF-A expression could not be detected in M2 macrophages (**Figure 6.2A**). Treatment of M1 macrophages with FaDu-IL-35 CM had no significant effect on VEGF-A expression (**Figure 6.2B**). The data therefore indicated that HNSCC-derived IL-35 may not promote M2 repolarisation via upregulation of VEGF-A expression, though additional repeats are required to confirm this.

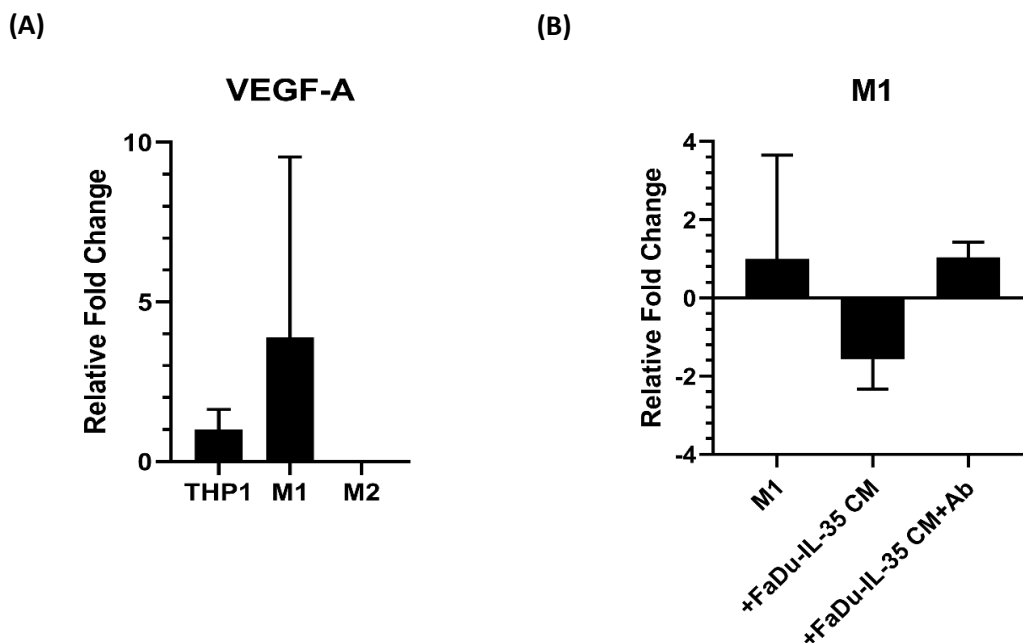


Figure 6.2 Effects of HNSCC-derived IL-35 on gene expression of VEGF-A in M1 macrophages. (A) THP1, M1 and M2 macrophages were analysed by RT-qPCR to assess changes in VEGF-A expression relative to untreated THP1 cells. (B) M1 macrophages were treated for 48 h with FaDu-IL-35 CM (10%) alone or with an anti-EBI3 monoclonal antibody (4 μ g). RT-qPCR was used to measure fold changes in gene expression relative to untreated M1 macrophages. Data represents mean+SD. (n=1). Samples run in triplicate.

6.4.2 Upregulation of M2 surface marker expression

Cultured M1 macrophages were treated for 48 h with FaDu-IL-35 CM alone, or in combination with an anti-EBI3 blocking antibody. RT-qPCR data showed that neither treatment had any significant effect on gene expression of CD206 in M1 macrophages (**Figure 6.3A**).

M1 macrophages were mixed 1:4 with FaDu or FaDu-IL-35 cells and cultured for 48 h, stained with fluorescent antibodies, and analysed by Flow Cytometry. Macrophages were distinguished from FaDu cells by using a CD326⁻ gate. It was then assessed whether co-culture with FaDu-IL-35 cells significantly increased the percentage of CD326⁻ macrophages that expressed CD206.

Flow cytometry data shown in **Figure 6.3C** demonstrated that IL-35 overexpression had no significant effect on CD206 expression in M1 macrophages. CD206 expression was low in monocultured M1 macrophages (mean 14%). M1/FaDu culture reduced the mean CD326⁻ CD206⁺ macrophage population (14% to 8%). M1/FaDu-IL-35 culture partially mitigated this (12%). However, as none of these differences were statistically significant, the data suggested that co-culture with FaDu cells, nor those that overexpressed IL-35, had any effect on CD206 expression in M1 macrophages.

A low mean percentage of M2 macrophages in monoculture expressed CD206 (16%) (**Figure 6.3C**). IL-35 overexpression in co-cultured FaDu cells had no significant effect (**Figure 6.3C**). The data followed a similar trend as with M1 macrophages, whereby M2/FaDu culture reduced CD206 expression relative to control M2 culture (6% versus 16% respectively), which was partially mitigated by IL-35 overexpression (9%) (**Figure 6.3C**). None of these differences were statistically significant. Therefore, the overall data indicated that HNSCC-derived IL-35 may not promote M2 polarisation via induction of CD206 gene or protein expression.

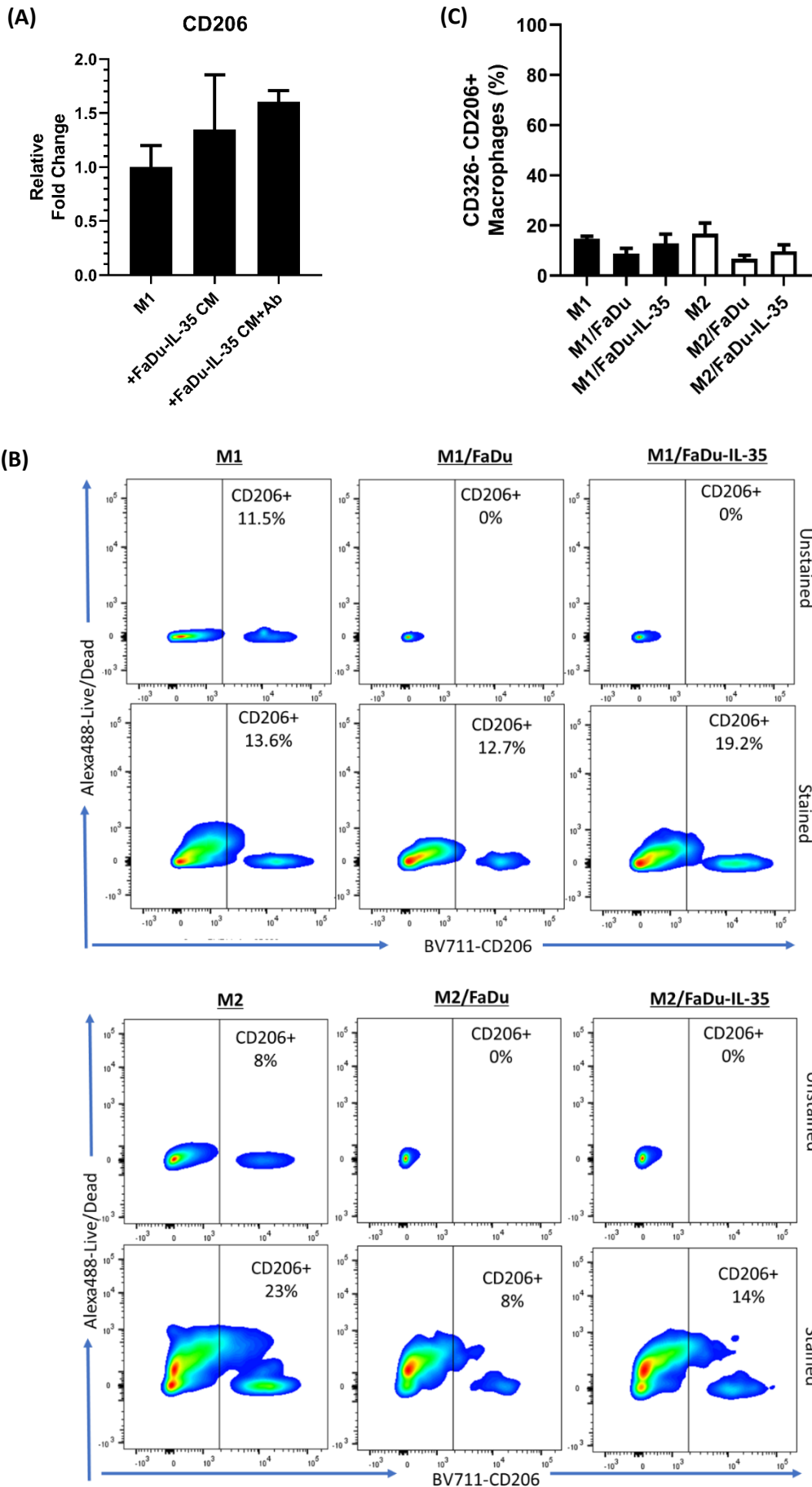


Figure 6.3 Effects of FaDu-derived IL-35 on CD206 expression in macrophages. M1 macrophages were stimulated for 48 h with 10% FaDu-IL-35 CM alone, or in combination with blocking antibody (anti-EBI3, 4 µg). RT-qPCR was used to measure changes in gene expression of CD206, relative to that in untreated M1 macrophages (**A**). Data shown represents mean fold changes + SD. (N=1). Samples were run in triplicate. To validate findings via analysis of changes in protein expression, M1 or M2 macrophages were cultured alone, or mixed in a 1:4 ratio with FaDu or FaDu-IL-35 cells. Cells were stained with antibodies and analysed by Flow Cytometry. CD326- macrophages were identified and then gated to discriminate CD206+ and CD206- cells. A representative image of this discrimination in all test samples is shown (**B**). A bar chart is displayed which depicts mean percentages (+SEM) of CD326- CD206+ macrophages within each test group (**C**). M1, (n=2). All other test samples (n=3). One Way ANOVA and Tukey's test was used to determine significance in differences observed between M1 and M2 sample groups.

It was next evaluated whether HNSCC-derived IL-35 upregulated CD163 expression in M1 macrophages. RT-qPCR data demonstrated that neither treatment of M1 macrophages with FaDu-IL-35 CM alone, or with a blocking antibody, had any significant effect on CD163 gene expression (**Figure 6.4A**).

Flow cytometry data showed that there was a low mean percentage of CD326- M1 macrophages that expressed CD163 in monoculture (25%). M1/FaDu (26%) nor M1/FaDu-IL-35 mixed culture (25%) had any significant effect (**Figure 6.4C**). CD163 expression was also low in M2 macrophages (mean 22%) (**Figure 6.4C**). In agreement with M1 data, mixed culture with FaDu cells (M2/FaDu, 30%) nor those that overexpressed IL-35 (M2/FaDu-IL-35, 30%) had any statistically significant effect on CD163 expression in M2 macrophages (**Figure 6.4C**). The data thus indicated that HNSCC-derived IL-35 may not promote M1 to M2 repolarisation via upregulation of the M2 markers CD206 or CD163 in M1 macrophages. It also may not enhance the M2 phenotype by upregulating expression of these markers.

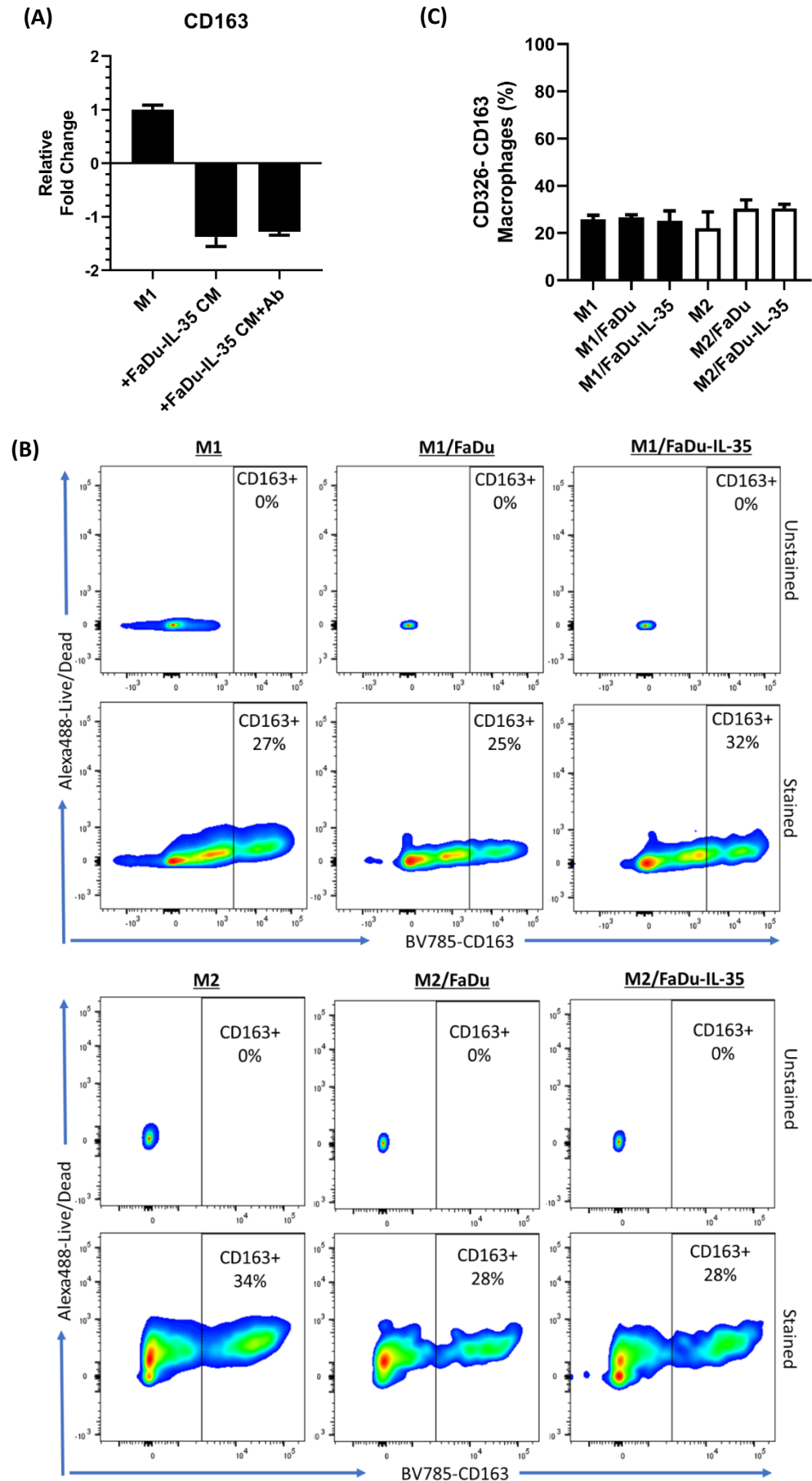


Figure 6.4 Effects of FaDu-derived IL-35 on CD163 expression in macrophages. M1 macrophages were stimulated for 48 h with 10% FaDu-IL-35 CM alone, or in combination with blocking antibody (anti-EBI3, 4 µg). RT-qPCR was used to measure changes in gene expression of CD163, relative to that in untreated M1 macrophages (**A**). Data shown represents mean fold changes + SD. N=1. Samples run in triplicate. To validate findings via analysis of changes in protein expression, M1 or M2 macrophages were cultured alone, or mixed in a 1:4 ratio with FaDu or FaDu-IL-35 cells. Cells were stained with antibodies and analysed by Flow Cytometry. CD326- macrophages were identified and then gated to discriminate CD163+ and CD163- cells. A representative image of this discrimination in all test samples is shown in (**B**). Gates were uniformly set across all samples, axes were adjusted to enable visualisation of all events. A bar chart is displayed which depicts mean percentages (+ SEM) of CD326- CD163+ macrophages within each test group (**C**). M1, (n=2). All other test samples (n=3). One Way ANOVA and Tukey's test was used to determine significance in differences observed between M1 and M2 sample groups.

6.4.3 Upregulation of M2-TAM biomarker expression

The final aim of the Chapter was to investigate whether HNSCC-derived IL-35 promoted the repolarisation of M1 macrophages to an M2-TAM phenotype via upregulation of the candidate M2-TAM markers PD-L1, B7-H4 and CD204.

RT-qPCR data showed that while M0 differentiation had no effect on PD-L1 expression relative to THP1 cells, IFN γ -induced M1 polarisation caused a 493-fold elevation in expression (**Figure 6.5A**). IL-4-mediated M2 polarisation also increased PD-L1 expression but to a lesser extent (62-fold). Treatment of M1 macrophages with FaDu-IL-35 CM reduced PD-L1 expression by a 3-fold magnitude (**Figure 6.5B**). This effect was abrogated when M1 macrophages were co-stimulated with both FaDu-IL-35 CM and a blocking antibody (**Figure 6.5B**). Thus, the data demonstrated that HNSCC-derived IL-35 may not promote M1 to M2-TAM repolarisation via upregulation of PD-L1, instead causing a reduction in expression. Additional repeats are required to confirm this.

It was analysed whether HNSCC-derived IL-35 increased in B7-H4 expression in M1 macrophages. However, RT-qPCR data demonstrated that gene expression could not be detected in THP1 cells, M0, M1 and M2 macrophages, and in M1 macrophages treated with FaDu-IL-35 CM (**data not shown**). Therefore, HNSCC-derived IL-35 may not promote M2-TAM polarisation via upregulation of B7-H4 expression.

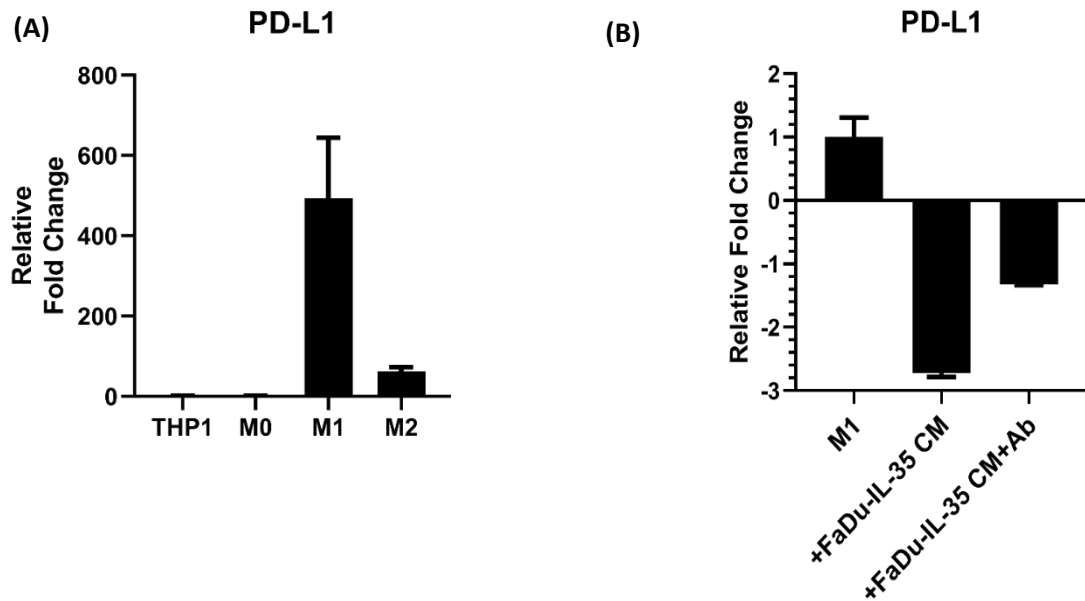


Figure 6.5 Effects of HNSCC-derived IL-35 on gene expression of PD-L1 in M1 macrophages. (A) THP1, M0, M1 and M2 macrophages were analysed by RT-qPCR to assess fold changes in PD-L1 expression relative to untreated THP1 cells. (B) M1 macrophages were treated for 48 h with FaDu-IL-35 CM (10%) alone or with an anti-EBI3 monoclonal antibody (4 μ g). RT-qPCR was used to measure fold changes in gene expression relative to untreated M1 macrophages. Data represents mean + SD. n=1. Samples run in triplicate.

It was examined whether HNSCC-derived IL-35 upregulated CD204 expression in M1 macrophages. M1 or M2 macrophages were mixed 1:4 with FaDu or FaDu-IL-35 cells and cultured for 48 h, stained with antibodies, and analysed by Flow Cytometry. Macrophages were identified by gating on CD326⁻ cells. They were then analysed to investigate if co-culture with FaDu-IL-35 induced significant increases in CD204 expression when compared to co-culture with FaDu cells, and when in monoculture.

The data showed that a large percentage of CD326⁻ M1 macrophages expressed CD204 in monoculture (mean = 69%) (**Figure 6.6B**). M1/FaDu mixed culture had no effect (mean = 68%) (**Figure 6.6B**). M1/FaDu-IL-35 culture caused a reduction that was not statistically significant when compared to the other groups (mean = 59%) (**Figure 6.6B**). The data therefore suggested that HNSCC-derived IL-35 may not promote M2-TAM repolarisation via upregulation of CD204 expression.

Half of the examined M2 macrophages in monoculture expressed CD204 (mean = 50%) (**Figure 6.6B**). M2/FaDu mixed culture increased this slightly (mean = 56%)

(**Figure 6.6B**). IL-35 overexpression had no additional effect (M2/FaDu-IL-35, mean = 57%) (**Figure 6.6B**). When analysed statistically, there was no significant difference between any of the tested groups. Thus, the data suggested that HNSCC-derived IL-35 may not elevate CD204 expression in M1 or M2 macrophages.

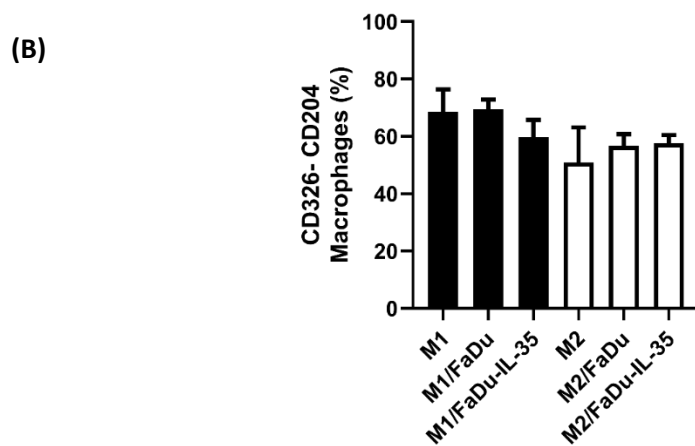
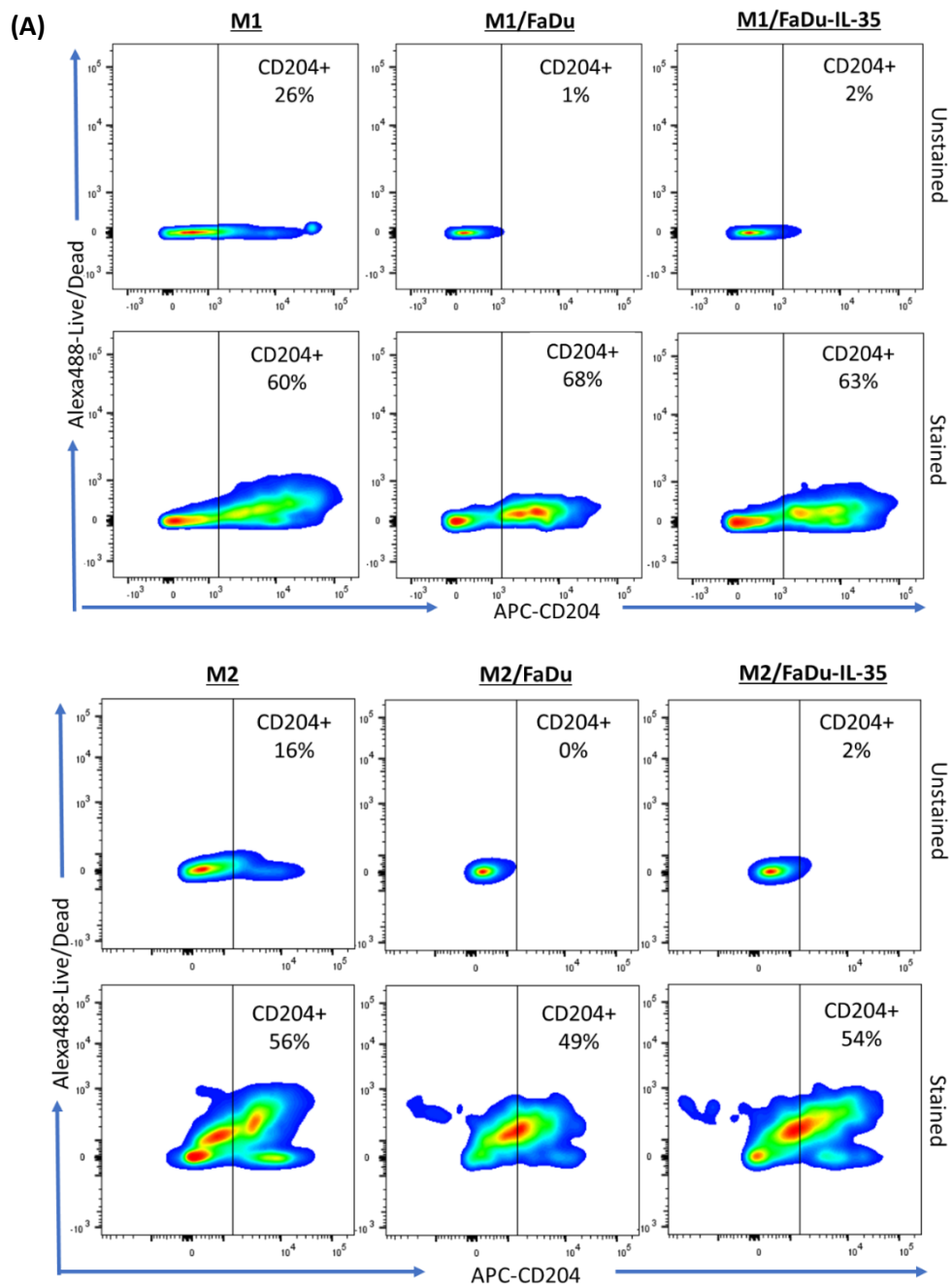


Figure 6.6 Effects of FaDu-derived IL-35 on CD204 expression in macrophages. M1 or M2 macrophages were cultured alone, or mixed in a 1:4 ratio with FaDu or FaDu-IL-35 cells. Cells were stained with antibodies and analysed by Flow Cytometry. CD326- macrophages were identified and then gated to discriminate CD204+ and CD204- cells. A representative image of this discrimination in all test samples is shown in (A). Gates were uniformly set across all samples, axes were adjusted to enable visualisation of all events. A bar chart is displayed which depicts mean percentages (+ SEM) of CD326- CD204+ macrophages within each test group (B). M1, (n=2). All other test samples (n=3). One Way ANOVA and Tukey's test was used to determine significance in differences observed between M1 and M2 sample groups.

6.5 Discussion

In inflamed HNSCCs, macrophages are often polarised to M2. M2-TAMs are associated with immune suppression and cancer progression (Mori et al. 2011; Weber et al. 2014; Hu et al. 2016; Okubo et al. 2016; Alves et al. 2018; Kumar et al. 2019; Kalogirou et al. 2021). While in different biological contexts, previous literature has reported that IL-35 may promote M2 repolarisation (Liu et al. 2019b; Peng et al. 2019; Jiang et al. 2020; He et al. 2021; Chen et al. 2022; Luo et al. 2022). The Chapter purported a mechanism used by tumour cells to facilitate the prevalence of M2-TAMs in the TME. It hypothesised that HNSCC-derived IL-35 promotes the repolarisation of M1 macrophages to an M2-TAM phenotype by inducing the upregulation of M2 genes. It was tested whether this could be evidenced by observing raised expression of M2 cytokines, surface markers and candidate TAM markers. While key findings were found, the data ultimately did not support this hypothesis, as HNSCC-derived IL-35 did not upregulate M2 cytokines, surface markers or tested immune-suppressing M2-TAM markers.

6.5.1 Upregulation of M2 cytokine production

IL-10 is an immunosuppressive cytokine that can be secreted by M2-TAMs (Mosser and Zhang 2008; Smith et al. 2018). In HNSCC, high densities of M2-TAMs which produce IL-10 can have negative implications prognostically (Costa et al. 2013). In the current study, it was purported that IL-35 produced by tumour cells could repolarise M1 macrophages to an M2 phenotype, which would encompass upregulation of IL-10. The Chapter data found that IL-35 secreted from FaDu cells did not increase gene expression of IL-10 in stimulated M1 macrophage models, nor did it enhance secretion in M1, M0 or M2 macrophage models.

These observations contrasted with those previously reported. Studies by Peng and Jiang found that mice M1 macrophage models treated with recombinant IL-35 increased expression of IL-10 (Peng et al. 2019; Jiang et al. 2020). Furthermore, He and Liu observed similar results when human M1 or M2 macrophage models, derived from primary MDMs or THP1 cells, were treated with recombinant IL-35 (Liu et al. 2019b; He et al. 2021). The study by He used a similar differentiation and polarisation protocol to that in the Chapter. Therefore, differences in these results, to those in the Chapter, suggest that other soluble factors produced by FaDu cells could have modulated the ability of IL-35 to regulate IL-10 signalling in stimulated macrophages. To assess this, the study could have been improved by testing the effects of recombinant human IL-35 on IL-10 gene expression and secretion as an additional positive control. At the time these experiments were performed however, recombinant IL-35 was unavailable for purchase from the manufacturer as a result of the COVID-19 pandemic. Thus, what can currently be deduced from the available Chapter data, is that IL-35 secreted from hypopharyngeal HNSCC cells may not repolarise M1 macrophages to an M2 phenotype via IL-10 upregulation.

A key novel finding was that CM from FaDu cells which overexpressed p35, but not EB13, induced a marked elevation in IL-10 secretion in M0 macrophages, and to a lesser extent, M1 macrophages. This suggested that the p35 subunit of IL-35 may be secreted independently of EB13 in HNSCC cells, where it could regulate macrophage polarisation and anti-tumour immunity. While no previous studies have investigated this role in macrophages, a study has shown that treatment of cultured B cells with a recombinant form of p35, caused increases in IL-10 and IL-35 expression (Dambuza et al. 2017). It is important to note however, that these studies were performed in mice, which may not reflect roles in humans.

The Chapter data showed that FaDu-p35 CM had a stronger effect on IL-10 induction in stimulated M0 macrophages when compared to M1 and M2. This may be due to differences in receptor expression or downstream signalling induced by differentiation and polarisation agents. Thus, to validate these effects, these experiments could be performed using alternative macrophage models, such as the M1-like model or MDMs.

Mechanistically, it must be considered whether secreted p35 can perform these roles in isolation, as described by Dambuza, perhaps when it is not associated with EBI3, or upregulated without EBI3 (such as via IFN γ stimulation, Chapter 3), or whether it requires an additional binding partner produced by FaDu cells, to become secreted and perform this function. Studies have shown that to become secreted, p35 requires co-expression of a binding partner which can stabilise it and permit its trafficking out of the cell (Devergne et al. 1997; Murphy et al. 2000; Reitberger et al. 2017). Therefore, it is possible that p35 utilises a binding partner produced by FaDu cells, other than EBI3, to become secreted, after which it was able to regulate macrophage phenotypes. Future studies are required to investigate these possibilities.

To test whether p35 acts in isolation, or requires co-expression of a FaDu cell factor, CM from a non-human cell line transfected to overexpress p35 may be used. A CHO-p35 cell line would have been relevant for this purpose but this was not developed during the project. Furthermore, it may be important to identify potential p35 binding partners in FaDu cells. In Chapter 5, it was found that neither p19, EBI3, nor p28, were overexpressed in the FaDu-p35 cell line. To identify other candidate binding partners, proteomic interactome data could be consulted as done with EBI3, or RNA-seq performed. Candidates could then be validated using co-immunoprecipitation experiments to detect interactions with p35 in lysates or culture supernatants.

In conclusion, the data showed that overexpression of p35 from HNSCC cells, perhaps under the stimulation of IFN γ (shown in Chapter 3), may, independently of EBI3, become secreted, where it may promote M2 macrophage polarisation and suppress anti-tumour immunity. Further research on other M2 markers and macrophage models is required to confirm this and to delineate underlying mechanisms.

The Chapter data demonstrated that CHO-EBI3 CM reduced IL-10 secretion in M2 macrophages, and to a lesser extent, M1 macrophages. In Chapter 5, CHO-EBI3 CM was also shown to increase TNF α secretion in M1 macrophages. This suggests that factors secreted by CHO cells may be recognised as foreign, triggering an inflammatory response in stimulated macrophages. These macrophages may then increase production of M1 markers such as TNF α , and reduce M2 markers including IL-10. Further research, possibly analysing additional M1 and M2 markers with CHO and CHO-EBI3 CM, may be required to confirm this.

There were limitations in the study of IL-10 expression. While this was not feasible due to cost restrictions, qPCR data could have been improved by repeating the experiments with statistical analysis and involving the use of additional controls, including recombinant IL-35, and CM from EB13/p35-overexpressing cell lines. Another limitation of this study was the secretion of IL-10 in the tested macrophage models. If at all, it was expected that IL-10 would be secreted most from M2 macrophages. While the protocols used were common in the literature, IL-10 was found to be secreted at low levels in all models, with M1 showing highest secretion levels. This matched qPCR data from Chapter 5, which suggested that PMA induced IL-10 expression, and that IL-4 had no effect. Low secretion therefore, could be due to the dissipating effects of PMA stimulation used for differentiation. Higher secretion in M1 compared to M0 and M2 may reflect the higher dose of PMA used for M1 differentiation. Furthermore, a major limitation of the IL-10 data is that all concentrations detected, with the exception of FaDu-p35 CM-treated M0 and M1 macrophages, were below the detection limit of the assay (2 pg/mL). Therefore, analyses inferred from these data may not be valid. To validate these findings in future, it may be beneficial to repeat experiments with concentrated samples (for example by freeze drying large volumes of culture supernatant) to potentially increase IL-10 concentrations above the assay sensitivity limit, or by using alternative models. Nevertheless, regardless of these limitations, the assays performed were still valid for the purpose of investigating whether HNSCC-derived IL-35 upregulated IL-10 expression above the detection limits.

VEGF-A is a pro-angiogenic factor produced by M2-TAMs to support tumour progression (Riabov et al. 2014). IL-35 had previously been demonstrated to negatively regulate VEGF-A expression in rheumatoid synoviocytes (Li et al. 2016). It has not been researched whether IL-35 can regulate VEGF-A expression in macrophages. In the current Chapter, it was investigated whether HNSCC-derived IL-35 could promote repolarisation of M1 macrophages to an M2 phenotype via upregulation of VEGF-A expression. Despite being an M2 marker, VEGF-A was shown to be expressed in M1 macrophages but not M2. Previous studies have demonstrated that PMA may negatively regulate VEGF-A expression in THP1-derived macrophages (Aldo et al. 2013). While no studies have analysed the effects of

IFN γ , the data in this Chapter suggests that when used to polarise macrophages to M1, it may have induced VEGF-A expression. Future dose-response studies could be performed to confirm this.

The hypothesis purported that VEGF-A expression may be upregulated by HNSCC-derived IL-35. The data obtained did not agree, as treatment with FaDu-IL-35 CM did not affect VEGF-A expression in cultured M1 macrophages. However, a major limitation in this study was the high degree of variation in data. Samples (n=1) were loaded in triplicate during qPCR. It is possible therefore, that variation was due to pipetting error. Ideally, this would be repeated in future with the inclusion of statistical analysis. Alternatively, a VEGF-A ELISA could be used. Therefore, from the data obtained, it cannot yet be concluded that IFN γ induced significant changes in VEGF-A expression, or that HNSCC-derived IL-35 has no effect on VEGF-A expression.

6.5.2 Upregulation of M2 surface marker expression

CD163 and CD206 are commonly described as M2 surface markers. CD163 is also used to identify M2-TAMs in-vivo (Kumar et al. 2019; Peltanova et al. 2019). It was purported that HNSCC-derived IL-35 could promote M2 polarisation by inducing expression of these markers, thus contributing to the prevalence of CD163+ M2-TAMs observed in HNSCC (Kumar et al. 2019; Peltanova et al. 2019).

It was expected that as M2 markers, CD163 and CD206 would be highly expressed in M2 macrophages, and less so in M1 macrophages. Flow Cytometry in Chapter 5 showed that, immediately after polarisation protocols, CD206 was expressed in 20% of M1 macrophages and 16% of M2. When used as controls in the current Chapter, these cells underwent 48 h of extended culture without additional stimulation. After this, 14% of M1 macrophages expressed CD206, and 16% of M2 macrophages. In both instances, expression was very low in M2 macrophages, and similar to M1. This suggests that stimulation protocols used for M2 polarisation may be insufficient to induce a strong M2 phenotype that persisted for the duration of the experiment. CD163 was shown in Chapter 5 to be strongly induced by PMA, as gene expression was high in M0 macrophages, and protein expression was higher in M1 macrophages (89% of cells) when compared to M2 macrophages (43%). When used as controls (48 h of

additional culture), 25% of M1 macrophages, and 22% of M2 macrophages expressed CD163. This suggests that the effects of polarisation may have dissipated.

Low expression of CD163, CD206 and IL-10 indicated the M2 model could have been improved. This could be done by increasing IL-4 dose and stimulation time, and/or adding IL-13 (Baxter et al. 2020). Alternatively, higher doses of polarisation agents, and performing mixed culture at an earlier timepoint, may have maintained polarisation during these experiments. Nevertheless, while a limitation of the model, it was still valid to assess whether HNSCC-derived IL-35 induced expression of these markers.

Both RT-qPCR and Flow Cytometry data showed that HNSCC-derived IL-35 had no effect on either CD206 or CD163 expression in M1 macrophages. This contrasted to previous studies. Jiang and others illustrated that injected mice, or treatment of mice microglial cell lines with recombinant IL-35, increased expression of CD206 (Jiang et al. 2020). He (using THP1 cells) and Peng (using MDMs) also showed in human models that M1 macrophages could be induced to increase CD206 expression following stimulation with recombinant IL-35 (Peng et al. 2019; He et al. 2021). Furthermore, Liu and others showed that MDM-derived M1 macrophages treated with recombinant IL-35 increased CD163 expression (Liu et al. 2019b).

Differences to the findings in the Chapter could possibly be due to the culture conditions used. Mixed culture enables crosstalk between FaDu cells and macrophages that recombinant IL-35 studies do not. FaDu cells may express factors on their surface and/or secrete soluble factors, which could modulate the ability of IL-35 to upregulate CD206 and CD163 in stimulated macrophages. Alternatively, differences could be due to variances in methods used to derive macrophage models. To determine whether differences in results were due to FaDu-derived factors, the Chapter studies could be performed with the inclusion of recombinant IL-35 controls.

There were limitations in the qPCR and flow cytometry approaches used that are relevant to the entire Chapter. These are detailed in the section below. Regardless, the data obtained indicated that HNSCC-derived IL-35 may not promote M2 polarisation by upregulating expression of the surface markers CD206 or CD163. Studies using alternative models and in-vivo samples may be required to validate these findings.

6.5.3 Upregulation of M2-TAM biomarker expression

It was purported that HNSCC-derived IL-35 could repolarise M1 macrophages to an immunosuppressive M2-TAM phenotype by elevating expression of PD-L1, CD204 and B7-H4. PD-L1 is an immune checkpoint protein that negatively regulates anti-tumour immunity. It is often overexpressed in HNSCC, and its expression in MDM models has been shown to be induced by co-culture with oral cancer cells in a mechanism dependent upon IL-10 (Jiang et al. 2017).

Prior to this Chapter, it had not been investigated whether HNSCC-derived IL-35 could upregulate PD-L1 expression in TAMs. Here, it was found that IL-35 secreted from FaDu cells reduced PD-L1 expression in M1 macrophages. This agreed with a previous study, where an MDM-derived M1 model was treated with recombinant IL-35. This also caused a marked reduction in PD-L1 expression (Liu et al. 2019b). Thus, the data disagreed with the Chapter hypothesis, and suggested that HNSCC-derived IL-35 may reduce PD-L1 expression in M1 macrophages. However, this finding was limited as the experiment was performed once. Thus, additional repeats are required to substantiate this finding.

RT-qPCR studies could have been improved by adding additional repeats, using recombinant IL-35 controls, and by analysing the effects of EB13 and p35 overexpression in FaDu cells. Furthermore, Flow Cytometry could be used to assess changes in surface expression, as regulation of PD-L1 trafficking to the cell surface could present an additional mechanism that regulates PD-L1 activity in TAMs.

From the perspective of macrophage polarisation, both the Chapter studies, and those previously reported, have shown that stimulation of macrophages with IFN γ , which polarises them to M1, strongly induces PD-L1 expression (Mattox et al. 2017; Liu et al. 2019b). This is somewhat unexpected, as M1 macrophages function to promote immunity and T cell activity, which is in contradiction to the role of upregulated PD-L1, which inhibits T cell activity. To explain this, reports have suggested that engagement and downstream signalling of PD-L1 in TAMs may promote cell survival, proliferation and activation (Hartley et al. 2018). Thus, rather than negating T-cell activity, it is possible that M1-TAMs use PD-L1 to increase the number of active cells, hence enhancing their ability to amplify anti-tumour immune responses.

How these effects are balanced with its role in negating T cell activity is not yet understood, but it is possible that M1-TAMs preferentially engage other cells that express the PD-L1 receptor PD-1, such as B cells, regulatory T cells and other macrophages (Okazaki and Honjo 2007), to favour enhancement of immunity rather than suppression. What can be inferred from these studies, is that HNSCC-derived IL-35 could suppress PD-L1 expression in M1-TAMs, which reduces their activation and survival. This may constitute a potential mechanism used by tumour cells to lower the ratio of M1:M2 TAMs in HNSCC.

From a therapeutic perspective, the finding that HNSCC-derived IL-35 suppressed PD-L1 expression is important. Low PD-L1 expression in HNSCC (from tumour or immune cells) is associated with poor responses to immunotherapy and overall survival (Burtneß et al. 2019). This may implicate overexpression of IL-35, not only in reduction of M1-TAMs, but also in reduced overall expression of PD-L1, responses to immunotherapy, and overall survival. In future, in addition to additional repeats that will confirm the chapter findings, it may be important to investigate whether IL-35 overexpression in HNSCC is associated with these effects in-vivo. Should this be the case, IL-35 may present an attractive therapeutic target to improve responses to immunotherapy.

Studies have shown that PD-L1 is overexpressed in HNSCC cells exposed to IFN γ (Tsushima et al. 2006; Ritprajak and Azuma 2015; Qiao et al. 2020). Future studies could also investigate whether IFN γ -induced PD-L1 expression is reduced in transfected cell lines that overexpress EB13, p35 or IL-35. This may be important as, if IL-35 overexpression reduces both tumour-derived and immune-derived PD-L1 expression, it further validates the targeting of IL-35 as a method of improving responses to anti-PD1/PD-L1 immunotherapy.

CD204 and B7-H4 are also biomarkers expressed in M2-TAMs that have been detected in HNSCC (Wu et al. 2016a; Kubota et al. 2017). Prior to the current Chapter, no literature had investigated the role of IL-35 in the regulation of either of these genes in TAMs. It was found that M2 macrophages expressed less CD204 than M1 macrophages. However, both PMA and PMA+IL-4 have been shown to induce CD204 expression (Soldano et al. 2016). As higher PMA concentrations were used to develop M1 macrophages, and a low concentration of IL-4 was used for M2 macrophages, this

may explain the differences observed. Nevertheless, HNSCC-derived IL-35 had no effect on CD204 expression in either M1 or M2 models, suggesting that it does not promote M2 polarisation via upregulation of this gene.

B7-H4 gene expression could not be detected in any of the macrophage models before or after addition of IL-35. This could be due to the primers used, or that the macrophage models used simply did not express this gene. Based on the data, it can be suggested that HNSCC-derived IL-35 may not upregulate its expression. However, a previous study has shown that B7-H4 is overexpressed in oral cancers, and that downregulation of expression in tumour cells is associated with increased M1 macrophage polarisation (Chi et al. 2022). It may therefore be of interest to assess expression in H357 cells (oral carcinoma), and whether IL-35 overexpression affects this to indirectly regulate macrophage polarisation.

Overall, the data did not agree with the hypothesis, and suggested that IL-35 secreted from tumour cells in HNSCC may not promote repolarisation of M1 macrophages to an M2-TAM phenotype via upregulation of B7-H4 or CD204.

6.5.4 Limitations

While important findings were observed in this Chapter, there were limitations in the approaches used. RT-qPCR may have been improved by performing additional repeats with the inclusion of statistical analysis. Recombinant IL-35, CHO-EBI3, FaDu, FaDu-EBI3 and FaDu-p35 controls may also have been useful, particularly as EBI3 and p35 overexpression were shown to have effects on cytokine production. While useful, the use of a blocking antibody may have been affected by expression of FC receptors in macrophages. It may have been prudent to use an isotype control and/or CMs pre-treated with antibodies by immunoprecipitation to remove EBI3 and/or p35.

Flow cytometry data obtained was limited by the presence of autofluorescence in unstained cells. When setting gates for CD206 and CD204, autofluorescence was high in control samples. This was not the case in mixed culture samples. Therefore, gates were set for CD206 expression between two populations that were common across all samples, with inferences from previous controls (Chapter 5) that were less affected by autofluorescence. For CD204, gates were placed between dense populations common across samples. These were also at boundaries of signal from unstained populations

where a single common population was present. This meant that in some control samples, there was spillover of autofluorescent signal into the positive population. This may have affected population statistics. Autofluorescence may have come from macrophages, which are known to display this. Alternatively, even though compensation was optimised, this may be due to fluorescence spillover from other channels. To mitigate this, and improve gating, fluorescence-minus-one (FMO) controls could be used, antibodies changed, or compensation altered. Though, due to the costs required for FMO controls or reconfiguring of antibody panels, this was not feasible. Studies could be repeated with these included in future, to confirm the findings from Flow Cytometry studies in this thesis. As mentioned in Chapter 5, the number of events captured during experiments could have been increased, as the number of events in gated macrophage populations were low and may have affected the significance of data.

The macrophage models used in this thesis could have been improved. Polarisation markers were lowly expressed, particularly during mixed culture studies. In future, similar models could be improved by increasing doses or time stimulated with PMA/IFN γ /IL-4. Mixed culture could also be performed at an earlier stage to prevent loss of marker expression. Alternatively, MDMs could be used. Despite low expression of polarisation markers, the models used were still relevant to assess the effects of HNSCC-derived IL-35 on macrophage polarisation, and important findings have successfully been elucidated.

6.6 Conclusions

The Chapter hypothesised that HNSCC-derived IL-35 promotes the repolarisation of M1 macrophages to an M2-TAM phenotype. This would be evidenced via upregulation of M2 cytokine secretion, M2 surface marker expression and M2-TAM marker expression.

The data obtained showed that HNSCC-derived IL-35 did not induce upregulation of M2 cytokines. CM from FaDu cells that overexpressed IL-35 had no effect on IL-10 gene expression or cytokine secretion in M1 macrophages. However, when p35 was overexpressed, FaDu-p35 CM upregulated IL-10 secretion in M0 and to a lesser extent, M1 macrophages. Future studies are required to assess whether overexpressed

p35 affects expression of other M2 markers. FaDu-IL-35 CM also may not induce VEGF-A expression in M1 macrophages. Additional experimental repeats are required to confirm this.

Treatment of M1 or M2 macrophages with FaDu-IL-35 CM, nor mixed culture with these cells, induced upregulation of the M2 surface markers CD163 and CD206. In a key finding, FaDu-IL-35 CM was shown to reduce PD-L1 expression in IFN γ -induced M1 macrophages, though additional repeats are required to confirm this. Further research using in-vivo models is required to assess whether IL-35 expression is associated with reduced PD-L1 expression, poor responses to immunotherapy and overall survival. HNSCC-derived IL-35 had no effect on expression of the M2-TAM markers CD204 or B7-H4. Further studies are required to confirm the findings in this Chapter.

While the hypothesis was not supported by the data, it is possible that HNSCC-derived IL-35 may indirectly promote M2 polarisation. In-vivo studies would be required to first validate an association between IL-35 expression and M2-TAM polarisation in HNSCC. Following this, it could be investigated whether HNSCC-derived IL-35 indirectly promotes M2 polarisation via reprogramming of other immune cells, which in turn produce Th2 cytokines that induce M1 to M2 repolarisation. The data found, and future research, could have a wider impact of validating IL-35 as a therapeutic target for HNSCC, which when modulated, could improve responses to immunotherapies, particularly considering its role in negative regulation of PD-L1 expression.

Chapter 7
General Discussion

7.1 Overview

The basis of the research was to assess whether the IL-35 cytokine, produced from tumour cells, contributes to the suppression of anti-tumour immunity in HNSCC. By stimulating HNSCC cell lines with pro-inflammatory and anti-inflammatory cytokines, the effects of inflammation in the TME on IL-35 expression from tumour cells was investigated. A HNSCC cell model that overexpressed IL-35 was developed. Treatment with conditioned medium taken from this cell line, and mixed culture of this cell line with THP1-derived macrophage models, were both used to explore whether HNSCC-derived IL-35 contributed to immune suppression and the prevalence of M2 macrophages by repolarising M1 macrophages to an M2 phenotype.

Despite advances in surgical and oncological management, and use of immunotherapies for the treatment of HNSCC, patient responses and overall survival rates remain unsatisfactory (Ferris et al. 2016; Forster and Devlin 2018; Cohen et al. 2019; Siegel et al. 2020; Sung et al. 2021). Poor responses can be associated with a dysfunctional immune profile in the TME. HNSCCs are often inflamed, containing TMEs enriched with immune cells. These immune cells can be edited by tumour cells to display phenotypes that suppress both anti-tumour immunity and responses to immunotherapy, and promote tumour progression (Elmusrati et al. 2021). To improve this, it is important to identify novel regulators of immune dysfunction in HNSCC.

This thesis sought to provide evidence suggesting that IL-35, derived from tumour cells, may contribute to immune dysfunction by promoting M2 macrophage polarisation. The rationale came from preliminary studies performed by the laboratory group. It was found that gene expression of the IL-35 subunits, EB13 and p35, were upregulated in HNSCC cells in response to stimulation with pro-inflammatory cytokines. This suggested the possibility that HNSCC cells produce IL-35 as an adaptive negative feedback response to inflammation. As an immunosuppressive cytokine, its production may help tumours evade immunity by inhibiting the activity of immune cells in the TME. In the HNSCC TME, macrophages are often polarised to an M2 activation state, which functions to suppress immunity and promote tumour progression (Wondergem et al. 2020). Based on these points, the thesis hypothesised that HNSCC cells, within an inflamed microenvironment, are under stimulation by inflammatory cytokines. These tumour cells respond by upregulating gene expression

of EBI3 and p35, culminating in IL-35 production. As an immunosuppressive cytokine, IL-35 may protect tumour cells from anti-tumour immunity by repolarising M1 macrophages, which are pro-inflammatory, to the immunosuppressive M2 phenotype.

7.2 Evaluation of the thesis studies

7.2.1 Regulation of IL-35 expression in HNSCC cells by inflammatory cytokines

Chapter 3 investigated the effects of inflammatory stimuli on IL-35 expression in HNSCC cell lines. Prior to the thesis, both the expression of IL-35 in HNSCC cells, and its regulation, were poorly studied. Preliminary studies showed that unstimulated HNSCC cell lines express varying mRNA levels of EBI3 and p35. As HNSCCs are often inflamed, it was important to assess whether IL-35 expression in tumour cells was affected by the prevalence of pro-inflammatory or anti-inflammatory cytokines in the TME. This may have suggested that tumour cells respond to inflammation by upregulating IL-35, which may contribute to suppression of anti-tumour immunity.

Pro-inflammatory cytokine stimulation was found to induce IL-35 gene expression in both hypopharyngeal carcinoma cells (FaDu) and oral carcinoma cells (H357). In both cell lines, IFN γ (at least 1 ng/mL) induced significant increases in gene expression of p35, but not EBI3. TNF α upregulated EBI3 gene expression in a dose and time dependent manner in FaDu cells but did not affect expression in H357 cells, nor did it affect p35 expression in either cell line. Stimulation with both IFN γ and TNF α increased gene expression of both IL-35 subunits in both cell lines. Moreover, these cytokines appeared to act synergistically, elevating gene expression of EBI3, but not p35, to greater magnitudes when added together, compared to individual cytokine stimulation. Gene expression data thus agreed with the thesis hypothesis and suggested that inflamed hypopharyngeal and oral carcinoma cells stimulated by IFN γ and TNF α may respond by upregulating IL-35 gene expression. In future, it may be beneficial to assess the effects of additional pro-inflammatory cytokines. For example, IL-1 has been shown to upregulate EBI3 and p35 expression, either alone, or in synergy with IFN γ , in other cancer cell lines (Maaser et al. 2004).

The differences in data between H357 and FaDu cells, particularly in response to TNF α stimulation, suggested that responses to inflammation may differ in HNSCC cells from different sites of origin. This may be influenced by the inflammatory nature of their TMEs, or genetic heterogeneity between cell lines. To date, there are no other published literature investigating this in other HNSCC cell lines. Therefore, future studies using additional HNSCC cell lines from a range of anatomical sites would be beneficial to further assess the hypothesis.

Beyond HNSCC, the published literature has described that stimulation of colorectal and hepatocellular carcinoma cell lines with pro-inflammatory cytokines may upregulate EBI3 and p35 expression (Maaser et al. 2004; Long et al. 2013; Wetzel et al. 2021). This suggests that production of IL-35 as an adaptive response to inflammation may be shared across cancer subtypes.

Additional gene expression studies were performed in this Chapter to provide evidence that upregulation of EBI3 and p35 gene upregulation was associated with IL-35 expression. EBI3 and p35 chains can also interact with other chains in the IL-12 family to form alternative cytokines (Mirlekar and Pylayeva-Gupta 2021). To substantiate that pro-inflammatory cytokine stimulation was associated with IL-35 expression, and not other IL-12 family cytokines, stimulated cells were also evaluated for upregulation of the remaining subunit chains (p19, p27 and p40).

In unstimulated HNSCC cells, expression of these chains was very low or undetectable. In stimulated H357 cells, IFN γ and TNF α did not induce upregulation of any of these chains. In FaDu cells, of the tested chains, IFN γ and TNF α were observed to only significantly affect p19 gene expression. Both TNF α and IFN γ +TNF α stimulation caused significant increases. Aside from IL-35 however, the only other known IL-12 family cytokine this could have induced was IL-39 (p19/EBI3), the existence of which has not been validated in humans (Ecoeur et al. 2020). Therefore, the data suggested that in inflamed hypopharyngeal carcinoma cells, the presence of IFN γ and TNF α may induce upregulation of EBI3, p35 and p19. EBI3 may favour interactions with p35 to form the IL-35 cytokine, which was in line with the hypothesis. Again, differences in data between FaDu and H357 cells may be explained by divergent responses to inflammation in different tissue sites and/or HNSCC cell lines, and thus warrants further investigation.

A major limitation of the Chapter studies was that protein expression of EBI3, p35, or the IL-35 cytokine, either in resting or stimulated FaDu cells, could not be detected. Prior to the thesis, there was a dearth of literature containing data which demonstrated detection of EBI3 and p35 protein expression in tumour cell lines via Western Blotting or ELISA. Nevertheless, there may be several reasons why protein could not be detected in the thesis studies.

Despite testing a range of stimulation conditions and increasing the sensitivity of detection assays, the concentration of full-length stable protein produced by pro-inflammatory cytokine stimulation may have been insufficient to enable detection. Additional stimulation, perhaps with other pro-inflammatory cytokines, or more sensitive assays, could be attempted in future to improve detection. The genes upregulated may not be translated. They could represent transgenes, which could be assessed by sequencing, or may be translated into misfolded and degraded proteins. Other HNSCC cell lines could be evaluated to assess whether lack of detection was due to the cell line tested. PCR and sequencing could be used to investigate whether alternative isoforms of the genes are transcribed, which may not be detectable with the tested antibodies. Binding epitopes in these proteins could be masked by misfolding or conformational changes. To detect several possible epitopes, polyclonal antibodies could be tried in future studies. Flow cytometry of live cells may also circumvent potential issues caused by cell lysis with RIPA buffer. Chapter data also showed that inflammation not only induces EBI3 and p35 expression in FaDu cells, but also that of IL-35 receptor chains. It cannot be ruled out therefore, that produced IL-35, or its subunits, may be internalised and degraded, thus preventing its protein detection. Future studies that detect IL-35 protein expression and secretion in HNSCC cell lines would be integral to the research area. As H357 cells also upregulated EBI3 and p35 in response to pro-inflammatory cytokine stimulation, protein studies in this cell line could be performed.

While protein expression could not be confirmed in-vitro, the hypothesis could be tested in-vivo. EBI3 and p35 have been detected in-vivo previously (Zhang et al. 2015). Here, its expression in tumour cells may be regulated by immune cells and a wider range of inflammatory cytokines than those tested in the Chapter. Thus, it could be evaluated whether IL-35 expression in tumour cells is detected at higher levels in

inflamed HNSCCs. While additional studies are required to further investigate induction of protein expression, gene expression data obtained in the Chapter supported the hypothesis that HNSCC cells may upregulate IL-35 expression in response to stimulation with pro-inflammatory cytokines.

This Chapter also investigated the effects of immunosuppressive cytokines on IL-35 expression in stimulated HNSCC cell lines. Reports had demonstrated that cultured T cells and tumour cells that produce IL-35, can also transduce exogenous IL-35, resulting in upregulation of endogenous expression (Collison et al. 2012; Wetzel et al. 2021). Thus, it was possible that IL-35, in an immunosuppressive TME, may upregulate endogenous expression in stimulated HNSCC cells. However, the data showed that recombinant IL-35 had no effect on endogenous expression in both FaDu and H357 cells.

It was considered that this may have been due to insufficient receptor expression. To transduce IL-35, cells must express homodimeric or heterodimeric receptors derived from gp130, which is ubiquitously expressed, and IL-12R β 2 (Collison et al. 2012; Lee et al. 2018; Wetzel et al. 2021). While gp130 was, as expected, expressed in both HNSCC cell lines, IL-12R β 2 was poorly expressed in FaDu cells and undetectable in H357 cells. Full biological effects of IL-35 signalling may require transduction via gp130/IL-12R β 2 heterodimers (Adam et al. 2009; Suthaus et al. 2011; Lee et al. 2018). Thus, the possible points were considered. (1) HNSCC cells that are not subjected to inflammatory stimuli may not express sufficient levels of both receptor chains. Both may be required to transduce IL-35 in a manner that promotes endogenous gene expression. (2) Inflammation may not only induce IL-35 expression, but may also promote upregulation of IL-35 receptor chains. This may be required to prime cells to respond to exogenous IL-35 in a manner that promotes endogenous expression.

When tested, the data showed that, in addition to induction of IL-35, IFN γ stimulation of FaDu cells, but not H357, increased gene expression of both gp130 and IL-12R β 2. TNF α stimulation significantly elevated gp130 expression in FaDu cells. Double stimulation with both cytokines significantly increased expression of both receptor chains in FaDu cells. Thus, inflammation may indeed prime hypopharyngeal carcinoma cells to respond to IL-35 signals. Protein expression of these receptor chains could be detected in future studies to further verify these findings. In addition, time-

course studies in H357 cells are required to confirm if the same effects are present in stimulated oral carcinoma cells beyond 6 h treatment.

While this was the first study to show this effect in HNSCC cells, previous studies have corroborated that pro-inflammatory cytokine stimulation increases IL-12R β 2 expression in other tumour cell lines. TNF α induced IL-12R β 2 upregulation in other HNSCC cell lines and a lung carcinoma cell line. Furthermore, this study further suggested that this chain was required for IL-35 signalling (Lee et al. 2018). What was not uncovered in the Chapter studies, and could be studied in future, is whether HNSCC cells primed by IFN γ +TNF α stimulation can transduce exogenous IL-35 (through autocrine or paracrine signalling) to further increase endogenous IL-35 expression as a method of both positive feedback, and amplification of immune suppression. To test this in future, FaDu cells could initially be stimulated with IFN γ and TNF α , followed by later stimulation with IL-35. RT-qPCR could then reveal whether IL-35 induced an additional increase in gene expression of EBI3 and p35.

It is important to reiterate that H357 cells did not respond to IFN γ and TNF α by upregulating IL-35 or its receptor chains. This further illustrated that tumour cells from varying anatomical sites in HNSCC may respond differently to inflammation. Thus, additional cell lines from other sites of origin should be tested.

Overall, findings in Chapter 3 contributed to the current understanding of immune escape in HNSCC. There was a need to identify novel regulators produced by tumour cells which may contribute to immune dysfunction. This Chapter potentially assisted in this by suggesting that inflamed tumour cells may upregulate IL-35. As an immunosuppressive cytokine, it may promote immunotolerance and affect responses to immunotherapy. Furthermore, the data suggested that the site of origin in HNSCC may affect responses to inflammation. Tumours presenting in similar sites and with similar pathological characteristics can behave differently. Thus, it is possible that the nature of the immune microenvironment may be a factor in this. Therefore, to further the Chapter research and investigate why such differences occur, it may be prudent to perform these studies in a larger range of HNSCC cell lines in future.

7.2.2 Establishment of a HNSCC cell line that overexpresses and secretes human Interleukin 35 (IL-35)

To study the immunoregulatory role of IL-35 produced by inflamed FaDu cells, Chapter 4 aimed to create a FaDu cell line that constitutively overexpressed IL-35. Structurally, IL-35 is a heterodimer composed of EBI3 and p35 subunits. Unlike IL-12 and IL-23, IL-35 subunits do not use disulphide linkages to physically interact. Instead, these interactions are thought to be non-covalent and are as such, considered unstable (Devergne et al. 1997; Jones and Vignali 2011; Jones et al. 2012).

Previous studies have circumvented this by transfecting host cells with vectors that facilitate the co-expression of EBI3 and p35 bound together covalently by linker peptides (Niedbala et al. 2007; Nakano et al. 2015; Wang et al. 2016; Haller et al. 2017). However, subunit heterodimerisation and the subsequent IL-35 cytokine produced may not accurately mimic the in-vivo form. An advantage of the Chapter 4 studies was that it relied upon natural associations between overexpressed EBI3 and p35 for overexpression of IL-35 in its native form.

Cells were first stably transfected with a plasmid that promoted overexpression of human EBI3. A monoclonal cell line derived from this was then stably transfected a second time with a vector that facilitated human p35 overexpression. When co-expressed in a monoclonal cell line, these subunits potentially used intrinsic cell machinery to naturally interact and become secreted as the native IL-35 heterodimer.

CHO cells that overexpressed EBI3 (CHO-EBI3) and IL-35 (CHO-IL-35) were established first and validated the approach. FaDu cells that overexpressed IL-35 (FaDu-IL-35), but also cell lines that individually overexpressed EBI3 (FaDu-EBI3) or p35 (FaDu-p35) were generated, both as controls, and to enable study of the potential roles of individual subunits in immunoregulation. To mitigate potential stability issues of native IL-35, conditioned medium samples taken from these cells were aliquoted, frozen at -80 °C, and used only once. In addition, the close proximity of cells in mixed culture may have enabled rapid signal transduction, and thus may have limited loss of IL-35 stability.

Development of these models benefited the field of study. Within the thesis, they were integral to testing of the hypothesis. The FaDu-IL-35 cell line was used to investigate the role of HNSCC-derived IL-35 in promoting immune suppression via repolarisation

of M1 macrophages to an immunosuppressive M2 phenotype. This model is also important for future studies. It could be used to further investigate the role of HNSCC-derived IL-35 in the regulation of other immune cells in the TME, or its potential effects on expressing tumour cells. FaDu-EBI3 and FaDu-p35 cell lines were important in uncovering potential immunoregulatory roles of each individual protein when overexpressed in HNSCC cells. CHO-EBI3 and CHO-IL-35 cell lines were important for use as controls, but could also be used to develop recombinant proteins. Stably transfected cell lines also have the potential advantage of prolonged overexpression. Therefore, the models developed could be provided to collaborators to help accelerate our understanding of the roles of both IL-35 in general, and HNSCC-derived IL-35.

The Chapter studies may have been improved by developing a control CHO-p35 cell line, as p35 overexpression in FaDu cells was found to have potential roles in M2 macrophage polarisation. In future, generation of HNSCC cell models whereby EBI3 and/or p35 have been knocked out via CRISPR-Cas9 technology may be useful.

7.2.3 Investigation of the role of HNSCC-derived IL-35 in M1 to M2 macrophage repolarisation via suppression of the M1 phenotype

Inflamed HNSCCs often contain a greater ratio of M2:M1 TAMs (Kumar et al. 2019; Peltanova et al. 2019; Wondergem et al. 2020). TAMs can be polarised to M1 following exposure to Th1 cytokines such as IFN γ . M1-TAMs antagonise tumour development by producing pro-inflammatory cytokines, presenting tumour antigens to effector CD4⁺ T cells, and by directly causing tumour cell death (reviewed in Chapter 5). On the other hand, TAMs can be polarised to M2 by stimulation with Th2 cytokines in the TME. These include IL-4, IL-10, TGF β and VEGF (Wheeler et al. 2018; Baxter et al. 2020). M2-TAMs suppress anti-tumour immunity and promote tumour progression by producing immunosuppressive cytokines, and by enhancing angiogenesis and tumour invasiveness (Hao et al. 2012; Sica and Mantovani 2012; Roszer 2015; Orecchioni et al. 2019). Thus, the prevalence of M2-TAMs in HNSCC TMEs has been associated with poor patient outcomes (Mori et al. 2011; Hu et al. 2016; Okubo et al. 2016; Alves et al. 2018; Kumar et al. 2019; Kalogirou et al. 2021). M2-TAMs are therefore an attractive target therapeutically, as altering their function, or reducing their numbers may improve anti-tumour immunity and overall survival.

The thesis hypothesised that HNSCC-derived IL-35 may contribute to immune suppression by repolarising M1-TAMs to the prevalent immunosuppressive M2-TAM phenotype. Prior to the project, reports had associated IL-35 with disease severity in several cancers (Nicholl et al. 2014; Ma et al. 2016; Ahmed et al. 2019; Larousserie et al. 2019; Zhu et al. 2020; Gu et al. 2021). Furthermore, IL-35 had been reported to convert the phenotype of immune cells to immunosuppressive subtypes. This includes the reprogramming of CD4+ T cells to regulatory T cells, B cells to regulatory B cells, neutrophils to the N2 phenotype, and dendritic cells to an immunosuppressive phenotype. However, before the start of the thesis, there was a gap in the literature pertaining to the role of IL-35 in the regulation of M2 macrophage polarisation.

Chapter 5 investigated whether HNSCC-derived IL-35 contributed to the prevalence of M2 macrophages in the TME by suppressing the M1 phenotype. M0, M1 and M2 macrophage models were generated using THP1 cells. While expression of M1 and M2 markers may have been improved by optimising polarisation protocols, these models were relevant for the purposes of the study. In line with the hypothesis, CM from FaDu-IL-35 cells was shown to suppress TNF α secretion from M1 macrophages. Similar findings were observed in other studies published during the course of the project (Peng et al. 2019; Jiang et al. 2020; He et al. 2021). This suggested that secreted IL-35 may have a role in reducing inflammation in the TME.

In Chapter 3, TNF α stimulation of FaDu cells induced EBI3 upregulation. In Chapter 5, a potential negative feedback response may have been uncovered. Similar to FaDu-IL-35 CM, treatment of M1 macrophages with FaDu-EBI3 CM also suppressed TNF α secretion. CHO-EBI3 CM however, did not induce these effects. It was possible that overexpressed EBI3 required interactions with additional factors produced by FaDu cells to modulate macrophage activity. The identity of these potential binding partners could not be determined, but RT-qPCR data suggested that it may not involve p19 or p28. Future studies could assess whether other candidates such as HLA-G, are upregulated in FaDu cells that overexpress EBI3. Nonetheless, the data obtained suggested that HNSCC cells may respond to TNF α , or both IFN γ and TNF α in the TME, by overexpressing EBI3, or IL-35, respectively, to suppress inflammation. This may have important clinical implications as lack of inflammation in HNSCC is

associated with poor outcomes. In-vivo experiments could determine whether IL-35 expression is associated with poor inflammation and survival.

While the above agreed with the thesis hypothesis, the remainder of the Chapter studies did not. FaDu-derived IL-35 did not reduce expression of the antigen presentation marker HLA-DR, or the co-stimulatory molecules CD80 or CD86, suggesting that HNSCC-derived IL-35 may not reduce the capacity of M1 macrophages to present antigens, or activate engaged CD4+ T cells in the TME. Future studies may evaluate whether CM or mixed culture experiments with FaDu cells that overexpress EB13 or p35 overexpression have any effect on these M1 markers.

It was assessed whether macrophages could directly induce tumour cell apoptosis and/or necrosis. However, FaDu and FaDu-IL-35 cells were highly apoptotic when analysed. This was possibly due to sample handling before Flow Cytometry, and thus alternative methods may be required to evaluate this further.

In conclusion, the data suggested that overexpression of IL-35 in HNSCC cells may not contribute to suppression of the M1 phenotype in HNSCC. What was elucidated however, was that HNSCC-derived IL-35 may reduce pro-inflammatory cytokine secretion from these macrophages, which may suppress inflammation in the TME. Whether tumour-derived IL-35 mediates M1 to M2 polarisation in the context of other cancers has not yet been studied, so at this juncture, it cannot be deduced whether the thesis findings are common. To further this research, alternative macrophage models could be tested such as those derived from human blood. The effects of FaDu-EB13 or FaDu-p35 CM on HLA-DR, CD80 and CD86 expression could also be analysed to investigate potential roles of individual IL-35 subunits upregulated by inflamed HNSCC cells. It could also be assessed whether IL-35 overexpression in-vivo is correlated with reduced M1 marker expression, reduced inflammation and/or reduced overall survival.

7.2.4 Investigation of the role of HNSCC-derived IL-35 in M1 to M2 macrophage repolarisation via promotion of the M2-TAM phenotype

Studies in Chapter 6 investigated whether HNSCC-derived IL-35 could repolarise M1 macrophages in the TME to an M2-TAM phenotype by upregulating expression of classical M2 and M2-TAM markers. The published literature has indicated that

stimulation of M1 macrophages with recombinant IL-35 causes them to repolarise to an M2 phenotype. This was observed via upregulation of the M2 markers CD206, CD163 and IL-10 (Liu et al. 2019; Peng et al. 2019; Jiang et al. 2020; He et al. 2021; Chen et al. 2022; Luo et al. 2022). Before the thesis, this had not been studied within the context of HNSCC or other tumours.

The Chapter studies attempted to fill this gap in the literature. Ultimately the data did not agree with the thesis hypothesis. Chapter 5 showed that HNSCC-derived IL-35 did not downregulate M1 markers. Chapter 6 demonstrated that it did not increase expression of the M2 cytokines IL-10 or VEGF-A in stimulated M1 macrophages. Furthermore, CM treatment, or mixed culture using FaDu-IL-35 cells did not increase expression of the classical M2 surface markers CD206 or CD163, nor did it upregulate the M2-TAM markers PD-L1, CD204 or B7-H4. As these results contrasted with previous studies, it may be important to use recombinant IL-35 and/or alternative macrophage models in future studies. Recombinant IL-35 may elucidate whether IL-35 activity in the CM is modulated by other factors produced by FaDu cells.

Despite disagreeing with the hypothesis, the Chapter did reveal important novel findings. In a notable study, the secretome of FaDu cells that overexpressed p35, but not EBI3, caused significant increases in IL-10 secretion in stimulated M0 macrophages, and to a lesser extent, M1 macrophages. It is possible therefore, that hypopharyngeal carcinoma cells that are induced to overexpress p35, perhaps when stimulated by IFN γ (as shown in Chapter 3), may promote M2 polarisation. To investigate this further, FaDu-p35 CM or mixed culture experiments could be used to evaluate changes in expression of additional M2 and M2-TAM markers.

In Chapter 5, it was shown that the secretome of FaDu cells that overexpressed EBI3, but not p35, suppressed TNF α production from M1 macrophages. It is possible therefore, that when FaDu cells are under stimulation with varying inflammatory signals, they can demonstrate flexibility in their responses. They may overexpress p35 (in response to IFN γ), which may promote M2 polarisation, EBI3 (in response to TNF α), which may suppress pro-inflammatory cytokine production, or both (IL-35), which may have similar effects. Further studies are required to confirm this possibility.

A key observation in this study was that FaDu-IL-35 CM reduced gene expression of PD-L1 in M1 macrophages. As an immune checkpoint ligand which suppresses

immunity, it was expected that PD-L1 would be poorly expressed in M1 macrophages. However, its expression both in this study, and those previously published, was shown to be markedly increased when polarising macrophages to M1 using IFN γ (Mattox et al. 2017; Liu et al. 2019). It is possible that these macrophages use PD-L1 to engage with PD-1, expressed on other macrophages, to signal for increased survival and activation, rather than inhibiting T cell activity (Okazaki and Honjo 2007; Hartley et al. 2018). As an immunosuppressive cytokine, it was also expected that HNSCC-derived IL-35 may induce further upregulation of PD-L1 expression in M1 macrophages as a means of inhibiting T cell activity. As suggested in a previous study (Liu et al. 2019), FaDu-IL-35 CM instead reduced PD-L1 expression in stimulated macrophages.

Additional experimental repeats are needed to confirm this data, but the findings may have important implications. Despite downregulation of PD-L1-mediated T cell inhibition, it is possible that HNSCC cells use IL-35 to suppress M1-mediated immunity by suppressing PD-1/PD-L1 signalling that promotes survival and activation (Okazaki and Honjo 2007; Hartley et al. 2018). Furthermore, from a clinical perspective, this finding may suggest a role for HNSCC-derived IL-35 in the reduced overall survival associated with lack of both inflammation (via TNF α downregulation), and PD-L1 expression (Burtneß et al. 2019). Additional in-vitro and in-vivo studies are required to confirm these associations, but this may suggest there could be potential benefit in targeting IL-35 in combination with anti-PD-L1/PD-1 therapies.

The findings from Chapter 5 and 6 ultimately disagreed with previous studies that suggested IL-35 can repolarise M1 macrophages to the M2 phenotype (Liu et al. 2019; Peng et al. 2019; Jiang et al. 2020; He et al. 2021; Chen et al. 2022; Luo et al. 2022). It is important to consider that these studies involved either the treatment of in-vitro macrophage models with recombinant IL-35, or injection of in-vivo models with the same. Differences between those reports and the thesis data may be attributed to the regulation of IL-35 activity by other HNSCC-derived factors. FaDu cells may express and/or secrete factors that modulate the M2-polarising effects of IL-35 signalling in stimulated macrophages. Future studies could use IL-35 overexpression in other HNSCC cell lines and evaluate whether similar results are observed. Alternatively,

these differences could be due to the recombinant nature of IL-35 used in the reported literature, which may not reflect the native form, and variances in macrophage models used. Nevertheless, what can be concluded from the thesis studies, is that IL-35 produced from inflamed hypopharyngeal carcinoma cells may not promote repolarisation of M1 macrophages in the TME to an M2 phenotype.

An important avenue to further this research, is the hypothesis that HNSCC-derived IL-35 may indirectly promote M1 to M2 repolarisation. Previous studies using recombinant IL-35 has shown that it may convert M1 macrophages to M2 in-vitro (Liu et al. 2019; Peng et al. 2019; Jiang et al. 2020; He et al. 2021; Chen et al. 2022; Luo et al. 2022). Furthermore, studies using breast cancer cell lines showed that tumour-derived IL-35 may convert CD4⁺ T cells to iTreg cells (Hao et al. 2018). It is possible that, while HNSCC-derived IL-35 did not directly repolarise M1 macrophages, it may induce iTreg cells. These iTreg cells may then produce high concentrations of IL-35 that is possibly accumulated in the TME via extracellular vesicle-mediated infectious tolerance (Sullivan et al. 2020a). IL-35 from iTreg and other producing cells may then polarise macrophages in the TME to an M2 phenotype.

7.3 Conclusion

The thesis hypothesised that in an inflamed HNSCC TME, pro-inflammatory cytokines present are able to stimulate tumour cells. These tumour cells respond by producing the immunosuppressive cytokine IL-35. IL-35 may be used to protect tumour cells from host immunity. IL-35 may contribute to immune escape in the TME by stimulating M1 macrophages, converting them to an immunosuppressive M2 phenotype, which are high in density in advanced HNSCC. Gene expression data from Chapter 3 studies supported this, demonstrating that stimulation of the hypopharyngeal cell line FaDu and oral carcinoma cell line H357, with IFN γ and TNF α , induces upregulation of EB13 and p35 gene expression, subunits of which comprise the IL-35 cytokine. Furthermore, these stimulations also increased gene expression of the IL-35 receptor chains gp130 and IL-12R β 2 in FaDu cells. Transduction of exogenous IL-35 using these receptors may further increase endogenous gene expression as a positive feedback mechanism. Using a FaDu cell line that overexpresses IL-35 (generated in Chapter 4), studies in Chapter 5 and 6

gathered data that ultimately did not agree with the thesis hypothesis. Regarding downregulation of the M1 phenotype, while FaDu-derived IL-35 suppressed secretion of the pro-inflammatory cytokine TNF α in stimulated M1 macrophages, it did not reduce expression of the antigen presentation and co-stimulatory genes HLA-DR, CD80 or CD86. FaDu-derived IL-35 also did not cause M2 repolarisation in M1 macrophages, as stimulated M1 macrophages did not display upregulation of M2 cytokines, surface markers or candidate M2-TAM markers. IL-35 may suppress PD-L1 expression but this requires additional data to confirm. Furthermore, the data showed that HNSCC-derived IL-35, or overexpression of EBI3 or p35 individually, may suppress inflammation. This may affect responses to immunotherapy and overall survival. Future studies are warranted to investigate this further.

7.4 Future studies

There are many areas which could be investigated to advance the thesis studies. To continue testing the thesis hypothesis, other HNSCC cell lines, sourced from different anatomical sites, and with different characteristics (such as HPV involvement), could be tested. Differences in IL-35 expression and upregulation in response to inflammation could be explored here. It may of interest to ascertain whether other HNSCC cell lines produce detectable protein under the tested conditions. Regulation of macrophage polarisation via tumour-derived IL-35 overexpression from other HNSCC cell lines could be evaluated in MDM models.

It is important to assess the potential clinical significance of IL-35 expression in HNSCC. This would entail using immunohistochemistry or ELISA to detect co-expression of EBI3 and p35 in patient tissue samples, or IL-35 in patient serum, respectively (healthy vs disease). It could be analysed whether IL-35 overexpression is associated with poor survival, and whether this is also associated with reduced inflammation and PD-L1 expression. Comparison of IL-35 levels in pre-treatment, during and post-treatment samples, may suggest an association of IL-35 with resistance to therapy and disease recurrence. How IL-35 expression is associated with the density of M2 macrophages could be investigated. This could be tested by determining whether tumours with high IL-35 concentrations correlates with high densities of M2 macrophages (CD68+ and CD163+). HPV-associated HNSCC tend

to have better prognoses when compared to HPV-negative HNSCC (who are more likely to have co-morbidities such as heart disease). Differences in IL-35 expression in these tumours may suggest a role here.

In-vitro, it could be hypothesised that HNSCC-derived IL-35 blocks M1 polarisation of infiltrating macrophages. This could be tested by culturing M0 macrophages in the presence of IFN γ with or without FaDu-IL-35 CM. Recombinant IL-35, FaDu, FaDu-EBI3 and FaDu-p35 CM, or FaDu-IL-35+antibody treatments could be used as controls. Treated macrophages could then be analysed for suppression of M1 gene upregulation and potential increases in M2 gene expression. The importance of this is that it may reveal a novel method of immune escape. It suggests macrophages that are recruited by inflammatory signals into the TME, may be prevented from acquiring an anti-tumour phenotype by tumour-derived IL-35.

As previously mentioned, another hypothesis is that HNSCC-derived IL-35 may indirectly promote repolarisation of M1 to M2 macrophages via conversion of CD4⁺ T cells to induced Tregs (iTr35 cells). Unlike the tested HNSCC cells, IL-35 from these cells may be able to repolarise M1 macrophages to M2. To test this, CD4⁺ T cells could be isolated from peripheral human blood (using Ficoll gradient centrifugation to separate cells from buffy coats, and then purified using a CD4 T cell isolation kit). Naïve CD4⁺ T cells would then be activated using CD3/CD28 activator reagent. Activated cells would be treated with recombinant IL-35 or FaDu-IL-35 CM with or without blocking antibody. To validate iTr35 conversion in treated CD4⁺ T cells, cultured cells would be analysed for reduced proliferation (MTT, alamar blue assay) and decreased IFN γ secretion (ELISA). Next, to validate conversion of M1 macrophages to M2, treated cells could be washed to remove stimulants, and transwell inserts used to enable co-culture with M1 macrophage models. After co-culture, harvested RNA or cells could be analysed for changes in M1 and M2 marker expression. These studies would evidence new roles for HNSCC-derived IL-35 in immune escape, not only via suppression of CD4⁺ T cell activity and conversion to immunosuppressive Tregs, but also via consequent M2 macrophage polarisation.

Finally, it could be important to study the effects of IL-35 overexpression in the expressing tumour cell. Inflammation was shown to increase IL-35 and IL-35 receptor expression. Previous studies have suggested that transduction of IL-35 signals in

tumour cells may be used to facilitate metastatic colonisation via mesenchyme to epithelial transition (MET) (Lee et al. 2018; He et al. 2021). It could be hypothesised therefore that, in an inflamed HNSCC TME, tumour-derived IL-35 stimulates receptors to promote MET. This would be an important finding, as it implicates it both in metastatic colonisation and immune suppression at secondary tumour sites. Data has already been generated which demonstrates that IFN γ and TNF α stimulate gene expression of IL-35 and its receptor chains. To validate its role in MET, FaDu or FaDu-IL-35 cells could be stimulated with IFN γ and TNF α , with or without recombinant IL-35 as a control. EBI3 and p35 overexpression models could also be used as controls. These cells could then be evaluated for increased expression of E-cadherin (RT-qPCR, Western Blot or ELISA) or increased migratory capacity (wound assay or transwell migration assay). Next, it could be tested whether inflammation-induced receptor expression enabled transduction of IL-35 to promote endogenous IL-35 gene expression, which could infer a role in immune suppression at metastatic sites. To evaluate this, FaDu cells stimulated with IFN γ and TNF α could later be treated with recombinant IL-35 and assessed for significant increases in gene or protein expression of EBI3 and p35. It could then be evaluated whether targeting of the IL-35 receptor chain IL-12R β 2, blocks IL-35 upregulation and MET. These studies would implicate both IL-35 and its receptor chains as potential targets to modulate in combination with existing immunotherapies. This could benefit patients by improving host immunity and reducing metastatic colonisation.

7.5 Contribution of the thesis study

Compared to the prognostic improvements in other cancers such as breast and prostate, survival rates attributed to HNSCC are unsatisfactory. While immunotherapies have provided some benefit, responses to such treatments need to be improved. To do this, there is an urgent requirement to identify novel regulators of immune suppression in HNSCC. This thesis contributed to achieving this goal.

The studies performed added to the current understanding of immune escape in HNSCC. It elucidated a potential novel mechanism, whereby tumour cells in inflamed TMEs of hypopharyngeal and oral carcinoma may respond to stimulation from pro-inflammatory cytokines by upregulating expression of the immunosuppressive

cytokine IL-35. This suggested that IL-35 may be a novel promoter of immune escape and dysfunction in HNSCC. The thesis generated novel study models, to which the roles of HNSCC-derived IL-35, and its individual subunits, could be studied as it pertains to the regulation of anti-tumour immunity. While studies using these models demonstrated that HNSCC-derived IL-35 may not repolarise M1 macrophages to M2, the value in this finding is that it opens up the possibility that HNSCC-derived IL-35 may indirectly increase the ratio of M2:M1 macrophages in the TME via promotion of iTr35 differentiation. These cells suppress immune responses and produce IL-35 which may polarise macrophages to the M2 phenotype.

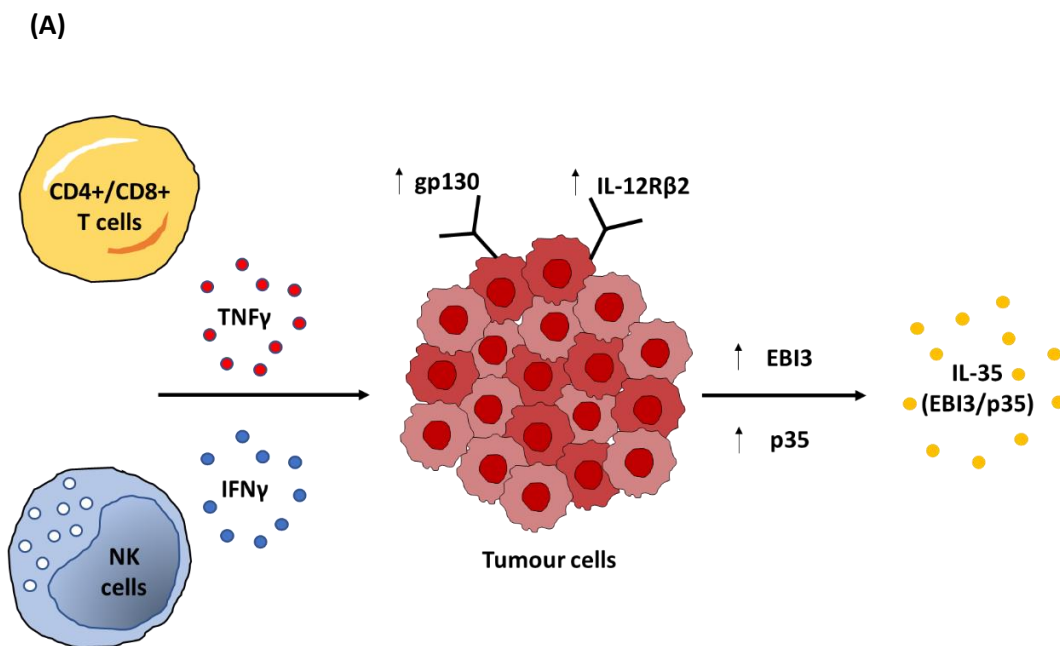
Outside the scope of the hypothesis, the thesis obtained key findings. It described potential roles for tumour-derived EBI3 and p35 in suppression of inflammation via TNF α downregulation and IL-10 upregulation in macrophages, respectively. HNSCC-derived IL-35 was shown to downregulate PD-L1 gene expression, which may have implications in resistance to immunotherapies such as nivolumab and pembrolizumab. Thus, in conclusion, the thesis studies made a valuable contribution to the field and has implicated IL-35 as a potential target, that could be modulated in combination with other immunotherapies, to improve both host immunity and overall survival rates.

The key novel findings from this thesis and possible findings from future studies have been collated into a potential model (**Figure 7.1**). In an inflamed hypopharyngeal squamous cell carcinoma, immune cells including CD4⁺ T cells, CD8⁺ T cells and natural killer cells, may produce pro-inflammatory cytokines including IFN γ and TNF α . These cytokines stimulate tumour cells. IFN γ signal transduction promotes increases in p35 expression. TNF α stimulation causes upregulation of EBI3 expression. Together, these cytokines induce elevation in expression of both genes, culminating in IL-35 production (**Figure 7.1A**). In addition to stimulating IL-35 expression, these pro-inflammatory cytokines may upregulate the IL-35 receptor chains gp130 and IL-12R β 2 (**Figure 7.1A**).

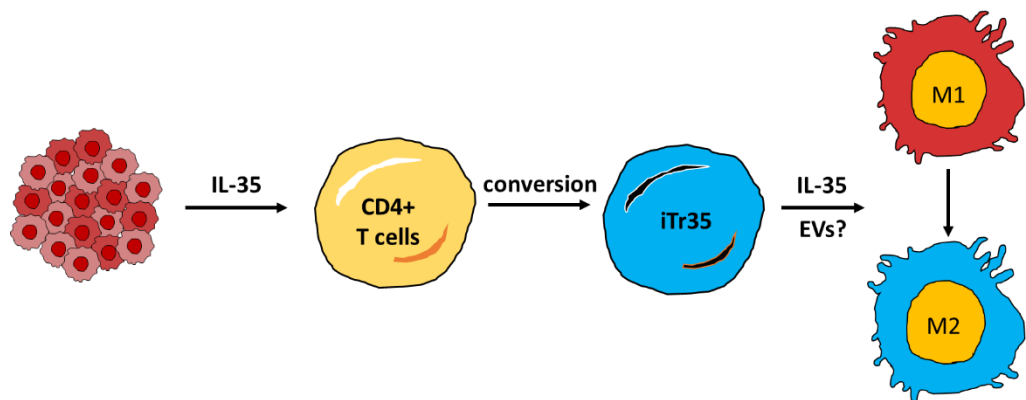
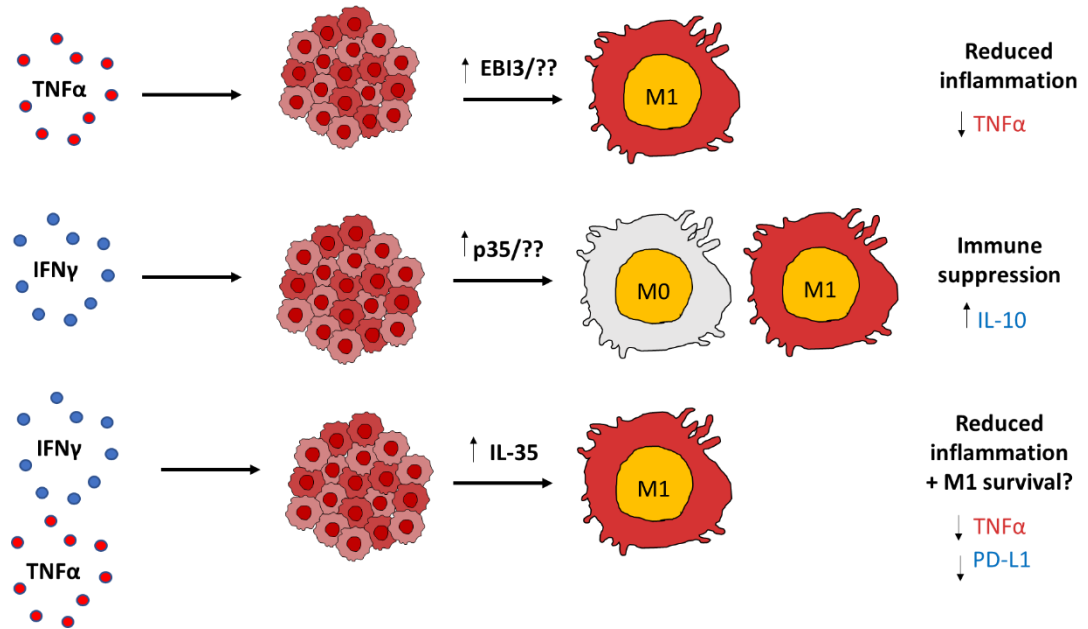
Regulation of macrophage activity by HNSCC cells may vary depending on the inflammatory nature of the TME (**Figure 7.1B**). High levels of TNF α , but not IFN γ , may induce EBI3 expression and secretion, possibly with an unknown binding partner. These may suppress inflammation in the TME via downregulation of TNF α secretion in M1 macrophages. IFN γ , but not TNF α in the TME, may induce upregulation of p35,

presumably in association with a binding partner which enables secretion. P35 may then suppress inflammation and anti-tumour immunity by promoting upregulation of IL-10 in M0 and M1 macrophages. When both IFN γ and TNF α are present, tumour cells may produce IL-35, which suppresses inflammation by blocking TNF α production from M1 macrophages. IL-35 may also lower the density of M1 macrophages in the TME by reducing PD-L1 expression, which may increase their susceptibility to cell death. HNSCC-derived IL-35 could also suppress immunity and indirectly contribute to the prevalence of M2 macrophages by converting CD4 $^+$ T cells in the TME to iT_{reg} cells. These cells may produce IL-35 in extracellular vesicles, which could repolarise M1 macrophages to M2.

HNSCC-derived IL-35 may also regulate tumour cell activity (**Figure 7.1C**). Inflammation was demonstrated to upregulate the IL-35 receptor chains. Inflammation may also promote EMT and tumour invasiveness (Lee et al. 2018; He et al. 2021). Upregulation of IL-35 receptor chains may facilitate transduction of IL-35 signals produced from inflamed tumour cells, Bregs and Tregs at metastatic sites, potentially resulting in mesenchyme to epithelial transition and metastatic colonisation (Lee et al. 2018). At secondary sites, tumour cells may also transduce IL-35 to promote endogenous expression, which could amplify immune suppression.



(B)



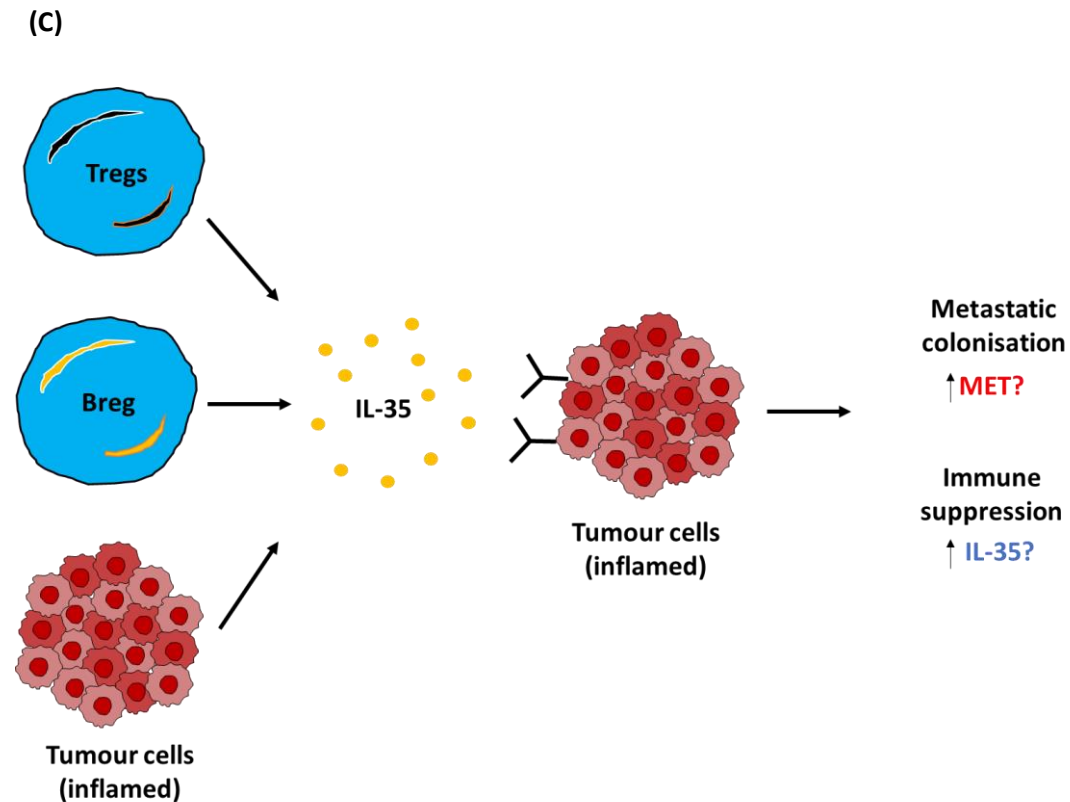


Figure 7-1 Summary of the thesis findings into a potential model.

(A) **Hypopharyngeal carcinoma cells may upregulate IL-35 in response to stimulation with pro-inflammatory cytokines in the TME.** Immune cells in the HNSCC TME, including CD4⁺ T cells, CD8⁺ T cells and natural killer cells (NK cells), secrete IFN γ and TNF α which stimulate tumour cells. TNF α stimulation upregulates EB13 expression. IFN γ causes p35 upregulation. Together, these cytokines stimulate production of the IL-35 cytokine (EB13/p35 heterodimer). In addition, they also upregulate expression of the IL-35 receptor chains gp130 and IL-12R β 2. (B) **The effects of IL-35 induction in immune suppression by regulating immune cells.** Tumour cells may adapt to inflammatory stimuli by upregulating IL-35, or its individual components EB13 or p35. TNF α causes upregulation of EB13. EB13 may interact with an unknown binding partner produced by tumour cells (labelled ??) to stimulate M1 macrophages in the TME, leading to reduced inflammation via suppression of TNF α secretion. IFN γ may induce p35 expression in tumour cells. p35 is likely secreted with an unknown binding partner, after which it stimulates macrophages. Unpolarised M0 macrophages, or M1 macrophages, are induced to increase IL-10 secretion, which suppresses inflammation and immunity in the TME. IFN γ +TNF α in the TME causes tumour cells to upregulate IL-35. HNSCC-derived IL-35 reduces TNF α and potentially PD-L1 expression in M1 macrophages, suppressing both inflammation and potentially M1 macrophage survival. Future studies may show that IL-35 could also convert CD4⁺ T cells to induced Tregs (iT_{reg}35). These, in turn, produce IL-35, possibly via extracellular vesicle formation, which may convert M1 macrophages to immunosuppressive, tumour-promoting M2 macrophages in the TME. (C) **Effects of tumour-derived IL-35 on tumour cell behaviour.** Inflamed tumour cells upregulate IL-35 receptor expression. Future studies could elucidate that IL-35 produced by inflamed tumour cells, Bregs or Tregs, may stimulate these receptors, leading to mesenchyme-to-epithelial transition and metastatic colonisation, and immune suppression at metastatic sites via upregulation of endogenous IL-35 expression. EVs; Extracellular vesicles.

References

- Adam, N., Rabe, B., Suthaus, J., Grötzinger, J., Rose-John, S. and Scheller, J. 2009. Unraveling Viral Interleukin-6 Binding to gp130 and Activation of STAT-Signaling Pathways Independently of the Interleukin-6 Receptor. *Journal of Virology* 83(10), pp. 5117–5126. doi: 10.1128/jvi.01601-08.
- Aharinejad, S. et al. 2004. Colony-stimulating factor-1 blockade by antisense oligonucleotides and small interfering RNAs suppresses growth of human mammary tumor xenografts in mice. *Cancer Research* 64(15), pp. 5378–5384. Available at: <https://pubmed.ncbi.nlm.nih.gov/15289345/> [Accessed: 5 March 2022].
- Ahmed, H.A., Maklad, A.M., Khaled, S.A.A. and Elyamany, A. 2019. Interleukin-27 and interleukin-35 in de novo acute myeloid leukemia: Expression and significance as biological markers. *Journal of Blood Medicine* 10, pp. 341–349. Available at: </pmc/articles/PMC6783395/> [Accessed: 31 March 2022].
- Aldo, P.B., Craveiro, V., Guller, S. and Mor, G. 2013. Effect of culture conditions on the phenotype of THP-1 monocyte cell line. *American Journal of Reproductive Immunology* 70(1), pp. 80–86. Available at: </pmc/articles/PMC3703650/> [Accessed: 23 November 2021].
- Allen, C.T., Clavijo, P.E., Van Waes, C. and Chen, Z. 2015. Anti-tumor immunity in head and neck cancer: Understanding the evidence, how tumors escape and immunotherapeutic approaches. *Cancers* 7(4), pp. 2397–2414. Available at: <https://pubmed.ncbi.nlm.nih.gov/26690220/> [Accessed: 21 June 2022].
- Almand, B. et al. 2001. Increased Production of Immature Myeloid Cells in Cancer Patients: A Mechanism of Immunosuppression in Cancer. *The Journal of Immunology* 166(1), pp. 678–689. Available at: <https://pubmed.ncbi.nlm.nih.gov/11123353/> [Accessed: 22 February 2022].
- Alves, A.M., Diel, L.F. and Lamers, M.L. 2018. Macrophages and prognosis of oral squamous cell carcinoma: A systematic review. *Journal of Oral Pathology and Medicine* 47(5), pp. 460–467. Available at: <https://pubmed.ncbi.nlm.nih.gov/28940738/> [Accessed: 9 December 2021].
- Aminin, D. and Wang, Y.M. 2021. Macrophages as a “weapon” in anticancer cellular immunotherapy. *Kaohsiung Journal of Medical Sciences* 37(9), pp. 749–758. Available at: <https://onlinelibrary-wiley-com.abc.cardiff.ac.uk/doi/full/10.1002/kjm2.12405> [Accessed: 20 July 2022].
- Amouzegar, A., Chelvanambi, M., Filderman, J.N., Storkus, W.J. and Luke, J.J. 2021. Sting agonists as cancer therapeutics. *Cancers* 13(11). Available at: </pmc/articles/PMC8198217/> [Accessed: 7 March 2022].
- Anfray, C., Ummarino, A., Andón, F.T. and Allavena, P. 2020. Current strategies to target tumor-associated-macrophages to improve anti-tumor immune responses. *Cells* 9(1). Available at: </pmc/articles/PMC7017001/> [Accessed: 11 September 2022].
- Ang, K.K. et al. 2010. Human Papillomavirus and Survival of Patients with Oropharyngeal Cancer. *New England Journal of Medicine* 363(1), pp. 24–35. Available at: <http://www.ncbi.nlm.nih.gov/pubmed/20530316> [Accessed: 2 May 2019].
- Aparicio-Siegmund, S. et al. 2014. Recombinant p35 from bacteria can form interleukin (IL-)12, but not IL-35. Moser, M. ed. *PLoS ONE* 9(9), p. e107990. Available at: <https://dx.plos.org/10.1371/journal.pone.0107990> [Accessed: 30 July 2020].
- Aras, S. and Raza Zaidi, M. 2017. TAMEless traitors: Macrophages in cancer progression and metastasis. *British Journal of Cancer* 117(11), pp. 1583–1591. Available at: <https://pubmed.ncbi.nlm.nih.gov/29065107/> [Accessed: 3 March 2022].
- Arlaukas, S.P. et al. 2017. In vivo imaging reveals a tumor-associated macrophage-mediated resistance pathway in anti-PD-1 therapy. *Science Translational Medicine* 9(389). Available at: <https://pubmed.ncbi.nlm.nih.gov/28490665/> [Accessed: 3 March 2022].
- Auffray, C. et al. 2007. Monitoring of blood vessels and tissues by a population of monocytes with patrolling behavior. *Science* 317(5838), pp. 666–670. Available at: <https://pubmed.ncbi.nlm.nih.gov/17673663/> [Accessed: 3 August 2020].
- Azizi, E. et al. 2018. Single-Cell Map of Diverse Immune Phenotypes in the Breast Tumor Microenvironment. *Cell* 174(5), pp. 1293–1308.e36. Available at: <https://pubmed.ncbi.nlm.nih.gov/29961579/> [Accessed: 4 August 2020].

Badoual, C. et al. 2006. Prognostic value of tumor-infiltrating CD4+ T-cell subpopulations in head and neck cancers. *Clinical Cancer Research* 12(2), pp. 465–472. Available at: <https://pubmed.ncbi.nlm.nih.gov/16428488/> [Accessed: 22 February 2022].

Baghban, R. et al. 2020. Tumor microenvironment complexity and therapeutic implications at a glance. *Cell Communication and Signaling* 18(1), pp. 1–19. Available at: <https://biosignaling-biomedcentral.com.abc.cardiff.ac.uk/articles/10.1186/s12964-020-0530-4> [Accessed: 19 February 2022].

Bak, S.P., Walters, J.J., Takeya, M., Conejo-Garcia, J.R. and Berwin, B.L. 2007. Scavenger receptor-A-targeted leukocyte depletion inhibits peritoneal ovarian tumor progression. *Cancer Research* 67(10), pp. 4783–4789. Available at: <https://aacrjournals-org.abc.cardiff.ac.uk/cancerres/article/67/10/4783/533005/Scavenger-Receptor-A-Targeted-Leukocyte-Depletion> [Accessed: 17 March 2022].

Banchereau, J., Pascual, V. and O'Garra, A. 2012. From IL-2 to IL-37: The expanding spectrum of anti-inflammatory cytokines. *Nature Immunology* 13(10), pp. 925–931. doi: 10.1038/ni.2406.

Baxter, E.W., Graham, A.E., Re, N.A., Carr, I.M., Robinson, J.I., Mackie, S.L. and Morgan, A.W. 2020. Standardized protocols for differentiation of THP-1 cells to macrophages with distinct M(IFN γ +LPS), M(IL-4) and M(IL-10) phenotypes. *Journal of Immunological Methods* 478. Available at: <https://pubmed.ncbi.nlm.nih.gov/32033786/> [Accessed: 23 November 2021].

Beatty, G.L. et al. 2011. CD40 agonists alter tumor stroma and show efficacy against pancreatic carcinoma in mice and humans. *Science* 331(6024), pp. 1612–1616. Available at: <https://www-science-org.abc.cardiff.ac.uk/doi/abs/10.1126/science.1198443> [Accessed: 17 March 2022].

Benci, J.L. et al. 2016. Tumor Interferon Signaling Regulates a Multigenic Resistance Program to Immune Checkpoint Blockade. *Cell* 167(6), pp. 1540–1554.e12. Available at: <https://pubmed-ncbi-nlm-nih-gov.abc.cardiff.ac.uk/27912061/> [Accessed: 21 June 2022].

Benoit, M., Desnues, B. and Mege, J.-L. 2008. Macrophage Polarization in Bacterial Infections. *The Journal of Immunology* 181(6), pp. 3733–3739. Available at: <https://pubmed.ncbi.nlm.nih.gov/18768823/> [Accessed: 3 August 2020].

Benson, E., Li, R., Eisele, D. and Fakhry, C. 2014. The clinical impact of HPV tumor status upon head and neck squamous cell carcinomas. *Oral Oncology* 50(6), pp. 565–574. Available at: <https://pubmed.ncbi.nlm.nih.gov/24134947/> [Accessed: 9 August 2020].

Bergers, G. and Benjamin, L.E. 2003. Tumorigenesis and the angiogenic switch. *Nature Reviews Cancer* 3(6), pp. 401–410. Available at: www.nature.com/reviews/cancer [Accessed: 4 August 2020].

Bezu, L. et al. 2018. Trial watch: Peptide-based vaccines in anticancer therapy. *OncoImmunology* 7(12). Available at: <https://pmc/articles/PMC6279318/> [Accessed: 14 February 2022].

Bhatia, S. et al. 2001. Solid cancers after bone marrow transplantation. *Journal of Clinical Oncology* 19(2), pp. 464–471. Available at: <http://ascopubs.org/doi/10.1200/JCO.2001.19.2.464> [Accessed: 6 May 2019].

Biswas, S.K. and Mantovani, A. 2010. Macrophage plasticity and interaction with lymphocyte subsets: Cancer as a paradigm. *Nature Immunology* 11(10), pp. 889–896. Available at: <https://pubmed.ncbi.nlm.nih.gov/20856220/> [Accessed: 3 January 2022].

Blot, W.J. et al. 1988. Smoking and Drinking in Relation to Oral and Pharyngeal Cancer. *Cancer Research* 48(11), pp. 3282–3287.

Bode, J., Schlake, T., Iber, M., Schübeler, D., Seibler, J., Snezhkov, E. and Nikolaev, L. 2000. The Transgeneticist's Toolbox: Novel Methods for the Targeted Modification of Eukaryotic Genomes. *Biological Chemistry* 381(9–10), pp. 801–813. Available at: <https://www-degruyter-com.abc.cardiff.ac.uk/document/doi/10.1515/BC.2000.103/html> [Accessed: 31 January 2023].

Brand, T.M. et al. 2015. AXL is a logical molecular target in head and neck squamous cell carcinoma. *Clinical cancer research : an official journal of the American Association for Cancer Research* 21(11), p. 2601. Available at: <https://pmc/articles/PMC5032632/> [Accessed: 27 July 2022].

Bray, F., Ferlay, J., Soerjomataram, I., Siegel, R.L., Torre, L.A. and Jemal, A. 2018. Global cancer statistics 2018: GLOBOCAN estimates of incidence and mortality worldwide for 36 cancers in 185 countries. *CA: A Cancer Journal for Clinicians* 68(6), pp. 394–424. Available at: <https://pubmed.ncbi.nlm.nih.gov/30207593/> [Accessed: 17 January 2022].

Bruno, A., Pagani, A., Pulze, L., Albini, A., Dallaglio, K., Noonan M., D.M. and Mortara, L. 2014. Orchestration of angiogenesis by immune cells. *Frontiers in Oncology* 4 JUL. Available at: <https://pubmed.ncbi.nlm.nih.gov/25072019/> [Accessed: 4 August 2020].

Bu, L.L. et al. 2016. Targeting STAT3 signaling reduces immunosuppressive myeloid cells in head and neck squamous cell carcinoma. *OncoImmunology* 5(5). Available at: <https://pubmed.ncbi.nlm.nih.gov/27467947/> [Accessed: 22 February 2022].

Buchbinder, E.I. and Desai, A. 2016. CTLA-4 and PD-1 pathways similarities, differences, and implications of their inhibition. *American Journal of Clinical Oncology: Cancer Clinical Trials* 39(1), pp. 98–106. Available at: </pmc/articles/PMC4892769/?report=abstract> [Accessed: 26 July 2020].

Burnet, F.M. 1970. The concept of immunological surveillance. *Progress in experimental tumor research. Fortschritte der experimentellen Tumorforschung. Progres de la recherche experimentale des tumeurs* 13, pp. 1–27. doi: 10.1159/000386035.

Burnet, M. 1964. Immunological factors in the process of carcinogenesis. *British Medical Bulletin* 20(2), pp. 154–158. Available at: <https://academic.oup.com/bmb/article/285310/IMMUNOLOGICAL> [Accessed: 24 July 2020].

Burtneess, B. et al. 2019. Pembrolizumab alone or with chemotherapy versus cetuximab with chemotherapy for recurrent or metastatic squamous cell carcinoma of the head and neck (KEYNOTE-048): a randomised, open-label, phase 3 study. *The Lancet* 394(10212), pp. 1915–1928. Available at: <https://pubmed.ncbi.nlm.nih.gov/31679945/> [Accessed: 12 February 2022].

Bustin, S.A. et al. 2009. The MIQE guidelines: Minimum information for publication of quantitative real-time PCR experiments. *Clinical Chemistry* 55(4), pp. 611–622. Available at: <https://academic.oup.com/clinchem/article/55/4/611/5631762> [Accessed: 29 October 2021].

Canning, M., Guo, G., Yu, M., Myint, C., Groves, M.W., Byrd, J.K. and Cui, Y. 2019. Heterogeneity of the head and neck squamous cell carcinoma immune landscape and its impact on immunotherapy. *Frontiers in Cell and Developmental Biology* 7(APR). Available at: </pmc/articles/PMC6465325/> [Accessed: 9 September 2021].

Carmeliet, P. 2005. VEGF as a key mediator of angiogenesis in cancer. *Oncology* 69(SUPPL. 3), pp. 4–10. Available at: <https://pubmed.ncbi.nlm.nih.gov/16301830/> [Accessed: 6 January 2022].

Di Caro, G. et al. 2015. Dual prognostic significance of tumour-Associated macrophages in human pancreatic adenocarcinoma treated or untreated with chemotherapy. *Gut* 65(10), pp. 1710–1720. Available at: <https://pubmed.ncbi.nlm.nih.gov/26156960/> [Accessed: 4 August 2020].

Carra, G., Gerosa, F. and Trinchieri, G. 2000. Biosynthesis and Posttranslational Regulation of Human IL-12. *The Journal of Immunology* 164(9), pp. 4752–4761. Available at: <https://pubmed.ncbi.nlm.nih.gov/10779781/> [Accessed: 28 September 2021].

Cassetta, L. and Pollard, J.W. 2018. Targeting macrophages: Therapeutic approaches in cancer. *Nature Reviews Drug Discovery* 17(12), pp. 887–904. Available at: <https://pubmed.ncbi.nlm.nih.gov/30361552/> [Accessed: 4 August 2020].

Chabanon, R.M., Pedrero, M., Lefebvre, C., Marabelle, A., Soria, J.C. and Postel-Vinay, S. 2016. Mutational landscape and sensitivity to immune checkpoint blockers. *Clinical Cancer Research* 22(17), pp. 4309–4321. Available at: <https://pubmed.ncbi.nlm.nih.gov/27390348/> [Accessed: 31 August 2022].

Chang, K.P. et al. 2011. Overexpression of macrophage inflammatory protein-3 α in oral cavity squamous cell carcinoma is associated with nodal metastasis. *Oral Oncology* 47(2), pp. 108–113. Available at: <https://pubmed.ncbi.nlm.nih.gov/21163685/> [Accessed: 3 March 2022].

Chanput, W., Mes, J.J. and Wichers, H.J. 2014. THP-1 cell line: An in vitro cell model for immune modulation approach. *International Immunopharmacology* 23(1), pp. 37–45. Available at: <https://pubmed.ncbi.nlm.nih.gov/25130606/> [Accessed: 23 November 2021].

Chatrabnous, N., Ghaderi, A., Ariafar, A., Razeghinia, M.S., Nemati, M. and Jafarzadeh, A. 2019. Serum concentration of interleukin-35 and its association with tumor stages and FOXP3 gene polymorphism in patients with prostate cancer. *Cytokine* 113, pp. 221–227. Available at: <https://pubmed.ncbi.nlm.nih.gov/30057362/> [Accessed: 17 January 2022].

Chaturvedi, A.K. et al. 2011. Human papillomavirus and rising oropharyngeal cancer incidence in the United States. *Journal of Clinical Oncology* 29(32), pp. 4294–4301. Available at: </pmc/articles/PMC3221528/?report=abstract> [Accessed: 9 August 2020].

Chen, D.S. and Mellman, I. 2017. Elements of cancer immunity and the cancer-immune set point. *Nature* 541(7637), pp. 321–330. Available at: <https://www-nature-com.abc.cardiff.ac.uk/articles/nature21349> [Accessed: 21 June 2022].

Chen, G. et al. 2016. Circulating low IL-23: IL-35 cytokine ratio promotes progression associated with poor prognosis in breast cancer. *American Journal of Translational Research* 8(5), pp. 2255–2264. Available at: </pmc/articles/PMC4891437/> [Accessed: 17 January 2022].

Chen, S., Xia, J., Zhang, Y. and Zhan, Q. 2022. IL-35 attenuated LPS-induced acute lung injury by regulating macrophage polarization. *Molecular Biology Reports* 49(7), pp. 5811–5820. Available at: <https://link-springer-com.abc.cardiff.ac.uk/article/10.1007/s11033-022-07293-5> [Accessed: 1 August 2022].

Chen, Y. et al. 2021. CAR-macrophage: A new immunotherapy candidate against solid tumors. *Biomedicine and Pharmacotherapy* 139, p. 111605. doi: 10.1016/j.biopha.2021.111605.

Chen, Y., Song, Y., Du, W., Gong, L., Chang, H. and Zou, Z. 2019. Tumor-associated macrophages: An accomplice in solid tumor progression. *Journal of Biomedical Science* 26(1), pp. 1–13. Available at: <https://doi.org/10.1186/s12929-019-0568-z> [Accessed: 5 August 2020].

Cheng, N. et al. 2018. A nanoparticle-incorporated STING activator enhances antitumor immunity in PD-L1-insensitive models of triple-negative breast cancer. *JCI insight* 3(22). doi: 10.1172/jci.insight.120638.

Chi, J., Liu, Y., Yang, L. and Yang, J. 2022. Silencing of B7H4 Represses the Development of Oral Squamous Cell Carcinoma Through Promotion of M1 Macrophage Polarization. *Journal of Oral and Maxillofacial Surgery* 80(8), pp. 1408–1423. doi: 10.1016/j.joms.2022.03.019.

Choi, I.-H. et al. 2003. Genomic Organization and Expression Analysis of B7-H4, an Immune Inhibitory Molecule of the B7 Family. *The Journal of Immunology* 171(9), pp. 4650–4654. Available at: <https://www-jimmunol-org.abc.cardiff.ac.uk/content/171/9/4650> [Accessed: 6 January 2022].

Choi, J.K. and Egwuagu, C.E. 2021. Interleukin 35 Regulatory B Cells. *Journal of Molecular Biology* 433(1), p. 166607. doi: 10.1016/j.jmb.2020.07.019.

Cieslewicz, M. et al. 2013. Targeted delivery of proapoptotic peptides to tumor-associated macrophages improves survival. *Proceedings of the National Academy of Sciences of the United States of America* 110(40), pp. 15919–15924. Available at: <https://www.pnas.org/content/110/40/15919.short> [Accessed: 15 March 2022].

Cohen, E.E.W. et al. 2019. Pembrolizumab versus methotrexate, docetaxel, or cetuximab for recurrent or metastatic head-and-neck squamous cell carcinoma (KEYNOTE-040): a randomised, open-label, phase 3 study. *The Lancet* 393(10167), pp. 156–167. Available at: <https://pubmed-ncbi-nlm-nih-gov.abc.cardiff.ac.uk/30509740/> [Accessed: 21 June 2022].

Collison, L.W. et al. 2007. The inhibitory cytokine IL-35 contributes to regulatory T-cell function. *Nature* 450(7169), pp. 566–569. doi: 10.1038/nature06306.

Collison, L.W. et al. 2010. IL-35-mediated induction of a potent regulatory T cell population. *Nature Immunology* 11(12), pp. 1093–1101. doi: 10.1038/ni.1952.

Collison, L.W. et al. 2012. The composition and signaling of the IL-35 receptor are unconventional. *Nature Immunology* 13(3), pp. 290–299. doi: 10.1038/ni.2227.

Concha-Benavente, F. et al. 2016. Identification of the cell-intrinsic and -extrinsic pathways downstream of EGFR and IFN γ that induce PD-L1 expression in head and neck Cancer. *Cancer Research* 76(5), pp. 1031–1043. Available at: <https://cancerres.aacrjournals.org/content/76/5/1031> [Accessed: 12 February 2022].

Concha-Benavente, F., Kansy, B., Moskovitz, J., Moy, J., Chandran, U. and Ferris, R.L. 2018. PD-L1 mediates dysfunction in activated PD-1 $^+$ NK cells in head and neck cancer patients. *Cancer Immunology Research* 6(12), pp. 1548–1560. Available at: <https://aacrjournals-org.abc.cardiff.ac.uk/cancerimmunolres/article/6/12/1548/468830/PD-L1-Mediates-Dysfunction-in-Activated-PD-1-NK> [Accessed: 19 February 2022].

Corrales, L. et al. 2015. Direct Activation of STING in the Tumor Microenvironment Leads to Potent and Systemic Tumor Regression and Immunity. *Cell Reports* 11(7), pp. 1018–1030. doi: 10.1016/j.celrep.2015.04.031.

Costa, N.L., Valadares, M.C., Souza, P.P.C., Mendonça, E.F., Oliveira, J.C., Silva, T.A. and Batista, A.C. 2013. Tumor-associated macrophages and the profile of inflammatory cytokines in oral squamous cell carcinoma. *Oral Oncology* 49(3), pp. 216–223. Available at: <http://www.ncbi.nlm.nih.gov/pubmed/23089461> [Accessed: 6 May 2019].

- D'Souza, G. et al. 2007. Case–Control Study of Human Papillomavirus and Oropharyngeal Cancer. *New England Journal of Medicine* 356(19), pp. 1944–1956. Available at: <http://www.nejm.org/doi/abs/10.1056/NEJMoa065497> [Accessed: 1 May 2019].
- Dacoba, T.G., Anfray, C., Mainini, F., Allavena, P., Alonso, M.J., Torres Andón, F. and Crecente-Campo, J. 2020. Arginine-Based Poly(I:C)-Loaded Nanocomplexes for the Polarization of Macrophages Toward M1-Antitumoral Effectors. *Frontiers in Immunology* 11, p. 1412. doi: 10.3389/fimmu.2020.01412.
- Daigneault, M., Preston, J.A., Marriott, H.M., Whyte, M.K.B. and Dockrell, D.H. 2010. The identification of markers of macrophage differentiation in PMA-stimulated THP-1 cells and monocyte-derived macrophages. *PLoS ONE* 5(1). Available at: <https://pubmed.ncbi.nlm.nih.gov/20084270/> [Accessed: 6 October 2021].
- Dal Maso, L. et al. 2016. Combined effect of tobacco smoking and alcohol drinking in the risk of head and neck cancers: a re-analysis of case–control studies using bi-dimensional spline models. *European Journal of Epidemiology* 31(4), pp. 385–393. Available at: <http://www.ncbi.nlm.nih.gov/pubmed/25855002> [Accessed: 1 May 2019].
- Dambuzza, I.M. et al. 2017. IL-12p35 induces expansion of IL-10 and IL-35-expressing regulatory B cells and ameliorates autoimmune disease. *Nature Communications* 8(1). Available at: <https://pubmed.ncbi.nlm.nih.gov/315620058/> [Accessed: 23 September 2021].
- DeNardo, D.G. and Ruffell, B. 2019. Macrophages as regulators of tumour immunity and immunotherapy. *Nature Reviews Immunology* 19(6), pp. 369–382. Available at: <https://www-nature-com.abc.cardiff.ac.uk/articles/s41577-019-0127-6> [Accessed: 17 March 2022].
- Deola, S. et al. 2008. Helper B Cells Promote Cytotoxic T Cell Survival and Proliferation Independently of Antigen Presentation through CD27/CD70 Interactions. *The Journal of Immunology* 180(3), pp. 1362–1372. Available at: <https://www.jimmunol.org/content/180/3/1362> [Accessed: 22 February 2022].
- Devergne, O., Birkenbach, M. and Kieff, E. 1997. Epstein-Barr virus-induced gene 3 and the p35 subunit of interleukin 12 form a novel heterodimeric hematopoietin. *Proceedings of the National Academy of Sciences of the United States of America* 94(22), pp. 12041–12046. Available at: <http://www.ncbi.nlm.nih.gov/pubmed/9342359> [Accessed: 30 April 2019].
- Devergne, O., Coulomb-L'Herminé, A., Capel, F., Moussa, M. and Capron, F. 2001. Expression of Epstein-Barr virus-induced gene 3, an interleukin-12 p40-related molecule, throughout human pregnancy: Involvement of syncytiotrophoblasts and extravillous trophoblasts. *American Journal of Pathology* 159(5), pp. 1763–1776. doi: 10.1016/S0002-9440(10)63023-4.
- Devergne, O., Hummel, M., Koeppen, H., Le Beau, M.M., Nathanson, E.C., Kieff, E. and Birkenbach, M. 1996. A novel interleukin-12 p40-related protein induced by latent Epstein-Barr virus infection in B lymphocytes. *Journal of Virology* 70(2), pp. 1143–1153. Available at: <https://pubmed.ncbi.nlm.nih.gov/189923/>?report=abstract [Accessed: 15 September 2021].
- Dixon, K.O., van der Kooij, S.W., Vignali, D.A.A. and van Kooten, C. 2015. Human tolerogenic dendritic cells produce IL-35 in the absence of other IL-12 family members. *European Journal of Immunology* 45(6), pp. 1736–1747. doi: 10.1002/eji.201445217.
- Downey, C.M., Aghaei, M., Schwendener, R.A. and Jirik, F.R. 2014. DMXAA causes tumor site-specific vascular disruption in murine non-small cell lung cancer, and like the endogenous non-canonical cyclic dinucleotide STING agonist, 2'3'-cGAMP, induces M2 macrophage repolarization. *PLoS ONE* 9(6), p. e99988. Available at: <https://journals.plos.org/plosone/article?id=10.1371/journal.pone.0099988> [Accessed: 17 March 2022].
- Dumitru, C.A., Bankfalvi, A., Gu, X., Eberhardt, W.E., Zeidler, R., Lang, S. and Brandau, S. 2013. Neutrophils activate tumoral CORTACTIN to enhance progression of oropharyngeal carcinoma. *Frontiers in Immunology* 4(FRB), p. 33. doi: 10.3389/fimmu.2013.00033.
- Dunn, G.P., Bruce, A.T., Ikeda, H., Old, L.J. and Schreiber, R.D. 2002. Cancer immunoediting: From immunosurveillance to tumor escape. *Nature Immunology* 3(11), pp. 991–998. Available at: <http://www.nature.com/articles/ni1102-991> [Accessed: 6 May 2019].
- Dunn, G.P., Old, L.J. and Schreiber, R.D. 2004. The three Es of cancer immunoediting. *Annual Review of Immunology* 22(1), pp. 329–360. Available at: <http://www.ncbi.nlm.nih.gov/pubmed/15032581> [Accessed: 6 May 2019].
- Ecoeur, F., Weiss, J., Schlegel, S. and Guntermann, C. 2020. Lack of evidence for expression and function of IL-39 in human immune cells. *PLoS ONE* 15(12 December), p. e0242329. Available at: <https://journals.plos.org/plosone/article?id=10.1371/journal.pone.0242329> [Accessed: 15 September 2021].

- Ehrlich, P. 1909. Ueber den jetzigen Stand der Karzinomforschung | *Nederlands Tijdschrift voor Geneeskunde*. *Ned. Tijdschr. Geneeskd.* 5, pp. 273–290. Available at: <https://www.ntvg.nl/artikelen/ueber-den-jetzig-stand-der-karzinomforschung> [Accessed: 1 August 2020].
- Elmusrati, A., Wang, J. and Wang, C.Y. 2021. Tumor microenvironment and immune evasion in head and neck squamous cell carcinoma. *International Journal of Oral Science* 13(1), pp. 1–11. Available at: <https://www-nature-com.abc.cardiff.ac.uk/articles/s41368-021-00131-7> [Accessed: 21 June 2022].
- Engelhard, V.H. 1994. Structure of peptides associated with class I and class II MHC molecules. *Annual Review of Immunology* 12, pp. 181–207. Available at: <https://pubmed.ncbi.nlm.nih.gov/7516668/> [Accessed: 6 August 2020].
- Etzerodt, A. et al. 2019. Specific targeting of CD163+ TAMs mobilizes inflammatory monocytes and promotes T cell-mediated tumor regression. *Journal of Experimental Medicine* 216(10), pp. 2394–2411. Available at: <https://doi.org/10.1084/jem.20182124> [Accessed: 17 March 2022].
- Eyles, J. et al. 2010. Tumor cells disseminate early, but immunosurveillance limits metastatic outgrowth, in a mouse model of melanoma. *Journal of Clinical Investigation* 120(6), pp. 2030–2039. Available at: <http://www.jci.org> [Accessed: 26 July 2020].
- Fan, Y.G., Zhai, J.M., Wang, W., Feng, B., Yao, G.L., An, Y.H. and Zeng, C. 2015. IL-35 over-expression is associated with genesis of gastric cancer. *Asian Pacific Journal of Cancer Prevention* 16(7), pp. 2845–2849. Available at: <https://pubmed-ncbi-nlm-nih-gov.abc.cardiff.ac.uk/25854372/> [Accessed: 9 September 2021].
- Farquhar, D.R., Divaris, K., Mazul, A.L., Weissler, M.C., Zevallos, J.P. and Olshan, A.F. 2017. Poor oral health affects survival in head and neck cancer. *Oral Oncology* 73, pp. 111–117. Available at: <https://pubmed.ncbi.nlm.nih.gov/28939062/> [Accessed: 9 August 2020].
- Feins, S., Kong, W., Williams, E.F., Milone, M.C. and Fraietta, J.A. 2019. An introduction to chimeric antigen receptor (CAR) T-cell immunotherapy for human cancer. *American Journal of Hematology* 94(S1), pp. S3–S9. Available at: <https://pubmed.ncbi.nlm.nih.gov/30680780/> [Accessed: 12 February 2022].
- Ferlay, J. et al. 2019. Estimating the global cancer incidence and mortality in 2018: GLOBOCAN sources and methods. *International Journal of Cancer* 144(8), pp. 1941–1953. Available at: <https://pubmed.ncbi.nlm.nih.gov/30350310/> [Accessed: 31 August 2022].
- Ferris, R.L. 2015. Immunology and immunotherapy of head and neck cancer. *Journal of Clinical Oncology* 33(29), pp. 3293–3304. doi: 10.1200/JCO.2015.61.1509.
- Ferris, R.L. et al. 2016. Nivolumab for Recurrent Squamous-Cell Carcinoma of the Head and Neck. *New England Journal of Medicine* 375(19), pp. 1856–1867. Available at: <https://www-nejm-org.abc.cardiff.ac.uk/doi/10.1056/NEJMoa1602252> [Accessed: 21 June 2022].
- Ferris, R.L. et al. 2018. Nivolumab vs investigator’s choice in recurrent or metastatic squamous cell carcinoma of the head and neck: 2-year long-term survival update of CheckMate 141 with analyses by tumor PD-L1 expression. *Oral Oncology* 81, pp. 45–51. Available at: <https://pubmed.ncbi.nlm.nih.gov/29884413/> [Accessed: 31 August 2022].
- Ferris, R.L. et al. 2020. Durvalumab with or without tremelimumab in patients with recurrent or metastatic head and neck squamous cell carcinoma: EAGLE, a randomized, open-label phase III study. *Annals of Oncology* 31(7), pp. 942–950. doi: 10.1016/j.annonc.2020.04.001.
- Ferris, R.L., Hunt, J.L. and Ferrone, S. 2005. Human leukocyte antigen (HLA) class I defects in head and neck cancer: Molecular mechanisms and clinical significance. *Immunologic Research* 33(2), pp. 113–133. doi: 10.1385/IR:33:2:113.
- Ferris, R.L., Whiteside, T.L. and Ferrone, S. 2006. Immune escape associated with functional defects in antigen-processing machinery in head and neck cancer. *Clinical Cancer Research* 12(13), pp. 3890–3895. Available at: <http://www.ncbi.nlm.nih.gov/pubmed/16818683> [Accessed: 6 May 2019].
- Fesnak, A.D., June, C.H. and Levine, B.L. 2016. Engineered T cells: The promise and challenges of cancer immunotherapy. *Nature Reviews Cancer* 16(9), pp. 566–581. Available at: <https://www-nature-com.abc.cardiff.ac.uk/articles/nrc.2016.97> [Accessed: 15 March 2022].
- Fife, B.T. and Bluestone, J.A. 2008. Control of peripheral T-cell tolerance and autoimmunity via the CTLA-4 and PD-1 pathways. *Immunological Reviews* 224(1), pp. 166–182. Available at: <https://pubmed.ncbi.nlm.nih.gov/18759926/> [Accessed: 7 August 2020].

- Finn, G.K., Kurz, B.W., Cheng, R.Z. and Shmookler Reis, R.J. 1989. Homologous plasmid recombination is elevated in immortalized transformed cells. *Molecular and Cellular Biology* 9(9), pp. 4009–4017. Available at: <https://pubmed.ncbi.nlm.nih.gov/2550810/> [Accessed: 29 January 2023].
- Forrester, M.A., Wassall, H.J., Hall, L.S., Cao, H., Wilson, H.M., Barker, R.N. and Vickers, M.A. 2018. Similarities and differences in surface receptor expression by THP-1 monocytes and differentiated macrophages polarized using seven different conditioning regimens. *Cellular Immunology* 332, pp. 58–76. Available at: <https://pubmed.ncbi.nlm.nih.gov/30077333/> [Accessed: 23 November 2021].
- Forster, M.D. and Devlin, M.J. 2018. Immune checkpoint inhibition in head and neck cancer. *Frontiers in Oncology* 8(AUG). Available at: <https://pubmed.ncbi.nlm.nih.gov/30211111/> [Accessed: 17 January 2022].
- Foster, C.C. et al. 2018. Definitive chemoradiation for locally-advanced oral cavity cancer: A 20-year experience. *Oral Oncology* 80, pp. 16–22. doi: 10.1016/j.oraloncology.2018.03.008.
- Fuertes, M.B., Kacha, A.K., Kline, J., Woo, S.R., Kranz, D.M., Murphy, K.M. and Gajewski, T.F. 2011. Host type I IFN signals are required for antitumor CD8⁺ T cell responses through CD8 α ⁺ dendritic cells. *Journal of Experimental Medicine* 208(10), pp. 2005–2016. Available at: </pmc/articles/PMC3182064/> [Accessed: 17 March 2022].
- van Furth, R. and Cohn, Z.A. 1968. The origin and kinetics of mononuclear phagocytes. *The Journal of experimental medicine* 128(3), pp. 415–435. Available at: <https://pubmed.ncbi.nlm.nih.gov/5666958/> [Accessed: 3 August 2020].
- van Furth, R., Cohn, Z.A., Hirsch, J.G., Humphrey, J.H., Spector, W.G. and Langevoort, H.L. 1972. The mononuclear phagocyte system: a new classification of macrophages, monocytes, and their precursor cells. *Bulletin of the World Health Organization* 46(6), pp. 845–852. Available at: </pmc/articles/PMC2480884/?report=abstract> [Accessed: 3 August 2020].
- Gabrilovich, D. 2004. Mechanisms and functional significance of tumour-induced dendritic-cell defects. *Nature Reviews Immunology* 4(12), pp. 941–952. Available at: <http://www.ncbi.nlm.nih.gov/pubmed/15573129> [Accessed: 6 May 2019].
- Gallo, O., Libonati, G.A., Gallina, E., Fini Storchi, O., Giannini, A., Urso, C. and Bondi, R. 1991. Langerhans Cells Related to Prognosis in Patients With Laryngeal Carcinoma. *Archives of Otolaryngology--Head and Neck Surgery* 117(9), pp. 1007–1010. Available at: <https://jamanetwork.com/journals/jamaotolaryngology/fullarticle/620011> [Accessed: 22 February 2022].
- Galvis, M.M. et al. 2020. Immunotherapy improves efficacy and safety of patients with HPV positive and negative head and neck cancer: A systematic review and meta-analysis. *Critical Reviews in Oncology/Hematology* 150, p. 102966. doi: 10.1016/j.critrevonc.2020.102966.
- Gao, L. et al. 2016. CCL2/EGF positive feedback loop between cancer cells and macrophages promotes cell migration and invasion in head and neck squamous cell carcinoma. *Oncotarget* 7(52), pp. 87037–87051. Available at: <https://pubmed.ncbi.nlm.nih.gov/27888616/> [Accessed: 5 March 2022].
- Gavrieliatou, N., Vathiotis, I., Economopoulou, P. and Psyrris, A. 2021. The role of b cells in head and neck cancer. *Cancers* 13(21). Available at: <https://pubmed.ncbi.nlm.nih.gov/34771546/> [Accessed: 22 February 2022].
- Gazi, U. and Martinez-Pomares, L. 2009. Influence of the mannose receptor in host immune responses. *Immunobiology* 214(7), pp. 554–561. doi: 10.1016/j.imbio.2008.11.004.
- Gazzaniga, S. et al. 2007. Targeting tumor-associated macrophages and inhibition of MCP-1 reduce angiogenesis and tumor growth in a human melanoma xenograft. *Journal of Investigative Dermatology* 127(8), pp. 2031–2041. Available at: <https://pubmed.ncbi.nlm.nih.gov/17460736/> [Accessed: 5 August 2020].
- Gelboin, H. V. 1980. Benzo[alpha]pyrene metabolism, activation and carcinogenesis: role and regulation of mixed-function oxidases and related enzymes. *Physiological reviews* 60(4), pp. 1107–1166. Available at: <https://pubmed.ncbi.nlm.nih.gov/7001511/> [Accessed: 7 August 2020].
- Genin, M., Clement, F., Fattaccioli, A., Raes, M. and Michiels, C. 2015. M1 and M2 macrophages derived from THP-1 cells differentially modulate the response of cancer cells to etoposide. *BMC Cancer* 15(1), pp. 1–14. Available at: <https://bmccancer.biomedcentral-com.abc.cardiff.ac.uk/articles/10.1186/s12885-015-1546-9> [Accessed: 23 November 2021].
- Gerace, E. and Moazed, D. 2014. Coimmunoprecipitation of proteins from yeast. *Methods in Enzymology* 541, pp. 13–26. Available at: </pmc/articles/PMC4370295/> [Accessed: 9 May 2022].

- Germano, G. et al. 2013. Role of Macrophage Targeting in the Antitumor Activity of Trabectedin. *Cancer Cell* 23(2), pp. 249–262. Available at: <http://www.cell.com.abc.cardiff.ac.uk/article/S1535610813000330/fulltext> [Accessed: 15 March 2022].
- Gershon, R.K. and Kondo, K. 1971. Infectious immunological tolerance. *Immunology* 21(6), pp. 903–914.
- Godin-Ethier, J., Hanafi, L.A., Piccirillo, C.A. and Lapointe, R. 2011. Indoleamine 2,3-dioxygenase expression in human cancers: Clinical and immunologic perspectives. *Clinical Cancer Research* 17(22), pp. 6985–6991. Available at: <https://clincancerres-aacrjournals-org.abc.cardiff.ac.uk/content/17/22/6985> [Accessed: 12 February 2022].
- Goldenberg, D., Lee, J., Koch, W.M., Kim, M.M., Trink, B., Sidransky, D. and Moon, C.S. 2004. Habitual risk factors for head and neck cancer. *Otolaryngology - Head and Neck Surgery* 131(6), pp. 986–993. Available at: <http://journals.sagepub.com/doi/10.1016/j.otohns.2004.02.035> [Accessed: 9 August 2020].
- Goldman, S.A., Baker, E., Weyant, R.J., Clarke, M.R., Myers, J.N. and Lotze, M.T. 1998. Peritumoral CD1a-positive dendritic cells are associated with improved survival in patients with tongue carcinoma. *Archives of Otolaryngology - Head and Neck Surgery* 124(6), pp. 641–646. Available at: <https://pubmed.ncbi.nlm.nih.gov/9639473/> [Accessed: 22 February 2022].
- Gomez-Roca, C.A. et al. 2019. Phase i study of emactuzumab single agent or in combination with paclitaxel in patients with advanced/metastatic solid tumors reveals depletion of immunosuppressive M2-like macrophages. *Annals of Oncology* 30(8), pp. 1381–1392. Available at: <https://pubmed.ncbi.nlm.nih.gov/31114846/> [Accessed: 17 March 2022].
- Gomez Perdiguero, E. et al. 2015. Tissue-resident macrophages originate from yolk-sac-derived erythro-myeloid progenitors. *Nature* 518(7540), pp. 547–551. Available at: <https://pubmed.ncbi.nlm.nih.gov/25470051/> [Accessed: 3 August 2020].
- Gordon, S. 2003. Alternative activation of macrophages. *Nature Reviews Immunology* 3(1), pp. 23–35. Available at: www.nature.com/reviews/immunol [Accessed: 3 August 2020].
- Gordon, S. 2008. Elie Metchnikoff: Father of natural immunity. *European Journal of Immunology* 38(12), pp. 3257–3264. Available at: <http://doi.wiley.com/10.1002/eji.200838855> [Accessed: 3 August 2020].
- Goswami, S. et al. 2005. Macrophages promote the invasion of breast carcinoma cells via a colony-stimulating factor-1/epidermal growth factor paracrine loop. *Cancer Research* 65(12), pp. 5278–5283. Available at: <http://cancerres.aacrjournals.org/> [Accessed: 4 August 2020].
- Green, S.E., McCusker, M.G. and Mehra, R. 2020. Emerging immune checkpoint inhibitors for the treatment of head and neck cancers. *Expert Opinion on Emerging Drugs* 25(4), pp. 501–514. Available at: [https://www-tandfonline-com.abc.cardiff.ac.uk/doi/abs/10.1080/14728214.2020.1852215](https://www.tandfonline-com.abc.cardiff.ac.uk/doi/abs/10.1080/14728214.2020.1852215) [Accessed: 12 February 2022].
- Greten, F.R. and Grivennikov, S.I. 2019. Inflammation and Cancer: Triggers, Mechanisms, and Consequences. *Immunity* 51(1), pp. 27–41. Available at: <https://pubmed.ncbi.nlm.nih.gov.abc.cardiff.ac.uk/31315034/> [Accessed: 21 June 2022].
- Von Groll, A., Levin, Y., Barbosa, M.C. and Ravazzolo, A.P. 2006. Linear DNA low efficiency transfection by liposome can be improved by the use of cationic lipid as charge neutralizer. *Biotechnology Progress* 22(4), pp. 1220–1224. Available at: <http://www.ncbi.nlm.nih.gov/pubmed/16889402> [Accessed: 30 April 2019].
- De Gruijl, T.D., Van Den Eertwegh, A.J.M., Pinedo, H.M. and Scheper, R.J. 2008. Whole-cell cancer vaccination: From autologous to allogeneic tumor- and dendritic cell-based vaccines. *Cancer Immunology, Immunotherapy* 57(10), pp. 1569–1577. Available at: <https://link-springer-com.abc.cardiff.ac.uk/article/10.1007/s00262-008-0536-z> [Accessed: 5 September 2022].
- Gu, J.H. et al. 2021. Serum level of interleukin-35 as a potential prognostic factor for gastric cancer. *Asia-Pacific Journal of Clinical Oncology* 17(1), pp. 52–59. Available at: <https://pubmed.ncbi.nlm.nih.gov/33044052/> [Accessed: 17 January 2022].
- Gu, S. et al. 2018. CD47 Blockade Inhibits Tumor Progression through Promoting Phagocytosis of Tumor Cells by M2 Polarized Macrophages in Endometrial Cancer. *Journal of Immunology Research* 2018. Available at: <https://pubmed.ncbi.nlm.nih.gov/30525058/> [Accessed: 17 March 2022].
- Gu, X. et al. 2015. Elevated plasma interleukin-35 levels predict poor prognosis in patients with non-small cell lung cancer. *Tumor Biology* 36(4), pp. 2651–2656. Available at: <http://www.ncbi.nlm.nih.gov/pubmed/25480413> [Accessed: 6 May 2019].

- Guerriero, J.L. 2019. Macrophages: Their Untold Story in T Cell Activation and Function. *International Review of Cell and Molecular Biology* 342, pp. 73–93. doi: 10.1016/bs.ircmb.2018.07.001.
- Guha, N., Warnakulasuriya, S., Vlaanderen, J. and Straif, K. 2014. Betel quid chewing and the risk of oral and oropharyngeal cancers: A meta-analysis with implications for cancer control. *International Journal of Cancer* 135(6), pp. 1433–1443. Available at: <https://pubmed.ncbi.nlm.nih.gov/24302487/> [Accessed: 7 August 2020].
- Haabeth, O.A.W. et al. 2019. Local delivery of OX40L, CD80, and CD86 mRNA kindles global anticancer immunity. *Cancer Research* 79(7), pp. 1624–1634. Available at: <https://pubmed.ncbi.nlm.nih.gov/30692215/> [Accessed: 15 March 2022].
- Haigentz, M. 2005. Aerodigestive cancers in HIV infection. *Current Opinion in Oncology* 17(5), pp. 474–478. Available at: <http://www.ncbi.nlm.nih.gov/pubmed/16093799> [Accessed: 6 May 2019].
- Haller, S., Duval, A., Migliorini, R., Stevanin, M., Mack, V. and Acha-Orbea, H. 2017. Interleukin-35-producing CD8 α ⁺ dendritic cells acquire a tolerogenic state and regulate T cell function. *Frontiers in Immunology* 8(FEB), p. 98. doi: 10.3389/fimmu.2017.00098.
- Hamaker, N.K. and Lee, K.H. 2018. Site-specific integration ushers in a new era of precise CHO cell line engineering. *Current Opinion in Chemical Engineering* 22, pp. 152–160. Available at: </pmc/articles/PMC6510493/> [Accessed: 31 January 2023].
- Hanna, E., Abadi, R. and Abbas, O. 2016. Imiquimod in dermatology: an overview. *International Journal of Dermatology* 55(8), pp. 831–844. Available at: <https://onlinelibrary-wiley-com.abc.cardiff.ac.uk/doi/full/10.1111/ijd.13235> [Accessed: 17 March 2022].
- Hao, N.B., Lü, M.H., Fan, Y.H., Cao, Y.L., Zhang, Z.R. and Yang, S.M. 2012. Macrophages in tumor microenvironments and the progression of tumors. *Clinical and Developmental Immunology* 2012. Available at: <https://pubmed.ncbi.nlm.nih.gov/22778768/> [Accessed: 8 December 2021].
- Hao, Q., Vadgama, J. V. and Wang, P. 2020. CCL2/CCR2 signaling in cancer pathogenesis. *Cell Communication and Signaling* 18(1), pp. 1–13. Available at: <https://biosignaling.biomedcentral.com/articles/10.1186/s12964-020-00589-8> [Accessed: 1 March 2022].
- Hao, S. et al. 2018. Breast cancer cell-derived IL-35 promotes tumor progression via induction of IL-35-producing induced regulatory T cells. *Carcinogenesis* 39(12), pp. 1488–1496. Available at: <https://academic-oup-com.abc.cardiff.ac.uk/carcin/article/39/12/1488/5128955> [Accessed: 23 November 2021].
- Haraf, D.J. et al. 1996. Human papilloma virus and p53 in head and neck cancer: Clinical correlates and survival. *Clinical Cancer Research* 2(4), pp. 755–762.
- Harney, A.S. et al. 2015. Real-time imaging reveals local, transient vascular permeability, and tumor cell intravasation stimulated by TIE2hi macrophage-derived VEGFA. *Cancer Discovery* 5(9), pp. 932–943. Available at: </pmc/articles/PMC4560669/?report=abstract> [Accessed: 4 August 2020].
- Hartley, G.P., Chow, L., Ammons, D.T., Wheat, W.H. and Dow, S.W. 2018. Programmed cell death ligand 1 (PD-L1) signaling regulates macrophage proliferation and activation. *Cancer Immunology Research* 6(10), pp. 1260–1273. Available at: <https://aacrjournals-org.abc.cardiff.ac.uk/cancerimmunolres/article/6/10/1260/466720/Programmed-Cell-Death-Ligand-1-PD-L1-Signaling> [Accessed: 27 July 2022].
- Hashibe, M. et al. 2009. Interaction between tobacco and alcohol use and the risk of head and neck cancer: Pooled analysis in the international head and neck cancer Epidemiology consortium. *Cancer Epidemiology Biomarkers and Prevention* 18(2), pp. 541–550. Available at: <http://www.ncbi.nlm.nih.gov/pubmed/19190158> [Accessed: 1 May 2019].
- He, K.F. et al. 2014. CD163⁺ tumor-associated macrophages correlated with poor prognosis and cancer stem cells in oral squamous cell carcinoma. *BioMed Research International* 2014. Available at: <https://pubmed.ncbi.nlm.nih.gov/24883329/> [Accessed: 9 December 2021].
- He, Y., Pei, J. hong, Li, X. qing and Chi, G. 2021. IL-35 promotes EMT through STAT3 activation and induces MET by promoting M2 macrophage polarization in HCC. *Biochemical and Biophysical Research Communications* 559, pp. 35–41. Available at: <https://pubmed.ncbi.nlm.nih.gov/33932898/> [Accessed: 23 November 2021].
- Heim, L. et al. 2019. Increased expression of the immunosuppressive interleukin-35 in patients with non-small cell lung cancer. *British Journal of Cancer* 120(9), pp. 903–912. Available at: <https://pubmed.ncbi.nlm.nih.gov/30956278/> [Accessed: 4 April 2022].

Hirano, H., Tanioka, K., Yokoyama, S., Akiyama, S.I. and Kuratsu, J.I. 2001. Angiogenic effect of thymidine phosphorylase on macrophages in glioblastoma multiforme. *Journal of Neurosurgery* 95(1), pp. 89–95. Available at: <https://pubmed.ncbi.nlm.nih.gov/11455962/> [Accessed: 4 August 2020].

Hoves, S. et al. 2018. Rapid activation of tumor-associated macrophages boosts preexisting tumor immunity. *Journal of Experimental Medicine* 215(3), pp. 859–876. Available at: <https://pubmed.ncbi.nlm.nih.gov/29436396/> [Accessed: 5 August 2020].

Hu, Y. et al. 2016. Tumor-associated macrophages correlate with the clinicopathological features and poor outcomes via inducing epithelial to mesenchymal transition in oral squamous cell carcinoma. *Journal of Experimental and Clinical Cancer Research* 35(1). Available at: <https://pubmed.ncbi.nlm.nih.gov/26769084/> [Accessed: 26 July 2020].

Hughes, R. et al. 2015. Perivascular M2 macrophages stimulate tumor relapse after chemotherapy. *Cancer Research* 75(17), pp. 3479–3491. Available at: <https://pubmed.ncbi.nlm.nih.gov/26269531/> [Accessed: 4 August 2020].

Ichimura, T. et al. 2014. Prognostic significance of CD204-positive macrophages in upper urinary tract cancer. *Annals of Surgical Oncology* 21(6), pp. 2105–2112. Available at: <https://pubmed.ncbi.nlm.nih.gov/abc.cardiff.ac.uk/24492923/> [Accessed: 6 January 2022].

Ikehara, S., Pahwa, R.N., Fernandes, G., Hansen, C.T. and Good, R.A. 1984. Functional T cells in athymic nude mice. *Proceedings of the National Academy of Sciences of the United States of America* 81(3 I), pp. 886–888. Available at: [/pmc/articles/PMC344943/?report=abstract](https://pubmed.ncbi.nlm.nih.gov/pmc/articles/PMC344943/?report=abstract) [Accessed: 24 July 2020].

Ishikawa, H., Ma, Z. and Barber, G.N. 2009. STING regulates intracellular DNA-mediated, type I interferon-dependent innate immunity. *Nature* 461(7265), pp. 788–792. Available at: <https://www-nature-com.abc.cardiff.ac.uk/articles/nature08476> [Accessed: 17 March 2022].

Ishizu, T. et al. 2021. Head and neck squamous cell carcinoma cell lines have an immunomodulatory effect on macrophages independent of hypoxia and toll-like receptor 9. *BMC Cancer* 21(1). Available at: <https://pubmed.ncbi.nlm.nih.gov/34479492/> [Accessed: 28 December 2021].

Jaiswal, S. et al. 2009. CD47 Is Upregulated on Circulating Hematopoietic Stem Cells and Leukemia Cells to Avoid Phagocytosis. *Cell* 138(2), pp. 271–285. Available at: <https://pubmed.ncbi.nlm.nih.gov/19632178/> [Accessed: 5 August 2020].

Jalah, R. et al. 2013. The p40 subunit of interleukin (IL)-12 promotes stabilization and export of the p35 subunit: Implications for improved IL-12 cytokine production. *Journal of Biological Chemistry* 288(9), pp. 6763–6776. doi: 10.1074/jbc.M112.436675.

Jardim, J.F., Gondak, R., Galvis, M.M., Pinto, C.A.L. and Kowalski, L.P. 2018. A decreased peritumoral CD1a+ cell number predicts a worse prognosis in oral squamous cell carcinoma. *Histopathology* 72(6), pp. 905–913. Available at: <https://pubmed.ncbi.nlm.nih.gov/29023924/> [Accessed: 22 February 2022].

Jayaram, S.C., Muzaffar, S.J., Ahmed, I., Dhanda, J., Paleri, V. and Mehanna, H. 2016. Efficacy, outcomes, and complication rates of different surgical and nonsurgical treatment modalities for recurrent/residual oropharyngeal carcinoma: A systematic review and meta-analysis. *Head and Neck* 38(12), pp. 1855–1861. Available at: <https://pubmed.ncbi.nlm.nih.gov/27405247/> [Accessed: 12 February 2022].

Jayasingam, S.D., Citartan, M., Thang, T.H., Mat Zin, A.A., Ang, K.C. and Ch'ng, E.S. 2020. Evaluating the Polarization of Tumor-Associated Macrophages Into M1 and M2 Phenotypes in Human Cancer Tissue: Technicalities and Challenges in Routine Clinical Practice. *Frontiers in Oncology* 9, p. 1512. doi: 10.3389/fonc.2019.01512.

Jiang, C., Yuan, F., Wang, J. and Wu, L. 2017. Oral squamous cell carcinoma suppressed antitumor immunity through induction of PD-L1 expression on tumor-associated macrophages. *Immunobiology* 222(4), pp. 651–657. doi: 10.1016/j.imbio.2016.12.002.

Jiang, H., Zhang, T., Yan, M.X. and Wu, W. 2019. IL-35 inhibits CD8+ T cells activity by suppressing expression of costimulatory molecule CD28 and Th1 cytokine production. *Translational Cancer Research* 8(4), pp. 1319–1325. Available at: [/pmc/articles/PMC8797787/](https://pubmed.ncbi.nlm.nih.gov/pmc/articles/PMC8797787/) [Accessed: 30 March 2022].

Jiang, Q.Y., Ma, L., Li, R.C. and Sun, J.H. 2018. Colon cancer-induced interleukin-35 inhibits beta-catenin mediated pro-oncogenic activity. *Oncotarget* 9(15), pp. 11989–11998. Available at: <https://www.oncotarget.com/lookup/doi/10.18632/oncotarget.22857> [Accessed: 30 July 2020].

Jiang, Y., Wang, J., Li, H. and Xia, L. 2020. IL-35 promotes microglial M2 polarization in a rat model of diabetic neuropathic pain. *Archives of Biochemistry and Biophysics* 685. Available at: <https://pubmed.ncbi.nlm.nih.gov/32156533/> [Accessed: 7 December 2021].

Jimenez-Duran, G. et al. 2020. Pharmacological validation of targets regulating CD14 during macrophage differentiation. *EBioMedicine* 61, p. 103039. Available at: <https://doi.org/10.1016/j.ebiom.2020.103039> [Accessed: 4 February 2022].

Jin, L., Xu, X., Ye, B., Pan, M., Shi, Z. and Hu, Y. 2015. Elevated serum Interleukin-35 levels correlate with poor prognosis in patients with clear cell renal cell carcinoma. *International Journal of Clinical and Experimental Medicine* 8(10), pp. 18861–18866. Available at: www.ijcem.com/ [Accessed: 29 July 2020].

Jin, P., Ren, H., Sun, W., Xin, W., Zhang, H. and Hao, J. 2014. Circulating IL-35 in pancreatic ductal adenocarcinoma patients. *Human Immunology* 75(1), pp. 29–33. Available at: <http://www.ncbi.nlm.nih.gov/pubmed/24121041> [Accessed: 6 May 2019].

Johnson, D.E., Burtneess, B., Leemans, C.R., Lui, V.W.Y., Bauman, J.E. and Grandis, J.R. 2020. Head and neck squamous cell carcinoma. *Nature Reviews Disease Primers* 6(1), pp. 1–22. Available at: <https://www.nature.com/articles/s41572-020-00224-3> [Accessed: 31 August 2022].

Jones, L.L., Chaturvedi, V., Uyttenhove, C., Van Snick, J. and Vignali, D.A.A. 2012. Distinct subunit pairing criteria within the heterodimeric IL-12 cytokine family. *Molecular Immunology* 51(2), pp. 234–244. Available at: [/pmc/articles/PMC3341524/](http://pmc/articles/PMC3341524/) [Accessed: 22 June 2022].

Jones, L.L. and Vignali, D.A.A. 2011. Molecular interactions within the IL-6/IL-12 cytokine/receptor superfamily. *Immunologic Research* 51(1), pp. 5–14. doi: 10.1007/s12026-011-8209-y.

Jorgovanovic, D., Song, M., Wang, L. and Zhang, Y. 2020. Roles of IFN- γ in tumor progression and regression: A review. *Biomarker Research* 8(1), pp. 1–16. Available at: <https://biomarkerres-biomedcentral.com.abc.cardiff.ac.uk/articles/10.1186/s40364-020-00228-x> [Accessed: 21 June 2022].

Joshi, S. et al. 2014. Rac2 controls tumor growth, metastasis and M1-M2 macrophage differentiation in vivo. Chrzanosowska-Wodnicka, M. ed. *PLoS ONE* 9(4), p. e95893. Available at: <https://dx.plos.org/10.1371/journal.pone.0095893> [Accessed: 3 August 2020].

Kakoschky, B. et al. 2018. Selective targeting of tumor associated macrophages in different tumor models. *PLoS ONE* 13(2). Available at: <https://pubmed-ncbi.nlm.nih-gov.abc.cardiff.ac.uk/29447241/> [Accessed: 17 March 2022].

Kalogirou, E.M., Tosios, K.I. and Christopoulos, P.F. 2021. The Role of Macrophages in Oral Squamous Cell Carcinoma. *Frontiers in Oncology* 11, p. 733. doi: 10.3389/fonc.2021.611115.

Kalos, M. and June, C.H. 2013. Adoptive T Cell Transfer for Cancer Immunotherapy in the Era of Synthetic Biology. *Immunity* 39(1), pp. 49–60. doi: 10.1016/j.immuni.2013.07.002.

Kaneda, M.M. et al. 2016. PI3K γ is a molecular switch that controls immune suppression. *Nature* 539(7629), pp. 437–442. Available at: <https://www-nature-com.abc.cardiff.ac.uk/articles/nature19834> [Accessed: 17 March 2022].

Karabajakian, A., Toussaint, P., Neidhardt, E.M., Paulus, V., Saintigny, P. and Fayette, J. 2017. Chemotherapy for recurrent/metastatic head and neck cancers. *Anti-Cancer Drugs* 28(4), pp. 357–361. Available at: https://journals.lww.com/anti-cancerdrugs/Fulltext/2017/04000/Chemotherapy_for_recurrent_metastatic_head_and.1.aspx [Accessed: 2 September 2022].

Karpathiou, G. et al. 2017. Prognostic impact of immune microenvironment in laryngeal and pharyngeal squamous cell carcinoma: Immune cell subtypes, immuno-suppressive pathways and clinicopathologic characteristics. *Oncotarget* 8(12), pp. 19310–19322. Available at: <https://pubmed.ncbi.nlm.nih.gov/28038471/> [Accessed: 22 February 2022].

Kaufmann, S.H.E. 2008. Immunology's foundation: The 100-year anniversary of the Nobel Prize to Paul Ehrlich and Elie Metchnikoff. *Nature Immunology* 9(7), pp. 705–712. Available at: <http://www.nature.com/natureimmunology> [Accessed: 3 August 2020].

Kim, H.J. and Cantor, H. 2014. CD4 T-cell subsets and tumor immunity: the helpful and the not-so-helpful. *Cancer immunology research* 2(2), pp. 91–98. Available at: <https://pubmed.ncbi.nlm.nih.gov/24778273/> [Accessed: 22 February 2022].

- Kitamura, T., Qian, B.Z. and Pollard, J.W. 2015. Immune cell promotion of metastasis. *Nature Reviews Immunology* 15(2), pp. 73–86. Available at: <https://pubmed.ncbi.nlm.nih.gov/25614318/> [Accessed: 4 August 2020].
- Klichinsky, M. et al. 2020. Human chimeric antigen receptor macrophages for cancer immunotherapy. *Nature Biotechnology* 38(8), pp. 947–953. Available at: <https://www-nature-com.abc.cardiff.ac.uk/articles/s41587-020-0462-y> [Accessed: 15 March 2022].
- Kobayashi, M. et al. 1989. Identification and purification of natural killer cell stimulatory factor (NKSF), a cytokine with multiple biologic effects on human lymphocytes. *Journal of Experimental Medicine* 170(3), pp. 827–845. doi: 10.1084/jem.170.3.827.
- Koebel, C.M. et al. 2007. Adaptive immunity maintains occult cancer in an equilibrium state. *Nature* 450(7171), pp. 903–907. Available at: <https://pubmed.ncbi.nlm.nih.gov/18026089/> [Accessed: 26 July 2020].
- Kohro, T., Tanaka, T., Murakami, T., Wada, Y., Aburatani, H., Hamakubo, T. and Kodama, T. 2004. A Comparison of Differences in the Gene Expression Profiles of Phorbol 12-myristate 13-acetate Differentiated THP-1 Cells and Human Monocyte-derived Macrophage. *Journal of Atherosclerosis and Thrombosis* 11(2), pp. 88–97. Available at: <http://www.med.rcast.u-tokyo.ac.jp/> [Accessed: 19 July 2022].
- Kong, L., Zhou, Y., Bu, H., Lv, T., Shi, Y. and Yang, J. 2016. Deletion of interleukin-6 in monocytes/macrophages suppresses the initiation of hepatocellular carcinoma in mice. *Journal of Experimental and Clinical Cancer Research* 35(1). Available at: </pmc/articles/PMC5009700/?report=abstract> [Accessed: 5 August 2020].
- Kubota, K. et al. 2017. CD163+CD204+ tumor-associated macrophages contribute to T cell regulation via interleukin-10 and PD-L1 production in oral squamous cell carcinoma. *Scientific Reports* 7(1), pp. 1–12. Available at: <https://www-nature-com/articles/s41598-017-01661-z> [Accessed: 7 December 2021].
- Kulkarni, A. et al. 2018. A designer self-assembled supramolecule amplifies macrophage immune responses against aggressive cancer. *Nature Biomedical Engineering* 2(8), pp. 589–599. Available at: <https://www-nature-com.abc.cardiff.ac.uk/articles/s41551-018-0254-6> [Accessed: 17 March 2022].
- Kumar, A.T. et al. 2019. Prognostic Significance of Tumor-Associated Macrophage Content in Head and Neck Squamous Cell Carcinoma: A Meta-Analysis. *Frontiers in Oncology* 9, p. 656. Available at: </pmc/articles/PMC6663973/?report=abstract> [Accessed: 26 July 2020].
- Kurahara, H. et al. 2011. Significance of M2-polarized tumor-associated macrophage in pancreatic cancer. *Journal of Surgical Research* 167(2), pp. e211–e219. doi: 10.1016/j.jss.2009.05.026.
- Laha, D., Grant, R., Mishra, P. and Nilubol, N. 2021. The Role of Tumor Necrosis Factor in Manipulating the Immunological Response of Tumor Microenvironment. *Frontiers in Immunology* 12, p. 1415. doi: 10.3389/fimmu.2021.656908.
- Larkins, E. et al. 2017. FDA Approval Summary: Pembrolizumab for the Treatment of Recurrent or Metastatic Head and Neck Squamous Cell Carcinoma with Disease Progression on or After Platinum-Containing Chemotherapy. *The Oncologist* 22(7), pp. 873–878. Available at: <https://academic-oup-com.abc.cardiff.ac.uk/oncolo/article/22/7/873/6444392> [Accessed: 21 June 2022].
- Larousserie, F., Kebe, D., Huynh, T., Audebourg, A., Tamburini, J., Terris, B. and Devergne, O. 2019. Evidence for IL-35 expression in diffuse large B-cell lymphoma and impact on the patient's prognosis. *Frontiers in Oncology* 9(JUN), p. 563. doi: 10.3389/fonc.2019.00563.
- Lawrence, M.S. et al. 2013. Mutational heterogeneity in cancer and the search for new cancer-associated genes. *Nature* 499(7457), pp. 214–218. Available at: <https://pubmed.ncbi.nlm.nih.gov/23770567/> [Accessed: 31 August 2022].
- Leblond, M.M. et al. 2017. M2 macrophages are more resistant than M1 macrophages following radiation therapy in the context of glioblastoma. *Oncotarget* 8(42), pp. 72597–72612. Available at: </pmc/articles/PMC5641155/?report=abstract> [Accessed: 5 August 2020].
- Lee, C.C. et al. 2018a. Macrophage-secreted interleukin-35 regulates cancer cell plasticity to facilitate metastatic colonization. *Nature Communications* 9(1), pp. 1–18. Available at: www-nature-com/naturecommunications [Accessed: 29 July 2020].
- Lee, N.C.J., Kelly, J.R., Park, H.S., An, Y., Judson, B.L., Burtness, B.A. and Husain, Z.A. 2018b. Patterns of failure in high-metastatic node number human papillomavirus-positive oropharyngeal carcinoma. *Oral Oncology* 85, pp. 35–39. doi: 10.1016/j.oraloncology.2018.08.001.

- Lee, S.Y. et al. 2022. A novel cytokine consisting of the p40 and EB13 subunits suppresses experimental autoimmune arthritis via reciprocal regulation of Th17 and Treg cells. *Cellular and Molecular Immunology* 19(1), pp. 79–91. Available at: <https://pubmed.ncbi.nlm.nih.gov/34782759/> [Accessed: 20 July 2022].
- Lewin, F., Norell, S.E., Johansson, H., Gustavsson, P., Wennerberg, J., Biörklund, A. and Rutqvist, L.E. 1998. Smoking tobacco, oral snuff, and alcohol in the etiology of squamous cell carcinoma of the head and neck: A population-based case-referent study in Sweden. *Cancer* 82(7), pp. 1367–1375. Available at: <https://pubmed.ncbi.nlm.nih.gov/9529030/> [Accessed: 7 August 2020].
- Li, B., Ren, M., Zhou, X., Han, Q. and Cheng, L. 2020. Targeting tumor-associated macrophages in head and neck squamous cell carcinoma. *Oral Oncology* 106, p. 104723. doi: 10.1016/j.oraloncology.2020.104723.
- Li, J. et al. 2019a. Prognostic impact of tumor-associated macrophage infiltration in esophageal cancer: A meta-analysis. *Future Oncology* 15(19), pp. 2303–2317. Available at: <https://pubmed.ncbi.nlm.nih.gov/31237146/> [Accessed: 4 August 2020].
- Li, N. et al. 2015. PTEN inhibits macrophage polarization from M1 to M2 through CCL2 and VEGF-A reduction and NHERF-1 synergism. *Cancer Biology and Therapy* 16(2), pp. 297–306. Available at: </pmc/articles/PMC4622010/> [Accessed: 9 December 2021].
- Li, W. et al. 2017. C-Terminal Modification and Multimerization Increase the Efficacy of a Proline-Rich Antimicrobial Peptide. *Chemistry - A European Journal* 23(2), pp. 390–396. Available at: <https://pubmed.ncbi.nlm.nih.gov/27862429/> [Accessed: 14 February 2022].
- Li, Y. et al. 2016. Interleukin-35 (IL-35) inhibits proliferation and promotes apoptosis of fibroblast-like synoviocytes isolated from mice with collagen-induced arthritis. *Molecular Biology Reports* 43(9), pp. 947–956. doi: 10.1007/s11033-016-4034-7.
- Li, Y. et al. 2019b. TMEM203 is a binding partner and regulator of STING-mediated inflammatory signaling in macrophages. *Proceedings of the National Academy of Sciences of the United States of America* 116(33), pp. 16479–16488. Available at: www.pnas.org/cgi/doi/10.1073/pnas.1901090116 [Accessed: 17 March 2022].
- Liang, Y.J., Liu, H.C., Su, Y.X., Zhang, T.H., Chu, M., Liang, L.Z. and Liao, G.Q. 2011. Foxp3 expressed by tongue squamous cell carcinoma cells correlates with clinicopathologic features and overall survival in tongue squamous cell carcinoma patients. *Oral Oncology* 47(7), pp. 566–570. Available at: <https://pubmed.ncbi.nlm.nih.gov/21641272/> [Accessed: 22 February 2022].
- Liguori, M., Solinas, G., Germano, G., Mantovani, A. and Allavena, P. 2011. Tumor-associated macrophages as incessant builders and destroyers of the cancer stroma. *Cancers* 3(4), pp. 3740–3761. Available at: <https://pubmed.ncbi.nlm.nih.gov/24213109/> [Accessed: 3 March 2022].
- Lin, D.J., Ng, J.C.K., Huang, L., Robinson, M., O'Hara, J., Wilson, J.A. and Mellor, A.L. 2021. The immunotherapeutic role of indoleamine 2,3-dioxygenase in head and neck squamous cell carcinoma: A systematic review. *Clinical Otolaryngology* 46(5), pp. 919–934. Available at: <https://pubmed.ncbi.nlm.nih.gov/34053179/> [Accessed: 29 August 2022].
- Lin, E.Y. and Pollard, J.W. 2007. Tumor-associated macrophages press the angiogenic switch in breast cancer. *Cancer Research* 67(11), pp. 5064–5066. Available at: <https://pubmed.ncbi.nlm.nih.gov/17545580/> [Accessed: 4 August 2020].
- Lin, Y., Xu, J. and Lan, H. 2019. Tumor-associated macrophages in tumor metastasis: Biological roles and clinical therapeutic applications. *Journal of Hematology and Oncology* 12(1), pp. 1–16. Available at: <https://doi.org/10.1186/s13045-019-0760-3> [Accessed: 4 August 2020].
- Linsley, P.S., Brady, W., Grosmaire, L., Aruffo, A., Damle, N.K. and Ledbetter, J.A. 1991. Binding of the B cell activation antigen B7 to CD28 costimulates T cell proliferation and interleukin 2 mRNA accumulation. *Journal of Experimental Medicine* 173(3), pp. 721–730. Available at: </pmc/articles/PMC2118836/?report=abstract> [Accessed: 7 August 2020].
- Liu, K., Huang, A., Nie, J., Tan, J., Xing, S., Qu, Y. and Jiang, K. 2021a. IL-35 Regulates the Function of Immune Cells in Tumor Microenvironment. *Frontiers in Immunology* 12. Available at: </pmc/articles/PMC8176033/> [Accessed: 9 December 2021].
- Liu, M., Wang, X., Wang, L., Ma, X., Gong, Z., Zhang, S. and Li, Y. 2018a. Targeting the IDO1 pathway in cancer: From bench to bedside. *Journal of Hematology and Oncology* 11(1), pp. 1–12. Available at: <https://jhoonline.biomedcentral.com/articles/10.1186/s13045-018-0644-y> [Accessed: 12 February 2022].

- Liu, M.X., Liu, Q.Y., Liu, Y., Cheng, Z.M., Liu, L., Zhang, L. and Sun, D.H. 2019a. Interleukin-35 suppresses antitumor activity of circulating CD8+ T cells in osteosarcoma patients. *Connective Tissue Research* 60(4), pp. 367–375. Available at: <https://pubmed.ncbi.nlm.nih.gov/30616389/> [Accessed: 30 March 2022].
- Liu, X. et al. 2018b. Administration of interleukin-35-conditioned autologous tolerogenic dendritic cells prolong allograft survival after heart transplantation. *Cellular Physiology and Biochemistry* 49(3), pp. 1221–1237. Available at: <https://www.karger.com/Article/FullText/493298> [Accessed: 5 April 2022].
- Liu, X. et al. 2019b. Interleukin-35 promotes early endothelialization after stent implantation by regulating macrophage activation. *Clinical Science* 133(7), pp. 869–884. Available at: </clinsci/article/133/7/869/218853/Interleukin-35-promotes-early-endothelialization> [Accessed: 29 July 2022].
- Liu, X., Ren, H., Guo, H., Wang, W. and Zhao, N. 2021b. Interleukin-35 has a tumor-promoting role in hepatocellular carcinoma. *Clinical and Experimental Immunology* 203(2), pp. 219–229. Available at: <https://academic.oup.com/cei/article/203/2/219/6403094> [Accessed: 30 March 2022].
- Liu, Z., Liang, Y., Ang, E.L. and Zhao, H. 2017. A New Era of Genome Integration - Simply Cut and Paste! *ACS Synthetic Biology* 6(4), pp. 601–609. Available at: <https://pubs-acscardiff.ac.uk/doi/full/10.1021/acssynbio.6b00331> [Accessed: 31 January 2023].
- Ljunggren, H.G. and Kärre, K. 1990. In search of the “missing self”: MHC molecules and NK cell recognition. *Immunology Today* 11(C), pp. 237–244. Available at: <http://www.ncbi.nlm.nih.gov/pubmed/2201309> [Accessed: 6 May 2019].
- Loberg, R.D. et al. 2007. Targeting CCL2 with systemic delivery of neutralizing antibodies induces prostate cancer tumor regression in vivo. *Cancer Research* 67(19), pp. 9417–9424. Available at: <https://aacrjournals-org.abc.cardiff.ac.uk/cancerres/article/67/19/9417/533845/Targeting-CCL2-with-Systemic-Delivery-of> [Accessed: 5 March 2022].
- Long, J. et al. 2016. IL-35 expression in hepatocellular carcinoma cells is associated with tumor progression. *Oncotarget* 7(29), pp. 45678–45686. Available at: </pmc/articles/PMC5216752/?report=abstract> [Accessed: 30 July 2020].
- Long, J., Zhang, X., Wen, M., Kong, Q., Lv, Z., An, Y. and Wei, X.Q. 2013. IL-35 over-expression increases apoptosis sensitivity and suppresses cell growth in human cancer cells. *Biochemical and Biophysical Research Communications* 430(1), pp. 364–369. doi: 10.1016/j.bbrc.2012.11.004.
- López-Albaitero, A. et al. 2006. Role of Antigen-Processing Machinery in the In Vitro Resistance of Squamous Cell Carcinoma of the Head and Neck Cells to Recognition by CTL. *The Journal of Immunology* 176(6), pp. 3402–3409. Available at: <http://www.ncbi.nlm.nih.gov/pubmed/16517708> [Accessed: 6 May 2019].
- Luo, Y. et al. 2006. Targeting tumor-associated macrophages as a novel strategy against breast cancer. *Journal of Clinical Investigation* 116(8), pp. 2132–2141. Available at: <http://www.jci.org> [Accessed: 17 March 2022].
- Luo, Z., Soläng, C., Larsson, R. and Singh, K. 2022. Interleukin-35 Prevents the Elevation of the M1/M2 Ratio of Macrophages in Experimental Type 1 Diabetes. *International Journal of Molecular Sciences* 23(14), p. 7970. Available at: </pmc/articles/PMC9320761/> [Accessed: 29 July 2022].
- Lyford-Pike, S. et al. 2013. Evidence for a role of the PD-1:PD-L1 pathway in immune resistance of HPV-associated head and neck squamous cell carcinoma. *Cancer Research* 73(6), pp. 1733–1741. doi: 10.1158/0008-5472.CAN-12-2384.
- Ma, X. et al. 2017. LncRNAs as an intermediate in HPV16 promoting myeloid-derived suppressor cell recruitment of head and neck squamous cell carcinoma. *Oncotarget* 8(26), pp. 42061–42075. Available at: </pmc/articles/PMC5522049/> [Accessed: 22 February 2022].
- Ma, Y. et al. 2016. Elevated level of Interleukin-35 in colorectal cancer induces conversion of T cells into iTreg35 by activating STAT1/STAT3. *Oncotarget* 7(45), pp. 73003–73015. Available at: <http://www.ncbi.nlm.nih.gov/pubmed/27682874> [Accessed: 6 May 2019].
- Maaser, C., Egan, L.J., Birkenbach, M.P., Eckmann, L. and Kagnoff, M.F. 2004. Expression of Epstein-Barr virus-induced gene 3 and other interleukin-12-related molecules by human intestinal epithelium. *Immunology* 112(3), pp. 437–445. Available at: <https://pubmed.ncbi.nlm.nih.gov/15196212/> [Accessed: 2 August 2020].
- Maeda, A., Digifico, E., Andon, F.T., Mantovani, A. and Allavena, P. 2019. Poly(I:C) stimulation is superior than Imiquimod to induce the antitumoral functional profile of tumor-conditioned macrophages. *European Journal of Immunology* 49(5), pp. 801–811. Available at: <https://onlinelibrary-wiley-com.abc.cardiff.ac.uk/doi/full/10.1002/eji.201847888> [Accessed: 17 March 2022].

- Maleckar, J.R. and Sherman, L.A. 1987. The composition of the T cell receptor repertoire in nude mice. *Journal of immunology* (Baltimore, Md. : 1950) 138(11), pp. 3873–6. Available at: <http://www.ncbi.nlm.nih.gov/pubmed/2953792> [Accessed: 24 July 2020].
- Malphettes, L. et al. 2010. Highly efficient deletion of FUT8 in CHO cell lines using zinc-finger nucleases yields cells that produce completely nonfucosylated antibodies. *Biotechnology and Bioengineering* 106(5), pp. 774–783. Available at: <https://onlinelibrary-wiley-com.abc.cardiff.ac.uk/doi/full/10.1002/bit.22751> [Accessed: 31 January 2023].
- Mandal, R. et al. 2016. The head and neck cancer immune landscape and its immunotherapeutic implications. *JCI Insight* 1(17). Available at: </pmc/articles/PMC5070962/> [Accessed: 9 September 2021].
- Mantovani, A., Marchesi, F., Malesci, A., Laghi, L. and Allavena, P. 2017. Tumour-associated macrophages as treatment targets in oncology. *Nature Reviews Clinical Oncology* 14(7), pp. 399–416. Available at: <https://pubmed.ncbi.nlm.nih.gov/28117416/> [Accessed: 17 March 2022].
- Marcus, B. et al. 2004. Prognostic factors in oral cavity and oropharyngeal squamous cell carcinoma: The impact of tumor-associated macrophages. *Cancer* 101(12), pp. 2779–2787. Available at: <http://doi.wiley.com/10.1002/cncr.20701> [Accessed: 6 May 2019].
- Martinez, F.O. and Gordon, S. 2014. The M1 and M2 paradigm of macrophage activation: Time for reassessment. *F1000Prime Reports* 6. Available at: <https://pubmed.ncbi.nlm.nih.gov/24669294/> [Accessed: 3 August 2020].
- Martinez, F.O., Sica, A., Mantovani, A. and Locati, M. 2008. Macrophage activation and polarization. *Frontiers in Bioscience* 13(2), pp. 453–461. Available at: <https://pubmed.ncbi.nlm.nih.gov/17981560/> [Accessed: 3 August 2020].
- Massarelli, E. et al. 2019. Combining Immune Checkpoint Blockade and Tumor-Specific Vaccine for Patients with Incurable Human Papillomavirus 16-Related Cancer: A Phase 2 Clinical Trial. *JAMA Oncology* 5(1), pp. 67–73. Available at: <https://jamanetwork-com.abc.cardiff.ac.uk/journals/jamaoncology/fullarticle/2703886> [Accessed: 12 February 2022].
- von Mässenhausen, A. et al. 2016. MERTK as a novel therapeutic target in head and neck cancer. *Oncotarget* 7(22), p. 32678. Available at: </pmc/articles/PMC5078043/> [Accessed: 27 July 2022].
- von Mässenhausen, A. et al. 2017. Implication of the Receptor Tyrosine Kinase AXL in Head and Neck Cancer Progression. *International Journal of Molecular Sciences* 18(1). Available at: </pmc/articles/PMC5297642/> [Accessed: 27 July 2022].
- Masucci, M.T., Minopoli, M. and Carriero, M.V. 2019. Tumor Associated Neutrophils. Their Role in Tumorigenesis, Metastasis, Prognosis and Therapy. *Frontiers in Oncology* 9. Available at: <https://pubmed-ncbi-nlm-nih-gov.abc.cardiff.ac.uk/31799175/> [Accessed: 19 February 2022].
- Mattox, A.K. et al. 2017. PD-1 Expression in Head and Neck Squamous Cell Carcinomas Derives Primarily from Functionally Anergic CD4 + TILs in the Presence of PD-L1 + TAMs. *Cancer research* 77(22), pp. 6365–6374. Available at: <https://pubmed.ncbi.nlm.nih.gov/28947422/> [Accessed: 1 August 2022].
- Matzke, M.A., Mette, M.F. and Matzke, A.J.M. 2000. Transgene silencing by the host genome defense: implications for the evolution of epigenetic control mechanisms in plants and vertebrates. *Plant molecular biology* 43(2–3), pp. 401–415. Available at: <https://pubmed.ncbi.nlm.nih.gov/10999419/> [Accessed: 25 June 2022].
- Mazul, A.L. et al. 2017. Oral health and human papillomavirus-associated head and neck squamous cell carcinoma. *Cancer* 123(1), pp. 71–80. Available at: </pmc/articles/PMC5161679/?report=abstract> [Accessed: 9 August 2020].
- Mazzieri, R. et al. 2011. Targeting the ANG2/TIE2 Axis Inhibits Tumor Growth and Metastasis by Impairing Angiogenesis and Disabling Rebounds of Proangiogenic Myeloid Cells. *Cancer Cell* 19(4), pp. 512–526. Available at: <https://pubmed.ncbi.nlm.nih.gov/21481792/> [Accessed: 4 August 2020].
- Mbongue, J.C., Nicholas, D.A., Torrez, T.W., Kim, N.S., Firek, A.F. and Langridge, W.H.R. 2015. The role of indoleamine 2, 3-dioxygenase in immune suppression and autoimmunity. *Vaccines* 3(3), pp. 703–729. doi: 10.3390/vaccines3030703.
- McBride, S. et al. 2021. Randomized phase II trial of nivolumab with stereotactic body radiotherapy versus nivolumab alone in metastatic head and neck squamous cell carcinoma. *Journal of Clinical Oncology* 39(1), pp. 30–37. doi: 10.1200/JCO.20.00290.

- McLenachan, S., Sarsero, J.P. and Ioannou, P.A. 2007. Flow-cytometric analysis of mouse embryonic stem cell lipofection using small and large DNA constructs. *Genomics* 89(6), pp. 708–720. Available at: <http://www.ncbi.nlm.nih.gov/pubmed/17449222> [Accessed: 30 April 2019].
- Mei, Z., Huang, J., Qiao, B. and Lam, A.K. yin 2020. Immune checkpoint pathways in immunotherapy for head and neck squamous cell carcinoma. *International Journal of Oral Science* 12(1), pp. 1–9. Available at: <https://www.nature.com/articles/s41368-020-0084-8> [Accessed: 31 August 2022].
- Mellor, A.L., Keskin, D.B., Johnson, T., Chandler, P. and Munn, D.H. 2002. Cells Expressing Indoleamine 2,3-Dioxygenase Inhibit T Cell Responses. *The Journal of Immunology* 168(8), pp. 3771–3776. Available at: <https://pubmed.ncbi.nlm.nih.gov/11937528/> [Accessed: 5 August 2020].
- Meng, Y., Beckett, M.A., Liang, H., Mauceri, H.J., Van Rooijen, N., Cohen, K.S. and Weichselbaum, R.R. 2010. Blockade of tumor necrosis factor α signaling in tumor-associated macrophages as a radiosensitizing strategy. *Cancer Research* 70(4), pp. 1534–1543. Available at: <https://pubmed.ncbi.nlm.nih.gov/20145121/> [Accessed: 5 August 2020].
- Metschnikoff, E. 1878. Über die Verdauungsorgane einiger Süßwasserturbellarien. *Zool. Anz* 1, pp. 387–390.
- Metschnikoff, E. 1884. Untersuchungen über die intracelluläre Verdauung bei wirbellosen Thieren. *Arb. Zool. Inst. Univ. wien. u. Zool. Stat. Triest* 5, p. 141.
- Metschnikoff, E. 1887. Ueber den Kampf der Zellen gegen Erysipel-kokken - Ein Beitrag zur Phagocytenlehre. *Archiv für Pathologische Anatomie und Physiologie und für Klinische Medicin* 107(2), pp. 209–249. Available at: <https://link-springer-com.abc.cardiff.ac.uk/article/10.1007/BF01926053> [Accessed: 3 August 2020].
- Miao, L. et al. 2020. Targeting the STING pathway in tumor-associated macrophages regulates innate immune sensing of gastric cancer cells. *Theranostics* 10(2), pp. 498–515. doi: 10.7150/THNO.37745.
- Mills, C.D., Kincaid, K., Alt, J.M., Heilman, M.J. and Hill, A.M. 2000. M-1/M-2 Macrophages and the Th1/Th2 Paradigm. *The Journal of Immunology* 164(12), pp. 6166–6173. Available at: <https://pubmed.ncbi.nlm.nih.gov/10843666/> [Accessed: 3 August 2020].
- Minami, K. et al. 2018. Prognostic significance of CD68, CD163 and Folate receptor- β positive macrophages in hepatocellular carcinoma. *Experimental and Therapeutic Medicine* 15(5), pp. 4465–4476. Available at: </pmc/articles/PMC5920942/> [Accessed: 9 December 2021].
- Mirlekar, B. and Pylayeva-Gupta, Y. 2021. IL-12 family cytokines in cancer and immunotherapy. *Cancers* 13(2), pp. 1–23. Available at: <https://pubmed.ncbi.nlm.nih.gov/33418929/> [Accessed: 21 June 2022].
- Mitchell, T.C. et al. 2018. Epacadostat plus pembrolizumab in patients with advanced solid tumors: Phase I results from a multicenter, open-label phase I/II trial (ECHO-202/KEYNOTE-037). *Journal of Clinical Oncology* 36(32), pp. 3223–3230. doi: 10.1200/JCO.2018.78.9602.
- Mitchem, J.B. et al. 2013. Targeting tumor-infiltrating macrophages decreases tumor-initiating cells, relieves immunosuppression, and improves chemotherapeutic responses. *Cancer Research* 73(3), pp. 1128–1141. Available at: <https://pubmed.ncbi.nlm.nih.gov/23221383/> [Accessed: 5 March 2022].
- Mittal, D., Gubin, M.M., Schreiber, R.D. and Smyth, M.J. 2014. New insights into cancer immunoediting and its three component phases—elimination, equilibrium and escape. *Current Opinion in Immunology* 27(1), pp. 16–25. doi: 10.1016/j.coi.2014.01.004.
- Miyasato, Y. et al. 2017. High density of CD204-positive macrophages predicts worse clinical prognosis in patients with breast cancer. *Cancer Science* 108(8), pp. 1693–1700. Available at: <https://pubmed.ncbi.nlm.nih.gov/28574667/> [Accessed: 6 January 2022].
- Morandi, F. and Pistoia, V. 2014. Interactions between HLA-G and HLA-E in physiological and pathological conditions. *Frontiers in Immunology* 5(AUG). Available at: </pmc/articles/PMC4141331/?report=abstract> [Accessed: 5 August 2020].
- Mori, K., Hiroi, M., Shimada, J. and Ohmori, Y. 2011. Infiltration of M2 tumor-associated macrophages in oral squamous cell carcinoma correlates with tumor malignancy. *Cancers* 3(4), pp. 3726–3739. Available at: </pmc/articles/PMC3763393/> [Accessed: 9 December 2021].
- Morrison, C. 2016. Immuno-oncologists eye up macrophage targets. *Nature Reviews Drug Discovery* 15(6), pp. 373–374. Available at: <https://pubmed.ncbi.nlm.nih.gov/27245386/> [Accessed: 4 August 2020].
- Mosser, D.M. 2003. The many faces of macrophage activation. *Journal of Leukocyte Biology* 73(2), pp. 209–212. Available at: <https://pubmed.ncbi.nlm.nih.gov/12554797/> [Accessed: 3 August 2020].

- Mosser, D.M. and Zhang, X. 2008. Interleukin-10: New perspectives on an old cytokine. *Immunological Reviews* 226(1), pp. 205–218. Available at: [/pmc/articles/PMC2724982/](#) [Accessed: 6 January 2022].
- Muntjewerff, E.M., Meesters, L.D. and van den Bogaart, G. 2020. Antigen Cross-Presentation by Macrophages. *Frontiers in Immunology* 11, p. 1276. Available at: <https://www.frontiersin.org/article/10.3389/fimmu.2020.01276/full> [Accessed: 6 August 2020].
- Murata, Y., Kotani, T., Ohnishi, H. and Matozaki, T. 2014. The CD47-SIRP α signalling system: Its physiological roles and therapeutic application. *Journal of Biochemistry* 155(6), pp. 335–344. Available at: <https://pubmed.ncbi.nlm.nih.gov/24627525/> [Accessed: 17 March 2022].
- Murphy, F.J., Hayes, M.P. and Burd, P.R. 2000. Disparate Intracellular Processing of Human IL-12 Preprotein Subunits: Atypical Processing of the P35 Signal Peptide. *The Journal of Immunology* 164(2), pp. 839–847. Available at: <https://www.jimmunol-org.abc.cardiff.ac.uk/content/164/2/839> [Accessed: 15 September 2021].
- Nakano, S., Morimoto, S., Suzuki, S., Tsushima, H., Yamanaka, K., Sekigawa, I. and Takasaki, Y. 2015. Immunoregulatory role of IL-35 in T cells of patients with rheumatoid arthritis. *Rheumatology (United Kingdom)* 54(8), pp. 1498–1506. Available at: <https://academic.oup.com/rheumatology/article/54/8/1498/1798723> [Accessed: 30 September 2021].
- Nathan, C.F., Murray, H.W., Wlebe, I.E. and Rubin, B.Y. 1983. Identification of interferon- γ , as the lymphokine that activates human macrophage oxidative metabolism and antimicrobial activity. *Journal of Experimental Medicine* 158(3), pp. 670–689. Available at: [/pmc/articles/PMC2187114/?report=abstract](#) [Accessed: 3 August 2020].
- Nayak-Kapoor, A. et al. 2018. Phase Ia study of the indoleamine 2,3-dioxygenase 1 (IDO1) inhibitor navoximod (GDC-0919) in patients with recurrent advanced solid tumors. *Journal for ImmunoTherapy of Cancer* 6(1), p. 61. Available at: <https://jitc-bmj-com.abc.cardiff.ac.uk/content/6/1/61> [Accessed: 12 February 2022].
- Ngambenjawang, C., Cieslewicz, M., Schellinger, J.G. and Pun, S.H. 2016. Synthesis and evaluation of multivalent M2pep peptides for targeting alternatively activated M2 macrophages. *Journal of Controlled Release* 224, pp. 103–111. Available at: [/pmc/articles/PMC4747818/](#) [Accessed: 17 March 2022].
- Nguyen, N. et al. 2016. Tumor infiltrating lymphocytes and survival in patients with head and neck squamous cell carcinoma. *Head and Neck* 38(7), pp. 1074–1084. Available at: <https://pubmed.ncbi.nlm.nih.gov/26879675/> [Accessed: 3 March 2022].
- Ni, Y.H., Ding, L., Huang, X.F., Dong, Y. chun, Hu, Q.G. and Hou, Y.Y. 2015. Microlocalization of CD68+ tumor-associated macrophages in tumor stroma correlated with poor clinical outcomes in oral squamous cell carcinoma patients. *Tumor Biology* 36(7), pp. 5291–5298. Available at: <https://pubmed.ncbi.nlm.nih.gov/25666753/> [Accessed: 3 March 2022].
- Nicholl, M.B. et al. 2014. IL-35 promotes pancreas cancer growth through enhancement of proliferation and inhibition of apoptosis: Evidence for a role as an autocrine growth factor. *Cytokine* 70(2), pp. 126–133. Available at: <https://pubmed.ncbi.nlm.nih.gov/25073578/> [Accessed: 29 July 2020].
- Niedbala, W., Wei, X.Q., Cai, B., Hueber, A.J., Leung, B.P., McInnes, I.B. and Liew, F.Y. 2007. IL-35 is a novel cytokine with therapeutic effects against collagen-induced arthritis through the expansion of regulatory T cells and suppression of Th17 cells. *European Journal of Immunology* 37(11), pp. 3021–3029. Available at: <http://www.ncbi.nlm.nih.gov/pubmed/17874423> [Accessed: 30 April 2019].
- Noy, R. and Pollard, J.W. 2014. Tumor-Associated Macrophages: From Mechanisms to Therapy. *Immunity* 41(1), pp. 49–61. doi: 10.1016/j.immuni.2014.06.010.
- Obreque, J. et al. 2017. Autologous tolerogenic dendritic cells derived from monocytes of systemic lupus erythematosus patients and healthy donors show a stable and immunosuppressive phenotype. *Immunology* 152(4), pp. 648–659. Available at: <https://pubmed.ncbi.nlm.nih.gov/28763099/> [Accessed: 5 August 2020].
- Oguejiofor, K., Galletta-Williams, H., Dovedi, S.J., Roberts, D.L., Stern, P.L. and West, C.M.L. 2017. Distinct patterns of infiltrating CD8+ T cells in HPV+ and CD68 macrophages in HPV- oropharyngeal squamous cell carcinomas are associated with better clinical outcome but PD-L1 expression is not prognostic. *Oncotarget* 8(9), pp. 14416–14427. Available at: <https://www.oncotarget.com/article/14796/text/> [Accessed: 19 April 2022].
- Ohtaki, Y. et al. 2010. Stromal macrophage expressing CD204 is associated with tumor aggressiveness in lung adenocarcinoma. *Journal of Thoracic Oncology* 5(10), pp. 1507–1515. Available at: <https://pubmed-ncbi-nlm-nih-gov.abc.cardiff.ac.uk/20802348/> [Accessed: 6 January 2022].
- Okazaki, T. and Honjo, T. 2007. PD-1 and PD-1 ligands: From discovery to clinical application. *International Immunology* 19(7), pp. 813–824. doi: 10.1093/intimm/dxm057.

- Okubo, M. et al. 2016. M2-polarized macrophages contribute to neovascuogenesis, leading to relapse of oral cancer following radiation. *Scientific Reports* 6(1), pp. 1–12. Available at: <https://www.nature.com/articles/srep27548> [Accessed: 9 December 2021].
- Old, L.J. and Boyse, E.A. 1964. Immunology of Experimental Tumors. *Annual review of medicine* 15(1), pp. 167–186. Available at: <http://www.annualreviews.org/doi/10.1146/annurev.me.15.020164.001123> [Accessed: 24 July 2020].
- Oppmann, B. et al. 2000. Novel p19 protein engages IL-12p40 to form a cytokine, IL-23, with biological activities similar as well as distinct from IL-12. *Immunity* 13(5), pp. 715–725. doi: 10.1016/S1074-7613(00)00070-4.
- Orecchioni, M., Ghosheh, Y., Pramod, A.B. and Ley, K. 2019. Macrophage polarization: Different gene signatures in M1(Lps+) vs. Classically and M2(LPS-) vs. Alternatively activated macrophages. *Frontiers in Immunology* 10(MAY), p. 1084. Available at: <http://bioinfogp.cnb.csic.es/tools/venny/index.html> [Accessed: 3 August 2020].
- Ostrand-Rosenberg, S. and Sinha, P. 2009. Myeloid-Derived Suppressor Cells: Linking Inflammation and Cancer. *The Journal of Immunology* 182(8), pp. 4499–4506. Available at: <https://pubmed.ncbi.nlm.nih.gov/19342621/> [Accessed: 22 February 2022].
- De Palma, M., Venneri, M.A., Galli, R., Sergi, L.S., Politi, L.S., Sampaolesi, M. and Naldini, L. 2005. Tie2 identifies a hematopoietic lineage of proangiogenic monocytes required for tumor vessel formation and a mesenchymal population of pericyte progenitors. *Cancer Cell* 8(3), pp. 211–226. Available at: <https://pubmed.ncbi.nlm.nih.gov/16169466/> [Accessed: 4 August 2020].
- Pan, Y., Yu, Y., Wang, X. and Zhang, T. 2020. Tumor-Associated Macrophages in Tumor Immunity. *Frontiers in Immunology* 11, p. 3151. doi: 10.3389/fimmu.2020.583084.
- Parfenov, M. et al. 2014. Characterization of HPV and host genome interactions in primary head and neck cancers. *Proceedings of the National Academy of Sciences of the United States of America* 111(43), pp. 15544–15549. Available at: <https://pubmed.ncbi.nlm.nih.gov/25313082/> [Accessed: 31 August 2022].
- Park, E.K., Jung, H.S., Yang, H.I., Yoo, M.C., Kim, C. and Kim, K.S. 2007. Optimized THP-1 differentiation is required for the detection of responses to weak stimuli. *Inflammation Research* 56(1), pp. 45–50. Available at: <https://link-springer-com.abc.cardiff.ac.uk/article/10.1007/s00011-007-6115-5> [Accessed: 19 July 2022].
- Paulus, P., Stanley, E.R., Schäfer, R., Abraham, D. and Aharinejad, S. 2006. Colony-stimulating factor-1 antibody reverses chemoresistance in human MCF-7 breast cancer xenografts. *Cancer Research* 66(8), pp. 4349–4356. doi: 10.1158/0008-5472.CAN-05-3523.
- Peltanova, B., Raudenska, M. and Masarik, M. 2019. Effect of tumor microenvironment on pathogenesis of the head and neck squamous cell carcinoma: A systematic review. *Molecular Cancer* 18(1), pp. 1–24. Available at: <https://molecular-cancer.biomedcentral.com/articles/10.1186/s12943-019-0983-5> [Accessed: 13 September 2021].
- Peña, C.G. et al. 2015. LKB1 loss promotes endometrial cancer progression via CCL2-dependent macrophage recruitment. *Journal of Clinical Investigation* 125(11), pp. 4063–4076. Available at: <https://pubmed.ncbi.nlm.nih.gov/26413869/> [Accessed: 5 August 2020].
- Peng, M., Qiang, L., Xu, Y., Li, C., Li, T. and Wang, J. 2019. IL-35 ameliorates collagen-induced arthritis by promoting TNF- α -induced apoptosis of synovial fibroblasts and stimulating M2 macrophages polarization. *FEBS Journal* 286(10), pp. 1972–1985. Available at: <https://onlinelibrary.wiley.com/doi/full/10.1111/febs.14801> [Accessed: 7 December 2021].
- Perry, C.J. et al. 2018. Myeloid-targeted immunotherapies act in synergy to induce inflammation and antitumor immunity. *Journal of Experimental Medicine* 215(3), pp. 877–893. Available at: <https://doi.org/10.1084/jem.20171435> [Accessed: 5 August 2020].
- Petruzzi, M.N.M.R., Cherubini, K., Salum, F.G. and de Figueiredo, M.A.Z. 2017. Role of tumour-associated macrophages in oral squamous cells carcinoma progression: An update on current knowledge. *Diagnostic Pathology* 12(1), pp. 1–7. Available at: <https://diagnosticpathology-biomedcentral-com.abc.cardiff.ac.uk/articles/10.1186/s13000-017-0623-6> [Accessed: 23 November 2021].
- Pezzuto, F. et al. 2015. Update on head and neck cancer: Current knowledge on epidemiology, risk factors, molecular features and novel therapies. *Oncology (Switzerland)* 89(3), pp. 125–136. Available at: <https://pubmed.ncbi.nlm.nih.gov/25967534/> [Accessed: 7 August 2020].

- Pflanz, S. et al. 2002. IL-27, a heterodimeric cytokine composed of EB13 and p28 protein, induces proliferation of naive CD4+T cells. *Immunity* 16(6), pp. 779–790. doi: 10.1016/S1074-7613(02)00324-2.
- Pinto, M.L. et al. 2019. The two faces of tumor-associated macrophages and their clinical significance in colorectal cancer. *Frontiers in Immunology* 10(AUG), p. 1875. doi: 10.3389/fimmu.2019.01875.
- Pinto, S.M. et al. 2021. Comparative Proteomic Analysis Reveals Varying Impact on Immune Responses in Phorbol 12-Myristate-13-Acetate-Mediated THP-1 Monocyte-to-Macrophage Differentiation. *Frontiers in Immunology* 12, p. 2241. doi: 10.3389/fimmu.2021.679458.
- Pirilä, E. et al. 2015. Macrophages modulate migration and invasion of human tongue squamous cell carcinoma. *PLoS ONE* 10(3). Available at: <https://pubmed.ncbi.nlm.nih.gov/25811194/> [Accessed: 11 January 2022].
- Platanias, L.C. 2005. Mechanisms of type-I- and type-II-interferon-mediated signalling. *Nature reviews. Immunology* 5(5), pp. 375–386. Available at: <https://pubmed.ncbi.nlm.nih.gov/abc.cardiff.ac.uk/15864272/> [Accessed: 21 June 2022].
- Prendergast, G.C., Malachowski, W.J., Mondal, A., Scherle, P. and Muller, A.J. 2018. Indoleamine 2,3-Dioxygenase and Its Therapeutic Inhibition in Cancer. *International Review of Cell and Molecular Biology* 336, pp. 175–203. doi: 10.1016/bs.ircmb.2017.07.004.
- Pries, R., Thiel, A., Brocks, C. and Wollenberg, B. 2006. Secretion of tumor-promoting and immune suppressive cytokines by cell lines of head and neck squamous cell carcinoma. *In Vivo* 20(1), pp. 45–48.
- Pua, K.H., Chew, C.L., Lane, D.P. and Tergaonkar, V. 2020. Inflammation-associated genomic instability in cancer. *Genome Instability & Disease* 1(1), pp. 1–9. Available at: <https://link-springer-com.abc.cardiff.ac.uk/article/10.1007/s42764-019-00006-6> [Accessed: 21 June 2022].
- Pylayeva-Gupta, Y., Das, S., Handler, J.S., Hajdu, C.H., Coffre, M., Koralov, S.B. and Bar-Sagi, D. 2016. IL35-producing b cells promote the development of pancreatic neoplasia. *Cancer Discovery* 6(3), pp. 247–255. doi: 10.1158/2159-8290.CD-15-0843.
- Qian, B.Z. and Pollard, J.W. 2010. Macrophage Diversity Enhances Tumor Progression and Metastasis. *Cell* 141(1), pp. 39–51. Available at: <https://pubmed.ncbi.nlm.nih.gov/20090554/> [Accessed: 4 August 2020].
- Qiao, X.W., Jiang, J., Pang, X., Huang, M.C., Tang, Y.J., Liang, X.H. and Tang, Y.L. 2020. The Evolving Landscape of PD-1/PD-L1 Pathway in Head and Neck Cancer. *Frontiers in Immunology* 11, p. 1721. doi: 10.3389/fimmu.2020.01721.
- Qin, S., Cobbold, S.P., Pope, H., Elliott, J., Kioussis, D., Davies, J. and Waldmann, H. 1993. “Infectious” transplantation tolerance. *Science* 259(5097), pp. 974–977. Available at: <https://pubmed.ncbi.nlm.nih.gov/8094901/> [Accessed: 5 April 2022].
- Qiu, S.Q., Waaijer, S.J.H., Zwager, M.C., de Vries, E.G.E., van der Vegt, B. and Schröder, C.P. 2018. Tumor-associated macrophages in breast cancer: Innocent bystander or important player? *Cancer Treatment Reviews* 70, pp. 178–189. Available at: <https://pubmed.ncbi.nlm.nih.gov/30227299/> [Accessed: 4 August 2020].
- Ramesh, A., Kumar, S., Nandi, D. and Kulkarni, A. 2019. CSF1R- and SHP2-Inhibitor-Loaded Nanoparticles Enhance Cytotoxic Activity and Phagocytosis in Tumor-Associated Macrophages. *Advanced Materials* 31(51), p. 1904364. Available at: <https://onlinelibrary.wiley.com/doi/full/10.1002/adma.201904364> [Accessed: 17 March 2022].
- Reitberger, S., Haimerl, P., Aschenbrenner, I., Esser-von Bieren, J. and Feige, M.J. 2017. Assembly-induced folding regulates interleukin 12 biogenesis and secretion. *The Journal of biological chemistry* 292(19), pp. 8073–8081. Available at: <https://pubmed.ncbi.nlm.nih.gov/28325840/> [Accessed: 31 July 2022].
- Riabov, V., Gudima, A., Wang, N., Mickley, A., Orekhov, A. and Kzhyshkowska, J. 2014. Role of tumor associated macrophages in tumor angiogenesis and lymphangiogenesis. *Frontiers in Physiology* 5 MAR. Available at: <https://pubmed.ncbi.nlm.nih.gov/24634660/> [Accessed: 7 December 2021].
- Ries, C.H. et al. 2014. Targeting tumor-associated macrophages with anti-CSF-1R antibody reveals a strategy for cancer therapy. *Cancer Cell* 25(6), pp. 846–859. Available at: <https://pubmed.ncbi.nlm.nih.gov/abc.cardiff.ac.uk/24898549/> [Accessed: 5 March 2022].
- Ritprajak, P. and Azuma, M. 2015. Intrinsic and extrinsic control of expression of the immunoregulatory molecule PD-L1 in epithelial cells and squamous cell carcinoma. *Oral Oncology* 51(3), pp. 221–228. doi: 10.1016/J.ORALONCOLOGY.2014.11.014.

- Rivera, C. 2015. Essentials of oral cancer. *International Journal of Clinical and Experimental Pathology* 8(9), pp. 11884–11894. Available at: [/pmc/articles/PMC4637760/](#) [Accessed: 10 February 2022].
- Rock, K.L., Reits, E. and Neefjes, J. 2016. Present Yourself! By MHC Class I and MHC Class II Molecules. *Trends in Immunology* 37(11), pp. 724–737. Available at: [/pmc/articles/PMC5159193/?report=abstract](#) [Accessed: 6 August 2020].
- Rohan, T.E. et al. 2014. Tumor microenvironment of metastasis and risk of distant metastasis of breast cancer. *Journal of the National Cancer Institute* 106(8). doi: 10.1093/jnci/dju136.
- Rosalia, R.A. et al. 2013. Dendritic cells process synthetic long peptides better than whole protein, improving antigen presentation and T-cell activation. *European Journal of Immunology* 43(10), pp. 2554–2565. Available at: <https://pubmed.ncbi.nlm.nih.gov/abc.cardiff.ac.uk/23836147/> [Accessed: 5 September 2022].
- Roszer, T. 2015. Understanding the mysterious M2 macrophage through activation markers and effector mechanisms. *Mediators of Inflammation* 2015. Available at: <http://dx.doi.org/10.1155/2015/816460> [Accessed: 15 July 2020].
- Rousseau, F., Basset, L., Froger, J., Dinguirard, N., Chevalier, S. and Gascan, H. 2010. IL-27 structural analysis demonstrates similarities with ciliary neurotrophic factor (CNTF) and leads to the identification of antagonistic variants. *Proceedings of the National Academy of Sciences of the United States of America* 107(45), pp. 19420–19425. doi: 10.1073/pnas.1005793107.
- Rowshanravan, B., Halliday, N. and Sansom, D.M. 2018. CTLA-4: A moving target in immunotherapy. *Blood* 131(1), pp. 58–67. Available at: <https://ashpublications.org/blood/article/131/1/58/107717/CTLA-4-a-moving-target-in-immunotherapy> [Accessed: 2 September 2022].
- Ruicci, K.M. et al. 2020. TAM family receptors in conjunction with MAPK signalling are involved in acquired resistance to PI3K α inhibition in head and neck squamous cell carcinoma. *Journal of Experimental & Clinical Cancer Research : CR* 39(1). Available at: [/pmc/articles/PMC7559997/](#) [Accessed: 27 July 2022].
- Sankaranarayanan, R., Masuyer, E., Swaminathan, R., Ferlay, J. and Whelan, S. 1998. Head and neck cancer: A global perspective on epidemiology and prognosis. *Anticancer Research* 18(6 B), pp. 4779–4786.
- Sansom, D.M., Manzotti, C.N. and Zheng, Y. 2003. What's the difference between CD80 and CD86? *Trends in Immunology* 24(6), pp. 313–318. Available at: <https://pubmed.ncbi.nlm.nih.gov/12810107/> [Accessed: 7 August 2020].
- Santarpia, M. and Karachaliou, N. 2015. Tumor immune microenvironment characterization and response to anti-PD-1 therapy. *Cancer Biology and Medicine* 12(2), pp. 74–78. Available at: <https://www.ncbi.nlm.nih.gov/pmc/articles/PMC4493379/> [Accessed: 5 August 2020].
- Sathawane, D., Kharat, R.S., Halder, S., Roy, S., Swami, R., Patel, R. and Saha, B. 2013. Monocyte CD40 expression in head and neck squamous cell carcinoma (HNSCC). *Human Immunology* 74(1), pp. 1–5. doi: 10.1016/j.humimm.2012.09.004.
- Saussez, S., Duray, A., Demoulin, S., Hubert, P. and Delvenne, P. 2010. Immune suppression in head and neck cancers: A review. *Clinical and Developmental Immunology* 2010, pp. 1–15. Available at: <http://www.ncbi.nlm.nih.gov/pubmed/21437225> [Accessed: 6 May 2019].
- Sawant, D. V. et al. 2019. Adaptive plasticity of IL-10⁺ and IL-35⁺ Treg cells cooperatively promotes tumor T cell exhaustion. *Nature Immunology* 20(6), pp. 724–735. Available at: <http://www.ncbi.nlm.nih.gov/pubmed/30936494> [Accessed: 6 May 2019].
- Schaer, D.J., Schaer, C.A., Buehler, P.W., Boykins, R.A., Schoedon, G., Alayash, A.I. and Schaffner, A. 2006. CD163 is the macrophage scavenger receptor for native and chemically modified hemoglobins in the absence of haptoglobin. *Blood* 107(1), pp. 373–380. Available at: <http://ashpublications.org/blood/article-pdf/107/1/373/1279907/zh800106000373.pdf> [Accessed: 6 January 2022].
- Schiavoni, G., Mattei, F. and Gabriele, L. 2013. Type I interferons as stimulators of DC-mediated cross-priming: Impact on anti-tumor response. *Frontiers in Immunology* 4(DEC). Available at: [/pmc/articles/PMC3872318/](#) [Accessed: 17 March 2022].
- Schuette, V. et al. 2016. Mannose receptor induces T-cell tolerance via inhibition of CD45 and up-regulation of CTLA-4. *Proceedings of the National Academy of Sciences of the United States of America* 113(38), pp. 10649–10654. Available at: <https://pubmed.ncbi.nlm.nih.gov/abc.cardiff.ac.uk/27601670/> [Accessed: 27 July 2022].
- Schulz, C. et al. 2012. A lineage of myeloid cells independent of myb and hematopoietic stem cells. *Science* 335(6077), pp. 86–90. Available at: <https://pubmed.ncbi.nlm.nih.gov/22442384/> [Accessed: 3 August 2020].

- Schürch, C.M. et al. 2019. Targeting CD47 in Anaplastic Thyroid Carcinoma Enhances Tumor Phagocytosis by Macrophages and Is a Promising Therapeutic Strategy. *Thyroid* 29(7), pp. 979–992. Available at: <https://www.liebertpub-com.abc.cardiff.ac.uk/doi/abs/10.1089/thy.2018.0555> [Accessed: 17 March 2022].
- Seliger, B., Massa, C., Yang, B., Bethmann, D., Kappler, M., Eckert, A.W. and Wickenhauser, C. 2020. Immune escape mechanisms and their clinical relevance in head and neck squamous cell carcinoma. *International Journal of Molecular Sciences* 21(19), pp. 1–17. Available at: [/pmc/articles/PMC7582858/](https://pubmed.ncbi.nlm.nih.gov/30781400/) [Accessed: 15 February 2022].
- Seminario, I. et al. 2018. High infiltration of CD68+ macrophages is associated with poor prognoses of head and neck squamous cell carcinoma patients and is influenced by human papillomavirus. *Oncotarget* 9(13), pp. 11046–11059. Available at: <http://www.ncbi.nlm.nih.gov/pubmed/29541395> [Accessed: 6 May 2019].
- Seminario, I. et al. 2019. Infiltration of FoxP3+ regulatory T cells is a strong and independent prognostic factor in head and neck squamous cell carcinoma. *Cancers* 11(2). Available at: <https://pubmed.ncbi.nlm.nih.gov/30781400/> [Accessed: 22 February 2022].
- Shang, B., Liu, Y., Jiang, S.J. and Liu, Y. 2015. Prognostic value of tumor-infiltrating FoxP3+ regulatory T cells in cancers: A systematic review and meta-analysis. *Scientific Reports* 5(1), pp. 1–9. Available at: <https://www.nature.com/articles/srep15179> [Accessed: 22 February 2022].
- Shankaran, V., Ikeda, H., Bruce, A.T., White, J.M., Swanson, P.E., Old, L.J. and Schreiber, R.D. 2001. IFN γ , and lymphocytes prevent primary tumour development and shape tumour immunogenicity. *Nature* 410(6832), pp. 1107–1111. Available at: www.nature.com [Accessed: 24 July 2020].
- Sharma, P., Hu-Lieskovan, S., Wargo, J.A. and Ribas, A. 2017. Primary, Adaptive, and Acquired Resistance to Cancer Immunotherapy. *Cell* 168(4), pp. 707–723. Available at: <https://pubmed.ncbi.nlm.nih.gov/28187290/> [Accessed: 21 June 2022].
- She, L. et al. 2018. Tumor-associated macrophages derived CCL18 promotes metastasis in squamous cell carcinoma of the head and neck. *Cancer Cell International* 18(1), pp. 1–14. Available at: <https://cancerjournalcentral-com.abc.cardiff.ac.uk/articles/10.1186/s12935-018-0620-1> [Accessed: 7 December 2021].
- Shen, P. et al. 2014. IL-35-producing B cells are critical regulators of immunity during autoimmune and infectious diseases. *Nature* 507(7492), pp. 366–370. doi: 10.1038/nature12979.
- Shibata, H., Zhou, L., Xu, N., Egloff, A.M. and Uppaluri, R. 2021. Personalized cancer vaccination in head and neck cancer. *Cancer Science* 112(3), pp. 978–988. Available at: <https://onlinelibrary-wiley-com.abc.cardiff.ac.uk/doi/full/10.1111/cas.14784> [Accessed: 14 February 2022].
- Shigeoka, M. et al. 2013. Tumor associated macrophage expressing CD204 is associated with tumor aggressiveness of esophageal squamous cell carcinoma. *Cancer Science* 104(8), pp. 1112–1119. Available at: <https://pubmed.ncbi.nlm.nih.gov/23648122/> [Accessed: 6 January 2022].
- Shinkai, Y. et al. 1992. RAG-2-deficient mice lack mature lymphocytes owing to inability to initiate V(D)J rearrangement. doi: 10.1016/0092-8674(92)90029-C.
- Shiraishi, D. et al. 2018. CD163 is required for protumoral activation of macrophages in human and murine sarcoma. *Cancer Research* 78(12), pp. 3255–3266. Available at: <https://aacrjournals-org.abc.cardiff.ac.uk/cancerres/article/78/12/3255/625113/CD163-Is-Required-for-Protumoral-Activation-of> [Accessed: 17 March 2022].
- Shiratori, H. et al. 2017. THP-1 and human peripheral blood mononuclear cell-derived macrophages differ in their capacity to polarize in vitro. *Molecular Immunology* 88, pp. 58–68. doi: 10.1016/j.molimm.2017.05.027.
- Sica, A. and Mantovani, A. 2012. Macrophage plasticity and polarization: In vivo veritas. *Journal of Clinical Investigation* 122(3), pp. 787–795. Available at: <https://pubmed.ncbi.nlm.nih.gov/22378047/> [Accessed: 3 August 2020].
- Siegel, R.L., Miller, K.D. and Jemal, A. 2017. Cancer statistics, 2017. *CA: A Cancer Journal for Clinicians* 67(1), pp. 7–30. Available at: <http://doi.wiley.com/10.3322/caac.21387> [Accessed: 1 May 2019].
- Siegel, R.L., Miller, K.D. and Jemal, A. 2020. Cancer statistics, 2020. *CA: A Cancer Journal for Clinicians* 70(1), pp. 7–30. Available at: <https://pubmed.ncbi.nlm.nih.gov/31912902/> [Accessed: 17 January 2022].
- Sieweke, M.H. and Allen, J.E. 2013. Beyond stem cells: Self-renewal of differentiated macrophages. *Science* 342(6161). Available at: <http://dx.doi.org/10.1126/science.1242974> [Accessed: 3 August 2020].

- Siu, L.L. et al. 2019. Safety and Efficacy of Durvalumab with or Without Tremelimumab in Patients with PD-L1-Low/Negative Recurrent or Metastatic HNSCC: The Phase 2 CONDOR Randomized Clinical Trial. *JAMA Oncology* 5(2), pp. 195–203. Available at: <https://jamanetwork.com.abc.cardiff.ac.uk/journals/jamaoncology/fullarticle/2711892> [Accessed: 12 February 2022].
- Smith, L.K. et al. 2018. Interleukin-10 Directly Inhibits CD8 + T Cell Function by Enhancing N-Glycan Branching to Decrease Antigen Sensitivity. *Immunity* 48(2), pp. 299–312.e5. Available at: <https://pubmed.ncbi.nlm.nih.gov.abc.cardiff.ac.uk/29396160/> [Accessed: 27 July 2022].
- Smith, M., Young, H., Hurlstone, A. and Wellbrock, C. 2015. Differentiation of THP1 Cells into Macrophages for Transwell Co-culture Assay with Melanoma Cells. *Bio-Protocol* 5(21). Available at: </pmc/articles/PMC4811304/> [Accessed: 11 October 2021].
- Snijders, P.J.F., Cromme, F. V., Van Brule, A.J.C.D., Schrijnemakers, H.F.J., Snow, G.B., Meijer, C.J.L.M. and Walboomers, J.M.M. 1992. Prevalence and expression of human papillomavirus in tonsillar carcinomas, indicating a possible viral etiology. *International Journal of Cancer* 51(6), pp. 845–850. Available at: <https://pubmed.ncbi.nlm.nih.gov/1322374/> [Accessed: 9 August 2020].
- Soldano, S. et al. 2016. Alternatively Activated (M2) Macrophage Phenotype Is Inducible by Endothelin-1 in Cultured Human Macrophages. *PLoS ONE* 11(11). Available at: </pmc/articles/PMC5112853/> [Accessed: 1 August 2022].
- Song, Y., Tang, C. and Yin, C. 2018. Combination antitumor immunotherapy with VEGF and PIGF siRNA via systemic delivery of multi-functionalized nanoparticles to tumor-associated macrophages and breast cancer cells. *Biomaterials* 185, pp. 117–132. doi: 10.1016/j.biomaterials.2018.09.017.
- Starr, T., Bauler, T.J., Malik-Kale, P. and Steele-Mortimer, O. 2018. The phorbol 12-myristate-13-acetate differentiation protocol is critical to the interaction of THP-1 macrophages with Salmonella Typhimurium. *PLoS ONE* 13(3). Available at: <https://pubmed.ncbi.nlm.nih.gov/29538403/> [Accessed: 25 November 2021].
- Stein, M., Keshav, S., Harris, N. and Gordon, S. 1992. Interleukin 4 potently enhances murine macrophage mannose receptor activity: A marker of alternative immunologic macrophage activation. *Journal of Experimental Medicine* 176(1), pp. 287–292. Available at: <https://pubmed.ncbi.nlm.nih.gov/1613462/> [Accessed: 3 August 2020].
- Stout, R.D., Jiang, C., Matta, B., Tietzel, I., Watkins, S.K. and Suttles, J. 2005. Macrophages Sequentially Change Their Functional Phenotype in Response to Changes in Microenvironmental Influences. *The Journal of Immunology* 175(1), pp. 342–349. Available at: <https://www.jimmunol.org/content/175/1/342> [Accessed: 1 March 2022].
- Stutman, O. 1974. Tumor development after 3-methylcholanthrene in immunologically deficient athymic-nude mice. *Science* 183(4124), pp. 534–536. Available at: <https://pubmed.ncbi.nlm.nih.gov/4588620/> [Accessed: 24 July 2020].
- Stutman, O. 1979. Chemical carcinogenesis in nude mice: Comparison between nude mice from homozygous matings and heterozygous matings and effect of age and carcinogen dose. Available at: <https://academic.oup.com/jnci/article-abstract/62/2/353/924356> [Accessed: 24 July 2020].
- Suárez-Sánchez, F.J. et al. 2020. Macrophages in Oral Carcinomas: Relationship with Cancer Stem Cell Markers and PD-L1 Expression. *Cancers* 12(7), pp. 1–14. Available at: </pmc/articles/PMC7408350/> [Accessed: 27 July 2022].
- Sullivan, J.A. et al. 2020. Treg-Cell-Derived IL-35-Coated Extracellular Vesicles Promote Infectious Tolerance. *Cell Reports* 30(4), pp. 1039–1051.e5. doi: 10.1016/j.celrep.2019.12.081.
- Sullivan, R.J. et al. 2018. Initial results from first-in-human study of IPI-549, a tumor macrophage-targeting agent, combined with nivolumab in advanced solid tumors. *Journal of Clinical Oncology* 36(15_suppl), pp. 3013–3013. doi: 10.1200/jco.2018.36.15_suppl.3013.
- Sullivan, T.J. et al. 2001. Lack of a role for transforming growth factor- β in cytotoxic T lymphocyte antigen-4-mediated inhibition of T cell activation. *Proceedings of the National Academy of Sciences of the United States of America* 98(5), pp. 2587–2592. Available at: <https://pubmed.ncbi.nlm.nih.gov/11226283/> [Accessed: 2 September 2022].
- Sun, H., Miao, C., Liu, W., Qiao, X., Yang, W., Li, L. and Li, C. 2018. TGF- β 1/T β RII/Smad3 signaling pathway promotes VEGF expression in oral squamous cell carcinoma tumor-associated macrophages. *Biochemical and biophysical research communications* 497(2), pp. 583–590. Available at: <https://pubmed.ncbi.nlm.nih.gov/29462614/> [Accessed: 27 July 2022].

- Sun, Z., Sun, X., Chen, Z., Du, J. and Wu, Y. 2022. Head and Neck Squamous Cell Carcinoma: Risk Factors, Molecular Alterations, Immunology and Peptide Vaccines. *International Journal of Peptide Research and Therapeutics* 28(1), pp. 1–18. Available at: <https://link.springer.com/article/10.1007/s10989-021-10334-5> [Accessed: 6 February 2022].
- Sung, H., Ferlay, J., Siegel, R.L., Laversanne, M., Soerjomataram, I., Jemal, A. and Bray, F. 2021. Global Cancer Statistics 2020: GLOBOCAN Estimates of Incidence and Mortality Worldwide for 36 Cancers in 185 Countries. *CA: A Cancer Journal for Clinicians* 71(3), pp. 209–249. Available at: <https://onlinelibrary.wiley.com/doi/full/10.3322/caac.21660> [Accessed: 17 January 2022].
- Sunshine, J. and Taube, J.M. 2015. PD-1/PD-L1 inhibitors. *Current Opinion in Pharmacology* 23, pp. 32–38. doi: 10.1016/j.coph.2015.05.011.
- Suthaus, J., Adam, N., Grötzinger, J., Scheller, J. and Rose-John, S. 2011. Viral Interleukin-6: Structure, pathophysiology and strategies of neutralization. *European Journal of Cell Biology* 90(6–7), pp. 495–504. doi: 10.1016/j.ejcb.2010.10.016.
- Tagliamonte, M., Petrizzo, A., Tornesello, M.L., Buonaguro, F.M. and Buonaguro, L. 2014. Antigen-specific vaccines for cancer treatment. *Human Vaccines and Immunotherapeutics* 10(11), pp. 3332–3346. Available at: <https://pubmed.ncbi.nlm.nih.gov/25483639/> [Accessed: 5 September 2022].
- Tao, Q. et al. 2015. Regulatory T cells-derived IL-35 promotes the growth of adult acute myeloid leukemia blasts. *International Journal of Cancer* 137(10), pp. 2384–2393. Available at: <http://www.ncbi.nlm.nih.gov/pubmed/25866142> [Accessed: 6 May 2019].
- Taylor, P.R. and Gordon, S. 2003. Monocyte heterogeneity and innate immunity. *Immunity* 19(1), pp. 2–4. Available at: <https://pubmed.ncbi.nlm.nih.gov/12871633/> [Accessed: 3 August 2020].
- Tedder, T.F. and Leonard, W.J. 2014. Autoimmunity: Regulatory B cells - IL-35 and IL-21 regulate the regulators. *Nature Reviews Rheumatology* 10(8), pp. 452–453. doi: 10.1038/nrrheum.2014.95.
- Tedesco, S. et al. 2018. Convenience versus biological significance: Are PMA-differentiated THP-1 cells a reliable substitute for blood-derived macrophages when studying in vitro polarization? *Frontiers in Pharmacology* 9(FEB). Available at: <https://pubmed.ncbi.nlm.nih.gov/29520230/> [Accessed: 23 November 2021].
- Teng, M.W.L., Vesely, M.D., Duret, H., McLaughlin, N., Towne, J.E., Schreiber, R.D. and Smyth, M.J. 2012. Opposing roles for IL-23 and IL-12 in maintaining occult cancer in an equilibrium state. *Cancer Research* 72(16), pp. 3987–3996. Available at: <http://cancerres.aacrjournals.org/> [Accessed: 26 July 2020].
- Terayama, H. et al. 2014. Contribution of IL-12/IL-35 common subunit p35 to maintaining the testicular immune privilege. *PLoS ONE* 9(4). Available at: [/pmc/articles/PMC3997559/?report=abstract](https://pubmed.ncbi.nlm.nih.gov/25483639/) [Accessed: 3 August 2020].
- Troiano, G. et al. 2019. Prognostic significance of CD68+ and CD163+ tumor associated macrophages in head and neck squamous cell carcinoma: A systematic review and meta-analysis. *Oral Oncology* 93, pp. 66–75. doi: 10.1016/j.oraloncology.2019.04.019.
- Trujillo, J.A., Sweis, R.F., Bao, R. and Luke, J.J. 2018. T cell–inflamed versus Non-T cell–inflamed tumors: a conceptual framework for cancer immunotherapy drug development and combination therapy selection. *Cancer Immunology Research* 6(9), pp. 990–1000. Available at: <https://aacrjournals-org.abc.cardiff.ac.uk/cancerimmunolres/article/6/9/990/469087/T-Cell-Inflamed-versus-Non-T-Cell-Inflamed-Tumors> [Accessed: 21 June 2022].
- Tsushima, F., Tanaka, K., Otsuki, N., Youngnak, P., Iwai, H., Omura, K. and Azuma, M. 2006. Predominant expression of B7-H1 and its immunoregulatory roles in oral squamous cell carcinoma. *Oral Oncology* 42(3), pp. 268–274. doi: 10.1016/J.ORALONCOLOGY.2005.07.013.
- Turan, S., Zehe, C., Kuehle, J., Qiao, J. and Bode, J. 2013. Recombinase-mediated cassette exchange (RMCE) - A rapidly-expanding toolbox for targeted genomic modifications. *Gene* 515(1), pp. 1–27. doi: 10.1016/j.gene.2012.11.016.
- Turnis, M.E. et al. 2016. Interleukin-35 Limits Anti-Tumor Immunity. *Immunity* 44(2), pp. 316–329. Available at: <http://www.ncbi.nlm.nih.gov/pubmed/26872697> [Accessed: 30 April 2019].
- Venneri, M.A. et al. 2007. Identification of proangiogenic TIE2-expressing monocytes (TEMs) in human peripheral blood and cancer. *Blood* 109(12), pp. 5276–5285. Available at: <https://pubmed.ncbi.nlm.nih.gov/17327411/> [Accessed: 3 March 2022].

- Verma, A., Warner, S.L., Vankayalapati, H., Bearss, D.J. and Sharma, S. 2011. Targeting Axl and Mer kinases in cancer. *Molecular cancer therapeutics* 10(10), pp. 1763–1773. Available at: <https://pubmed.ncbi.nlm.nih.gov/abc.cardiff.ac.uk/21933973/> [Accessed: 27 July 2022].
- Vokes, E.E., Agrawal, N. and Seiwert, T.Y. 2015. HPV-Associated Head and Neck Cancer. *Journal of the National Cancer Institute* 107(12), p. djv344. Available at: <https://doi.org/10.1093/jnci/djv344>.
- Vonderheide, R.H. 2020. CD40 Agonist Antibodies in Cancer Immunotherapy. *Annual Review of Medicine* 71, pp. 47–58. Available at: <https://www-annualreviews-org.abc.cardiff.ac.uk/doi/abs/10.1146/annurev-med-062518-045435> [Accessed: 17 March 2022].
- Wang, H. et al. 2021. Immunotherapy Advances in Locally Advanced and Recurrent/Metastatic Head and Neck Squamous Cell Carcinoma and Its Relationship With Human Papillomavirus. *Frontiers in Immunology* 12. Available at: </pmc/articles/PMC8296140/> [Accessed: 12 February 2022].
- Wang, H.M. et al. 2018a. Interleukin-35 suppresses the antitumor activity of T cells in patients with non-small cell lung cancer. *Cellular Physiology and Biochemistry* 47(6), pp. 2407–2419. Available at: <https://pubmed.ncbi.nlm.nih.gov/29991058/> [Accessed: 23 November 2021].
- Wang, J.Y. and Wang, W.P. 2020. B7-H4, a promising target for immunotherapy. *Cellular Immunology* 347, p. 104008. doi: 10.1016/j.cellimm.2019.104008.
- Wang, L. et al. 2016a. Gene expression and antiviral activity of interleukin-35 in response to influenza A virus infection. *Journal of Biological Chemistry* 291(32), pp. 16863–16876. doi: 10.1074/jbc.M115.693101.
- Wang, M., Xiao, C., Ni, P., Yu, J.J., Wang, X.W. and Sun, H. 2018b. Correlation of Betel Quid with Oral Cancer from 1998 to 2017: A Study Based on Bibliometric Analysis. *Chinese Medical Journal* 131(16), pp. 1975–1982. Available at: <https://pubmed.ncbi.nlm.nih.gov/30082530/> [Accessed: 9 August 2020].
- Wang, R.X. et al. 2014. Interleukin-35 induces regulatory B cells that suppress autoimmune disease. *Nature Medicine* 20(6), pp. 633–641. Available at: <http://www.nature.com/doi/10.1038/nm.3554>.
- Wang, S., Zou, Z., Luo, X., Mi, Y., Chang, H. and Xing, D. 2018c. LRH1 enhances cell resistance to chemotherapy by transcriptionally activating MDC1 expression and attenuating DNA damage in human breast cancer. *Oncogene* 37(24), pp. 3243–3259. Available at: <https://pubmed.ncbi.nlm.nih.gov/29545602/> [Accessed: 5 August 2020].
- Wang, X. et al. 2016b. A novel IL-23p19/Ebi3 (IL-39) cytokine mediates inflammation in Lupus-like mice. *European Journal of Immunology* 46(6), pp. 1343–1350. Available at: <http://doi.wiley.com/10.1002/eji.201546095> [Accessed: 27 July 2020].
- Wang, X. et al. 2017. The EF-1 α promoter maintains high-level transgene expression from episomal vectors in transfected CHO-K1 cells. *Journal of Cellular and Molecular Medicine* 21(11), pp. 3044–3054. Available at: <https://onlinelibrary-wiley-com.abc.cardiff.ac.uk/doi/full/10.1111/jcmm.13216> [Accessed: 25 June 2022].
- Wang, Z. et al. 2013. Tumor-Derived IL-35 Promotes Tumor Growth by Enhancing Myeloid Cell Accumulation and Angiogenesis. *The Journal of Immunology* 190(5), pp. 2415–2423. Available at: <http://www.ncbi.nlm.nih.gov/pubmed/23345334> [Accessed: 30 April 2019].
- Weber, M. et al. 2014. Small oral squamous cell carcinomas with nodal lymphogenic metastasis show increased infiltration of M2 polarized macrophages - An immunohistochemical analysis. *Journal of Cranio-Maxillofacial Surgery* 42(7), pp. 1087–1094. Available at: <https://pubmed.ncbi.nlm.nih.gov/24556525/> [Accessed: 9 December 2021].
- Wetzel, A., Scholtka, B., Schumacher, F., Rawel, H., Geisendörfer, B. and Kleuser, B. 2021. Epigenetic dna methylation of ebi3 modulates human interleukin-35 formation via nfkb signaling: A promising therapeutic option in ulcerative colitis. *International Journal of Molecular Sciences* 22(10). Available at: </pmc/articles/PMC8158689/> [Accessed: 15 September 2021].
- Wheeler, K.C. et al. 2018. VEGF may contribute to macrophage recruitment and M2 polarization in the decidua. *PLoS ONE* 13(1). Available at: </pmc/articles/PMC5764356/> [Accessed: 23 November 2021].
- Whiteside, T.L. 2002. Tumor-induced death of immune cells: Its mechanisms and consequences. *Seminars in Cancer Biology* 12(1), pp. 43–50. doi: 10.1006/scbi.2001.0402.
- Whiteside, T.L. 2005. Immunobiology of head and neck cancer. *Cancer and Metastasis Reviews* 24(1), pp. 95–105. Available at: <https://link.springer.com/article/10.1007/s10555-005-5050-6> [Accessed: 9 September 2021].

- Wierzbicka, M., Józefiak, A., Jackowska, J., Szydłowski, J. and Goździcka-Józefiak, A. 2014. HPV vaccination in head and neck HPV-related pathologies. *Otolaryngologia Polska* 68(4), pp. 157–173. Available at: <https://pubmed.ncbi.nlm.nih.gov/24981297/> [Accessed: 14 February 2022].
- Wing, J.B., Ise, W., Kurosaki, T. and Sakaguchi, S. 2014. Regulatory T cells control antigen-specific expansion of T_H cell number and humoral immune responses via the coreceptor CTLA-4. *Immunity* 41(6), pp. 1013–1025. Available at: <https://pubmed.ncbi.nlm.nih.gov/25526312/> [Accessed: 2 September 2022].
- von Witzleben, A., Wang, C., Laban, S., Savelyeva, N. and Ottensmeier, C.H. 2020. HNSCC: Tumour Antigens and Their Targeting by Immunotherapy. *Cells* 9(9). Available at: [/pmc/articles/PMC7564543/](https://pubmed.ncbi.nlm.nih.gov/25526312/) [Accessed: 5 September 2022].
- Wong, N.E., Nauta, I.H., Muijlwijk, T., Leemans, C.R. and van de Ven, R. 2020. The Immune Microenvironment in Head and Neck Squamous Cell Carcinoma: on Subsets and Subsites. *Current Oncology Reports* 22(8). Available at: <https://pubmed.ncbi.nlm.nih.gov/32602047/> [Accessed: 8 December 2021].
- Wood, P. 2011. *Understanding immunology*. Third Edit. Pearson Education Limited. doi: 10.1201/b13504-10.
- Wu, L. et al. 2016a. B7-H4 expression indicates poor prognosis of oral squamous cell carcinoma. *Cancer immunology, immunotherapy* : CII 65(9), pp. 1035–1045. Available at: <https://pubmed.ncbi.nlm.nih.gov/27383830/> [Accessed: 27 July 2022].
- Wu, P. et al. 2016b. Inverse role of distinct subsets and distribution of macrophage in lung cancer prognosis: A meta-analysis. *Oncotarget* 7(26), pp. 40451–40460. Available at: www.impactjournals.com/oncotarget [Accessed: 4 August 2020].
- Wu, W., Jiang, H., Li, Y. and Yan, M.X. 2017. IL-35 expression is increased in laryngeal squamous cell carcinoma and in the peripheral blood of patients. *Oncology Letters* 13(5), pp. 3303–3308. Available at: <https://www.ncbi.nlm.nih.gov/pmc/articles/PMC5431269/>.
- Wu, X. et al. 2013. Immune microenvironment profiles of tumor immune equilibrium and immune escape states of mouse sarcoma. *Cancer Letters* 340(1), pp. 124–133. Available at: <https://linkinghub.elsevier.com/retrieve/pii/S0304383513005582> [Accessed: 26 July 2020].
- Wurm, F.M. 2004. Production of recombinant protein therapeutics in cultivated mammalian cells. *Nature Biotechnology* 22(11), pp. 1393–1398. Available at: <https://www-nature-com.abc.cardiff.ac.uk/articles/nbt1026> [Accessed: 30 June 2022].
- Wyckoff, J. et al. 2004. A paracrine loop between tumor cells and macrophages is required for tumor cell migration in mammary tumors. *Cancer Research* 64(19), pp. 7022–7029. Available at: <https://pubmed.ncbi.nlm.nih.gov/15466195/> [Accessed: 4 August 2020].
- Wyss, A. et al. 2013. Cigarette, cigar, and pipe smoking and the risk of head and neck cancers: Pooled analysis in the international head and neck cancer epidemiology consortium. *American Journal of Epidemiology* 178(5), pp. 679–690. doi: 10.1093/aje/kwt029.
- Xu, X., Ye, J., Huang, C., Yan, Y. and Li, J. 2019. M2 macrophage-derived IL6 mediates resistance of breast cancer cells to hedgehog inhibition. *Toxicology and Applied Pharmacology* 364, pp. 77–82. Available at: <https://pubmed.ncbi.nlm.nih.gov/30578886/> [Accessed: 5 August 2020].
- Xue, J. et al. 2014. Transcriptome-Based Network Analysis Reveals a Spectrum Model of Human Macrophage Activation. *Immunity* 40(2), pp. 274–288. Available at: <https://pubmed-ncbi-nlm-nih-gov.abc.cardiff.ac.uk/24530056/> [Accessed: 3 January 2022].
- Yang, H., Shao, R., Huang, H., Wang, X., Rong, Z. and Lin, Y. 2019a. Engineering macrophages to phagocytose cancer cells by blocking the CD47/SIRPα axis. *Cancer Medicine* 8(9), pp. 4245–4253. Available at: <https://onlinelibrary-wiley-com.abc.cardiff.ac.uk/doi/full/10.1002/cam4.2332> [Accessed: 17 March 2022].
- Yang, L., Shao, X., Jia, S., Zhang, Q. and Jin, Z. 2019b. Interleukin-35 dampens CD8+ T cells activity in patients with non-viral hepatitis-related hepatocellular carcinoma. *Frontiers in Immunology* 10(MAY), p. 1032. doi: 10.3389/fimmu.2019.01032.
- Yang, L. and Zhang, Y. 2017. Tumor-associated macrophages, potential targets for cancer treatment. *Biomarker Research* 5(1), pp. 1–6. Available at: <https://biomarkerres-biomedcentral-com.abc.cardiff.ac.uk/articles/10.1186/s40364-017-0106-7> [Accessed: 9 December 2021].
- Yao, M., Epstein, J.B., Modi, B.J., Pytynia, K.B., Mundt, A.J. and Feldman, L.E. 2007. Current surgical treatment of squamous cell carcinoma of the head and neck. *Oral Oncology* 43(3), pp. 213–223. Available at: <https://pubmed.ncbi.nlm.nih.gov/16978911/> [Accessed: 10 February 2022].

Yeo, E.J. et al. 2014. Myeloid wnt7b mediates the angiogenic switch and metastasis in breast cancer. *Cancer Research* 74(11), pp. 2962–2973. Available at: [/pmc/articles/PMC4137408/?report=abstract](https://pubmed.ncbi.nlm.nih.gov/24819861/) [Accessed: 4 August 2020].

Yu, M. et al. 2019. Prognostic value of tumor-associated macrophages in pancreatic cancer: A meta-analysis. *Cancer Management and Research* 11, pp. 4041–4058. Available at: [/pmc/articles/PMC6504556/?report=abstract](https://pubmed.ncbi.nlm.nih.gov/31111111/) [Accessed: 4 August 2020].

Yuan, X., Zhang, J., Li, D., Mao, Y., Mo, F., Du, W. and Ma, X. 2017. Prognostic significance of tumor-associated macrophages in ovarian cancer: A meta-analysis. *Gynecologic Oncology* 147(1), pp. 181–187. Available at: <https://pubmed.ncbi.nlm.nih.gov/28698008/> [Accessed: 4 August 2020].

Zandberg, D.P. and Strome, S.E. 2014. The role of the PD-L1:PD-1 pathway in squamous cell carcinoma of the head and neck. *Oral Oncology* 50(7), pp. 627–632. Available at: <https://pubmed.ncbi.nlm.nih.gov/24819861/> [Accessed: 16 February 2022].

Zeisberger, S.M., Odermatt, B., Marty, C., Zehnder-Fjällman, A.H.M., Ballmer-Hofer, K. and Schwendener, R.A. 2006. Clodronate-liposome-mediated depletion of tumour-associated macrophages: A new and highly effective antiangiogenic therapy approach. *British Journal of Cancer* 95(3), pp. 272–281. Available at: <https://www-nature-com.abc.cardiff.ac.uk/articles/6603240> [Accessed: 15 March 2022].

Zeng, J.C. et al. 2013. Assessing the role of IL-35 in colorectal cancer progression and prognosis. *International Journal of Clinical and Experimental Pathology* 6(9), pp. 1806–1816. Available at: [/pmc/articles/PMC3759487/](https://pubmed.ncbi.nlm.nih.gov/24819861/) [Accessed: 9 September 2021].

Zhang, F. et al. 2019. Genetic programming of macrophages to perform anti-tumor functions using targeted mRNA nanocarriers. *Nature Communications* 10(1), pp. 1–16. Available at: <https://www-nature-com.abc.cardiff.ac.uk/articles/s41467-019-11911-5> [Accessed: 15 March 2022].

Zhang, H. et al. 2015a. HIF-1 regulates CD47 expression in breast cancer cells to promote evasion of phagocytosis and maintenance of cancer stem cells. *Proceedings of the National Academy of Sciences of the United States of America* 112(45), pp. E6215–E6223. Available at: <https://pubmed.ncbi.nlm.nih.gov/26512116/> [Accessed: 5 August 2020].

Zhang, J. et al. 2016a. IL-35 Decelerates the Inflammatory Process by Regulating Inflammatory Cytokine Secretion and M1/M2 Macrophage Ratio in Psoriasis. *The Journal of Immunology* 197(6), pp. 2131–2144. Available at: <https://www-jimmunol-org.abc.cardiff.ac.uk/content/197/6/2131> [Accessed: 5 January 2022].

Zhang, J., Mao, T., Wang, S., Wang, D., Niu, Z., Sun, Z. and Zhang, J. 2017. Interleukin-35 expression is associated with colon cancer progression. *Oncotarget* 8(42), pp. 71563–71573. Available at: <http://www.ncbi.nlm.nih.gov/pubmed/29069729> [Accessed: 6 May 2019].

Zhang, J.Q. et al. 2018. Macrophages and CD8+ T cells mediate the antitumor efficacy of combined CD40 ligation and imatinib therapy in gastrointestinal stromal tumors. *Cancer Immunology Research* 6(4), pp. 434–447. Available at: <https://aacrjournals-org.abc.cardiff.ac.uk/cancerimmunolres/article/6/4/434/469193/Macrophages-and-CD8-T-Cells-Mediate-the-Antitumor> [Accessed: 17 March 2022].

Zhang, N. and Bevan, M.J. 2011. CD8+ T Cells: Foot Soldiers of the Immune System. *Immunity* 35(2), pp. 161–168. Available at: <https://pubmed.ncbi.nlm.nih.gov/21867926/> [Accessed: 22 February 2022].

Zhang, T. et al. 2021. Correlation Analysis Among the Level of IL-35, Microvessel Density, Lymphatic Vessel Density, and Prognosis in Non-Small Cell Lung Cancer. *Clinical and Translational Science* 14(1), pp. 389–394. Available at: <https://onlinelibrary.wiley.com/doi/full/10.1111/cts.12891> [Accessed: 31 March 2022].

Zhang, X., Zhang, W., Yuan, X., Fu, M., Qian, H. and Xu, W. 2016b. Neutrophils in cancer development and progression: Roles, mechanisms, and implications (Review). *International Journal of Oncology* 49(3), pp. 857–867. Available at: <http://www.spandidos-publications.com/10.3892/ijo.2016.3616/abstract> [Accessed: 19 February 2022].

Zhang, Y., Sun, H., Wu, H., Tan, Q. and Xiang, K. 2015b. Interleukin 35 is an independent prognostic factor and a therapeutic target for nasopharyngeal carcinoma. *Wspolczesna Onkologia* 19(2), pp. 120–124. Available at: <http://www.ncbi.nlm.nih.gov/pmc/articles/PMC4444442/>.

Zhao, X. et al. 2017a. Prognostic significance of tumor-associated macrophages in breast cancer: A meta-analysis of the literature. *Oncotarget* 8(18), pp. 30576–30586. Available at: <https://pubmed.ncbi.nlm.nih.gov/28427165/> [Accessed: 4 August 2020].

Zhao, Z. et al. 2017b. Increased interleukin-35 expression in tumor-infiltrating lymphocytes correlates with poor prognosis in patients with breast cancer. *Cytokine* 89, pp. 76–81. Available at: <http://www.ncbi.nlm.nih.gov/pubmed/27681506> [Accessed: 6 May 2019].

Zheng, X., Turkowski, K., Mora, J., Brüne, B., Seeger, W., Weigert, A. and Savai, R. 2017. Redirecting tumor-associated macrophages to become tumoricidal effectors as a novel strategy for cancer therapy. *Oncotarget* 8(29), pp. 48436–48452. Available at: </pmc/articles/PMC5564660/> [Accessed: 3 January 2022].

Zhou, H., Liu, Z. gang, Sun, Z. wei, Huang, Y. and Yu, W. yuan 2010. Generation of stable cell lines by site-specific integration of transgenes into engineered Chinese hamster ovary strains using an FLP-FRT system. *Journal of Biotechnology* 147(2), pp. 122–129. doi: 10.1016/j.jbiotec.2010.03.020.

Zhou, J., Tang, Z., Gao, S., Li, C., Feng, Y. and Zhou, X. 2020. Tumor-Associated Macrophages: Recent Insights and Therapies. *Frontiers in Oncology* 10, p. 188. Available at: www.frontiersin.org [Accessed: 4 August 2020].

Zhu, J., Wang, Y., Li, D., Zhang, H., Guo, Z. and Yang, X. 2020. Interleukin-35 promotes progression of prostate cancer and inhibits anti-tumour immunity. *Cancer Cell International* 20(1), pp. 1–13. Available at: <https://cancerci.biomedcentral.com/articles/10.1186/s12935-020-01583-3> [Accessed: 17 January 2022].

Zhu, J., Yang, X., Wang, Y., Zhang, H. and Guo, Z. 2019. Interleukin-35 is associated with the tumorigenesis and progression of prostate cancer. *Oncology Letters* 17(6), pp. 5094–5102. Available at: </pmc/articles/PMC6507472/> [Accessed: 17 January 2022].

Zolkind, P. et al. 2018. Cancer immunogenomic approach to neoantigen discovery in a checkpoint blockade responsive murine model of oral cavity squamous cell carcinoma. *Oncotarget* 9(3), pp. 4109–4119. Available at: <https://pubmed.ncbi.nlm.nih.gov/29423108/> [Accessed: 31 August 2022].

Zou, J.M. et al. 2017. IL-35 induces N2 phenotype of neutrophils to promote tumor growth. *Oncotarget* 8(20), pp. 33501–33514. Available at: <https://pubmed.ncbi.nlm.nih.gov/28432279/> [Accessed: 30 July 2020].

Supplementary Data

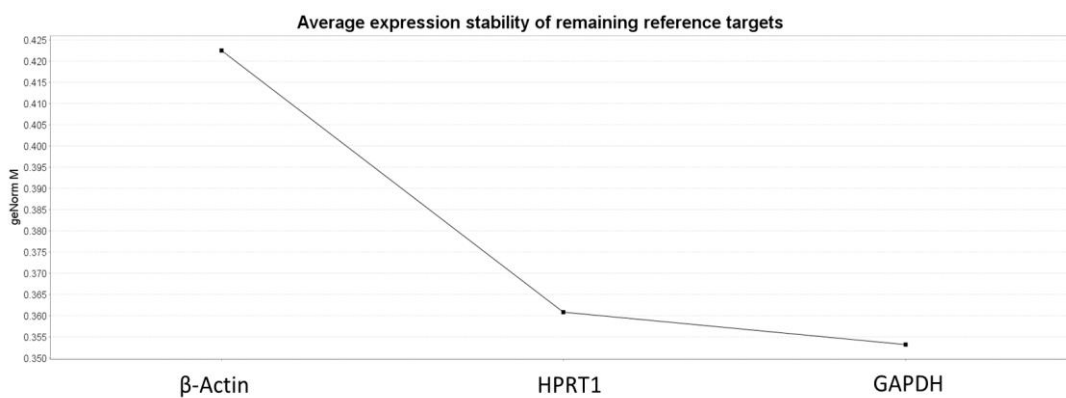
9.1 Supplementary data 1 - RNA Integrity Scores (Chapter 3)

Sample	RNA Integrity Number (RIN)
FaDu	10
FaDu+IFN γ +TNF α (1 ng/mL, 6 h)	10
FaDu+IFN γ +TNF α (10 ng/mL, 6 h)	10
FaDu+IFN γ +TNF α (100 ng/mL, 6 h)	10
FaDu+IFN γ +TNF α (100 ng/mL, 24 h)	10
FaDu+IFN γ +TNF α (100 ng/mL, 48 h)	10
FaDu+IFN γ (100 ng/mL, 48 h)	10
FaDu+TNF α (100 ng/mL, 48 h)	10
H357+IFN γ +TNF α (100 ng/mL, 6h)	9.90

9.2 Supplementary data 2 - Selection of a stable reference gene for qPCR normalisation (Chapter 3)

FaDu cells

Target	Stability Score
β -Actin	0.514
HPRT1	0.353
GAPDH	0.337



H357 cells

Target	Stability Score
β -Actin	0.517
HPRT1	0.301
GAPDH	0.300

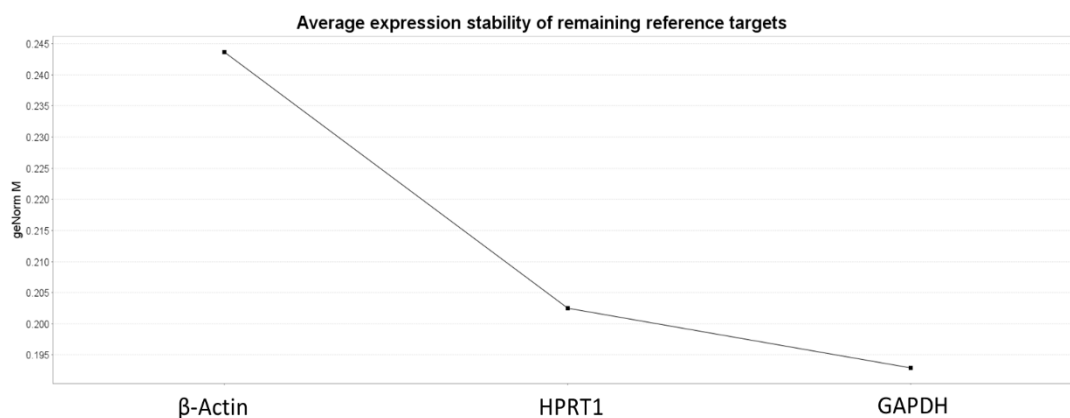


Figure 9.1 Selection of β -Actin as the reference gene for qPCR.

FaDu and H357 cells were treated with IFN γ /TNF α or IL-35/IL-10. cDNA was mixed with each primer and analysed by qPCR. Stability scores calculated by the Thermo Fisher Connect, and the Genorm M graphs, are shown. The most stable gene for each cell type was used as the reference gene in Chapter 3 qPCR studies.

9.3 Supplementary data 3 - Primer Efficiencies for gene targets in Chapter 3

During optimisation of RT-qPCR in Chapter 3, where sufficient gene expression was detected to generate standard curves using RNA dilution series, RT-qPCR efficiencies were calculated for designed primers (**Table 9.1**). High efficiencies may have been a result of impurities in RNA sample preparations. Gp130 could not be determined, possibly due to pipetting error as low volumes were used, or insufficient mixing of RNA in water before loading into qPCR plates. Sufficient data points to generate standard curves could not be obtained for p28 and p40, and as such, data could not be shown.

Table 9-1 qPCR efficiencies calculated for primers used in Chapter 3

Gene	Amplification factor	Efficiency
β -Actin	2.46	146%
EBI3	2.8	180%
p35	2.08	108%
p19	1.94	94%
IL-12R β 2	2.13	113%

9.4 Supplementary data 4 - Estimations of basal gene expression by RT-qPCR (Chapter 3)

Table 9-2 - Mean CT values of all target genes in Chapter 3 within resting FaDu and H357 cells (n=3)

Gene	Mean CT (FaDu)	Mean CT (H357)
β -Actin	15	15
EBI3	31	28
p35	30	30
p19	30	31
p28	Undetectable	32
p40	Undetectable	Undetectable
GP130	25	22
IL-12R β 2	Undetectable	Undetectable

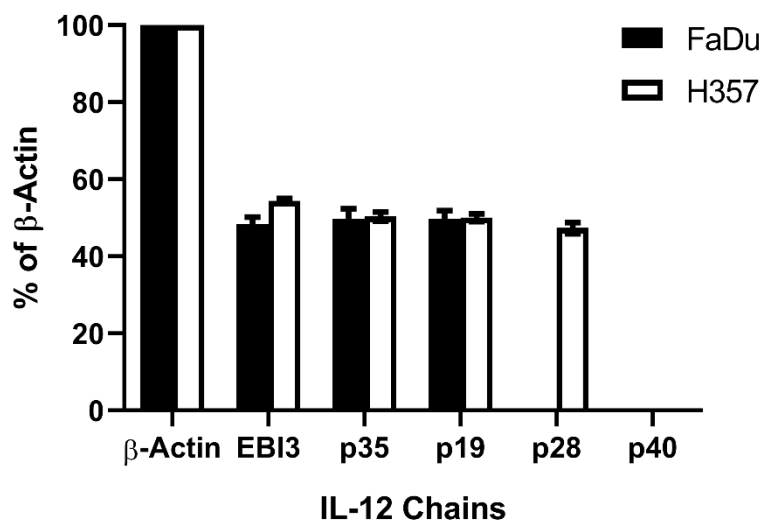
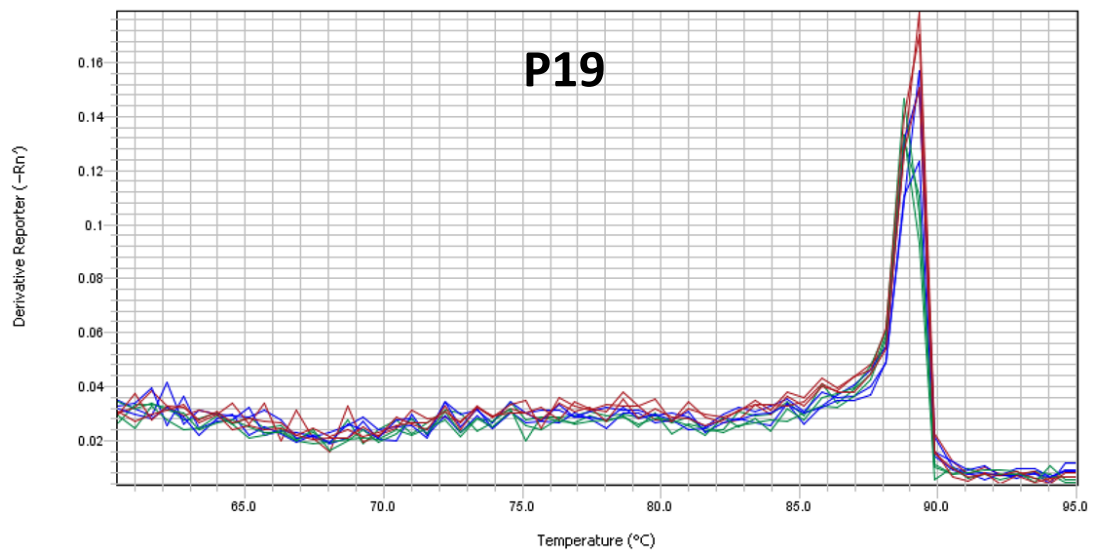
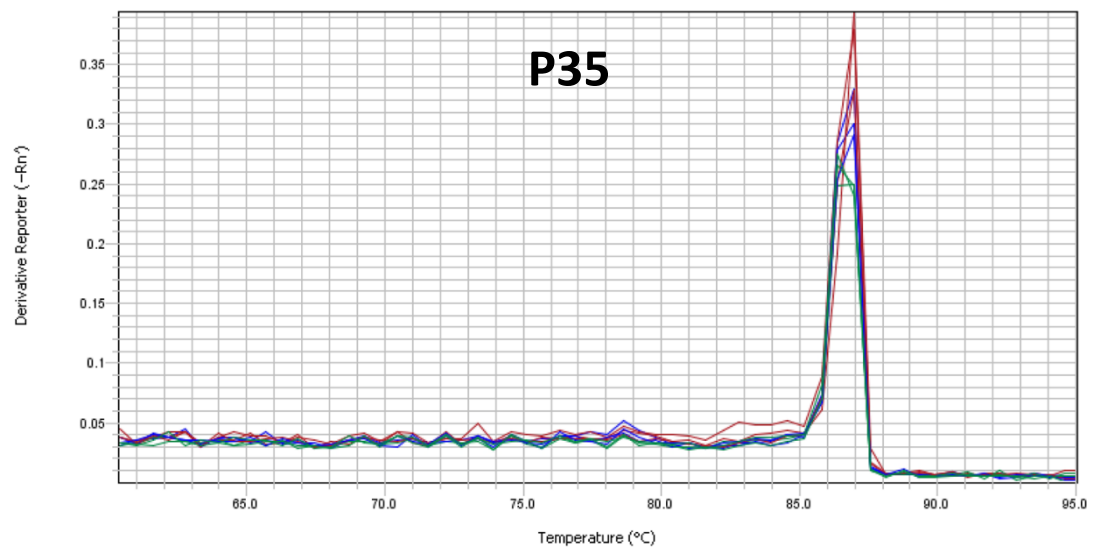
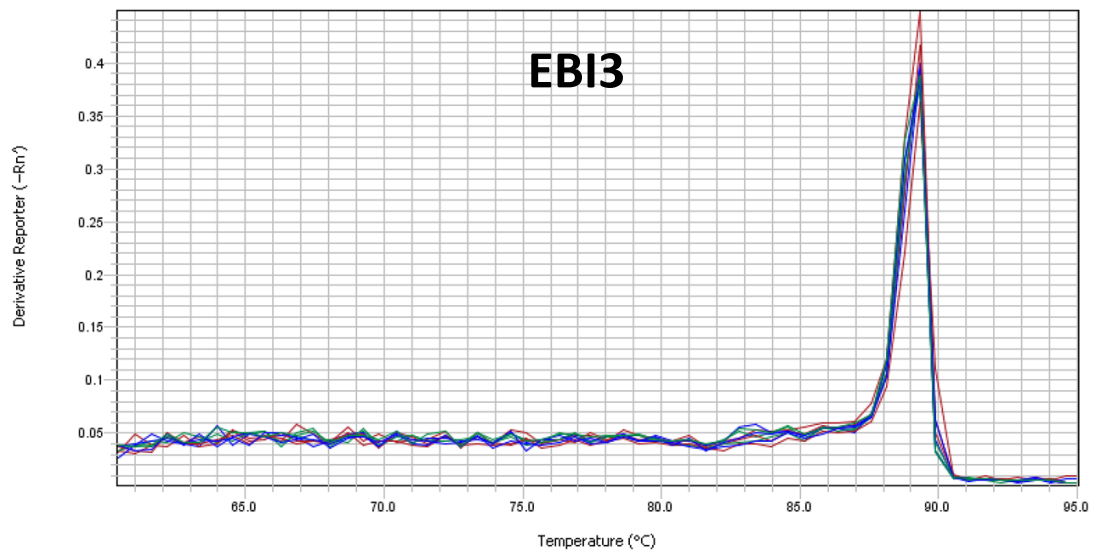
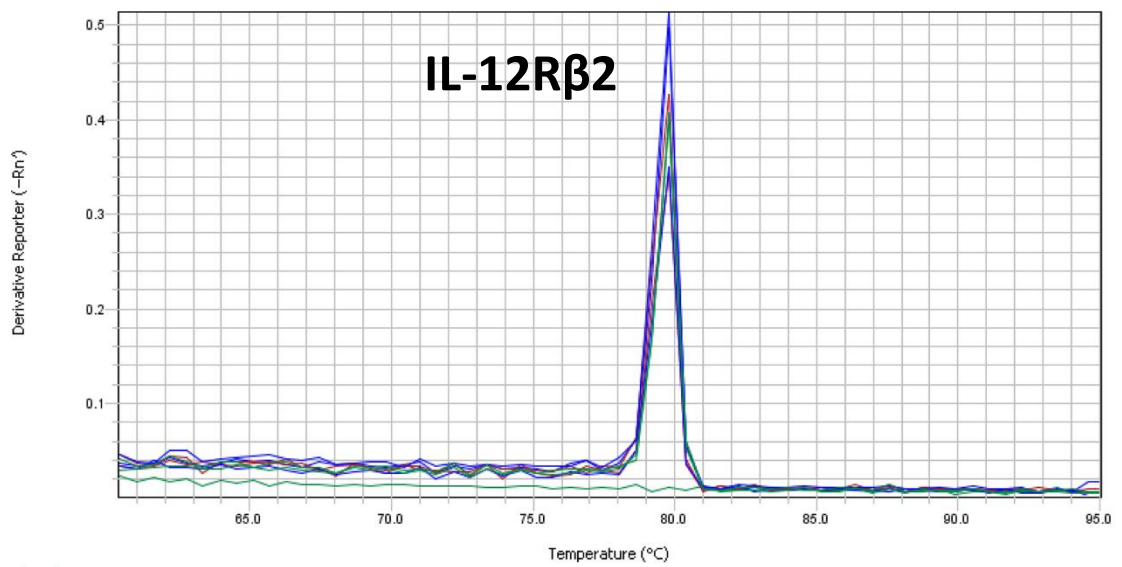
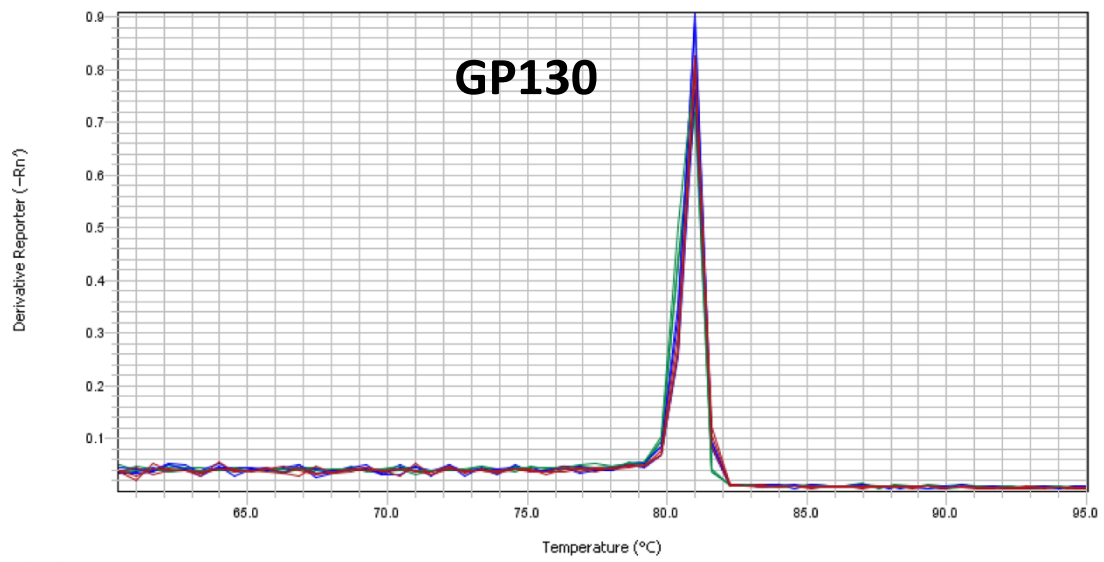
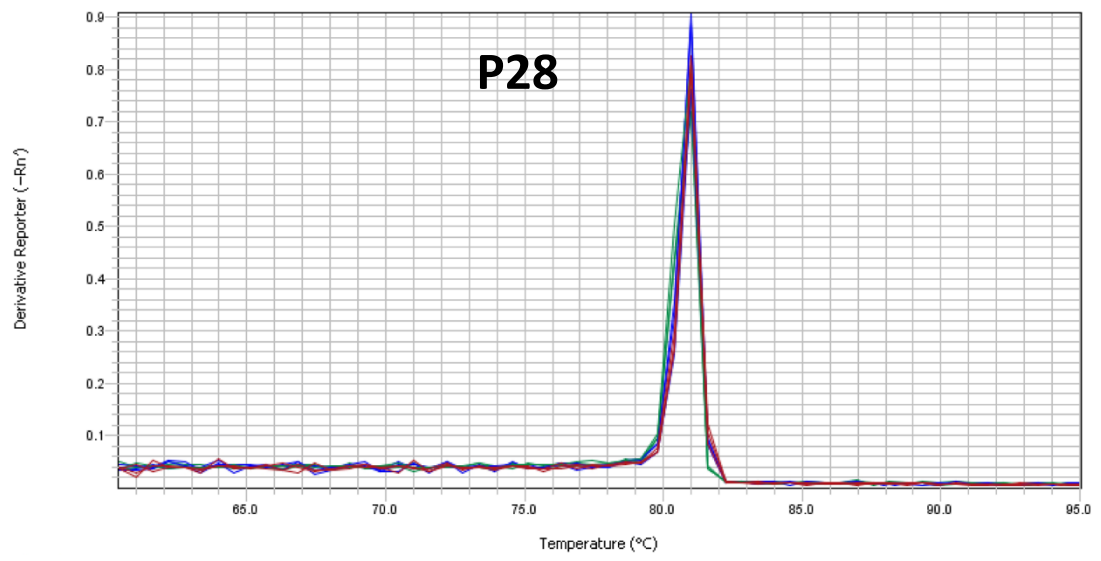


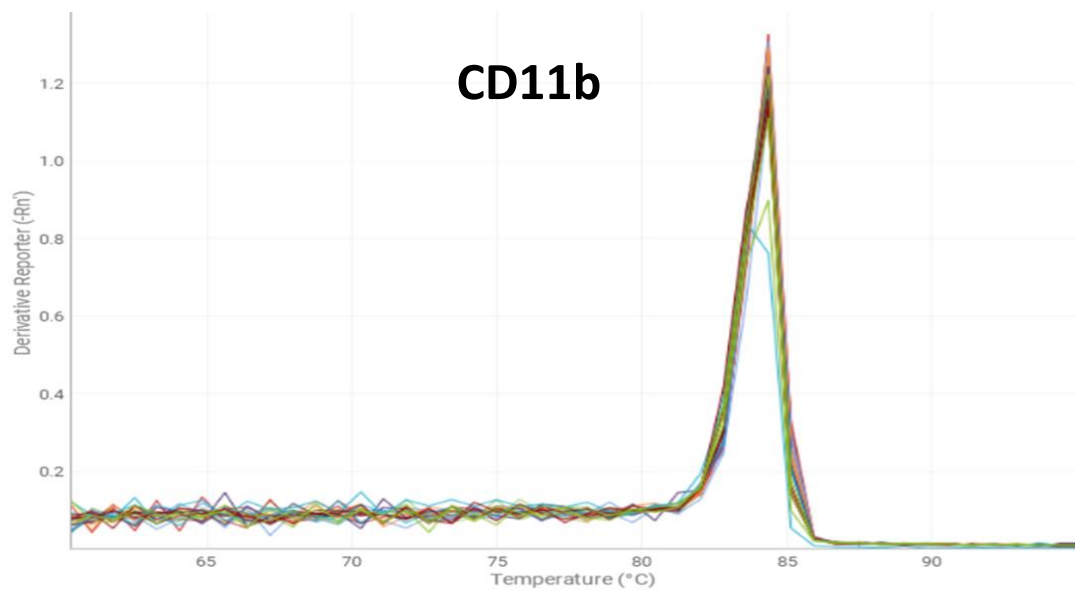
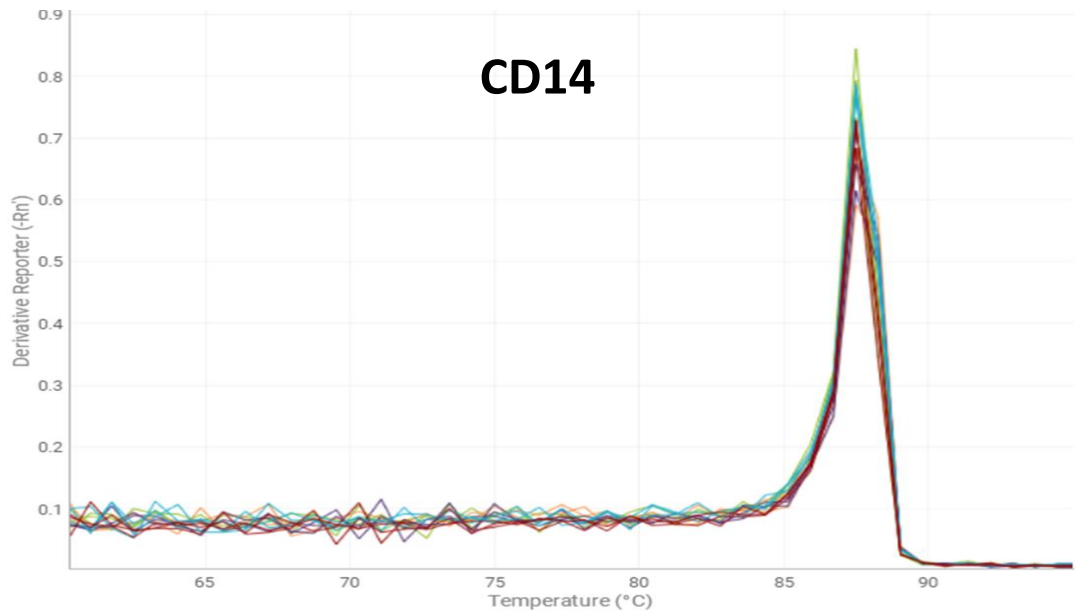
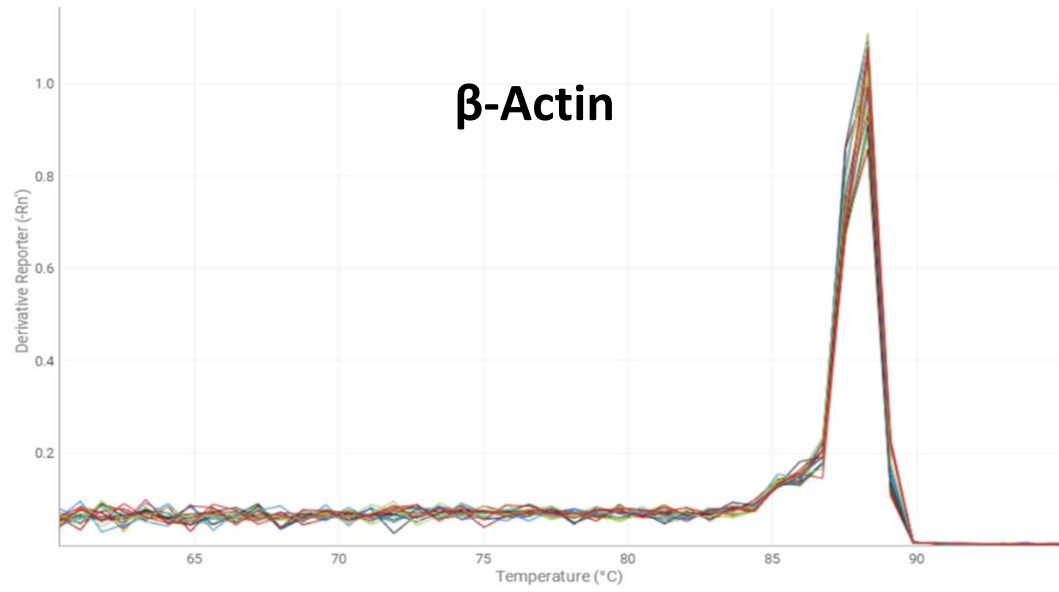
Figure 9.2 Expression of IL-12 chains in HNSCC cell lines.

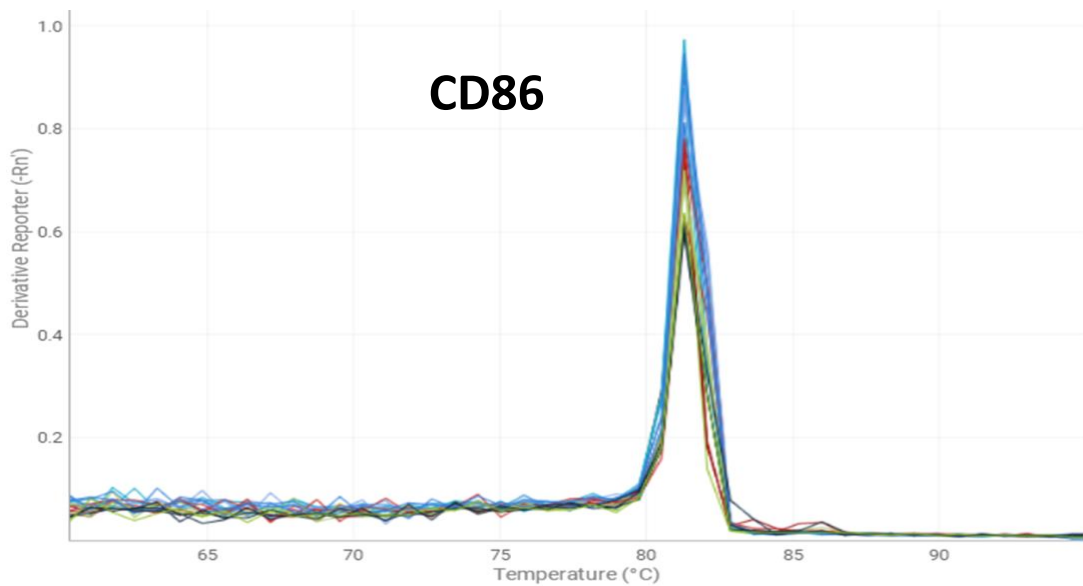
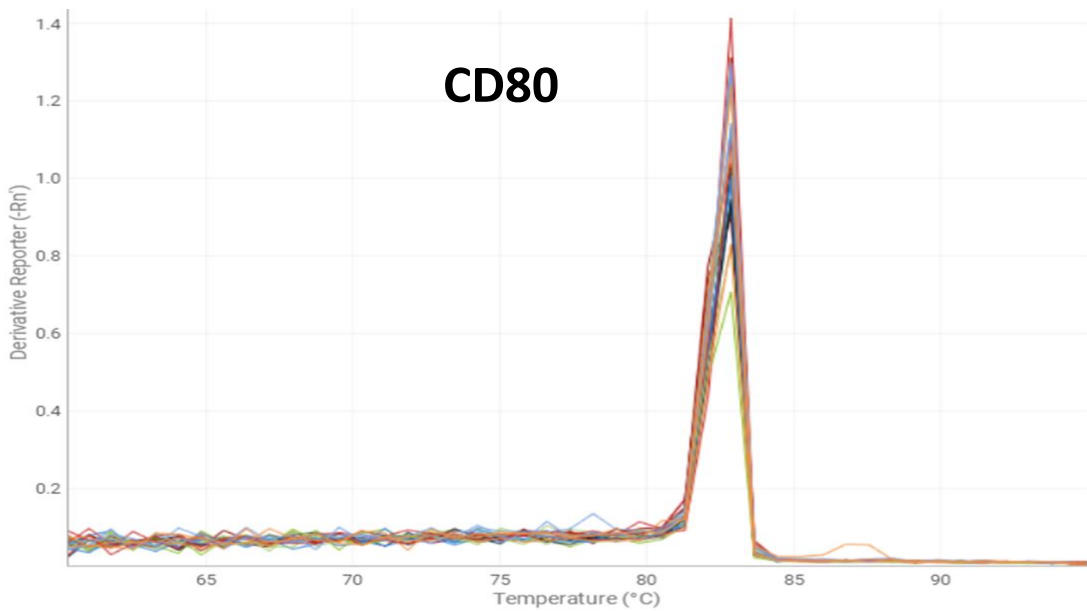
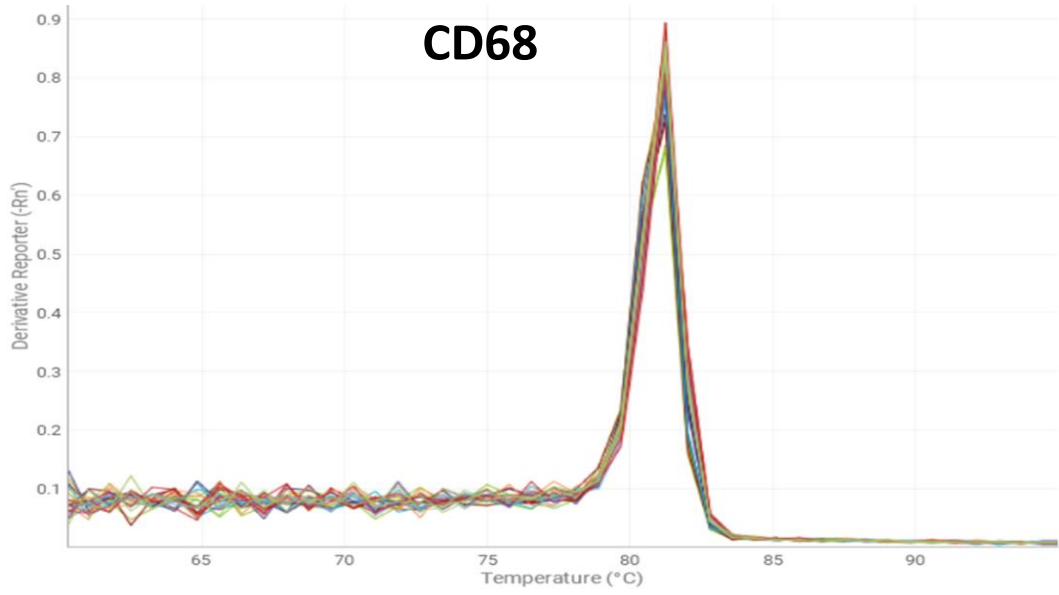
Gene expression of IL-12 chains were analysed by qPCR in resting FaDu and H357 cells (n=3). β -Actin was used as an endogenous control. β -Actin-CT values were divided by CT values for each target gene and multiplied by 100. Expression of each gene is represented as mean % of β -Actin \pm SEM of the mean.

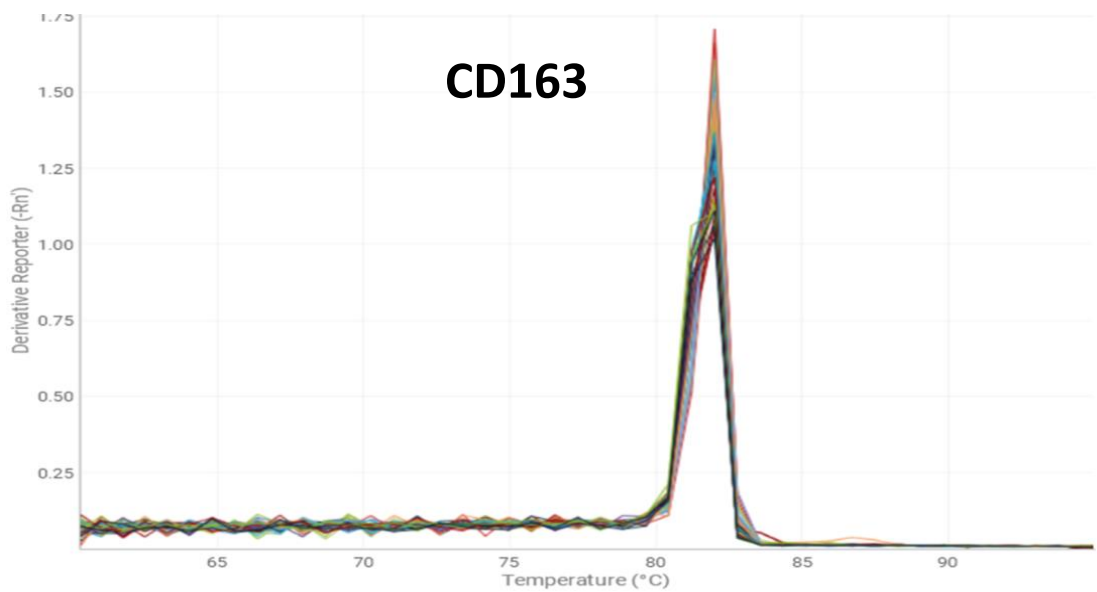
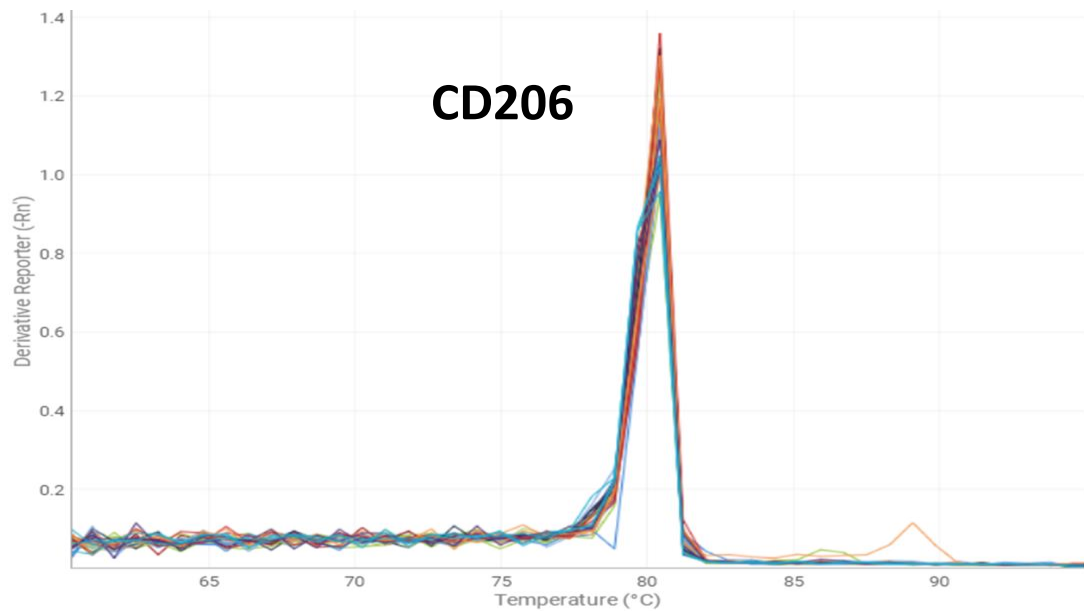
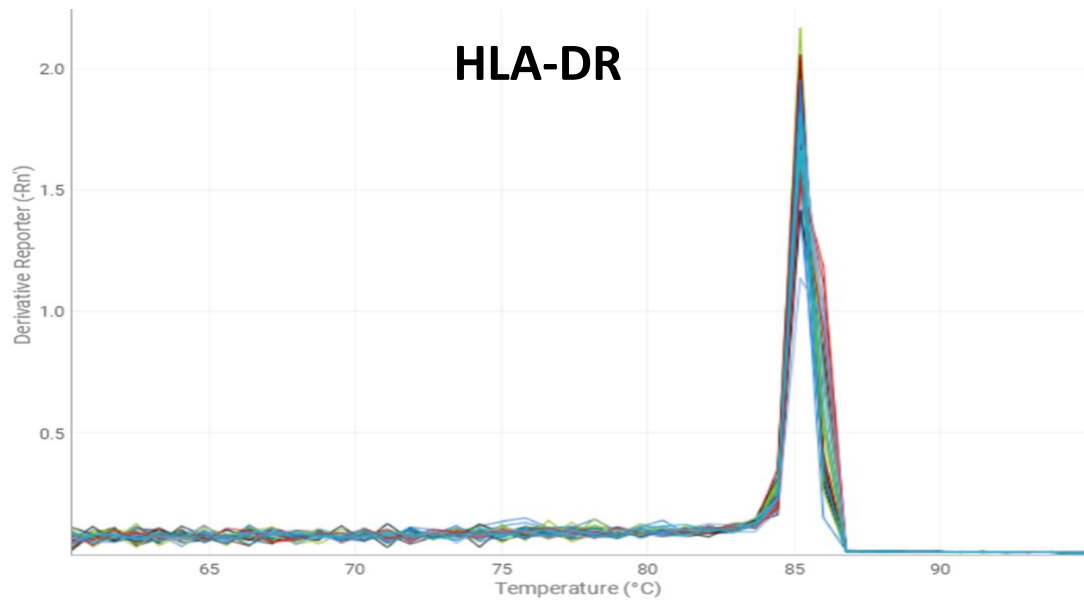
9.5 Supplementary data 5 – RT-qPCR Dissociation (Melt) Curves











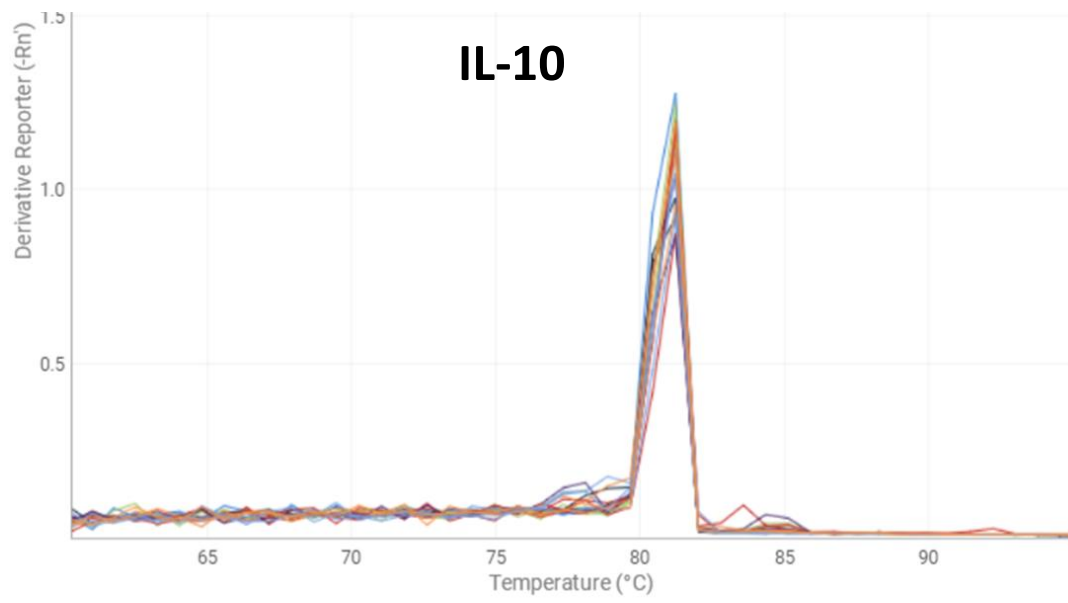


Figure 9-3 Dissociation curves for targets detected by qPCR.

For all genes analysed by qPCR, representative melt curves are shown.

9.6 Supplementary data 6 - Immunoprecipitation/Western blot detection of p35 in FaDu cells stimulated with IFN γ

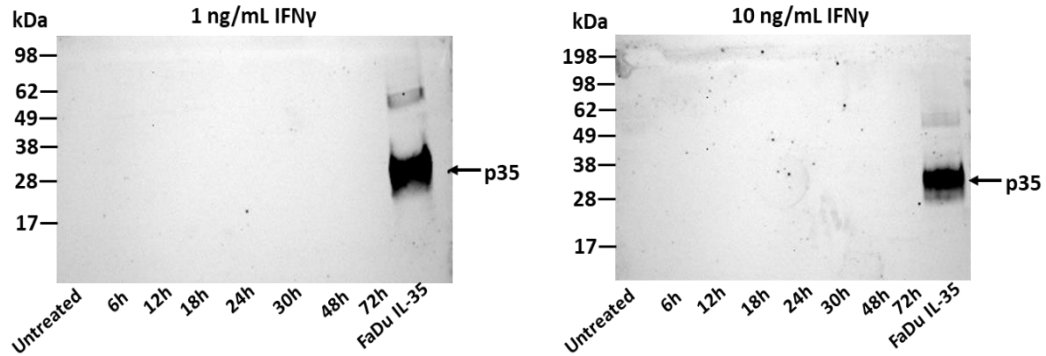


Figure 9.4 Detection of p35 protein in FaDu cells stimulated with IFN γ by immunoprecipitation. FaDu cells were stimulated with IFN γ (1 or 10 ng/mL). Lysates were immunoprecipitated with anti-p35 and pulled down p35 detected by Western Blot.

9.7 Supplementary data 7 – Co-immunoprecipitation/Western blot to detect EB13 and p35 using the Veriblot antibody

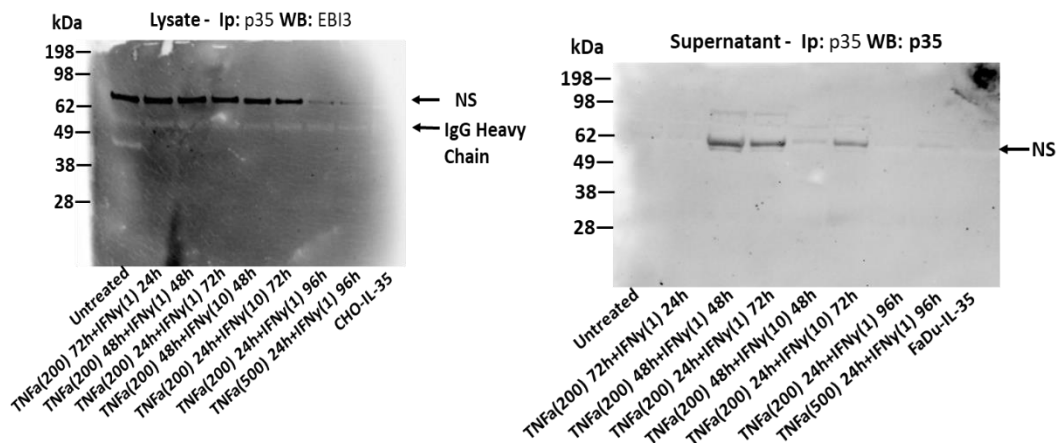


Figure 9.5 Detection of IL-35 protein by co-immunoprecipitation of p35 and EB13. FaDu cells were stimulated with IFN γ and TNF α with concentrations (ng/mL) and times as shown. P35 was immunoprecipitated from lysates and supernatants. P35 and EB13 were detected from eluates using Western Blotting using anti-p35 and anti-EB13 and the veriblot secondary antibody. Blot data is shown. P35 data from lysates and EB13 data from supernatants could not be retrieved.

9.8 Supplementary Data 8 – Gating strategy to identify single, live THP1 or M1/M2 macrophages in monoculture when validating M1 or M2 polarisation

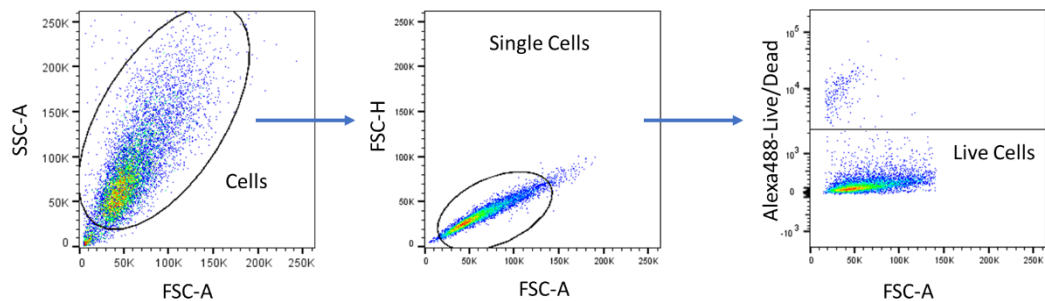


Figure 9.6 Identification of single, live THP1 or macrophage cells in monoculture. Cultured THP1 M1 or M2 macrophages were stained with a Live/Dead kit and antibodies that detect M1 and M2 polarisation markers. The image shows a representative example of the gating strategy used to identify single live THP1 or macrophage cells in monoculture. Cells were first identified by exclusion of debris. Doublet discrimination was used to gate on single cells. Live cells were obtained by gating on those negative for Live/Dead staining.

9.9 Supplementary Data 9 – Gating strategy to identify single, live CD326-macrophages when co-cultured with FaDu or FaDu-IL-35 cells

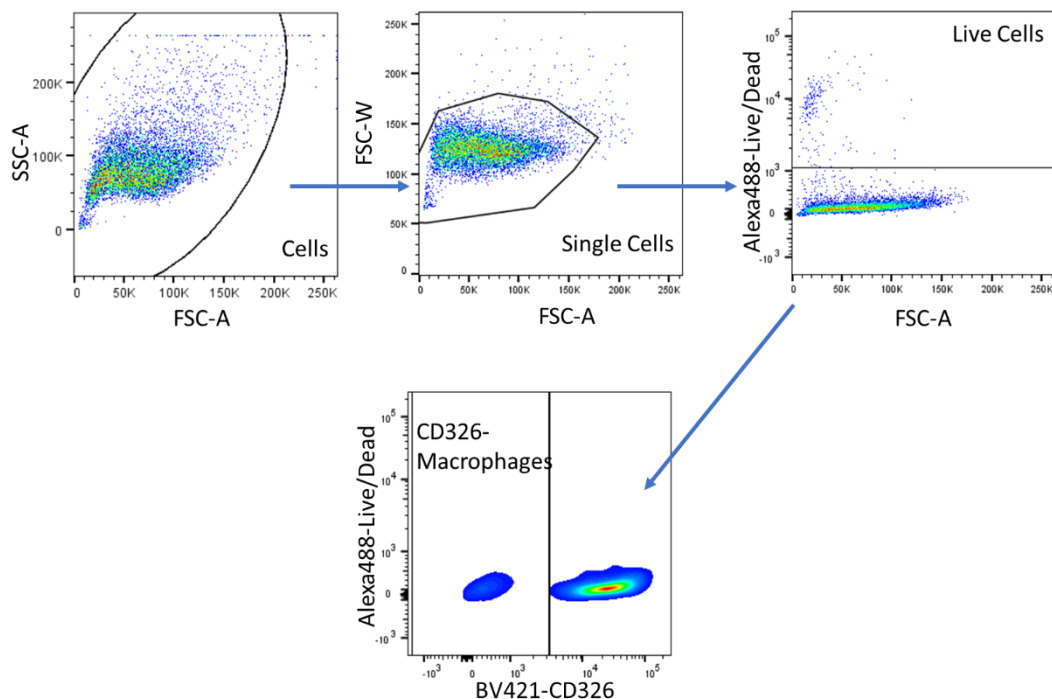


Figure 9.7 Identification of macrophages from the mixed cell population. M1 or M2 macrophages were co-cultured with FaDu or FaDu-IL-35 cells and stained with a Live/Dead kit and the macrophage polarisation antibody panel. The image shows a representative example of the gating strategy used to identify live macrophages from the mixed cell population. Cells were obtained via exclusion of debris. Doublet exclusion enabled gating on single cells. Live cells were obtained via inclusion of Live/Dead negative cells only. Macrophages were then isolated from FaDu cells by gating on the CD326- population.

9.10 Supplementary Data 10 – Gating strategy to identify single, CD326+ CD14- FaDu cells when co-cultured with M1 or M2 macrophages

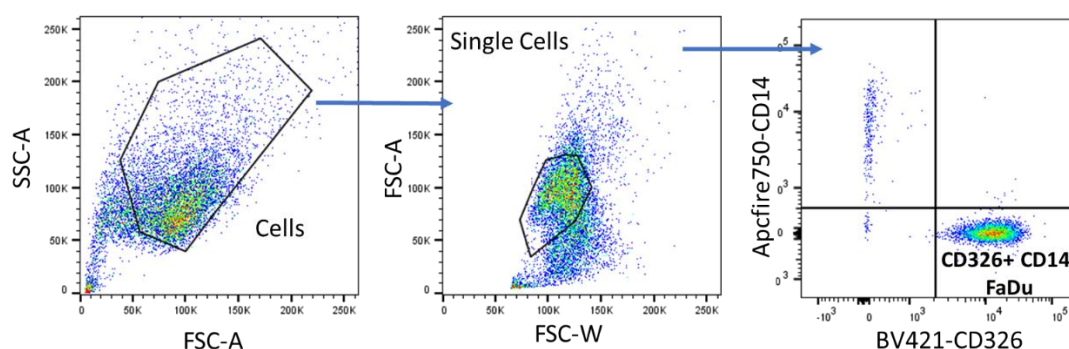
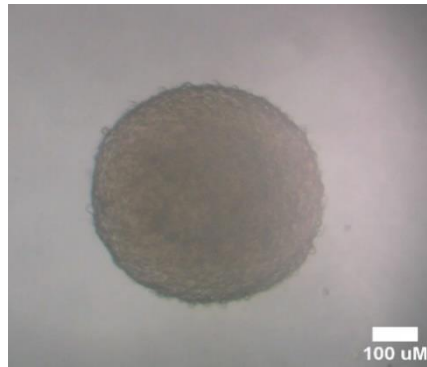


Figure 9.8 Gating strategy used to identify CD326+ FaDu or FaDu-IL-35 cells. FaDu or FaDu-IL-35 cells were mixed in culture with M1 or M2 macrophages. To identify FaDu or FaDu-IL-35 cells, debris was first excluded before doublet discrimination to gate on single cells. FaDu/FaDu-IL-35 cells were then identified using CD326+ CD14- gating.

9.11 Supplementary Data 11 – 3D tumour spheroids

3D tumour spheroids were generated using the hanging drop method. FaDu cells successfully aggregated to form densely packed spheroids with smooth edges. A representative image of spheroids formed after 24 h is shown in **Figure 9.9A**. FaDu cells mixed 20:1 with M1 macrophages (**Figure 9.9B**) and M2 macrophages (**Figure 9.9C**) also successfully formed spheroids. To test for macrophage-mediated inhibition of FaDu 3D spheroid growth, FaDu monoculture, FaDu/M1 and FaDu/M2 mixed cultures were prepared and used to seed hanging drops. Drops were incubated for 72 h, with images captured every 24 h. Mean surface area at each time point was calculated from measurements taken from ten individual spheroids per culture setting. Mean spheroid areas are shown in **Figure 9.10**. The data shows that M1 and M2 macrophages may reduce the rate at which FaDu spheroids grow.

(A)



(B)



(C)



Figure 9.9 Representative images of 3D spheroids derived from FaDu monoculture and FaDu/macrophage co-culture, using the hanging drop technique. (A) FaDu cell spheroid after 24 h (B) Spheroid formed from FaDu cells mixed 20:1 with M1 macrophages (C) Spheroid from FaDu cells mixed with M2 macrophages. Images captured using an inverted microscope. Magnification 4X. Scale bars = 100 μ M.

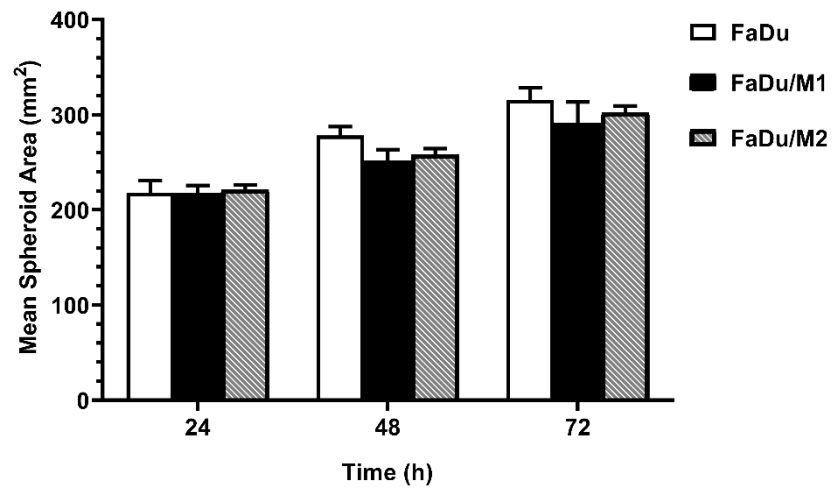


Figure 9.10 Mean areas of 3D spheroids formed from FaDu, FaDu/M1 or FaDu/M2 mixed cultures (20:1 ratio) after 24, 48 and 72 h. Data represents mean+SD. (N=1).

9.12 Supplementary data 12 - Morphology and scatter data for M1 and M2 macrophages

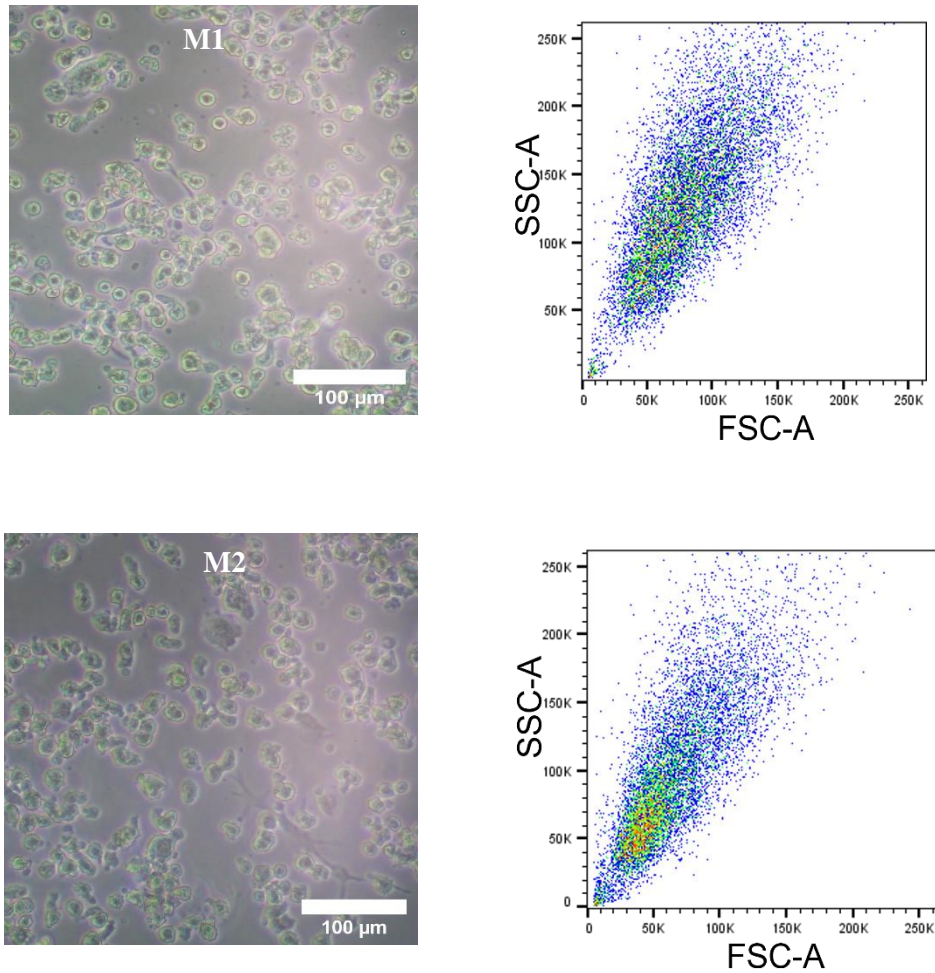


Figure 9.11 Cell morphologies and forward/side scatter data taken from M1 and M2 macrophages.

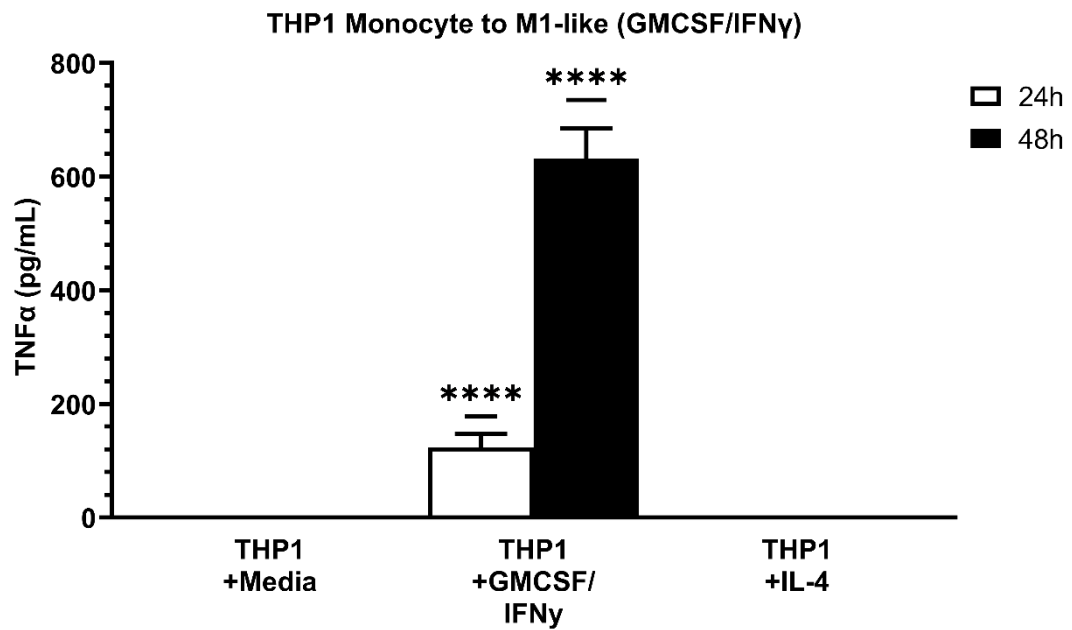
9.13 Supplementary data 13 – TNF α secretion in the M1-like cell model

Figure 9.12 TNF α secretion in M1-like cells. M1-like cells were generated. 24 h and 48 h after addition of IFN γ , supernatant was collected and analysed by ELISA. Mock treated THP1 cells and those treated with IL-4 (20 ng/mL) were used as controls. Data shown represents mean + standard error. N=3. Statistics analysed using One Way Anova and Dunnetts post hoc test. **** = $p < 0.0001$

9.14 Supplementary data 14 – Preliminary IL-10 ELISA data

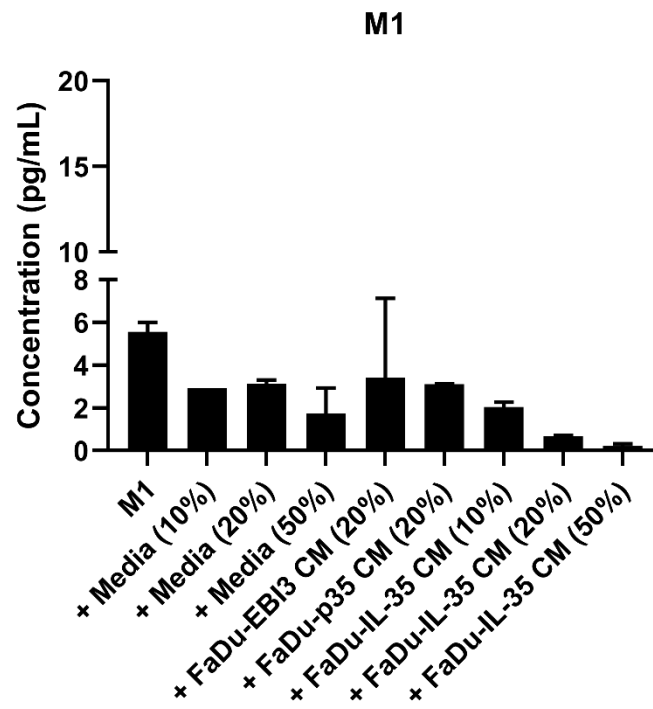
It was investigated whether HNSCC-derived IL-35, at increasing concentrations (10%, 20% or 50% CM) could induce upregulation of IL-10 secretion in M1, M0 or M2 macrophages. Each macrophage model was treated with FaDu-IL-35 CM, or that taken from FaDu-EBI3 or FaDu-p35 cells (20% CM). After 48 h, supernatants were collected and analysed for secretion of IL-10 by ELISA.

IL-10 was produced at low levels in M1 macrophages (**Figure 9.13A**). Treatment with FaDu-IL-35 CM marginally decreased IL-10 production in a dose-dependent manner. Control CM treatments had no effect. Thus, the data suggested that HNSCC-derived IL-35 may not promote M1 to M2 repolarisation via upregulation of IL-10 secretion.

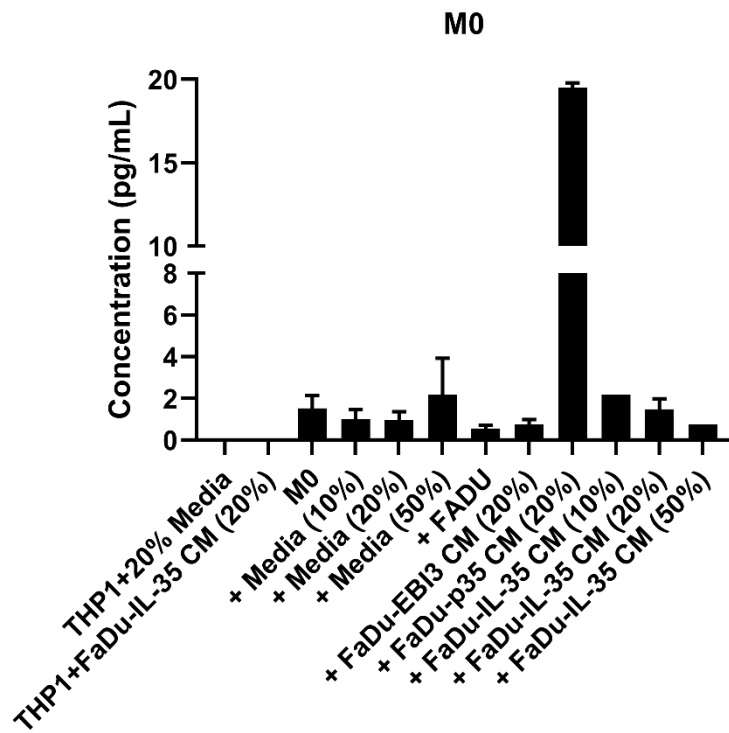
M0 macrophages produced low concentrations of IL-10 (**Figure 9.13B**). Treatment with FaDu-IL-35 CM had no effect regardless of the concentration added. FaDu-p35 CM markedly increased IL-10 secretion. Therefore HNSCC-derived IL-35 may have no effect on IL-10 secretion in resting M0 macrophages. However, when HNSCC cells overexpress p35, the secretome from these cells may potentially induce IL-10 secretion.

M2 macrophages expressed very low levels of IL-10 (**Figure 9.13C**). FaDu-IL-35 CM had no effect, nor did treatment with other CM samples. Thus, HNSCC-derived IL-35 may not promote IL-10 secretion in any of the tested macrophage models. The secretome from tumour cells that overexpress p35 however, may upregulate IL-10 secretion in stimulated macrophages.

(A)



(B)



(c)

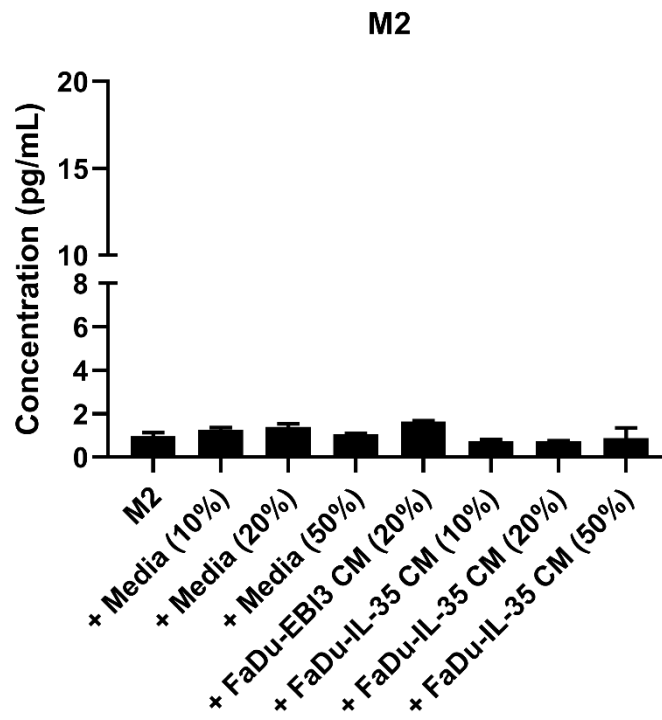


Figure 9.13 Assessment of the effects of HNSCC-derived IL-35 on IL-10 secretion in M1, M0 and M2 macrophage models. M1 (A), M0 (B) and M2 (C) macrophage models were seeded and treated for 48 h with CM from transfected FaDu cells lines at the percentages of the culture volumes shown. Changes in the concentration (pg/mL) of IL-10 secreted was analysed by ELISA. Data shown represents mean+SD. n=1. Samples run in duplicate.